

UNIVERSITÉ DU QUÉBEC À MONTRÉAL

NEW STRATEGY TOWARD THE SYNTHESIS OF
THERAPEUTIC GLYCONANOMATERIALS

THESIS
PRESENTED
AS PARTIAL REQUIREMENT
OF THE DOCTORATE OF CHEMISTRY

BY
SHUAY ABDULLAYEV

NOVEMBER 2021

UNIVERSITÉ DU QUÉBEC À MONTRÉAL

NOUVELLES STRATÉGIES DE SYNTHÈSE DE
GLYCONANOMATÉRIAUX THÉRAPEUTIQUES

THÈSE
PRÉSENTÉE
COMME EXIGENCE PARTIELLE
DU DOCTORAT EN CHIMIE

PAR
SHUAY ABDULLAYEV

NOVEMBRE 2021

UNIVERSITÉ DU QUÉBEC À MONTRÉAL
Service des bibliothèques

Avertissement

La diffusion de cette thèse se fait dans le respect des droits de son auteur, qui a signé le formulaire *Autorisation de reproduire et de diffuser un travail de recherche de cycles supérieurs* (SDU-522 – Rév.04-2020). Cette autorisation stipule que «conformément à l'article 11 du Règlement no 8 des études de cycles supérieurs, [l'auteur] concède à l'Université du Québec à Montréal une licence non exclusive d'utilisation et de publication de la totalité ou d'une partie importante de [son] travail de recherche pour des fins pédagogiques et non commerciales. Plus précisément, [l'auteur] autorise l'Université du Québec à Montréal à reproduire, diffuser, prêter, distribuer ou vendre des copies de [son] travail de recherche à des fins non commerciales sur quelque support que ce soit, y compris l'Internet. Cette licence et cette autorisation n'entraînent pas une renonciation de [la] part [de l'auteur] à [ses] droits moraux ni à [ses] droits de propriété intellectuelle. Sauf entente contraire, [l'auteur] conserve la liberté de diffuser et de commercialiser ou non ce travail dont [il] possède un exemplaire.»

ACKNOWLEDGEMENTS

Firstly, I would like to thank my supervisor, Professor René Roy, for all his support, patience, and guidance throughout my entire Ph.D studies and for giving me an opportunity to join his research group. He always opened his mind for any help and discussions. Moreover, I have to say that during writing my thesis and reviewing anterior and present research works in the field, I became one more time sure how creative and imaginative scientist and supervisor he is. I really appreciate your supervision and will always remember you.

I sincerely thank Prof. Alexandre Gagnon who accepted me to his group in 2016 and helped me to continue my academic carrier at UQAM.

I would like to thank Prof. Sylvain Canesi, Prof. Daniel Chapdelaine and Prof Steve Bourgault for being part of my thesis committee members and for their valuable help and suggestions regarding the project.

I am thankful to all technical and administrative staff of the chemistry department of UQAM. Special thanks to Pascal Beauchemin (Department Secretary), Luc Arsenault, (ChemStore) Dr. Alexandre Arnold (NMR) for their help.

I am also grateful to Leanne Ohlund for providing HRMS and HPLC analysis of my samples, Dr. Phuong Trang Nguyen, and Dr. Ximena Zottig from Bourgault's group for their help in HPLC analysis.

Thanks also go to former and present Roy group members, especially to Dr. Rabindra Rej and Tze-Chieh Siao for their support and encouragement.

I must also thank Laman Seyidova, Nargiz Novruzova, Elchin Isgandarov, Leyla Adishirinli, Narmin Babayeva, Havva Mammadova, Behzad Ahmadov, Samir Garayev, Orxan Aliyev, Elshan Mustafayev, Célia Sehad, Guillaume Michaud, Dr. Adrien Le Roch and all my other friends and colleagues for standing by my side during the Ph.D program.

Finally, I would like to thank my family members and relatives: Tunzala Ahmadova, Svetlana Abdullayeva, Anjella Abdullayeva, Sabina Javadova, Ravan Hajimammadli, Turkhan Hadiyev for their continuous encouragement and support throughout my study. Without their moral support especially after my father's sudden death, it would have been really a hard task to finish my Ph.D. I also thank Aytan Pirverdiyeva who came into my life in 2019 and guided me through. I deeply apologize that I could not afford you enough time especially during writing period of my thesis. Thank you that you have been there for me all the time.

DEDICATED

Dedicated to my lovely father who passed
away during my Ph.D in 2018

TABLE OF CONTENTS

LIST OF FIGURES	ix
LIST OF SCHEMES	xxv
LIST OF TABLES.....	xxviii
LIST OF ABBREVIATIONS	xxix
RÉSUMÉ	xxxiii
ABSTRACT	xxxv
CHAPTER I INTRODUCTION TO CARBOHYDRATE-PROTEIN INTERACTIONS	
1.1 Fundamentals of carbohydrate-protein interaction	1
1.1.1 Chelation of metals.....	1
1.1.2 Hydrogen bonding	2
1.1.3 Hydrophobic interactions	3
1.1.4 Ionic interactions	4
1.2 Lectins	5

1.2.1	Plant Lectins	6
1.2.2	Microbial Lectins.....	7
1.2.3	Animal Lectins	8
1.2.4	Carbohydrate-specific Enzymes	11
1.3	Multivalency in Protein-Carbohydrate Recognition	12
1.4	Multivalent Neoglycoconjugates	15
CHAPTER II INTRODUCTION TO DENDRIMERSOMES.....		18
2.1	Nanosized drug carriers and dendrimersomes	19
2.2	Lidocaine-loaded self-assembling amphiphilic Janus-dendrimer	21
2.2.1	Lidocaine as local anesthetic agent	22
2.3	Results and discussion.....	22
2.3.1	DLS studies.....	25
2.3.2	Infrared spectrum analysis.....	27
2.3.3	DSC studies	28
2.3.4	Atomic force microscopy (AFM) analysis	30
2.3.5	Transmission electron microscopy (TEM) analysis.....	31
2.4	Conclusion.....	31
2.5	Perspective	32
CHAPTER III Efficient and Regioselective 3'-O-Funtionnalization of Propargyl and <i>Para</i> -nitrophenyl-based Lactosides as Inhibitors of Galectins.....		34
3.1	Galectins and their role in biology	35
3.2	Monovalent Ligands of Galectins	40
3.3	Aim of the Project	46

3.3.1	Synthesis of a small library of <i>O</i> 1- and <i>O</i> 3'-derivatives of Lac and LacNAc.....	46
3.3.2	Results and discussion	51
3.4	Conclusion.....	72
CHAPTER IV Design and Synthesis of Glycodendrimersomes towards Cancer related Galectins		
		73
4.1	Bivalent ligands.....	74
4.2	Trivalent ligands.....	78
4.3	Tetravalent Ligands.....	81
4.4	Multivalent ligands.....	83
4.4.1	Neoglycoproteins.....	83
4.4.2	Neoglycopeptides	87
4.4.3	Glyco-gold nanoparticles.....	89
4.4.4	Glycopolymers.....	92
4.4.5	Glycodendrimers	95
4.4.6	Introduction to new class of neoglycoconjugates: Glycodendrimersomes	
	99	
4.5	Aim of the Project: Design and synthesis of LacNAc-decorated glycodendrimersomes	104
4.6	Result and Discussion	106
4.6.1	Synthesis LacNAc-conjugated amphiphilic Janus-Dendrimers (LacNAc-JDs) and generation glycodendrimersomes	106
4.7	Conclusion.....	123

CHAPTER V DESIGN AND SYNTHESIS OF SIALIC ACID-CONJUGATED DENDRIMERSOMES	124
5.1 Introduction to sialic acid.....	124
5.1.1 Sialic acid dependence of Influenza virus in host-cell invasion.....	126
5.1.2 Hemagglutinin of Influenza A viruses.....	127
5.1.3 Neuraminidase enzyme of Influenza A virus	129
5.1.4 Sialic acid binding Siglec family	131
5.2 Sialic acid in chemistry	136
5.2.1 Anomeric leaving groups.....	137
5.2.2 Influence of C5 protecting group modification	141
5.2.3 N5,O4-cyclic protecting group-mediated sialylation.....	142
5.2.4 Thiosialosides	145
5.2.5 Multivalent Sialoconjugates	148
5.3 Aim of the project: Synthesis of new class of sialoconjugates: Sialodendrimersomes.....	168
5.3.1 Synthesis of hydrophilic segments	168
5.3.2 S-sialoside synthesis	171
5.3.3 O-sialoside synthesis	187
5.3.4 Synthesis of amphiphilic Janus sialodendrimer and generation of sialodendrimersomes	203
5.4 Conclusion.....	210
CONCLUSION	213
CHAPTER VI EXPERIMENTAL PARTS.....	216
6.1 Materials and methods	216

6.2	Experimental Part of Chapter II	218
6.2.1	Synthesis and characterization.....	218
6.3	Experimental Part of Chapter III.....	257
6.3.1	Synthesis and characterization.....	257
6.4	Experimental Part of Chapter IV.....	364
6.4.1	Synthesis and characterization.....	364
6.5	Experimental Part of Chapter V	394
6.5.1	Synthesis and characterization.....	394
	REFERENCES	449

LIST OF FIGURES

Figure	Page
1.1 Coordination of Ca ²⁺ in sugar binding region. <i>Cratylia mollis</i> seed lectin in complex with methyl α-D-mannoside (pdb code: 1MVQ). ¹	2
1.2 Hydrogen network formation <i>via</i> crystal structure of human Galectin-7 in complex with galactosamine (pdb code: 3GAL). ⁹	3
1.3 Hydrophobic interactions <i>via</i> crystal structure of <i>Streptomyces avermitilis</i> α-L-rhamnosidase complexed with L -rhamnose (pdb code: 3W5N). ¹⁸	4
1.4 Ionic interactions <i>via</i> <i>Streptococcus sanguinis</i> SrpA adhesin complexation with the Neu5Ac-Gal (pdb code: 5IIY). ¹⁹	5
1.5 Plant lectins: A) Con A (pdb code: 6AHG); ³⁴ B) PNA (pdb code: 2PEL); ³⁵ C) WGA (pdb code: 1WGT). ³⁶	7
1.6 Attachment of various pathogens to the cell surface through lectin-glycan interactions. ³⁷	8
1.7 Schematic representation of monovalent and multivalent interactions between ligand and receptor. ⁶⁰	13
1.8 Binding mechanism of multivalent ligands on receptor site: a) Occupation of multiple binding site by multivalent ligands (chelate	

effect); b) Multivalent ligands-mediated receptor clustering on the cell surface; c) Occupation of primary and secondary binding sites by multivalent ligands; d) Binding of multivalent ligands to a receptors with higher local concentration of binding element. ⁶⁵	15
1.9 Example of scaffold-based constructed neoglycoconjugates. ¹¹²	17
2.1 Structural features of a dendrimer. ¹³⁰	19
2.2 Structural comparison of stealth liposome, polymersome and dendrimersome. ¹⁴⁸	21
2.3 FTIR spectra of JD, Dendrimersome, Lido, Lido/D.	28
2.4 DSC data of JD, Dendrimersomes, Lido, Lido/D.	29
2.5 AFM micrographs of Lidocaine-loaded dendrimersome: a) 2D and 3D micrographs of early Lido/D; b) 2D and 3D micrographs of dehydrated Lido/D.	30
2.6 Transmission electron micrographs of freeze-fractured replica of Lidocaine-loaded dendrimersomes.	31
3.1 Galectin subdivision in human according to structural feature of CRD. a) Monomer form of Galectins; b) Homodimerization of “proto-type”, oligomerization or pentamerization of “chimera-type”, dimerization of “tandem repeat-type”; c) Attribution of subtypes accordingly.	36
3.2 Galectin family members in the hallmarks of cancer. ¹⁷¹	38
3.3 Organization of CRDs of homodimeric galectins: side-by-side (Gal-1 and Gal-2), back-to-back (Gal-7).....	39
3.4 Binding of human Gal-1 and Gal-3 at CRDs with various disaccharides. A ₁) hGal-1 – Lac (pdb code: 1W6O); ²²³ A ₂) hGal-1 – LacNAc (pdb code: 1W6P); ²²³ A ₃) hGal-1 – 3.16 (pdb code: 6F83); ²²⁴ B ₁) hGal-3 – Lac (pdb code: 4RL7); ²²⁵ B ₂) hGal-3 – LacNAc(pdb code: 1KJL); ²¹¹ B ₃) hGal-3 – 3.12(pdb code: 5E89). ²¹⁷	44

3.5	Structure of CRD site within SiaLacNAc-galectin-8N interaction (PDB 3VKO): ionic interaction in orange between carboxyl group of Neu5Ac and Arg59 is crucial. ²³⁸	48
3.6	HRMS spectrum of compound 3.32.....	51
3.7	¹ H and ¹³ C NMR (300 MHz, CD ₃ OD) spectra of compound 3.34.	53
3.8	HRMS spectrum of compound 3.34.....	54
3.9	Comparison of ¹ H NMR (300 MHz, CD ₃ OD) spectra of compounds 3.34 and 3.37 with the appearance of deshielded <i>H</i> -3, <i>H</i> -4 (in red) of galactoside moiety after sulfation.	57
3.10	¹ H and ¹³ C NMR (600 and 150 MHz, CDCl ₃) spectra of compound 3.39.	58
3.11	Confirmation of regioselective <i>O</i> -alkylation through HMBC experiment of compound 3.39 with the correlation between <i>C</i> 3' (in yellow) and CH ₂ CO ₂ 'Bu.....	59
3.12	Comparison of ¹ H NMR (300 MHz, D ₂ O) spectra of compounds 3.32 and 3.38 with the appearance of deshielded <i>H</i> -3, <i>H</i> -4 (in red) of galactoside moiety after sulfation.	60
3.13	Comparison of ¹³ C NMR spectra (75 MHz, D ₂ O,) of compounds 3.32 and 3.38 with the appearance of deshielded <i>C</i> -3 (in red) of galactoside moiety after sulfation.	61
3.14	¹ H NMR (600 MHz, CDCl ₃) spectrum of compound 3.41.	62
3.15	HRMS spectrum of compound 3.41.....	63
3.16	¹ H and ¹³ C NMR (300 and 75 MHz, CDCl ₃) spectra of compound 3.48. ..	65
3.17	HMBC spectrum of compound 3.48, correlation between <i>H</i> 1 (in yellow) and <i>C</i> 4 (in blue).....	66

3.18	Comparison of ^1H NMR (600 MHz, D_2O) spectra of compounds 3.52 and 3.53 with the appearance of deshielded <i>H</i> -3, <i>H</i> -4 (in yellow) of galactoside moiety after sulfation.	68
3.19	Comparison of ^1H NMR (300 MHz, D_2O) spectra of compounds 3.58 and 3.61 with the appearance of deshielded <i>H</i> -3, <i>H</i> -4 (in yellow) of galactoside moiety after sulfation.	71
4.1	Schematic representation of receptor binding mechanism of bivalent glycocluster and galectins and formation of lectin-carbohydrate lattice. ...	75
4.2	Schematic representation of receptor binding mechanism of trivalent glycocluster and galectins, and formation of lectin-carbohydrate lattice. ..	78
4.3	Application of AuNPs in biomedical science. ²⁹¹	89
4.4	Schematic representation of pentameric Gal-3 receptor binding mechanism of glycopolymers.	92
4.5	Schematic representation of pentameric Gal-3 receptor binding mechanism of glycodendrimers.	95
4.6	LacNAc-harbored glycodendrimersomes with three types of topologies : twin (left), twin-mixed (middle), physical-auto dilution of twin-mixed (right).....	104
4.7	^1H and ^{13}C NMR (300 and 75 MHz, CDCl_3) spectra of compound 4.119.	109
4.8	HRMS spectrum of compound 4.121.....	110
4.9	^1H and ^{13}C NMR (300 and 75 MHz, CDCl_3) spectra of compound 4.121.	111
4.10	^1H NMR (300 MHz, $\text{CDCl}_3+\text{CD}_3\text{OD}$, v/v = 1/1) spectrum of compound 4.109.....	113
4.11	^{13}C NMR (75 MHz, $\text{CDCl}_3+\text{CD}_3\text{OD}$, v/v = 1/1) spectrum of compound 4.109.....	114

4.12	¹ H NMR (300 MHz, CDCl ₃ +CD ₃ OD, v/v = 1/1) spectrum of compound 4.113.....	115
4.13	¹³ C NMR (150 MHz, CDCl ₃ +CD ₃ OD, v/v = 1/1) spectrum of compound 4.113.....	116
4.14	MALDI-TOF MS spectrum of compound 4.109.	117
4.15	MALDI-TOF MS spectrum of compound 4.113.	118
4.16	Plot of glycodendrimersome from 4.109, concentration versus size.	121
4.17	Plot of glycodendrimersome from 4.113, concentration versus size.	121
4.18	Plot of glycodendrimersome from 4.109, concentration versus Z _{avg} and Pdl.	122
4.19	Plot of glycodendrimersome from 4.113, concentration versus Z _{avg} and Pdl.	122
5.1	Sialic acid on cell surface.....	125
5.2	Attachment of Influenza Virus to the epithelial cell surface (HA ₃ – trimeric hemagglutinin, SA – sialic acid. ⁷²	127
5.3	Influenza virus HA binding to Sia residue with two different linkage. a) Schematic view of HA homotrimer; b) Binding specificity of RBS depending on species; c) Location of RBS on the top of HA ₁ ; d) Close-up view of HA-Neu5Ac interaction; e) Superposition of Avian Influenza HA with Neu5Acα(2→3')LacNAc and Human Influenza HA with Neu5Acα(2→6')LacNAc. ³²⁵	129
5.4	Structure of Neuraminidase (NA) surface glycoprotein on Influenza virus. ³²⁷	130
5.5	X-ray structure of NA-Neu5Ac complex (pdb code: 2BAT). ³²⁹	131
5.6	Siglec family subdivision. ³³¹	133

5.7	Siglec-Neu5Ac interactions <i>via</i> immune cells-tumor cells communications. ³⁴⁰	136
5.8	¹ H NMR (300 MHz, CDCl ₃) spectrum of compound 5.175.	175
5.9	¹ H NMR (300 MHz, CDCl ₃) spectrum of compound 5.174.	176
5.10	¹ H NMR (300 MHz, D ₂ O) spectrum of TBATA.	177
5.11	¹³ C NMR (75 MHz, D ₂ O) spectrum of TBATA.	178
5.12	¹ H NMR (300 MHz, CDCl ₃) spectrum of compound 5.126.	179
5.13	¹ H and ¹³ C NMR (300 and 75 MHz, CDCl ₃) spectra of compound 5.176.	181
5.14	¹ H NMR (300 MHz, CDCl ₃) spectrum of compound 5.177.	182
5.15	DEPT ¹³ C NMR (75 MHz, CDCl ₃) spectrum of compound 5.177.	183
5.16	2D-COSY spectrum of compound 5.177.	184
5.17	HSQC spectrum of compound 5.177.	185
5.18	HMBC spectrum of compound 5.177.	186
5.19	HRMS spectrum of compound 5.177.	187
5.20	¹ H and ¹³ C NMR (300 and 75 MHz, CDCl ₃) spectra of compound 5.180. ..	189
5.21	¹ H NMR (300 MHz, CDCl ₃) spectrum of compound 5.183.	191
5.22	DEPT ¹³ C NMR (75 MHz, CDCl ₃) spectrum of compound 5.183.	192
5.23	2D-COSY spectrum of compound 5.183.	193
5.24	HSQC spectrum of compound 5.183.	194

5.25	HMBC spectra of compound 5.183.	195
5.26	HRMS spectrum of compound 5.183.....	196
5.27	¹ H NMR (300 MHz, D ₂ O) spectrum of compound 5.171.....	197
5.28	¹ H NMR (300 MHz, CDCl ₃) spectrum of compound 5.184.	199
5.29	DEPT ¹³ C NMR (75 MHz, CDCl ₃) spectrum of compound 5.184.	200
5.30	2D COSY spectrum of compound 5.184.	201
5.31	HSQC spectrum of compound 5.184.	202
5.32	¹ H NMR (600 MHz, CD ₃ OD+CDCl ₃ (v/v : 1/1)) spectrum of compound 5.168.....	205
5.33	¹³ C NMR (150 MHz, CD ₃ OD+CDCl ₃ (v/v : 1/1)) spectrum of compound 5.168.....	206
5.34	DEPT ¹³ C NMR (150 MHz, CD ₃ OD+CDCl ₃ (v/v : 1/1)) spectrum of compound 4.109.....	207
5.35	Plot of sialodendrimerosome from 5.168, concentration versus PdI.	209
5.36	Plot of sialodendrimerosome from 5.168, concentration versus Z _{avg}	209
5.37	Plot of sialodendrimerosome from 5.168, concentration versus size.....	210
6.1	¹ H NMR (300 MHz, DMSO-d ₆) spectrum of compound 2.01.....	219
6.2	¹³ C NMR (75 MHz, DMSO-d ₆) spectrum of compound 2.01.....	220
6.3	¹ H NMR (300 MHz, CDCl ₃) spectrum of compound 2.02.	222
6.4	¹³ C NMR (75 MHz, CDCl ₃) spectrum of compound 2.02.....	223

6.5	^1H NMR (300 MHz, CDCl_3) spectrum of compound 2.03.....	225
6.6	^{13}C NMR (75 MHz, CDCl_3) spectrum of compound 2.03.....	226
6.7	^1H NMR (300 MHz, DMSO-d_6) spectrum of compound 2.04.....	228
6.8	^{13}C NMR (75 MHz, DMSO-d_6) spectrum of compound 2.04.....	229
6.9	^1H NMR (300 MHz, CDCl_3) spectrum of compound 2.05.....	231
6.10	^{13}C NMR (75 MHz, CDCl_3) spectrum of compound 2.05.....	232
6.11	^1H NMR (300 MHz, CDCl_3).spectrum of compound 2.06.....	234
6.12	^{13}C NMR (75 MHz, CDCl_3) spectrum of compound 2.06.....	235
6.13	^1H NMR (300 MHz, CDCl_3) spectrum of compound 2.07.....	237
6.14	^{13}C NMR (75 MHz, CDCl_3) spectrum of compound 2.07.....	238
6.15	^1H NMR (300 MHz, CDCl_3) spectrum of compound 2.08.....	240
6.16	^{13}C NMR (75 MHz, CDCl_3) spectrum of compound 2.08.....	241
6.17	^1H NMR (300 MHz, CDCl_3) spectrum of compound 2.09.....	243
6.18	^{13}C NMR (75 MHz, CDCl_3) spectrum of compound 2.09.....	244
6.19	^1H NMR (300 MHz, CDCl_3) spectrum of compound 2.10.....	246
6.20	^{13}C NMR (75 MHz, CDCl_3) spectrum of compound 2.10.....	247
6.21	^1H NMR (300 MHz, CDCl_3) spectrum of compound 2.11.....	250
6.22	^{13}C NMR (75 MHz, CDCl_3) spectrum of compound 2.11.....	251
6.23	HRMS spectrum of compound 2.11.....	252

6.24	^1H NMR (300 MHz, CDCl_3) spectrum of compound 2.12.	255
6.25	^{13}C NMR (75 MHz, CDCl_3) spectrum of compound 2.12.	256
6.26	^1H NMR (300 MHz, D_2O) spectrum of compound 3.32.	261
6.27	^{13}C NMR (75 MHz, D_2O) spectrum of compound 3.32.	262
6.28	HRMS spectrum of compound 3.32.	263
6.29	^1H NMR (300 MHz, CD_3OD) spectrum of compound 3.33.	265
6.30	^{13}C NMR (75 MHz, CD_3OD) spectrum of compound 3.33.	266
6.31	HRMS spectrum of compound 3.33.	267
6.32	^1H NMR (300 MHz, CD_3OD) spectrum of compound 3.34.	269
6.33	^{13}C NMR (75 MHz, CD_3OD) spectrum of compound 3.34.	270
6.34	HRMS spectrum of compound 3.34.	271
6.35	^1H NMR (300 MHz, CDCl_3) spectrum of compound 3.35.	273
6.36	^{13}C NMR (75 MHz, CDCl_3) spectrum of compound 3.35.	274
6.37	^1H NMR (300 MHz, CDCl_3) spectrum of compound 3.36.	276
6.38	^{13}C NMR (75 MHz, CDCl_3) spectrum of compound 3.36.	277
6.39	^1H NMR (300 MHz, CD_3OD) spectrum of compound 3.37.	279
6.40	^{13}C NMR (75 MHz, CD_3OD) spectrum of compound 3.37.	280
6.41	HRMS spectrum of compound 3.37.	281
6.42	^1H NMR (300 MHz, D_2O) spectrum of compound 3.38.	283

6.43	^{13}C NMR (75 MHz, D_2O) spectrum of compound 3.38.	284
6.44	HRMS spectrum of compound 3.38.....	285
6.45	^1H NMR (300 MHz, CDCl_3) spectrum of compound 3.39.	288
6.46	^{13}C NMR (75 MHz, CDCl_3) spectrum of compound 3.39.....	289
6.47	HRMS spectrum of compound 3.39.....	290
6.48	^1H NMR (600 MHz, D_2O) spectrum of compound 3.40.....	292
6.49	^{13}C NMR (150 MHz, D_2O) spectrum of compound 3.40.	293
6.50	HRMS spectrum of compound 3.40.....	294
6.51	^1H NMR (600 MHz, CD_3OD) spectrum of compound 3.41.	297
6.52	^{13}C NMR (150 MHz, CD_3OD) spectrum of compound 3.41.....	298
6.53	HRMS spectrum of compound 3.41.....	299
6.54	^1H NMR (300 MHz, D_2O) spectrum of compound 3.42.....	301
6.55	^{13}C NMR (75 MHz, D_2O) spectrum of compound 3.42.	302
6.56	HRMS spectrum of compound 3.42.....	303
6.57	^1H NMR (300 MHz, CDCl_3) spectrum of compound 3.44.	305
6.58	^{13}C NMR (75 MHz, CDCl_3) spectrum of compound 3.44.....	306
6.59	^1H NMR (300 MHz, CD_3OD) spectrum of compound 3.45.	308
6.60	^{13}C NMR (75 MHz, CD_3OD) spectrum of compound 3.45.....	309
6.61	^1H NMR (300 MHz, CDCl_3) spectrum of compound 3.46.	311

6.62	^{13}C NMR (75 MHz, CDCl_3) spectrum of compound 3.46.....	312
6.63	^1H NMR (600 MHz, CDCl_3) spectrum of compound 3.48.....	315
6.64	^{13}C NMR (150 MHz, CDCl_3) spectrum of compound 3.48.....	316
6.65	HRMS spectrum of compound 3.48.....	317
6.66	^1H NMR (300 MHz, CD_3OD) spectrum of compound 3.49.....	319
6.67	^{13}C NMR (75 MHz, CD_3OD) spectrum of compound 3.49.....	320
6.68	HRMS spectrum of compound 3.49.....	321
6.69	^1H NMR (300 MHz, CD_3OD) spectrum of compound 3.50.....	323
6.70	^{13}C NMR (75 MHz, CD_3OD) spectrum of compound 3.50.....	324
6.71	HRMS spectrum of compound 3.50.....	325
6.72	^1H NMR (300 MHz, CD_3OD) spectrum of compound 3.51.....	327
6.73	^{13}C NMR (75 MHz, CD_3OD) spectrum of compound 3.51.....	328
6.74	HRMS spectrum of compound 3.51.....	329
6.75	^1H NMR (600 MHz, D_2O) spectrum of compound 3.52.....	331
6.76	^{13}C NMR (75 MHz, D_2O) spectrum of compound 3.52.....	332
6.77	HRMS spectrum of compound 3.52.....	333
6.78	^1H NMR (300 MHz, D_2O) spectrum of compound 3.53.....	335
6.79	^{13}C NMR (75 MHz, D_2O) spectrum of compound 3.53.....	336
6.80	HRMS spectrum of compound 3.53.....	337

6.81	¹ H NMR (300 MHz, CDCl ₃) spectrum of compound 3.55.	340
6.82	¹³ C NMR (75 MHz, CDCl ₃) spectrum of compound 3.55.	341
6.83	¹ H NMR (600 MHz, D ₂ O) spectrum of compound 3.56.	343
6.84	¹³ C NMR (75 MHz, D ₂ O) spectrum of compound 3.56.	344
6.85	¹ H NMR (300 MHz, CDCl ₃) spectrum of compound 3.57.	347
6.86	¹³ C NMR (75 MHz, CDCl ₃) spectrum of compound 3.57.	348
6.87	¹ H NMR (600 MHz, D ₂ O) spectrum of compound 3.58.	350
6.88	¹³ C NMR (150 MHz, DMSO-d ₆) spectrum of compound 3.58.	351
6.89	¹ H NMR (300 MHz, CDCl ₃) spectrum of compound 3.59.	353
6.90	¹³ C NMR (75 MHz, CDCl ₃) spectrum of compound 3.59.	354
6.91	HRMS spectrum of compound 3.59.	355
6.92	¹ H NMR (600 MHz, CD ₃ OD) spectrum of compound 3.60.	357
6.93	¹³ C NMR (150 MHz, CD ₃ OD) spectrum of compound 3.60.	358
6.94	HRMS spectrum of compound 3.60.	359
6.95	¹ H NMR (600 MHz, D ₂ O) spectrum of compound 3.61.	361
6.96	¹³ C NMR (150 MHz, D ₂ O) spectrum of compound 3.61.	362
6.97	HRMS spectrum of compound 3.61.	363
6.98	¹ H NMR (300 MHz, CDCl ₃) spectrum of compound 4.117.	365
6.99	¹³ C NMR (75 MHz, CDCl ₃) spectrum of compound 4.117.	366

6.100 ^1H NMR (300 MHz, CDCl_3) spectrum of compound 4.118.	368
6.101 ^{13}C NMR (75 MHz, CDCl_3) spectrum of compound 4.118.	369
6.102 ^1H NMR (300 MHz, CDCl_3) spectrum of compound 4.119.	371
6.103 ^{13}C NMR (75 MHz, CDCl_3) spectrum of compound 4.119.	372
6.104 HRMS spectrum of compound 4.119.	373
6.105 ^1H NMR (300 MHz, CDCl_3) spectrum of compound 4.120.	375
6.106 ^{13}C NMR (75 MHz, CDCl_3) spectrum of compound 4.120.	376
6.107 HRMS spectrum of compound 4.120.	377
6.108 ^1H NMR (300 MHz, CDCl_3) spectrum of compound 4.121.	380
6.109 ^{13}C NMR (75 MHz, CDCl_3) spectrum of compound 4.121.	381
6.110 HRMS spectrum of compound 4.121.	382
6.111 ^1H NMR (300 MHz, $\text{CD}_3\text{OD}+\text{CDCl}_3$ (v/v : 1/1)) spectrum of compound 4.109.	384
6.112 ^{13}C NMR (150 MHz, $\text{CD}_3\text{OD}+\text{CDCl}_3$ (v/v : 1/1)) spectrum of compound 4.109.	385
6.113 MALDI-TOF MS spectrum of compound 4.109.	386
6.114 ^1H NMR (300 MHz, $\text{CD}_3\text{OD}+\text{CDCl}_3$ (v/v : 1/1)) spectrum of compound 4.113.	388
6.115 ^{13}C NMR (150 MHz, $\text{CD}_3\text{OD}+\text{CDCl}_3$ (v/v : 1/1)) spectrum of compound 4.113.	389
6.116 MALDI-TOF MS spectrum of compound 4.113.	390

6.117 DLS analysis of glycodendrimersomes of 4.109 with different concentration in EtOH.....	392
6.118 DLS analysis of glycodendrimersomes of 4.113 with different concentration in EtOH.....	393
6.119 ^1H NMR (300 MHz, CDCl_3) spectrum of compound 5.126.....	397
6.120 ^{13}C NMR (75 MHz, CDCl_3) spectrum of compound 5.126.....	398
6.121 ^1H NMR (300 MHz, D_2O) spectrum of compound TBATA.....	399
6.122 ^{13}C NMR (75 MHz, D_2O) spectrum of compound TBATA.....	400
6.123 ^1H NMR (300 MHz, CDCl_3) spectrum of compound 5.174.....	402
6.124 ^{13}C NMR (75 MHz, CDCl_3) spectrum of compound 5.174.....	403
6.125 ^1H NMR (300 MHz, CDCl_3) spectrum of compound 5.175.....	404
6.126 ^{13}C NMR (75 MHz, CDCl_3) spectrum of compound 5.175.....	405
6.127 ^1H NMR (300 MHz, CDCl_3) spectrum of compound 5.176.....	407
6.128 ^{13}C NMR (75 MHz, CDCl_3) spectrum of compound 5.176.....	408
6.129 ^1H NMR (300 MHz, CDCl_3) spectrum of compound 5.177.....	411
6.130 ^{13}C NMR (75 MHz, CDCl_3) spectrum of compound 5.177.....	412
6.131 ^1H NMR (300 MHz, CD_3OD) spectrum of compound 5.178.....	414
6.132 ^{13}C NMR (75 MHz, CDCl_3) spectrum of compound 5.178.....	415
6.133 ^1H NMR (300 MHz, CDCl_3) spectrum of compound 5.179.....	417
6.134 ^{13}C NMR (75 MHz, CDCl_3) spectrum of compound 5.179.....	418

6.135 ^1H NMR (300 MHz, CDCl_3) spectrum of compound 5.180.....	420
6.136 ^{13}C NMR (75 MHz, CDCl_3) spectrum of compound 5.180.....	421
6.137 ^1H NMR (300 MHz, CDCl_3) spectrum of compound 5.181.....	423
6.138 ^{13}C NMR (75 MHz, CDCl_3) spectrum of compound 5.181.....	424
6.139 ^1H NMR (300 MHz, CDCl_3) spectrum of compound 5.182.....	427
6.140 ^{13}C NMR (75 MHz, CDCl_3) spectrum of compound 5.182.....	428
6.141 ^1H NMR (300 MHz, CDCl_3) spectrum of compound 5.183.....	431
6.142 ^{13}C NMR (75 MHz, CDCl_3) spectrum of compound 5.183.....	432
6.143 ^1H NMR (300 MHz, D_2O) spectrum of compound 5.171.....	434
6.144 ^{13}C NMR (75 MHz, D_2O) spectrum of compound 5.171.....	435
6.145 ^1H NMR (300 MHz, CDCl_3) spectrum of compound 5.184.....	437
6.146 ^{13}C NMR (75 MHz, CDCl_3) spectrum of compound 5.184.....	438
6.147 ^1H NMR (300 MHz, CDCl_3) spectrum of compound 5.185.....	440
6.148 ^{13}C NMR (75 MHz, CDCl_3) spectrum of compound 5.185.....	441
6.149 ^1H NMR (300 MHz, D_2O) spectrum of compound 5.185b.....	443
6.150 ^{13}C NMR (75 MHz, D_2O) spectrum of compound 5.185b.....	444
6.151 ^1H NMR (600 MHz, $\text{CD}_3\text{OD}+\text{CDCl}_3$ (v/v : 1/1)) spectrum of compound 5.109.....	446
6.152 ^{13}C NMR (150 MHz, $\text{CD}_3\text{OD}+\text{CDCl}_3$ (v/v : 1/1)) spectrum of compound 5.109.....	447

6.153 DLS analysis of sialodendrimerosomes of 5.168 with different concentration in EtOH..... 448

LIST OF SCHEMES

Scheme	Page
1.1 Modification of carbohydrate moiety by three types of carbohydrate-specific enzymes: 1) Hydrolytic; 2) Phosphorolytic; 3) Synthetic. ⁵⁵	12
2.1 Synthesis of alkyne-functionalized JD precursor.....	24
2.2 Radical mediated thiol-yne coupling of JD dendrimer precursor and mercaptoethanol.	25
2.3 Formation of Lidocaine-loaded dendrimersome.	25
2.4 Synthesis of less polar analogue of 2.08.	33
3.1 Reported Gal-1 and Gal-3 inhibitors; (HI – Hemagglutination Inhibition assay; FP – Fluorescence Polarization assay; SP – Solid Phase assay). ²⁰⁴⁻²²²	42
3.2 Reported Gal-4, Gal-7, and Gal-8 inhibitors; (FP – Fluorescence Polarization assay; SPR – Surface Plasmon Resonance; SP – Solid Phase assay). ^{208, 220, 224, 226-230}	45
3.3 3'-O-funtionnalization of propargyl-based <i>N</i> -Acetyllactosamine.	49

3.4	Synthetic strategy for the preparation <i>para</i> -nitrophenyl and propargyl-based lactosides and their 3'- <i>O</i> -sulfated derivatives.....	50
3.5	Deprotection of compound 3.31 and preparation of the key intermediate 3.34.....	52
4.1	Reported bivalent ligands. ^{204, 209, 217, 260-276}	77
4.2	Reported trivalent ligands. ^{207, 263, 265, 269, 278-280}	80
4.3	Reported tetravalent ligands. ^{261, 265, 269, 276, 279-282}	82
5.1	Sialic acid family: a) Sia family members; b) Most common Sia family members; c) Commonly found terminal Neu5Ac linkage. ³¹⁶	126
5.2	Promoter mediated sialylation and formation of the glycal.	137
5.3	Under Koenig-Knoor condition, silver carbonate-promoted sialylation... ..	138
5.4	C1 auxiliary in stereoselective sialylation.....	139
5.5	C3 auxiliary-mediated α -sialylation.....	140
5.6	C5 stereodirecting effect in sialylation.	142
5.7	Oxazolidinone donors and conformational analysis of nucleophilic attack on oxocarbenium ion. ⁴⁶²	144
5.8	Synthesis of the analogue of CMP-Neu5Ac with sulfur as glycosidic atom. ⁴⁶⁷	145
5.9	Biologically active <i>S</i> -sialosides. ^{469, 471, 472}	147
5.10	Copolymerization of <i>O</i> -sialosides and acrylamide. ^{474, 475}	150
5.11	<i>S</i> - and <i>C</i> -sialoside acrylamide copolymerization. ^{477, 487}	150
5.12	Some examples to linear sialopolymers. ^{479, 481, 488, 497-508}	153

5.13	Some other reported sialopolymer. ^{509, 511-520}	156
5.14	Multi-antennary glycoprotein-like thiosialoside dendrimers. ^{385, 521}	158
5.15	Synthesis of PAMAM-based Sialo- <i>S</i> -dendrimers with various valencies. ⁵²²	160
5.16	Sialic acid bearing dendrimers. ^{526, 534-541}	161
5.17	Reported sialic acid containing liposomes. ^{542-546, 548-550}	164
5.18	Synthesis of <i>S</i> -Sialoliposome. ⁵⁵¹	167
5.19	Retrosynthetic analysis of amphiphilic Janus sialodendrimer.	169
5.20	Retrosynthetic analysis of hydrophilic segments.	170
5.21	Synthesis of α - <i>S</i> -sialosides by using various approaches. ⁴⁵⁸	171
5.22	Synthesis of α - <i>S</i> -alkyl sialosides within various thiol precursors.	172
5.23	Synthesis of thiosialosides under PTC conditions.	173
5.24	Synthesis of compound 5.170.	174
5.25	Synthesis of compound 5.171.	188
5.26	Stereoselective sialylation by using insoluble silver zeolite.	198
5.27	Click reaction between hydrophobic and hydrophilic intermediates.	204
5.28	Generation of sialodendrimersome via ethanol injection method.	208

LIST OF TABLES

Table	Page
1.1 Example of animal or mammalian lectin classification.	10
2.1 Comparative studies of free Lidocaine, free Dendrimersome, Lido/D and Lido/L.....	26
3.1 Amino acid sequence at CRD of Galectin-3, 4C, 8N. ⁷⁰	47
5.1 Human Siglec classification. ³⁴⁰	135
5.2 Thioaryl and thioalkyl sialosides donor in sialylation.	141

LIST OF ABBREVIATIONS

ACN	Acetonitrile
COSY	Correlation spectroscopy
CuAAC	Copper-catalyzed alkyne-azide cycloaddition
DCC	<i>N,N</i> -dicyclohexylcarbodiimide
DCM	Dichloromethane
DIPEA	Diisopropylethylamine
DLS	Dynamic light scattering
DMAP	4-(<i>N,N</i> -Dimethylamino)pyridine
DMF	<i>N,N</i> -Dimethylformamide
DMPA	2,2-Dimethoxy-2-phenylacetophenone
DMSO	Dimethylsulfoxide

ESI	Electrospray ionization
EtOAc	Ethyl acetate
FA	Fluorescence polarization
Fuc	Fucose
Gal	Galactose
Glc	Glucose
GlcNAc	<i>N</i> -Acetylglucosamine
HA	Hemagglutinin
HI	Hemagglutinin Inhibition
IC ₅₀	Half maximal inhibitory concentration
ITC	Isothermal titration calorimetry
Lac	Lactose
LacNAc	<i>N</i> -Acetyllactosamine
MALDI-TOF	Matrix-assisted laser desorption ionization-time of flight
Man	Mannose
MeOH	Methanol

MeONa	Sodium methoxide
NA	Neuraminidase
NaAsc	Sodium ascorbate
Neu5Ac	<i>N</i> -Acetylneuraminic acid
NMR	Nuclear magnetic resonance
on	Overnight
PAMAM	Poly(amidoamine)
PdI	Polydispersity index
PEG	Poly(ethyleneglycol)
PNP	<i>para</i> -Nitrophenol
PPI	Poly(propylene imine)
r.t.	Room temperature
Rha	Rhamnose
Sia	Sialic acid
SP	Solid phase
SPR	Surface plasmon resonance

TBAF	Tetra- <i>n</i> -butylammonium fluoride
TBDPSCI	<i>tert</i> -Butyldiphenylsilyl chloride
TBDPS	<i>tert</i> -Butyldiphenylsilylether
TEA	Triethylamine
TEC	Thiol-ene click
TEM	Transmission electron microscopy
TFA	Trifluoroacetic acid
THF	Tetrahydrofurane

RÉSUMÉ

Les interactions entre glucides et récepteurs ont un rôle crucial dans de nombreux processus biologiques y compris l'adhésion cellulaire, la prolifération, les infections bactériennes et virales. L'interaction monovalent entre un glycoconjugué et une protéine est généralement faible. Par contre de multiples interactions simultanées conduisent à de fortes avidités. Cependant, afin de créer des interactions protéine-glucide plus efficaces et de résoudre le problème de faible affinité (K_D dans la plage millimolaire ou micromolaire), certaines lectines possédant plus d'un domaine de reconnaissance des glucides, utilisent le mode de multivalence pour s'associer à leurs ligands de manière rigide et énergétique. Certains glycoconjugués multivalents synthétiques imitent les ligands naturels de glycanes, mais leurs synthèses en plusieurs étapes pour générer la multivalence et constructions sur des squelettes toxiques demeurent les inconvénients majeurs. Les vésicules et les liposomes possédant une cavité interne et portant les glucides, pouvant imiter la multivalence supramoléculaire des membranes cellulaires sont particulièrement avantageux. Les dendrimères amphiphiles Janus, portant mono- et disaccharides sur leurs extrémités, et possédant les structures tridimensionnelles contrôlables, ont attiré l'attention des chimistes médicaux.

Dans ce rapport le premier exemple de dendrimère amphiphile de type Janus décoré avec du *N*-acétyllactosamine et de l'acide *N*-acétylneuraminique a été rapporté. En utilisant la réaction de cycloaddition 1,3-dipolaire catalysée par le sel de cuivre, les intermédiaires hydrophiliques et hydrophobiques sont conjugués. En utilisant la méthode d'injection d'éthanol, des glycodendrimersomes ont été générés à partir de glycodendrimères et leurs tailles et l'indice de polydispersité de nanoparticules ont été mesurés par la technique de "la diffusion dynamique de la lumière". Des études biologiques sur les protéines correspondantes – spécifiques aux saccharides seront étudiées. Afin de trouver et étudier les interactions nouvellement créées entre Galectins et les di- et trisaccharides monovalents, nous avons également préparé une

série de dérivés lesquels sont générés en position *O*3 du lactose et *N*-acétyllactosamine.

De plus, la synthèse de « thiosialodendrimersomes » dans lesquels l'oxygène glycosidique est remplacé par un atome de soufre a été effectuée. Nous présentons ici une méthode stéréocontrôlée et hautement convergente pour synthétiser les molécules cibles avec une application potentielle dans le but de développer des agents antiadhésifs et inhibiteurs contre les glycoprotéines de surface de sous-types de virus de la grippe A. Les étapes clés de la synthèse ont impliqué une sialylation α -stéréosélective entre des donneurs de sialoside et divers accepteurs. Une méthode alternative, peu coûteuse et économique en atomes permettant d'avoir des α -sialosides PEGylés a été développée. Le groupement tosyl au point focal du PEG est particulièrement avantageux, car sa transformation en divers groupes fonctionnels peut être mise à profit.

Mots clés: Dendrimère de Janus, dendrimersome, *N*-acétyllactosamine, Lactose, sulfatation régiosélective, *O*-sialylation, *S*-sialylation, Galectines, virus de la grippe, Siglecs

ABSTRACT

In biology, Fischer's lock and key model is the basis for non-covalent interactions between ligands and receptors. Biomolecules with multiple locks and keys are leading to multivalent interactions. Homo- or multimer-structured lectins are the targets for studying interactions with glycosylated multivalent ligands. Conventional multivalent glycoconjugates provide some accessible mimics for the biodisplay of glycans, but all require complex multistep synthesis to generate multivalency and are often built on toxic scaffolds. Vesicles and liposomes presenting carbohydrates, avoiding such restrictions are endowed with internal cavity that can mimic supramolecular multivalency of biological cell membranes. Recently described, mono and disaccharide attached amphiphilic Janus dendrimer with those parameters and predictable size has attracted more attention.

Here we report the first synthesis of amphiphilic Janus dendrimer functionalized with *N*-Acetyllactosamine and *N*-Acetylneuraminic acid at the focal point. Using CuAAC-mediated click-chemistry hydrophilic and hydrophobic segments were conjugated to afford self-assembling amphiphilic Janus glycodendrimers. Size and PDI properties of generated glycodendrimersomes were studied *via* DLS technique. Multivalent glycodendrimersomes will be further evaluated in protein binding studies towards corresponding carbohydrate-specific receptors.

Moreover, for comparative study purpose, preparation of a small library constituted from *para*-nitrophenyl and propargyl-based *O*3'-functionalized lactosides have also been described. Their protein binding studies towards Galectin family members are currently under investigation. Additionally, the synthesis of thiosialodendrimersomes wherein the interglycosidic oxygen is replaced with enzymatically stable and nonhydrolyzable sulfur atom has been achieved. Herein, a stereocontrolled and highly convergent method for synthesizing the target molecules with potential application in host-pathogen, carbohydrate-lectin interaction is reported. The key steps in the

synthesis involved α -stereoselective sialylation between sialosyl donors and various acceptors. Alternatively, low-cost, atom-economical method for the synthesis of PEGylated sialosides have been developed. Especially, having versatile tosylate at the focal point is beneficial for further transformations to various functional groups.

Keywords: Janus dendrimer, dendrimersome, *N*-acetyllactosamine, Lactose, regioselective sulfation, *O*-sialylation, *S*-sialylation, Galectins, Influenza virus, Siglecs

CHAPTER I

INTRODUCTION TO CARBOHYDRATE-PROTEIN INTERACTIONS

1.1 Fundamentals of carbohydrate-protein interaction

Besides being most abundant biomolecules in nature, carbohydrates possess biological information storage and transfer capacity which is embodied as “sugar code.” Deciphering and interpreting these codes by carbohydrate receptors (lectins, carbohydrate-specific enzymes, antibodies) require special reading features which are characterized through diverse molecular interactions.

1.1.1 Chelation of metals

Certain sugar receptors (leguminous lectins, C-type lectins, sugar isomerase enzymes) bind to carbohydrates in a metal-dependent manner (Ca^{2+} , Mg^{2+} , Mn^{2+}). Therefore, it is universally known that lone pair electrons on oxygen, nitrogen, sulfur and π -electrons of double, triple bonds of amino acids interact non-covalently with metal ions. Bridging (or chelating) to metal with the vicinal hydroxyls of sugars, makes the association around metal energetically more favorable and at the same time allows the site to differentiate stereochemically binding groups. Remarkably, during

interactions between sugar and leguminous lectins Ca^{2+} and Mn^{2+} ions do not coordinate with sugar moiety, instead they make the site suitable for binding *via* chelating with amino acids at CRD (Figure 1.1).¹

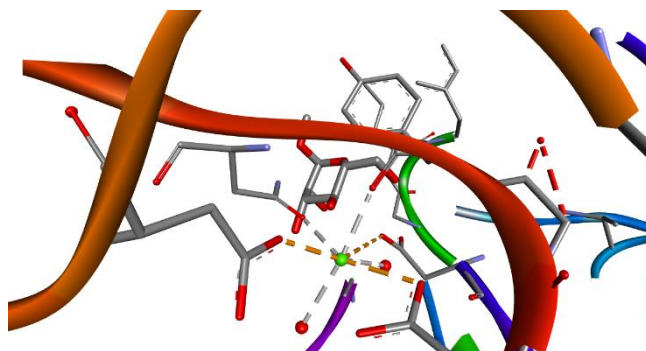


Figure 1.1 Coordination of Ca^{2+} in sugar binding region. *Cratylia mollis* seed lectin in complex with methyl α -D-mannoside (pdb code: 1MVQ).¹

1.1.2 Hydrogen bonding

Described for the first time by Linus Pauling,² hydrogen bonding is a unique electrostatic interaction between hydrogen atom of a donor (hydrogen donor) and an atom (hydrogen acceptor) with higher value of electronegativity (closer to 4.0 on the Pauling scale and mainly with *N*, *O*, *F*). Primarily referring to directional interaction, hydrogen bond has an energy ranging from 1 to 10 kcal/mol depending on distance (2.2 to 4.0 Å) between hydrogen of a donor and an acceptor. The hydrogen bond plays crucial modulator role in receptor-ligand interactions. Study shows that introducing more hydrogen acceptors and donors can significantly affect binding affinity.³⁻⁶ Consequently, high content of hydroxyl groups that are present on sugars allows them to create hydrogen bond network during association to a receptor (Figure 1.2).⁷⁻⁹ Having both hydrogen bond donor and acceptor characters, *OH* groups interact essentially with *OH*, *NH*, *C=O* functional groups of amino acids present at carbohydrate binding site. Another interesting fact is that, besides creating energetically favorable hydrogen bond, hydroxyl group can be involved cooperatively

in second and third bond formation which may affect binding properties of primarily created hydrogen bond.^{10, 11}

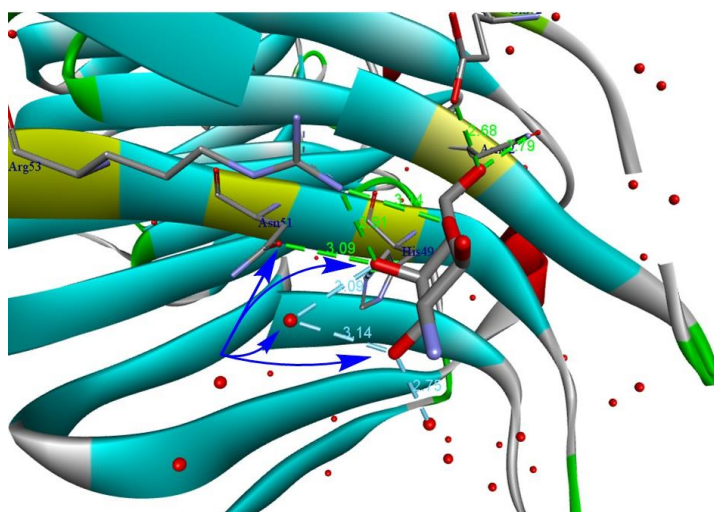


Figure 1.2 Hydrogen network formation *via* crystal structure of human Galectin-7 in complex with galactosamine (pdb code: 3GAL).⁹

1.1.3 Hydrophobic interactions

The phenomena of low water affinity of nonpolar functional groups and poor solubility of nonpolar solute in water had been known long before they become hot topic to investigate. In 1959 American chemist Walter J. Kauzmann by describing attraction between nonpolar groups of proteins in aqueous solution, introduced the term “hydrophobic bond” as stabilizing factor in protein folding.¹² However, at the end of 60s the term has been replaced by “hydrophobic interactions” due to association of apolar groups in aqueous solution and minimization of the contact with neighboring water molecules.¹³ Nevertheless, the precise molecular mechanism of formation of hydrophobic interactions remains controversial and a particular explanation has been reported thermodynamically through positive entropy effect profile.^{14, 15} Highly ordered water molecules around non-polar solute have a negative impact in entropy, hence despite of destabilizing effect on enthalpy, formation of

hydrophobic interactions between nonpolar regions increases entropy by freeing water molecules and making them less ordered and energetically more favorable. So far, it is widely known that hydrophobic interactions (0.5 to 2 kcal/mol) play prominent role in sugar-receptor interactions.¹⁶ Although, the presence of multiple hydroxyl groups on their scaffolds allows them to be classified as hydrophilic molecules, depending on their faces sugars also have substantial hydrophobic character. For example, studies revealed that α -face of β -D-galactose is stacking with aromatic rings in most of cases *via* making extensive hydrophobic contacts by virtue of 4-OH which is oriented to axial position whereas its 4-epimers (Glc, Man) are relatively more hydrophilic.¹⁷ Moreover, having methyl (Fuc, Rha) and acetyl (GlcNAc, GalNAc, Neu5Ac) groups on their scaffolds provides additional hydrophobic contacts in sugar-receptor interactions. For example as it is shown in Figure 1.3, C-H \cdots π interactions between CH_3 of L-rhamnose and aromatic side chains of Tyr, Trp plays pivotal role during binding to the enzyme.¹⁸

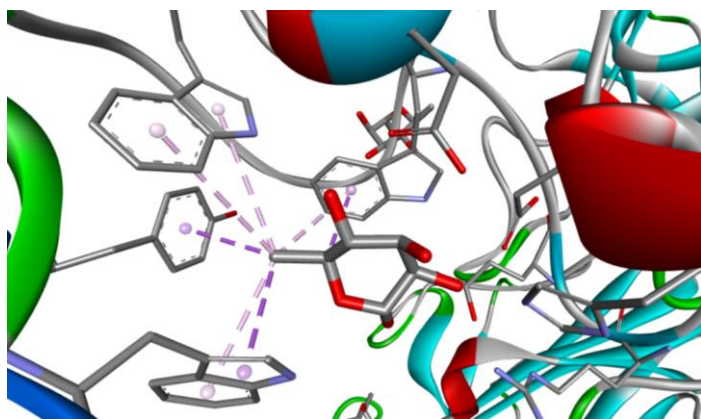


Figure 1.3 Hydrophobic interactions *via* crystal structure of *Streptomyces avermitilis* α -L-rhamnosidase complexed with L-rhamnose (pdb code: 3W5N).¹⁸

1.1.4 Ionic interactions

Besides being mainly neutral, some sugars (sialic acids, aminosugars) exist in charged form by involving ionic interactions with different amino acids. For example,

the carboxylate group of Neu5Ac residue is involved in strong electrostatic interaction with the guanidium residue of arginine in Figure 1.4, shows importance of salt bridge in sugar-receptor interactions.¹⁹ Therefore, introducing in a synthetic manner, carboxyl, sulfo, phosphoryl, amine groups to sugar frame as binding affinity enhancers, are widely used method in medicinal chemistry.²⁰

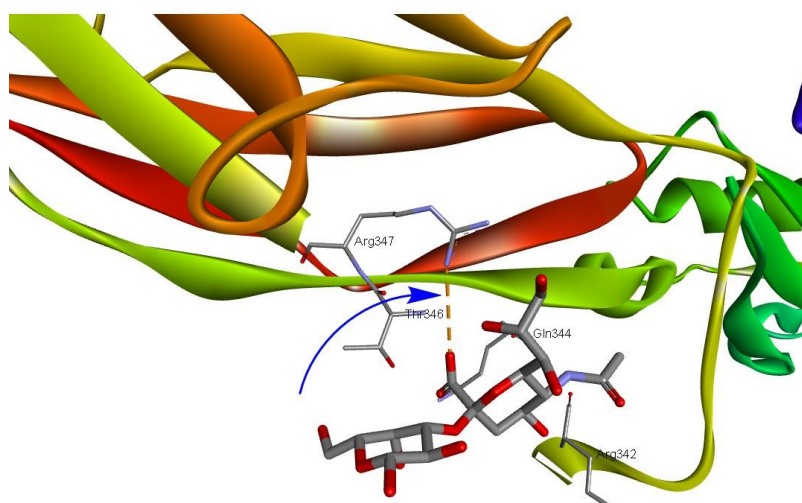


Figure 1.4 Ionic interactions via *Streptococcus sanguinis* SrpA adhesin complexation with the Neu5Ac-Gal (pdb code: 5I1Y).¹⁹

1.2 Lectins

Lectins are the carbohydrate binding proteins with non-immune origin. Depending on sources, they are classified into plant, microbial and animal lectins. Generally speaking, with their carbohydrate recognition domains (CRDs) lectins bind reversibly to specific mono- and oligosaccharides and cause agglutination of the affected cells.²¹ Most of the lectins possess more than one CRD with dimerizing, trimerizing or polymerizing tendencies.^{22,23}

1.2.1 Plant Lectins

As mentioned above, leguminous lectins are Ca^{2+} and Mn^{2+} dependent lectins which are mostly composed of 25-30 kDa of structurally similar 2 or 4 subunits, each with one carbohydrate binding site.²⁴ The precise function of leguminous lectins has not been clarified yet, but some research groups reported that they are involved in defense mechanism against parasitic microorganisms (bacteria, fungi) and also nodulation process with symbiotic (nitrogen fixing bacteria) bacteria.^{25, 26} On the other hand, due to similarity of binding to carbohydrates, extracted plant lectins have gained popularity as models of animal lectins in biotechnology and biomedical science. Especially, Concanavalin A (Con A) from *Canavalia ensiformis*, peanut agglutinin (PNA) from *Arachis hypogea* and wheat germ agglutinin (WGA) from *Triticum vulgare* are commercially available plant lectins which have been extensively employed in surface glycoconjugates characterizations of various cells (Figure 1.5).²⁷⁻³³

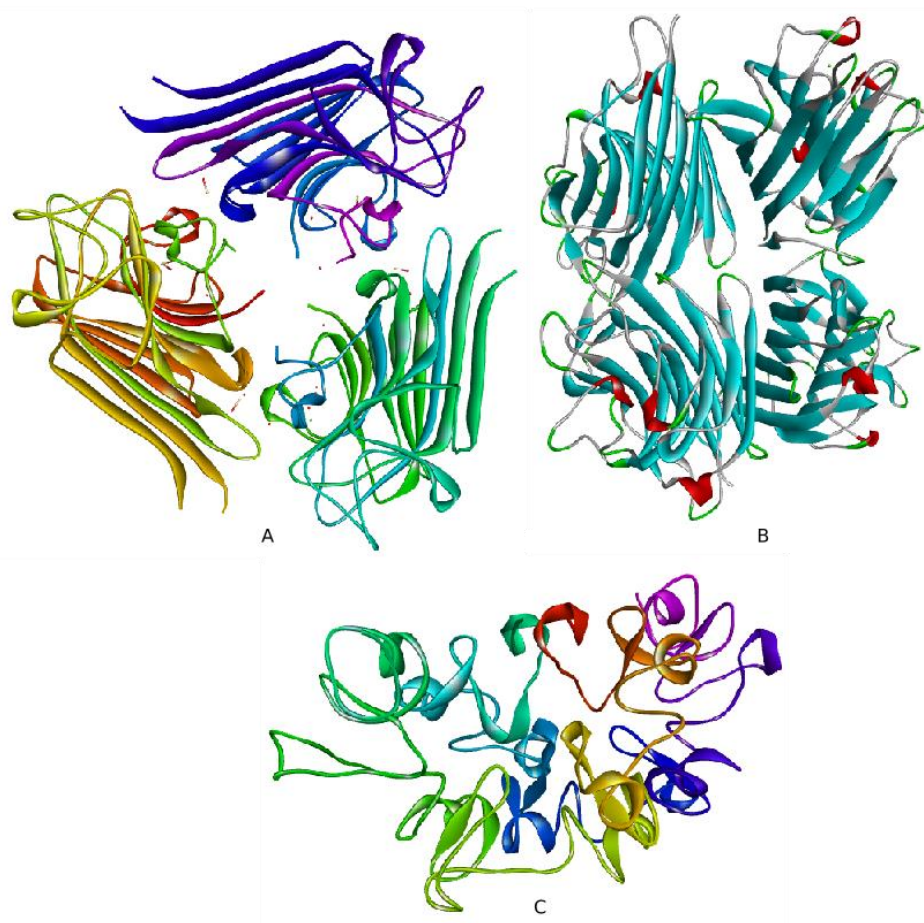


Figure 1.5 Plant lectins: A) Con A (pdb code: 6AHG);³⁴ B) PNA (pdb code: 2PEL);³⁵ C) WGA (pdb code: 1WGT).³⁶

1.2.2 Microbial Lectins

The extracellular surfaces of endothelial cells are covered by glycoconjugates or glycocalyx which are expressed as glycosaminoglycans (GAGs), glycoproteins and glycolipids. Thus, pathogens (bacteria, viruses, protozoa) using adhesion strategy attach to the surface of host cells *via* lectin-surface glycoconjugate interactions (Figure 1.6).³⁷⁻³⁹ Imberty and co-workers reported that in comparison with plant lectins and animal, microbial and fungal lectins show higher binding affinity towards monosaccharides.⁴⁰ Apart from this, multivalent binding mode (simultaneous binding

of multiple ligands) through lectin-surface glycan interactions remains key regulator for attachment.

So far, adhesion of influenza virus to the cell surface is the most studied interactions to date.⁴¹⁻⁴³ Thus, attachment is mediated by multivalent interactions between trimeric envelop surface glycoprotein – hemagglutinin and terminal sialic acid containing surface glycoconjugates.⁴¹

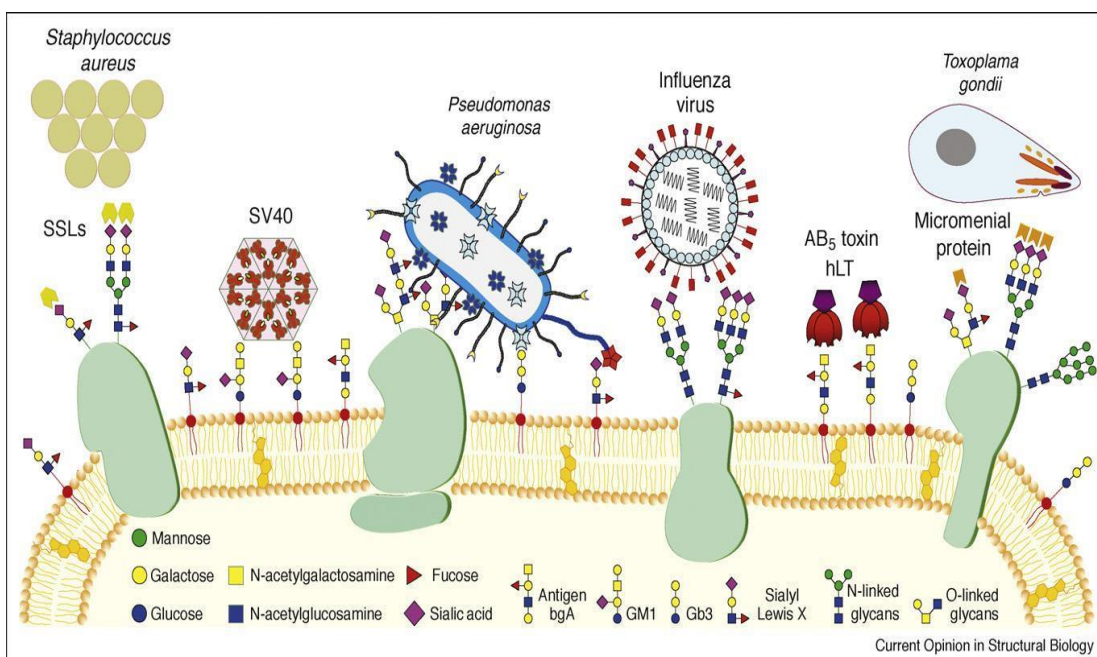


Figure 1.6 Attachment of various pathogens to the cell surface through lectin-glycan interactions.³⁷

1.2.3 Animal Lectins

Animal lectins are classified according to their carbohydrate recognition domains' (CRDs) which determine their sugar specificity, dependence of bivalent cations, localization on cellular sites and involved biological functions (Table 1.1).⁴⁴ C-type lectins are Ca^{2+} ion dependent lectin superfamily. Based on organization of the features of their CRD C-type lectins are divided into 14 groups.⁴⁵ The majority of the

family members possess similar structure of CRDs with 110-130 amino acids. In each group, the members share common amino acid sequences and sugar specificity (Table 1.1, Selectins).⁴⁶ Some members of the family are secreted and others are transmembrane proteins. Through protein-protein and protein-ligand interactions C-type lectins play numerous biological roles such as adhesion, signal transduction in the immune system.

I-type lectins are members of immunoglobulin superfamily that bind to glycan through recognizing glycosaminoglycans (GAGs) and sialic acid (Sia) residues.^{47, 48} Siglecs (Sialic acid-binding immunoglobulin-like lectins) are well-documented family which are essentially expressed on the immune system cells.⁴⁹ Siglecs themselves have been differentiated into subgroups based on their amino acid sequence similarity on *N*-terminal V-set and adjoining C2-set domains: Sialoadhesin (Sn) or Siglec-1, CD22 or Siglec-2, CD33 or Siglec-3, Myelin associated glycoprotein (MAG) or Siglec-4a, Schwann cell myelin protein (SMP) or Siglec-4b.⁵⁰

P-type lectins are categorized by their CRDs which recognize phosphorylated terminal mannose residues.⁴⁴ There are two types of P-lectins: cation-dependent mannose 6-phosphate receptor (CD-MPR) and cation-independent mannose 6-phosphate receptor (CI-MPR) with molecular weights of 46 and 300 kDa respectively.⁵¹ Being type I transmembrane glycoproteins, both receptors play important biological role by recognizing and transporting lysosomal enzymes to lysosomes.⁵²

S-type lectins are sulfhydryl-dependent class of lectins primarily binding to β -galactosides residues.⁴⁴ Also called as Galectin family, its members possess similar amino acid sequence on their CRDs. Based on structural feature of CRD they are grouped into 3 types: proto, tandem-repeat, chimeric.⁵³ There are 15 members of the mammalian galectins that have been discovered and numerated accordingly. Besides

being sulfhydryl-dependent, galectins are present intra- (cytoplasm and nucleus) and extra-cellularly (cell surface and medium).⁵⁴

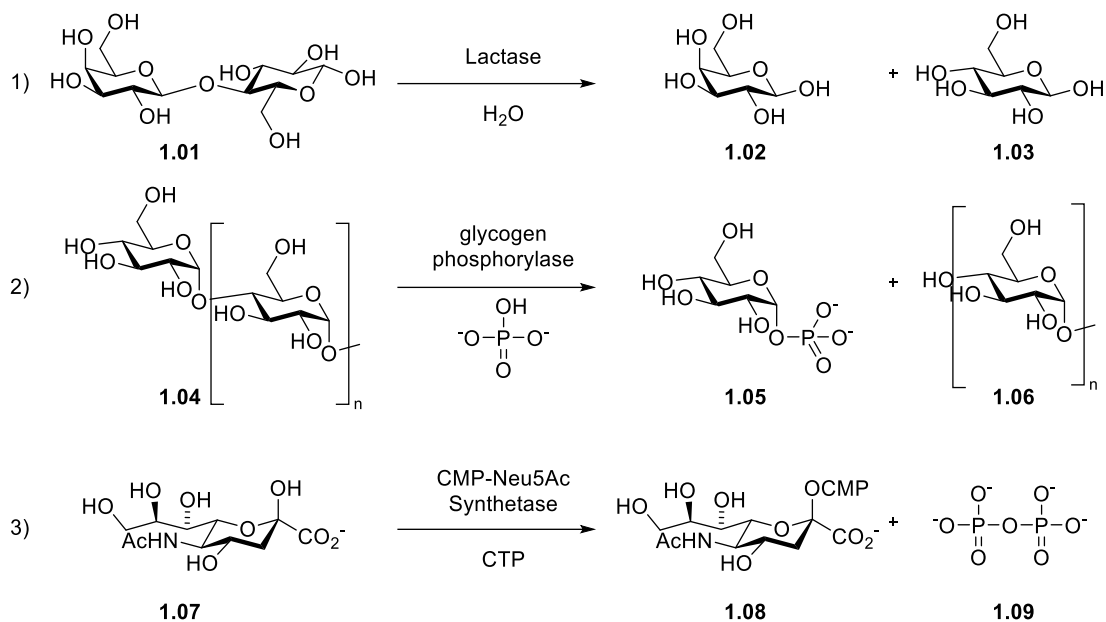
Table 1.1 Example of animal or mammalian lectin classification.

Lectin family	Subtypes	Dependence	Sugar specificity	Functions
C-type	E-selectin	Ca ²⁺	SLe ^x , SLe ^a	Adhesion of leucocytes on endothelial cells
	L-selectin			Adhesion of endothelial cells on leucocytes
	P-selectin			Adhesion of leucocytes on platelets
	Collectins		mannosides and galactosides	Endocytosis of mannosides by Man-specific lectin on macrophage, phagocytosis, elimination of aged desialylated erythrocytes by asialoglycoprotein receptor
I-type	Siglecs	-	sialosides	Regulation of immune cell-cell communications
P-type	CD-MPR	Bivalent cations (Ca ²⁺ ,	Mannose-6-phosphate	Direction or transport of M6P bearing lysosomal enzymes to

		Mg ²⁺)	residues (M6P)	lysosomes
	CI-MPR	-		
S-type	Galectins	Sulfhydryl	β-Gal	Host-pathogen interactions, regulation of cell cycle, immune response, autophagy, signaling

1.2.4 Carbohydrate-specific Enzymes

Based on properties that modify carbohydrate moieties, carbohydrate-specific enzymes are divided into 3 main types: hydrolytic, phosphorolytic and synthetic enzymes (Scheme 1.1).⁵⁵ For example, Neuraminidase enzyme (NA) of influenza virus is one of hydrolytic enzymes (Glycoside hydrolases (GHs)) that cleave terminal sialic acid residues from oligosaccharide chains within catalytic hydrolysis in order to release newly born virions from cells.⁵⁶ Phosphorolytic enzymes are involved in catalysis and regiospecific phosphorolysis of non-reducing end of certain types of glycosidic linkages.⁵⁷ Both synthetic and phosphorolytic enzymes are responsible for synthesis of new sugar chains and glycosidic bonds.



Scheme 1.1 Modification of carbohydrate moiety by three types of carbohydrate-specific enzymes: 1) Hydrolytic; 2) Phosphorolytic; 3) Synthetic.⁵⁵

1.3 Multivalency in Protein-Carbohydrate Recognition

Monovalent protein-carbohydrate interactions are generally characterized by low affinity where K_D values are in millimolar or micromolar range. K_D (M) ($K_D = 1/K_A$; K_A – equilibrium association constant) refers to equilibrium dissociation constant that measures propensity of the dissociation of a ligand-receptor complex (LR) into ligand (L) and receptor (R) (Equation 1.2).



$$K_A = \frac{[LR]}{[L][R]} \quad (\text{eq. 1.1})$$

$$K_D = \frac{[L][R]}{[LR]} \quad (\text{eq. 1.2})$$

However, in order to create effective protein-carbohydrate interactions and overcome the weak affinity, some lectins, which possess more than one CRD, utilize multivalent (simultaneous multiple binding) binding mode to associate with their ligands more rigidly while costing lower binding energy (Figure 1.7).^{7, 58, 59} Consequently, this type of communication event between receptors and sugars results in augmentation of binding affinity and diminution of dissociation constant (K_D) which is one of the main objective of medicinal organic chemists in designing potent synthetic ligands.

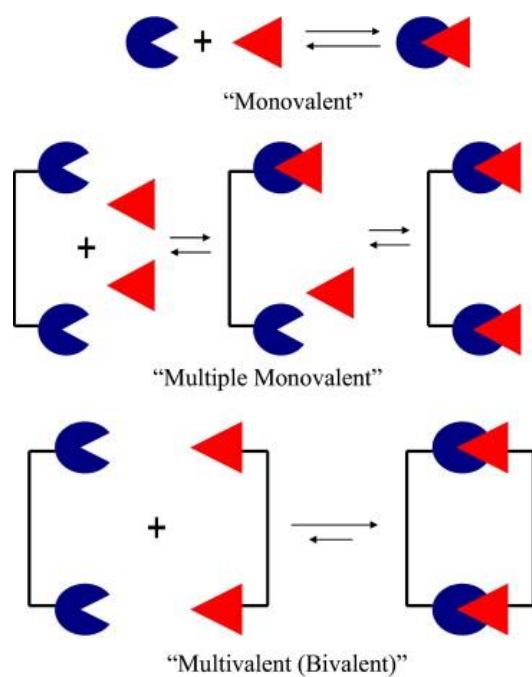


Figure 1.7 Schematic representation of monovalent and multivalent interactions between ligand and receptor.⁶⁰

In presence of multivalent ligands some lectins have oligomerizing tendencies. To bind to their multivalent ligands more energetically lectins usually use multivalency

mode. This phenomenon was first introduced by Lee and co-workers as the “glycoside cluster effect”.^{61 62} Multivalency has been considered as an existential phenomenon for pathogens attachment to cell surfaces. In order to clarify biological functions of naturally occurring ligands with multivalent binding properties, design and synthesis of low-cost synthetic ligands that mimic multivalent arrays have been in demand. Especially, for the purpose of competing natural ligands, since 90s peculiar architectural design (inspired by multivalent topology in nature, flora, and fauna) of ligands with unusual multivalent binding mechanism to receptors have been very popular. Nevertheless, not all synthetic ligands interact as expected in receptor sites, while chelating (Figure 1.8 a) some of them cause additional receptor clustering through bidimensional diffusion in the fluid bilayer (Figure 1.8 b).⁶³ In some cases a ligand chelates on monomeric receptor by creating interactions at the second site for binding (Figure 1.8 c).⁶⁴

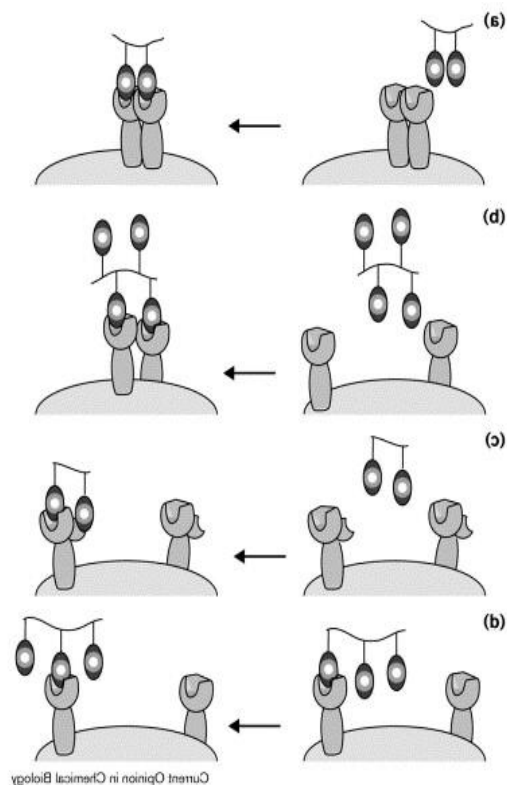


Figure 1.8 Binding mechanism of multivalent ligands on receptor site: a) Occupation of multiple binding site by multivalent ligands (chelate effect); b) Multivalent ligands-mediated receptor clustering on the cell surface; c) Occupation of primary and secondary binding sites by multivalent ligands; d) Binding of multivalent ligands to a receptors with higher local concentration of binding element.⁶⁵

1.4 Multivalent Neoglycoconjugates

Besides being expressed intra- and extra-cellularly, carbohydrates are primarily linked to peptides, proteins and lipids *via* covalent bonds. Interacting with proteins of various pathogens including fungi, bacteria and viruses through multivalent binding mode cell surface glycoconjugates mediate infection process.³⁷ To date, in order prevent attachment of pathogens to the cell surface or their replication in infected cells a wide variety of glycoconjugates and unnatural glycoconjugates

(neoglycoconjugates) with various scaffolds, valencies and architectural design have been constructed (Figure 1.9).⁶⁵⁻⁷² Built on different scaffold, neoglycoconjugates (glycoproteins,⁷³⁻⁷⁶ glycodendrimers,⁷⁷⁻⁸¹ glycopolymers,⁸²⁻⁸⁵ glyconanoparticles,⁸⁶⁻⁹¹ glycoliposomes⁹²⁻⁹⁵ etc.) have been shown as an alternative therapeutic strategy fighting pathogens by reaching preclinical⁹⁶⁻⁹⁸ and clinical trials.⁹⁹⁻¹⁰³ For example reported by Roy and collaborators in 2004 synthetic glycoconjugate vaccine against *Haemophilus influenzae* type b (Hib) was successfully tested in adults and children in Cuba.¹⁰⁴ Moreover, it is widely known that while designing and synthesizing potent inhibitors throughout most advantageous avidity and selectivity, several factors including length and nature of employed linkers for conjugation, nature of scaffolds, sugar densities at focal points, hydrophilic and hydrophobic balance and most importantly cost of synthesis for reaching final products play significant roles and should be absolutely taken into consideration.^{67, 105-107} However, optimal and efficient synthesis of multivalent glycoconjugates still remain a challenging task,¹⁰⁸⁻¹¹⁰ whereas some vaccine development projects have been aborted due to their higher costs.¹¹¹

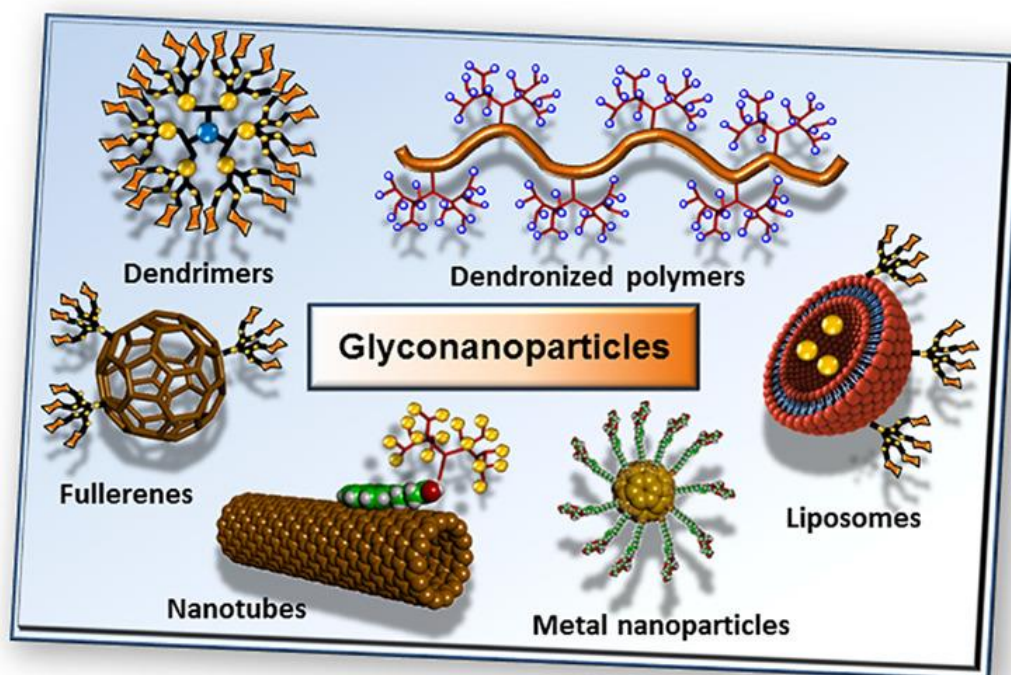


Figure 1.9 Example of scaffold-based constructed neoglycoconjugates.¹¹²

CHAPTER II

INTRODUCTION TO DENDRIMERSOMES

As discussed above, a variety of multivalent neoglycoconjugates have been developed in last thirty years which provided some accessible mimics for the biodisplay of glycans and also bind or interact with proteins of pathogens. But still some issues related with those unnatural ligands including high polydispersity, poor physical and mechanical properties, time- and money-consuming multistep synthesis, toxic scaffolds, poor bioavailability *etc.* remain key obstacles to overcome. Recently reported self-assembly of carbohydrate-harbored amphiphilic Janus dendrimers gained attention due to their excellent mechanical properties and capacity of mimicking biological membranes as well as classical liposomes.¹¹³⁻¹²¹

In this chapter we will mainly focus on dendrimersomes as a nanosized carrier and some recent results that we have obtained.

2.1 Nanosized drug carriers and dendrimersomes

Nanoscale drug carriers^{122, 123} serve as vehicles for transporting various drugs through biological barriers¹²⁴ to a necessary site for a required period of time. Nanosized carriers are promising agents to provide some enhanced *in-vivo* efficiency to drugs including half-life in blood circulation, stability and solubility, controlled release while simultaneously diminishing unwanted side-effects of some drugs in certain area of a body.¹²⁵ To date, regarding to natural bionanomaterials, nano-based drug delivery system with various synthetic drug carriers has contributed to significant advances in nanomedicine and biomedical sciences.¹²⁶ But not all drug carriers respect fundamental guidelines for the administration of biomolecules. For example, after delivering drugs, there are some harmful toxicity including epidermal and dermal sensitization (in case of delivery through the skin) associated with carriers themselves.¹²⁷ This phenomenon is explained that while using dermal and transdermal delivery some carriers may provoke production of cytokine and adhesion molecules by epidermal cells as immunological barrier which result erythema and oedema etc.^{128, 129}

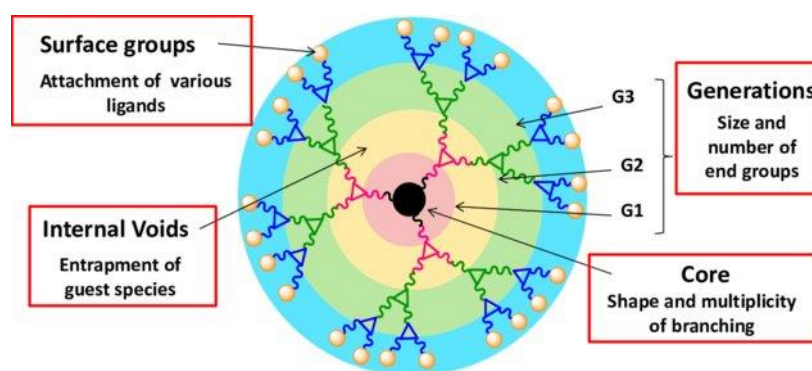


Figure 2.1 Structural features of a dendrimer.¹³⁰

Liposomes are most studied biomolecules consisting of phospholipid bilayers which are similar to the structure of cell membranes.¹³¹ Liposomal encapsulation of drugs

has opened large spectrum of application and has been employed in a few marketed formulations (e.g. liposomal doxorubicin: Doxil[®], Caelyx[®]).¹³² More recently, the surface functionalization or PEGylation (polyethylenglycol-PEG) of liposomal carriers (natural or synthetic) which are embodied as stealth liposomes (refers to furtive liposomes that avoid uptake by mononuclear phagocyte system) has demonstrated better half-life blood circulation than conventional liposomes while reducing mononuclear phagocyte system uptake.¹³³⁻¹³⁶ Even though stealth liposomes are widely used in transdermal delivery of local anesthesia¹³⁷⁻¹³⁹ and chemotherapy,¹⁴⁰⁻¹⁴² they still face various major drawbacks including controlled drug release, lower entrapment efficiency, shorter shelf-life *etc.*¹⁴³ Another noteworthy class of multifunctional nanocarriers is dendrimer by virtue of their hyperbranched, monodisperse, polyfunctional and tridimensional properties.¹⁴⁴ Besides being synthetic macromolecules and having functionalizable periphery, dendrimers possess internal cavity (Figure 2.1) where essentially hydrophobic drug molecules can be encapsulated (physical encapsulation). On the other hand, more hydrophilic drugs can be attached to the surface through covalent conjugation. Among other nanocarriers, polymersomes¹⁴⁵ should be cited, thus self-assemblies from amphiphilic block copolymers form vesicular shells which have shown to be promising candidates for a wide range of various applications including drug delivery system. However, aforementioned synthetic drug carriers suffer from some limitations including polydispersity, lower biocompatibility, multistep synthesis, toxicity *etc.*

Dendrimersomes – generated from self-assembling amphiphilic Janus-dendrimers (JDs) are particularly interesting by their character of mimicking biological membrane as well as liposomes and possessing strength and stability of polymersomes (Figure 2.2). JD refers to a dendrimer constituted of two different dendrimeric wedges with double-faced head, each possesses different properties. Reported by Percec and co-workers, amphiphilic JDs are monodisperse, stable over

time, impermeable dendrimers which have demonstrated excellent mechanical properties.¹⁴⁶ Constituted of hydrophilic and hydrophobic segments (hydrophilic and hydrophobic), amphiphilic dendrimers self-assembly to form dendrimersome through injection from a water-miscible organic solution into water or biological buffers.¹⁴⁶ Most interestingly dimensions and size distribution of generated dendrimersomes are predictable depending on concentration. Over a decade numerous researches related to biomedical applications of JDs have been published. Among them carbohydrate-branched Janus dendrimers or Janus glycodendrimers (JGDs) *via* forming unilamellar and multilamellar vesicles called as glycodendrimersomes (GDs) have demonstrated excellent biological activity towards some lectins.^{113-115, 121, 147} More on GDs will be discussed in next chapters. In this chapter the compatibility of dendrimersome as a hydrophobic drug carrier have been investigated.

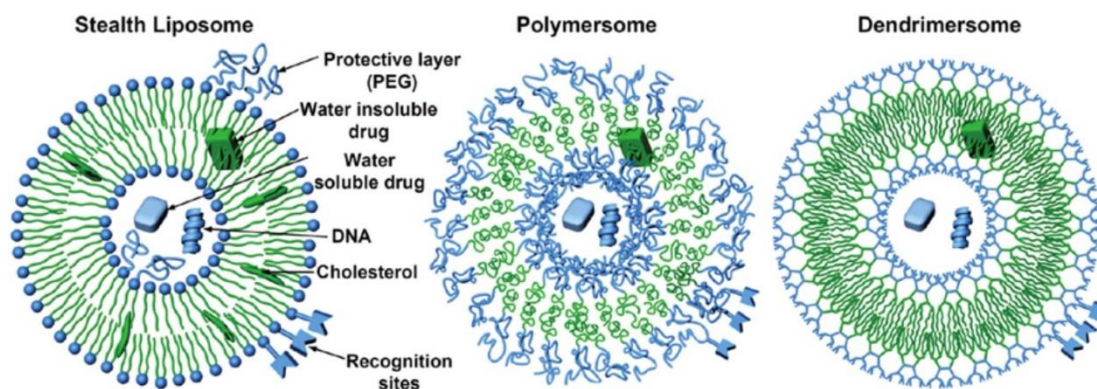


Figure 2.2 Structural comparison of stealth liposome, polymersome and dendrimersome.¹⁴⁸

2.2 Lidocaine-loaded self-assembling amphiphilic Janus-dendrimer

Herein we present our recent studies on “Liposome formulation optimization of Lidocaine-loaded self-assembling amphiphilic Janus-dendrimers”.

Composed of multiple lipid bilayers and having a thickness of up to 30 μm *Stratum Corneum* (SC, outermost layer of the epidermis) acts as main barrier of the skin for the dermal and transdermal drug delivery.¹⁴⁹ Hence, developing a nanoparticulate drug-delivery system, particularly lipid-based carriers that can efficiently enable drugs to pass through the SC and provide high drug concentration at the site of action with minor uptake, while increasing the duration of analgesia with long-lasting stability, and reducing undesirable side effects remained a challenging task to accomplish.^{97, 150, 151}

2.2.1 Lidocaine as local anesthetic agent

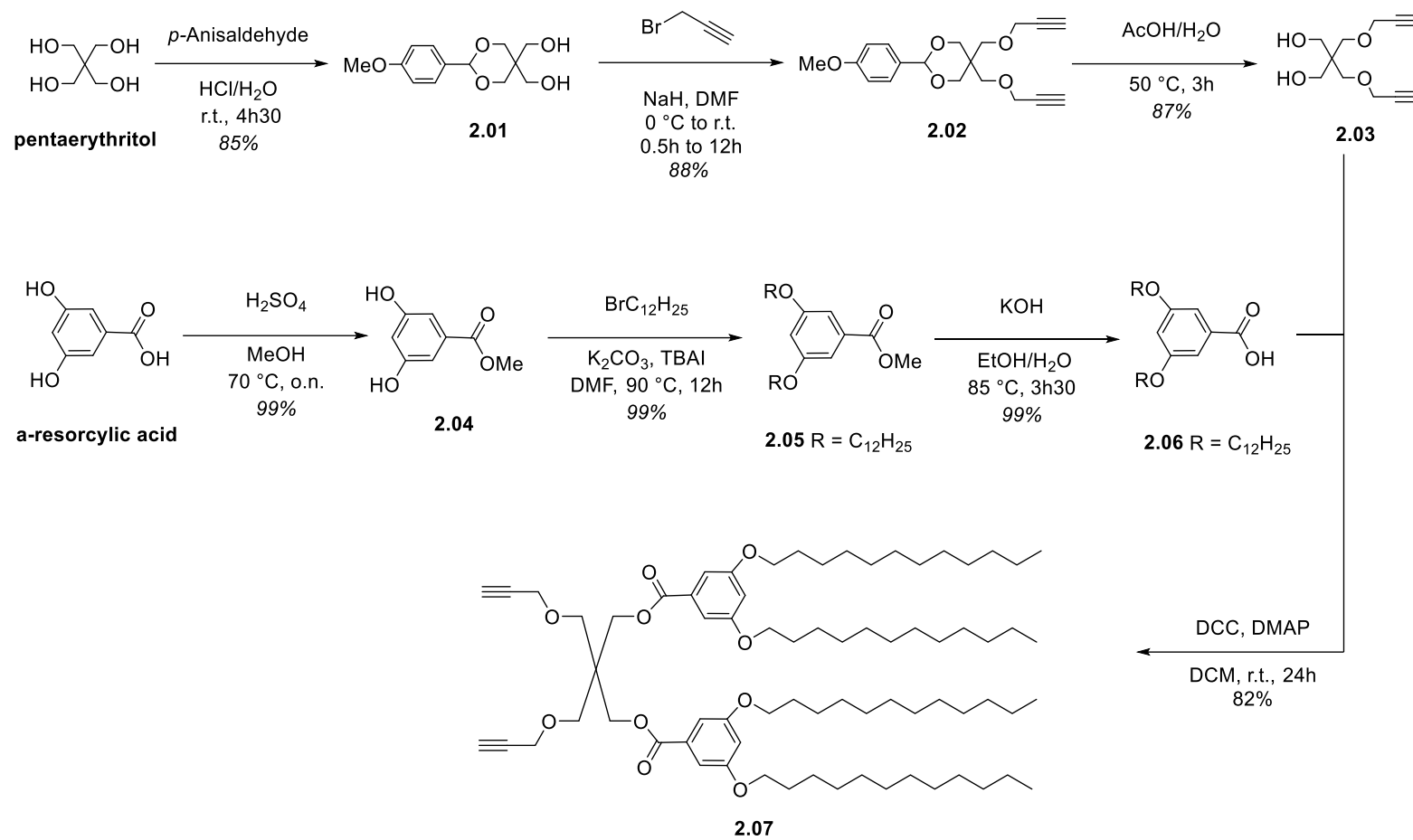
Lidocaine (Lido), [2-(diethylamino)-*N*-(2,6-dimethyl phenyl)-acetamide] formerly lignocaine is an effective topical and local anesthetics in dentistry with moderate and rapid action.^{152, 153} During anesthetic injection of Lido in the palatal mucosa^{154, 155} and intraligamentary region¹⁵⁶ and gingival probing¹⁵⁷ interruption of pain perception and blocking sensitive and motor nerves have been previously reported. Nevertheless, hydrophilic protonated form of lidocaine limits its bioavailability through SC. To this goal, development of a carrier able to deliver and provide long-lasting effect and slow release of lidocaine was established as an alternative way. Although several reports confirmed that local anesthetics, including lidocaine, provide efficient topical anesthesia for the skin when encapsulated into lipid vesicles,^{158, 159} to our knowledge topical delivery of lidocaine, incorporated in dendrimersome is not known.

Here, we report comparative studies of two types of lidocaine formulations: classic liposomal (L) and Dendrimersomal (D).

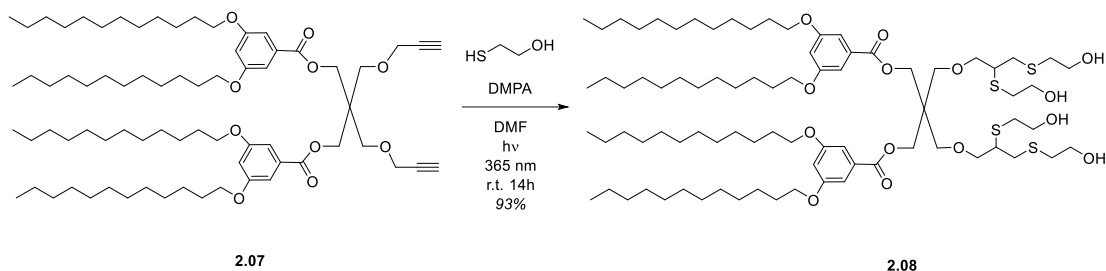
2.3 Results and discussion

Our synthesis began by preparation of alkyne-functionalized JD precursor **2.07** in light of previously reported protocol (Scheme 2.1).¹¹³ Hydroxyl-functionalized

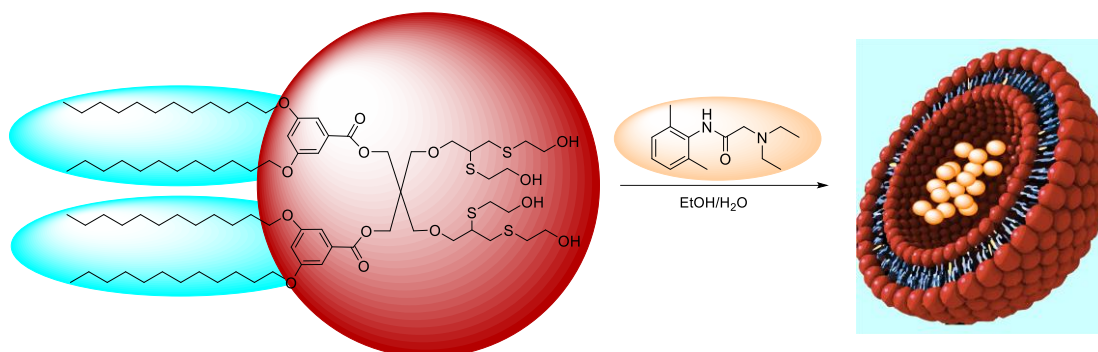
amphiphilic JD **2.08** was synthesized by using radical-initiated thiol-yne (TYC) coupling in presence of 2,2-dimethoxy-2-phenylacetophenone photoinitiator (DMPA; Scheme 2.2).¹⁶⁰ Although earliest thiol-yne coupling protocol appeared in mid-20th century,¹⁶¹ nowadays, especially in macrocyclization reactions,¹⁶² glycodendrimer,¹⁶³ polymer¹⁶⁵ and material¹⁶⁶ synthesis it has become more in demand. Possessing click chemistry character thiol-yne coupling is an efficient method in hydrothiolation of alkyne by functionalizing bis-thioether which can be used in lipid mimetic synthesis.



Scheme 2.1 Synthesis of alkyne-functionalized JD precursor.



Scheme 2.2 Radical mediated thiol-yne coupling of JD dendrimer precursor and mercaptoethanol.



Scheme 2.3 Formation of Lidocaine-loaded dendrimersome.

2.3.1 DLS studies

For comparative study purpose, lidocaine was loaded into both dendrimersomes (D) and classical liposomes (L, which are generated from mixture of commercially available soybean lecithin phospholipid and cholesterol in a ratio of 67:33 w/w) by the Ethanol injection method. Direct impact of concentration of the dendrimersome on particle size, Zeta potential, and encapsulation efficiency (EE) were studied. Dendrimersomal formulation of lidocaine with optimized concentration (D/Lido ratio

6/1 (w/w), C_m (D) = 0.05 mg/mL, C_m (Lido) = 0.008 mg/mL in H₂O) have been found to exhibit to date highest value of Entrapment Efficiency (EE %, Table 2.1). Moreover, formulations were evaluated in terms of particle size, polydispersion index (PDI) and stability. While having almost similar PDI, Z_{avg} , it was observed that after 60 days the size of liposomal formulation increased 3.5 times whereas Lido/D had only 1.5 times growth. *In-vitro* release (by using dialysis membrane) and *ex-vivo* permeation studies (by using Franz diffusion cell) of Lido/D versus free Lido have been also studied. As result, enhanced values in both parameters have been observed.

Table 2.1 Comparative studies of free Lidocaine, free Dendrimersome, Lido/D and Lido/L.

	DLS studies		EE(%)	<i>In-vitro</i> release	<i>Ex-vivo</i> skin permeation	Stability (60 days)
	PdI	Z_{avg} (nm)				
Lido	N/A	N/A	N/A	38 % in 4h ^a	43 % in 6h ^a	N/A
D	0.086 ^b	92.50 ^b	N/A	N/A	N/A	-
Lido/D	0.147 ^c	76.57 ^c	97.0	83 % in 8h ^a	85 % in 10h ^a	f
Lido/L	0.210 ^d	98.10 ^d	21.6 ^e	N/A	N/A	f

a) no changes after 24h; b) C_m = 0.05 mg/mL in H₂O (obtained minimum size); c) D/Lido ratio 6/1 (w/w), C_m (D) = 0.05 mg/mL, C_m (Lido) = 0.008 mg/mL in H₂O; d) parameters of c was applied for Lido/L; e) Literature value¹⁶⁷ f) after 60 days the sizes of Lido/D and Lido/L were increased ~1.5 and ~3.5 times.

2.3.2 Infrared spectrum analysis

FTIR was employed for studying the interaction between lidocaine and JD in generated Lido/D formulation. Spectra of JD, Dendrimersomes, Lido, Lido/D suspension are reported respectively in Figure 2.3. The main functional groups in JD are C=O (1720 cm^{-1}), C=C (1595 cm^{-1}), $C_{sp^3}\text{-H}$ ($2922, 2853\text{ cm}^{-1}$), O-H (3357 cm^{-1}). IR of the generated dendrimersome shows only two significant bands at 1622 and $3342, 3246\text{ cm}^{-1}$ corresponding to carbonyl of the ester and hydroxyl groups of outer surfaces of the nanovesicles.

Lido contains a tertiary amine connected to a benzene ring ($C=C, 1425\text{ cm}^{-1}$) by an amide ($C=O, 1662\text{ cm}^{-1}$ and $N\text{-H}, 3335\text{ cm}^{-1}$) bond. The bands at 2970 and 3050 cm^{-1} could be assigned respectively to $C_{sp^3}\text{-H}$ aliphatic and $C_{sp^2}\text{-H}$ aromatic stretching modes of lidocaine. Remarkable, during FTIR analysis of Lido/D, it was observed that as a result of incorporation of Lidocaine in JD, the C=O band of Lido at 1667 cm^{-1} disappeared due to strong C=O stretching band of JD. Spectral changes were also observed in the region corresponding to the polar heads of the JD during FTIR analysis of the generated Lido/D. Therefore, the N-H stretching band of Lido at 3335 cm^{-1} was disappeared due to strong stretching vibrations of O-H. During comparative studies between Lido/D and D, we also observed slight shifting at assigned wavenumber for C=O and O-H.

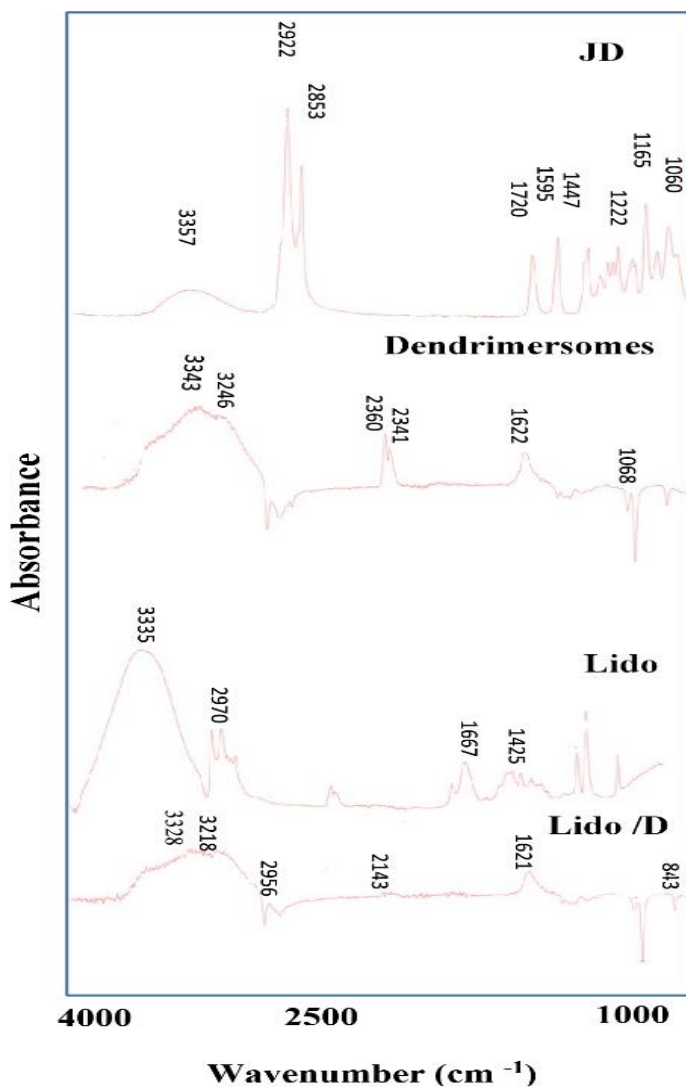


Figure 2.3 FTIR spectra of JD, Dendrimerosome, Lido, Lido/D.

2.3.3 DSC studies

The DSC study was carried out to determine the difference in melting points of vesicular structures of dendrimerosome and lidocaine loaded dendrimerosome. As it is shown in Figure 2.4 thermal profile of JD clearly showed a single endothermic peak at -16.01 °C ($\Delta H = -24.48$ J/g), that was shifted after dendrimerosome formation. However, generated dendrimerosome exhibited a melting point at 7.15°C ($\Delta H = -$

210.99 J/g) which is due to hydrogen bonding between surface hydroxyl groups of vesicular structures. DSC thermograms also revealed endothermic melting peaks at 68°C ($\Delta H=66.45\text{J/g}$) and 2.17 °C ($\Delta H = -59.06 \text{ J/g}$) for crystalline lidocaine and Lido/D suspension, respectively. This decrement shows occurring interaction between lidocaine and dendrimersomes, we presume that the presence of lidocaine can be played a disruptive role in hydrogen bonding.

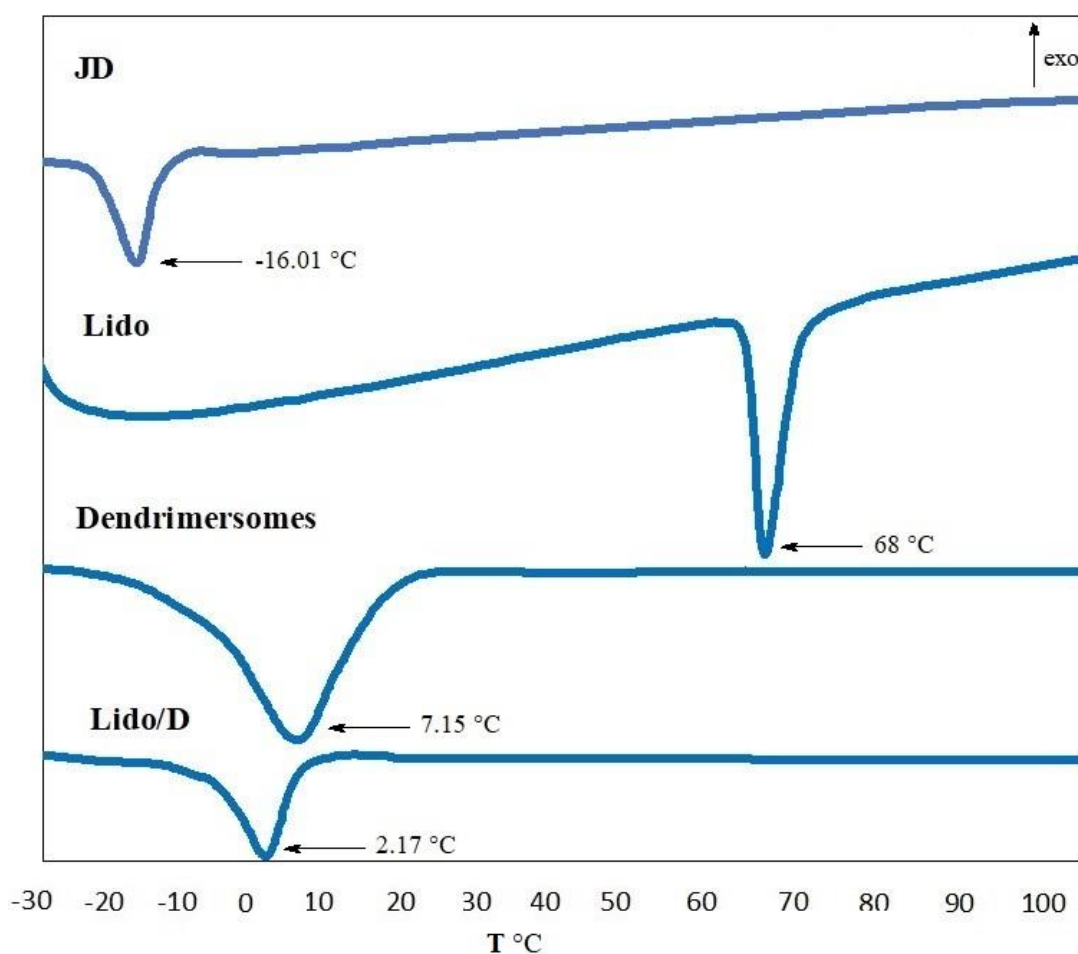


Figure 2.4 DSC data of JD, Dendrimersomes, Lido, Lido/D.

2.3.4 Atomic force microscopy (AFM) analysis

For AFM analysis, one drop from optimized Lido/D formulation was deposited on a fresh mica surface and left to be evaporated at room temperature. During analysis it was revealed that despite dilution and evaporation, dendrimersomal formulation maintained their spherical shapes (Figure 2.5). Additionally, opposite to micelles, our dendrimersomal nanoparticles were not in equilibrium with their monomers which is observed by AFM. Furthermore, calculated dimensions of the particles demonstrated that, while decreasing diameter from 77 nm to approximately 45 nm *via* dehydration, their heights were slightly changed (4.7 nm). This implies that the nanoparticles were “soft” and that their volumes dramatically shrunk during dehydration.¹⁵⁰

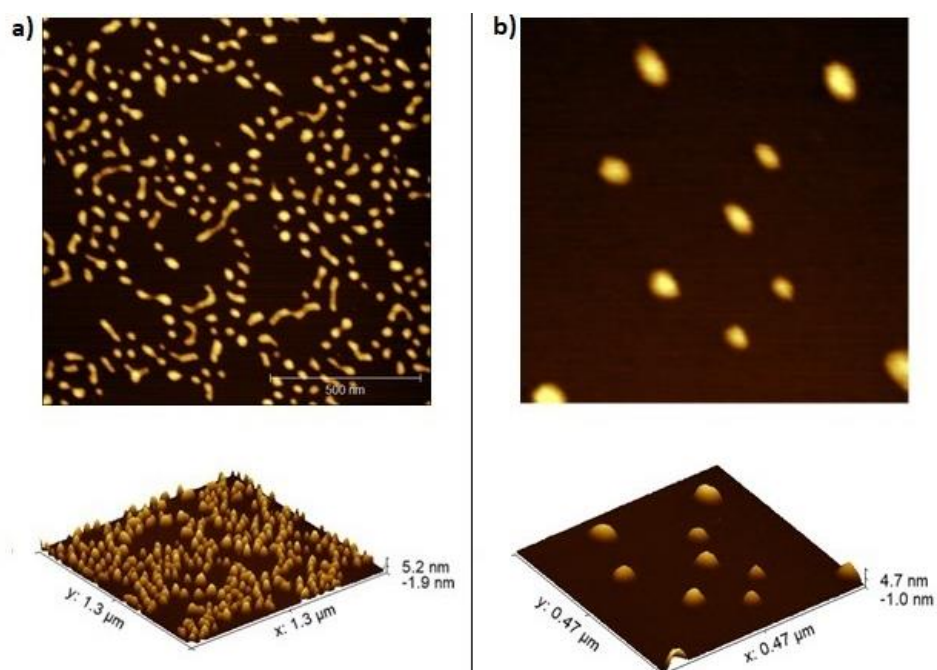


Figure 2.5 AFM micrographs of Lidocaine-loaded dendrimersome: a) 2D and 3D micrographs of early Lido/D; b) 2D and 3D micrographs of dehydrated Lido/D.

2.3.5 Transmission electron microscopy (TEM) analysis

Transmission electron microscope (TEM) of freeze-fractured replica was used to obtain a visual information on Lido/D suspensions. During analysis, it was observed that particles with a diameter of 70 nm are homogeneous, regular and in spherical shapes. Moreover, as it was confirmed by DLS, agglomeration of nanoparticles was not detected.

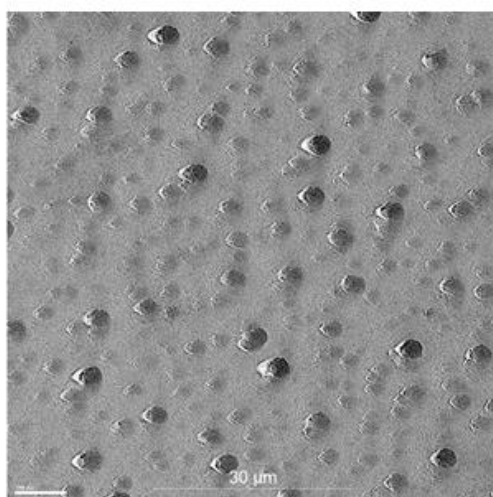


Figure 2.6 Transmission electron micrographs of freeze-fractured replica of Lidocaine-loaded dendrimersomes.

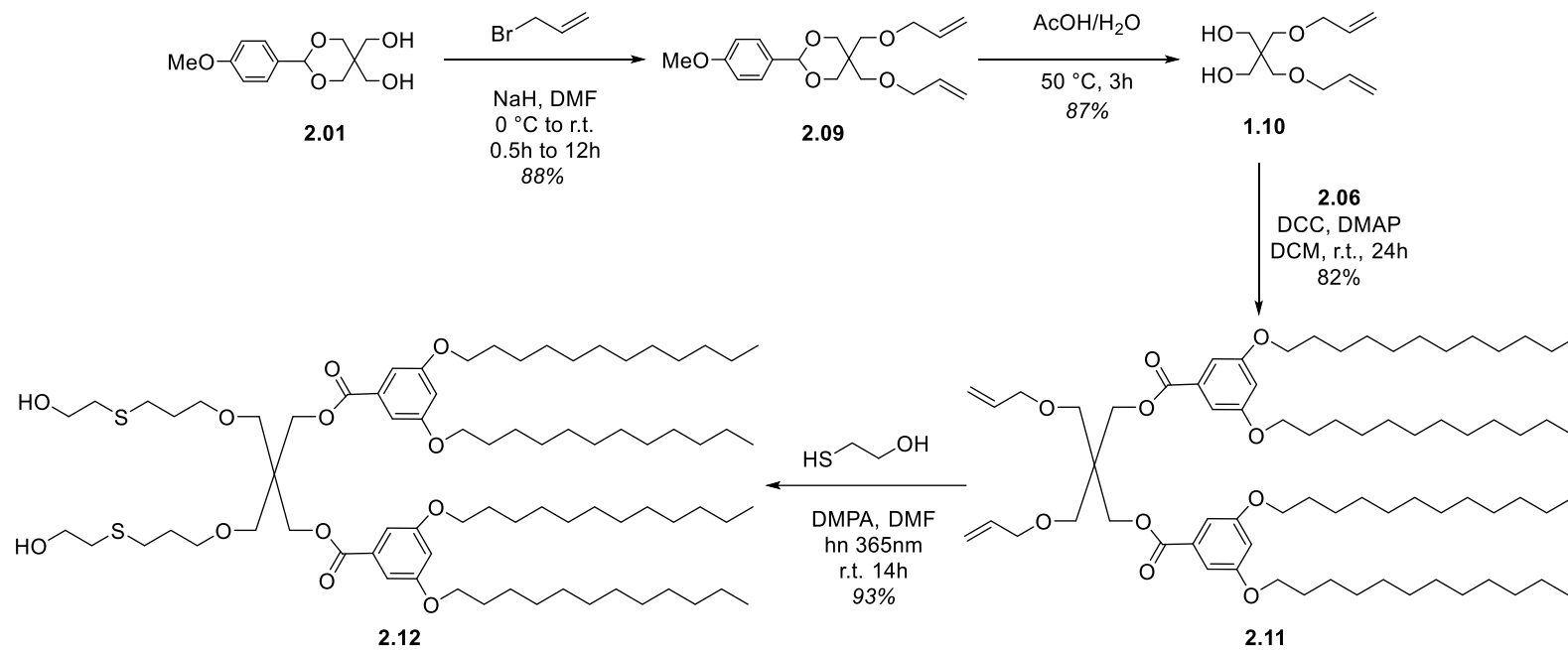
2.4 Conclusion

In the present study, Lidocaine was successfully loaded into two types of nanocarriers: dendrimersomes and classical liposomes. Both colloidal systems Lido/D and Lido/L suspensions showed superiority over the free drug solution for dermal delivery. Compared to free Lido solution, Lido/D suspension presented higher drug release in a sustained manner. Observed higher value of Lidocaine permeation through human skin indicates that the Lido/D formulation could improve the anesthesia efficiency of

Lidocaine. Moreover, Lido/D formulation is more stable than Lido/L formulation after 60 days. Results also revealed that skin permeation of dendrimersomal formulation and controlled release of Lido are much greater than pure Lido. Generated from amphiphilic Janus-dendrimer, dendrimersomes can be used for dermal drug delivery and immediate skin numbing. Extensive investigation and experimentation on potential application of dendrimersomes, which exhibited more promising characteristics including Entrapment Efficiency (EE% is defined by the quantity of the incorporated drug detected in the formulation over the free or untrapped quantity of the drug used to make the formulation), shelf-life stability, mechanical properties than the classical liposomes are strongly recommended.

2.5 Perspective

Additionally, for comparative study purpose, less polar amphiphilic Janus dendrimer **2.12** was synthesized *via* thiol-ene mediated click reaction between allyl functionalized JD precursor **2.11** and mercaptoethanol (Scheme 2.4). The synthesis of **2.11** itself began from bis allylation of **2.01** followed by deacetalization and Steglich-Neises esterification. Furthermore, synthesis both propargyl and allyl functionalized JD precursor are particularly interesting. Therefore, click reaction with carbohydrate moieties through CuAAC and thiol-ene could be comparatively explored.

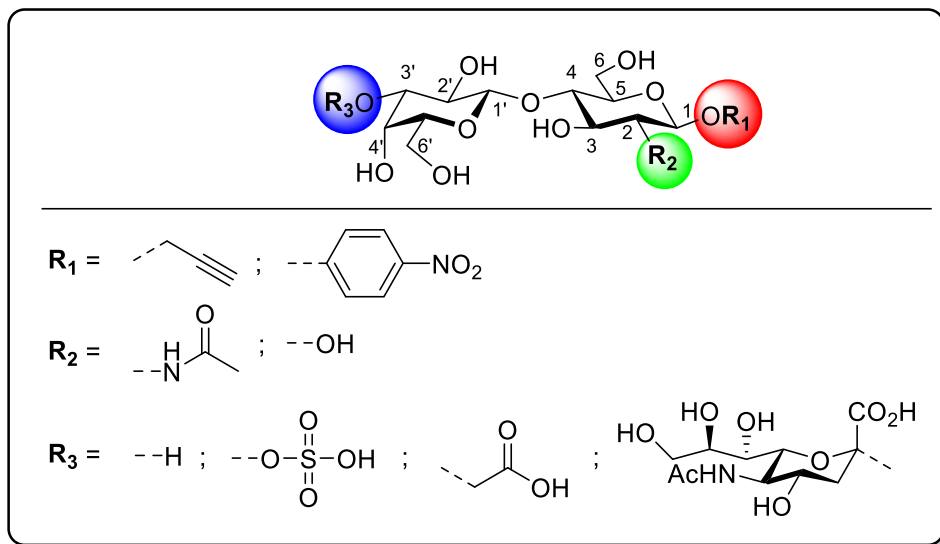


Scheme 2.4 Synthesis of less polar analogue of **2.08**.

CHAPTER III

EFFICIENT AND REGIOSELECTIVE 3'-*O*-FUNCTIONNALIZATION OF PROPARGYL AND *PARA*-NITROPHENYL-BASED LACTOSIDES AS INHIBITORS OF GALECTINS

An efficient and regioselective 3'-*O*-functionnalization of propargyl and *para*-nitrophenyl-based lactosides (Scheme 3.1) as inhibitors of galectins was described. The regioselective sulfo and alkyl-lactosides synthesis highlights the use of the dibutyltin oxide mediated acetalization protocol from 6,6'-di-TBDPSi-protected intermediates (**3.34**, **3.50**, **3.59**). The α -stereoselective sialylation reaction was performed in light of the previously reported method using thiophenylsialoside donor (**3.36**) and LacNAc acceptor (**3.34**) under Lewis acidic condition, followed by deprotection steps to afford the SialylLacNAc (sialyl-LacNAc) trisaccharide (**3.42**). The regioselective β -D-(1 \rightarrow 4) galactosylation of the 4-nitrophenyl- β -D-*N*-acetylglucopyranoside acceptor (**3.46**) provided efficient access to the PNP-LacNAc precursor (**3.48**).



Scheme 3.1 Aimed 3'-*O*-derivatives of propargyl and *para*-nitrophenyl-based lactosides.

3.1 Galectins and their role in biology

Galectins known as S-type¹⁶⁸ (sulfhydryl-dependent) lectins and one of the extensive class of the lectin family identified in vertebrates in 90s of last century.¹⁶⁹ The term Galectin was given for the first time in 1994 due to properties of the carbohydrate recognition domain (CRD) of the glycoprotein that binds to galactose-containing oligosaccharides.¹⁷⁰ So far, all extracted galectins from vertebrate tissues have shown similar core of amino acid sequence and β -galactosides binding, homologous and mostly conserved CRDs.

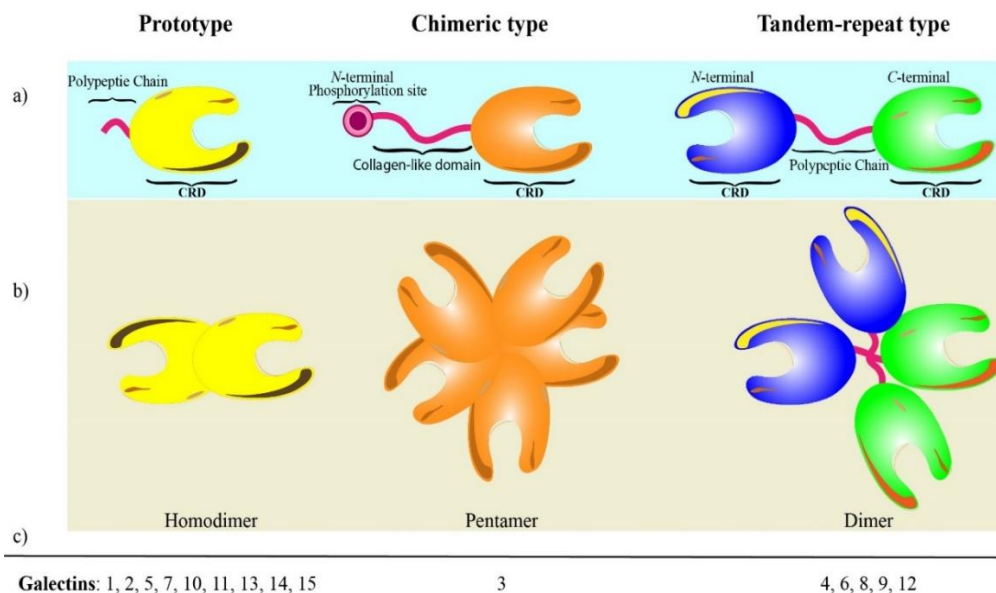


Figure 3.1 Galectin subdivision in human according to structural feature of CRD. a) Monomer form of Galectins; b) Homodimerization of “proto-type”, oligomerization or pentamerization of “chimera-type”, dimerization of “tandem repeat-type”; c) Attribution of subtypes accordingly.

Although 20 members of galectin have been discovered in mammals to date, only 15 are expressed in human tissues and all of them consist of about 130-135 amino acids including at least one CRD which is conjugated to single polypeptide chain. Based on the organization of CRD, galectins are subdivided in 3 types: “proto”, “chimera”, “tandem repeat” and all subtypes have been numbered according to the chronology of their discovery (Figure 3.1).⁵³ The Proto-type galectins have only one CRD per subunit and tends to form homodimer, whereas tandem-repeat have two non-identical CRDs linked each other by polypeptide chain and dimerize. Exclusive chimera-type galectin which is Gal-3 has a single CRD linked to phosphorylation site in *N*-terminal region within collagen-like polypeptide chain.⁷⁰ Expression of galectins are localized both in intracellular (nucleus, cytoplasm, cell membrane) and extracellular (outer cell surface) environments depending on galectin members. Secreted by nonclassical

pathway, galectins are implicated in adhesion, cell proliferation, apoptosis, immune response, angiogenesis including expression in cancer progression and metastasis. Especially overexpression of galectins in cancerous cells makes them to be considered the hallmarks of cancer (Figure 3.2).^{171, 172} Therefore, during immunosurveillance in the tumor microenvironment galectins serve as negative regulators of immune checkpoints by activating the secretion of immunosuppressive cytokines that weaken immune response toward cancerous cells. Among galectins most-studied Gal-1 (14.6 kDa) and Gal-3 (26 kDa) are highly expressed in immune cells, sensory neurons, epithelial and endothelial cells and nearly participate in all stages of tumor development and progression. First member of the family, Gal-1 binds to LacNAc residue of *N*- and *O*-glycans on the surface of various cells and modulates cell migration, adhesion and signaling *via* forming cross-linked lattice.¹⁷³ Gal-2 (15 kDa for monomer) is mainly present in gastric cells and its lowered expression is associated with lymph node metastasis in gastric cancer.^{174, 175} Unique, chimeric type Gal-3 is composed of *N*-terminal region consisting of 12 amino acids including serine (Ser6 and Ser12) and tyrosine which are responsible for phosphorylation site, collagen-like polypeptide chain consisting of ~110 amino acids rich in proline and glycine, and *C*-terminal region consisting of 135 amino acids and containing a CRD.^{176, 177} *N*-terminal domain affords flexibility and promotes pentamerization in presence of specific multivalent glycoconjugates. This ability contribute to form heterogenous disordered cross-linked complex on cell surface and in the extracellular matrix.¹⁷⁸ Interestingly, it has been reported that collagen-like domain of Gal-3 is susceptible to cleavage by matrix metalloproteinase (MMP-2 and MMP-9) that leads to truncated Gal-3 (trGal-3).¹⁷⁹

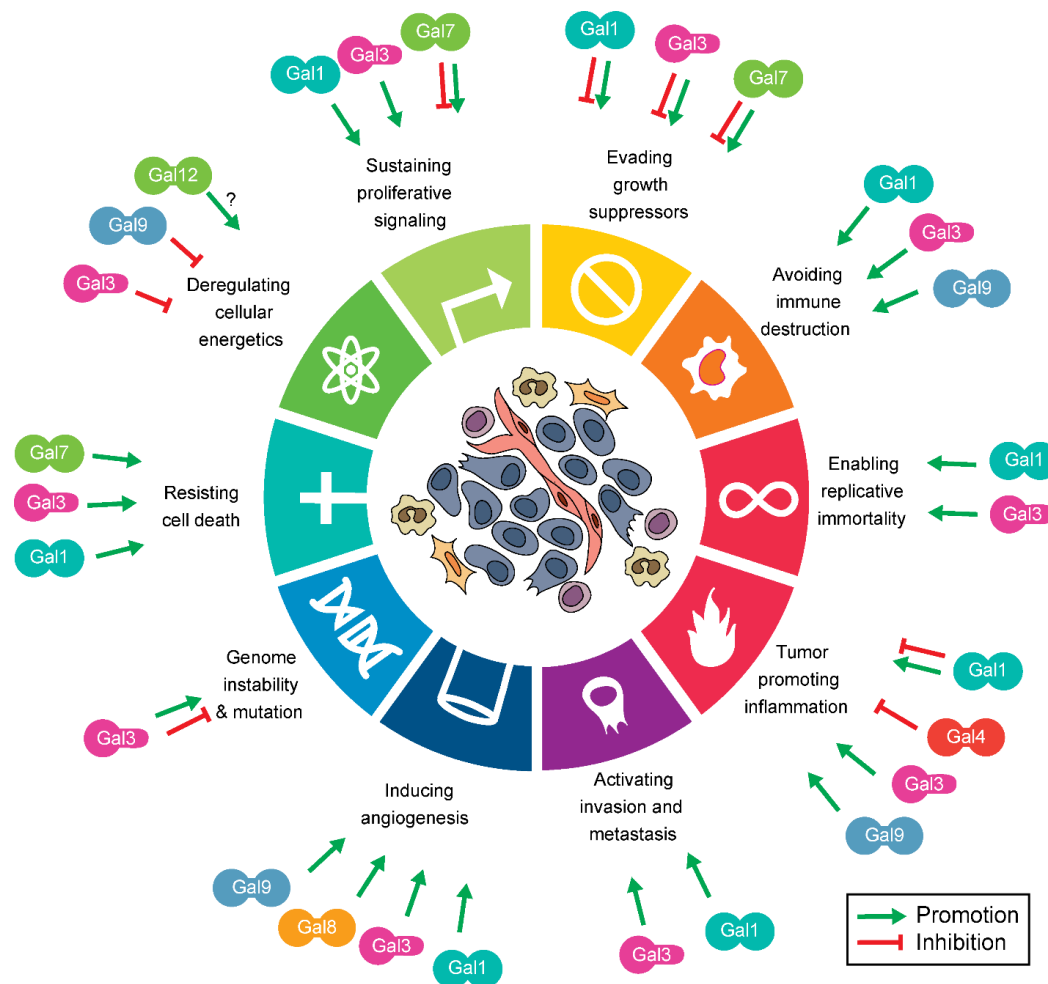


Figure 3.2 Galectin family members in the hallmarks of cancer.¹⁷¹

Although devoid of self-association, trGal-3 maintains carbohydrate-binding activity at C-terminal rendering it to act as dominant negative inhibitor of Gal-3 which can be beneficial for fighting cancer.¹⁸⁰ Gal-4 (36 kDa) is the third most studied galectin which plays numerous important biological roles including intestinal inflammation, protein trafficking, tumor progression, cell adhesion, wound healing *etc.*¹⁸¹⁻¹⁸³

Tandem-repeat type Gal-4 possesses two distinct CRDs (C- and N-terminals), and their amino acid sequences are 40 % identical, but they bind preferentially different saccharides. Main natural ligands of Gal-4 are human blood group antigens, MUC1

(mucin like membrane), glycosphingolipids and sulfated-cholesterol. Gal-7 (15 kDa for monomer) is an apoptosis regulator and modulates keratinocytes apoptosis, migration and proliferation during skin repair.¹⁸⁴ Its gene expression is induced by mutant p53 whose accumulation is considered as a hallmark of cancer cells.¹⁸⁵ Comparing to homodimeric Gal-1 (1094 Å²) and Gal-2 (1179 Å²), whose CRDs are associated side-by-side organization, Gal-7 (1484 Å²) possesses the largest interface among its proto-type homologues due to back-to-back arrangement (Figure 3.3).^{9, 186} This structural advantage may give Gal-7 play bridging role during cell-cell communication. Studies also showed that Gal-7 preferentially binds to LacNAc epitope over Lac, but its association is much weaker than Gal-1 and Gal-3.¹⁸⁷ Human Gal-8 (34 kDa) is another member of tandem-repeat type galectin whose CRDs are connected to each other with either short (33 amino acids, Gal-8L) or long (73 amino acids, Gal-8S) polypeptide chains.^{188, 189} By virtue of its multiple function in immune system, Gal-8 is suggested to be an immunostimulatory agent, thus co-stimulation of naïve helper T cell in presence of antigens and production of Interleukin 6 (IL6) have been observed.¹⁹⁰⁻¹⁹³

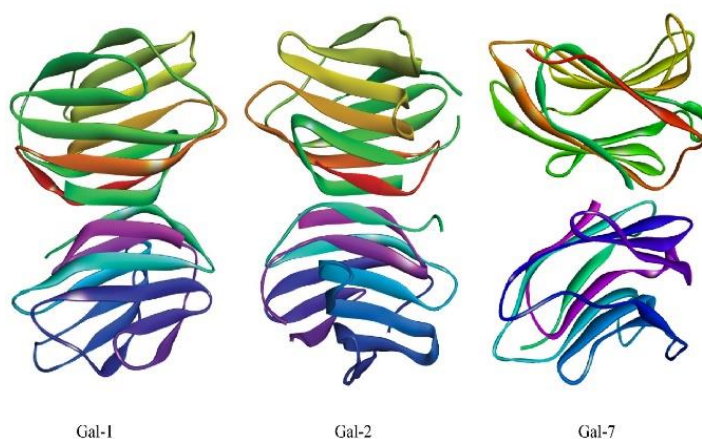
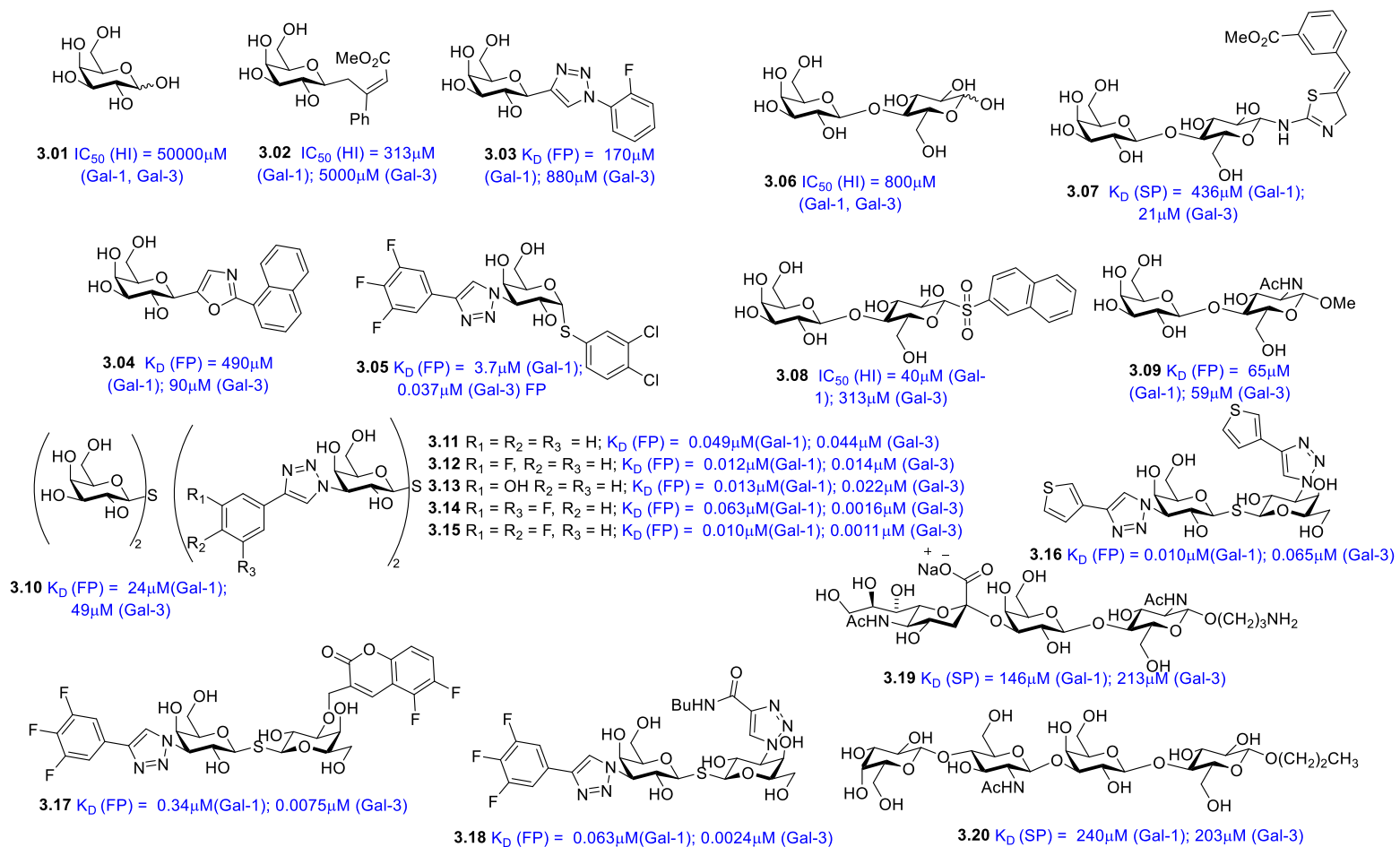


Figure 3.3 Organization of CRDs of homodimeric galectins: side-by-side (Gal-1 and Gal-2), back-to-back (Gal-7).

3.2 Monovalent Ligands of Galectins

The elucidation of biological roles of each galectin member have been studied individually by several research groups.^{173, 194-202} Although being natural ligands of galectins, galactose (Gal), lactose (Lac) and *N*-acetyllactosamine (LacNAc) exhibit low inhibitory potency toward galectins (K_D in millimolar and micromolar range Scheme 3.2). Alternatively, as we mentioned earlier, galectins dimerize and oligomerize in presence of their multivalent glycoconjugate ligands which are omnipresent at the outer surface of cells and form a lattice through crosslinking surface glycoproteins and glycolipids. In the past two decades, tremendous progress of structural elucidation of CRDs *via* multivalent glycoconjugates or small molecule glycomimetics led to encouraging breakthroughs in the development of cancer prognostics. Consequently, structural modification or derivatization of monomeric ligands (Gal, Lac, LacNAc) of galectins as the single presentation strategy (binding mode between a monovalent carbohydrate ligand and a lectin) has been demonstrated persuading advancement in development of potent inhibitor toward monomeric form of galectins. The carbohydrate ligand derivatization is oriented either to aglycon-based approach or SAR-(structure-activity relationship) based direct functionalization of sugar moiety. For the sake of clarity, we will give some examples of reported monomeric ligands and their inhibitory activity against most studied Galectin members (Gal-1, Gal-3, Gal-4, Gal-7 and Gal-8). To elucidate the role of aglycon within galactose moiety, Roy *et al.* developed a heterocyclic isoxazole functionalized β -galactoside, which demonstrated 20 times better activity toward Gal-1 than free galactose during qualitative hemagglutination inhibition assay.²⁰³ Taking into consideration that *C*- and *S*-glycosides are more stable against enzymatic hydrolysis than *O*-glycosides, galactosides with carbon and sulfur as glycosidic atom have been reported to show better stability and similar activity. Compared to natural galactose, *C*-galactoside **3.02**, containing phenyl and ester functional groups, have been reported

to show 160 times better activity against Gal-1.²⁰⁴ In another example, reported by Nilsson and co-workers, C1-heteroaryl galactosides **3.03** ($K_D = 170 \mu\text{M}$ for Gal-1) and **3.04** ($K_D = 90 \mu\text{M}$ for Gal-3) have exhibited superior binding activity versus methyl- β -lactoside ($K_D = 190 \mu\text{M}$ for Gal-1 and $220 \mu\text{M}$ for Gal-3) using fluorescence polarization assay.²⁰⁵ Moreover, it has been reported that double derivatization of galactopyranoside moiety at C3 and C1 positions was even more promising.^{206, 207} As a result, more recently developed by Nilsson and his co-workers, α -thio-galactopyranoside **3.05** showed surprisingly low nanomolar potency toward Gal-3 ($K_D = 31 \text{ nM}$) despite having unnatural aglycon at α -anomeric position.²⁰⁸ Naturally, Galectin family members bind preferentially to lactose over galactose, thus derivatization of commercially available lactose appears more beneficial for increasing the affinity toward galectins. Lactose derivative with rigid aglycon **3.07** developed by Pieters and co-workers, was observed to discriminate Gal-3 over Gal-1 with 14-fold enhancement relative to lactose in a solid phase assay.²⁰⁹



Scheme 3.1 Reported Gal-1 and Gal-3 inhibitors; (HI – Hemagglutination Inhibition assay; FP – Fluorescence Polarization assay; SP – Solid Phase assay).²⁰⁴⁻²²²

In another notable work, Roy *et al.* have developed small library of *S*-lactosides in order to evaluate impact of aglycons through hemagglutination inhibition assay. Therefore, among synthetic disaccharides 2-naphthylsulfonyl **3.08** and 2-nitrothiophenyl lactosides have shown respectively 20- and 10-fold enhanced inhibitory potency relative to lactose toward Gal-1.²¹⁰ X-ray elucidation of CRDs of Gal-1 and Gal-3 complexed with Lac (Figure 3.4, A₁ and B₁) and LacNAc (Figure 3.4, A₂ and B₂) shows both ligands bind at the same site, but somehow LacNAc possesses slightly better binding affinity. Pioneered by Nilsson and co-workers, introduction of aromatic moieties for additional interactions (cation- π interaction between Arginine and Arene) at C3' of LacNAc, have been reported to decrease dissociation constant to submicromolar value.^{211, 212}

In the past two decades, among synthetic monovalent ligands thiodigalactosides (TDGs) gained more attention. Thus, X-ray crystal structure of Gal-1 and Gal-3 complexed with thiodigalactoside derivatives **3.12** and **3.16** (Figure 3.4, A₃ and B₃) revealed that the second galactoside moiety replaced GlcNAc of LacNAc. Taking into account the previous studies, introduction of aromatic moieties through triazole or amide bond as single or double derivatization at C3 **3.11–3.18** have been reported more successful.^{206, 211, 213-216} Although reported disaccharides do not show distinct selectivity between Gal-1 and Gal-3, K_D have reached to a value below 10 nM in the fluorescence polarization assay.^{206, 214, 217} Possessing negatively charged sulfate at O3' position of lactosides²¹⁸⁻²²¹ and carboxyl containing SiaLacNAc²²² have significantly gained attention due to ionic interaction with positively charged lateral chain of amino acid within CRD. As result, trisaccharide **3.19** was observed to exhibit 6.3- (Gal-1) and 4.8-fold (Gal-3) enhancements relative to lactose in the solid phase assay. Additionally, tetrasaccharide (LNnT) containing Lac and LacNAc motifs **3.20** and demonstrating 3.8- (Gal-1) and 5-times (Gal-3) decreased IC_{50} values relative to lactose seems promising.

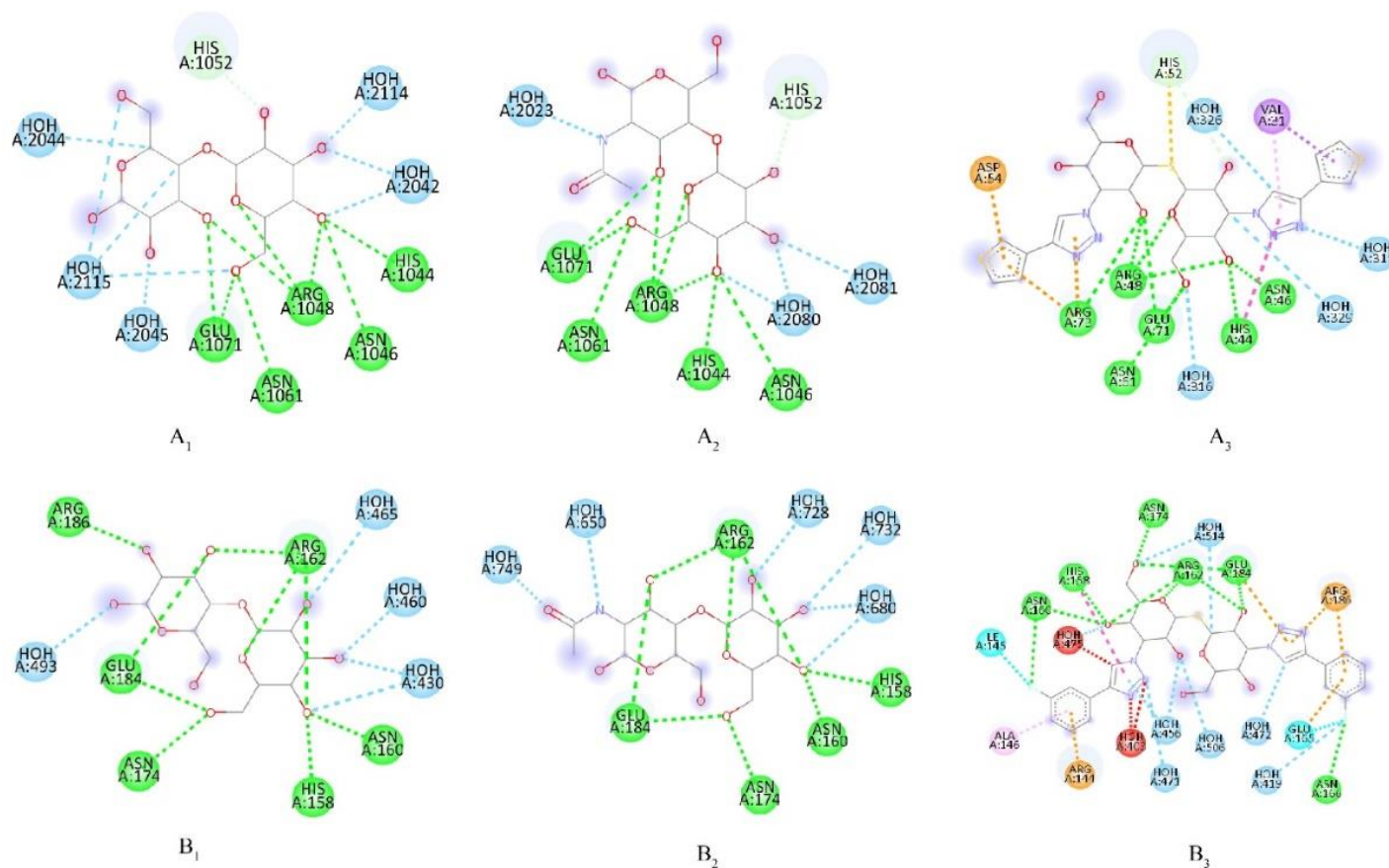
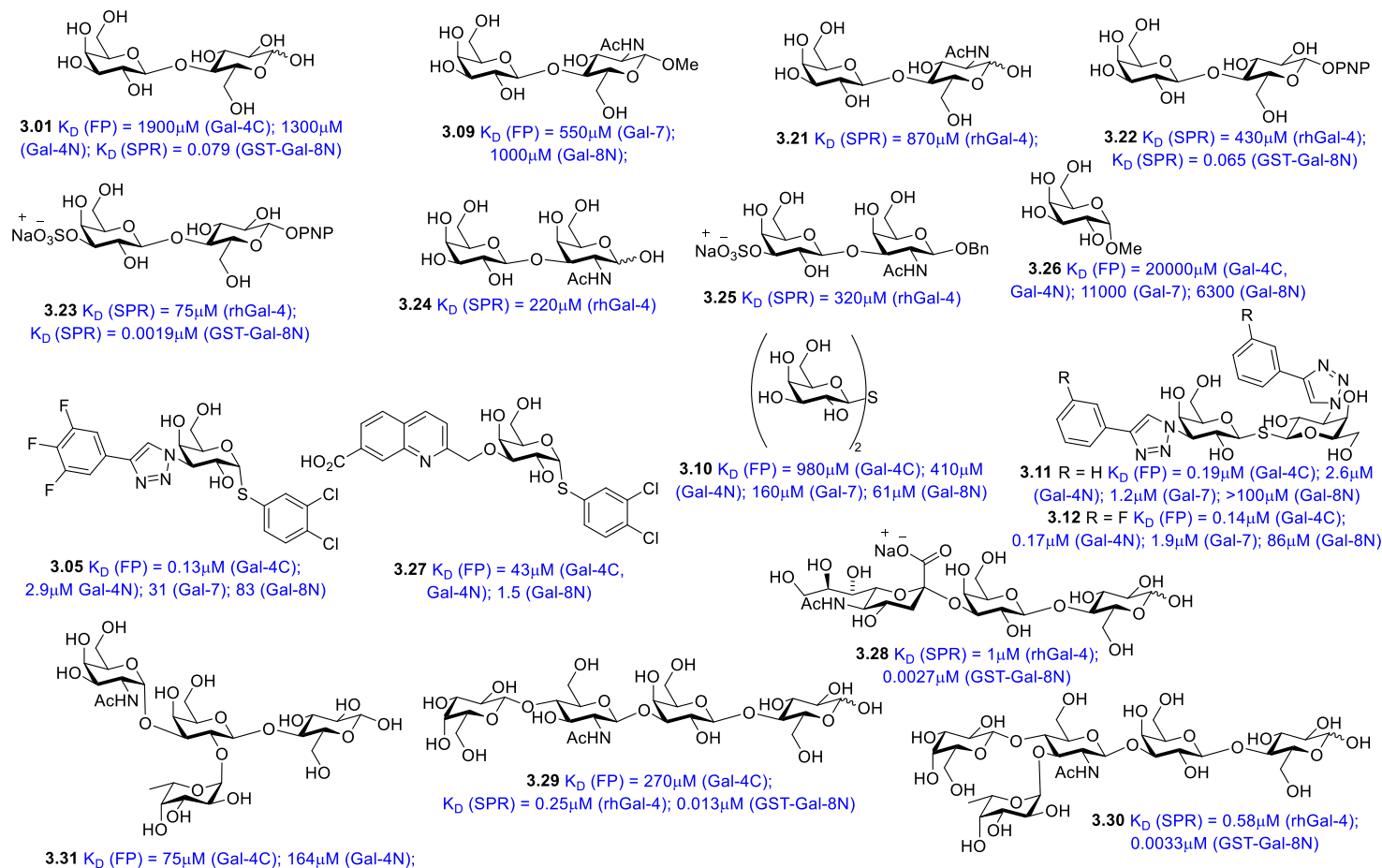


Figure 3.4 Binding of human Gal-1 and Gal-3 at CRDs with various disaccharides. A₁) hGal-1 – Lac (pdb code: 1W6O);²²³ A₂) hGal-1 – LacNAc (pdb code: 1W6P);²²³ A₃) hGal-1 – **3.16** (pdb code: 6F83);²²⁴ B₁) hGal-3 – Lac (pdb code: 4RL7);²²⁵ B₂) hGal-3 – LacNAc (pdb code: 1KJL);²¹¹ B₃) hGal-3 – **3.12** (pdb code: 5E89).²¹⁷



Scheme 3.2 Reported Gal-4, Gal-7, and Gal-8 inhibitors; (FP – Fluorescence Polarization assay; SPR – Surface Plasmon Resonance; SP – Solid Phase assay).^{208, 220, 224, 226-230}

Although both CRDs of tandem-repeat type Gal-4 possess 38 % amino acid sequence similarity, they bind preferentially different ligands as well as Gal-8 and Gal-9. Both Gal-4C and Gal-4N prefer Lac over LacNAc. *O*3'-sulfation of lactose readily improves binding affinity toward Gal-4 and Gal-8 due to salt bridge between guanidino of arginine residues (Arg59, Arg45) and sulfate (Scheme 3.3, compound **3.23**).^{226, 228, 231} Besides having poor binding affinity for LacNAc type-I (Gal β 1 \rightarrow 4GlcNAc), Gal-4 binds to LacNAc type-II (Gal β 1 \rightarrow 3GlcNAc) **3.24** with 3.9-fold increased affinity whereas sulfation at *O*3' position **3.25** have showed 250-fold enhancement relative to lactose.^{226, 227} Nilsson *et al.* have demonstrated that double derivatization of galactose and introduction of aromatic moieties are crucial for all galectin members.²⁰⁸ As result, α -thiogalactosides (**3.05** and **3.27**) and thiodigalactosides (**3.11-3.12**) outclass natural ligands (Gal, Lac, LacNAc) of galectins.^{208, 224, 229} During SPR analysis of oligosaccharide screening on immobilized glutathione-*S*-transferase (GST)-fused recombinant Gal-8, Ideo *et al.* have found that *p*NP-based *O*3'-sulfated lactose **3.23** and Sia(α 2 \rightarrow 3')Lac **3.28** show strongest binding affinity with lowest dissociation constants varying between 1-3 nM by virtue of salt bridge at *N*-terminal domain.²²⁸ Studies also demonstrated that, tetrasaccharide LNnT **3.29** and pentasaccharide LNF-III **3.30** have reached lower nanomolar potency toward GST-Gal-8N whereas GST-Gal-8C showed slightly weaker binding affinity.²²⁸ Blanchard *et al.* reported that **3.31** is the best known ligand for Gal-4C with 25-fold enhancement relative to lactose due to additionally created interactions *via* GalNAc residue which is utterly promising agent for further development.²³¹

3.3 Aim of the Project

3.3.1 Synthesis of a small library of *O*1- and *O*3'-derivatives of Lac and LacNAc

Thus, efficient, and low-cost synthesis of lactosides along with exclusive control of stereochemistry at anomeric position still remains a hot topic to develop. With the

aim of investigating newly created interactions, herein we report short chemical synthesis of small libraries of negatively charged *O*3'- derivatives of propargyl and *para*-nitrophenyl based lactose and LacNAc. Our initial targets are Galectins-3, -4C, -8N due to similarity up to 80 % of the amino acid sequence at CRD (Table 3.1)⁷⁰, but study shows that other galectin members would also be sensitive to the 3'-*O*-derivatives of Lactose and LacNAc.^{210, 222, 230}

Table 3.1 Amino acid sequence at CRD of Galectin-3, 4C, 8N.⁷⁰

<i>CRD-subsite</i>	Galectin 3	Galectin 4C	Galectin 8N
<i>A</i>	Arg144 (R)	Ser220	Arg45
<i>B</i>	Ala146 (A)	Ala222	Gln47
<i>C</i>	Asp148 (D)	Asn224	Asp49
<i>D</i>	Gln150 (Q)	Lys226	Gln51
<i>E</i>	-	-	Arg59
<i>F</i>	His158 (H)	His236	His65
<i>G</i>	Asn160 (N)	Asn238	Asn67
<i>H</i>	Arg162 (R)	Arg240	Arg69
<i>I</i>	-	-	-
<i>J</i>	Glu165 (E)	-	-
<i>K</i>	Asn174 (N)	Asn249	Asn79
<i>L</i>	Trp181 (W)	Trp256	Trp86
<i>M</i>	Glu184(E)	Glu259	Glu89
<i>N</i>	Arg186 (R)	Lys261	Ile91
<i>O</i>	Ser297 (S)	Gln313	Tyr141

To prepare targeted molecules, based on aglycon and availability of low-cost starting material, we initially divided our synthetic strategy in three parts: 1) series of β -propargyl-LacNAc and its 3'-*O*-derivatives (Scheme 3.4); 2) β -PNP-LacNAc and 3'-*O*-sulfo- β -PNP-LacNAc (Scheme 3.5); 3) β -PNP-Lactose and 3'-*O*-sulfo- β -PNP-Lactose (Scheme 3.5). Additionally, β -propargyl-lactoside was added to the list for further comparative study purpose with its LacNAc homologue.

While previous synthetic efforts have been mainly focused on direct synthesis of 3'-*O*-sulfate^{218, 232, 233} and -alkyl^{234, 235} of unprotected lactosides, our synthetic strategy requires protection of primary hydroxyl groups in order to avoid any formed side

products,^{236, 237} especially inseparable by classical column chromatography 6'-*O*-regioisomers (unpublished data), which is quite common in dibutyltin acetal-mediated functionalization.²³⁶ Among propargyl based LacNAc derivatives, the synthesis of Neu5Ac α (2 \rightarrow 3')LacNAc was particularly interesting. Presence of electron-withdrawing carboxyl group at anomeric position and absence of C3 neighboring participation group decrease the activity of sialyl donors and most of the case leads to obtention of exclusive 2,3-elimination product.

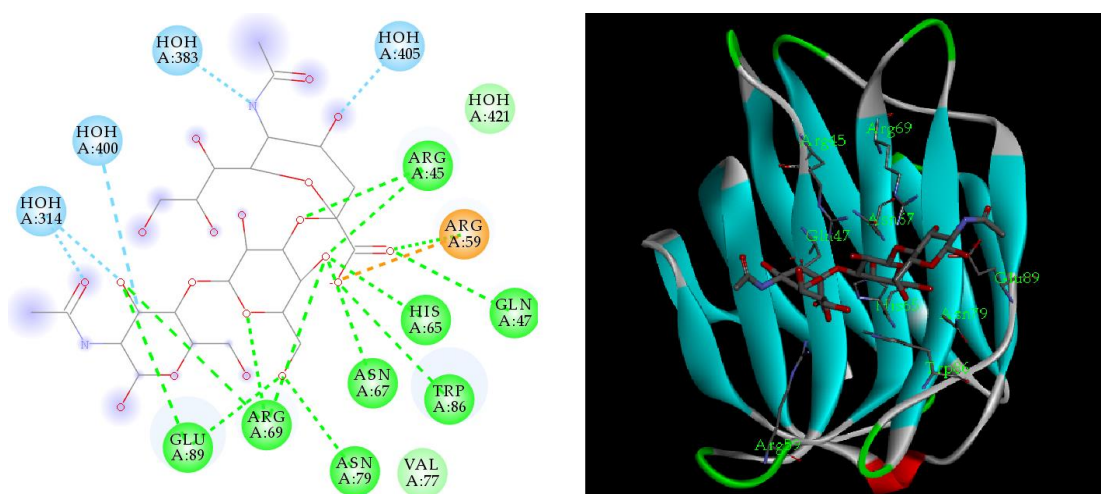
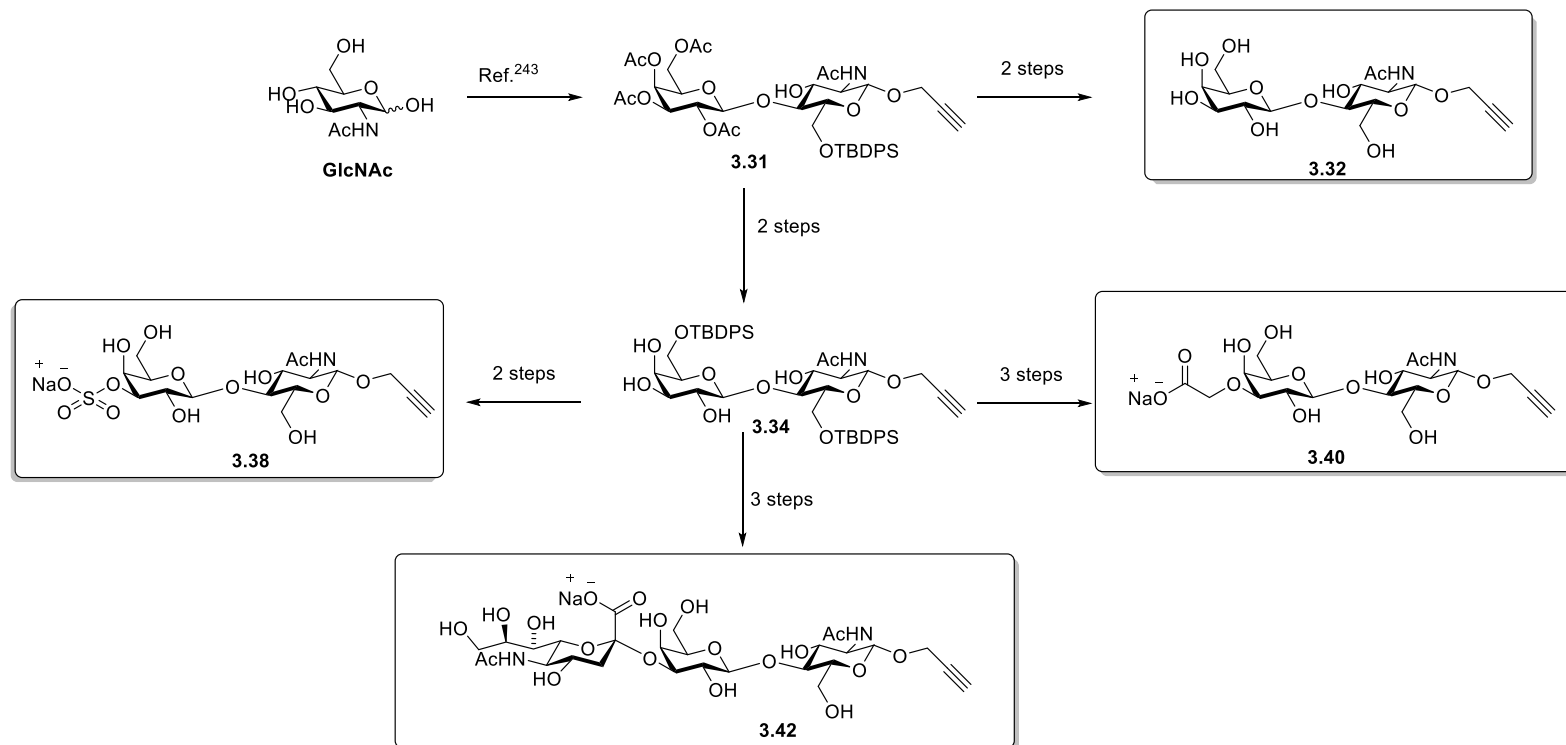
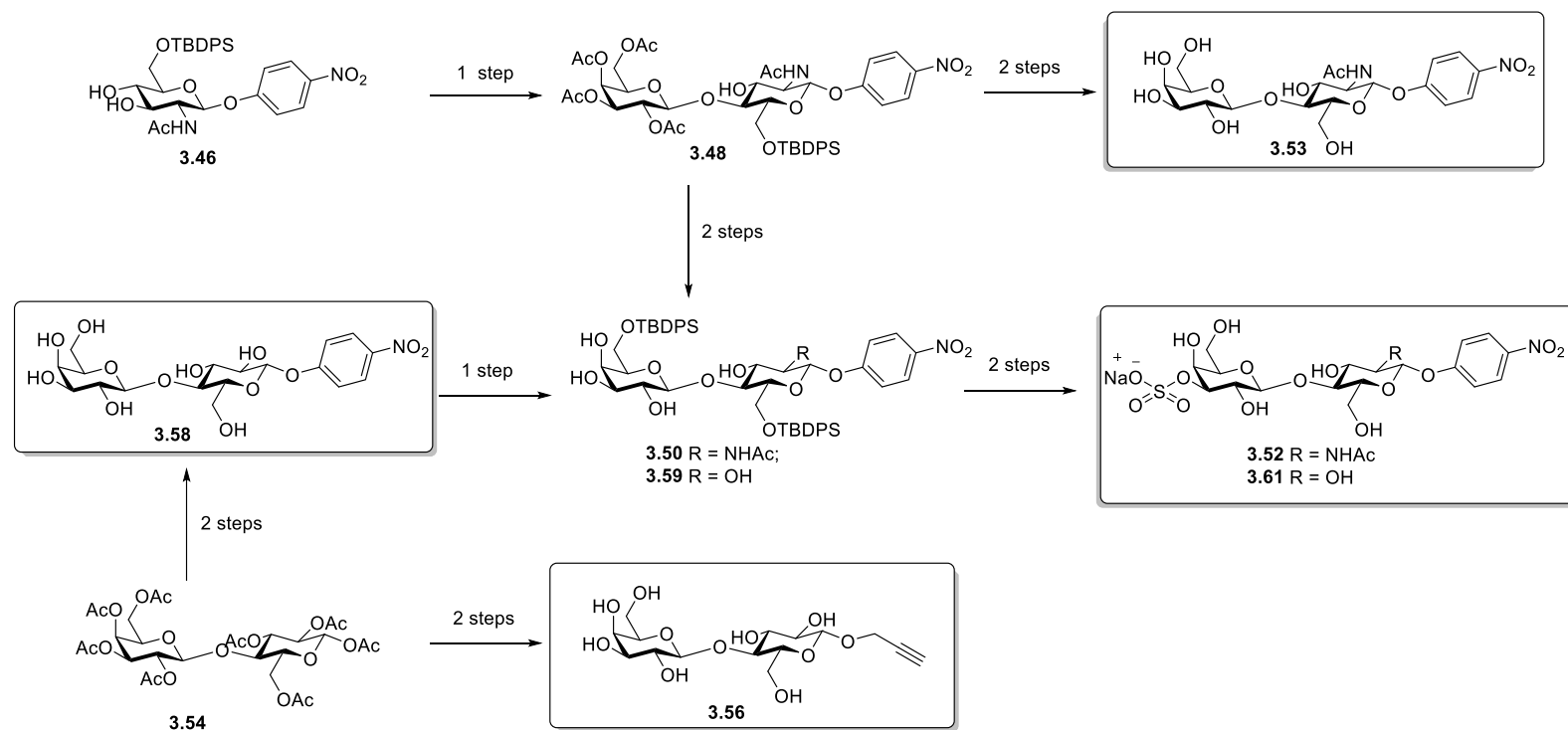


Figure 3.5 Structure of CRD site within SiaLacNAc-galectin-8N interaction (PDB 3VKO): ionic interaction in orange between carboxyl group of Neu5Ac and Arg59 is crucial.²³⁸

To date, several research groups have reported optimized methods²³⁹⁻²⁴² to sialylate LacNAc derivatives stereo- and regioselectively, but unfortunately, they all require additional protection/deprotection steps of the acceptor. Herein, we report the shortest, atom-economical, and less time-consuming path of preparation of Neu5Ac α (2 \rightarrow 3')LacNAc trisaccharide. On the other hand, inspiring by electrostatic contact between carboxylate of Sialic acid moiety and guanidinium of Arg59 (Gal-8N, Figure 3.5), preparation of an alternative **3.40** containing carboxylate at the same distance has been particularly interesting in further biological studies.



Scheme 3.3 3'-O-funtionnalization of propargyl-based *N*-Acetyllactosamine.



Scheme 3.4 Synthetic strategy for the preparation *para*-nitrophenyl and propargyl-based lactosides and their 3'-*O*-sulfated derivatives.

3.3.2 Results and discussion

In light of previously reported protocol by our group, we first resynthesized **3.31**.²⁴³ Subsequently, desilylation using tetrabutylammonium fluoride (TBAF) in THF, then treatment of crude product with sodium methanolate in MeOH/THF mixture at room temperature led to **3.32** in 88 % yield over 2 steps (Scheme 3.6). Described product was characterized by ¹H-NMR, ¹³C-NMR and ESI-HRMS (Figure 3.6).

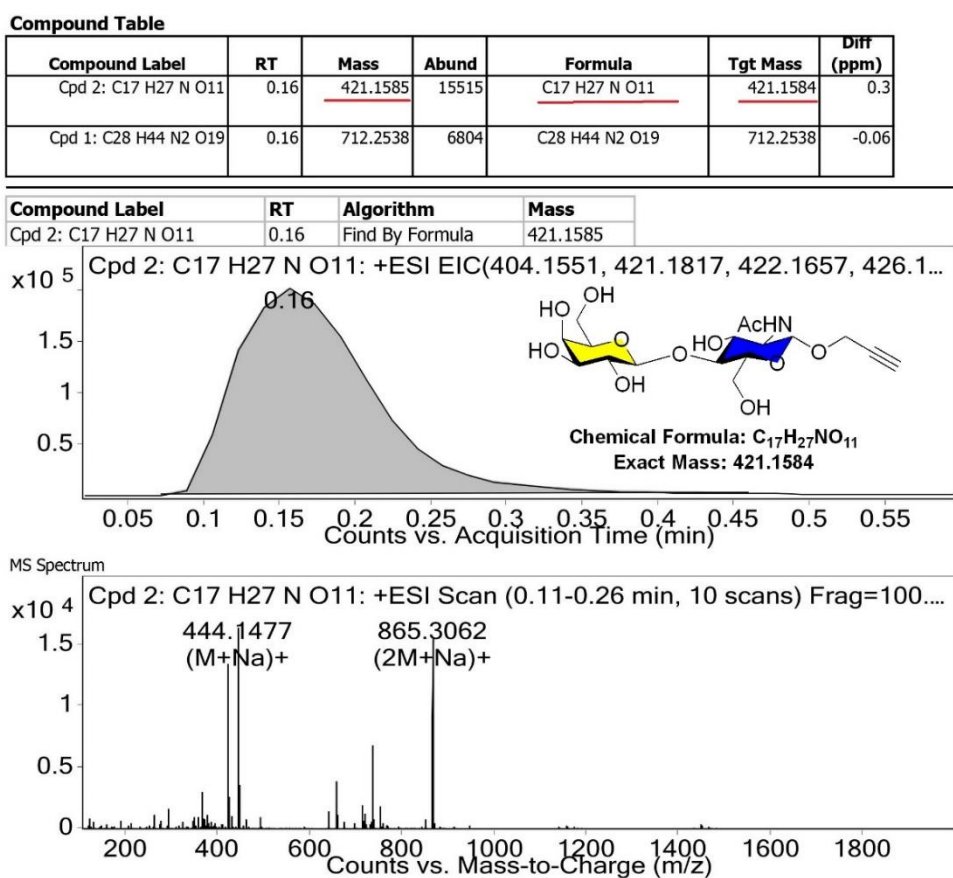
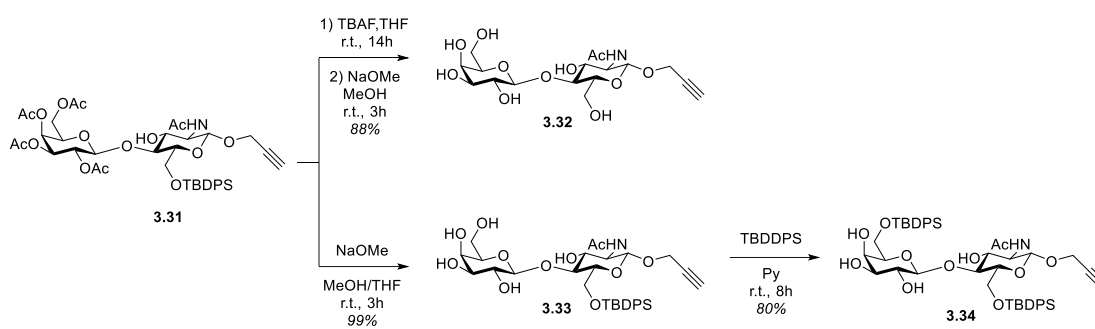


Figure 3.6 HRMS spectrum of compound **3.32**.

Deacetylation of **3.31** with catalytic quantity of sodium methanolate in methanol and tetrahydrofuran mixture at room temperature in 3 h gave 6-TBDPSi-protected-*N*-acetylglucosamine **3.33** in 99 % yield. Completion of deacetylation was confirmed by

$^1\text{H-NMR}$ and ESI-HRMS. Without any further purification step, the primary hydroxyl group of disaccharide **3.34** was protected with the bulky *tert*-butyldiphenylsilyl ether in the presence of pyridine at room temperature in 8 h to afford key intermediate **3.34** in good yield. Appearance of the second *tert*-butyldiphenylsilyl ether was confirmed by NMR and HRMS techniques (Figure 3.7 and 3.8).



Scheme 3.5 Deprotection of compound **3.31** and preparation of the key intermediate **3.34**.

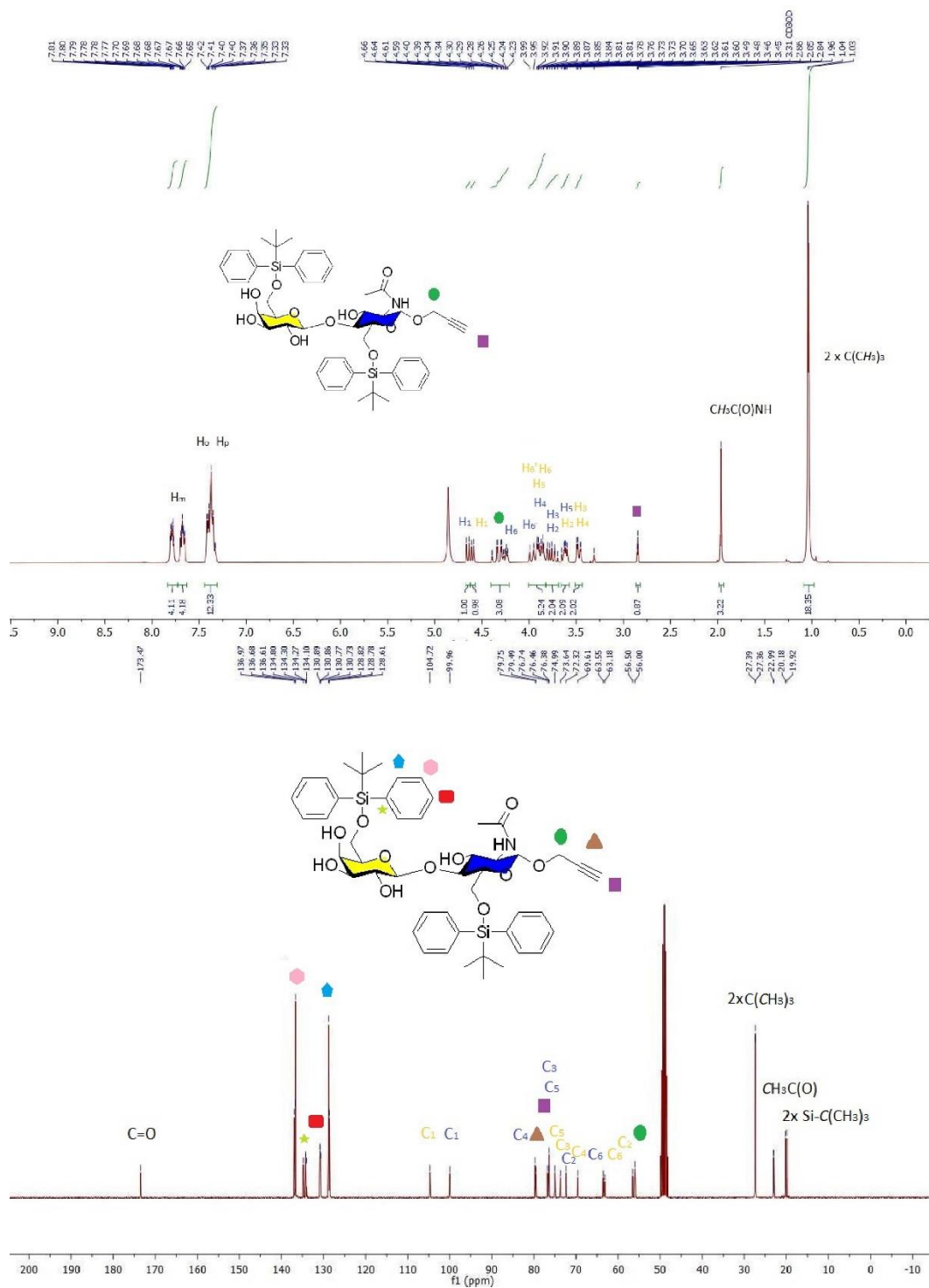


Figure 3.7 ¹H and ¹³C NMR (300 MHz, CD₃OD) spectra of compound 3.34.

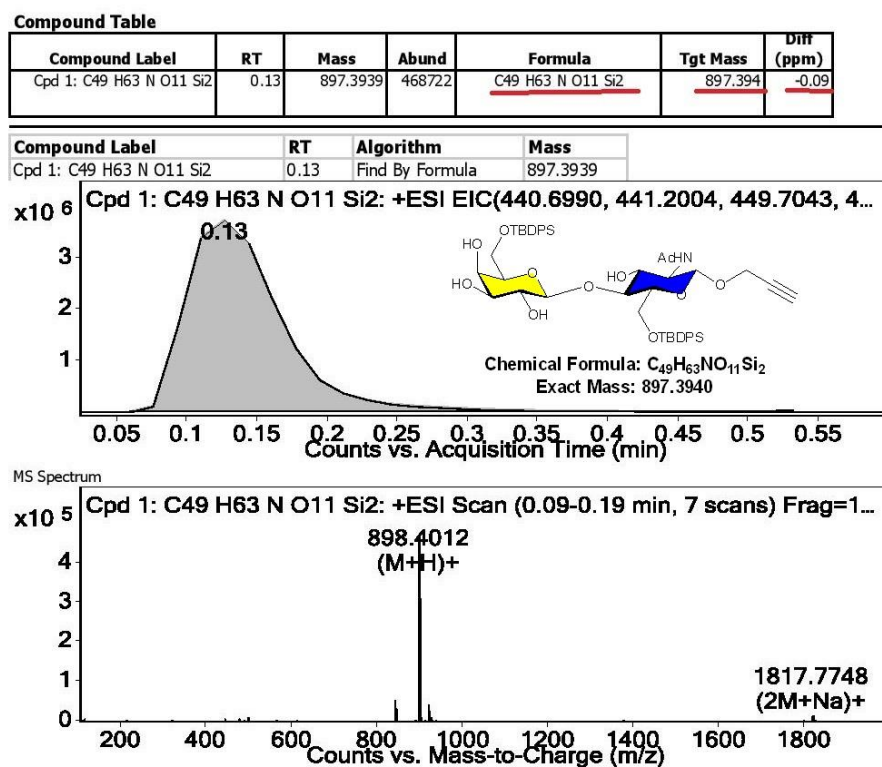
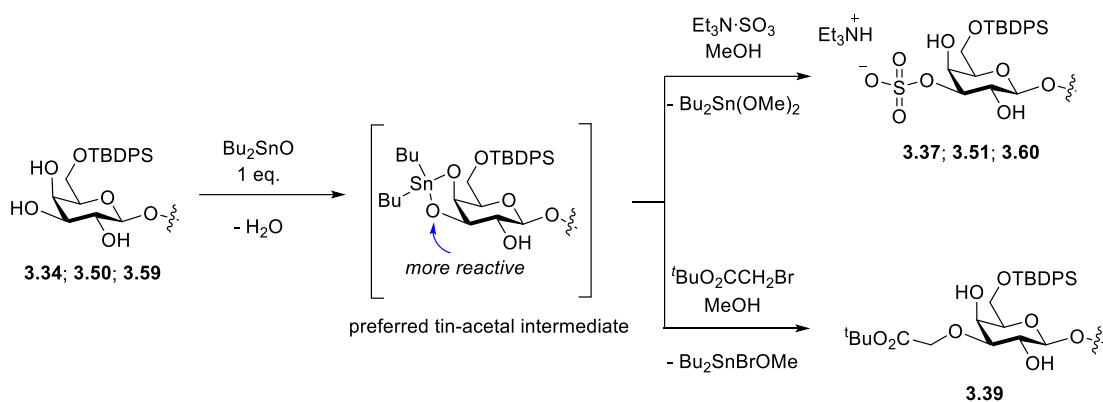


Figure 3.8 HRMS spectrum of compound **3.34**.

Regioselective sulfation and alkylation of C3' position of galactoside moiety without protecting other hydroxyl groups have been carried out by using dibutyltin oxide method.^{237, 244, 245} It was proposed that *cis*-vicinal diol preferentially chelates to the metal center and form dibutylstannylene acetal intermediate where oxygen atom (3'-O) at equatorial position is electronically and sterically more reactive (Scheme 3.6).²⁴⁶ The use of stoichiometric ratio between dibutyltin oxide and unprotected lactosides (in our case where primary hydroxyls are protected) are crucial, thus in case of excess amount of dibutyltin oxide additional formation of dibutyltin acetal intermediate through *trans*-vicinal diol could lead unwanted side products.

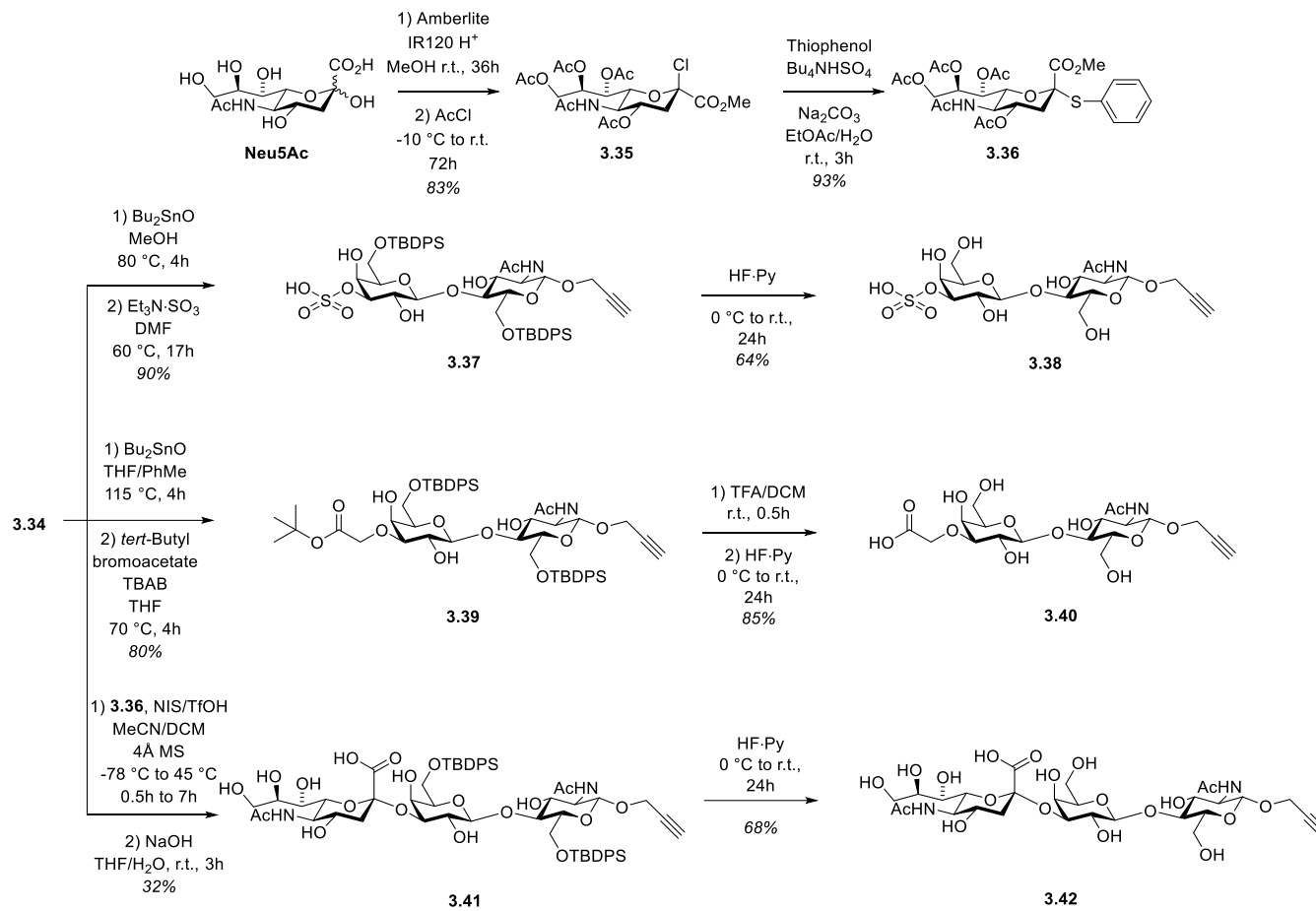
Toward this goal, dibutylstannylene acetal mediated regioselective sulfation and alkylation of the 6,6'-di-TBDPSi-protected-lactosides (**3.34**, **3.50**) were performed

using sulfur trioxide-triethylamine complex ($\text{Et}_3\text{N}\cdot\text{SO}_3$) and *tert*-butylbromoacetate²³⁵ to give respectively **3.37** and **3.39** in good to excellent yields (Scheme 3.7, 3.8 and 3.9). Each compound was characterized using NMR and HRMS techniques. The presence of *O*-sulfo group at *C3'* position was confirmed by downfield shift of 3'-*H* signal (Figure 3.9). *O*-alkylation at *C3'* position was confirmed *via* correlation between $\text{CH}_2\text{CO}_2^t\text{Bu}$ and *C3'* using HMBC (Heteronuclear Multiple Bond Correlation) experiment (Figure 3.11).



Scheme 3.6 Dibutyltin acetal mediated regioselective 3'-*O*-sulfation and alkylation of galactoside moiety of lactosides.

Efficient removal of silyl protected, especially acid-sensitive 3'-*O*-sulfated lactosides in basic media²⁴⁷ (in pyridine) using $\text{HF}\cdot\text{Py}$ yielded **3.38**, **3.40**. Desilylation reaction with the presence of TBAF in THF unfortunately led to cleavage of the sulfo group.



Scheme 3.7 Stereo- and regioselective sialylation and tin acetal catalyzed regioselective 3'-*O*-sulfation and 3'-*O*- etherification.

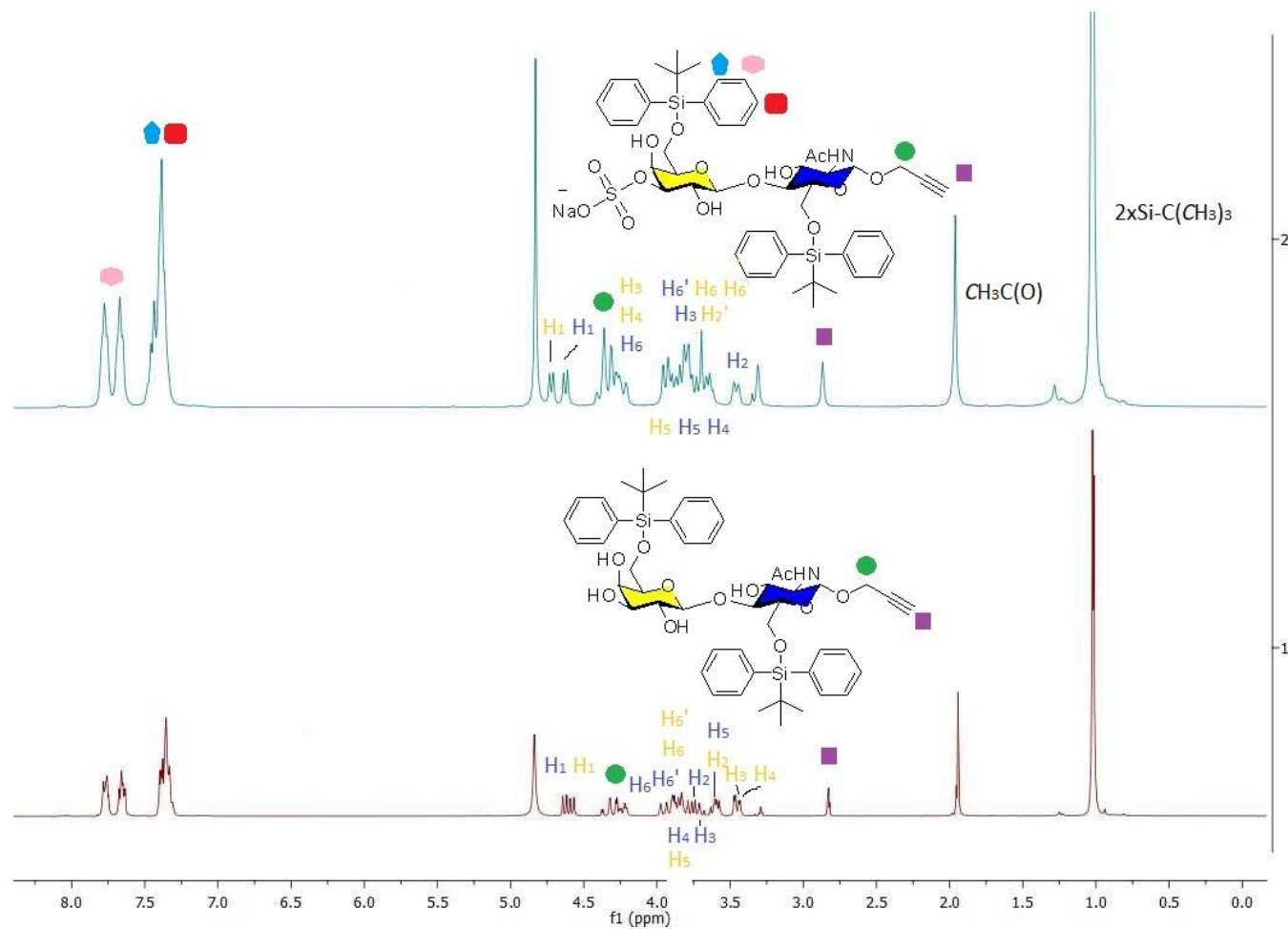


Figure 3.9 Comparison of ¹H NMR (300 MHz, CD₃OD) spectra of compounds 3.34 and 3.37 with the appearance of deshielded *H*-3, *H*-4 (in red) of galactoside moiety after sulfation.

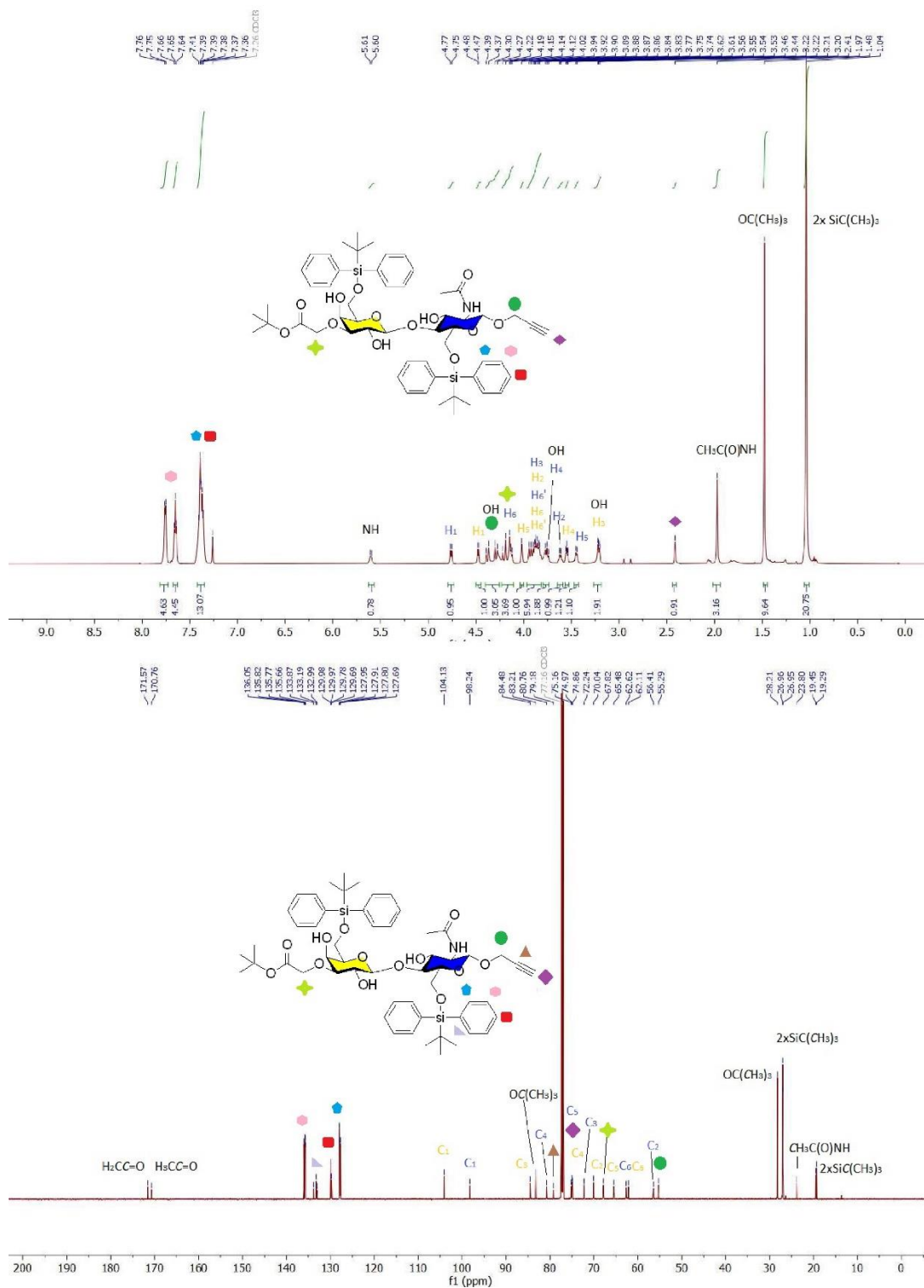


Figure 3.10 ¹H and ¹³C NMR (600 and 150 MHz, CDCl₃) spectra of compound 3.39.

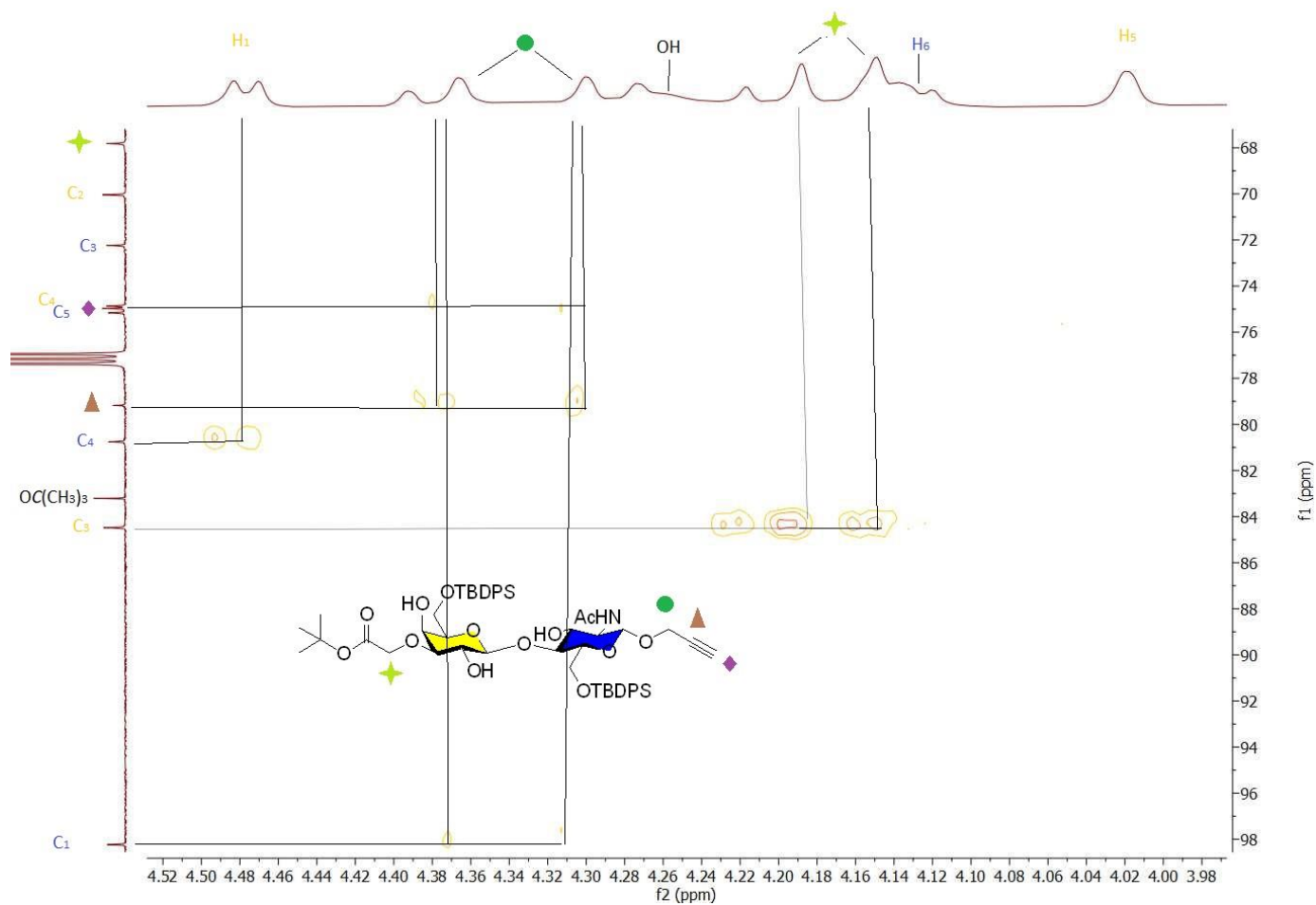


Figure 3.11 Confirmation of regioselective *O*-alkylation through HMBC experiment of compound **3.39** with the correlation between C3' (in yellow) and $\underline{\text{CH}}_2\text{CO}_2^t\text{Bu}$.

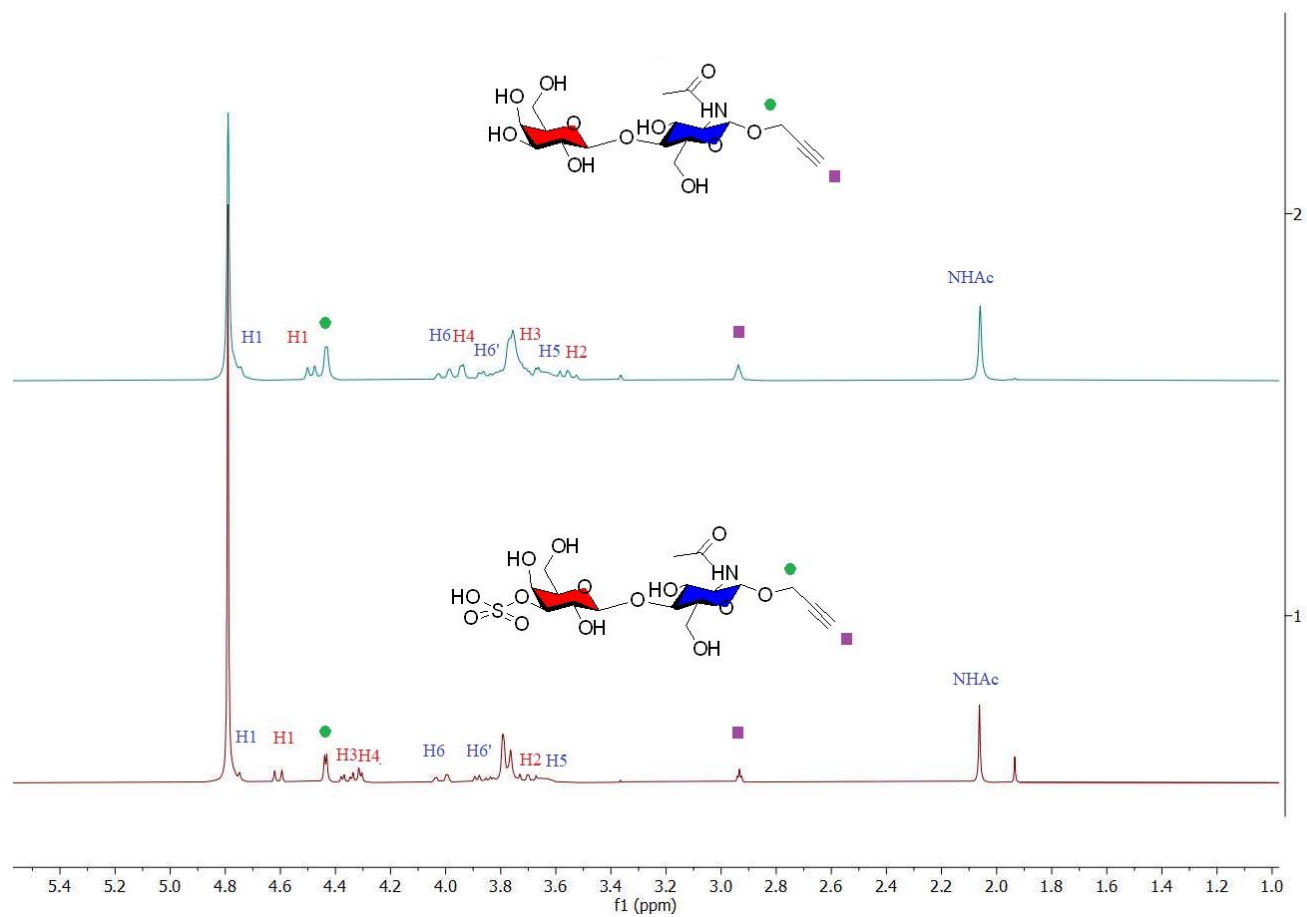


Figure 3.12 Comparison of ¹H NMR (300 MHz, D₂O) spectra of compounds 3.32 and 3.38 with the appearance of deshielded *H*-3, *H*-4 (in red) of galactoside moiety after sulfation.

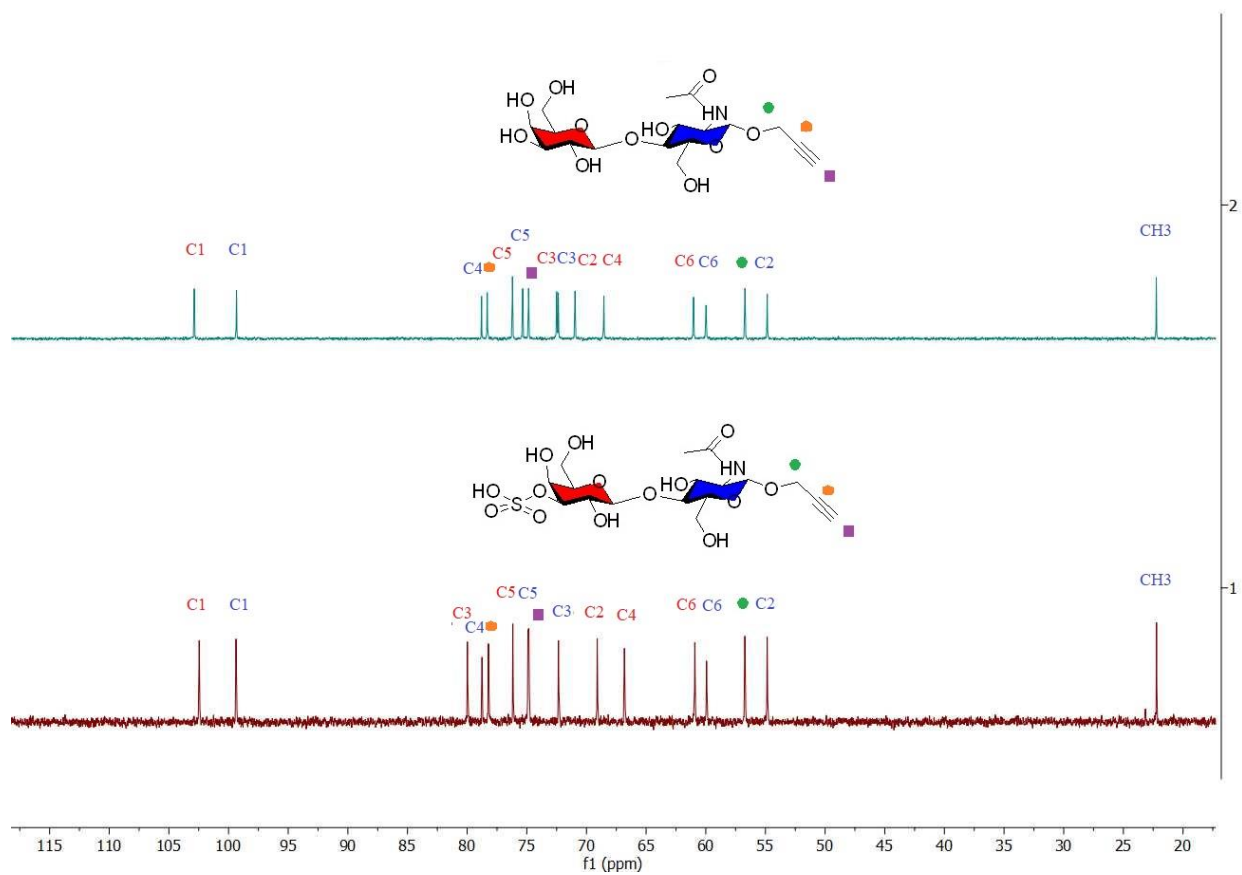


Figure 3.13 Comparison of ^{13}C NMR spectra (75 MHz, D_2O), of compounds 3.32 and 3.38 with the appearance of deshielded C-3 (in red) of galactoside moiety after sulfation.

The presence of the sulfate groups were readily confirmed on the basis of the $H-3'$ downfield shift from ~ 3.5 ppm to ~ 4.35 ppm (Figure 3.12) together with the characteristic ^{13}C NMR chemical shift displacement of the $C-3'$, which usually appears 7.5 ppm downfield ($\sim \delta$ 80 ppm) from the unsubstituted precursors at $\sim \delta$ 72.5 ppm (Figure 3.13).²³² NMR COSY and HSQC experiments were also used to unambiguously correlate the sulfation, alkylation process and regioselectivity.

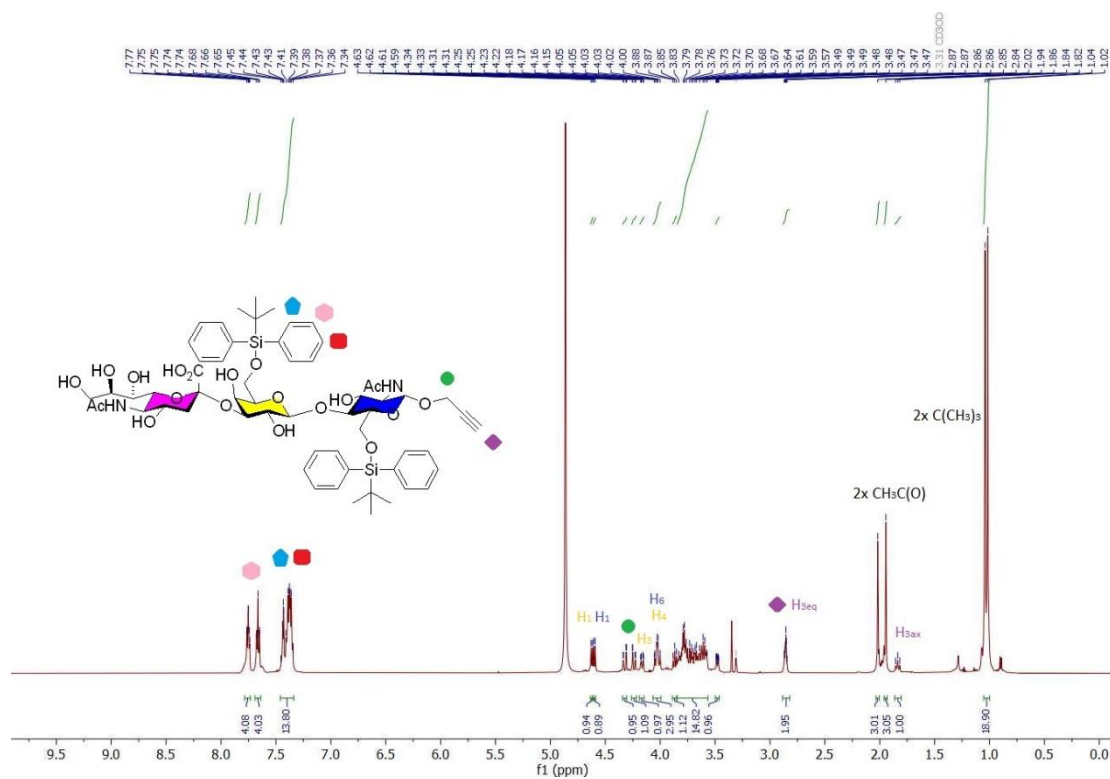


Figure 3.14 ^1H NMR (600 MHz, CDCl_3) spectrum of compound **3.41**.

For efficient α -sialylation, the anomeric leaving group (LG) at $C2$ position plays prominent role. Easily prepared from β -chloro sialoside **3.35** using phase transfer condition (PTC),²⁴⁸⁻²⁵¹ thiophenyl sialyl donor **3.36** have been used for the regio and α -stereoselective sialylation of LacNAc acceptor **3.34** in the presence N -iodosuccinimide (NIS), catalytic amount of triflic acid (TfOH) and 4Å molecular sieves (4Å MS) at -45 °C in DCM/MeCN solvent mixture.²³⁹ Before the purification

process, reaction mixture containing desired trisaccharide rather than peracetylation,²⁴² was subjected to high-yielding saponification followed by neutralization in presence of acidic resin to obtain **3.41** in 38 % yield over 2 steps. ¹H NMR spectra of **3.41** clearly showed the two proton signals corresponding to the H-3_{eq} and H-3_{ax} protons of neuraminyl residue at δ 2.86 and δ 1.84 ppm for the

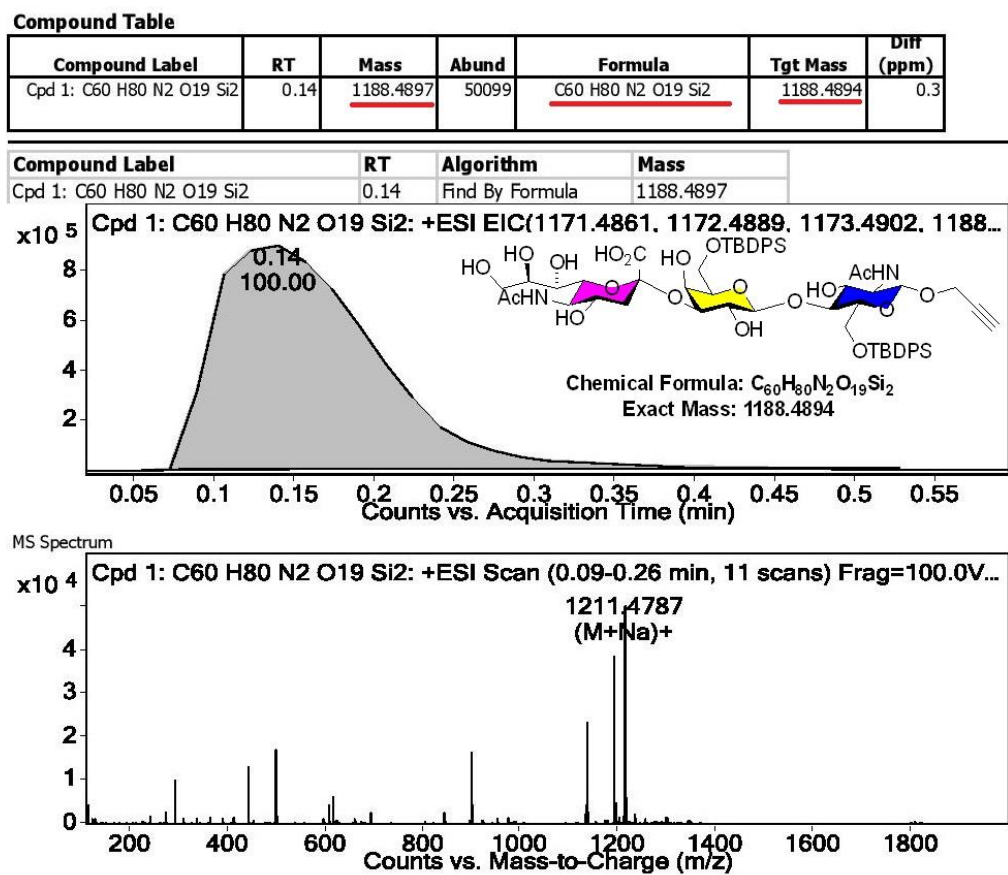


Figure 3.15 HRMS spectrum of compound **3.41**.

exclusive α -anomer according to well established empirical rules (Figure 3.14).²⁵²⁻²⁵⁶ Moreover, the regioselectivity was confirmed by downfield shift of 3'-H signal. Formation of the trisaccharide was also confirmed by HRMS technique (Figure 3.15). Efficient removal of silyl protecting groups in presence of HF in pyridine afforded **3.42** in 68 %.

After successful synthesis of propargyl-based LacNAc derivatives **3.32**, **3.38**, **3.40** and **3.42**, we turned our efforts to synthesize their *para*-nitrophenyl-based congeners. Starting with the preparation of galactoside acceptor **3.46**, we then focused on stereo- and regioselective glycosylation. We originally sought to synthesize β -*para*-nitrophenyl LacNAc derivative **3.48** following previously employed procedure²⁴³ for the preparation **3.31**, but unfortunately the solubility of **3.46** in DCM at low temperature was complicating glycosylation reaction (Scheme 3.8). We, therefore, solved this issue *via* mixing DCM with THF and increasing the reaction temperature to -35 °C to obtain desired disaccharide in moderate yield where unreacted **3.46** was recovered. The structure of **3.48** was fully characterized using ¹H and ¹³C NMR techniques (Figure 3.16). The regioselectivity of the formed interglycosidic linkage was determined by HMBC experiment where *H1* (Gal) – *C4* (Glc) correlation was observed (Figure 3.17). Deacetylation of **3.48** following general Zemplén transesterification condition (0.5 eq NaOMe in MeOH/THF mixture at room temperature, 3.5 h of stirring) afforded **3.49** in 97 % yield. Repeating above linear synthesis strategy (protection of 6'-*O* with TBDPSi, dibutylstannylene acetal-mediated regioselective sulfation at C3' position, desilylation in presence of HF in basic media) preparation of *para*-nitrophenyl-based 3'-*O*-sulfo-LacNAc **3.52** was achieved with 53 % yield over 3 steps. As illustrated in Figure 3.18 deshielded *H3'* and *H4'* signals clearly show the presence of sulfo group. Having successfully prepared **3.52** and **3.53**, we next focused on the synthesis of Lactose derivatives.

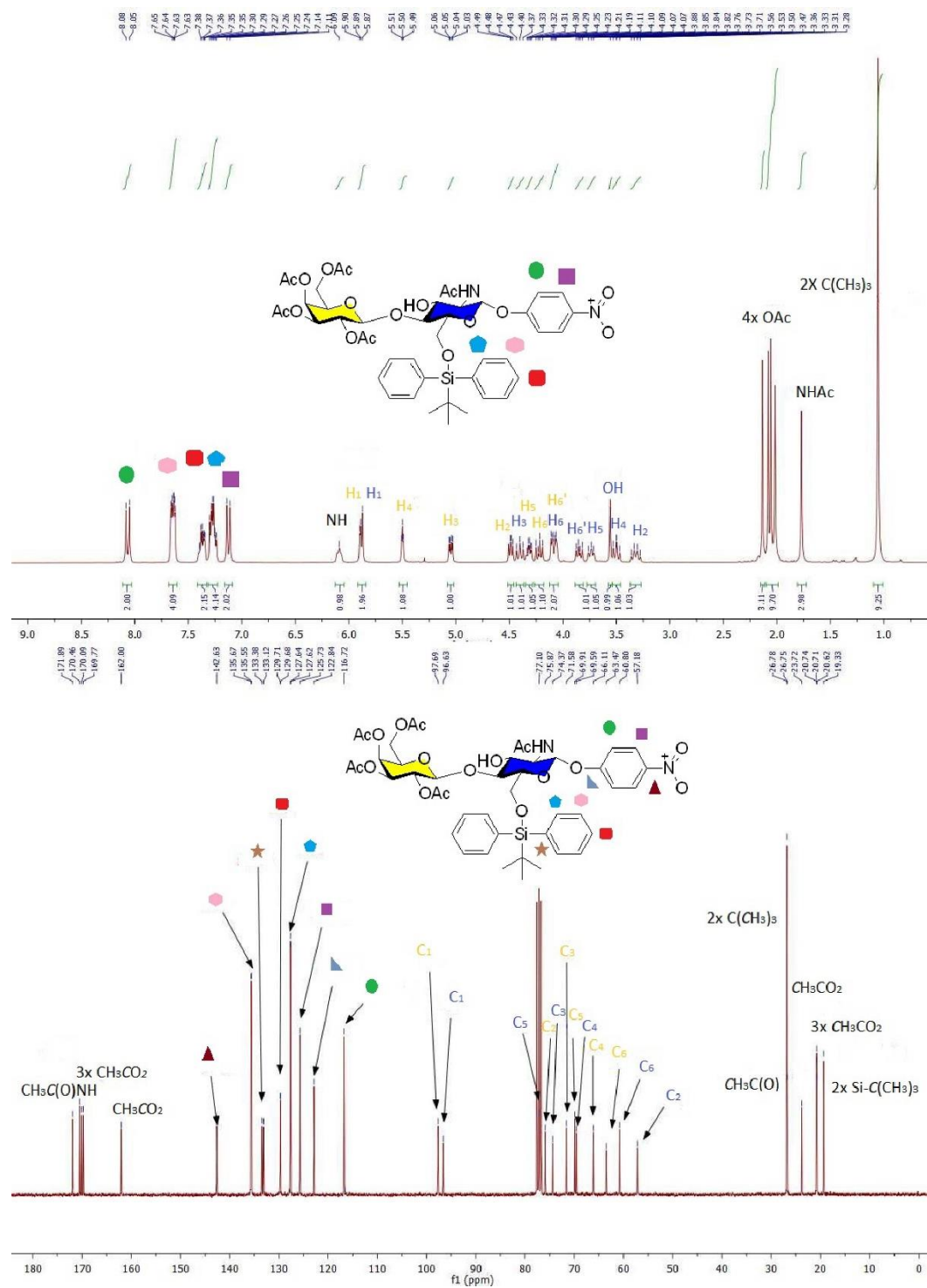


Figure 3.16 ^1H and ^{13}C NMR (300 and 75 MHz, CDCl_3) spectra of compound 3.48.

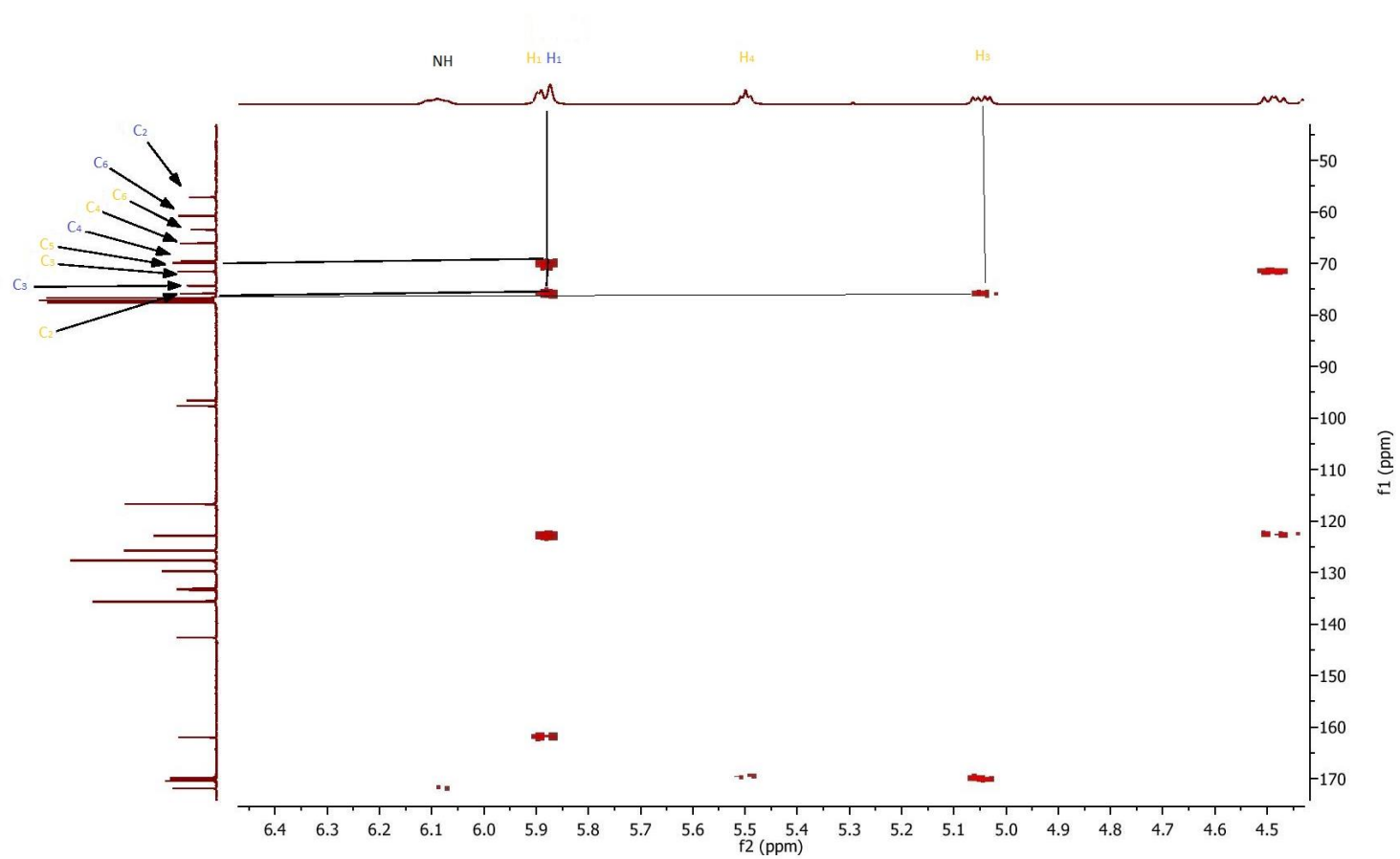
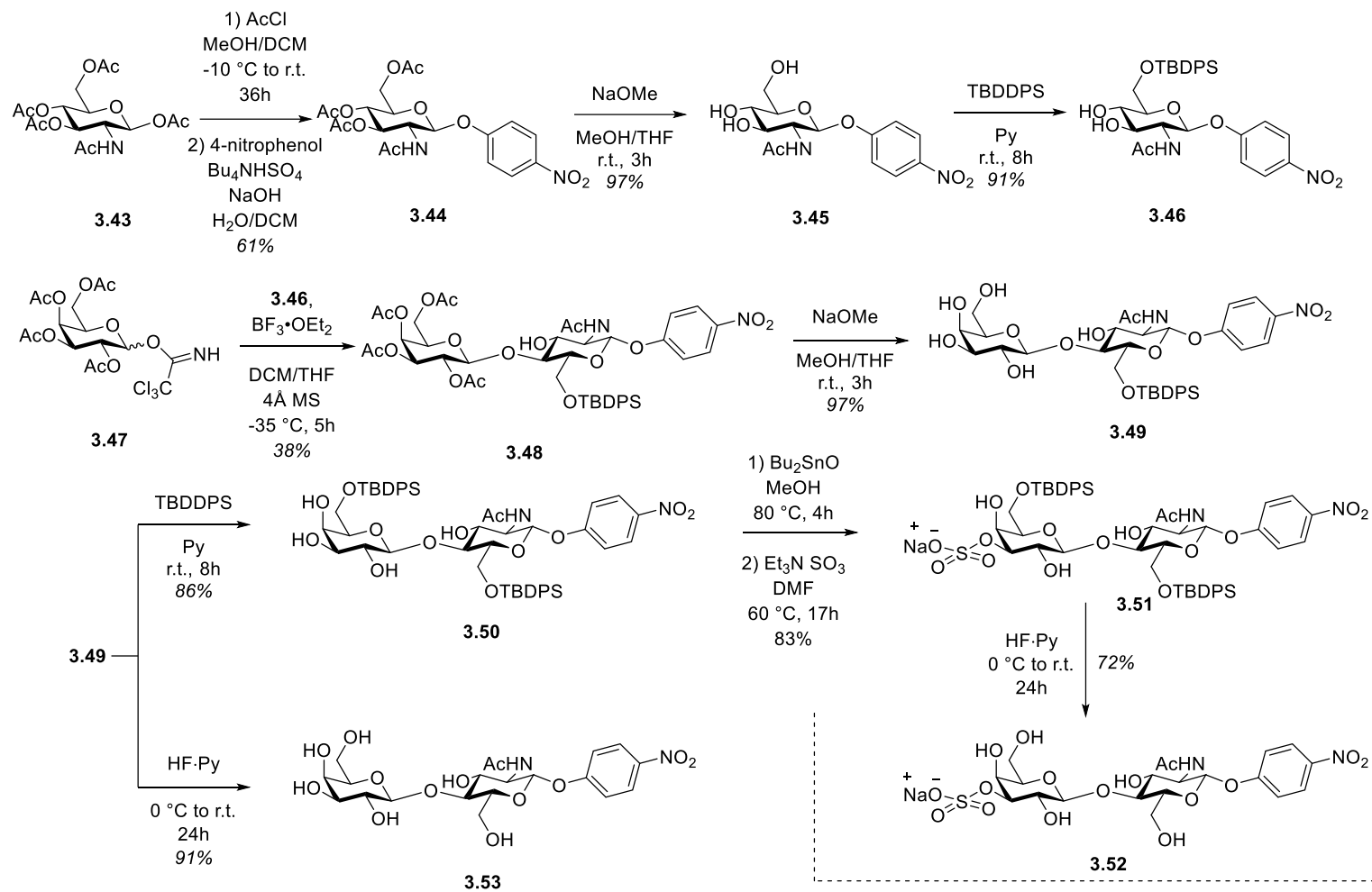


Figure 3.17 HMBC spectrum of compound **3.48**, correlation between *H*1 (in yellow) and *C*4 (in blue).



Scheme 3.8 Preparation of *para*-nitrophenyl-based LacNAc derivatives.

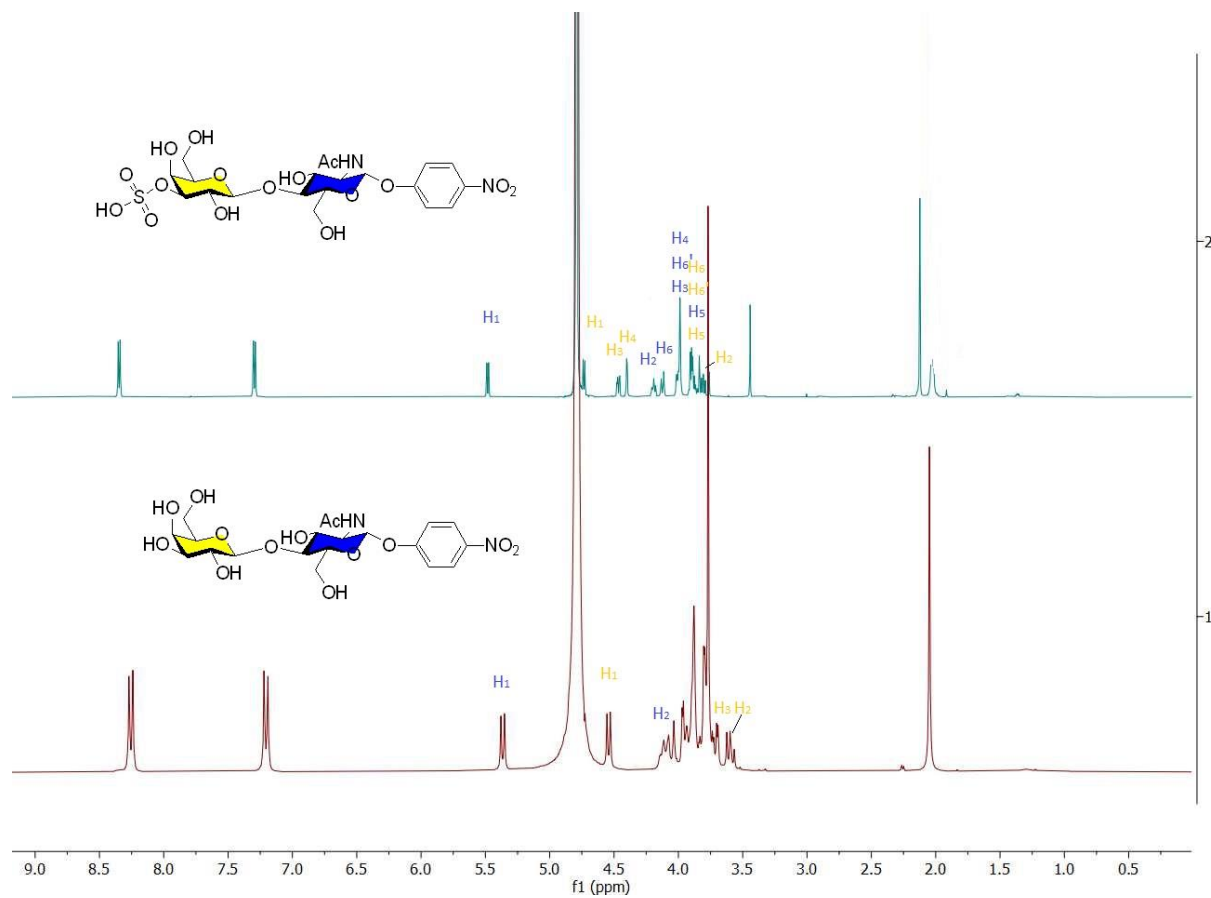
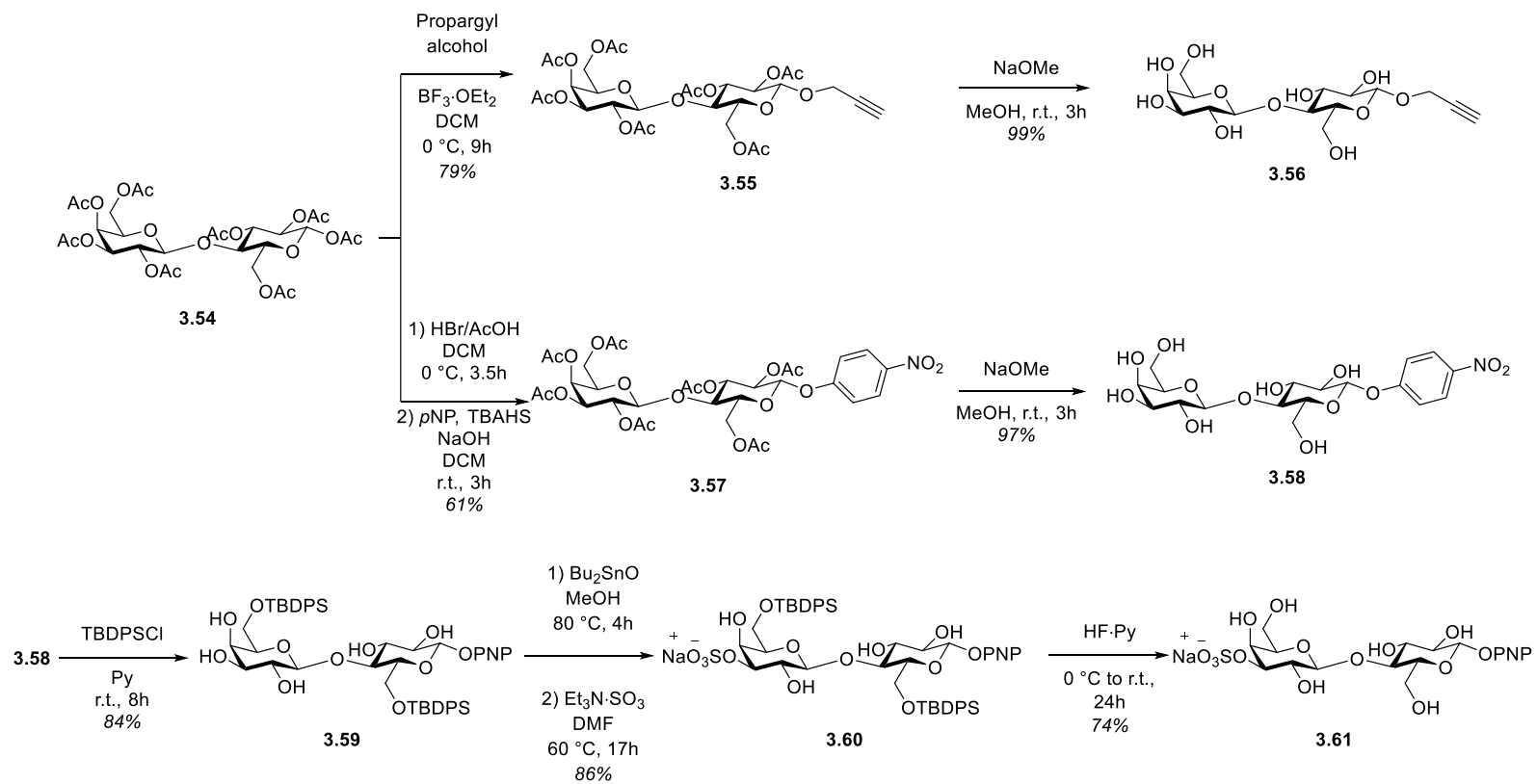


Figure 3.18 Comparison of ¹H NMR (600 MHz, D₂O) spectra of compounds **3.52** and **3.53** with the appearance of deshielded *H*-3, *H*-4 (in yellow) of galactoside moiety after sulfation.



Scheme 3.9 Preparation of propargyl and *para*-nitrophenyl-based lactosides.

Synthesis of β -propargyl lactoside **3.56** began with $\text{BF}_3 \cdot \text{OEt}_2$ promoted glycosylation of **3.54** with propargyl alcohol in DCM, followed by Zemplén deacetylation.²⁵⁷ The structures of **3.54** and **3.56** were confirmed with NMR and HRMS techniques. The final synthetic challenge was the stereoselective glycosylation and sulfation of β -*para*-nitrophenyl lactosides in an efficient manner. PTC condition using tetrabutylammonium hydrogensulfate (TBAHS) and *para*-nitrophenol have been previously found to be effective to get only β -anomer from α -glycosyl halides. Thus, slightly modifying of the known protocol,²¹⁰ we synthesized **3.57** in good yield. Unfortunately, due to the overlap of two protons between 5.19 and 5.17 ppm stereochemistry of the β -anomer *via* ^1H NMR could not be determined. Deacetylation of **3.57** under Zemplén transesterification condition gave **3.58** in 97 % yield. The structure of **3.58** was fully confirmed by ^1H NMR which showed a doublet with $J = 7.8$ Hz at 5.32 ppm corresponding to $H-1$ of β -anomer. To this end, repeating linear synthesis strategy, preparation of *para*-nitrophenyl-based 3'-*O*-sulfo-lactoside **3.61** as well as its LacNAc homologue **3.38** was successfully achieved by following general synthetic methods (Scheme 3.8 and 3.9). The presence of sulfo group at $C3'$ position was confirmed on the basis of the $H-3'$ and $H-4'$ downfield shift (Figure 3.19).

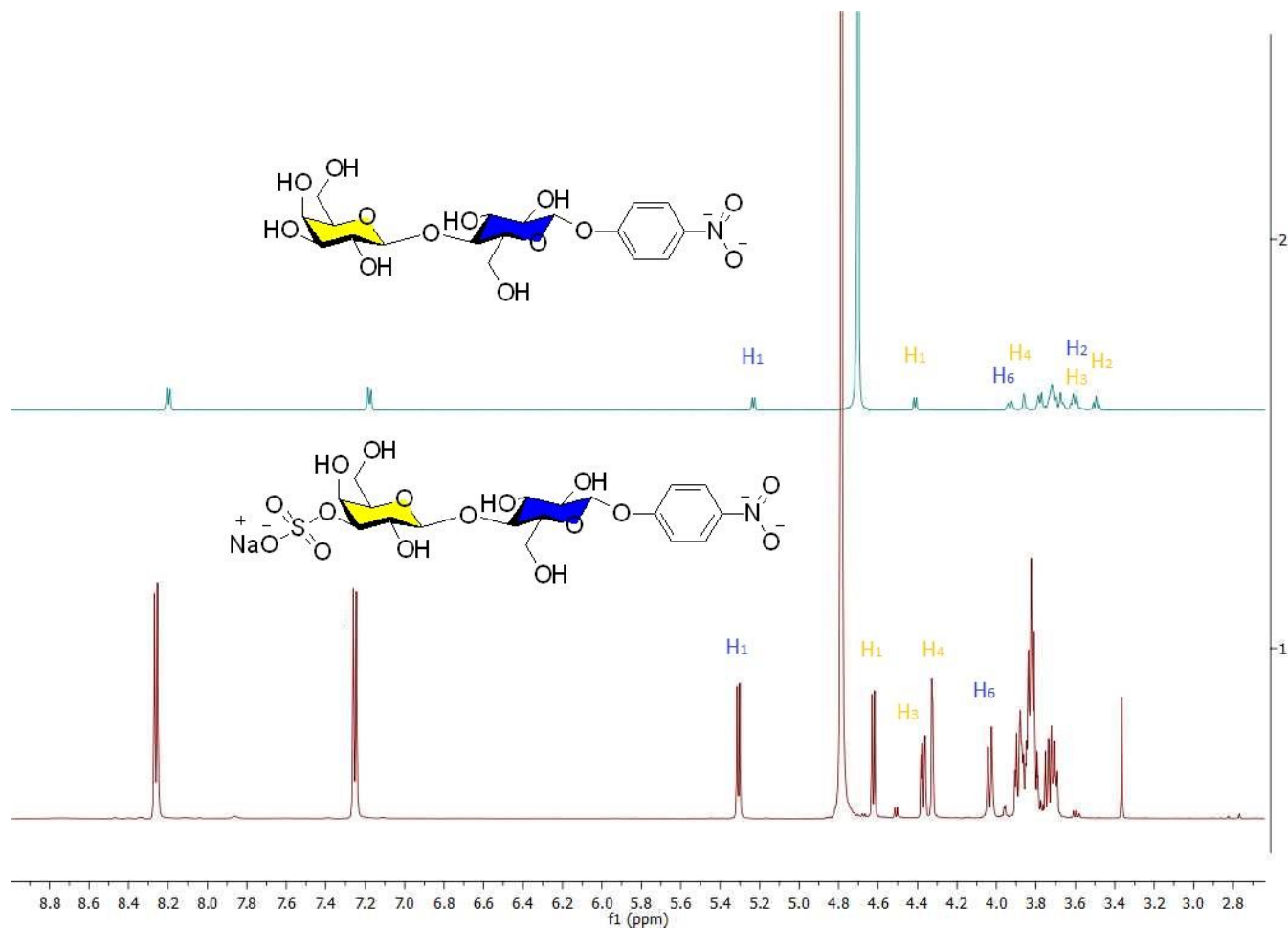


Figure 3.19 Comparison of ¹H NMR (300 MHz, D₂O) spectra of compounds **3.58** and **3.61** with the appearance of deshielded *H*-3, *H*-4 (in yellow) of galactoside moiety after sulfation.

3.4 Conclusion

Small library of β -*para*-nitrophenyl and β -propargyl-based Lactoside and LacNAc together with their 3'-*O*-derivatives was successfully prepared. Besides employing novel strategy for regioselective functionalization at 3'-*O*-position and avoiding potential formation of side products, desired final products were purified by only using classical column chromatography. Especially, efficient convergent synthesis of SiaLacNAc **3.42** has been achieved in a highly stereoselective manner. Additionally, based on previous studies,^{208, 224, 258, 259} relying on adaptation ability of binding site at CRDs, an extension brought at 3'-*O* and 1-*O* positions of lactosides would play affinity and selectivity-enhancing role further in the design of improved ligand. Using analogous derivatization synthesized β -vaniline-based lactose derivatives,²³³ together with our compounds are currently under biological investigation *via* Hemagglutination Inhibition (HI) assay toward Gal-4C, Gal-8N in collaboration with Prof. G. A. Rabinovich group (National University of Cordoba, Buenos-Aires, Argentina). Biological data will be published in peer-reviewed journal.

CHAPTER IV

DESIGN AND SYNTHESIS OF GLYCODENDRIMERSOMES TOWARDS CANCER RELATED GALECTINS

Synthetic multivalent glycoconjugates (neoglycoconjugates) built on wide variety of scaffolds have been designed and synthesized to compete natural ligands of galectins. Several parameters including architecture of multivalent display, spatial arrangement of sugar head groups, topology and valency have been found to play crucial roles in enhancement of avidity. Although some neoglycoconjugates have shown good binding properties, they suffer some limitations including construction on toxic scaffolds (*in-vivo* toxicity caused by certain artificial scaffolds, e.g. quantum dots, unmodified carbon nanotubes), multistep synthesis, lack of *in-vivo* mimicry of mobile cell surface *etc.* Taking into account these drawbacks, research groups are focused on more bioinspired programmable glyconanoparticles. In this chapter, for the sake of clarity we will review hitherto reported multivalent neoglycoconjugates as inhibitors of Galectins. Subsequently, our approach of designing and synthesizing programmable multivalent ligands as potential cancer-related Galectin inhibitors.

4.1 Bivalent ligands

In the past two decades, several research groups have been primarily focused on structure-activity relationship between a single CRD of galectins and galactoside-containing ligands in order to design highly potent and selective inhibitors. Alternative approach has been considered to mimic multivalency of naturally occurring galectins while creating and designing new potent ligands of therapeutic potential. It was therefore anticipated that well-defined multimeric ligands could be beneficial to better understand spatial arrangement of CRDs of galectins with dimerization and oligomerization tendencies. Toward this goal, targeting proto-type galectins with homodimerized CRDs, synthesis and bioevaluation of bivalent ligands as glycomimetic strategies have been reported by various research groups. Moreover, having nearly similar amino acid sequence at CRD of galectins, designed synthetic ligands could be potent inhibitors for several members of the family at the same time. Here we review reported to date, bivalent synthetic ligands built on wide variety of scaffolds with different spatial arrangement (Figure 4.1). To explore interactions between galectins and synthetic ligands in 2001 Gabius and co-workers designed and synthesized wedge-like glycodendrimers.²⁶⁰ Constructed on benzoic acid derivative and bearing lactoside moieties at the focal points of di-, tetra- and octavalent dendrons were tested at solid-phase inhibition assay toward proto-type homodimeric Gal-1, Gal-7, and chimera-type Gal-3. Remarkably, increasing sugar valency around Galectins have drastically augmented relative potency versus free lactose, thus, bivalent ligand **4.001** shown 750, 20 and 1.6 relative potency towards Gal-1, -3 and -7 respectively.²⁶⁰ Switching from more flexible thiourea to aminothiazole **4.002** *via* treating isothiocyanato-lactoside with corresponding propargylic amine, resulted enhancement in relative potency towards Gal-1, -3 and -5 and demonstrated selectivity for Gal-3.²⁰⁹

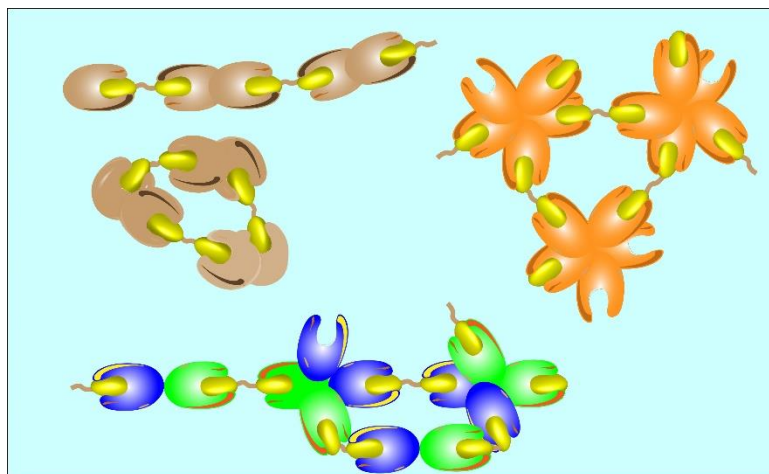
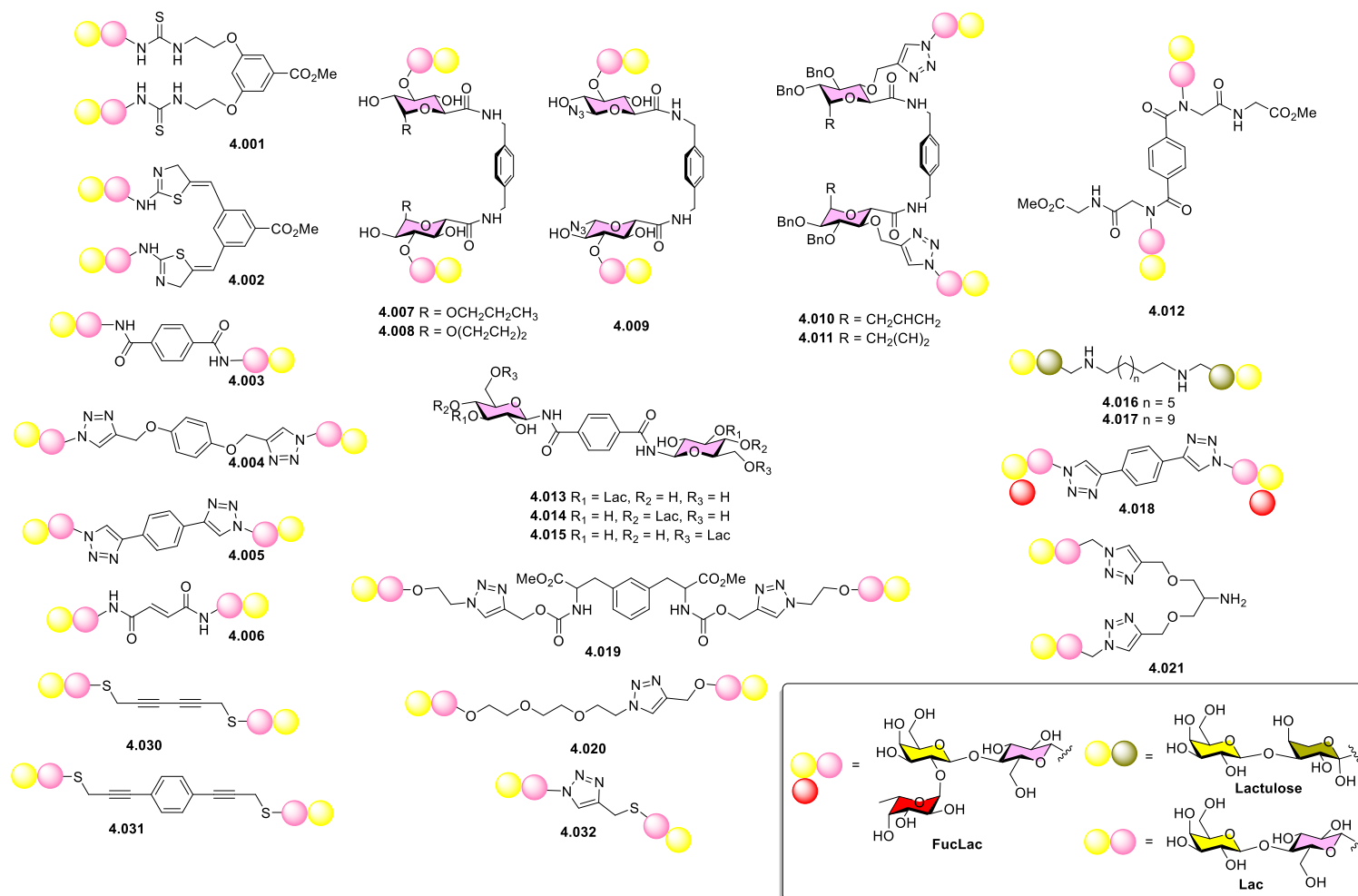


Figure 4.1 Schematic representation of receptor binding mechanism of bivalent glycocluster and galectins and formation of lectin-carbohydrate lattice.

Appealingly, extending library of flexible and rigid bivalent lactosides with various length of spacers helped to elucidate the distance between sugar headgroups and geometrical aspects of ligands more precisely. To meet this objective, flexible and rigid bivalent ligands based on various scaffolds including secondary (**4.003**), tertiary (**4.012**) and *N,N*-diglycosylterephthalamides (**4.013-4.015**), *p*-bispropargyloxybenzene (**4.004**), *p*-bisacetylenebenzene (**4.005**, **4.018**), fumaramide (**4.006**), glycocyclophane (**4.008**, **4.011**) and its acyclic derivatives (**4.007-4.010**), *m*-benzenedialanine (**4.019**), calixarene²⁶¹ have been synthesized.²⁶²⁻²⁶⁶ Interestingly, CuAAC click coupling of azide functionalized-PEGylated lactoside and propargyl lactose, afforded triazole-linked unsymmetric bivalent ligand which was observed to exhibit submicromolar affinity toward human Gal-3 ($K_{D1} = 0.15 \mu\text{M}$ / $K_{D2} = 19 \mu\text{M}$) whereas free lactose has $K_D = 92.6 \mu\text{M}$.²⁶⁷ Remarkably, synthesized H-trisaccharide (histo-blood group)-harbored rigid bivalent ligand **4.018** where fucosyl moiety bound to *O2'* position of galactoside has been found selective toward Gal-4 with $IC_{50} = 8 \mu\text{M}$ versus free lactose ($IC_{50} = 1600 \mu\text{M}$).²⁶⁶ Not only bivalent *N*- and *O*-lactosides demonstrated good affinity for certain galectins, but lactulose-bearing bivalent

ligands (**4.016-4.017**)²⁶⁸ and enzymatically more stable C-²⁶⁹ and S-lactosides (**4.021, 4.030-4.032**)²⁰⁴ and S- and Se-galactosides (**4.022-4.029**)^{217, 270-275} were seen to be promising. Among them thiodigalactosides (TDGs) are particularly interesting, thus *via* taking advantage of extra room at shallow binding pocket of CRD, C3-derivatives of galactosides have successfully inhibited Gal-1 and -3 by creating additional interactions that associated with an increase in the overall avidity.



Scheme 4.1 Reported bivalent ligands.^{204, 209, 217, 260-276}

4.2 Trivalent ligands

Increasing valency permits designing architecturally and geometrically more complex ligands that shed new light on multivalent sugar-receptor interactions. As we discussed that CRD of galectin family members tends to dimerize or oligomerize, synthesizing dimeric, tetrameric, and multimeric ligands seem more rational.

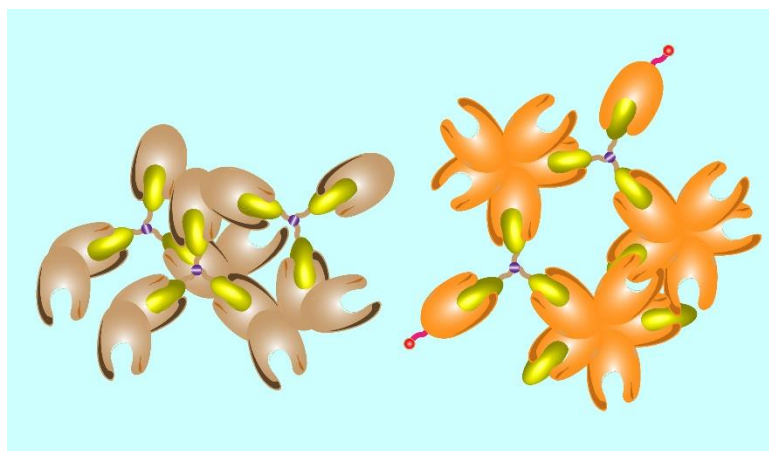
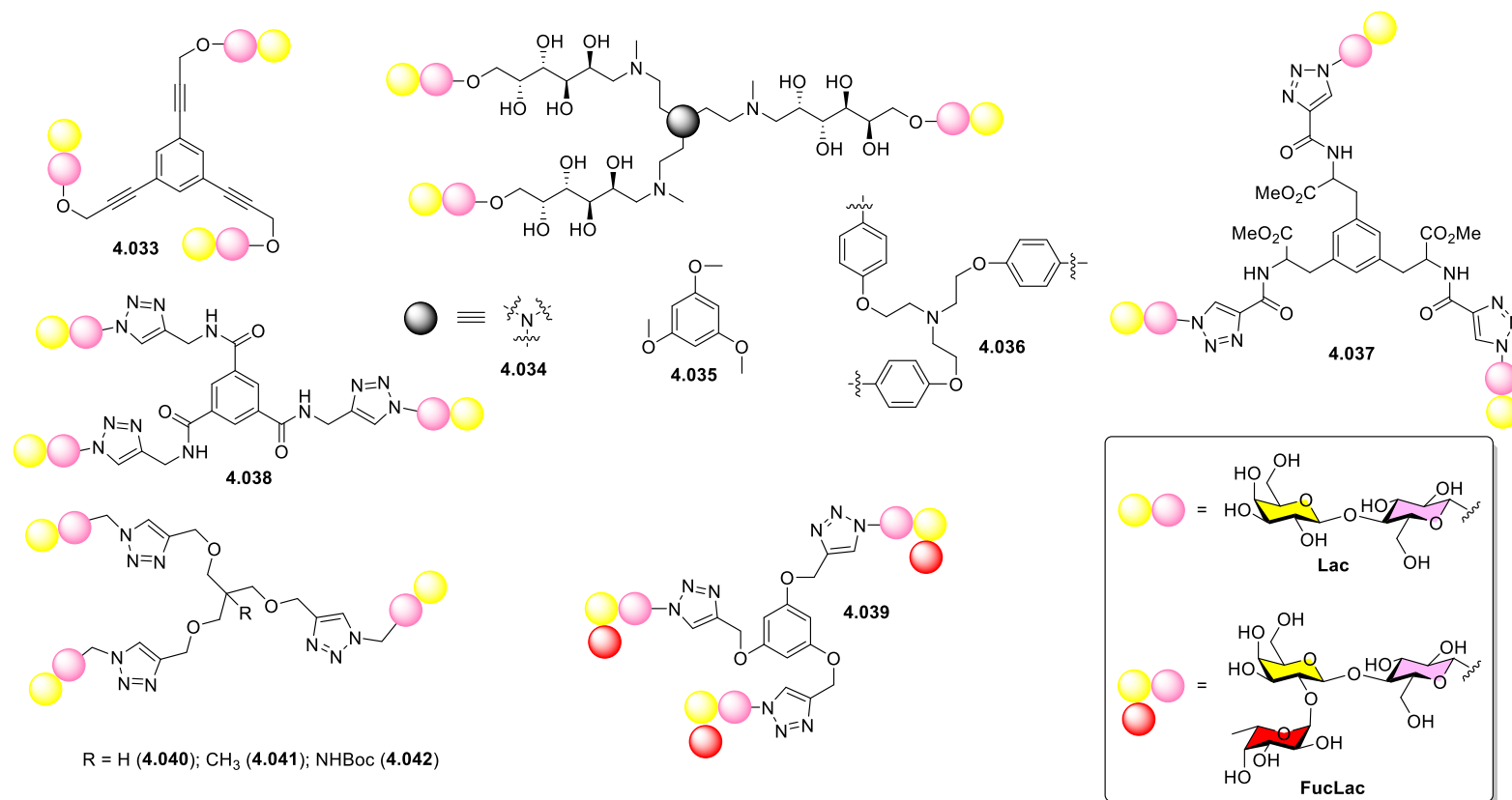


Figure 4.2 Schematic representation of receptor binding mechanism of trivalent glycocluster and galectins, and formation of lectin-carbohydrate lattice.

Due to the fact that galectins are generally soluble lectins, in normal cell membrane they are not highly ordered. The reason of designing less common trivalent ligands is to cluster galectin through cross-linked lattice (Figure 4.2). For the purpose, Roy *et al.*²⁷⁷ in 2003 designed and synthesized, trivalent glycocluster (Scheme 4.2. **4.033**) which was constructed on benzene *via* Sonogashira coupling between propargyl lactoside and triiodobenzene. Surprisingly, among bi- and tetravalent glycoclusters, trivalent ligand demonstrated its superiority toward Gal-3 with 7.6-fold increase in relative potency. After this event, a few examples of trivalent glycoclusters have been synthesized with various rigid and flexible frameworks including trialkylamine^{265, 278},

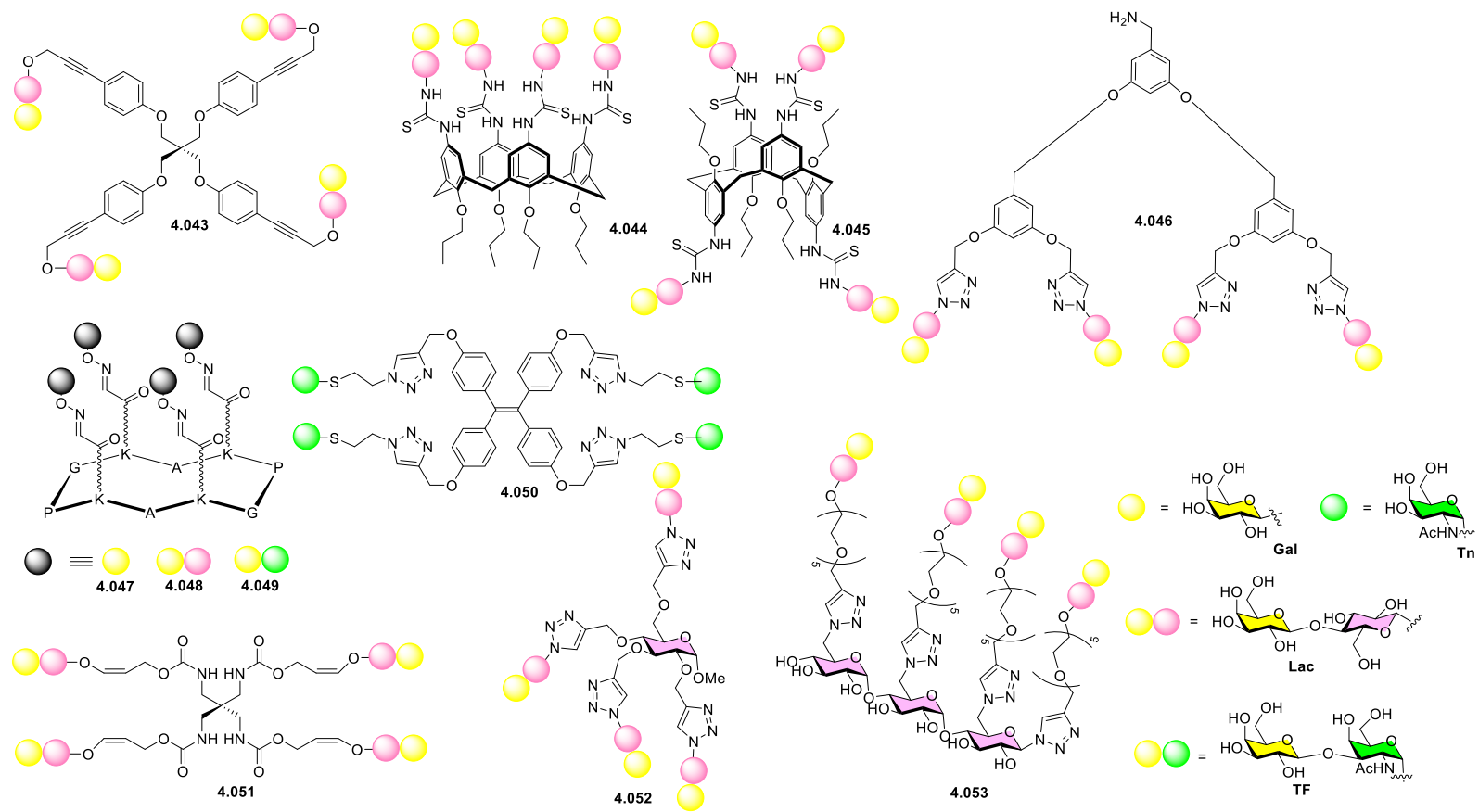
²⁷⁹ (4.034, 4.036), benzenetriols^{265, 278} (4.035, 4.039), benzotriamine²⁶³ (4.037), tricarboxyamido²⁰³ (4.038) and tris(hydroxymethyl)²⁶⁹ derivatives (4.040-4.042).



Scheme 4.2 Reported trivalent ligands.^{207, 263, 265, 269, 278-280}

4.3 Tetravalent Ligands

Systematically advancing in the context, tetravalent glycoclusters with various topology have been exhibited to impact substantially the binding properties of galectins. In aforementioned paper, homologue of **4.001**, wedge-like dendrimer with tetravalent lactoside ligand in comparison with free lactose have reached maximum value of 1667 relative potency for Gal-1.²⁶⁰ This result encouraged glycochemists to synthesize more tetravalent glycoclusters (Scheme 4.3). Tetravalent glycocluster based on pentaerythritol²⁷⁷ (**4.043**), rigid cyclic core of calix[4]arenes²⁶¹ (**4.044-4.045**), 3,5-dihydroxybenzylamine²⁶⁵ (**4.046**), rigid decapeptide²⁸¹ (**4.047-4.049**), fluorescent TPE²⁷⁶ (tetraphenylethylene, **4.050**) pentaerythrityltetraamine²⁷⁹ (**4.051**) and methyl 2,3,4,6-tetrapropargyl- α -D-glucoside²⁶⁹ (**4.052**) and trisaccharide²⁸² (**4.053**) have been hitherto reported. Among them cyclic decapeptide and TPE based tetravalent ligands, bearing not lactoside but disaccharide of TF (Thomsen-Friedenreich) and monosaccharide of T_n antigens have also showed some activity toward certain galectins. Generally speaking, synthesized all bi-to tetravalent ligands have shown better affinity than single lactoside and galactoside as their monovalent references in activity assays.



Scheme 4.3 Reported tetraivalent ligands.^{261, 265, 269, 276, 279-282}

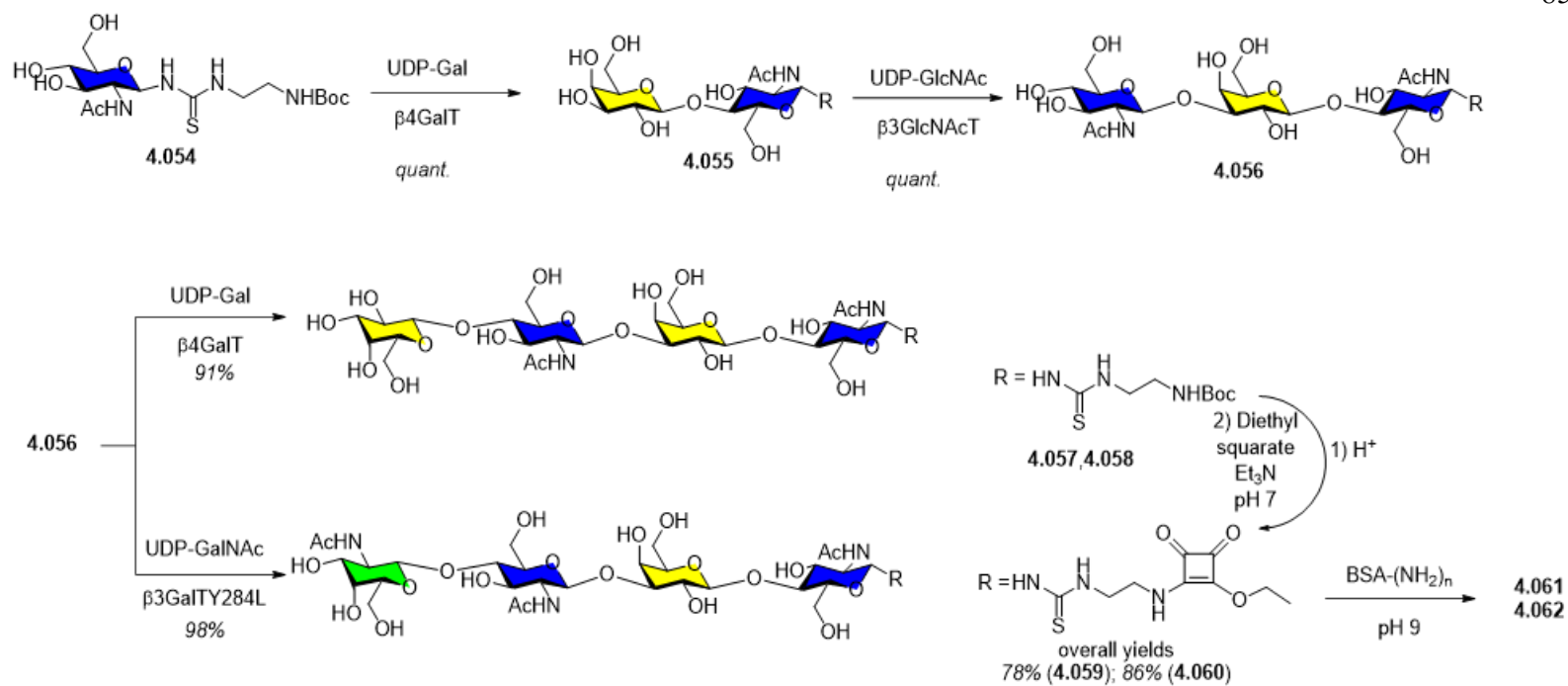
4.4 Multivalent ligands

The aim of augmentation of valencies of carbohydrate ligands gives rise exponentially to new glycoconjugates with various topologies which could be built on a wide variety of scaffolds. Low-valent neoglycoconjugates are appealing synthetic targets that have already been found to possess greater binding properties versus monovalent ligands nonetheless, there is a need of spatial and conformational optimization. Alternatively, multivalent ligands are mostly considered more potent inhibitors due to higher energetic glycoside cluster effect *via* inducing aggregation of protein receptors over randomly distributed heterogenic platform. Therefore, multivalent ligands are characterized to possess multiple copies of receptor-binding elements which results in high avidity while binding to a receptor. To date, constructed on various backbones multivalent neoglycoconjugates including glycoproteins, glycopeptides, glyco-gold nanoparticles, glycopolymers and glycodendrimers have been extensively reported. For the sake of clarity, we show the chemistry of an example of different class of reported multivalent glycoconjugates with enhanced affinity toward galectins.

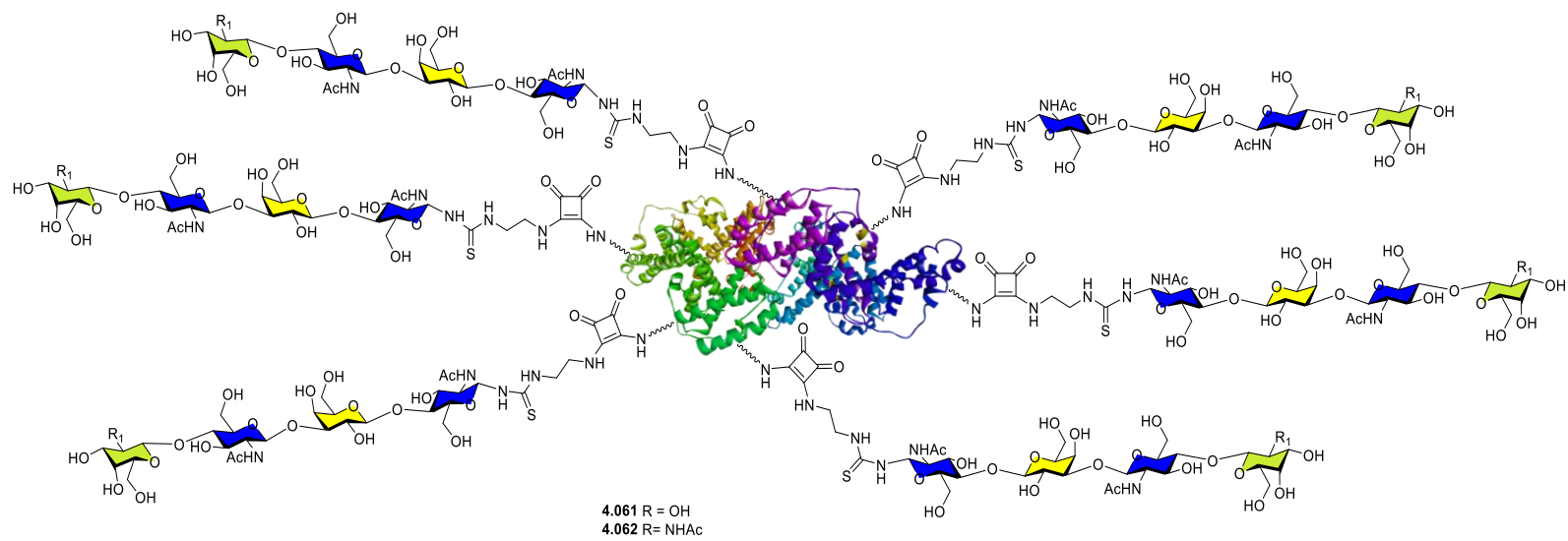
4.4.1 Neoglycoproteins

Starting with neo-glycoproteins, most popular proteins as carriers have been considered Serum Albumins (SAs) by virtue of their properties of being biodegradable and biocompatible and relatively easy for preparation over wide range of particle sizes. Bovine Serum Albumin (BSA) and Human Serum Albumin (HSA) are frequently employed carriers, which are reported to be low in toxicity.²⁸³⁻²⁸⁵ Additionally, these non-glycosylated proteins possess multiple lysine residues which can be functionalized for tunable multivalency. Among notable works, reported by Elling and co-workers, enzymatically synthesized tetrasaccharides which were composed of two types of lactoside motifs (LacdiNAc– LacNAc and LacNAc –

LacNAc) and conjugated to BSA through squarate spacer **4.061-4.062** discriminated Gal-3 (IC_{50} below 100 nM) over Gal-1 (Scheme 4.4).²⁸⁶ In another publication of same group, it has been revealed that cancer-related truncated Gal-3 selectively binds to LacNAc – LacNAc motif over LacdiNAc – LacNAc.²⁸⁷ As we previously mentioned that thiodigalactosides have been reported being most potent inhibitors for homo-dimeric Gal-1 (TDG, $K_D = 24\mu M$) and chimera-type Gal-3 (TDG, $K_D = 49\mu M$), especially after C3-functionnalization affinity in low nanomolar range have been achieved. Recently published by Pieters *et al.* BSA-conjugated thiodigalactoside have shown impressive high affinity toward Gal-3 with $IC_{50} = 1.8$ nM versus free thiodigalactoside with $IC_{50} = 9030$ nm at ELISA assay.²⁸⁸ Today neo-glycoproteins remain one of the strong and promising candidates for the development of galectin inhibitors.



Scheme 4.4 Enzymatic synthesis of tetrasaccharides and their conjugation to BSA.²⁸⁶



Scheme 4.5 Structure of tetrasaccharide-BSA conjugation.²⁸⁶

4.4.2 Neoglycopeptides

Alternative to neo-glycoproteins are glycopeptides, thus among polypeptides Q11 has been one of noteworthy synthetic peptide to cite. Q11 (QQKFQFQFEQQ) is a *de-novo* peptide composed of 11 amino acids that self-assembles into β -sheet nanofiber in aqueous media.²⁸⁹ In 2015, Hudalla *et al.* have successfully conjugated Asparagine-linked GlcNAc to Q11 through SGSG (Serine-Glycine-Serine-Glycine) linker. Obtained glycopeptide efficiently converted to LacNAc-Q11 *via* enzymatic glycosylation using β - (1 \rightarrow 4)-galactosyltransferase and UDP-galactose (Scheme 4.6). Interestingly LacNAc-Q11 has inhibited Gal-1-mediated apoptosis of Jurkat T-cells while exhibiting fruitless impact on Gal-3 activity.²⁹⁰

4.4.3 Glyco-gold nanoparticles

Among inorganic scaffolds bearing carbohydrates, gold nanoparticles (AuNPs) have been evaluated as useful medical nanovectors, transducers and nanosensors. Thus, with their properties of being relatively inert in biological environment, lower toxicity, and lower rate of clearance from circulation AuNPs have found their applications in biomedical sciences (Figure 4.3).²⁹¹

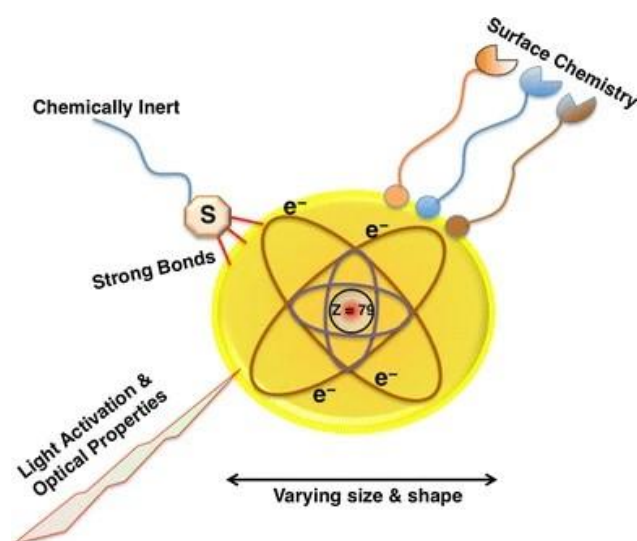
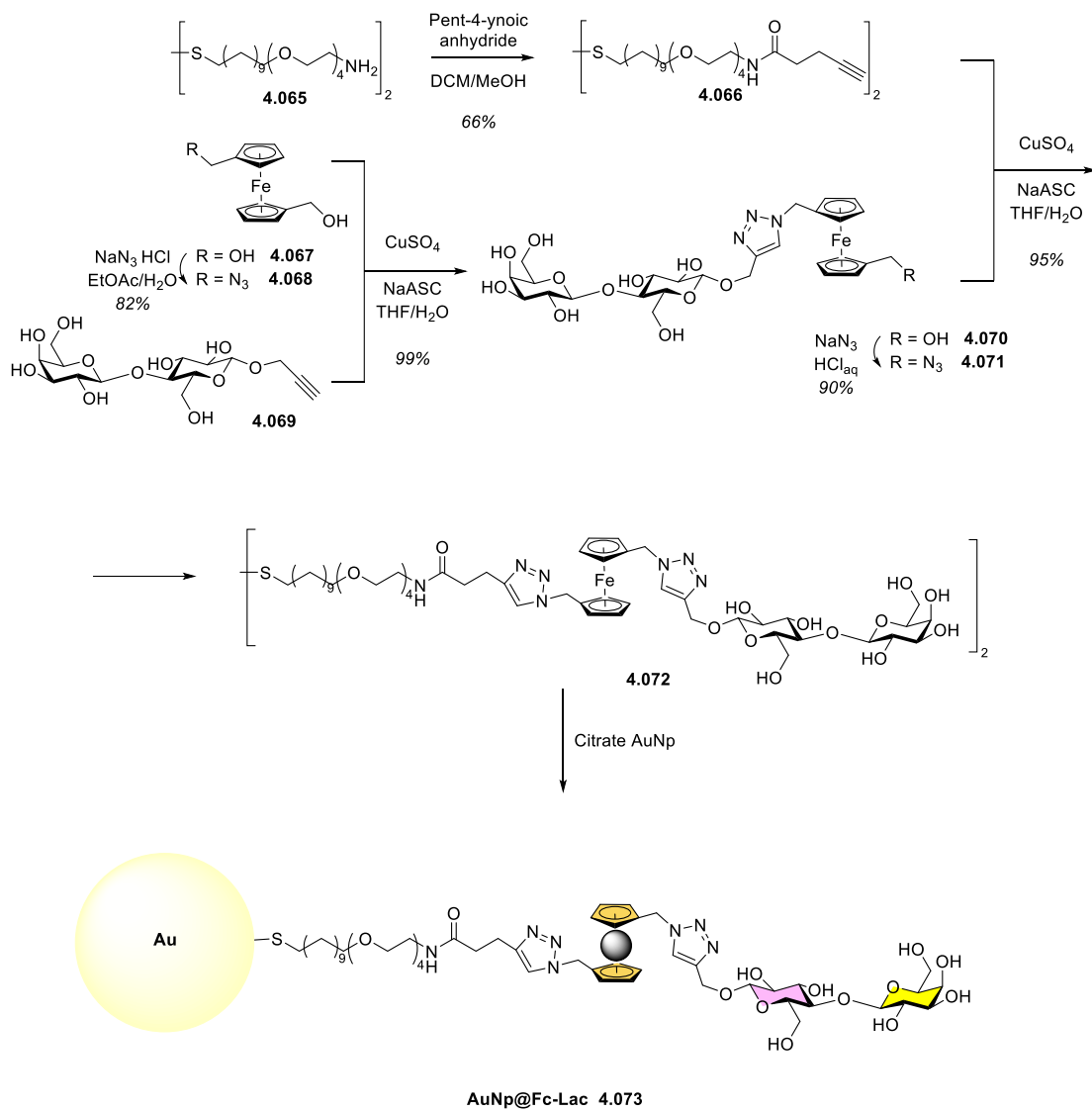


Figure 4.3 Application of AuNPs in biomedical science.²⁹¹

Besides having shape and size controlling capacity, AuNPs can be easily prepared through strong thiol-gold interaction.^{292, 293} Another advantage of AuNPs is that, while employing as a biosensor agent, they give access to detect biological entities at low concentrations.²⁹⁴ Furthermore, AuNPs have been broadly employed as carriers of glyco-epitopes in glycobiology *via* forming self-assembling monolayer (SAM) at the surface of nanoparticles by virtue of thiolated carbohydrates.^{90, 295} As detection and identification of galectins are crucial events during cancer diagnosis, prognosis and disease progression, there is need of highly sensitive detection methods. Toward this goal, successful application of Glyco-AuNPs in development of Galectin sensing

techniques have been hitherto realized. For example, Niwa and co-workers have achieved to detect nanomolar level (1 nM) of Gal-4 and Gal-8 over lactoside-bearing AuNPs by using Surface Plasmon Resonance (SPR) measurements.²⁹⁶ Experiments^{297, 298} show that when iron doped into AuNPs, plasmon absorption augment its capacity by virtue of increased optical and redox sensing ability. Toward this goal recently reported by Vargas-Berenguel *et al.* multivalent lactose-ferrocene-conjugated gold nanoparticles (AuNP@Fc-Lac) have exhibited excellent sensitivity to Gal-3, thus nanomolar concentration of glycoprotein have been detected (Scheme 4.7).²⁹⁹



Scheme 4.7 Ferrocene-containing gold-glyconanoparticles.²⁹⁹

4.4.4 Glycopolymers

An alternative class to Glyco-AuNPs are glycopolymers,³⁰⁰⁻³⁰² thus, this type of macromolecules possesses larger valency than any other glycoconjugates and demonstrates largest amplification effects in molecular recognition. They also effectively mimic multimeric display of oligosaccharides and serve as useful tool for probing carbohydrate-receptor interactions. During last decade, constructed on various building blocks glycopolymers with pendant carbohydrates (Figure 4.4) have been applied probing cancer-related Galectins.³⁰³⁻³⁰⁵ Especially, recent advances in living radical polymerization provide excellent opportunities to control bulk properties of targeted proteins with narrow polydispersity index. Among them Polyacrylic acid (PAA)- and *N*-(2-hydroxypropyl)methacrylamide(HMPA)-based glycopolymers are attractive due to their water solubility, less toxic or non-toxic and non-immunogenic properties.

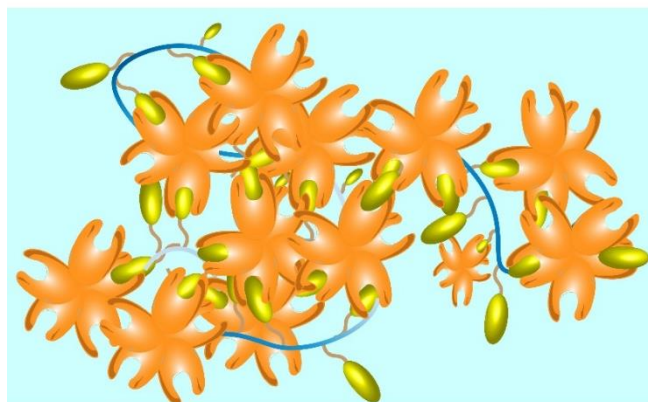
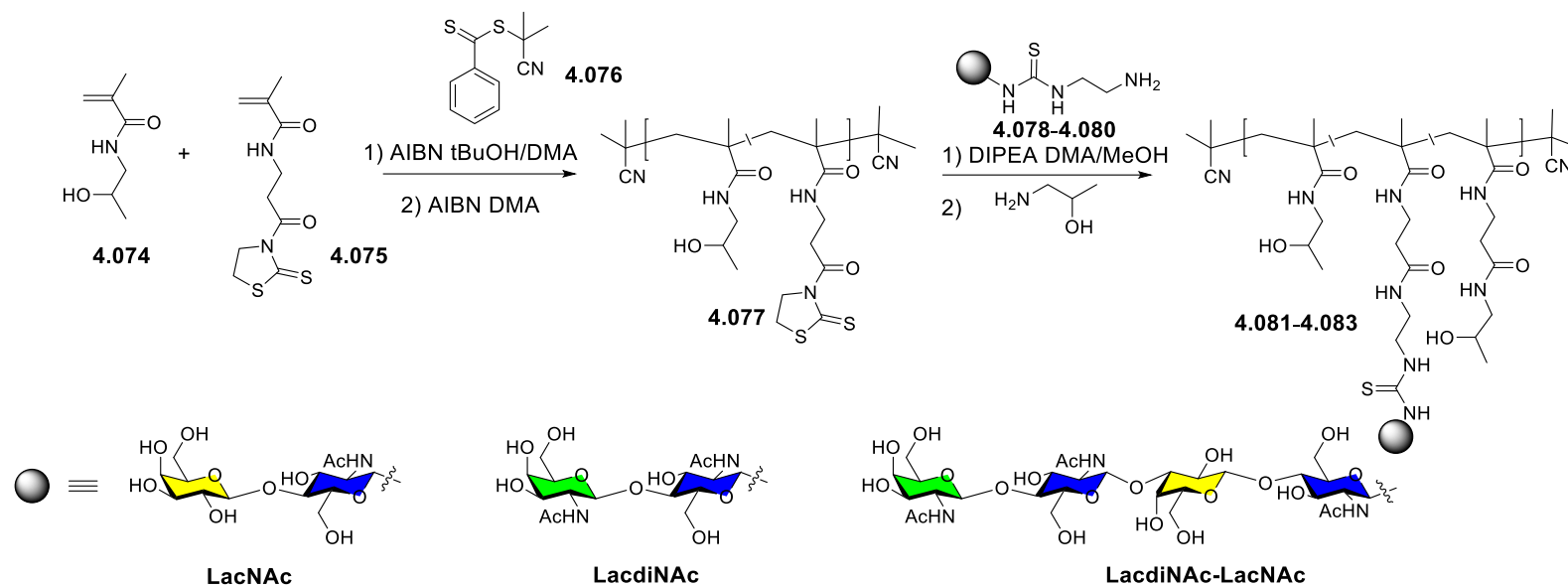


Figure 4.4 Schematic representation of pentameric Gal-3 receptor binding mechanism of glycopolymers.

Additionally, from a chemist point of view, they are facile to prepare and functionalize in post-polymerization phase. In recently reported work by Filipová and co-workers, toward Gal-3, HMPA-based polymers bearing disaccharides **4.079**, **4.080**

(LacNAc, LacdiNAc) and tetrasaccharide **4.080** (LacdiNAc-LacNAc) have shown 304-fold enhancement (IC_{50} in nanomolar range) in relative potency versus monomer (Scheme 4.8).³⁰⁴ In another publication, Chytil *et al.* have shown that while increasing epitope (LacNAc) density on HMPA-based polymer avidity increases for both Gal-1 and Gal-3 but dense glycoconjugate discriminates Gal-1 over Gal-3.³⁰⁶



Scheme 4.8 Synthesis of HMPA-based glycopolymers.³⁰⁴

4.4.5 Glycodendrimers

In general, what makes dendrimers appealing over linear polymers is that dendrimers are nearly monodisperse globular macromolecules, where molecular size, shape and branching multiplicity are controllable.

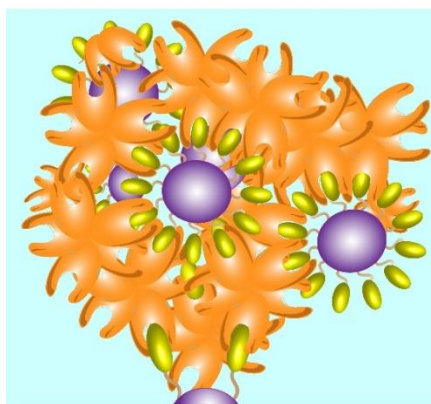
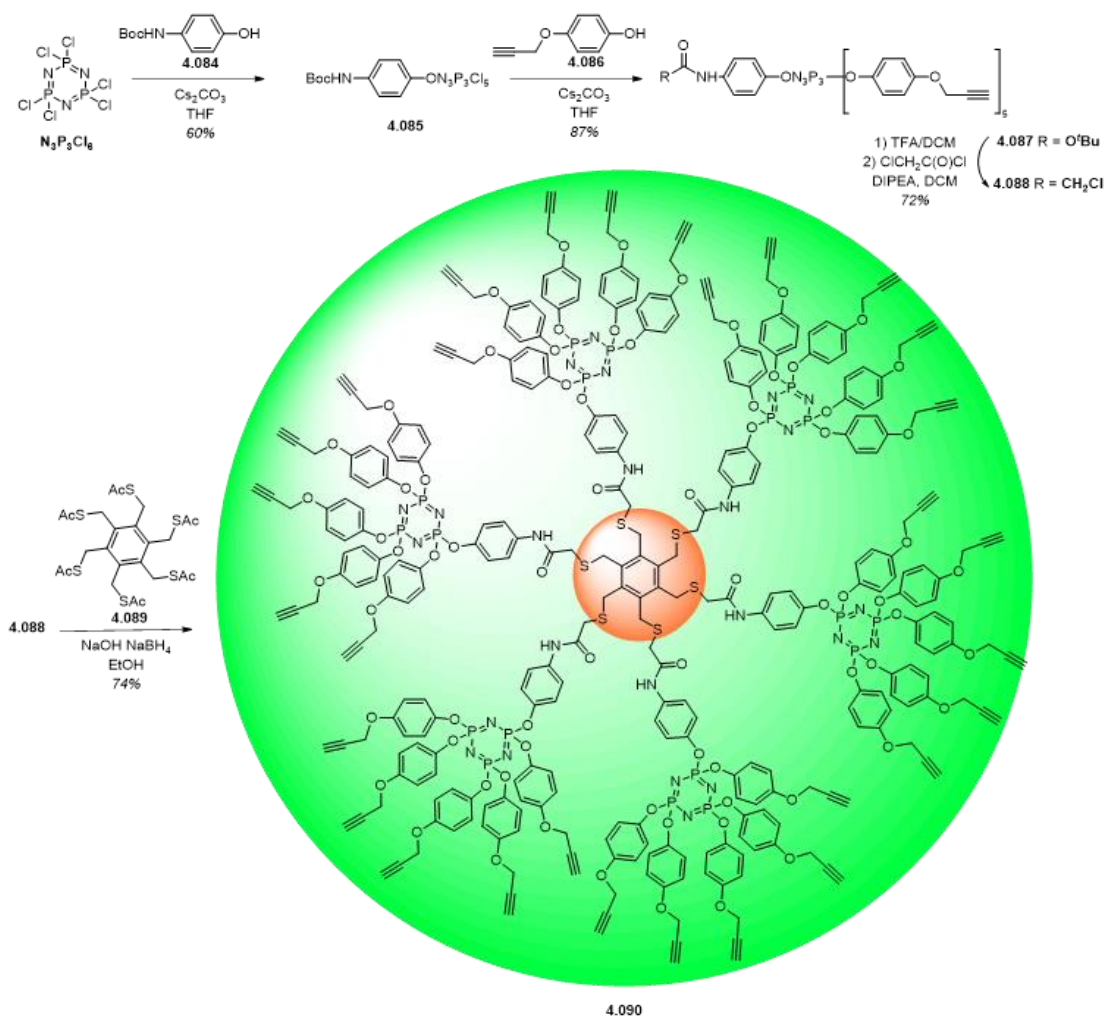


Figure 4.5 Schematic representation of pentameric Gal-3 receptor binding mechanism of glycodendrimers.

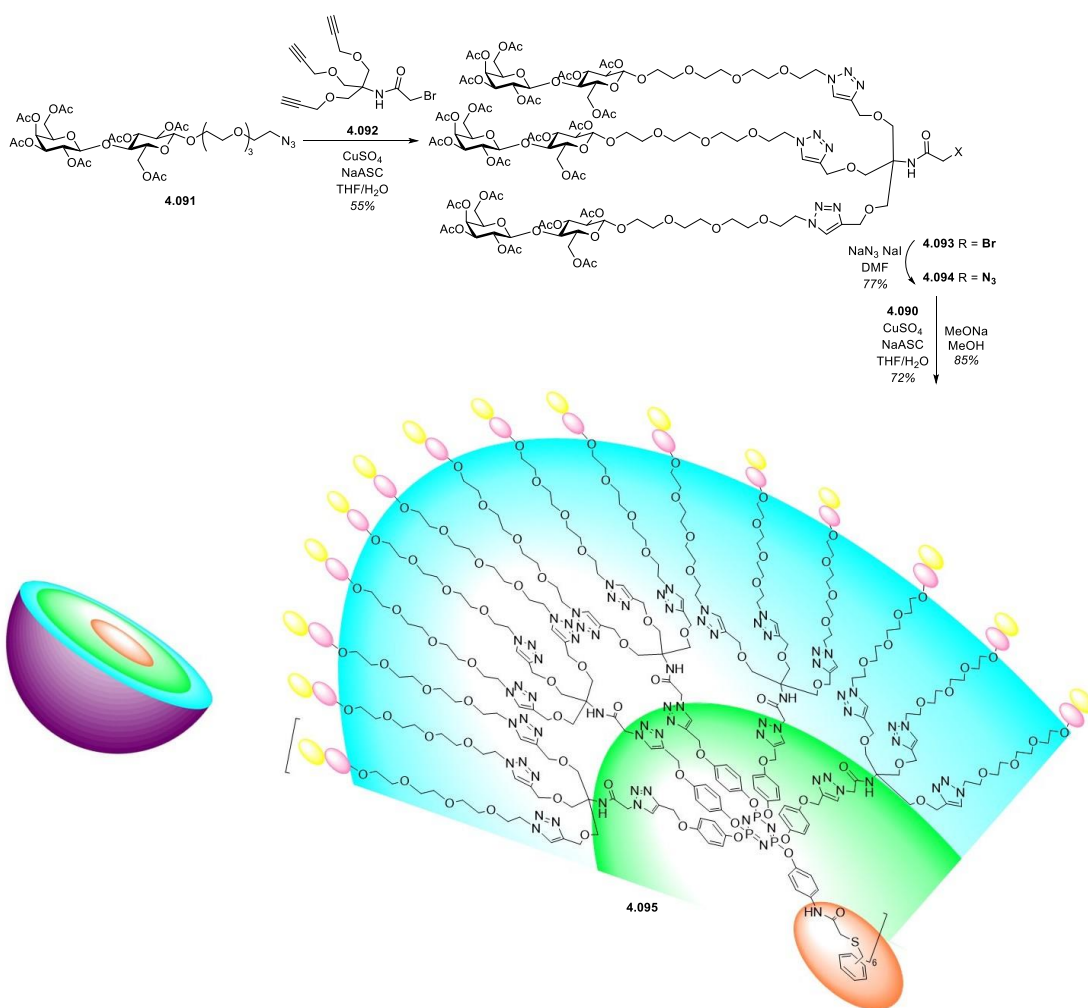
As reviewed previously, in the early 2000s Gabius *et al.*²⁶⁰ have published wedge-like dendrimer demonstrating better affinity than single monomer toward Gal-1. To this goal, several research groups have henceforth reported various dendrimers built on a wide variety of scaffolds including cyclotriphosphazene (CTP), poly(amidoamine) (PAMAM), hexaphenylbenzene, decapeptide, glucopyranoside *etc.* Among them most well-known PAMAM-based dendrimers with unique tunable physicochemical properties are interesting. Additionally, having functionalizable surface primary amine groups give access to growth easily the size of macromolecule by means of increased generation number. Cloninger *et al.*⁸⁰ have shown that PAMAM-based G(2)-dendrimer bearing lactose (15 Lac) inhibits Gal-3-induced aggregation *via* binding to the active site of Gal-3, instead G(6) dendrimer with 100 lactose units cause aggregation of cancer cells by means of Gal-3 pathway. In another published

work of same author, double functionalized PAMAM-based hybrid dendrimers bearing two different saccharides (Lac and Gal; GalNAc and Gal) exhibit IC_{50} in micromolar range for Gal-3 whereas 100-mer lactodendrimer has $IC_{50} = 1.74$ nM toward Gal-1.³⁰⁷ Alternatively, reported by Roy *et al.*⁸¹ lactose-bearing dendrimers, synthesized *via* novel “onion peel” strategy using different building blocks are quite appealing. Synthesis of AB₅-type of building block was started by desymmetrization of commercially available hexachlorocyclophosphazene *via* mono-incorporation of NBoc-protected *para*-amino phenol **4.084** in basic media to afford **4.085** (Scheme 4.9). Introduction of five units of monopropargylated hydroquinone **4.086** using under similar basic condition gave protected AB₅-type building block **4.087** in 87% yield. After deprotection of NBoc-protecting group in presence of trifluoroacetic acid in DCM, the compound **4.087** was readily converted to *N*-chloroacetamide-terminated dendron **4.088** through amidation reaction with chloroacetyl chloride. Synthesis of highly symmetrical tricontra-propargylated hypercore **4.090** was accomplished in 74% yield by treatment of **4.088** with **4.089** in basic and reductive condition (NaOH, NaBH₄ in EtOH). In the context, using standard CuAAC-assisted click chemistry reaction (CuSO₄, sodium ascorbate, THF/H₂O) between PEG₄-spaced lactoside **4.091** and propargyl-functionalized AB₃-type TRIS-based derivative **4.092** halogenated dendron **4.093** was synthesized in moderate yield (Scheme 4.10). After introduction of azido functional group at focal point *via* SN₂-type substitution, **4.094** and **4.090** were subjected to CuAAC-assisted click reaction under similar condition followed by Zemplén transesterification reaction to afford **4.095** in 62% yield over two steps.

Inhibition studies toward truncated Gal-3 (trGal-3) have revealed that versus PEGylated monomeric lactoside ($IC_{50} = 164$ μ M), 90-mer-lactosylated G(2)-dendrimer **4.095** demonstrated 1025-fold enhancement in affinity ($IC_{50} = 0.16$ μ M).⁸¹



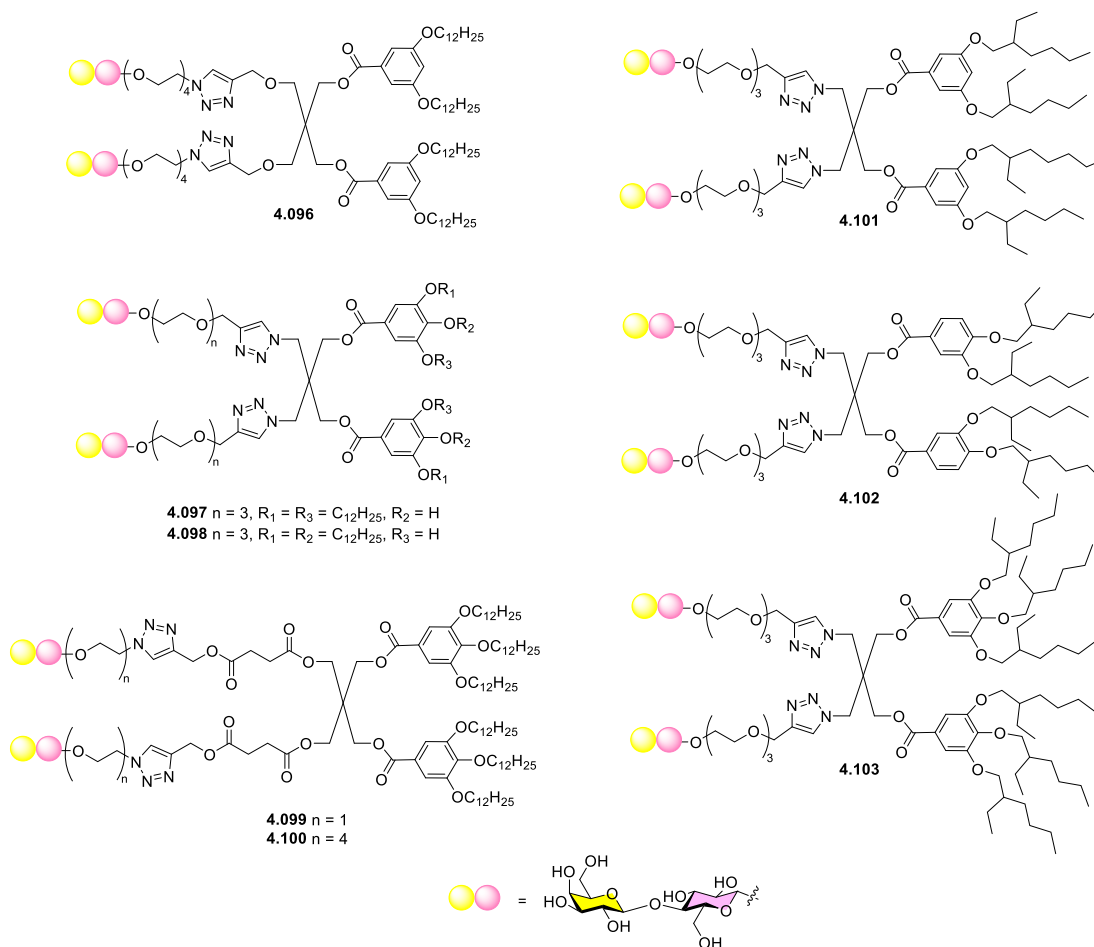
Scheme 4.9 Synthesis of triconta-propargylated hypercore **4.090**.⁸¹



Scheme 4.10 Convergent synthesis of 90-mer lactodendrimer *via* onion-peel strategy.⁸¹

4.4.6 Introduction to new class of neoglycoconjugates: Glycodendrimersomes

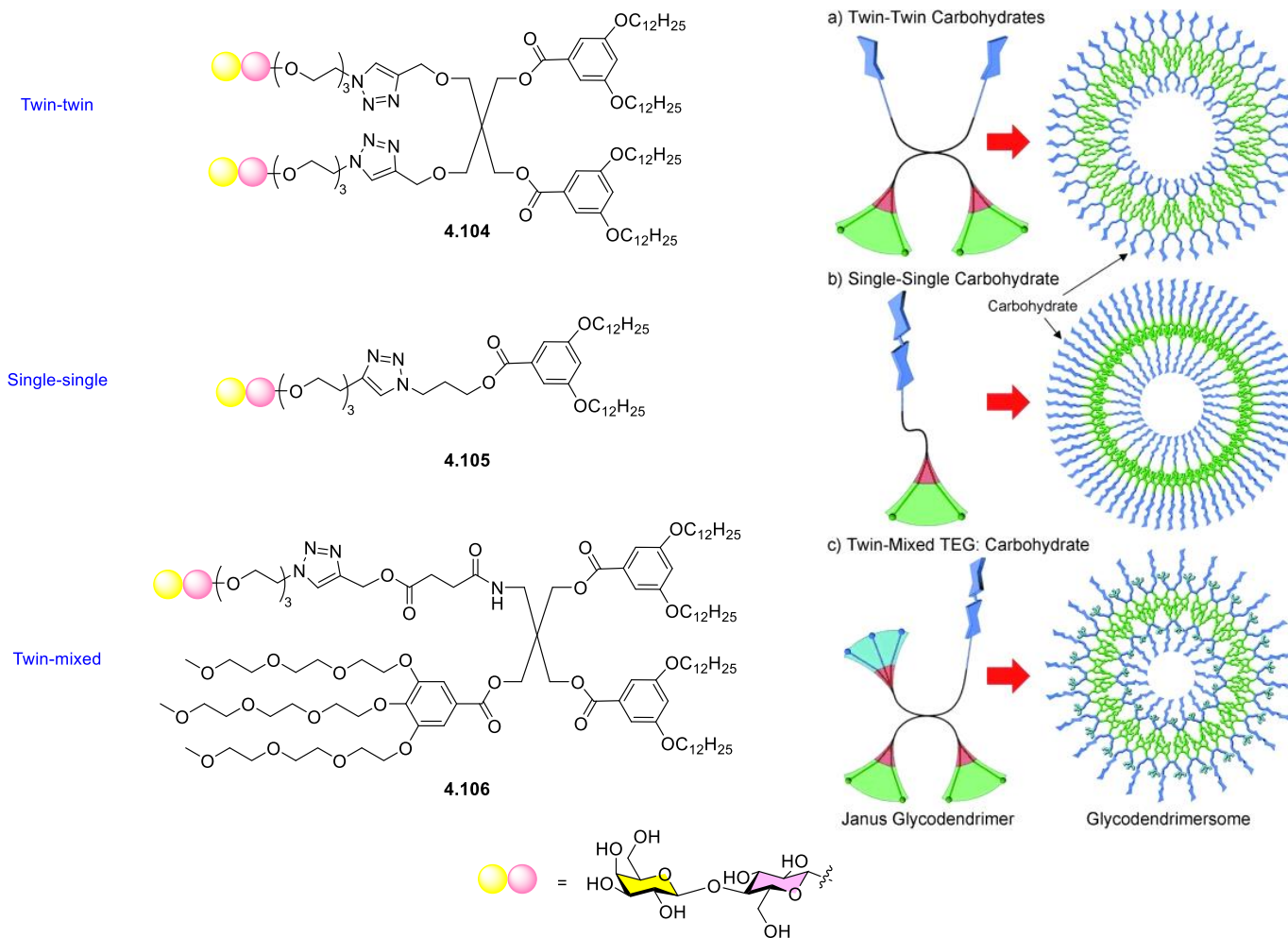
In the past three decades, the tremendous evolution of multivalent neoglycoconjugates built on a wide variety of scaffolds that mimic natural glycan architecture and compete natural ligands for binding to receptors have improved our understanding of “sugar codes”.¹⁰⁵ Nevertheless, mimicking supramolecular interactions with aforementioned synthetic glyconanoparticles have provided useful information about biological processes through carbohydrate-protein interactions. But not all multivalent platforms have been considered suitable for biological systems, yet, lack of certain essential properties including straightforward control of size, aqueous solubility, biocompatibility, biodegradation of scaffolds after delivery, non-toxicity of scaffolds for vital cells, *in-vivo* mimicry of mobile cell surface remain upsetting. With the aim of overcoming these challenges in novel synthetic multivalent display design leads to more bioinspired programmable glyconanoparticles. Recently reported carbohydrate-harbored dendrimersomes embodied as glycodendrimersomes possessing both dendrimer and liposome characters have gained more attention.¹¹³ Besides having internal cavity and programmable surface, self-assembled from glycodendrimers – glycodendrimersomes mimic supramolecular multivalency of biological membrane. In 2013 Percec and co-workers¹⁰⁵ have reported a library containing 51 amphiphilic Janus glycodendrimers with various spacers (propargyl, succinic ester, PEG-2, -3, -4) alkyl chains (linear and branched) and harbored with monosaccharides (Man, Gal) and disaccharide (Lac). Among them a few have demonstrated desired properties. Especially, single-type soft glycodendrimersomes (glycodendrimersomes with one type of shape e.g. spherical, polygonal, or tubular etc.) with narrow polydispersity and significant stability in buffer and water have shown excellent biological properties (Scheme 4.11).



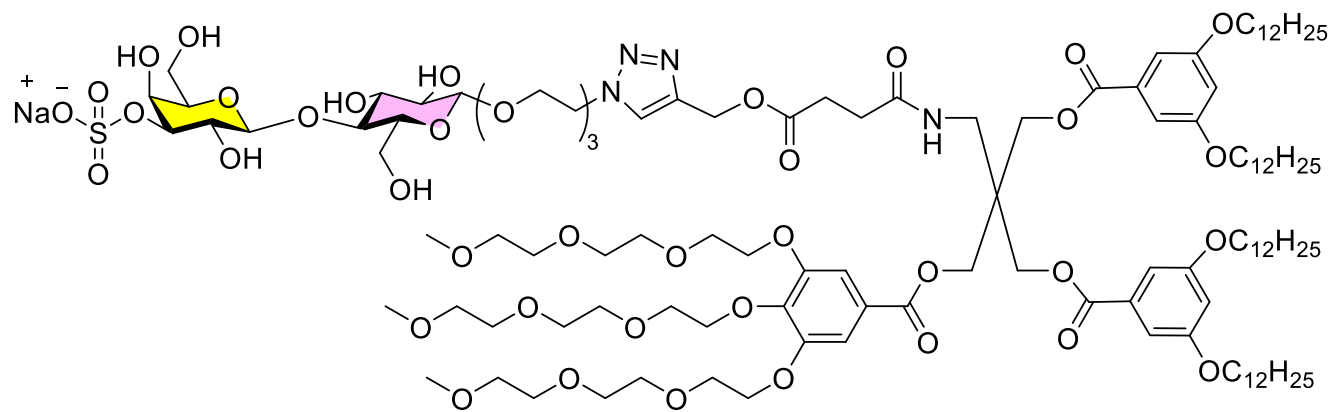
Scheme 4.11 Amphiphilic Janus Lactodendrimers self-assemble into single-type soft lactodendrimersomes.^{113-115, 118, 120, 121, 308}

For example, Lactodendrimersomes from **4.096** are agglutinated in presence of with different concentration of Gal-3 and Gal-4 where the concentration of generated glycodendrimersomes was maintained constant.¹¹³ Cryo-TEM images during interaction between lectin and glycodendrimersomes have also revealed that mechanical properties of multivalent display play major role thus, soft unilamellar glycodendrimersomes in terms of adaptability and topology are discriminated by lectins.¹⁰⁵ For the purpose of studying topology effect of glycodendrimersomes

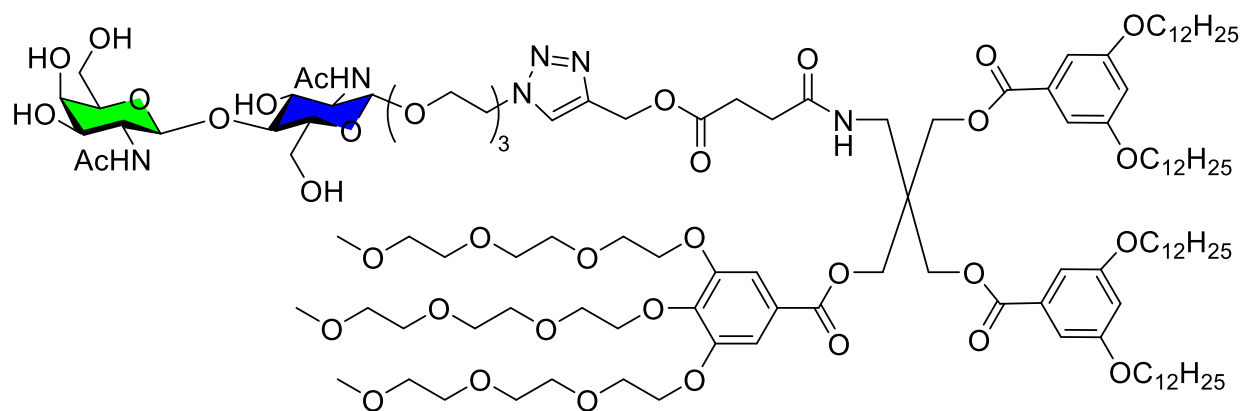
during carbohydrate-dependent aggregation, three types (twin-twin, single-single, twin-mixed) of surface presentation have been constructed (Scheme 4.12).¹¹⁴ Interestingly, it has been revealed that decreasing surface density of cognate sugar has a significant impact, thus much better results have been achieved with twin-mixed lactodendrimersome from **4.106** for human Gal-1, Gal-7 and Gal-8 by virtue of reduced steric hindrance.^{114, 115, 120, 121} Later, during aggregation assay toward prototype homodimeric (Gal-1), tandem-repeat-type heterodimeric (Gal-4 and Gal-8) and chimera-type monomeric (Gal-3) natural and engineered galectins, binding efficiency of **4.106** and its 3'-*O*-Sulfo analogue **4.107** (Scheme 4.13) have been compared.³⁰⁸ Results shows that, apart homodimeric Gal-1, rest of the galectins prefer to aggregate 3'-*O*-sulfo-Lac bearing dendrimersome generated from **4.107**.³⁰⁸ Switching from Lac epitope to LacdiNAc **4.108** have slightly influenced on PI (from 0.280 to 0.220 at optimal concentration (0.2 mM in THF)) and Z_{avg} (from 91 nm to 58 nm), but resulting glycodendrimersomes have demonstrated better activity towards WT (Wilms Tumor) engineered variants of Gal-1.³⁰⁸



Scheme 4.12 Self-assembly of lactodendrimers with various topologies: a) twin-twin b) single-single c) twin-mixed.¹¹⁴



4.107



4.108

Scheme 4.13 3'-O-sulfo-Lac and LacdiNAc harbored twin-mixed.³⁰⁸

4.5 Aim of the Project: Design and synthesis of LacNAc-decorated glycodendrimersomes

As we have reviewed reported multivalent ligands towards Galectins, to our knowledge there is no example of glycodendrimersomes with LacNAc disaccharides. In current chapter our objective has been set to design LacNAc and its *O*-3' derivatives (monomers have shown in Chapter 3) decorated dendrimersomes (Scheme 4.14). Moreover, generation of various topologies (Figure 4.6) and investigation of bioactivity for cancer-related human Galectins will be also realized.

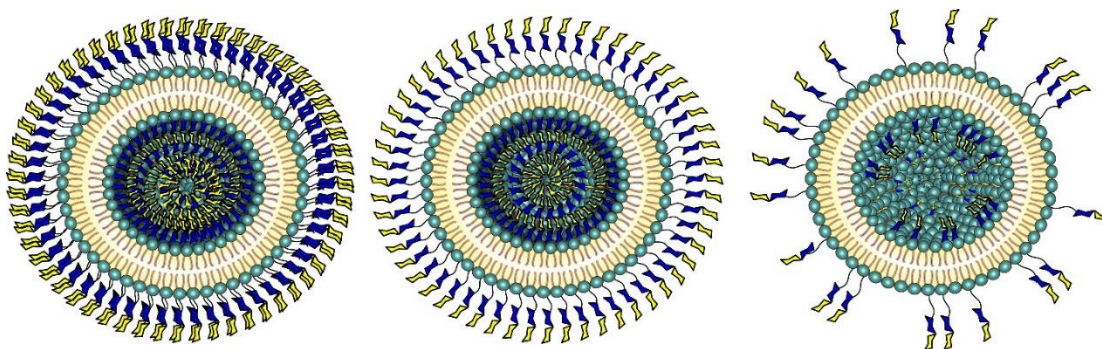
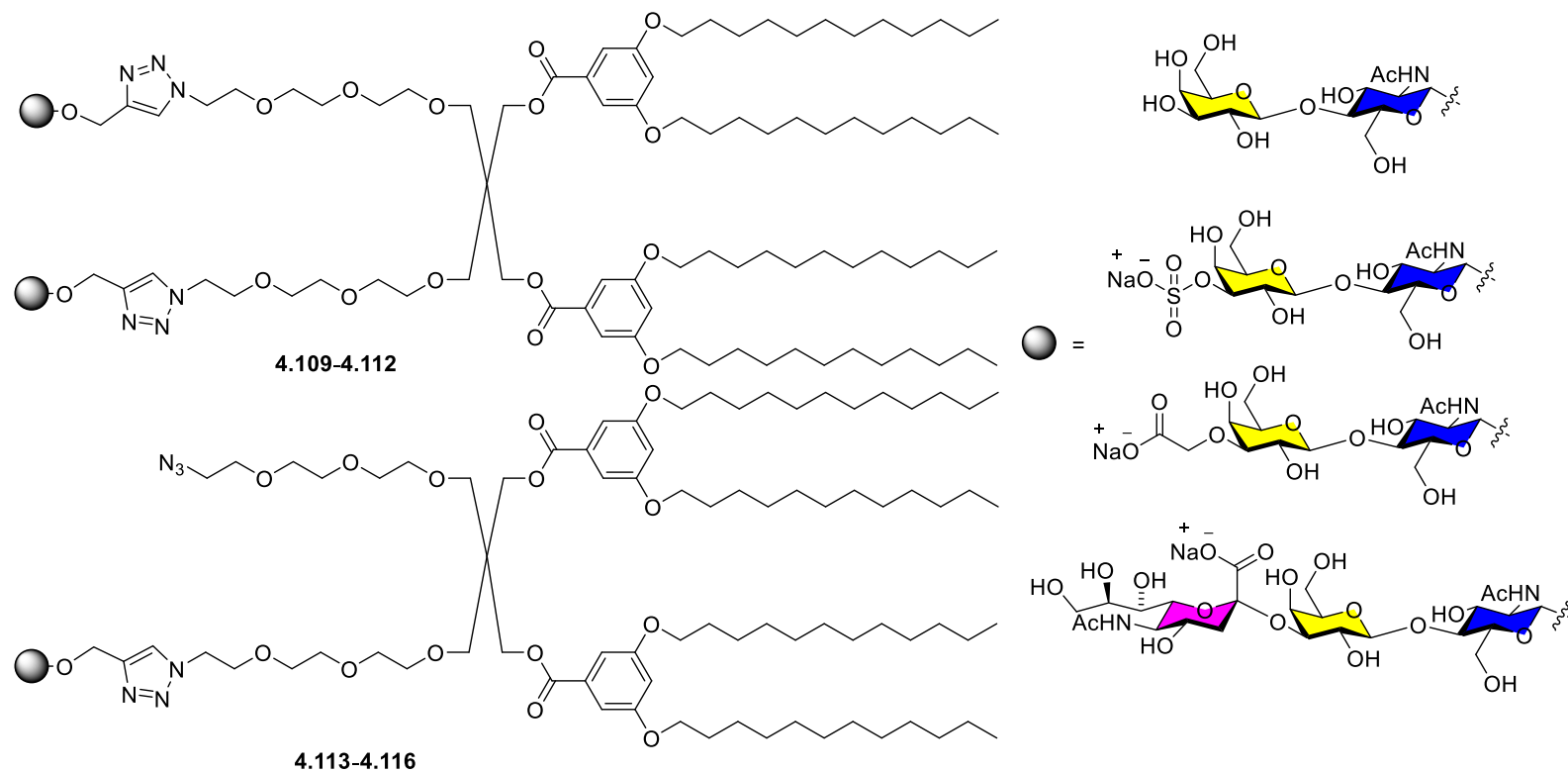


Figure 4.6 LacNAc-harbored glycodendrimersomes with three types of topologies : twin (left), twin-mixed (middle), physical-auto dilution of twin-mixed (right).



Scheme 4.14 Amphiphilic Janus Dendrimers bearing LacNAc and its 3'-O-derivatives at the focal points.

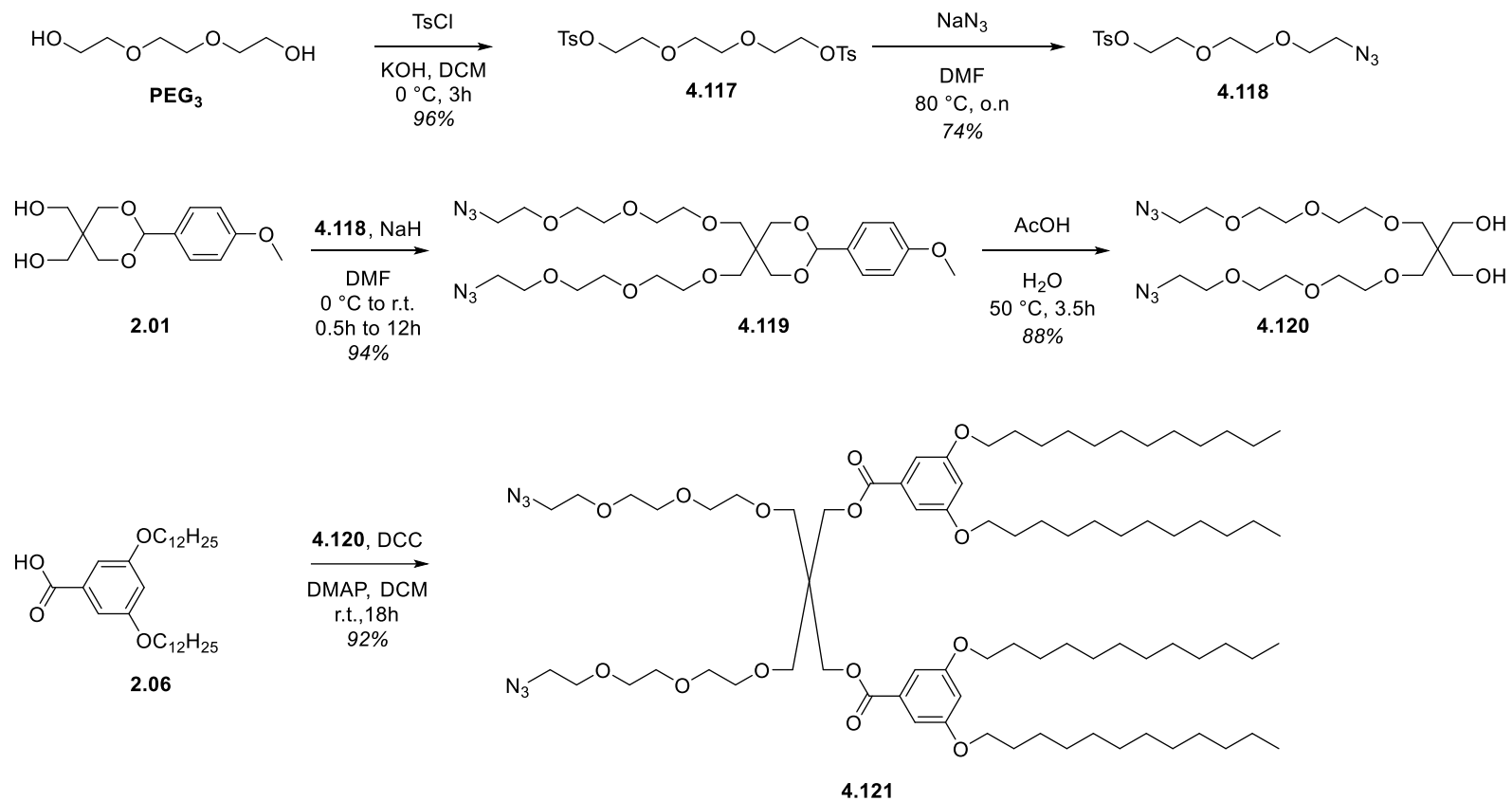
4.6 Result and Discussion

4.6.1 Synthesis LacNAc-conjugated amphiphilic Janus-Dendrimers (LacNAc-JDs) and generation glycodendrimersomes

As we have synthesized propargyl-functionalized tri- and disaccharides for CuAAC click reaction, synthesis of azido-functionalized Janus-Dendrimer precursor was in need (Scheme 4.15). Therefore, in order to get desired unilamellar soft glycodendrimersome, the hydrophobic and hydrophilic segments must be kept in balance.¹¹³ To this goal, we first synthesized the double functionalized (azido and tosylate functional groups at the focal points) **4.118** in two steps from commercially available PEG₃. Then, classical Williamson etherification *via* SN₂ – type substitution in presence of sodium hydride in DMF afforded **4.119** in 94 % yield. The structure of **4.119** was confirmed by ¹H and ¹³C NMR (Figure 4.119). Deprotection of anisacetal in AcOH/H₂O mixture (v/v = 7/3) at 50 °C followed by Steglich – Neises esterification with previously synthesized benzoic acid derivative **2.06** in presence of DCC, DMAP and DCM, at room temperature gave **4.121** in 81 % yield over two steps. The structure of **4.121** was confirmed by HRMS (Figure 4.8) and NMR (Figure 4.9). Additionally, NMR COSY, HSQC and HMBC experiments were used to assign the carbons and hydrogens.

Click reaction using standard CuAAC condition (catalytic quantity of CuSO₄·5H₂O, NaAsc in THF/H₂O mixture (v/v = 10/1) at room temperature) between **4.121** and **3.32** afforded bis-clicked **4.109** in 19 % yield. During purification stage mono-clicked **4.113** was isolated with 15 % yield (Scheme 4.16). Both products were easily purified *via* classical column chromatography on silica gel. The ratio between hydrophobic and hydrophilic segments determined by ¹H NMR analysis. As illustrated in Figure 4.10, hydrogen ratio (1:1) between singlet of the formed triazole at 7.86 ppm and triplet of the *Hp* (aromatic) at 6.80 ppm confirms the formation of bis-clicked product **4.109**. In case of isolated less polar compound, relative ratio for the same hydrogens

was observed to be 1:2 which was corresponding to mono-clicked product **4.113** (Figure 4.12). Both products were not soluble neither in CDCl_3 nor in CD_3OD . To resolve this issue, we used mixture of $\text{CDCl}_3/\text{CD}_3\text{OD}$ in a 1/1 volume ratio where peaks corresponding to two deuterated solvents were displayed in ^1H and ^{13}C NMR spectra. Unfortunately, high-resolution electrospray ionization mass spectrometry (ESI-HRMS) could not detect both dendrimers due to in-source cleavage, for this reason matrix-assisted laser desorption/ionization time of flight mass spectrometry (MALDI-TOF-MS) was chosen alternatively. Both methods, ESI-MS and MALDI-MS are considered “soft” ionization techniques and widely used in determination of molecular weight of various biomolecules. Nevertheless, compare to ESI, MALDI through generating single-charged quasi molecular ion and minimizing spectral complexity is considered to be more advantageous in molecular weight determination. As shown in Figure 4.14 and 4.15, molecular weight of sodium adducts $[\text{M}+\text{Na}]^+$ of the bis and mono-clicked products **4.109** and **4.113** were confirmed by MALDI-TOF MS.

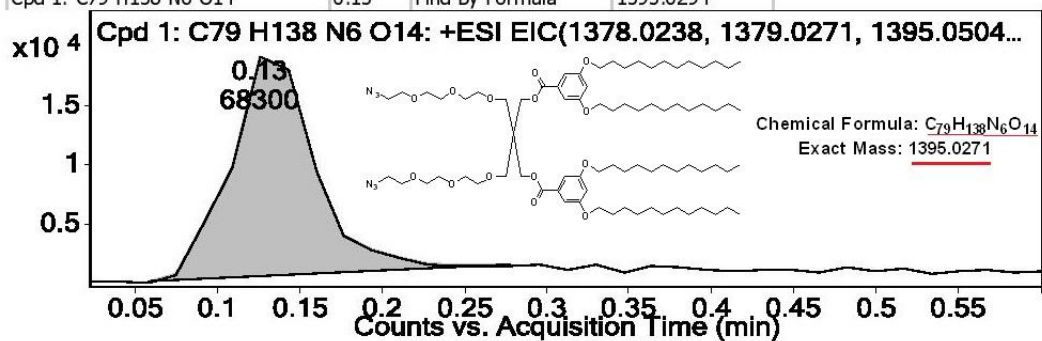


Scheme 4.15 Synthesis of azido-functionalized Janus-Dendrimer precursor.

Compound Table

Compound Label	RT	Mass	Abund	Formula	Tgt Mass	Diff (ppm)
Cpd 1: C ₇₉ H ₁₃₈ N ₆ O ₁₄	0.13	<u>1395.0294</u>	1087	<u>C₇₉ H₁₃₈ N₆ O₁₄</u>	<u>1395.0271</u>	<u>1.66</u>

Compound Label	RT	Algorithm	Mass
Cpd 1: C ₇₉ H ₁₃₈ N ₆ O ₁₄	0.13	Find By Formula	1395.0294



MS Spectrum

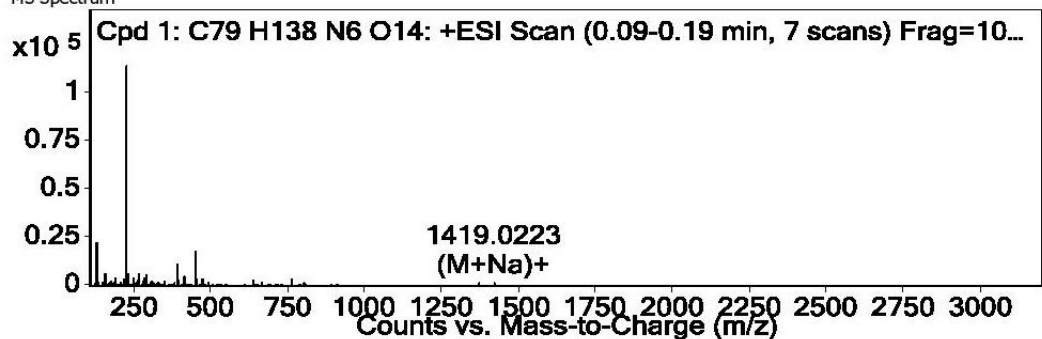
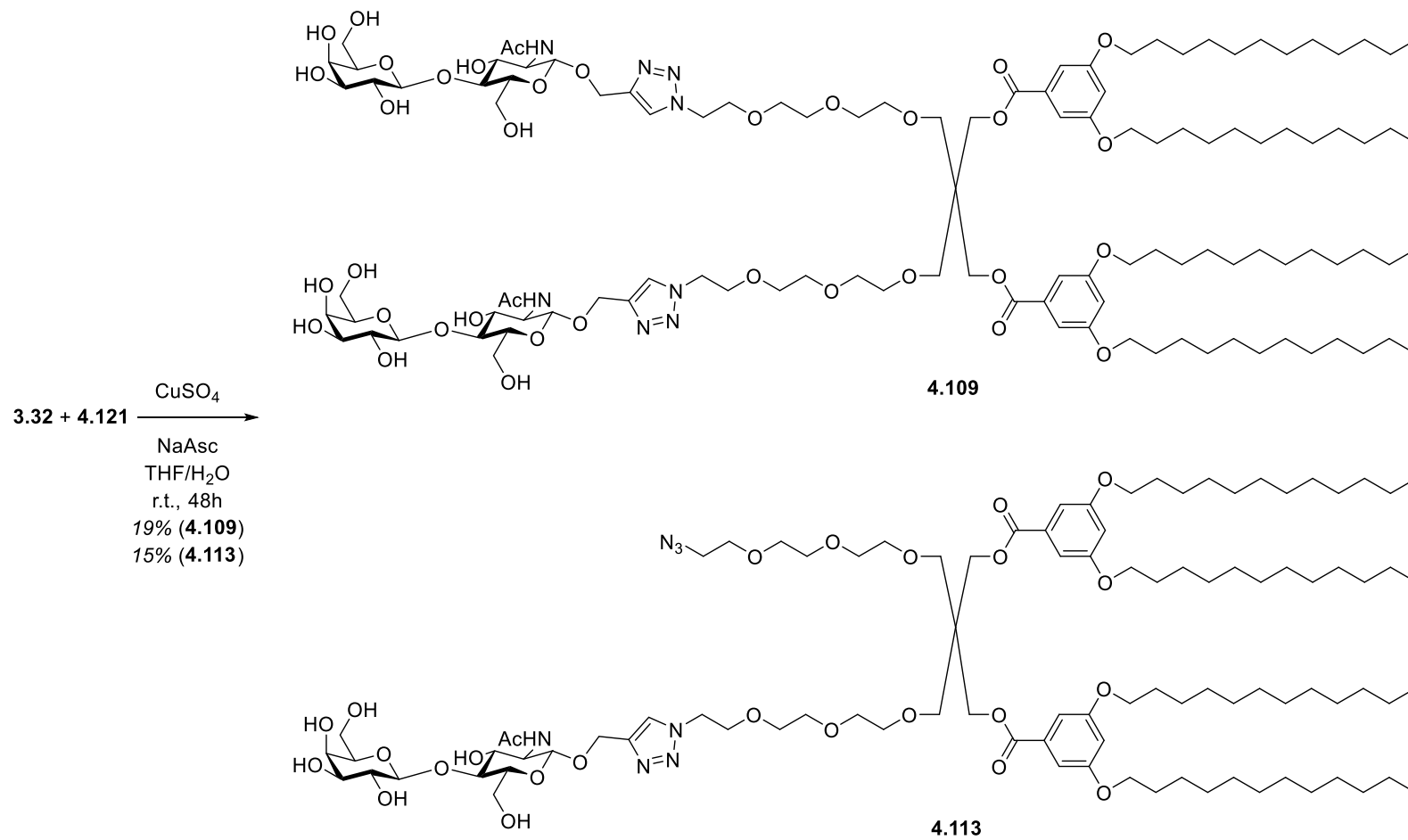


Figure 4.8 HRMS spectrum of compound 4.121.



Scheme 4.16 CuAAC-based click reaction between hydrophobic and hydrophilic segments.

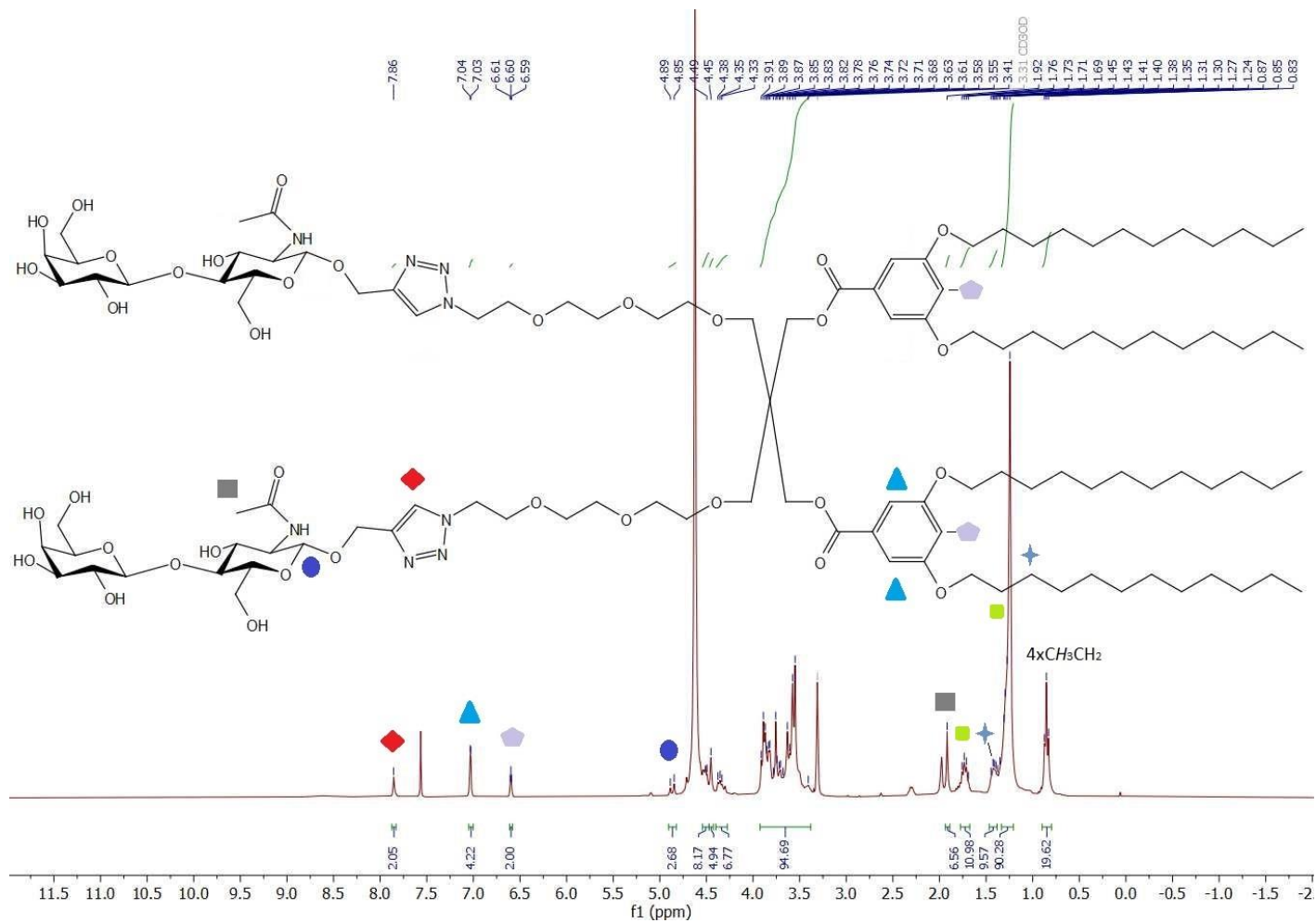


Figure 4.10 ¹H NMR (300 MHz, CDCl₃+CD₃OD, v/v = 1/1) spectrum of compound 4.109.

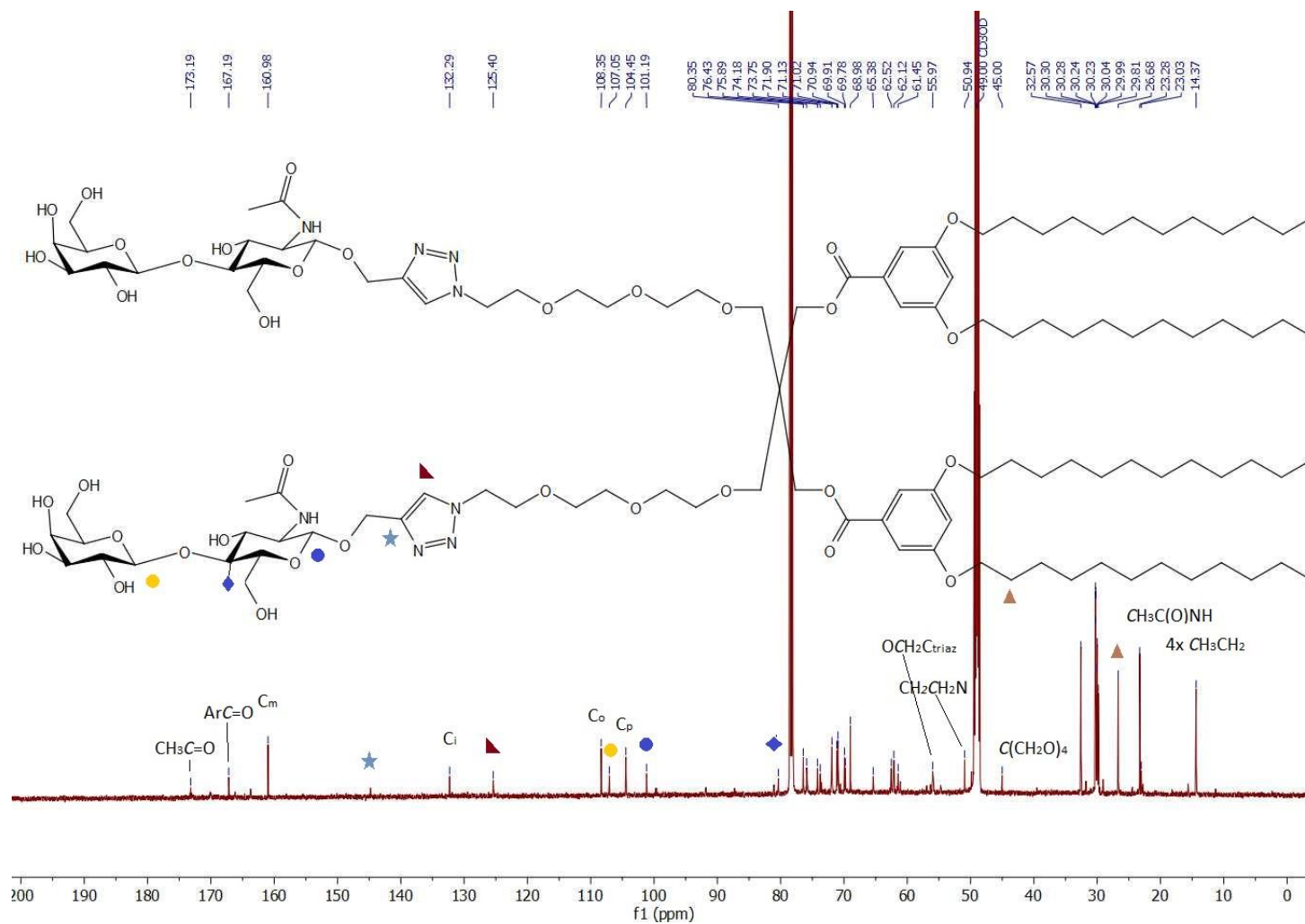


Figure 4.11 ¹³C NMR (75 MHz, CDCl₃+CD₃OD, v/v = 1/1) spectrum of compound **4.109**.

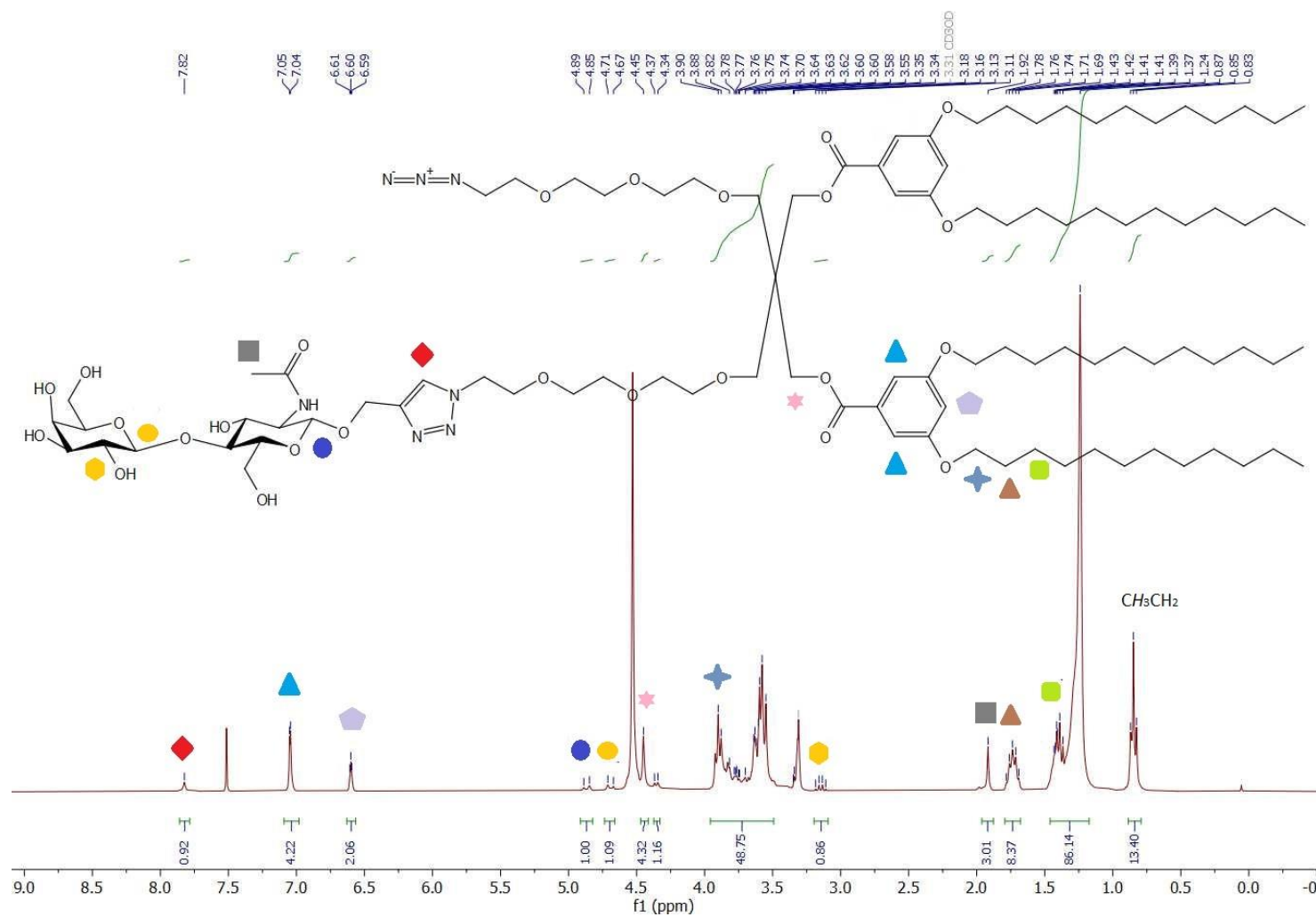


Figure 4.12 ¹H NMR (300 MHz, CDCl₃+CD₃OD, v/v = 1/1) spectrum of compound 4.113.

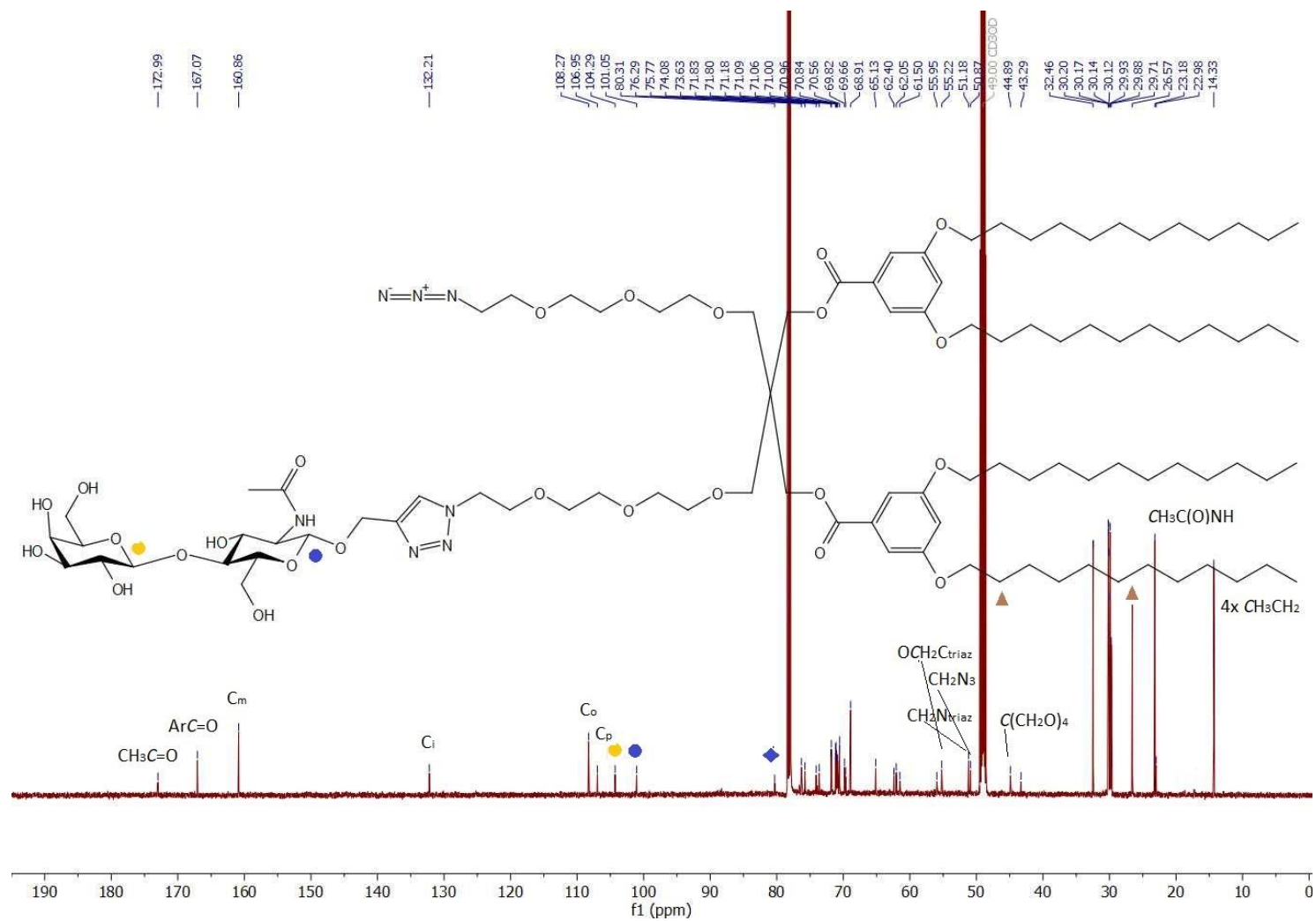


Figure 4.13 ¹³C NMR (150 MHz, CDCl₃+CD₃OD, v/v = 1/1) spectrum of compound **4.113**.

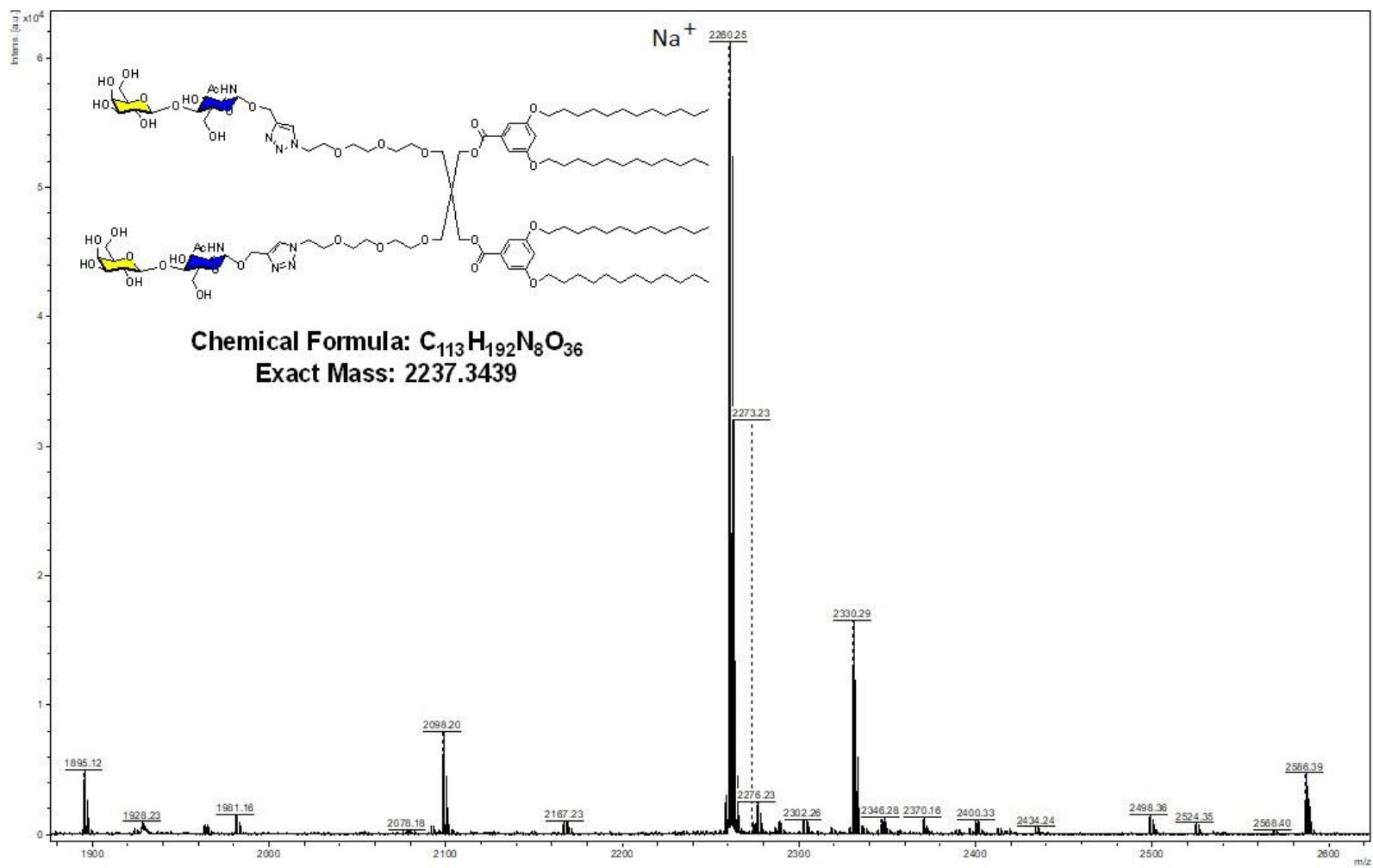


Figure 4.14 MALDI-TOF MS spectrum of compound 4.109.

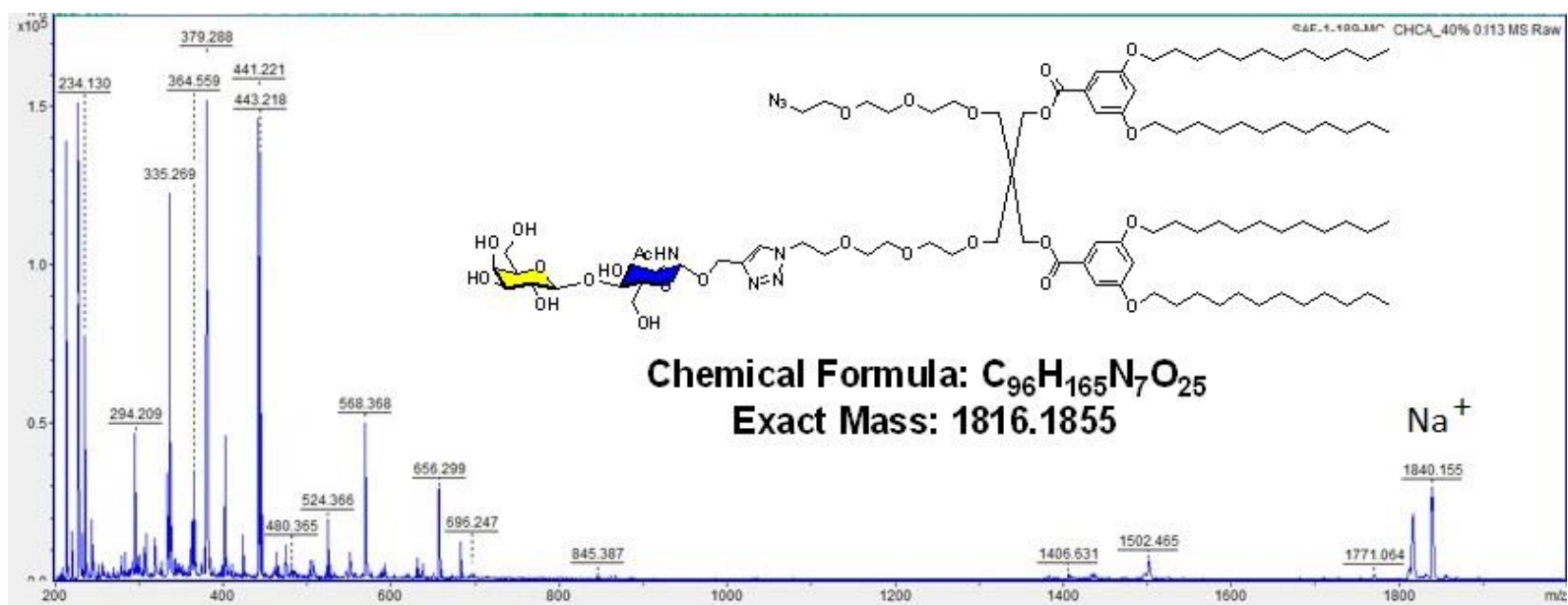


Figure 4.15 MALDI-TOF MS spectrum of compound 4.113.

Using ethanol injection method, different concentration of both glycodendrimersomes were prepared and Z_{avg} , particle size and polydispersity index (PDI) were measured by DLS technique. Understanding that size determines the fate of nanoparticles, therefore depending on concentration, prediction of size with narrow polydispersity is one of key advantageous properties of glycodendrimersomes. As shown in Figures 4.16 – 4.17, plots of self-assemblies from **4.109** and **4.113** demonstrate that hydrophobic/hydrophilic ratio influence directly the size of nanoparticles. While increasing concentration the size of glycodendrimersomes from **4.109** augments in a linear fashion. At the concentration of 0.2 mg/mL in EtOH (EtOH/H₂O ratio = 1/4 v/v) glycodendrimersome from **4.109** has broader size distribution with 0.468 of PDI value where the major vesicle size population is 8 nm. Surprisingly, while increasing concentration from 0.2 mg/mL to 0.5 mg/mL, the PDI value reached 1, and it means the suspension is highly polydisperse. In contrast, two times increment of concentration (at 1 mg/mL) leads to narrow size distribution (PDI = 0.131) with 130 nm of vesicle size. In the context, increment of concentration from 1 mg/mL to 5 mg/mL resulted highly monodisperse suspension with the vesicle size of 238 nm.

The changes in vesicle size and size distribution of dendrimersomes from **4.113** at similar concentrations show that all dendrimersomes were narrowly dispersed (Figure 4.17). However, the sizes of the generated dendrimersomes from Janus dendrimer with one hydrophilic head are much larger. The influence of polar head group on vesicle size has been already reported by several research groups.³⁰⁹⁻³¹² It has been suggested that higher concentration of polar head groups increase stability of vesicles and prevent their aggregation by covering the surface which leads to small vesicle size. Formation of large vesicles at lower head group concentration is explained due to the effect of decreased surface free energy and increased surface tension which leads to high bilayer stiffness and coalescence of bilayer membranes.

The difference between size and Z_{avg} can be explained by PDI (Figure 4.18). Ideally for monodisperse sample ($PDI \rightarrow 0$), particle size and Z_{avg} possess same peak size which is the case for glycodendrimersomes from **4.109** and **4.113** at $C_m = 1$ mg/mL and 5 mg/mL where PDI values are close to 0. Higher value of PDI of the sample could be explained that the distribution is broad and there are multiple particle size populations in the suspension.

During DLS study it was revealed that the balance between hydrophilic head and lipophilic tail affects the size of vesicles. Therefore, in the context, augmented hydrophobicity of Janus dendrimer leads to formation of larger vesicles.

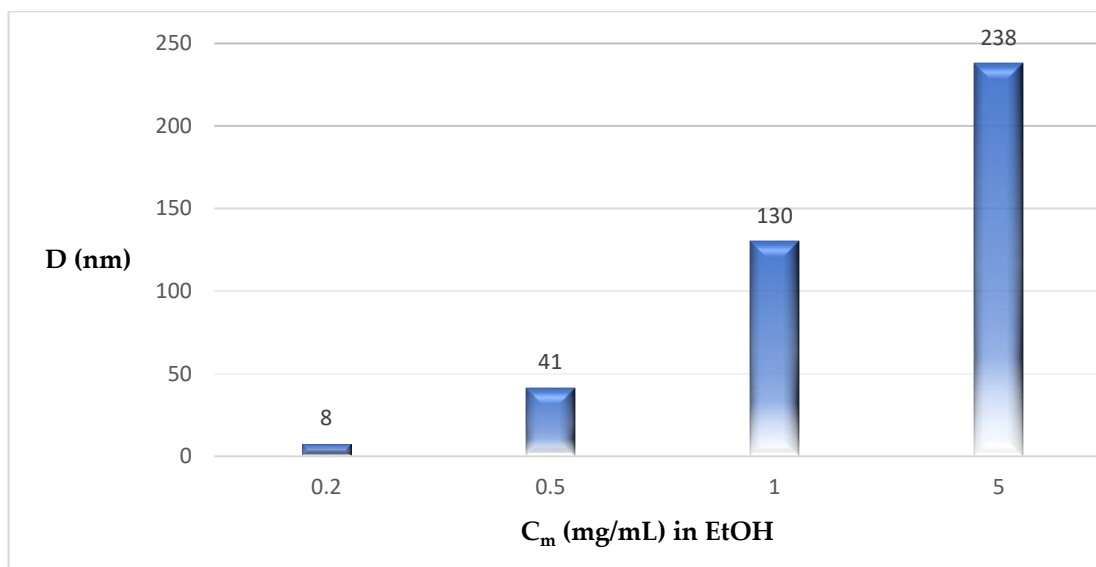


Figure 4.16 Plot of glycodendrimersome from 4.109, concentration versus size.

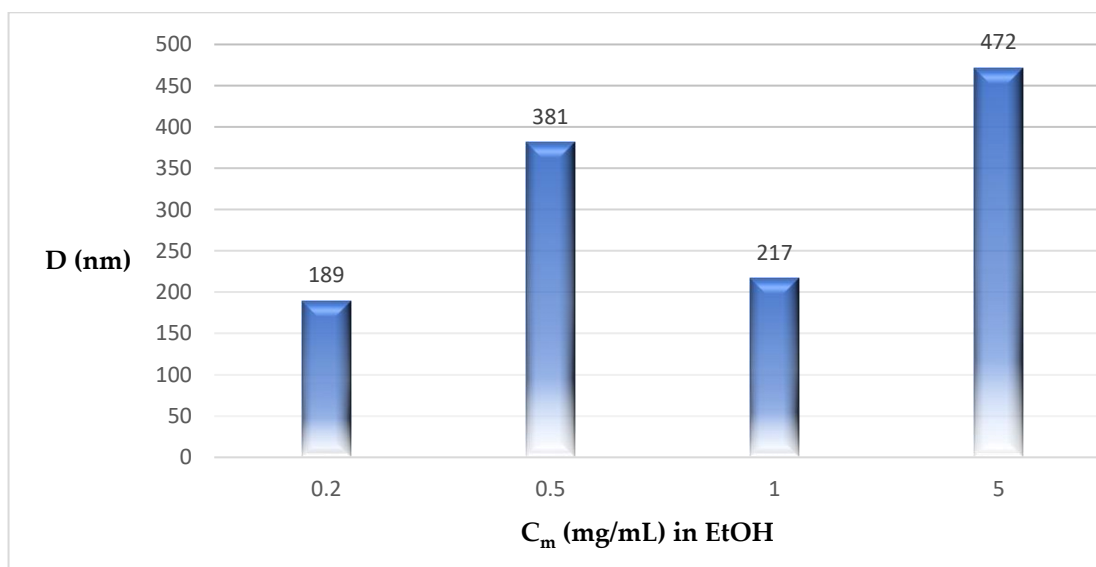


Figure 4.17 Plot of glycodendrimersome from 4.113, concentration versus size.

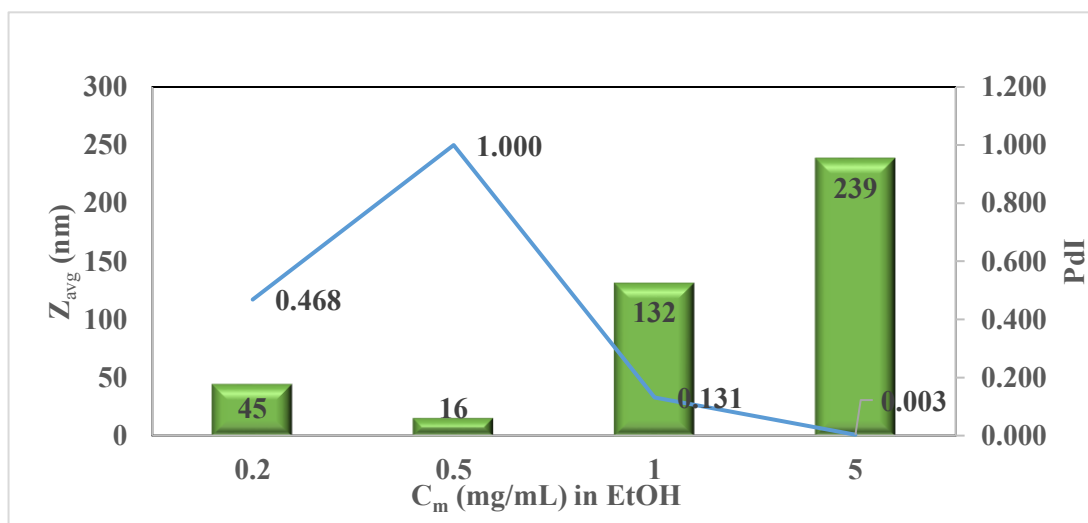


Figure 4.18 Plot of glycodendrimerosome from 4.109, concentration versus Z_{avg} and Pdl.

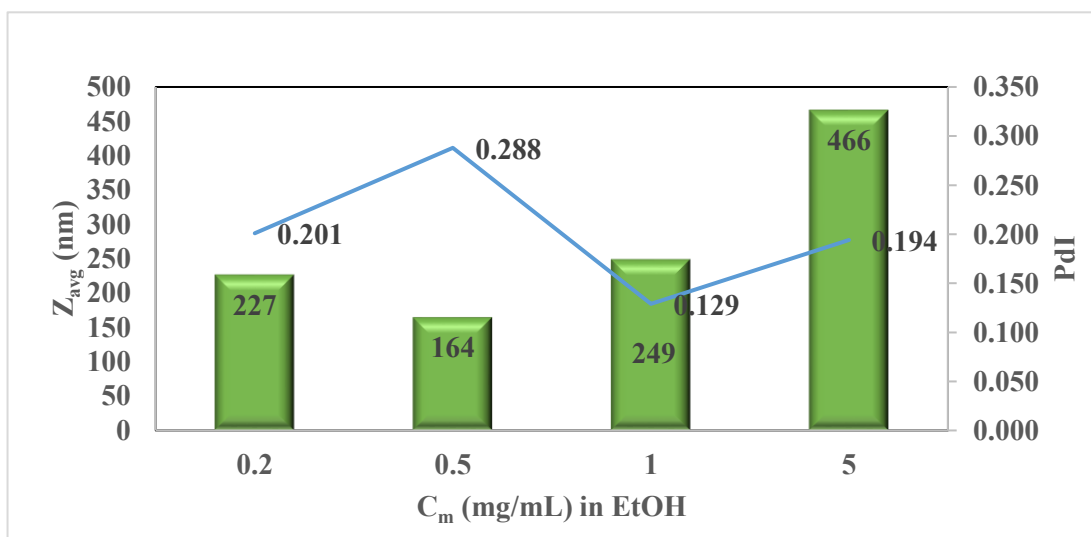


Figure 4.19 Plot of glycodendrimerosome from 4.113, concentration versus Z_{avg} and Pdl.

4.7 Conclusion

In summary, low-cost, straightforward synthesis of first example of LacNAc-bearing Janus-dendrimer was accomplished successfully. CuAAC-based click chemistry was chosen for coupling hydrophobic and hydrophilic segments. Obtained dendrimer were easily purifiable by classical column chromatography. Size and PDI properties of generated dendrimersomes were studied with DLS technique. As it is seen, for glycodendrimersomes from **4.109**, augmentation of the concentration has led to greater size and optimal PDI whereas at the similar concentrations dendrimersome vesicles from **4.113** have much larger sizes and narrow size distributions. Especially, glycodendrimersome from **4.109**. at the concentration of $C_m = 5$ mg/mL in EtOH and in a volume ratio of 1:4 with H₂O was observed to show higher monodispersity with PDI = 0.003 and $D = 238$ nm $Z_{avg} = 239$ nm which corresponds to perfectly uniform glycodendrimersome.

CHAPTER V

DESIGN AND SYNTHESIS OF SIALIC ACID-CONJUGATED DENDRIMERSOMES

5.1 Introduction to sialic acid

Sialic acids (Sias) are a family of nine-carbon acidic monosaccharides and typically found at the terminating branches of *N*-Glycans, *O*-Glycans and Gangliosides - a subgroup of Glycosphingolipids (Figure 5.1).³¹³ The family is also called “neuraminic acids” because of first isolation from neuronal glycolipid by German scientist E. Klenk.³¹⁴ Sialic acids play numerous biological roles in human physiology of cell-cell communication, cell-cell signaling, immune response, carbohydrate-protein interactions *etc.* For example, in human body during development and regeneration they serve as protecting group for some proteins against proteolytic enzymes.³¹⁵ There is high concentration of sialic acids in human milk and brain especially gangliosides which are very important in synaptogenesis and neural transmissions.

The sialic acid family hitherto contains more than 50 naturally occurring members including *N*-Acetylneuraminic acid (Neu5Ac) which is an aminosugar member of the

family and at the same time most abundant neuraminic acid in human body (Figure 5.1). *N*-Acetylneuraminic acid plays crucial role in intracellular and intercellular interactions including transport of ions, amino acids and pathogens. In this chapter we will focus on sialic acid chemistry, but brief information about major sialic acid-binding receptors will be also given.

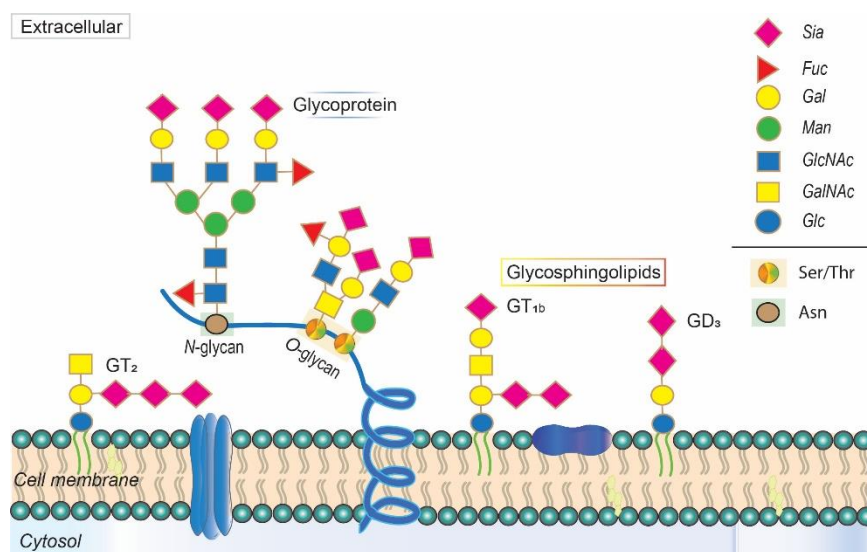
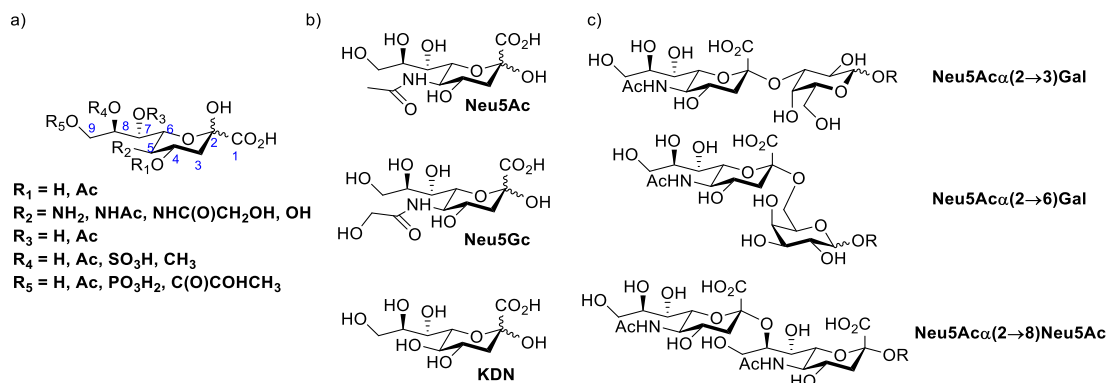


Figure 5.1 Sialic acid on cell surface.



Scheme 5.1 Sialic acid family: a) Sia family members; b) Most common Sia family members; c) Commonly found terminal Neu5Ac linkage.³¹⁶

5.1.1 Sialic acid dependence of Influenza virus in host-cell invasion

There are 4 subtypes (A, B, C, D) of negative-stranded RNA virus of Influenza. Being human viruses Influenza B and C can cause seasonal epidemics (known as seasonal flu) and mild illness, whereas Influenza A is most dangerous virus responsible for pandemics and global epidemics and they are mainly displaying in birds (known as avian viruses) and mammalians hosts. Finally, influenza D is mainly circulating in cattle and infection of human is not well-known up to date.

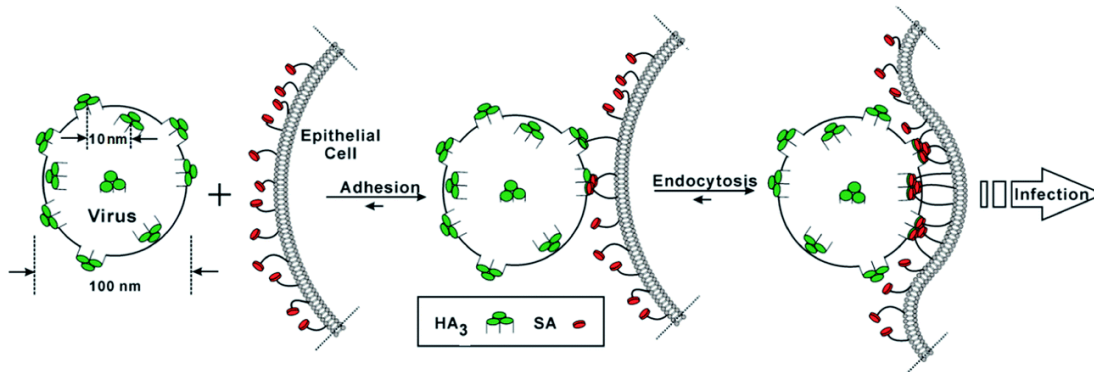


Figure 5.2 Attachment of Influenza Virus to the epithelial cell surface (HA₃ – trimeric hemagglutinin, SA – sialic acid).⁷²

Influenza viruses attach to the outer part of epithelial cells in the upper respiratory tract by using their surface glycoprotein hemagglutinin (HA) which recognizes terminal sialic acid residues (Figure 5.2). The enveloped virus enters cells *via* endocytosis followed by fusion of the endosomal membrane and this phenomenon is called infection. Based on membrane-bound surface glycoproteins (Hemagglutinin (HA) and Neuraminidase Enzyme (NA)) Influenza A viruses are subdivided: H₁ through H₁₉ and N₁ through N₁₁. In nature, up to date 131 Influenza A subtypes have been detected. Among them a few circulate in humans whereas in the past H₁N₁ (Spanish flu), H₂N₂ (Asian flu), H₃N₂ (Hong-Kong flu) caused pandemics by killing more than 50 million people globally.³¹⁷ More recently found in China avian influenza virus H₅N₁ has become a more deadly threat worldwide by killing humans and poultry.³¹⁸

5.1.2 Hemagglutinin of Influenza A viruses

HA plays an essential role in the adhesion strategy of the virus *via* recognizing surface glycolipids and glycoproteins terminating with sialic acid residues excluding gangliosides. Being a type-I transmembrane protein – homotrimeric HA is composed of an assembly of noncovalently-conjugated copies (HA₁, HA₂) of a single polypeptide precursor protein (HA₀). HA₁ has a molecular weight of approximately 55 kDa (in

H₁N₁, H₃N₂) and linked with HA₂ (25 kDa, H₁N₁, H₃N₂) by a disulfide bond.³¹⁹ Cleavage of biosynthetic precursor HA₀ (75 kDa) through basic amino acid residue (mostly Arg, rarely Lys) at cleavage site by proteolytic enzyme is vital for pathogenicity of the virus, thus at endosomal pH, it activates membrane fusion.^{319, 320} Globular head (HA₁) contains highly mutable receptor binding site (RBS) which is situated in shallow groove on the top of the subunit and responsible for the attachment of the virus to the cell surface (Figure 5.3a and 5.3c). The interactions between Neu5Ac and HA₁ are mostly similar in all Influenza A virus subtypes by virtue of conserved amino acid residues (Avian RBS: Ala138, Glu190, Leu194, Gly225, Gln226, Gly228).³²¹ Naturally, avian influenza binds predominantly to Neu5Ac α (2 \rightarrow 3)Gal linkage, whereas mammalian influenza has binding specificity for Neu5Ac α (2 \rightarrow 6)Gal (Figure 5.3 b, Scheme 5.1 c). Presence of low quantity of Neu5Ac α (2 \rightarrow 3)Gal at the upper trachea of pigs, makes them to be considered intermediary hosts or mixing vessels for both avian and mammalian influenza viruses. A single amino acid substitution at RBS can dramatically change HA binding specificity from α 2,3-linked Sia to α 2,6-linked Sia or vice-versa that occurs when HA₁ undergoes mutation.³²² Study shows that among conserved amino acids E190 and G225 play crucial role in determination of the specificity for RBS of avian influenza. Replacement of glutamic acid by aspartic acid at 190 position favors both specificities which is the case for pigs, whereas D190 and D225 support binding to α 2,6-linked Sia at human Influenza RBS.³²³ For example, H₁N₁ virus (Spanish flu) that caused 1918 pandemic, differs one or two conserved residues from avian influenza consensus depending on viral isolate.³²² Stem domain of HA contains HA₂ and fusion subdomain of HA₁ and serves for stabilization of the globular head. Mainly composed of conserved hydrophobic amino acids stem domain mediates entry of viral RNA and polymerase complex into the host cells through membrane co-fusion (target cell membrane and viral membrane).³²⁴

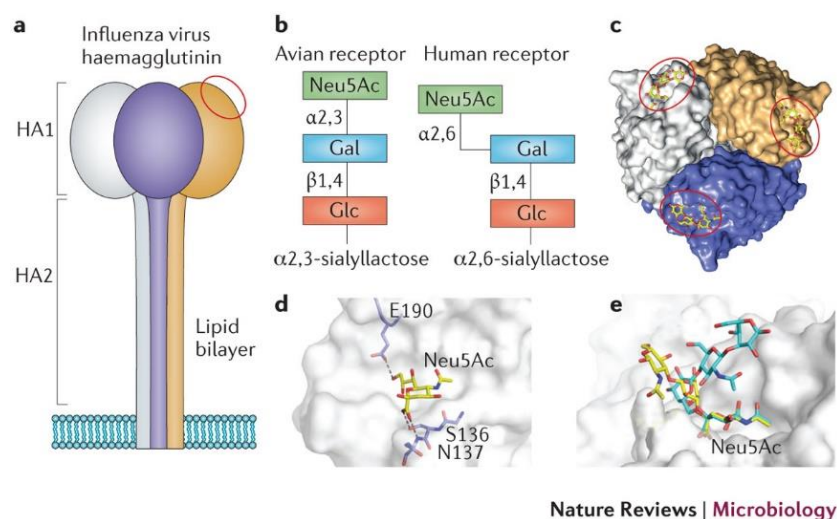


Figure 5.3 Influenza virus HA binding to Sia residue with two different linkage. a) Schematic view of HA homotrimer; b) Binding specificity of RBS depending on species; c) Location of RBS on the top of HA₁; d) Close-up view of HA-Neu5Ac interaction; e) Superposition of Avian Influenza HA with Neu5Ac $\alpha(2\rightarrow 3')$ LacNAc and Human Influenza HA with Neu5Ac $\alpha(2\rightarrow 6')$ LacNAc.³²⁵

5.1.3 Neuraminidase enzyme of Influenza A virus

Second major surface glycoprotein of Influenza virus is Neuraminidase (NA) and it mediates enzymatic cleavage of terminal Neu5Ac moiety from host and viral glycoproteins in order to release the virus from cells and prevent attachment of HA to other viral glycoproteins. Additionally, Matrosovich and co-workers reported that NA is taking part in early stage of virus invasion through degrading sialic acid-containing glycoprotein (mucin) and glycocalyx in human respiratory tract to clear the path for HA binding to the surface membrane of target cell.³²⁶ Mushroom-shaped homotetrameric NA is a type-II integral membrane glycoprotein composed of assembly of four identical polypeptides. Each monomer contains about 470 amino acids which are distributed in four domains: head, stalk, transmembrane region and cytoplasmic tail (Figure 33).

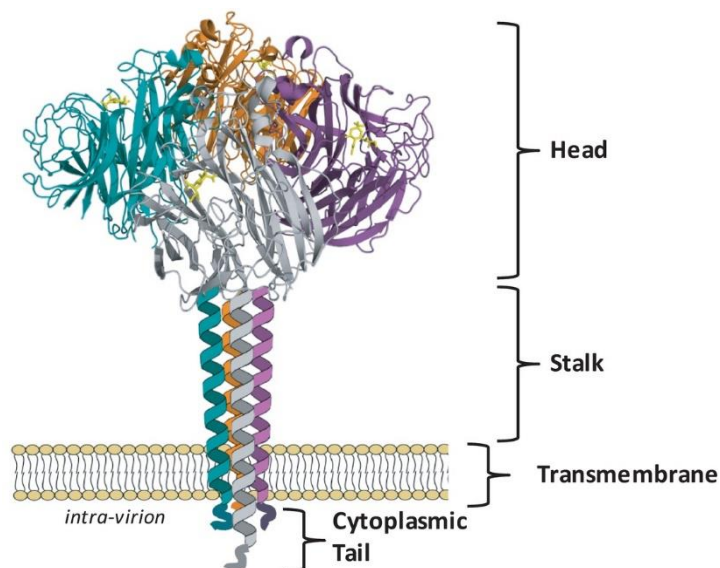


Figure 5.4 Structure of Neuraminidase (NA) surface glycoprotein on Influenza virus.³²⁷

Enzymatic activity of the protein occurs in the catalytic head domain where Neu5Ac recognizing surface is located sideward for facilitating the cleavage from nearby membrane glycoprotein. Compared to HA, NA does not possess any specificity toward α 2,3- or α 2,6-linked Sia by virtue of large polar cavity at binding pocket (Figure 5.5 left). Usually, the globular head domain has low mutation rate, therefore 50-90 % similarity between Influenza A virus subtypes has been reported by Colman *et al.*³²⁸ In sialic acid binding pocket, 8 highly conserved amino acid residues (Arg118, Asp151, Arg152, Arg224, Glu276, Arg292, Arg371, Tyr406) are responsible for the activity of enzyme (Figure 5.5).

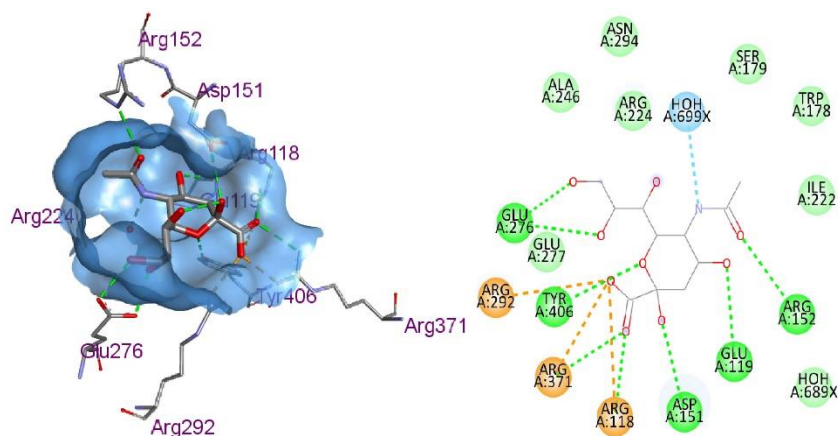


Figure 5.5 X-ray structure of NA-Neu5Ac complex (pdb code: 2BAT).³²⁹

However stalk domain is highly variable depending on subtypes but contains minimum one cysteine residue for stabilization of tetramer through creating disulfide bond.³³⁰ Although most subtypes possess up to 50 amino acids in stalk domain, deletion of around 20 residues in poultry have seen frequently. It has been hypothesized that diminished length of stalk domain decrease flexibility of NA nearby HA due to increased steric hindrance.³²⁷ Hydrophobic transmembrane domain is composed of highly variable amino acid sequence (7-29 amino acids) and mediates signal translocation from endothelial reticulum (ER) to apical surface. Cytoplasmatic or hydrophilic tail consists of highly conserved 6 amino acids (MNPNQK) in most Influenza A virus subtypes. To date it has been little known the exact role of cytoplasmatic tail. However, the lack of hydrophilic tail has been observed to affect negatively budding efficiency of the virus. Furthermore, together with transmembrane domain cytoplasmatic tail participate in lipid raft association that provides the transport of glycoprotein to the apical plasma membrane.³²⁷

5.1.4 Sialic acid binding Siglec family

Sialic acid terminated oligosaccharides are also recognized by endogenous receptors (selectins, siglecs, factor H). Among them, expressed on the surface of immune cells

including innate immune cells – I-type (Ig-type) siglec family has been found to bind only sialoglycans and generate inhibitory intercellular signaling. To date 15 members of family have been found in human. As we mentioned earlier depending on amino acid sequence in *N*-terminal V-set and C2-set domains siglec family members have been subdivided in two groups: 1) Classic siglecs containing Sialoadhesin (Siglec-1 or CD169), CD22 (Siglec-2), Myelin-associated glycoprotein (MAG, Siglec-4), Siglec-15; 2) CD33 (Siglec-3)-related siglecs which have been evolved from CD33 gene duplication (Figure 5.6). As well as Influenza A Virus hemagglutinin, each siglec member possess preferential binding specificity for terminal Neu5Ac linkage (Table 5.1). Therefore, CD22 and CD33 preferentially bind to α 2,6-linked Neu5Ac, whereas Sialoadhesin and MAG have strong binding specificity for α 2,3-linked Neu5Ac. Additionally, Siglec-5, -7, -11, -14 and -16 have been found to bind Neu5Ac α (2 \rightarrow 8)Neu5Ac linkage (Scheme 5.1 c).³³¹ Although certain siglec members have similar specificity for terminal sialic acid linkage, each member possess unique binding preference for specific sialoglycans.

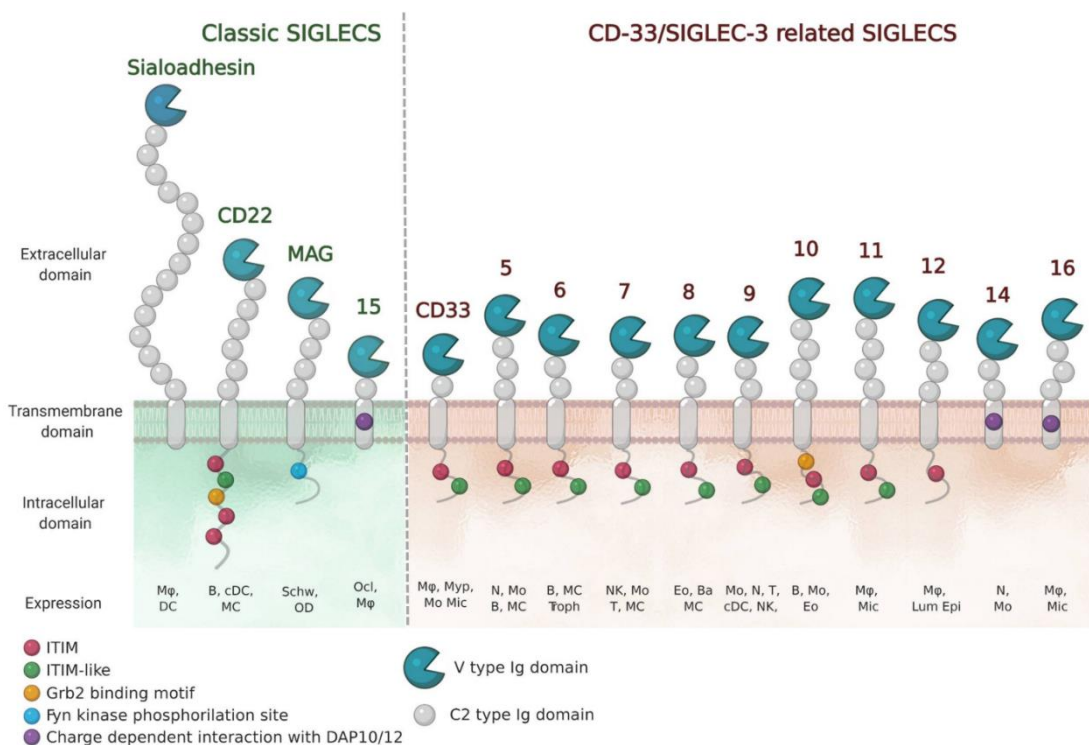


Figure 5.6 Siglec family subdivision.³³¹

In biology, glycosylation is the process by which proteins undergo post-translational modification mainly in the cytosol, the Golgi apparatus, the endoplasmic reticulum and the sarcolemmal membrane. Any abnormal change in glycosylation is considered a sign of malignant transformation. Aberrant glycosylation in cancer has been reported for the first time in 1969 by Meezan and co-workers.³³² Sialylation is one of the most widely occurring cancer-associated changes in glycosylation.³³³ Aberrant glycosylation and hypersialylation on the surface of cells are hallmarks of cancer that allow cancer cells to proliferate, survive and propagate tumor. Therefore, it has been suggested that during cancerous cell progression, hypersialylation is crucial for surface antigen masking. As siglecs are present on T cells, B cells, NK cells, macrophages, and dendritic cells, during immune surveillance sialylated glycans are recognized as immune checkpoint targets. The role of immune checkpoint is to

differentiate healthy from unhealthy cells and prevent an immune response that could destroy healthy ones. Hypersialylated cancer cells do not trigger an immune response as well as healthy cells. Therefore, interaction between sialylated glycan on cancer cell and corresponding siglecs on immune cells mediates immunosuppression and inhibition of apoptosis (Figure 5.7). Targeting siglecs for immunotherapy of certain types of cancer have been considered hot topic by virtue of their selective expressions.³³⁴ Although naturally siglec-sialic acid interactions have low binding affinity, creation of additional binding interactions *via* SAR or direct functionalization of sialic acid moiety have been considered powerful tools. More detailed information about sialobiology and sialic acid binding receptors originated from pathogens and intrinsic lectins have been described elsewhere.^{316, 335-338}

Table 5.1 Human Siglec classification.³³⁹

Siglec	Expression	Terminal Sia linkage specificity	Biological function
Siglec-1 (Sialoadhesin; CD169)	Macrophages	Neu5Ac α (2→3)Gal	Macrophage interaction with lymphocytes; internalization of sialylated pathogens
Siglec-2 (CD22)	B cells	Neu5Ac α (2→6)Gal	Negative regulation of B cell activation; B cell tolerance induction
Siglec-3 (CD33)	Myeloid cells, monocytes, microglia	Neu5Ac α (2→6)Gal	Regulation of myeloid cell development and function; Suppression of amyloid beta uptake by microglia in the brain
Siglec-4 (MAG)	Schwann cells, oligodendrocytes	Neu5Ac α (2→3)Gal	Maintenance of myelinated axons; suppression of axonal regeneration after injury
Siglec-5 (CD170)	Monocytes, neutrophils	Neu5Ac α (2→8)Neu5Ac Neu5Ac α (2→6)GalNAc	Recognition and internalization of sialylated pathogens; inhibition of immune cell activation
Siglec-6 (CD327)	Trophoblasts, B cell subset	Neu5Ac α (2→6)GalNAc	Regulation of trophoblast proliferation and invasiveness
Siglec-7 (CD328)	NK cells, monocytes, mast cells, basophils	Neu5Ac α (2→8)Neu5Ac	Attenuation of NK cell activation and function; inhibition of mast cell and basophils
Siglec-8 (SAF2)	Mast cells, basophils, eosinophils	Neu5Ac α (2→3)Gal6SO ₃ H	Induction of apoptosis in eosinophils
Siglec-9 (CD329)	NK cells, monocytes, macrophages, dendritic cells, neutrophils	Neu5Ac α (2→3)Gal	Inhibition of NK cell and neutrophil activation and function; immune modulation of myeloid cells
Siglec-10 (SLG2)	B cells, NK cells, monocytes, CD 4+ T cells	Neu5Ac α (2→6)Gal Neu5Gc α (2→6)Gal	Attenuation of immune activation and overreaction; suppression of CD4+ T cells
Siglec-11	Microglia, macrophages	Neu5Ac α (2→8)Neu5Ac	Inhibition of microglial activation
Siglec-14	Neutrophils, monocytes	Neu5Ac α (2→8)Neu5Ac Neu5Ac α (2→6)GalNAc	Activation of proinflammatory pathway in monocytes; recognition of sialylated pathogens
Siglec-15 (CD33L3)	Osteoclasts, macrophages	Neu5Ac α (2→6)GalNAc	Regulation of osteoclast differentiation and bone resorption; immune modulation of macrophages
Siglec-16	Macrophages	Neu5Ac α (2→8)Neu5Ac	Unknown

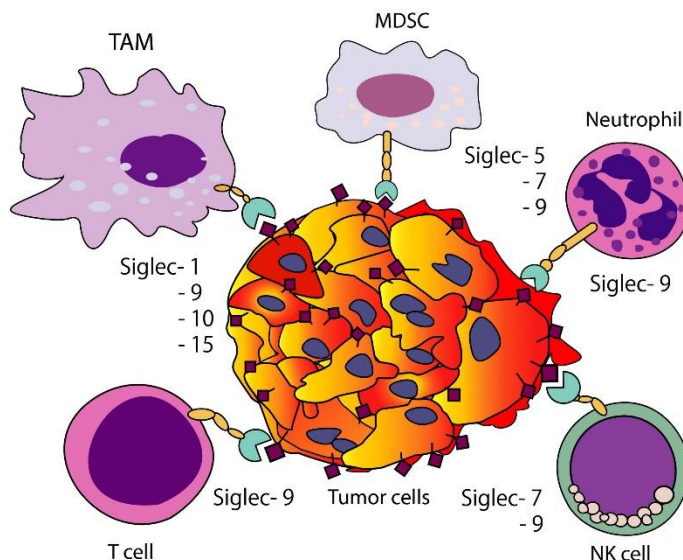
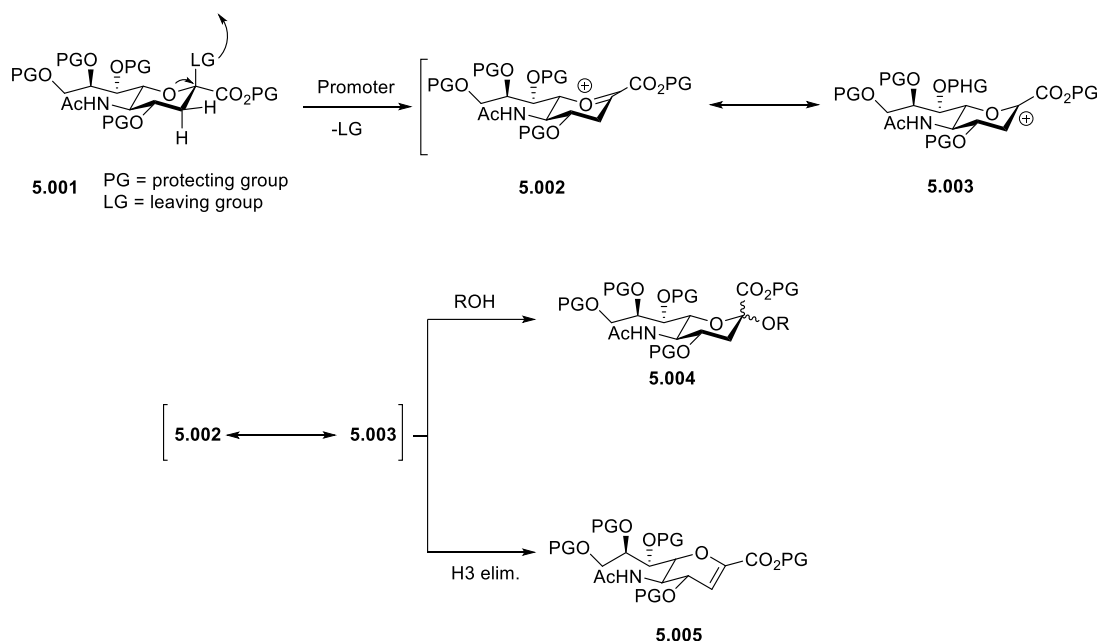


Figure 5.7 Siglec-Neu5Ac interactions *via* immune cells-tumor cells communications.³⁴⁰

5.2 Sialic acid in chemistry

In chemistry the stereoselective synthesis of sialosides has been considered to be one of the challenging reactions, especially that of the naturally occurring α -sialosides. The difficulties arise from the presence of electron withdrawing carboxyl group at anomeric position and lack of anchimeric assistance at neighboring C3 position which reduce reactivity of the donor and lead to low yield and poor stereoselectivity. Moreover, the leaving group at C2 position sometimes causes formation of undesired 2,3-eliminated product or glycal (Neu5Ac2en) through E1 mechanism (Scheme 5.2). Additionally, sterically hindered anomeric position makes sialidation more complicated for some bulky nucleophiles. However many advance have been made to obtain α -stereoselective sialosides either using chemoenzymatic³⁴¹⁻³⁴³ or synthetic chemical approaches.^{67, 344-352} In synthetic approach for desired stereoselectivity achievement several factors including anomeric leaving groups, nature of promoters,

reactivity of acceptors, stereodirecting ability of functional groups on Neu5Ac moiety and solvent system play determining roles.

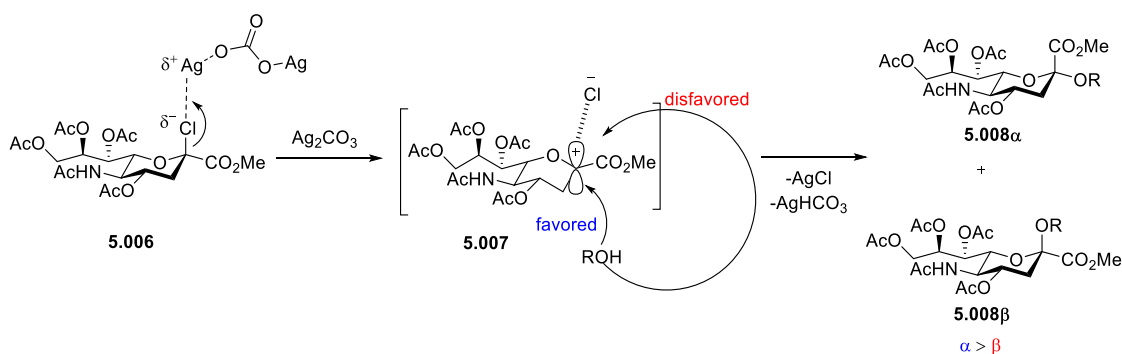


Scheme 5.2 Promoter mediated sialylation and formation of the glycal.

5.2.1 Anomeric leaving groups

Anomeric leaving group at C2 position plays prominent role for efficient α -sialylation. Earliest attempts for stereoselective synthesis were mostly based on promoter ($\text{Ag}^{\text{(I)}}$ - and $\text{Hg}^{\text{(II)}}$ -based salts) mediated SN_1 (Koenig-Knoor condition) and SN_2 (Helferich condition) type reactions *via* using halides as anomeric leaving group.^{253, 353-355} Although most successful results have been obtained using β -chloro sialoside donors and silver-based salt promoters, formation of undesired β -derivatives and glycals, and poor selectivity toward less reactive secondary, tertiary and primary higher alcohols (higher alcohols – those containing more than 4 carbon atoms) have been considered main drawbacks of this synthesis method (Scheme 5.3). To this end, introduction of

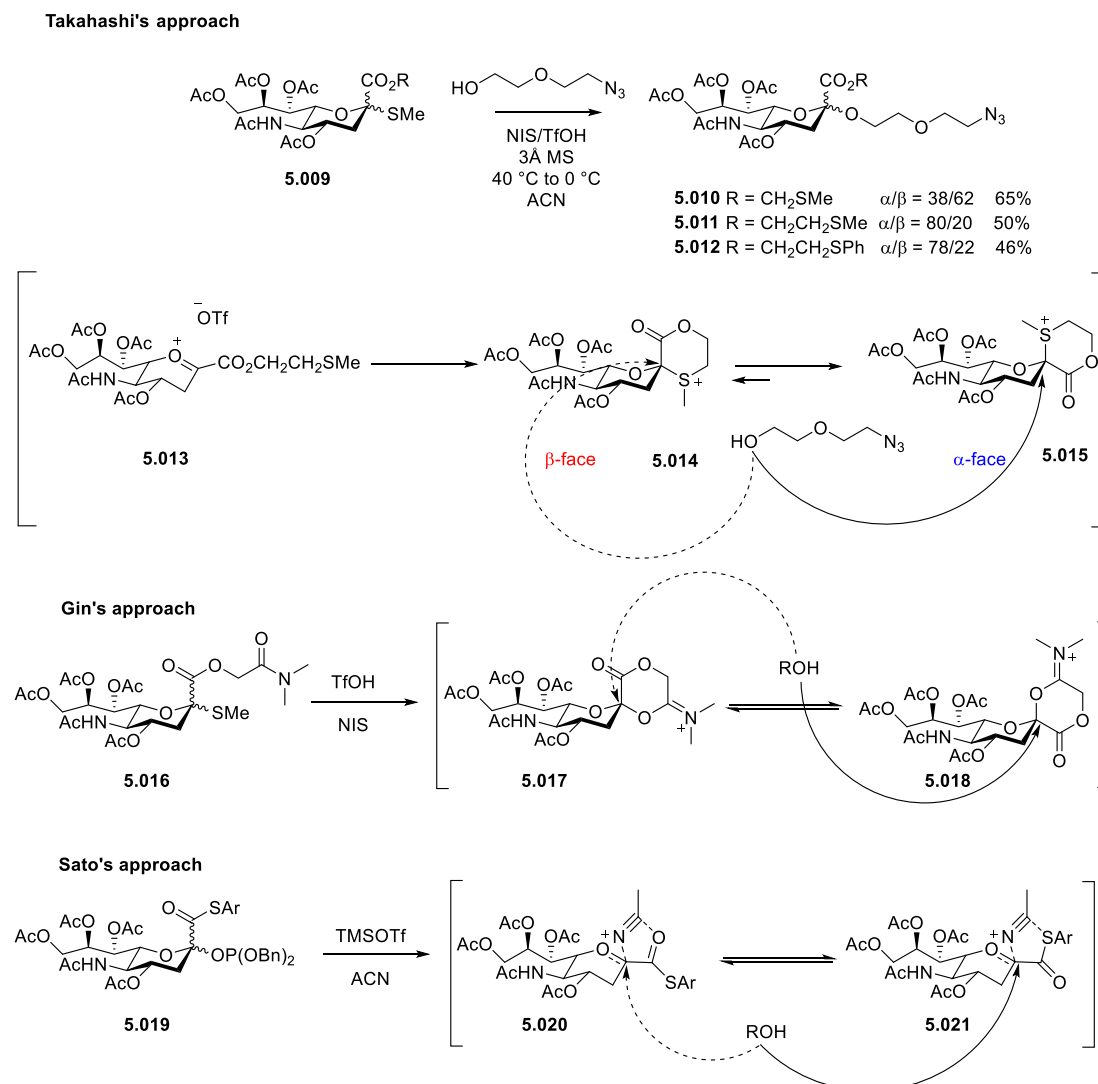
an auxiliary group at C1³⁵⁶⁻³⁶² and C3³⁶³⁻³⁷¹ positions have been reported improve stereoselectivity. Takahashi and co-workers reported that introduction of “long-range participation” of methylthioethyl ester at C1 position promotes modest α -sialylation through formation of sulfonium ion intermediate (Scheme 5.4).³⁵⁷ Further development has been reported by Gin and co-workers whereas *N,N*-dimethylglycolamide auxiliary leads to the formation of exclusive α -sialosides although suffers from weak stereoselectivity toward sterically more hindered secondary alcohol acceptors.³⁵⁸ In another published work by Sato *et al.* C1 arylthioesters in acetonitrile exhibit moderate to good α -selectivity toward primary alcohol acceptors.³⁶² Although C3 auxiliary have been successfully employed to obtain desired sialylation, this method requires introduction and removal of stereodirecting groups that cause additional difficulties (Scheme 5.5).



Scheme 5.3 Under Koenig-Knoor condition, silver carbonate-promoted sialylation.

Alternatively, from the beginning of 90s the use of sulfur-based functional groups (xanthate,³⁷²⁻³⁷⁷ sulfide,³⁷⁸⁻³⁸⁸ sulfoxide³⁸⁹⁻³⁹¹, thioamidoyl³⁹²⁻³⁹⁴) has opened new perspectives for sialic acid glycosylation. Due to their remarkable shelf-life stability, easy preparation and modest α -stereodirecting abilities, thioaryl and thioalkyl sulfides remain hitherto most employed anomeric leaving groups in sialylation reactions. During a study of “active” and “latent” thioglycoside donor strategy, Roy *et al.* have

demonstrated that electron withdrawing and donor groups on aryl ring affect the reactivity of thiosialoside donor in sialylation (Table 5.2).³⁹⁵

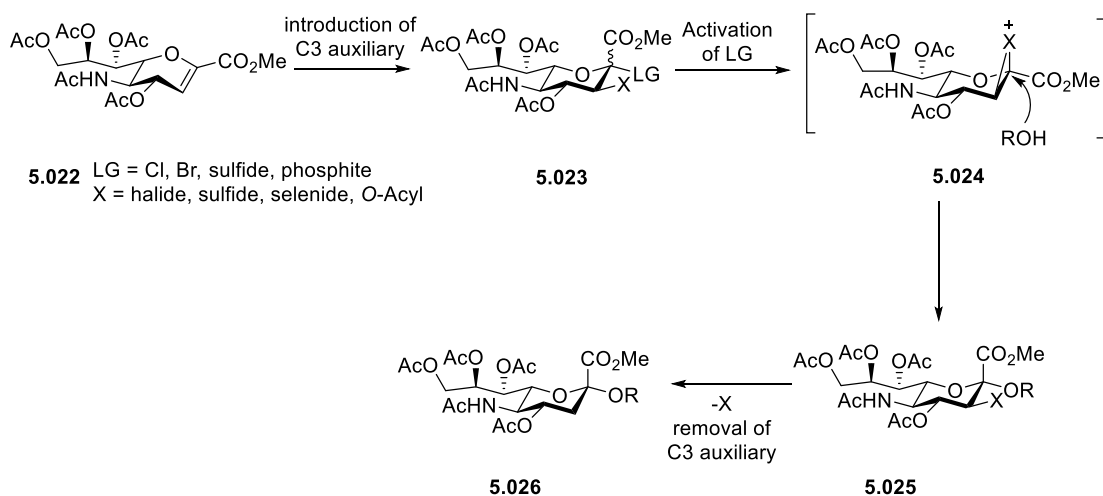


Scheme 5.4 C1 auxiliary in stereoselective sialylation.

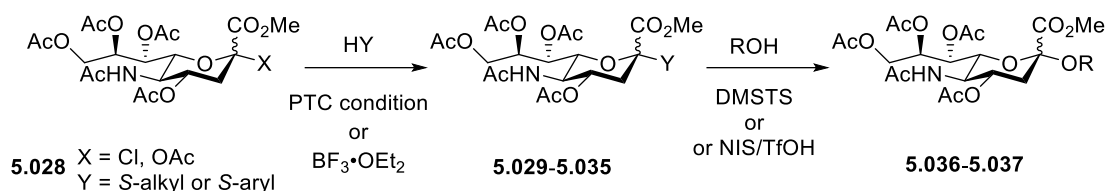
While DMTST promoted electron-rich *para*-acetamidophenyl thiosialoside donor shows modest stereoselectivity, electron-poor *para*-nitrophenyl thiosialoside remains intact. On the other hand, Crich and Li have reported that β -sialoside donor with

bulkier thioadamantyl group is more compatible with α -stereodirecting nitriles at low temperature whereas its thiotolyl analogue is ineffective.³⁹⁶

Among α -stereodirecting anomeric leaving groups phosphite,³⁹⁷⁻⁴⁰⁴ phosphate⁴⁰⁵⁻⁴¹¹ and phenyltrifluoroacetimidate⁴¹²⁻⁴¹⁴ should be also mentioned. Although they exhibit better α -stereodirecting activity, installation of these leaving groups requires additional synthetic steps.



Scheme 5.5 C3 auxiliary-mediated α -sialylation.

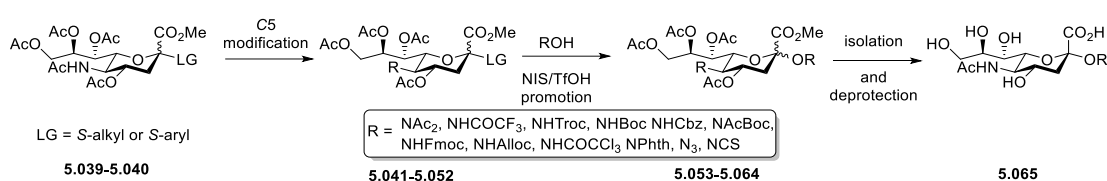
Table 5.2 Thioaryl and thioalkyl sialosides donor in sialylation.

Thiosialoside Donor (Y)		Acceptor (ROH)	Promoter	Solvent (temp.)	Yield (%)	α/β
5.029	—S—Me		DMTST	DCM (r.t.)	82	1.5/1
5.030	—S—				81	5.5/4.5
5.031	—S—				80	1/1
5.032	—S—			73	7/3	
5.033	—S—			81	3/1	
				MeCN:DCM 1:1 (r.t.)	Not reacted	
5.034	—S—		NIS/TfOH	DCM (-40 °C)	89	1/8
				MeCN (-40 °C)	89	1.6/1
5.035	—S—			EtCN	81	2.2/1
				DCM (-40 °C)	73	1/4
				MeCN (-40 °C)	Not reacted	
				EtCN	Not reacted	

5.2.2 Influence of C5 protecting group modification

To date C5 modification of sialyl donor has been considered to be most powerful method for efficient α -sialylation. Together combining with α -stereodirecting anomeric leaving group N5-modified donors have been observed to give desired sialoside compounds in stereoselective manner. Notable, replacement of acetamido with more electron withdrawing functional groups are more successful. Demchenko and Boons have observed that conversion of C5 acetamido group into N-diacetyl can dramatically affect stereoselective sialylation reaction.⁴¹⁵ Therefore, at -40 °C and in presence of acetonitrile NIS/TfOH promoted coupling between Neu5Ac₂ donor and

2-(trimethylsilyl)ethyl-6-O-benzoyl- β -D-galactopyranoside acceptor afforded only α -anomer with 72 % yield in less than 5 min whereas Neu5Ac acceptor gave same exclusive anomer with 61 % yield in 2-6h.⁴¹⁵ In another published work by Demchenko and Boons, where *N*-diacetyl methylthiosialoside donor gives Neu5Ac₂(2 \rightarrow 8)Neu5Ac with a ratio 1.7/1 – α/β whereas *N*-acetyl methylthiosialoside affords racemic mixture (Neu5Ac(2 \rightarrow 8)Neu5Ac, 1.7/1 – α/β) at -40 °C in presence of acetonitrile.⁴¹⁶ Since then, chemically converted C5 into various functional groups including *N*-trifluoroacetyl (NHCOCF₃),^{348, 417-424} *N*-trichloroethoxycarbonyl (NHTroc),⁴²⁵⁻⁴³³ *N*-*tert*-butyloxycarbonyl (NHBoc),^{434, 435} *N*-benzyloxycarbonyl (NHCbz),^{422, 427} *N,N*-*tert*-butyloxycarbonylacetamido (NAcBoc),⁴³⁶⁻⁴³⁸ *N*-fluorenylmethoxycarbonyl (NHFmoc),^{427, 435} *N*-allyloxycarbonyl (NHAlloc),⁴²⁷ *N*-trichloroacetyl (NHCOCCl₃),^{427, 439-441} *N*-phthalimido,^{413, 442-444} azido (N₃),^{359, 445-452} isothiocyanato (NCS)^{451, 453} have been tested for the synthesis of Neu5Ac α (2 \rightarrow 6)Gal, Neu5Ac α (2 \rightarrow 3)Gal, Neu5Ac α (2 \rightarrow 8)Neu5Ac and Neu5Ac α (2 \rightarrow 9)Neu5Ac dimers (Scheme 5.6). Although efficient α -sialylation achieved with aforementioned C5 electron withdrawing functional groups, most of them exhibit only modest stereoselectivity with unhindered primary alcohols.

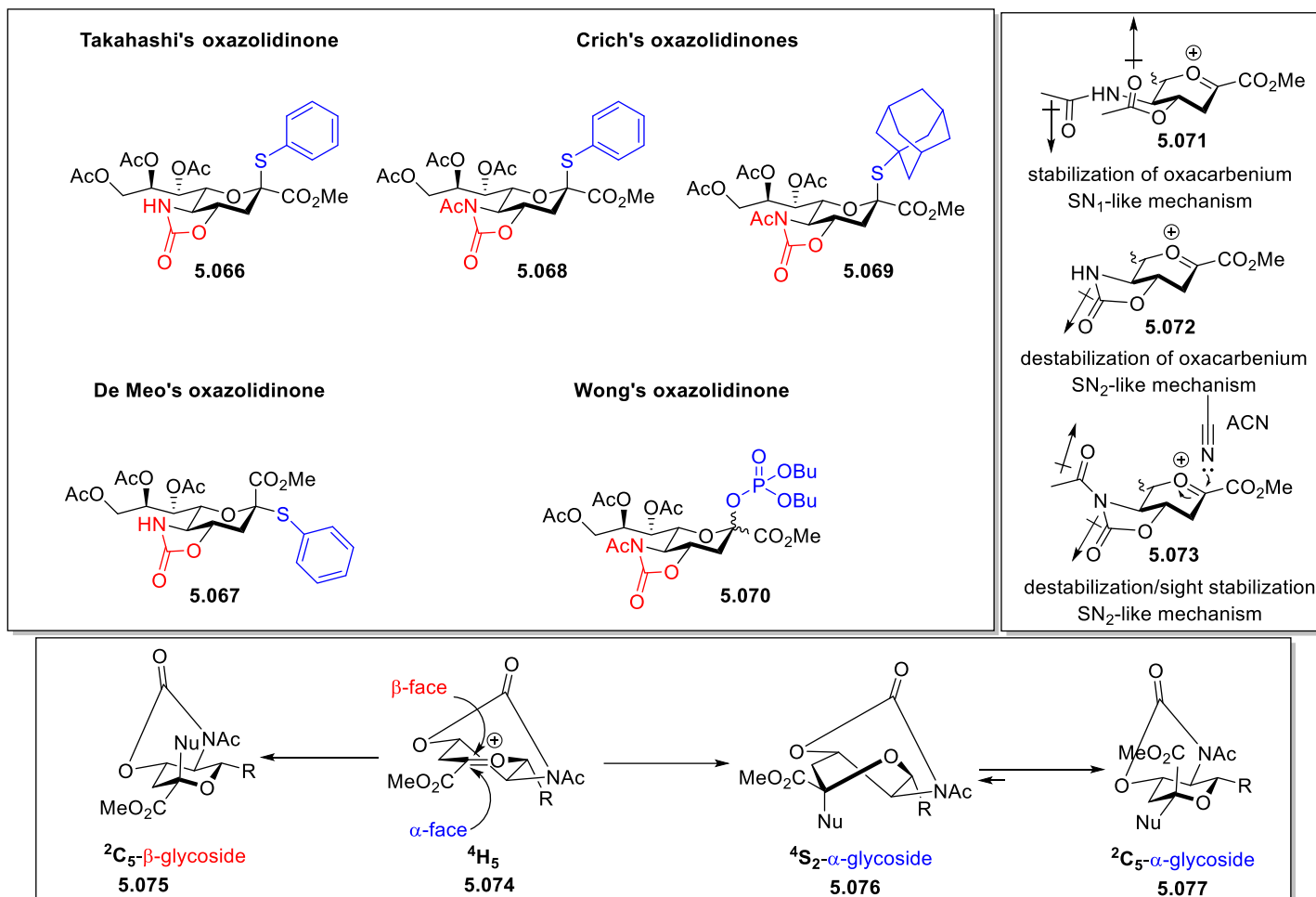


Scheme 5.6 C5 stereodirecting effect in sialylation.

5.2.3 N5,O4-cyclic protecting group-mediated sialylation

The installation of *trans*-fused cyclic oxazolidinone and its acetylated variation on sialoside moiety has been considered to be huge breakthrough in sialic acid glycosylation. Therefore, to improve α -stereoselectivity with unhindered primary and

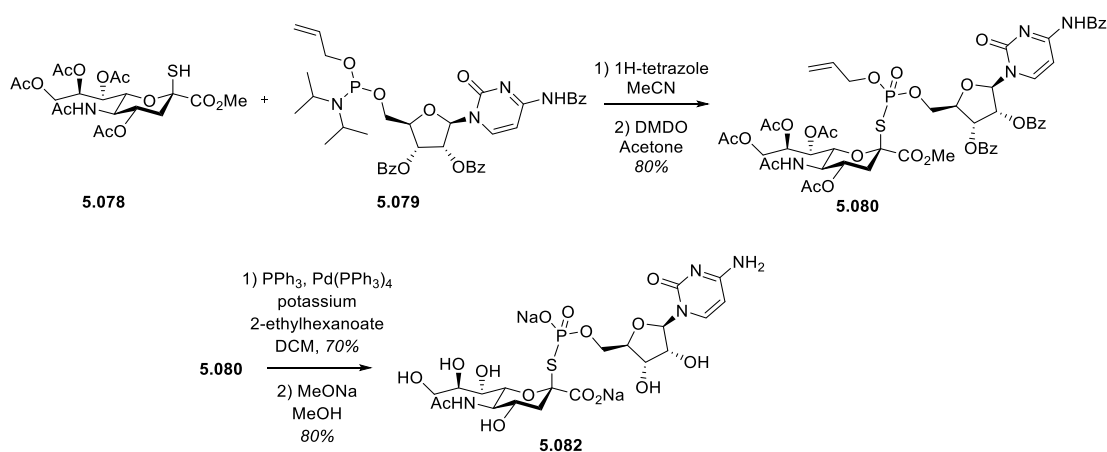
secondary alcohol acceptors, 5-*N*, 4-*O*-oxazolidinone *trans*-fused cyclic protecting group (Takahashi's oxazolidinone **5.066**, Scheme 5.7) with the best α -stereodirecting ability has been introduced for the first time by Takahashi *et al.*⁴⁵⁴ Subsequently, Farris and De Meo has confirmed the superiority of 5-*N*, 4-*O*-oxazolidinone- α -thiophenyl sialoside donor **5.067** in synthesis of α 2,6 Neu5Ac, α 2,3 Neu5Ac glycosidic bonds *via* obtaining sole α -anomer.⁴⁵⁵ At the same year Crich group has developed and examined *N*-acetylated variation of oxazolidinone ring with thiophenyl **5.068** and thioadamantyl **5.069** leaving groups.^{396, 456} The purpose of *N*-acetylation of the ring is to avoid post-glycosylation harsh deprotection condition. Wong and co-workers have reported that sialoside donor **5.070** with the combination of *trans*-fused cyclic *N*-acetyl-5*N*, 4-*O*-oxazolidinone and dibutyl phosphate as anomeric leaving group affords only α -anomer under Lewis acidic condition at -78 °C in DCM.⁴⁰⁵ Moreover, Crich *et al.* have successfully applied same condition for stereoselective *C*- and *S*-sialylation reactions.^{457, 458} According to plausible explanation has been given by Crich *et al.* 5*N*, 4-*O*-oxazolidinone ring **5.072** has larger dipole moment to slow down positive charge buildup at anomeric center and destabilize oxocarbenium ion that promotes SN₂-like mechanism.⁴⁵⁹ Furthermore, the presence of *trans*-fused oxazolidinone forces oxocarbenium to adapt half-chair conformation **5.074** (⁴H₅) where both faces are shielded equally. Consequently, attack of the nucleophile at either face is in equilibrium: β -face attack provides β -sialoside **5.075** whereas α -face attack passes through twist boat **5.076** (⁴S₂) and affords α -anomer **5.077**. More information on 5-*N*, 4-*O*-oxazolidinone and *N*-acetyl-5-*N*, 4-*O*-oxazolidinone and other α -stereodirecting sialylation factors have been reviewed by several research group.^{388, 391, 420, 459-466} In this chapter we are focused on synthesis of multivalent sialosides and their applications toward major sialic acid-specific receptors.



Scheme 5.7 Oxazolidinone donors and conformational analysis of nucleophilic attack on oxocarbenium ion.⁴⁶²

5.2.4 Thiosialosides

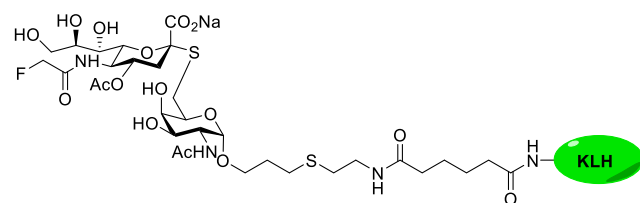
In carbohydrate chemistry, substitution of anomeric oxygen with sulfur atom has been widely exploited as enzymatically more resistant mimetic of *O*-glycosides. Besides being recognized as stable pharmacophores, *S*-glycosides have been observed to show similar or better biological activity.



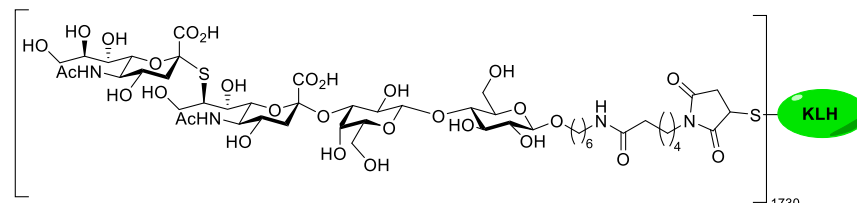
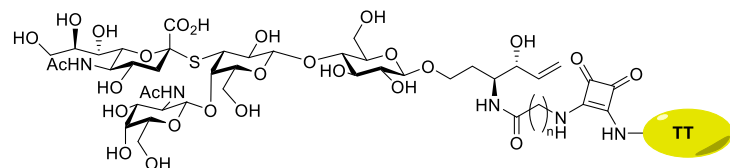
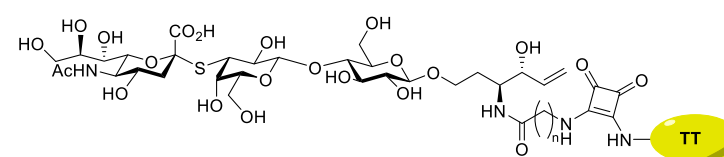
Scheme 5.8 Synthesis of the analogue of CMP-Neu5Ac with sulfur as glycosidic atom.⁴⁶⁷

Another salient particularity of thioglycoside is the bond distance between carbon and sulfur at the anomeric position. Therefore, the length of the C-S bond is 1.78 Å versus C-O with 1.42 Å which makes thioglycoside slightly more flexible.⁴⁶⁸ *S*-sialosides have been gained popularity due to their properties of being nonhydrolyzable mimics of *O*-sialosides and facile preparation. For comparative study purpose, Halcomb and Cohen have successfully synthesized thiosialoside analogue of CMP-Neu5Ac **5.082** after deprotection of **5.080** which is previously obtained through tetrazole-promoted coupling between β -mercaptosialoside **5.078** and cytidine-5'-phosphoramidite **5.079** followed by *in-situ* oxidation in presence of DMDO (Scheme 5.8).⁴⁶⁷ During determination of solvolysis rate in aqueous buffer, **5.082** has been found to be 50-times more slower than its natural analogue. Study also revealed that thiosialoside

exhibits 3-times less reactivity toward $\alpha(2,3)$ sialyl transfer. Taking advantage of enzymatic hydrolysis-resistant properties of the *S*-glycosidic bond, research groups have reported that *S*-sialosides exhibit excellent biological activities as well as natural sialosides. As an example, Ye et al. have shown that *N*-modified *S*-linked STn antigen – KLH (keyhole limpet hemocyanin) neoglycoconjugate **5.083** possesses good immunogenic response and induces anti-natural STn IgG titer.⁴⁶⁹ In other published work, Lin and co-workers have reported *S*-linked GD₃-KLH glycoconjugate **5.084** stimulates antibody production against both natural and unnatural GD₃, whereas Bundle and co-workers, have previously stated that tetanus toxoid (TT)-conjugated *S*-linked GM₂ **5.085** and GM₃ **5.086** analogues of natural gangliosides are also immunogenic antigens that exhibit similar results.^{470, 471} More on synthesis and application of thiosialosides will be discussed below.



5.083-STn analogue

5.084 GD₃-KLH5.085 GM₂ analogue5.086 GM₃ analogueScheme 5.9 Biologically active *S*-sialosides.^{469, 471, 472}

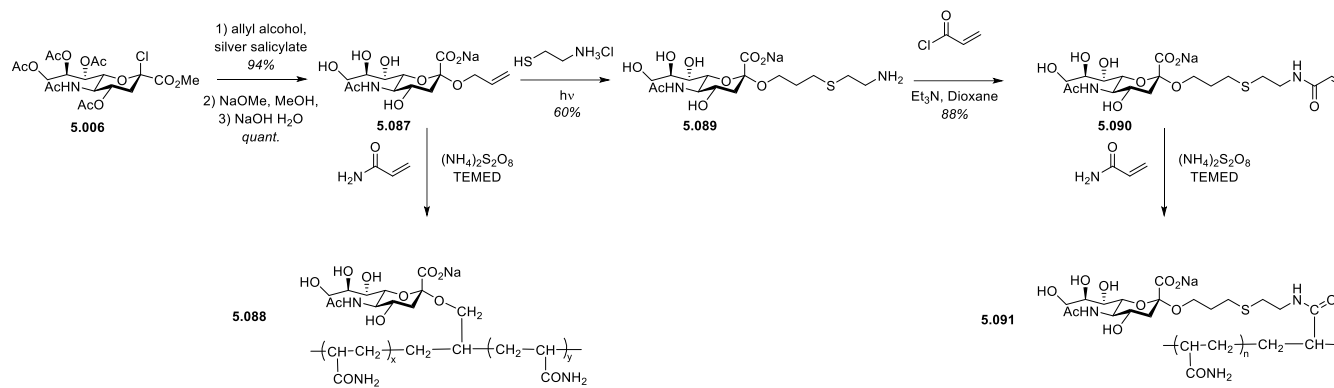
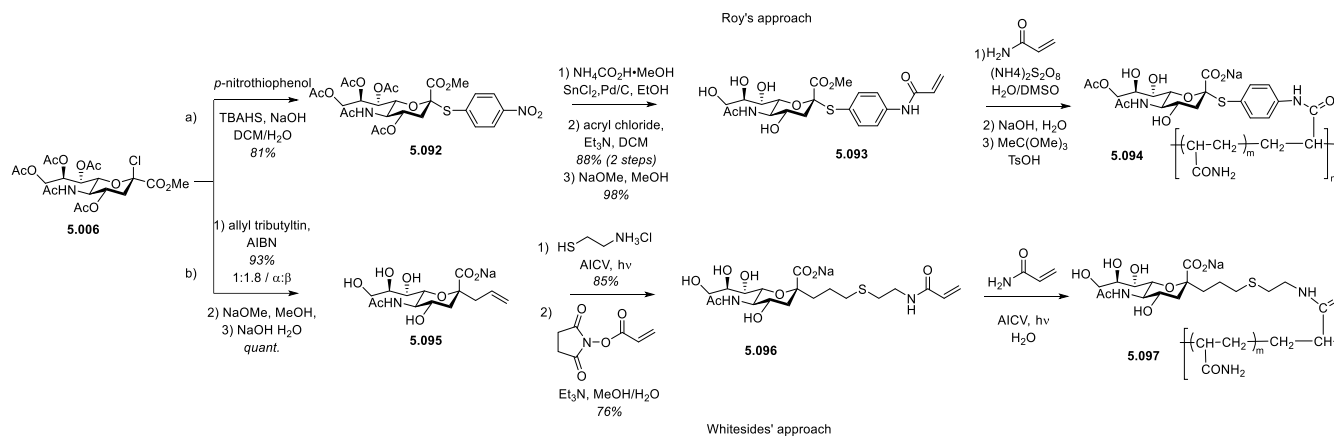
5.2.5 Multivalent Sialoconjugates

As mentioned earlier, usually monomeric saccharides including sialosides exhibit weak binding properties and poor specificity toward their natural receptors (K_D in μM and mM range).⁴⁷³ However multivalent presentation of sialosides has been considered to be powerful tool to overcome this limitation by virtue of glycoside cluster effect. To date, based on scaffolds, several sialic acid-containing neoglycoconjugates including sialoproteins, sialopeptides, sialopolymers, sialodendrimers, sialoliposomes and sialonanoparticles with different ligand valencies and spatial arrangement have been reported. In this chapter we are more focused on the synthesis of biologically active multiple Neu5Ac bearing synthetic scaffolds from organic chemist's point of view. For the sake of clarity, we will give an example of 3 most studied class of sialic acid-containing neoglycoconjugates: Sialopolymers, Sialodendrimers and Sialoliposomes

5.2.5.1 Sialopolymers

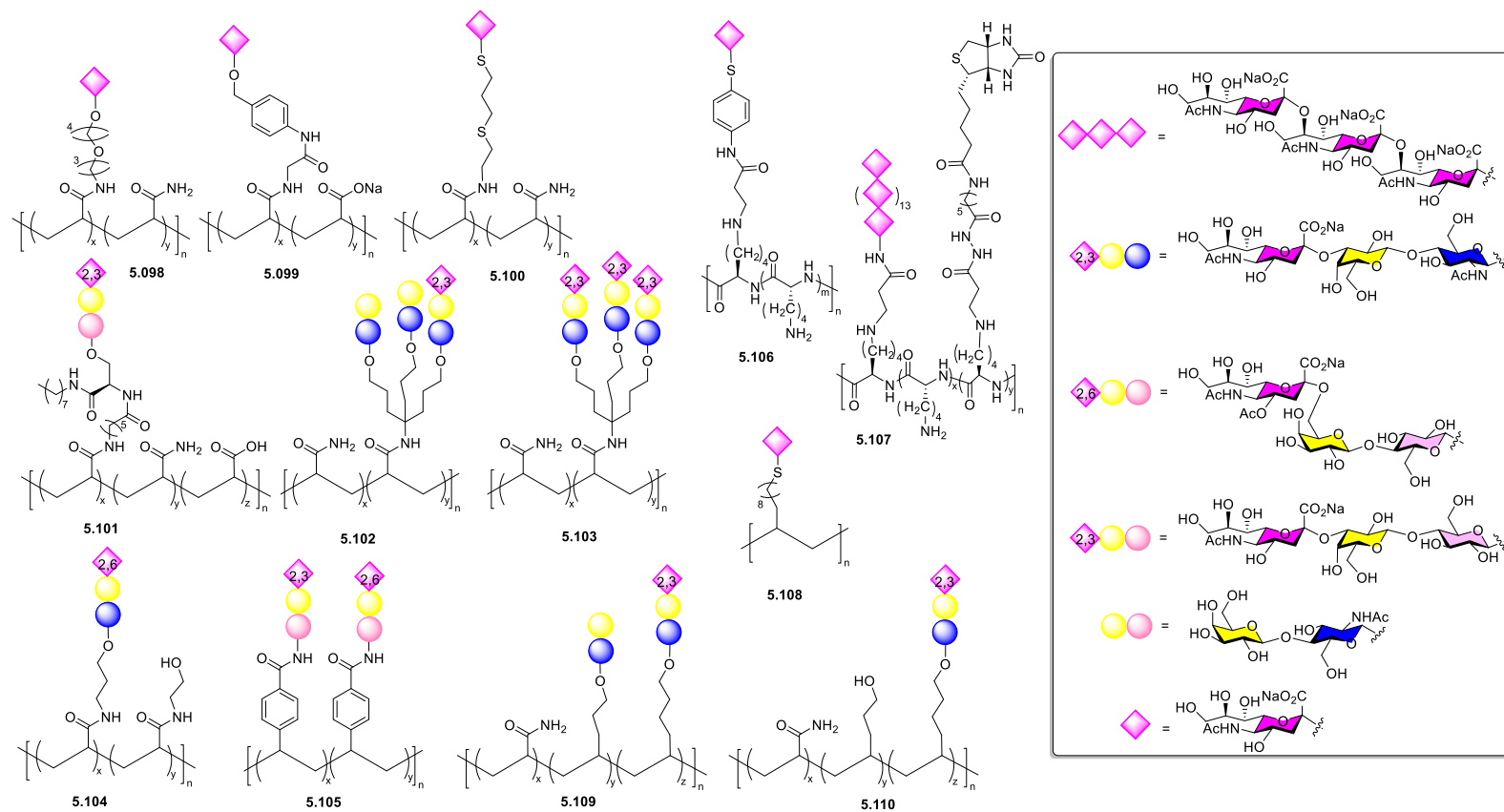
Sialic acid-containing polymers are one of the earliest synthetic macromolecules reported at the end of 80s. Sialopolymers are the most extensive studied class of synthetic sialomacromolecules that have been mainly targeted Influenza virus surface glycoproteins (HA, NA), Alzheimer's disease and cancer related siglec family members. The initial reports for sialopolymer synthesis were based on radical-initiated homo- or copolymerization of monomeric sialic acid with acrylamide backbone. However, the field have been dominated by few research groups Roy,⁴⁷⁴⁻⁴⁸⁰ Whitesides,⁴⁸¹⁻⁴⁸⁷ and Matrosovich⁴⁸⁸⁻⁴⁹⁰ for almost a decade through providing valuable information on the interactions between sialic acid and its receptors. Roy group have first reported the copolymerization of Neu5Ac derivatives and acrylamide using ammonium persulfate-initiated electron-transfer polymerization (Scheme 5.10).^{474, 475} The key product – exclusive α -allyl Neu5Ac **5.087** was synthesized in excellent yield using silver salicylate which was readily deprotected by

NaOMe/MeOH and aqueous NaOH. Subsequently, ammonium persulfate-initiated copolymerization with acryl amide in presence *N,N,N,N*-tetramethyldiamine (TEMED) led to formation of **5.088**. For comparative study purpose, more exposed – longer spacer possessing glycopolymer **5.091** was also synthesized in 3 steps (through thiol-ene click and amidification reactions then copolymerization). During study of biological activities, compare to neoglycoproteins Neu5Ac α (2 \rightarrow 6')Lac-BSA and Neu5Ac α (2 \rightarrow 3')Lac-BSA, more exposed sialopolymer **5.091** has been found to exhibit superior inhibitory potency. Although, Roy's sialopolymer have failed toward viral NA activity, HA (Influenza A virus (H3N2)) binding to chick red blood cells have been successfully inhibited.⁴⁷⁶ Matrosovich *et al.* have also observed that polyacrylate-based sialopolymers dominate on monomeric Neu5Ac α 2 \rightarrow 3'Lac and 4-NH₂-BnO Neu5Ac derivatives at fetuin binding (FB) assay toward H3 subtypes of Influenza A virus.⁴⁸⁹ As a result, the synthetic macromolecules containing 10 % Neu5Ac, have shown 408-fold enhanced relative potency versus monomeric Neu5Ac α (2 \rightarrow 6')Lac. Furthermore, taking advantage of enzymatically stable properties of *S*- and *C*-glycosidic bonds, Roy,⁴⁷⁷ Nagy^{491, 492} and Whitesides^{482, 485, 487} research groups have developed polymeric unnatural sialosides with excellent inhibitory potency. Generally, the stereoselective *S*-sialosides were synthesized either *via* direct SN₂-type substitution between thiol and glycosyl halide or through more sophisticated, high-yielding PTC (phase transfer catalyst) condition that have been developed by Roy research group.^{250, 377, 381, 395, 478, 493, 494} Interestingly, developed by the same group, 9-*O*-Acetyl poly-*S*-sialoside **5.094** have shown excellent inhibitory capacity toward esterase activity of Influenza C virus hemagglutinin.^{478, 495} Nagy and Whitesides have been copolymerized *C*-sialosides with 2-amidoglucose and acrylamide employing earlier described method by Paulsen and Matschulat which gives inseparable mixture (α : β / 1:1.8) and requires challenging chromatographic isolation.⁴⁹⁶

Scheme 5.10 Copolymerization of *O*-sialosides and acrylamide.^{474, 475}Scheme 5.11 *S*- and *C*-sialoside acrylamide copolymerization.^{477, 487}

Since 90s, a wide variety of polymeric *N*-, *C*-, *O*- and *S*-sialosides based on polyacrylamide (**5.098-5.104**),^{481, 488, 497-501} polyacrylic acid derivatives,⁵⁰² polystyrene (**5.105**),⁵⁰³ polylysine(**5.106-5.107**),^{479, 504} poly-*L*-glutamic acid,⁵⁰⁵ and others(**5.108-5.110**)^{498, 506, 507} have been synthesized and tested (Scheme 5.12). Among them, reported by Nagy and co-workers, *C*-sialoside constructed on 2-amidoglucose polymer, containing 5 % sugar moiety (IC₅₀ = 1mM) exhibited 4-fold enhanced inhibitory potency versus α -methyl Neu5Ac monomer (IC₅₀ = 4mM) whereas 30 % Neu5Ac-presented copolymer (IC₅₀ = 200 nM) demonstrated 20000-fold increased potency toward Influenza virus hemagglutinin.⁴⁹¹ In another research work, Inokouchi *et al.* reported polyvalent GM₃ epitope containing hydrophobic alkyl chain and constructed on polyacrylamide backbone **5.101** have shown strongly inhibit cell proliferation against NIH3T3 cells as GM₃ resistant cells.⁵⁰⁸ Furthermore, Usui and co-workers designed and synthesized glycopolyptide carrying $\alpha(2\rightarrow3')$ and $\alpha(2\rightarrow6')$ sialylated glycans with long and short spacer as inhibitors of human and avian influenza A virus hemagglutinin. As result glycopolyptide containing GlcNAc $\beta(1\rightarrow3')$ Gal repetitive units **5.111** (IC₅₀ = 38 μ M and 19 μ M for H5N1 and H3N2), and **5.112** (IC₅₀ = 0.29 μ M for H3N2) exhibited promising inhibitory potencies (Scheme 5.13).⁵⁰⁹ Synthesis of glycopolymers became more widespread last two decades due to their advantageous properties in biorecognition phenomenon. Although earlier polymerization technique was based on free radical polymerization, nowadays controllable polymerization techniques such as atom transfer radical polymerization (ATRP) and reversible addition-fragmentation chain-transfer polymerization (RAFT) have been more beneficial. A significant breakthrough in the area arose from the discovery of copper-assisted azide-alkyne cycloaddition (CuAAC) click reaction.⁵¹⁰ Therefore, controlled or living polymerization techniques together combining with click reactions give access to prepare glycopolymers with predicted weight and narrow sugar moiety distribution. Moreover, click reaction is compatible

with wide variety of functional groups and solvents and allows post polymerization modification attainable.



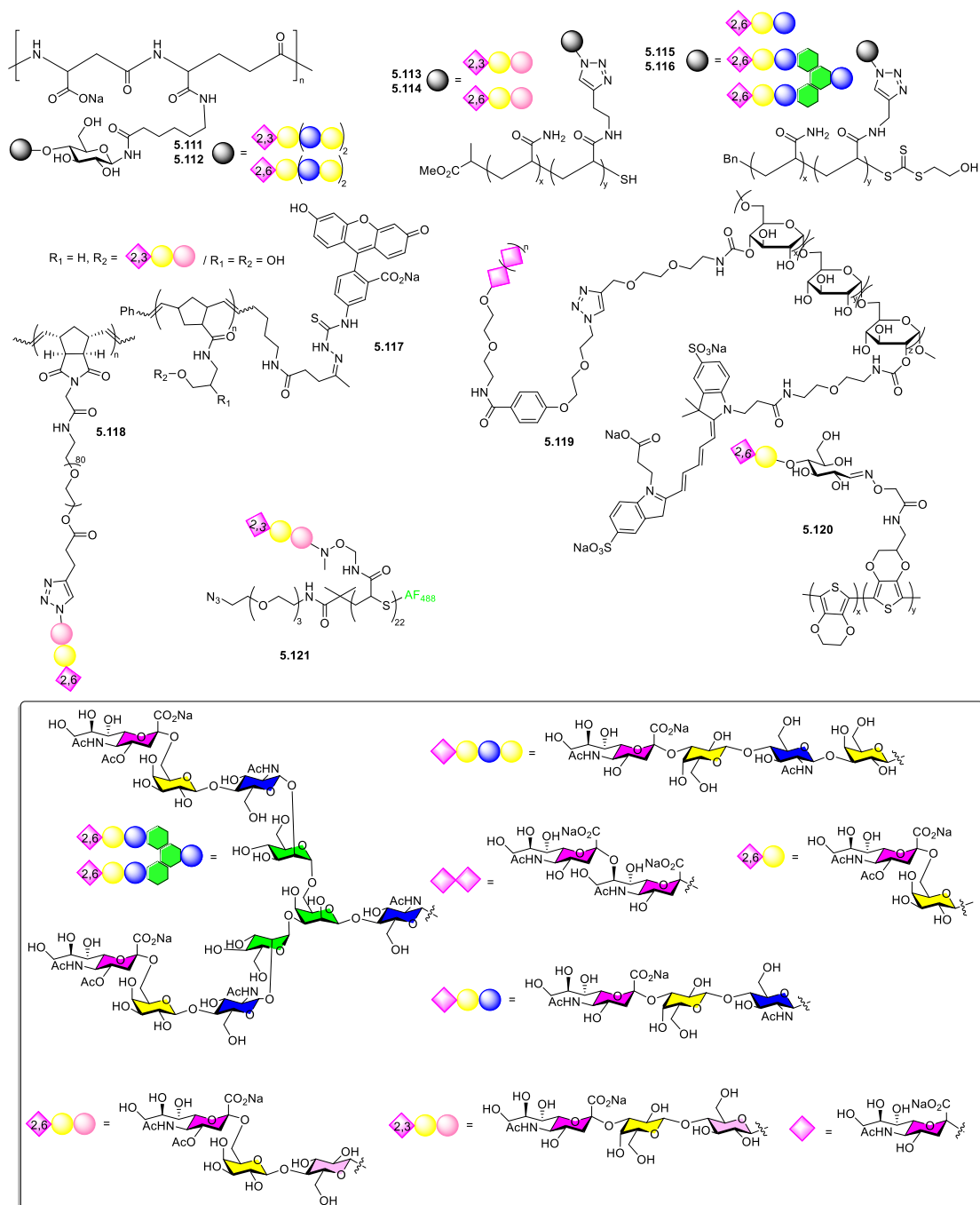
Scheme 5.12 Some examples to linear sialopolymers. 479, 481, 488, 497-508

Miura and co-workers synthesized Neu5Ac α (2 \rightarrow 3')Lac and Neu5Ac α (2 \rightarrow 6')Lac carrying polymers **5.113-5.114** *via* using “post-click” and living polymerization techniques.⁵¹¹ During biological evaluation, authors indicated that the density of sugar moiety around backbone has shown directly influence inhibitory potency. Therefore, at HI assays, lowest K_i values have been determined for α 2,3 and α 2,6 are 81 μ M (H1N1) and 48 μ M (H3N2) respectively. In another tremendous work by Tanaka and co-workers, without using protecting group RAFT polymerization in combination with click chemistry afforded 6'-sialyllactose **5.115** and complex-type sialyl *N*-linked oligosaccharide (*N*-glycan) **5.116**.⁵¹² The comparative biological study toward human and avian influenza at HI assay showed that *N*-glycan carrying polymer **5.116** binds to A/Memphis/1/1972 (H3N2) with $K_a = 4.9 \times 10^{-7}$ M whereas **5.114** ($K_a = 2.5 \times 10^{-4}$ M) and fetuin ($K_a = 7.8 \times 10^{-5}$ M) bind 510 and 160 times less tidily. Interestingly, **5.116** possessing biantennary Neu5Ac α (2 \rightarrow 6)Gal linkage has shown to bind to A/duck/Hong-Kong/313/4/1978 (H5N3) with $K_a = 6.3 \times 10^{-5}$ M which is specific for Neu5Ac α (2 \rightarrow 3)Gal linkage.

Ring-opening metathesis polymerization (ROMP) as an alternative to radical polymerization strategy has also applied in glycopolymer synthesis especially for signal transduction studies. Main drawbacks of this technique are possessing limited solubility in organic and aqueous solvents and allowing side-product formation. Additionally, using succinimide as a side chain can be beneficial in post-polymerization modification. For example, reported by Kiessling *et al.* fluorescein-labeled, trisaccharide-containing glycopolymer **5.117** which is synthesized through ROMP technique has used to visualize B cell surface glycoprotein CD22 and its role for *trans* interaction in B cell signaling.⁵¹³ Later, using same technique the group reported that designed 2,4-dinitrophenyl (DNP) and CD22 ligand presenting hapten successfully promotes B cell activation.⁵¹⁴ Olsen and co-workers synthesized Neu5Ac α (2 \rightarrow 6')Lac containing brush polymer **5.118** and tested toward influenza A virus A/WSN/1933(H1N1) hemagglutinin.⁵¹⁵ Biostudy revealed that at HI assay

monomeric trisaccharide does not show any inhibition on the contrary while using sialopolymer virions have seen to bind to brush polymer rather than erythrocytes.

To date, sialopolymers remain extensively studied class of neoglycoconjugates. Sialic acid presenting glycopolymers constructed on polydextran **5.119**,⁵¹⁶ PEDOT (poly(3,4-ethylenedioxythiophen)) **5.120**⁵¹⁷ and others **5.121**⁵¹⁸⁻⁵²⁰ have also synthesized and tested toward various sialic-acid binding receptors.

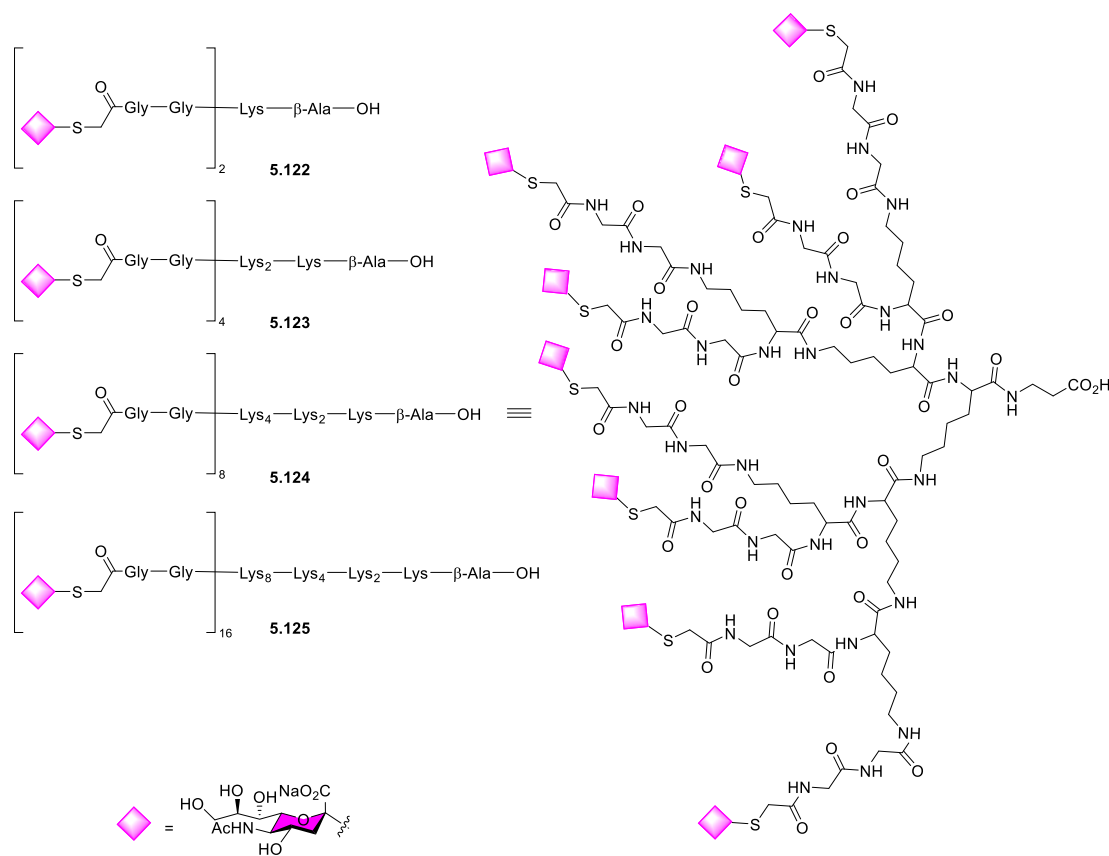


Scheme 5.13 Some other reported sialopolymer.^{509, 511-520}

5.2.5.2 Sialodendrimers

Efforts for blocking influenza virus attachment and replication have driven carbohydrate chemists to design and develop bioinspired synthetic polyvalent sialoconjugates as anti-adhesive agents and inhibitors. As mentioned above, with defined molecular weight, peripheral end group and internal cavities, three-dimensional and monodisperse dendrimers are best known for targeted and controllable drug delivery. Together with molecularly defined multivalent scaffolds and various architectural designs, glycodendrimers are considered to be potent adjuvant and immunostimulating agents. Synthetic sialic acid bearing polyvalent glycoconjugates have been showing strong binding properties are appealing synthetic targets since sialic acid-binding receptors are predominantly found on the surface of various cells. Being such glycoconjugates, sialodendrimers have emerged as promising antiviral agents in the literature early 1990s. Using phase transfer catalyst, Roy group first synthesized multi-antennary glycoprotein-like *S*-sialoside dendrimers.^{385, 521} Constructed on lysine core and glycine spacer, sialodendrimers **5.122-5.125** with 2-, 4-, 8- and 16-valencies have been observed to inhibit influenza virus binding to erythrocytes at concentrations of 625, 312.5, 156 and 19 mM respectively (Scheme 5.14). After these promising results, sialic acid-bearing dendrimers have gained more attention and synthesized by various research groups as potential polyvalent inhibitors of viral and bacterial glycoproteins. Roy and Zanini designed and synthesized up to hexadecameric α -thiosialoside-decorated PAMAM poly(amidoamine) dendrimer to investigate their inhibitory potency toward animal lectin (*Limax flavus* (FLA)) as a model for a large number of Neu5Ac-protein binding interactions.⁵²² The generations were conjugated through amino-acid coupling with orthogonally protected 3,3'-iminobis(propylamine) derivatives **5.128a** and **5.128b** which then deprotected (Scheme 5.15). To rapidly increase valency, **5.129** was coupled with hexamethylenediamine and tris(2-aminoethyl)amine to afford tetra- and hexavalent dendrimers. Subsequently, treatment of **5.127** with *N*-chloroacetylated

cores **5.130** and **5.132** in presence of triethylamine, following deacetylation and saponification reactions gave targeted thiosialoside dendrimers **5.131** and **5.133** with excellent yields. During biostudy at enzyme-linked lectin inhibition assay (ELLA), it was found that binding of human α 1-acid glycoprotein (Orosomucoid) to FLA was inhibited by sialodendrimers. Especially, versus monomer Neu5Ac α N₃ (IC₅₀ = 1.5 μ M), tetra- and dodecameric thiosialoside dendrimers were observed to exhibit 127- and 182-fold enhancement in relative potencies.

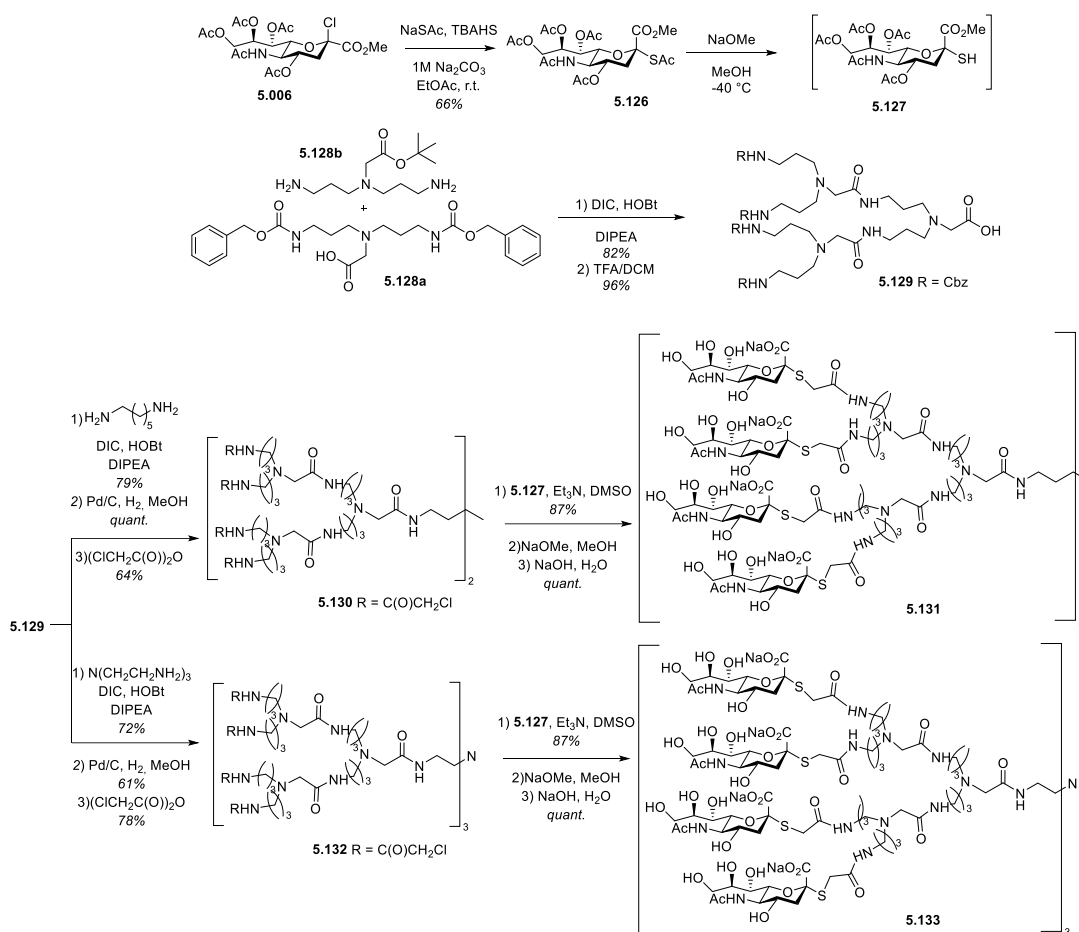


Scheme 5.14 Multi-antennary glycoprotein-like thiosialoside dendrimers.^{385, 521}

So far, PAMAM and PPI (polypropylene imine) cores are the most heavily exploited scaffolds by virtue of their less toxicity and commercial availability. Another

advantage of aminated scaffolds is that direct anchoring capacity of reducing sugar moieties into dendrimers through reductive amination, amidation and thioamidation reactions easily realizable. Sialic acid decorated PAMAM⁵²³⁻⁵³⁰ and PPI^{524, 531, 532} are the most cited sialodendrimers of the last two decades. As an example, tested against 3 subtypes (H1N1, H2N2 and H3N2) of influenza A virus using HI assay sialic acid attached to G4 PAMAM dendrimer **5.134** (Scheme 5.15) found inhibiting all H1N1 and 3 H3N2 subtype strains with up to 170-fold enhanced relative potency versus monomeric sialic acid.⁵²⁶ Good *et al.* synthesized two types of sialic acid conjugated PAMAM dendrimers through C_1 amidation and thioamidation of isothiocyanato-terminated spacer.^{527, 528} Bioevaluation revealed that both dendrimers inhibit almost equally β -amyloid A β -protein and reduce neurotoxicity. β -amyloid A β -protein has been considered a hallmark of Alzheimer's Disease and their abnormal aggregation leads to neurodegeneration and ultimately dementia.⁵³³ Moreover, authors demonstrate that free anomeric hydroxyl containing dendrimer shows modestly less efficiency versus free carboxylate. Using same strategy (C_1 amidation), McReynolds *et al.* synthesized sulfated sialo-PAMAM dendrimer in order to investigate their binding properties against HIV.⁵²⁵ Dendrimer possessing sulfo group at 6 position was observed to inhibit HIV1 through binding gp120 with $IC_{50} = 23 \mu M$ (ELISA). In another research work by Schengrund and Thompson, GM₁-conjugated PPI dendrimer was observed to inhibit cholera toxin B subunit and heat labile enterotoxin of *E. coli* with 15- and 1000-fold lower concentrations versus native GM₁ and free oligosaccharide.⁵²⁴ Although PAMAM and PPI dendrimers are highly investigated, these amine containing macromolecules still suffer from some limitations including toxicity in physiological conditions. To overcome this limitation and reduce toxicity of the PAMAM scaffold Roy *et al.* proposed and synthesized hybrid dendrimer through reductive amination reaction between thiosialoside decorated and PEGylated scaffold and naturally-occurring, non-toxic and biodegradable chitosan **5.135**.⁵³⁴ In 2011, Haag and co-workers introduced new class of sialodendrimer architecture as

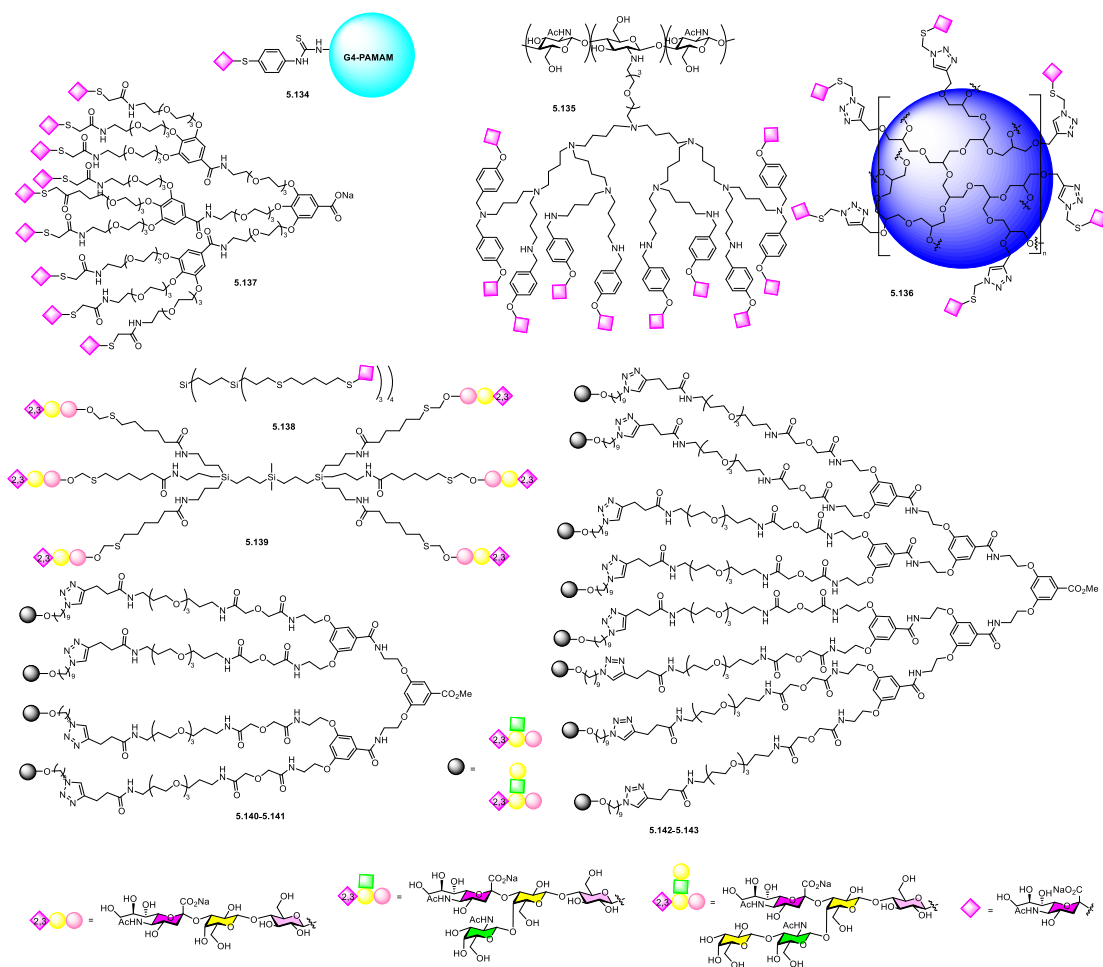
powerful tool to fight against influenza virus.⁵³⁵ Constructed on biodegradable polyglycerol backbone and decorated through click reaction, sialodendrimers were seen to inhibit binding and fusion of influenza A virus. During biostudy it has been uncovered that the size of the hyperbranched dendrimer is crucial. Thus, **5.136** with 50 nm was 7000-fold more effective than *O*-sialodendrimer with 3 nm.



Scheme 5.15 Synthesis of PAMAM-based Sialo-S-dendrimers with various valencies.⁵²²

The incorporation of a variety of scaffolds, differing building block, shapes, and spatial arrangement, contributed to broaden the arsenal of sialodendrimers. To this end, built on gallic acid **5.137**,⁵³⁶ carboxilene **5.138-5.139**⁵³⁷⁻⁵⁴⁰ and α -resorcylic acid

derivatives **5.140-5.143**,⁵⁴¹ sialic acid bearing dendrimer are the alternative sialoconjugates found in the literature.



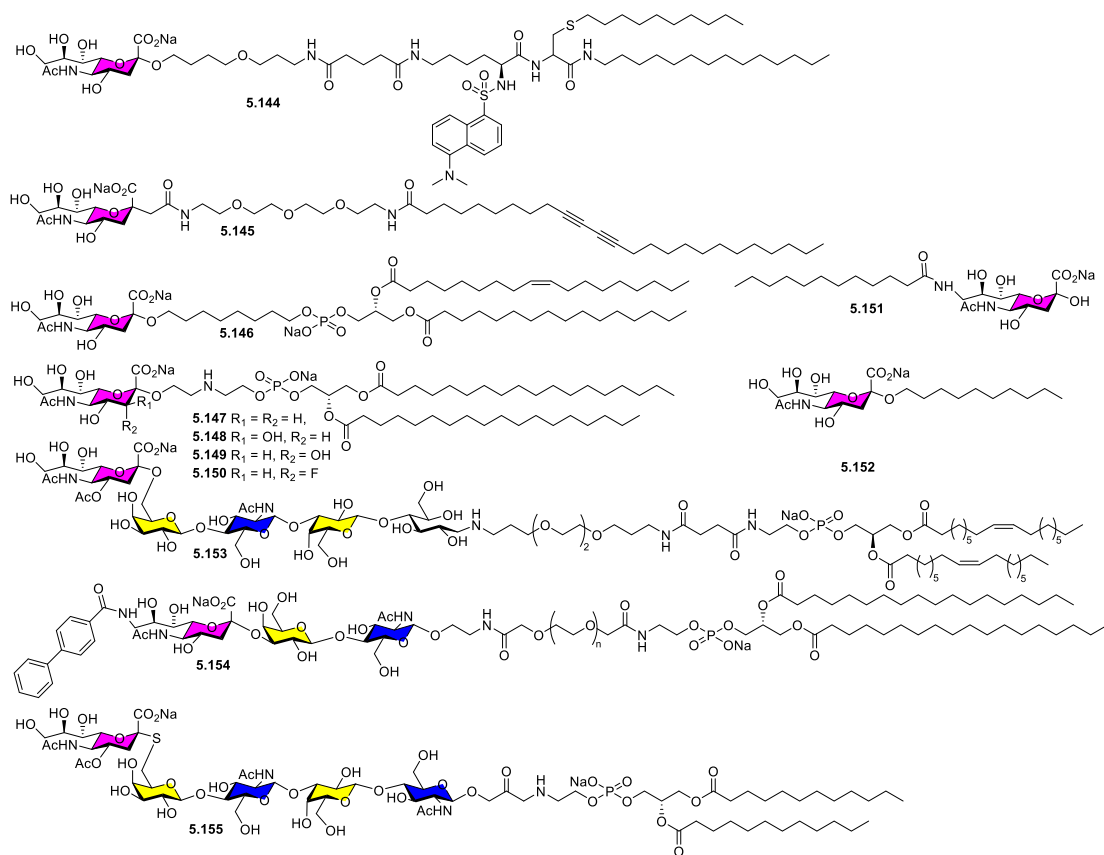
Scheme 5.16 Sialic acid bearing dendrimers.^{526, 534-541}

5.2.5.3 Sialoliposomes

Among multivalent sialoconjugates, self-assembling sialoliposomes or sialolipids have been widely studied due to their numerous advantages including biodegradability, biocompatibility and lower or non-specific toxicity. Moreover,

commercial availability of phospholipid segments such as DSPE-PEG (1,2-Distearoyl-sn-glycero-3-phosphoethanolamine-Poly(ethylene glycol)), DOPE (dioleoylphosphatidylethanol-amine), DOTAB (1,2-dioleoyl-3-trimethylammonium propane), DPPC (dipalmitoylphosphatidylcholine) is another facilitating feature that allows carbohydrate chemists to explore the field. Several research groups have hitherto designed and synthesized sialic acid containing liposomes for various receptors including influenza virus surface glycoproteins. In 1992, Whitesides and co-workers reported, synthetic liposome from **5.144** (Scheme 5.17) incorporated with fluorescent (5-dimethyl amino naphthalene-1-sulfonyl) group and containing sialic acid at focal point inhibits hemagglutination of erythrocytes with $K_i \approx 20$ nM at HI assay whereas monomer exhibits 10000-fold higher K_i value.⁵⁴² However multivalent sialoconjugates failed to block viral infectivity. One year later, Bednarski *et al.* synthesized and tested C-sialoside conjugated to single alkyl chain **5.145** which was elongated through alkyne-alkyne (Glaser) coupling, exhibited 30000-fold enhanced relative potency versus monovalent α -methyl Neu5Ac toward erythrocytes hemagglutination by Influenza virus.⁵⁴³ It was first time a synthetic sialoconjugates reached that much higher relative potency. Developed by Koketsu and co-workers, sialylation of β -chloro sialoside donor with octyl-linked phospholipid in presence of silver triflate generated new type of sialolipid **5.146**.⁵⁴⁴ Investigation of binding properties against human and simian rotaviruses, it was revealed that required sialoliposome concentrations for 50 % inhibition (IC_{50}) against MO (human) and SA-11(simian) strains were 16.1 and 4.35 μ M respectively. These results were corresponding 10000- and 1000-fold enhancement in relative potencies over monomeric Neu5Ac. With the aim to explore the role of hydrogens at C3 position, Guo and co-workers developed sialoliposome series **5.147-5.150** where either axial or equatorial hydrogen was substituted by fluorine atom or hydroxyl group.⁵⁴⁵ Among them axial fluorine containing sialoliposome **5.150** demonstrated much better binding properties toward influenza virus A/Aichi/2/68 (H3N2) hemagglutinin and inhibited

the catalytic hydrolysis of viral sialidase in lower micromolar range. Recently, Kikkeri and Yadav have prepared two types of sialomicelles from **5.151-5.152** to study orientation of sugar moieties during carbohydrate-protein interactions.⁵⁴⁶ SPR studies toward five different lectins (*Sambucus nigra* and *Limax Flavus* agglutinins, E- and P-selectins, CD22-Fc) have been compared. Although generated micelles demonstrated similar K_D toward E- and P-selectins, surprisingly plant and animal lectins were observed to bind more tidily to C9-derivative. In case of CD22-Fc, SPR assay demonstrated that C2-sialomicelles were discriminated. Overall, obtained these results were promising for further development of potent inhibitors for different types of sialic acid-specific receptors. An alternative strategy in preparation of effective sialoliposome was developed by Wang *et al.*⁵⁴⁷



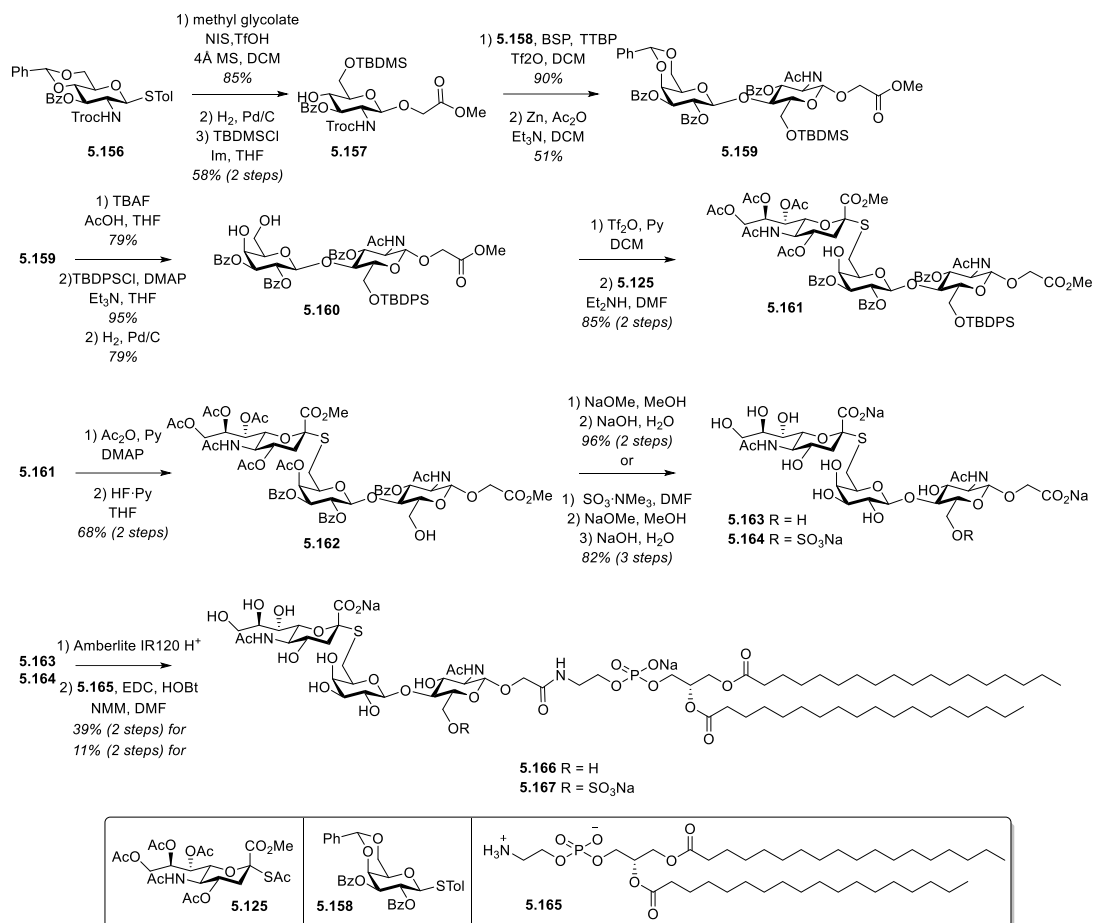
Scheme 5.17 Reported sialic acid containing liposomes.^{542-546, 548-550}

Therefore, using Fmoc method amine-terminated linker attached to commercially available DOPE which was subsequently coupled with Sialylneolacto-*N*-tetraose c (LSTc) through reductive amination reaction. Self-assemblies from 7.5 % LSTc containing **5.153** were observed to be best multivalent presentation that bind and inhibit efficiently Influenza A virus H1N1 and H3N2 strains at nanomolar concentrations. As we mentioned earlier, Sialoadhesin from Siglec superfamily has known to bind α 2,3 Neu5Ac terminated glycan. However, substitution of 9-OH by 9-*N*-biphenyl carboxamide (BPC) was previously seen to overthrow natural epitope with higher binding affinity.⁵⁴⁸ Therefore Paulson and co-workers designed and

synthesized sialolipid **5.154** with aim to investigate binding properties of multivalent 9BPC-Neu5Ac α (2 \rightarrow 3')LacNAc.⁵⁴⁹ Generated liposomal nanoparticles were observed to induce Sn-dependent activation of antigen specific T cells through targeting bone marrow derived macrophages.

In recent years, sialoliposomes incorporating the sulfur atom within glycosidic bond have been emphasized to be beneficial. Especially, during combatting against influenza virus sialidase, sulfur linked sialoconjugates have seen to be more effective. In 2018, Liang and co-workers synthesized and generated *S*-linked Neu5Ac α (2 \rightarrow 6')di-LacNAc containing sialolipid **5.155**.⁵⁵⁰ Generated liposome was determined to inhibit RBCs with K_i value at micromolar range. Disappointingly none of prepared liposomal formulations, could block A/WSN/33 (H1N1) infectivity. However, developed by same group *S*-linked Neu5Ac α (2 \rightarrow 6')LacNAc containing liposome moderately inhibits same IAV strains.⁵⁵¹ As it has shown in Scheme 5.18, linear synthesis began with glycosylation of **5.156** donor with methyl glycolate acceptor in presence of NIS and TfOH. Subsequently, opening benzylidene ring under hydrogenolysis condition and regioselective protection of primary alcohol with *tert*-butyldimethylsilyl chloride in presence of imidazole afforded **5.157** in moderate yield. Upon activation of thiogalactoside donor **5.158** using BSP/Tf₂O and TTBP led to formation of disaccharide in 90 % yield. Replacement of NHTroc by NHAc was performed under Zn/Ac₂O conditions. Replacement of acid sensitive TBDMS by more stable TBDPS was started by deprotection of **5.159** in presence TBAF/AcOH. After protection C6 hydroxyl in presence of TBDPSCl, Et₃N, resulted intermediate was subjected to hydrogenolysis. Treatment of diol **5.160** with triflic anhydride followed by *in-situ* substitution gave *S*-linked trisaccharide **5.161** in 85 % for 2 steps. Further, desilylation and saponification reactions gave fully deprotected trisaccharide **5.163**. For comparative study purpose authors also synthesized C6-sulfo derivative. After successful protection and deprotection steps, **5.162** was first treated with sulfur trioxide trimethylamine complex, then fully deprotected using Zemplén condition and

basic hydrolysis to give **5.164**. Although sulfo group was sensitive to acidic condition, using acidic resin, authors first acidified both hydrophilic segments, then amino acid coupling with amine functionalized phospholipid **5.165** was performed using EDC/HOBt. At virus neutralization and HI assays, liposome from **5.166** was observed to be more potent than its sulfo congener.

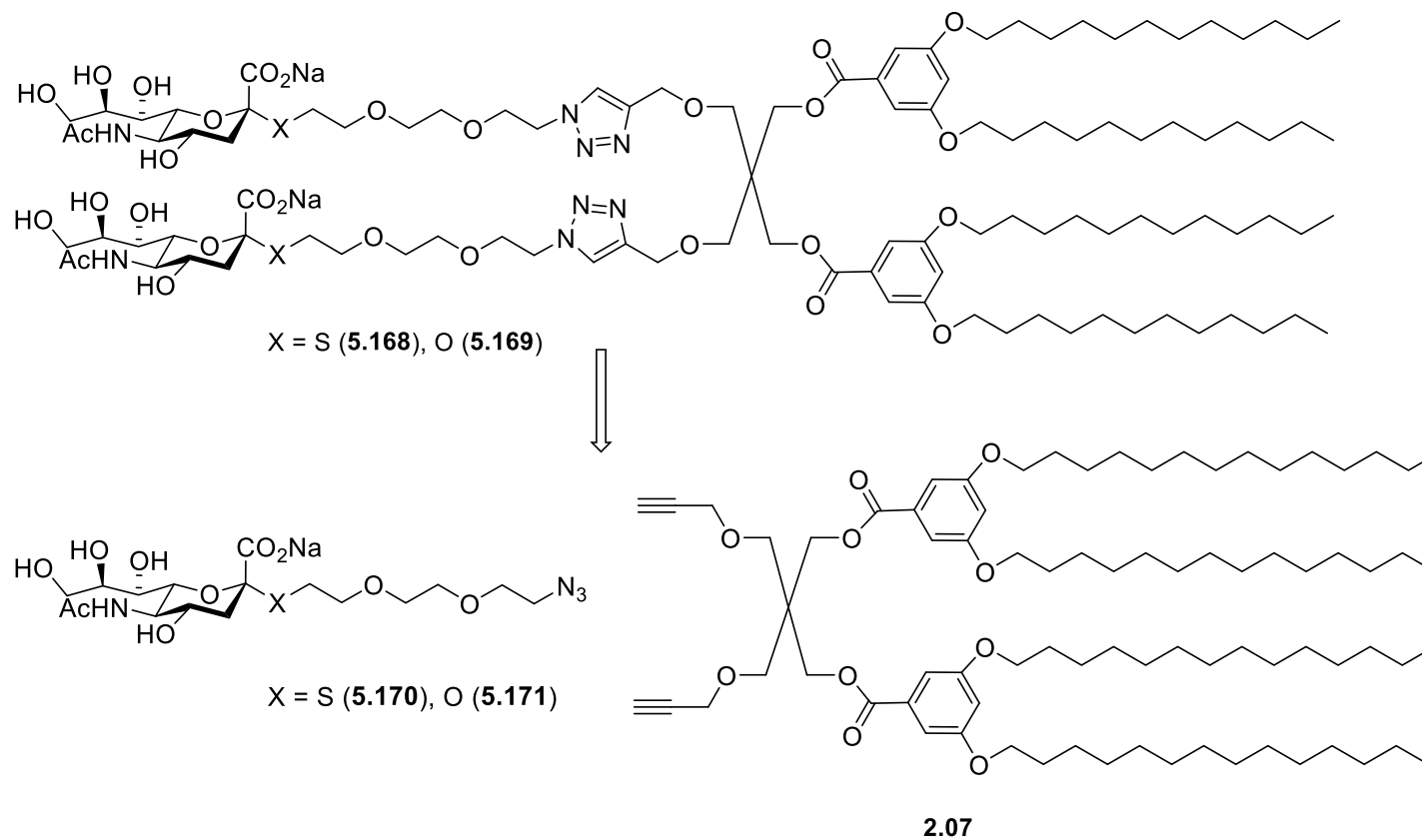
Scheme 5.18 Synthesis of *S*-Sialoliposome.⁵⁵¹

5.3 Aim of the project: Synthesis of new class of sialoconjugates: Sialodendrimersomes

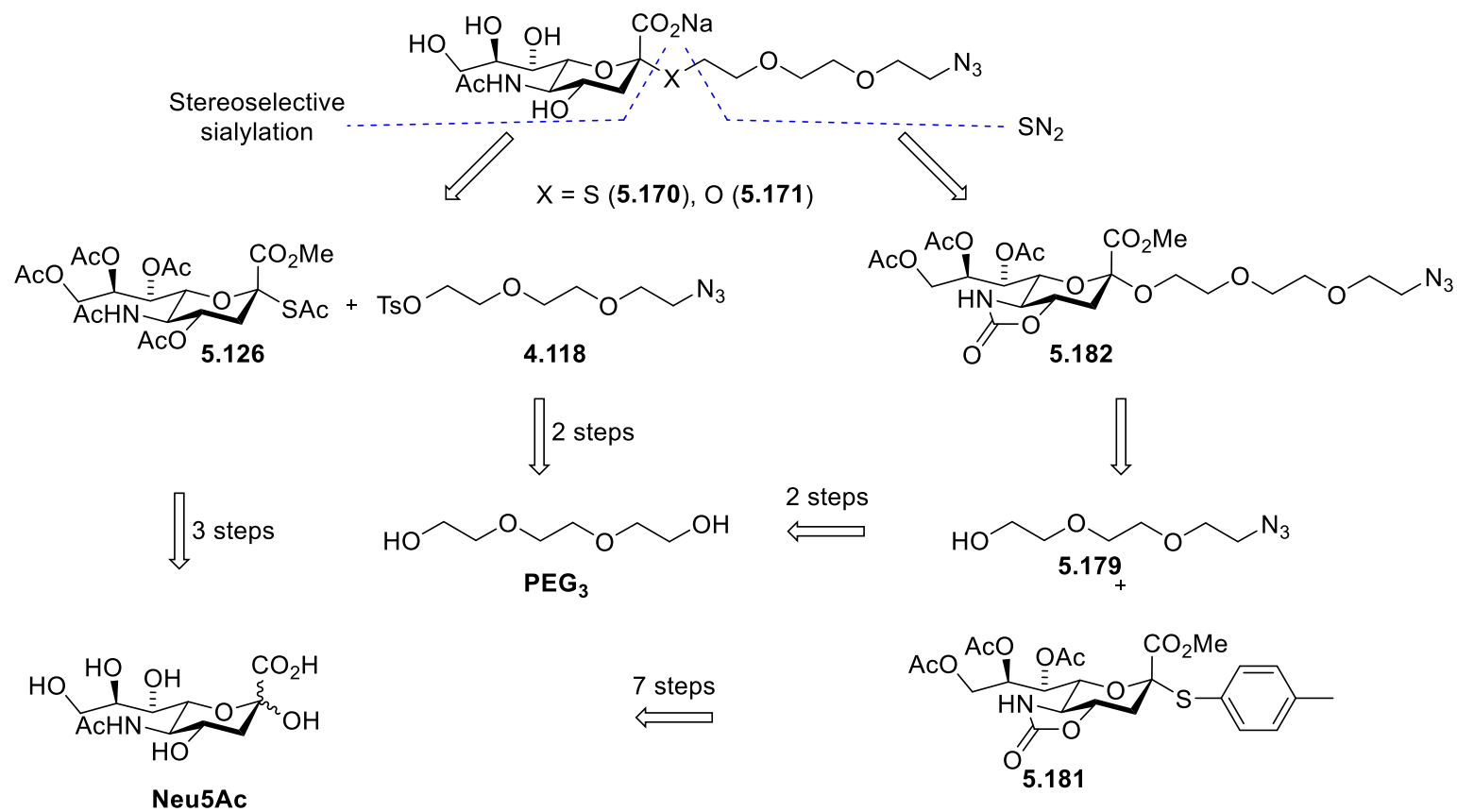
Although multivalent presentations of sialic acid on various synthetic scaffolds have been extensively studied, mimicking the functionality of the surface of biological membrane, imprecise spatial ligand presentation, chemical construction on toxic scaffolds, restricted synthetic approaches, and undesirable mechanical properties persists being main drawbacks. As an alternative, recently described glycodendrimersomes seem promising to trigger mimicking biological membranes with programmable glycan ligands. To our knowledge there is no reported evidence of sialic acid bearing dendrimersome or sialodendrimersome. To this end, our main goal was to synthesize and generate first example of sialodendrimersome and study its binding properties toward sialic acid specific lectins that we discussed above. Due to the fact that enzymatically stable *S*-sialosides are beneficial, we were interested in developing *S*-sialodendrimersome as well. As it is shown in Scheme 5.19, our initial approach for the synthesis of **5.168** and **5.169** is based on copper catalyzed azide-alkyne cycloaddition reaction (CuAAC) to couple hydrophilic **5.170**, **5.171** and hydrophobic **2.07** segments.

5.3.1 Synthesis of hydrophilic segments

As we discussed in Chapter 4, in order to obtain soft glycodendrimersomes with shape adaptability (during interactions with various lectins) hydrophilic and hydrophobic segments should be maintained in balance. To this goal, azido functionalized PEG₃ was chosen as a spacer. However, for *O*- and *S*-sialosides two distinct synthesis strategies were employed (Scheme 5.20).



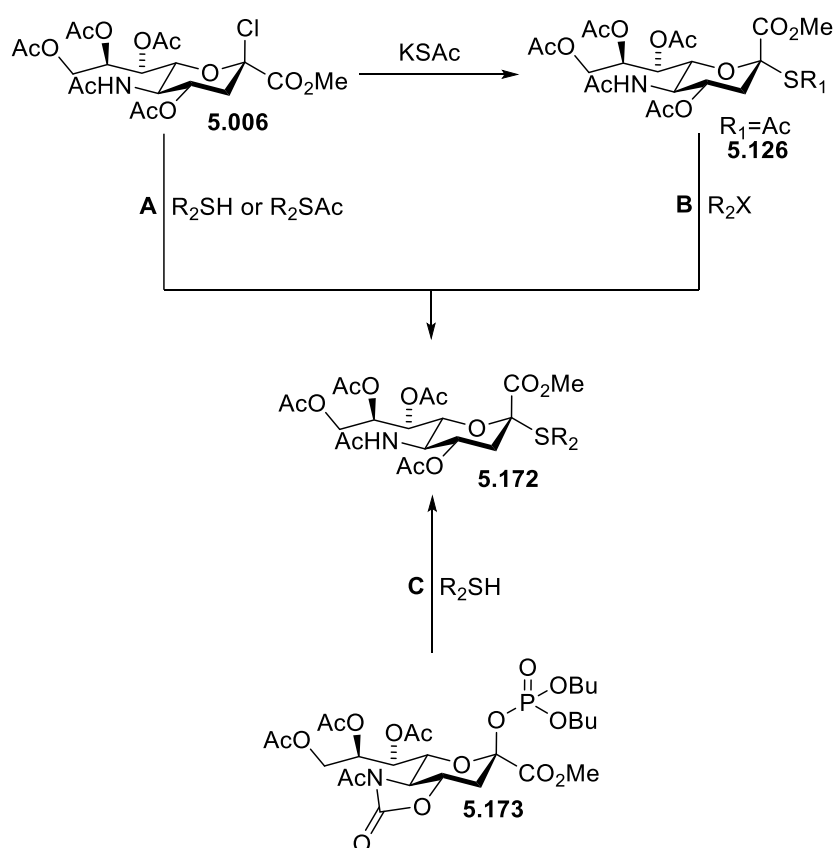
Scheme 5.19 Retrosynthetic analysis of amphiphilic Janus sialodendrimer.



Scheme 5.20 Retrosynthetic analysis of hydrophilic segments.

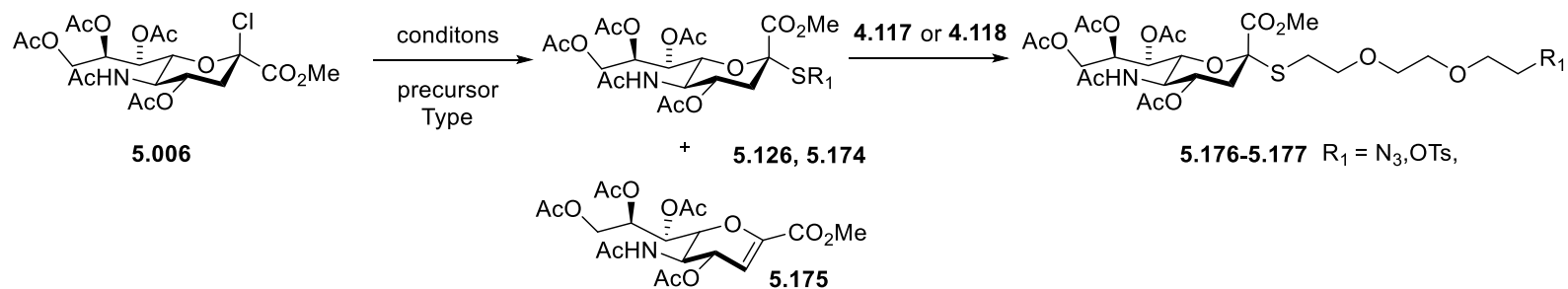
5.3.2 *S*-sialoside synthesis

Generally, α -*S*-sialoside synthesis involves either incorporation of the sulfur atom into sialoside acceptor (Scheme 5.21, route A) *via* a substitution reaction or chemoselective deprotection of anomeric thioacetyl following S_N2 type reaction with leaving group functionalized acceptor (route B). More recently an alternative substitution reaction has been introduced by Crich and co-workers (route C).⁴⁵⁸

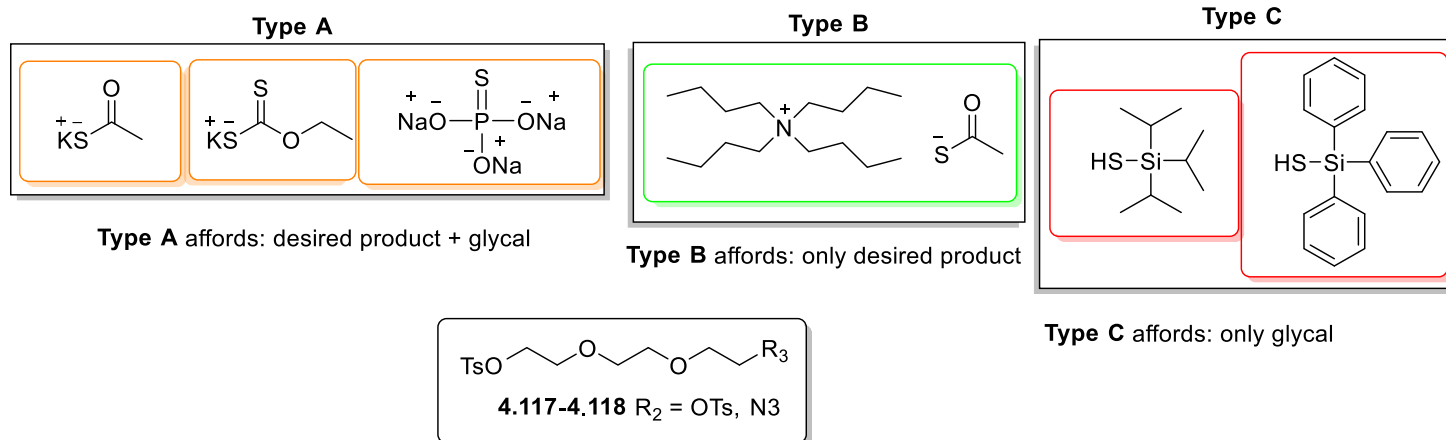


Scheme 5.21 Synthesis of α -*S*-sialosides by using various approaches.⁴⁵⁸

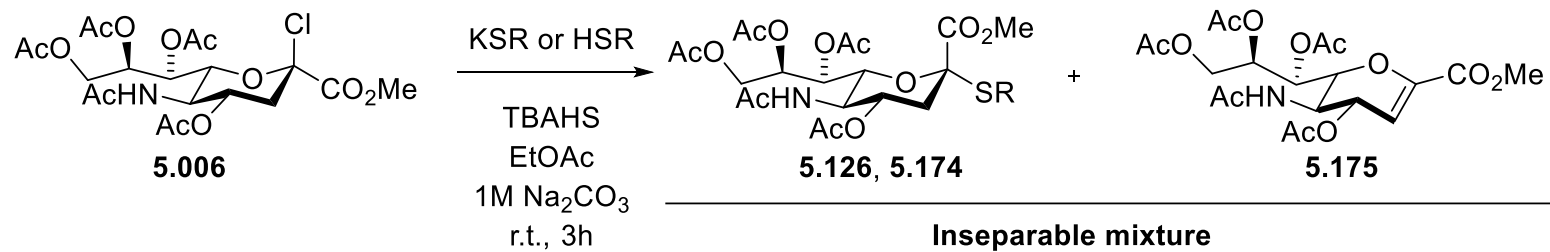
Thus, glycosylation of *N*-Acetyl-5-*N*, 4-*O*-oxazolidinone-protected dibutyl phosphate sialosyl donor with primary, secondary, and tertiary thiols under Lewis acidic condition gave exclusive α -*S*-sialosides in high yields.



Reaction with *S*-Sialosides precursors

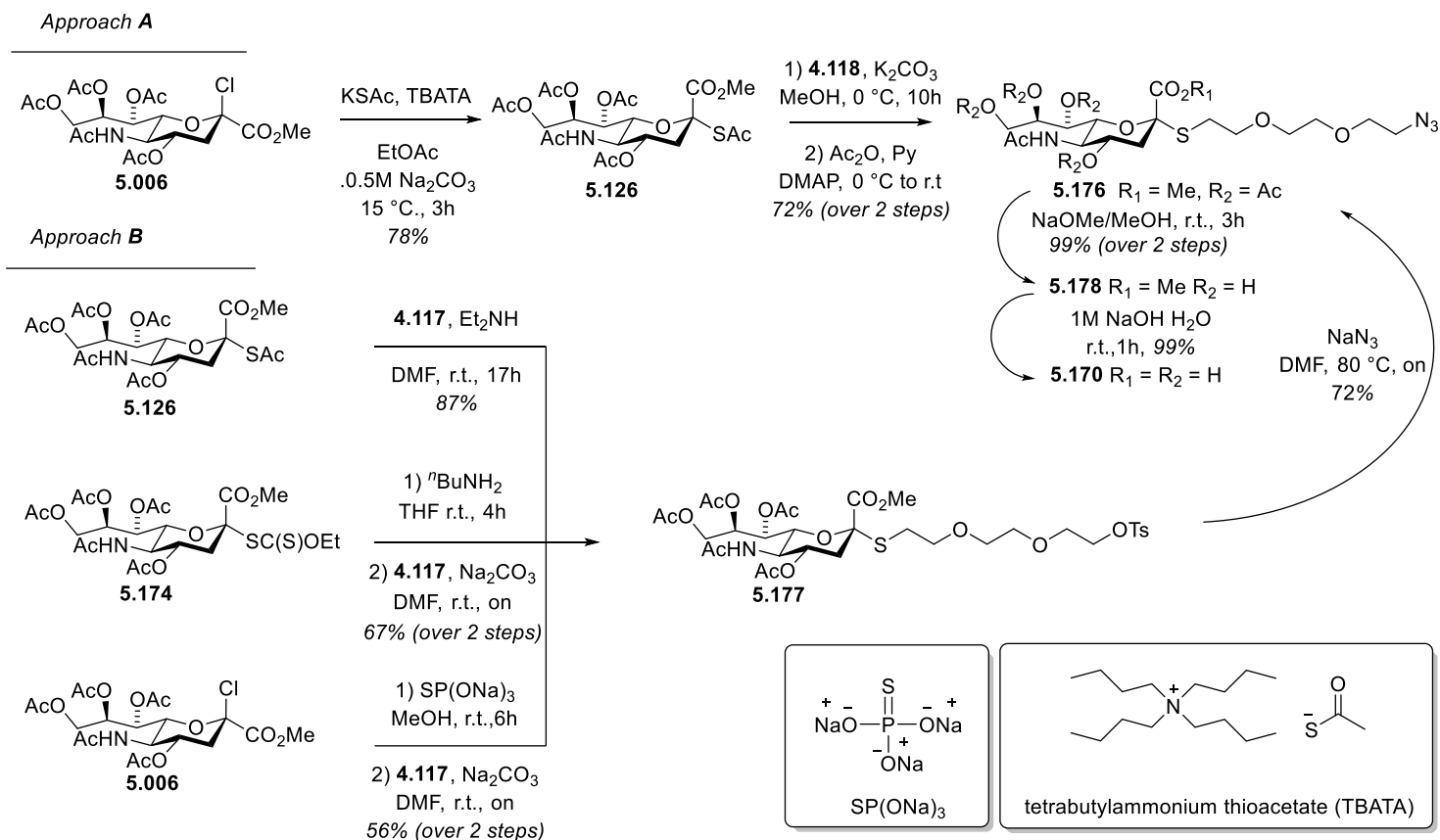


Scheme 5.22 Synthesis of α -*S*-alkyl sialosides within various thiol precursors.



R	C(O)CH ₃	C(S)OEt	Si ⁱ Pr ₃	SiPh ₃
Yield (%)	67	82	-	-
Glycal	+	+	+	+

Scheme 5.23 Synthesis of thiosialosides under PTC conditions.



Scheme 5.24 Synthesis of compound 5.170.

Synthesizing glycal-free azide functionalized *S*-sialoside **5.170** was challenging. We initially thought using standard PTC condition (tetrabutylammonium hydrogen sulfate (TBAHS) 1 eq., 1M Na₂CO₃, EtOAc)^{248, 249, 395, 477, 478, 536, 552} thioacetylation of **5.006** then deprotection and *in-situ* substitution on **4.118** would be ideal. Unfortunately, formation of inseparable glycal **5.175** in both steps is very common. As illustrated in Figure 5.8, the doublet (H₃) with 3 Hz at 5.91 ppm and disappearance of H_{3ax} and H_{3eq} peaks between 1.9-2.5 ppm confirmed the formation of **5.175**. Similar phenomenon using commercially available potassium thioacetate (KSAc) was observed by several research groups and even two research papers focusing on special purification methods were published.⁵⁵³⁻⁵⁵⁵

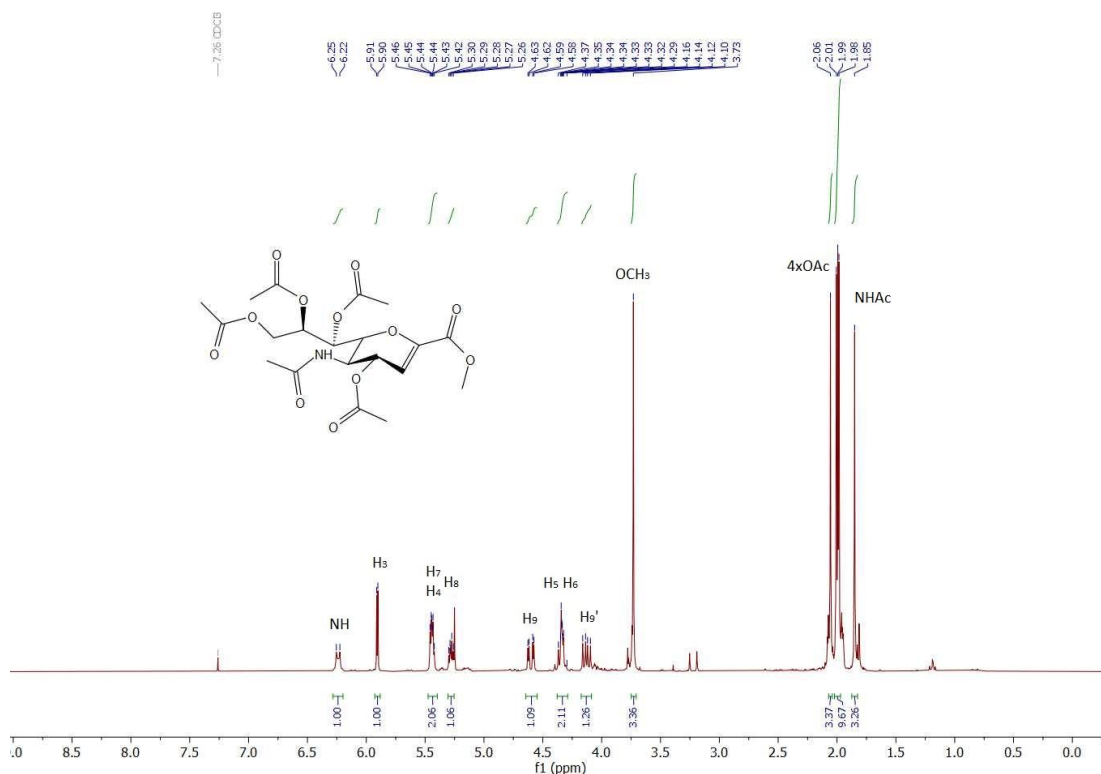


Figure 5.8 ¹H NMR (300 MHz, CDCl₃) spectrum of compound **5.175**.

To address this issue, we first tried to incorporate sulfur atom into α -position of sialic acid moiety *via* various commercial precursors (Scheme 5.22).

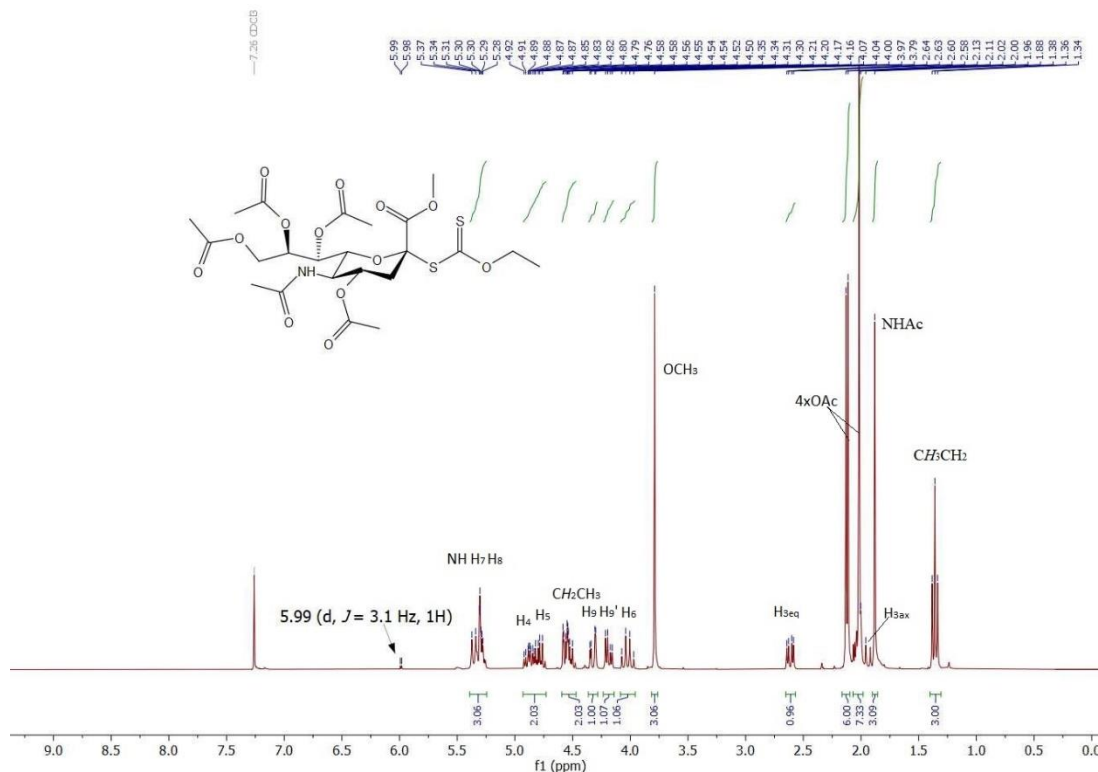


Figure 5.9 ^1H NMR (300 MHz, CDCl_3) spectrum of compound **5.174**.

Using PTC condition (2 eq. of potassium salt of thioacetic or ethylxanthic acids, 1 eq. of TBAHS, 1M Na_2CO_3 in EtOAc at room temperature, 3 h of stirring) *S*-acetyl **5.126** and *S*-xanthate-Neu5Ac **5.174** were first synthesized in 67 and 82 % yield respectively. The presence of glycal was confirmed *via* ^1H NMR analysis, thus doublet at 5.99 ppm with $J = 3.1$ Hz corresponds to H_3 of elimination product (Figure 5.9). Another commercial precursor as triisopropylsilanethiol (TIPSSH) was particularly interesting. In 2014, Nilsson and Mandal reported that TIPS-*S*-glycosides could be synthesized through either base promoted $\text{S}_{\text{N}}2$ type substitution from glycosyl halides or Lewis acid promoted substitution from glycosyl acetates.⁵⁵⁶ Subsequently *in-situ* substitution *via* activating with TBAF in acetonitrile, high-yielding thioalkylation were successfully achieved. However, its application in *S*-sialoside synthesis is not known. Unfortunately, thiosialylation with TIPSSH and less

bulky triphenylsilanethiol (TPSSH) was fruitless and after chromatographic purification only glycal was isolated. To address this issue, we thought using TBATA (tetrabutylammonium thioacetate) as an alternative phase transfer catalyst would be more efficient. After treatment of TBAB (tetrabutylammonium bromide) with potassium thioacetate in methanol at room temperature Bu_4NSAc was obtained in 94 % yield. The structure of TBATA was confirmed by ^1H and ^{13}C NMR. Appearance of singlet with 3 H at 2.44 ppm (Figure 5.10) and two more carbon peaks at 37.7 and 23.2 ppm (Figure 5.11) clearly shows presence of $\text{CH}_3\text{C}(\text{O})\text{S}^-$ counter anion. The spectroscopic data agreed well with those of the literature.⁵⁵⁵ Therefore, replacing TBAHS by freshly synthesized TBATA and reducing concentration of Na_2CO_3

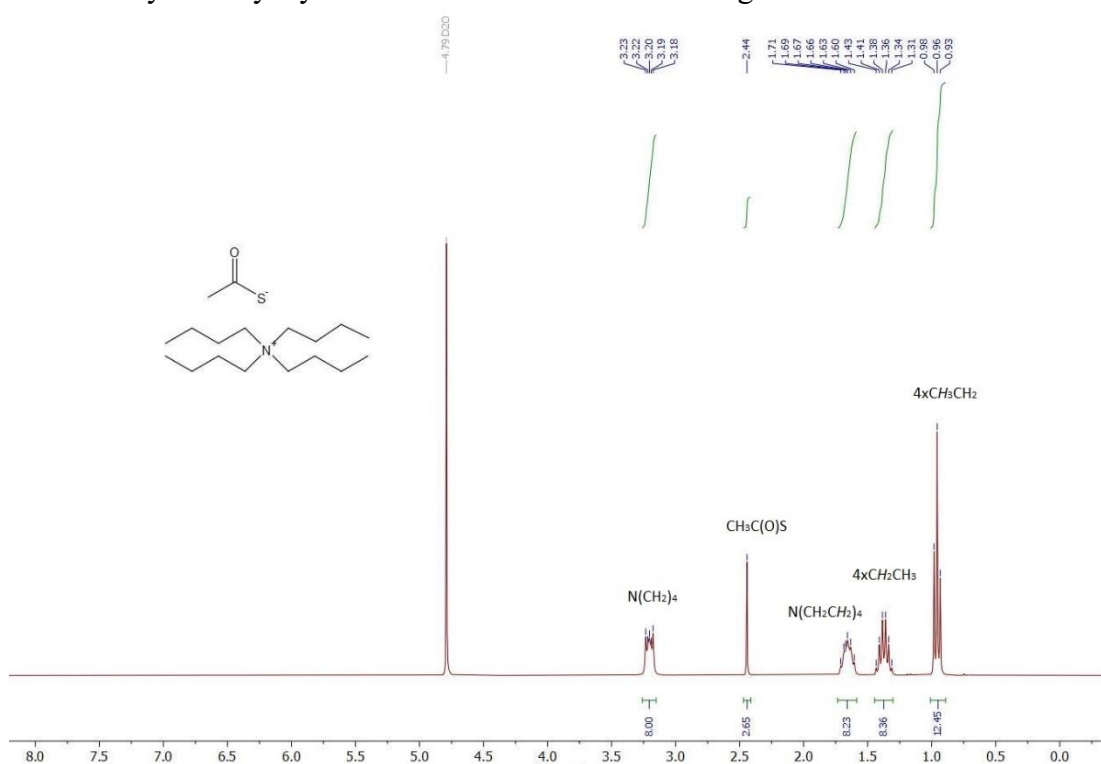


Figure 5.10 ^1H NMR (300 MHz, D_2O) spectrum of TBATA.

solution from 1M to 0.5 M afforded thioacetylsialoside **5.126** in 78 %. Surprisingly after chromatographic purification presence of glycal was not observed (Figure 5.12).

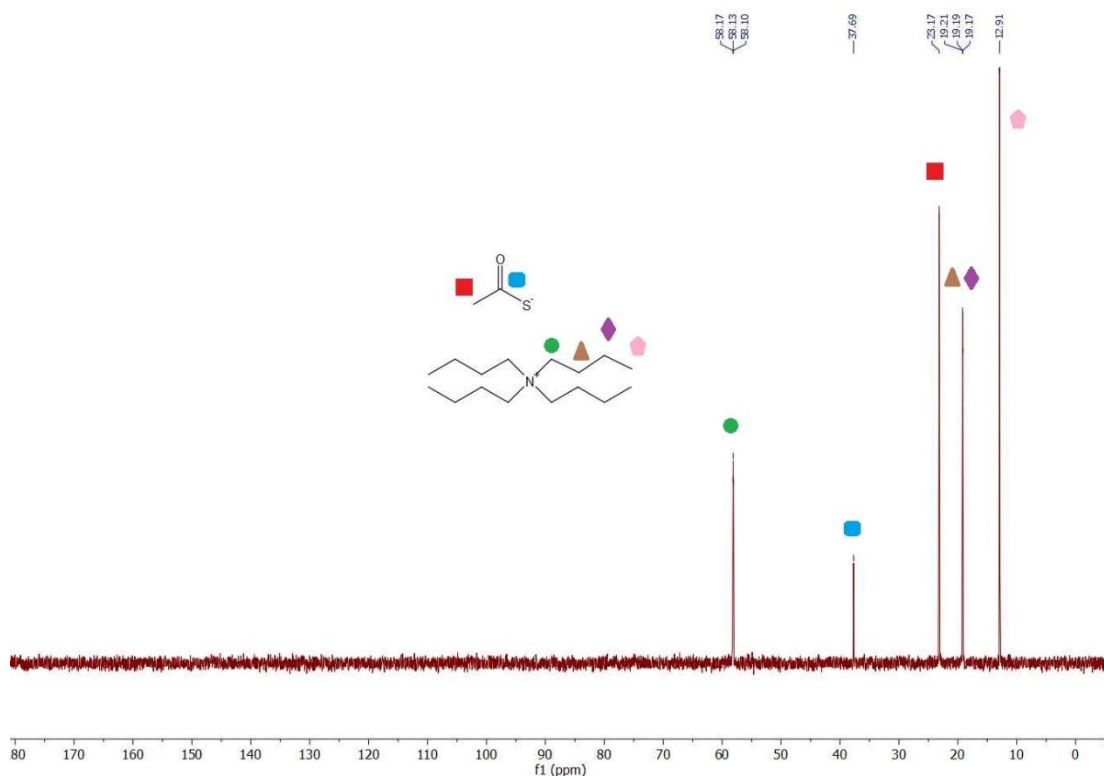


Figure 5.11 ^{13}C NMR (75 MHz, D_2O) spectrum of TBATA.

Subsequently, conversion of **5.126** into **5.176** *via* $\text{S}_{\text{N}}2$ was achieved in two steps (deacetylation, thioalkylation). The structure of the obtained product **5.176** was confirmed by ^1H and ^{13}C NMR experiments (Figure 5.13). As confirmation of previous reported work, getting rid of glycol (in case of presence) in this step through classical column chromatography is ineffective.⁵⁵⁴ Alternatively, we developed a new approach where glycol can be eliminated in purification stage. Therefore, treating **5.126** with ditosyl-PEG₃ **4.117** (instead of **4.118**) in presence of diethylamine afforded **5.177** in 87 % yield. All the ^1H and ^{13}C signal assignments were unambiguously determined using DEPT- ^{13}C (Figure 5.15) together with 2D-COSY (Figure 5.16), HSQC (Figure 5.17) and HMBC (Figure 5.18) experiments. As it is shown in Figure 5.14, multiplet at 2.93-2.71 ppm corresponding to two hydrogens of SCH_2 confirms *S*-alkylation. Additionally, the signals at 2.41, 7.31 and 7.76 ppm

corresponding to the tosylate shows monosubstitution which was positively confirmed by ESI-TOF HRMS technique (Figure 5.19).

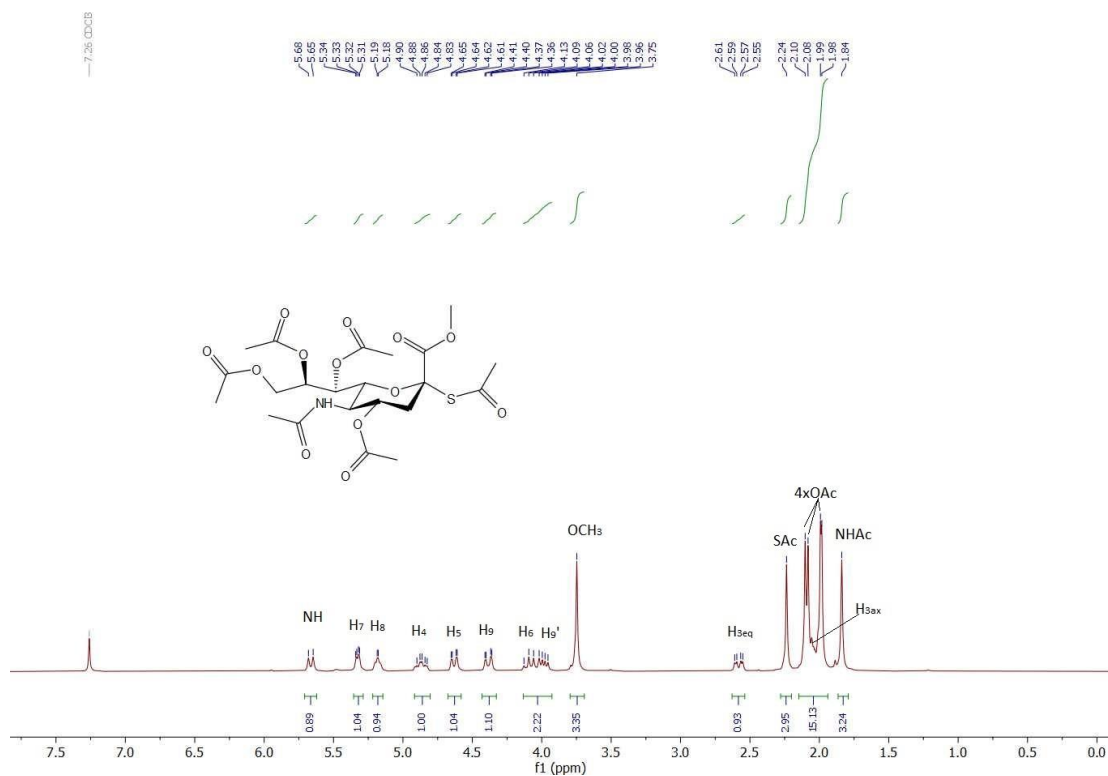


Figure 5.12 ^1H NMR (300 MHz, CDCl_3) spectrum of compound **5.126**.

Tosyl-functionalized PEG₃-S-sialoside **5.177** was synthesized also from **5.174** via selective deprotection of xanthate in presence of butyl amine in THF and substitution in presence of Na_2CO_3 in DMF at room temperature. Additionally, in light of previously reported protocol,⁵⁵⁷ sialyl halide donor **5.006** was first treated with sodium thiophosphate in methanol. Obtained free thiol containing crude residue was subjected to substitution reaction with the same condition (Na_2CO_3 in DMF, at room temperature, overnight stirring) to afford desired compound **5.177** in 56 % over two steps. Having versatile tosyl group at focal point is particularly interesting, thus via converting it to thiol group and subsequent thiol-ene click reaction with hydrophobic

segment as an alternative to CuAAC could be realizable. Further substitution of tosylate by azido using sodium azide in DMF at 80 °C overnight stirring, following Zemplén deprotection (NaOMe in MeOH at room temperature in 3 h of stirring) gave **5.178** in 71 % yield over 2 steps. Disappearance of tosylate and complete removal of *O*-acetyl groups were confirmed by NMR experiments. Subsequently, treatment of **5.178** in basic hydrolysis condition (1M NaOH in 1 h of stirring) afforded desired product **5.170**. Without further purification crude product was subjected to click reaction with hydrophobic tail that previously prepared.

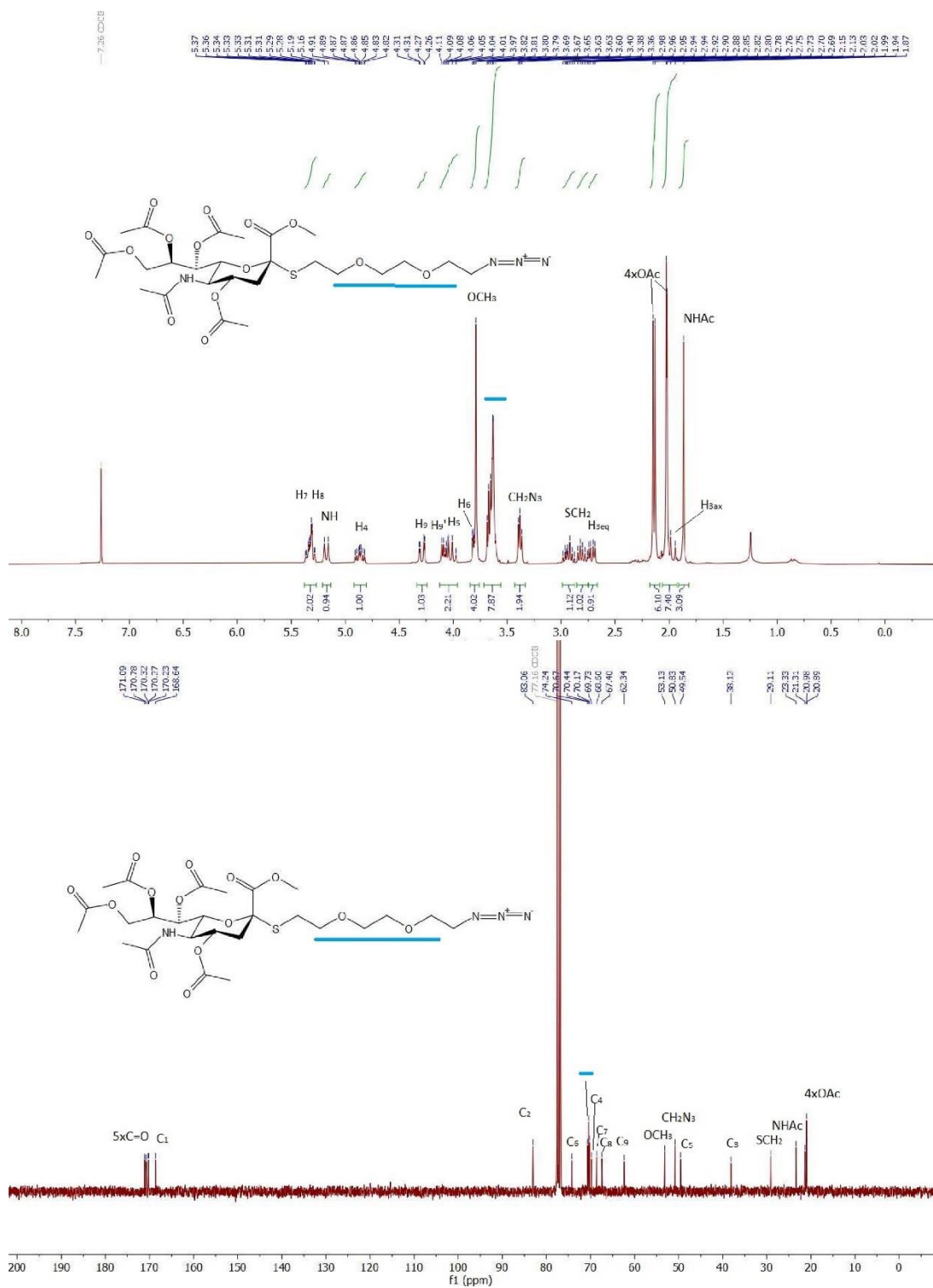


Figure 5.13 ¹H and ¹³C NMR (300 and 75 MHz, CDCl₃) spectra of compound 5.176.

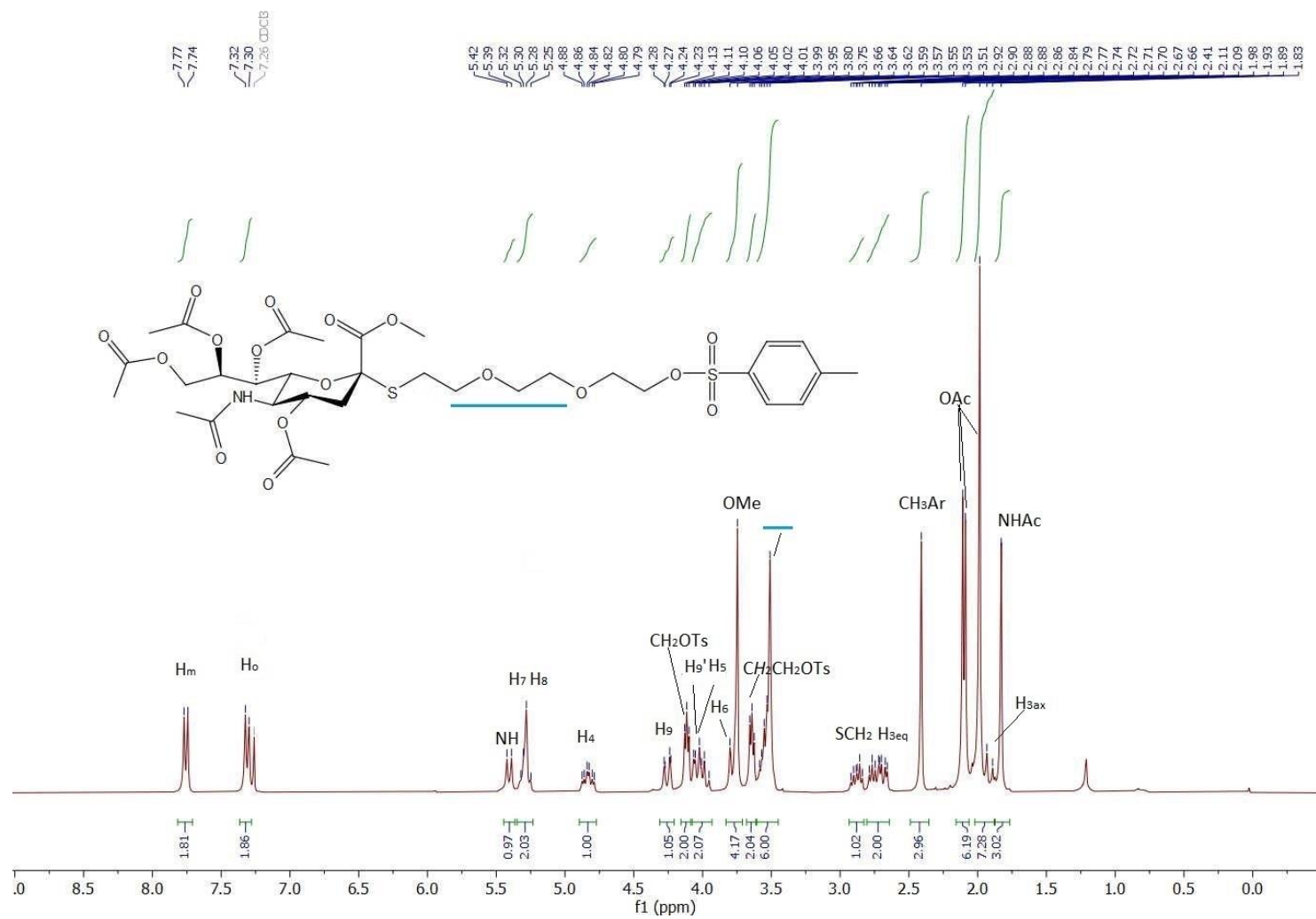


Figure 5.14 ^1H NMR (300 MHz, CDCl_3) spectrum of compound 5.177.

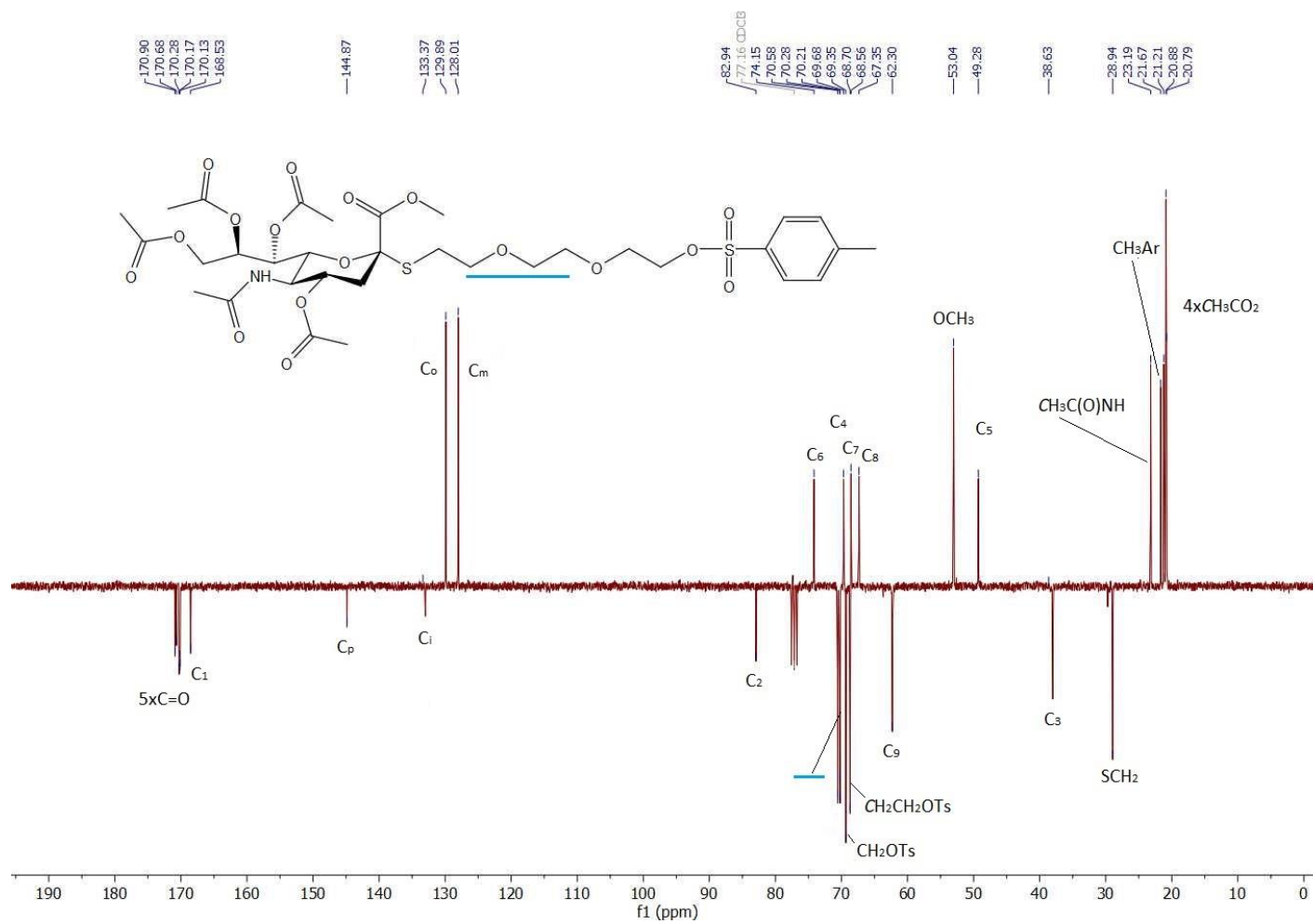


Figure 5.15 DEPT ¹³C NMR (75 MHz, CDCl₃) spectrum of compound 5.177.

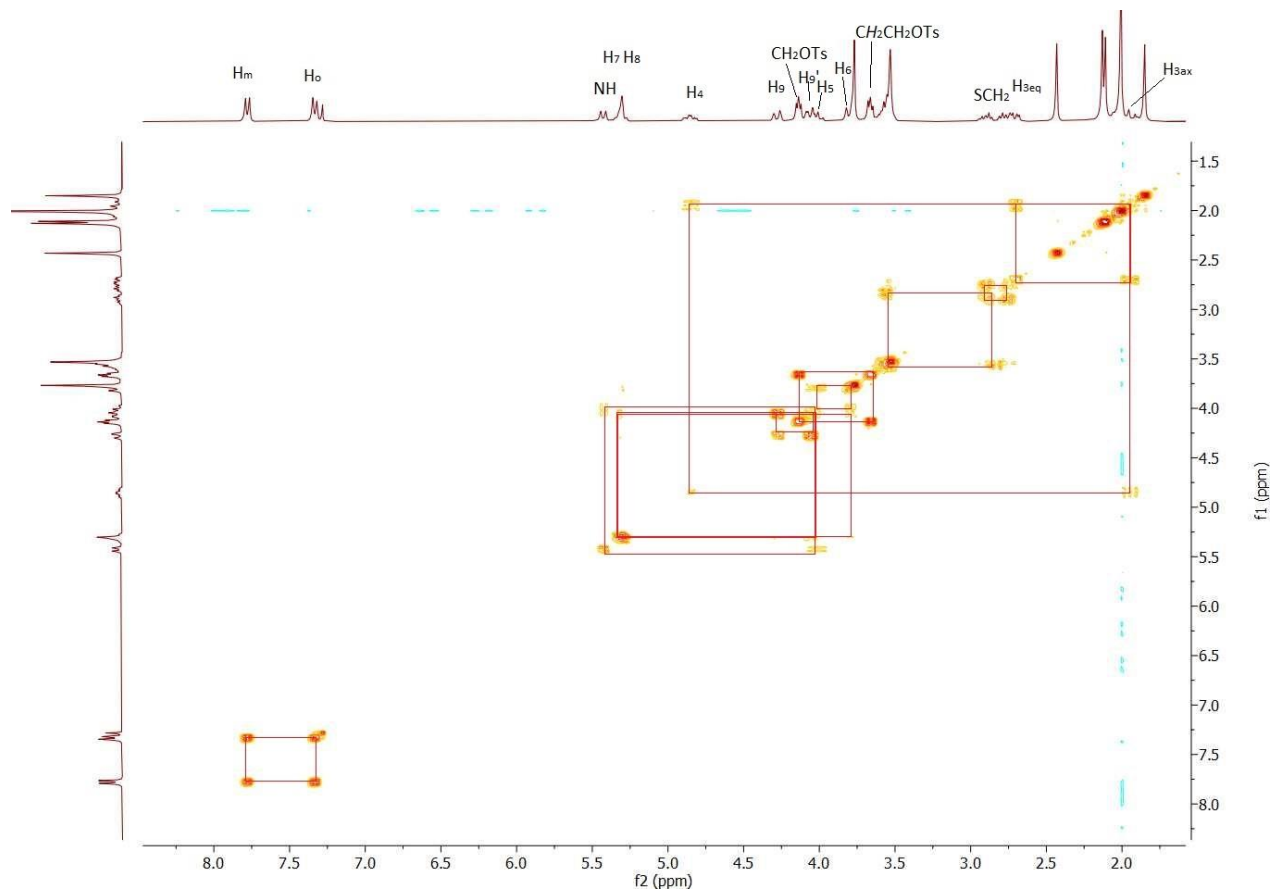


Figure 5.16 2D-COSY spectrum of compound 5.177.

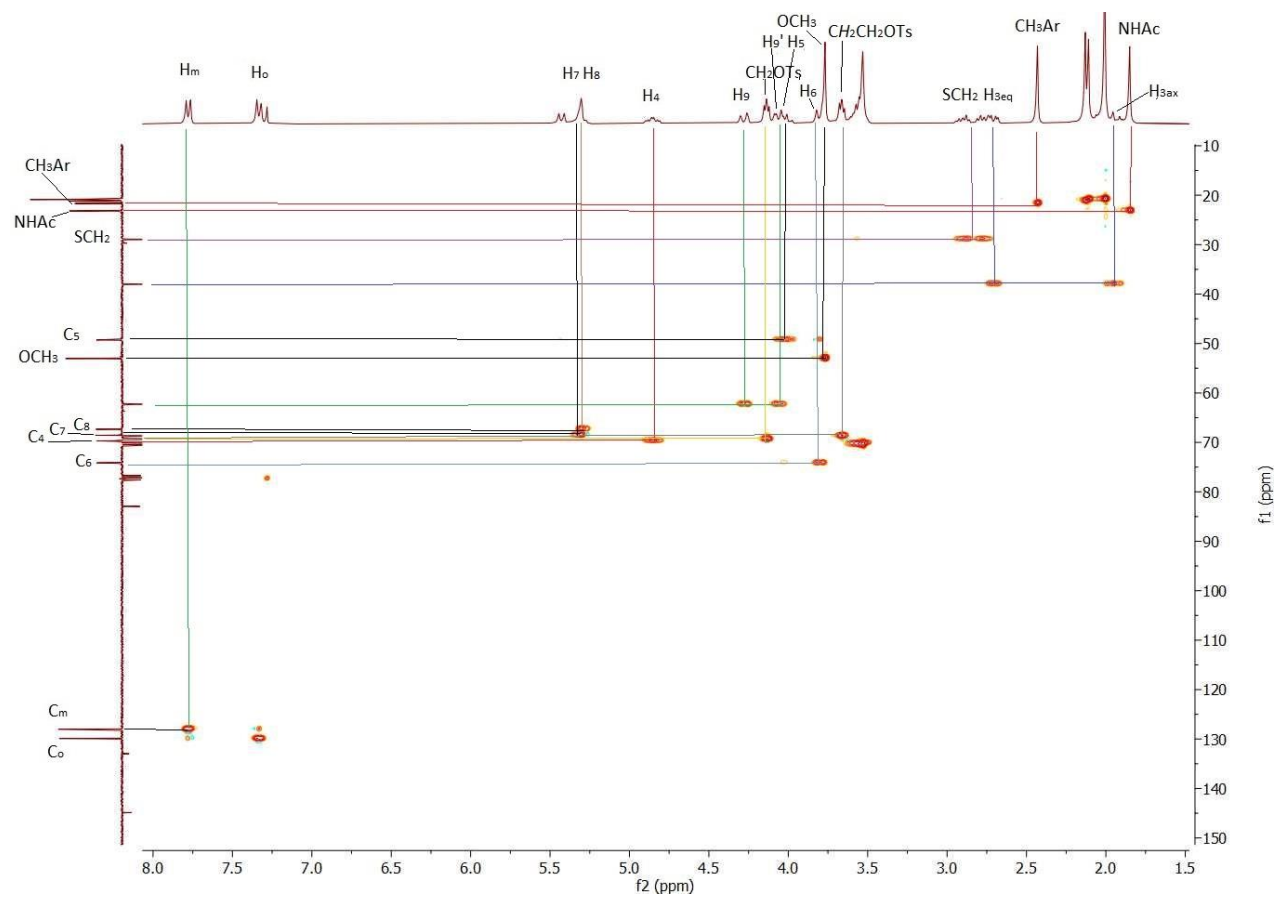


Figure 5.17 HSQC spectrum of compound 5.177.

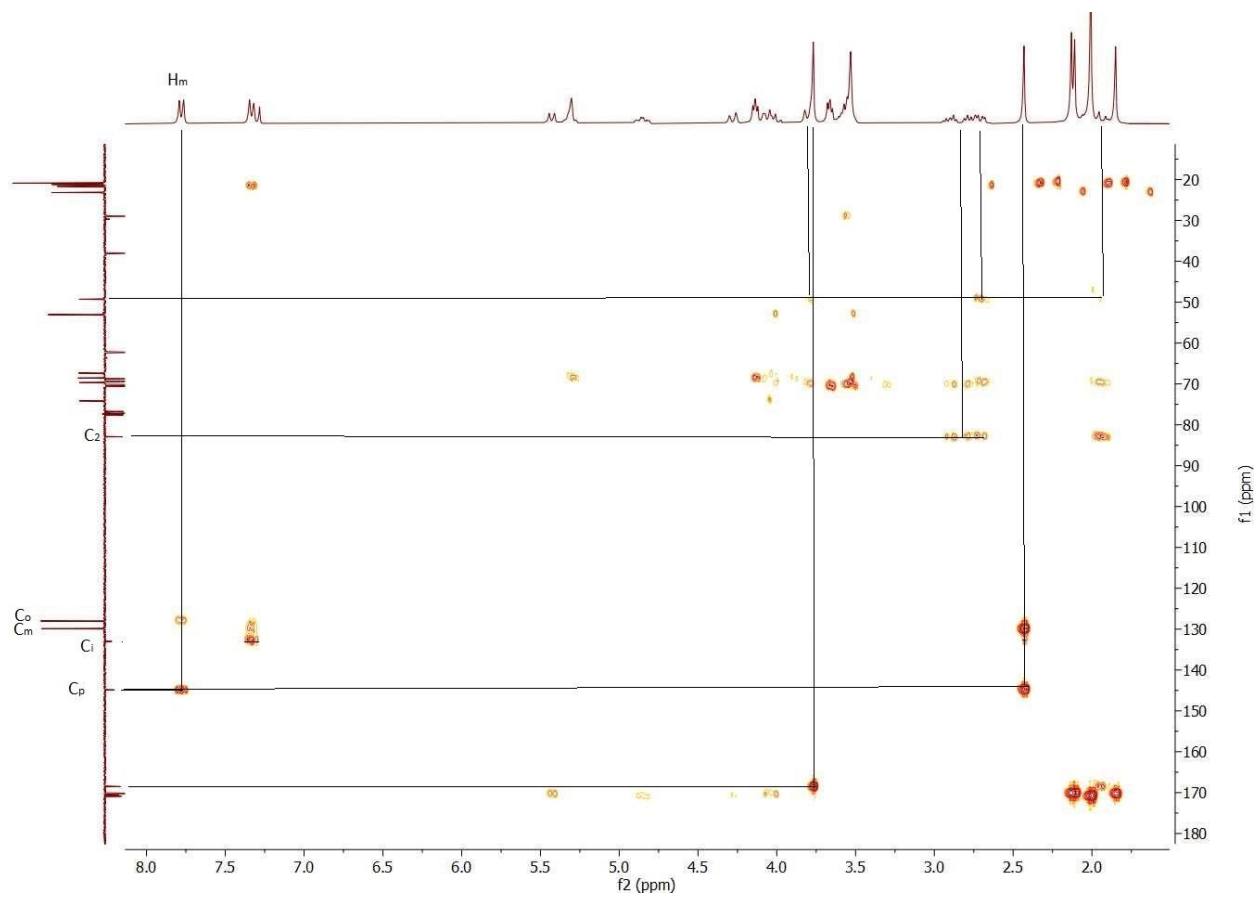


Figure 5.18 HMBC spectrum of compound **5.177**.

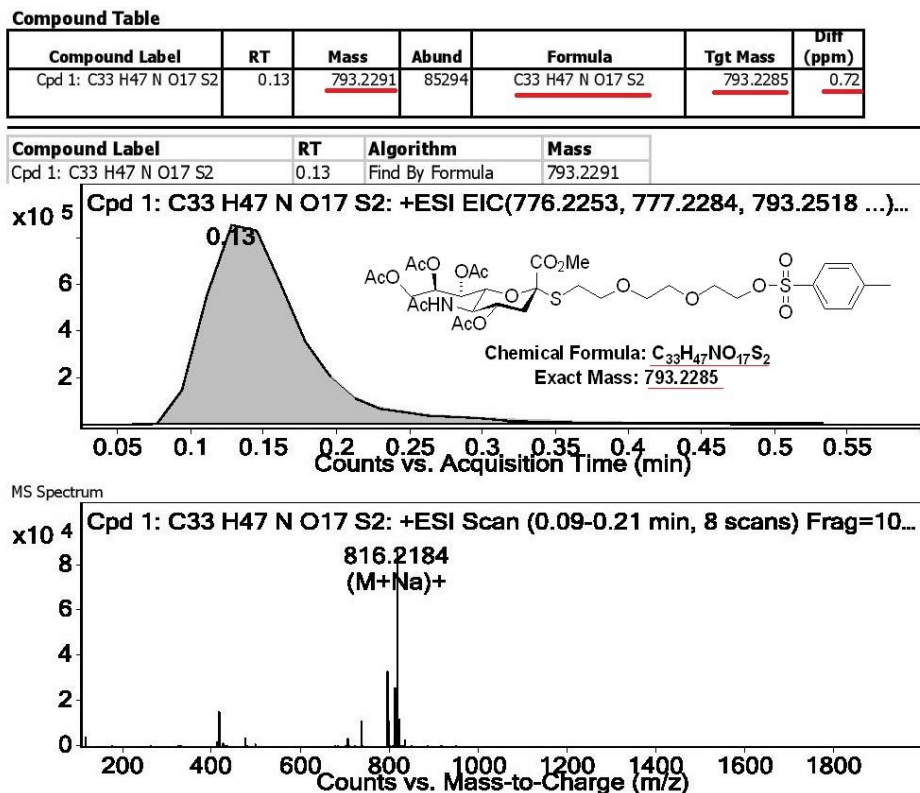
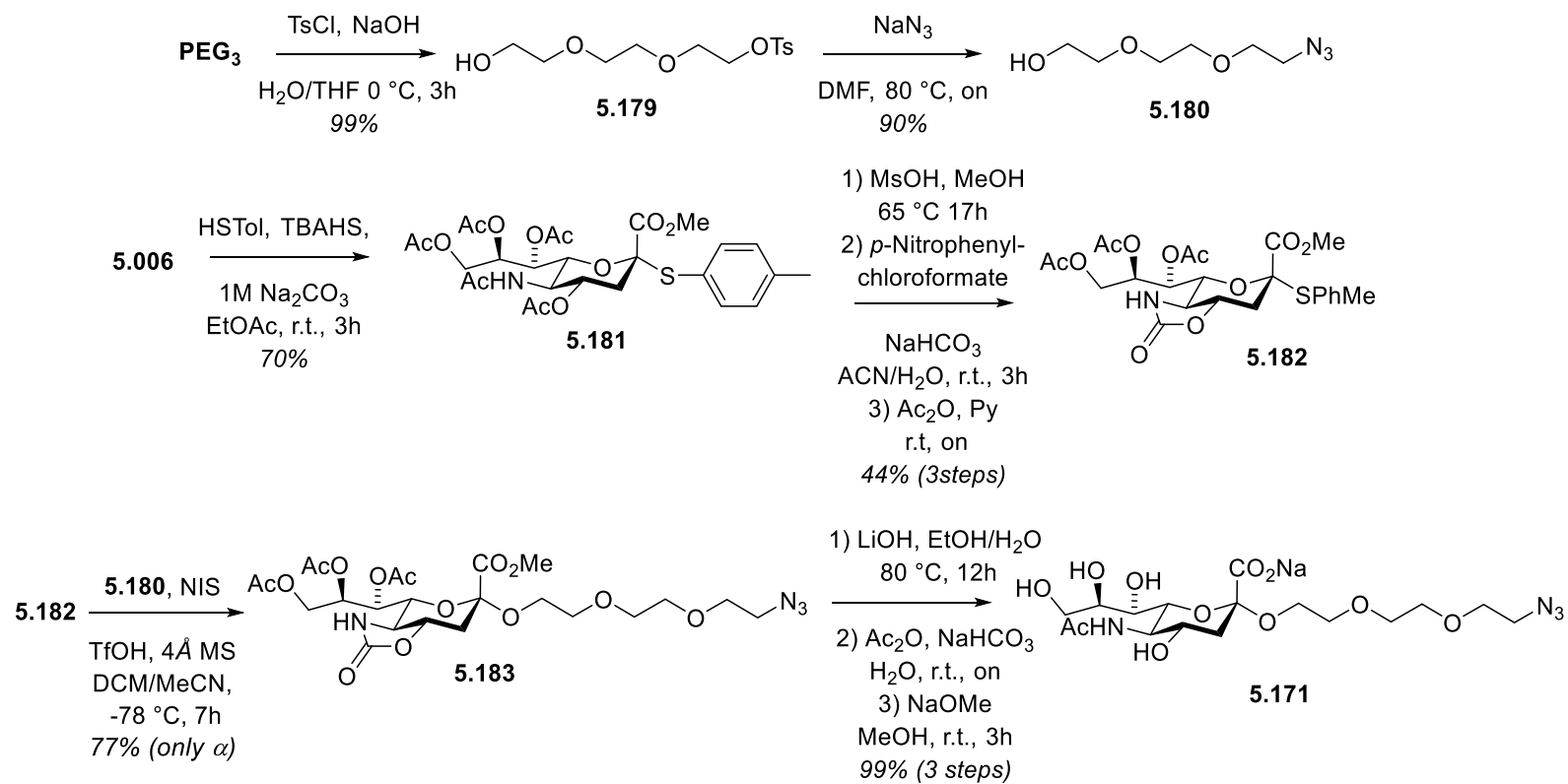


Figure 5.19 HRMS spectrum of compound 5.177.

5.3.3 O-sialoside synthesis

The synthesis of the naturally occurring α -sialoside constitutes the most challenging part of our project. The first step of our synthetic approach dealt with azido functionalization of acceptor at the focal point. Toward this goal, we first activated one of the hydroxyl groups by converting it to the tosylate group *via* treating PEG₃ with tosyl chloride and 40 % solution of NaOH in THF at 0 °C in 3h to get **5.179** (Scheme 5.25). The success of the monotosylation was confirmed by ¹H NMR. Subsequent substitution of tosylate by azido group under standard condition (NaN₃ in DMF at 80 °C, overnight stirring) afforded **5.180** in 90 %. Disappearance of the signals corresponding to the tosyl group at ¹H and ¹³C NMR confirmed the completion of the substitution (Figure 5.20).



Scheme 5.25 Synthesis of compound 5.171.

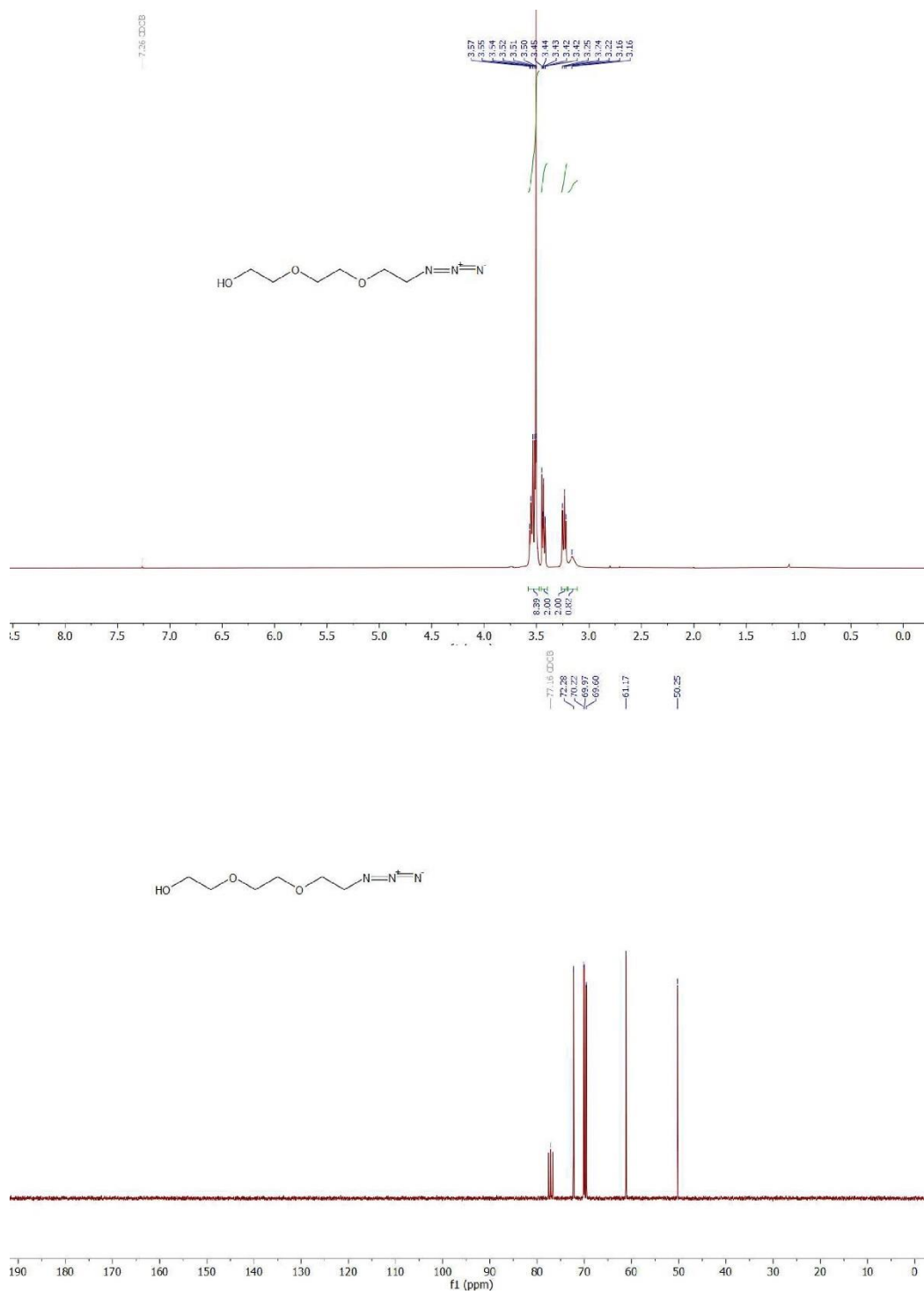


Figure 5.20 ¹H and ¹³C NMR (300 and 75 MHz, CDCl₃) spectra of compound **5.180**.

We next focused on synthesis of thiosialosyl donor. Using PTC condition (4-methyl phenyl thiol, TBAHS, 1M Na₂CO₃, in EtOAc at room temperature in 3h of stirring) **5.006** was converted to **5.181** in 70 % yield. The spectroscopic data agreed well with those of the literature.³⁸¹ We initially tried to synthesize the targeted α -sialoside directly from *N*-acetyl thiosialosyl donor **5.181** but the presence of the undesired β -anomer and elimination product **5.175** and difficulties in purification stage (which is quite common and has the same R_f as desired compound), led us to modify *N5* group from *N*-acetyl to 5-*N*, 4-*O*-oxazolidinone under standard De Meo conditions.⁴⁵⁵ De-*O* and *N*-acetylation of **5.181** was achieved by using 1 eq. of methanesulfonic acid (MsOH) in MeOH at 65 °C. Without further purification, obtained crude product was treated with 4-nitrophenyl chloroformate and NaHCO₃ in H₂O/MeCN (v/v : 1/4) mixture. After short column filtration and *in-vacuo* concentration, the residue was subjected to standard acetylation reaction (Py/Ac₂O (v/v : 4/1) overnight stirring at room temperature) to give **5.182** in 45 % yield over 3 steps. Subsequently by activation with *N*-iodosuccinimide (NIS) and trifluoromethanesulfonic acid (TfOH) sialosyl donor **5.182** was treated with acceptor **5.180** at -78 °C in DCM/MeCN (v/v : 2/1) mixture to afford **5.183** as a single anomer in 77 % yield. The α -configuration of **5.183** was determined on the basis of above mentioned established empirical rules. These rules include: a) $\delta H_{3\text{eq.}}(\alpha) > \delta H_{3\text{eq.}}(\beta)$; b) $\delta H_4(\alpha) < \delta H_4(\beta)$; c) $\delta H_9 - H_9(\alpha) < \delta H_9 - H_9(\beta)$; d) $J_{7,8}(\alpha) > J_{7,8}(\beta)$. Same rules are applicable for the determination of anomeric configuration of *S*-sialosides. Usually, the signals corresponding to H_{3eq.} of the α -anomer range between 2.5-2.8 ppm, whereas H_{3eq.} of the β -anomer appears at 2.2-2.5 ppm. In case of the presence of electron-withdrawing 5-*N*, 4-*O*-oxazolidinone protecting group for α -anomer, shifting of H_{3eq.} to lower field $\delta \sim 2.9$ ppm and upfield shift of H₅ toward $\delta \sim 3.0$ ppm have been already reported.^{455, 558} Study also revealed that the signal corresponding to H_{3eq.} of the 5-*N*, 4-*O*-oxazolidinone protected β -*O*-sialosides was deshielded to $\delta \sim 2.6$ ppm.⁵⁵⁸

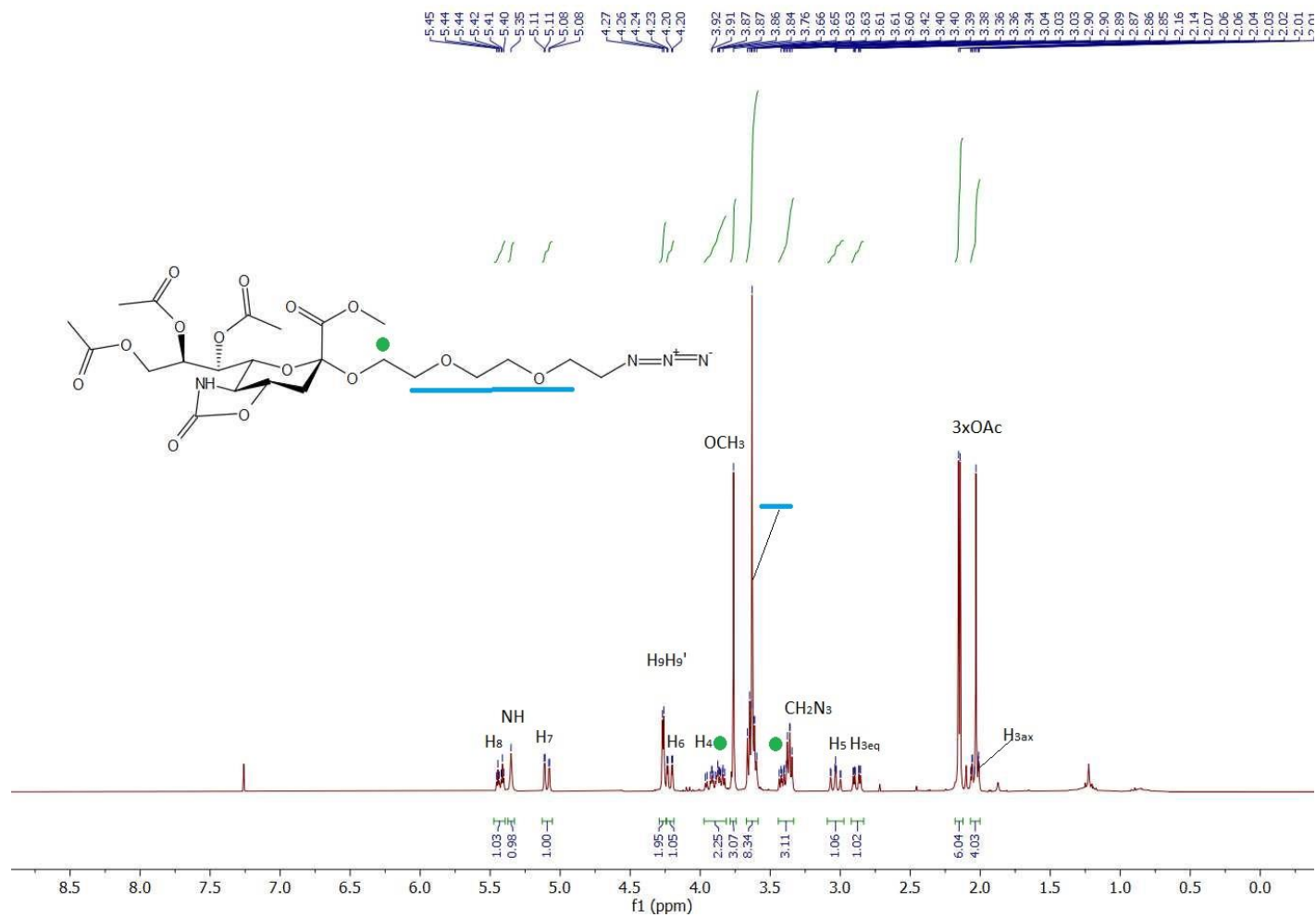


Figure 5.21 ¹H NMR (300 MHz, CDCl₃) spectrum of compound **5.183**.

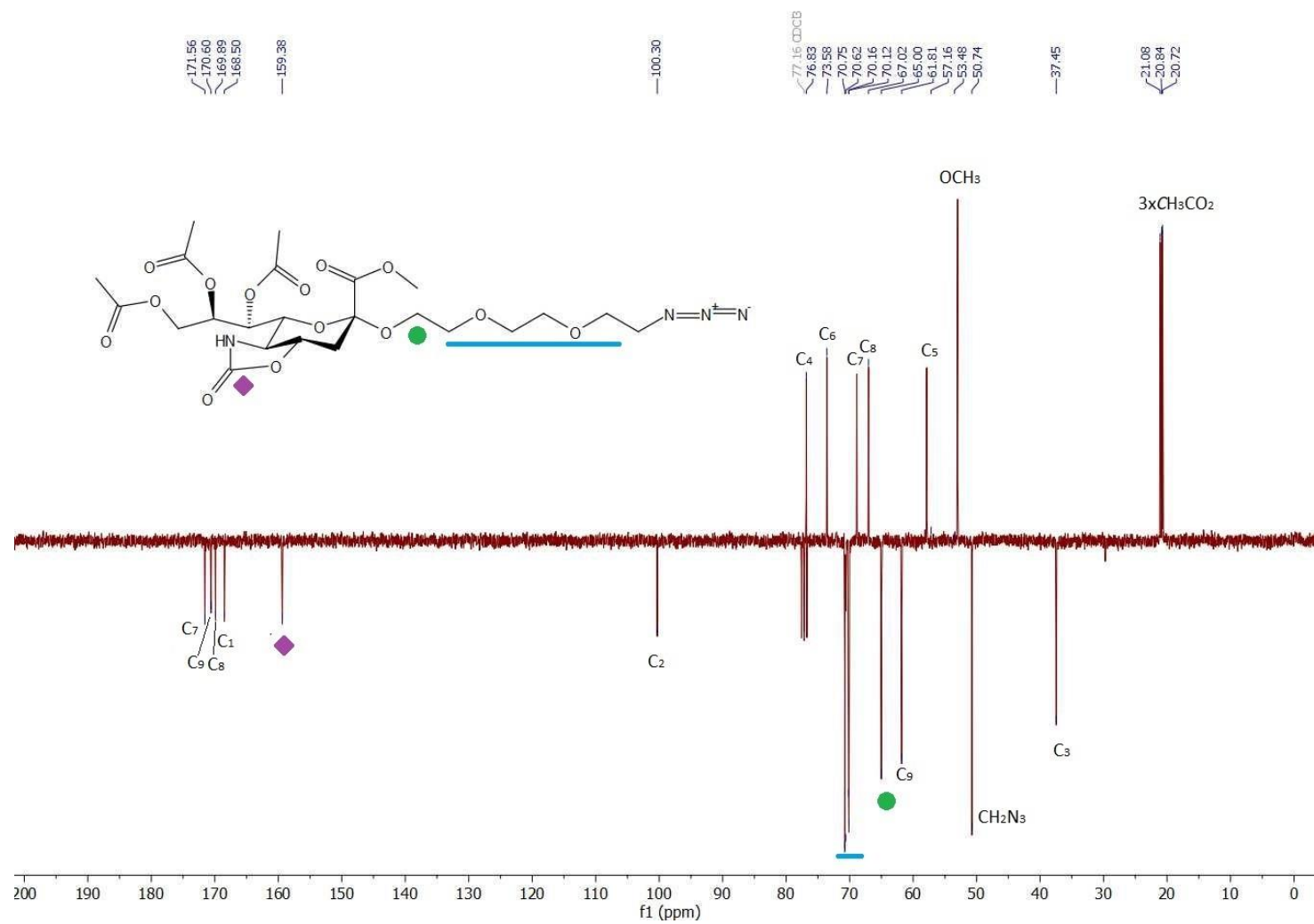


Figure 5.22 DEPT ¹³C NMR (75 MHz, CDCl₃) spectrum of compound **5.183**.

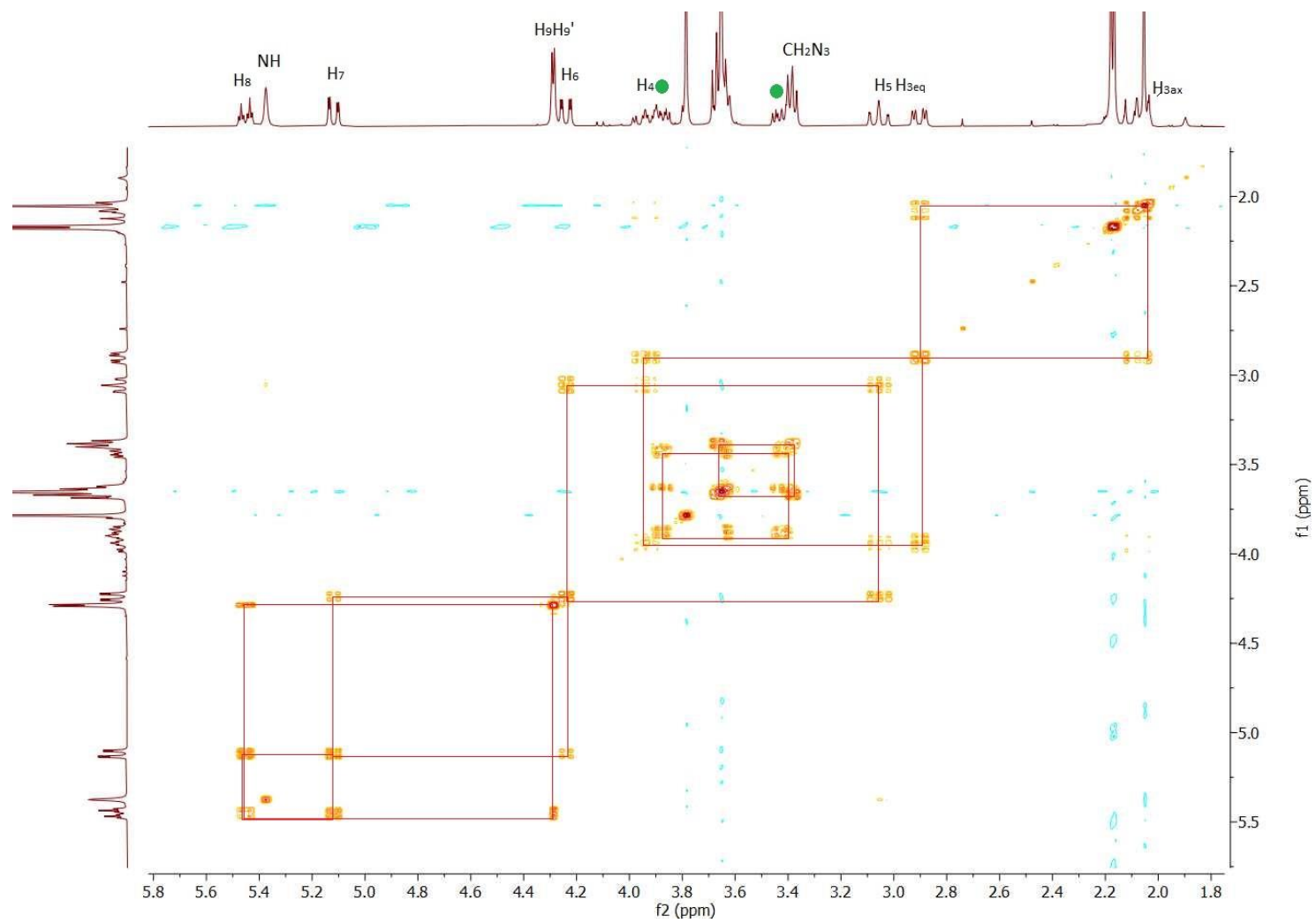


Figure 5.23 2D-COSY spectrum of compound **5.183**.

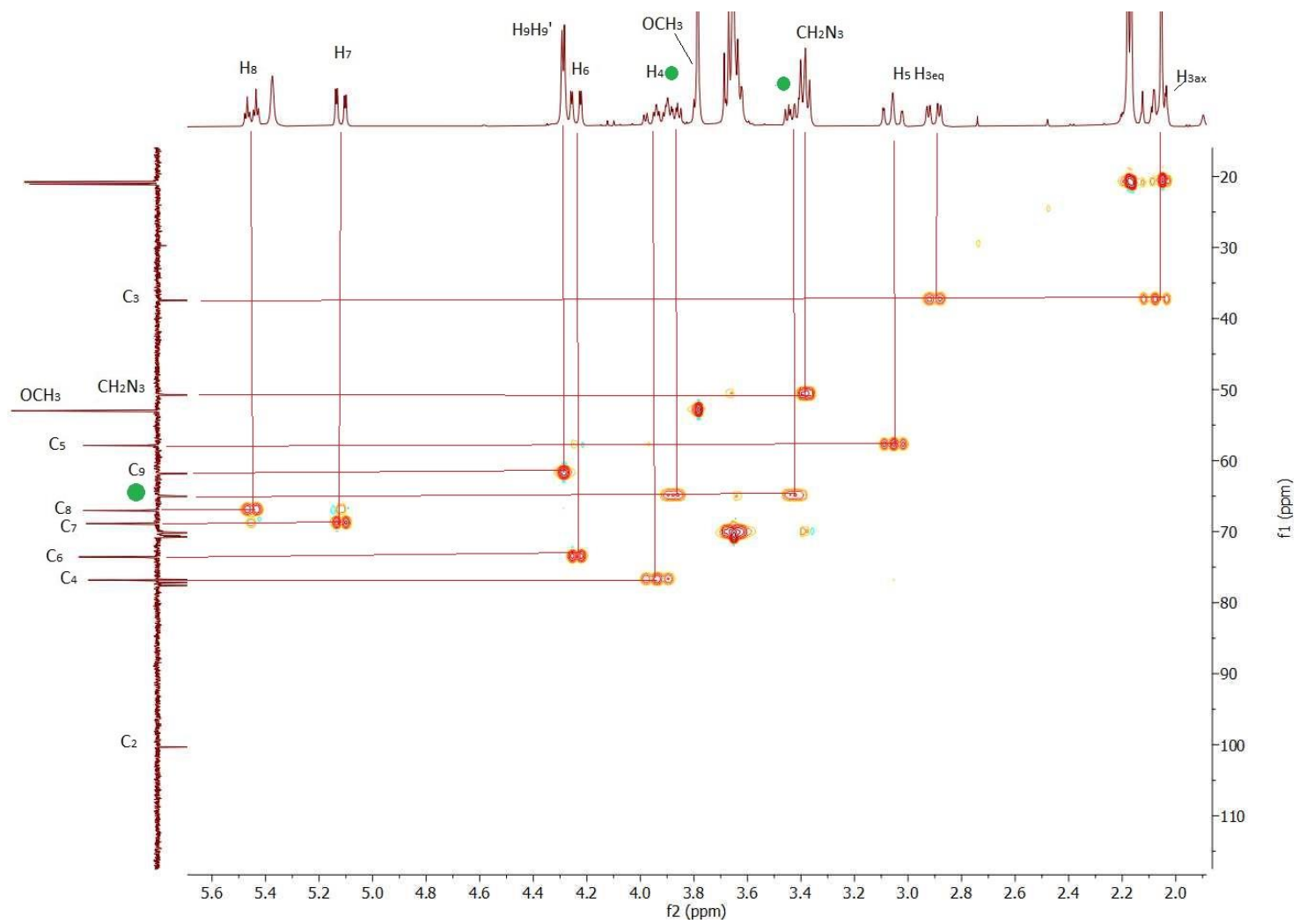


Figure 5.24 HSQC spectrum of compound 5.183.

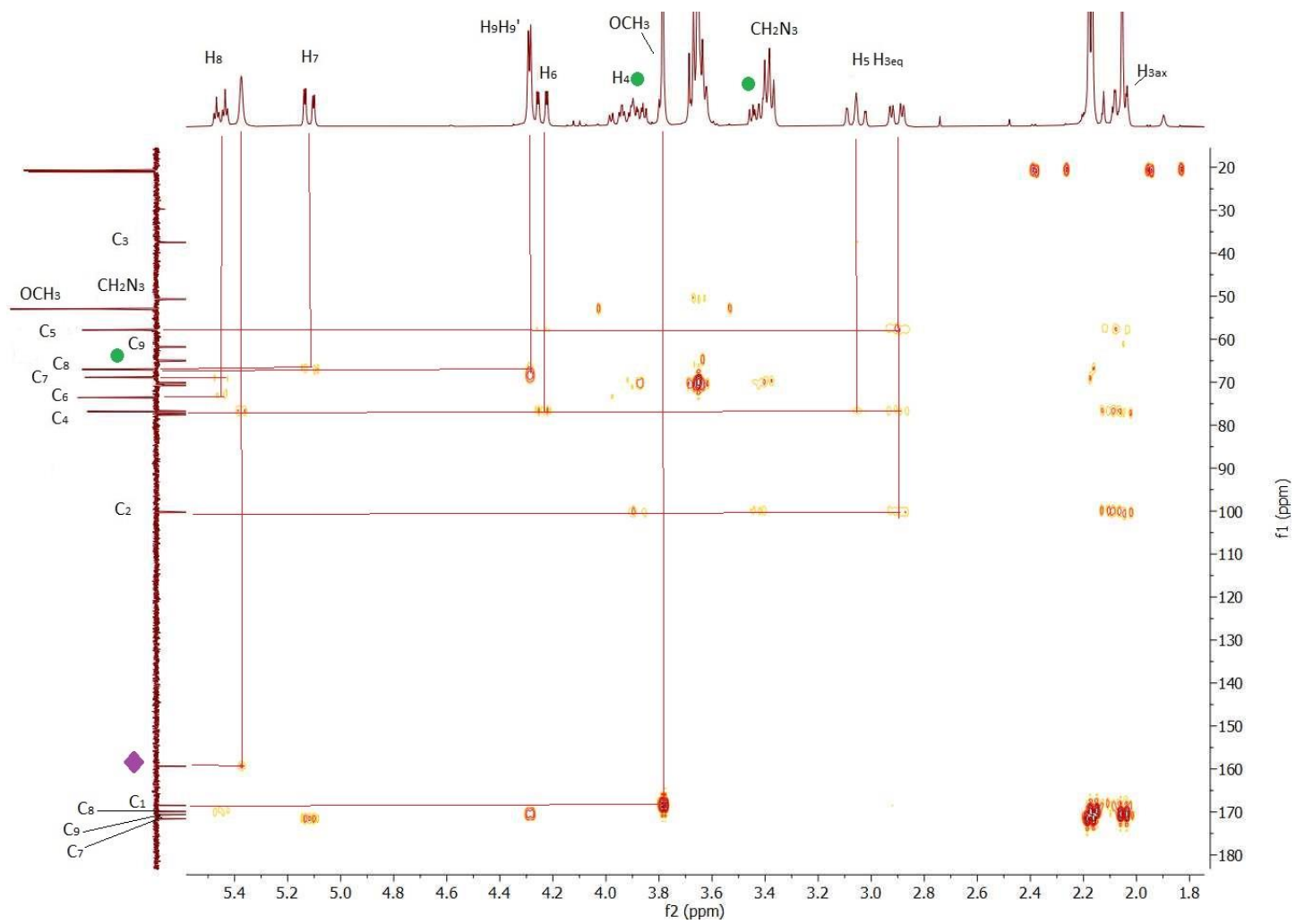


Figure 5.25 HMBC spectra of compound 5.183.

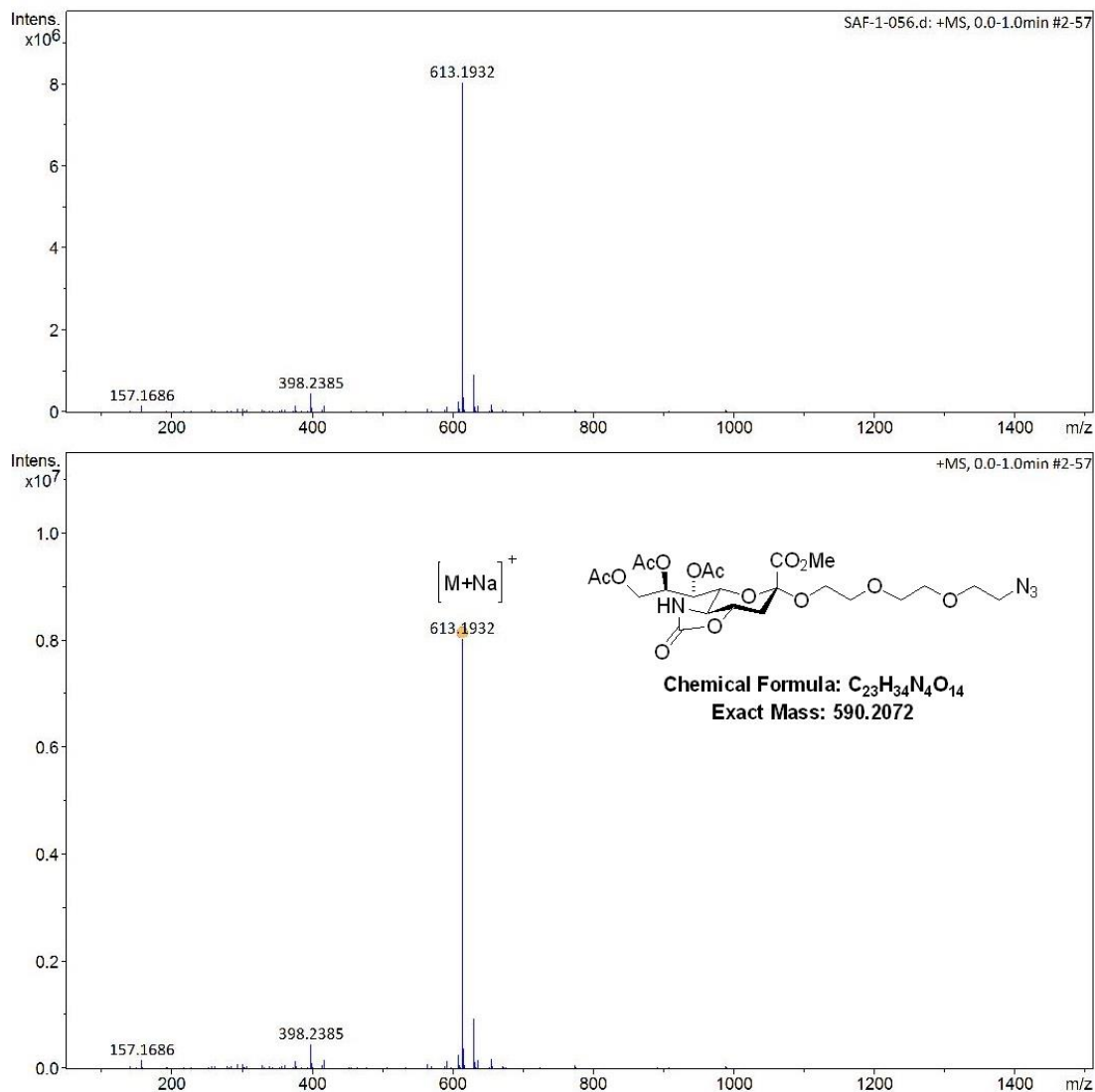


Figure 5.26 HRMS spectrum of compound **5.183**.

As illustrated in Figure 5.21, doublet of doublets of H_{3eq} at 2.88 ppm and triplet of H_5 at 3.03 ppm of clearly indicates α -anomer. All the 1H and ^{13}C signal assignments were unambiguously determined using DEPT- ^{13}C (Figure 5.22) together with 2D-COSY (Figure 5.23), HSQC (Figure 5.24) and HMBC (Figure 5.25) experiments. The structure of **5.183** was also confirmed by HMRS technique (Figure 5.26). To this end, total deprotection of sugar moiety with LiOH in EtOH/H₂O, following

chemoselective *N*-acetylation and Zemplén transesterification reactions provided **5.171** in almost quantitative yield. As confirmation of α -configuration of **5.183**, during ^1H NMR analysis of **5.171** doublet of doublets, at 2.74 ppm was found to correspond to $H_{3\text{eq}}$ α -anomer.

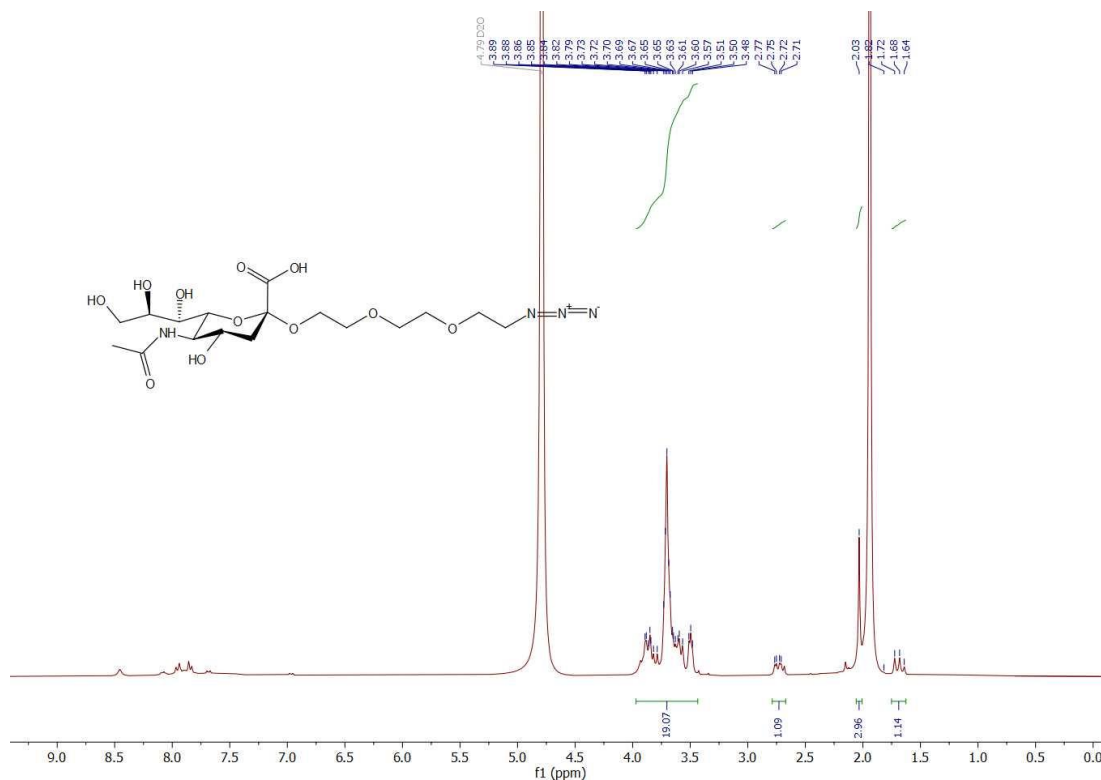
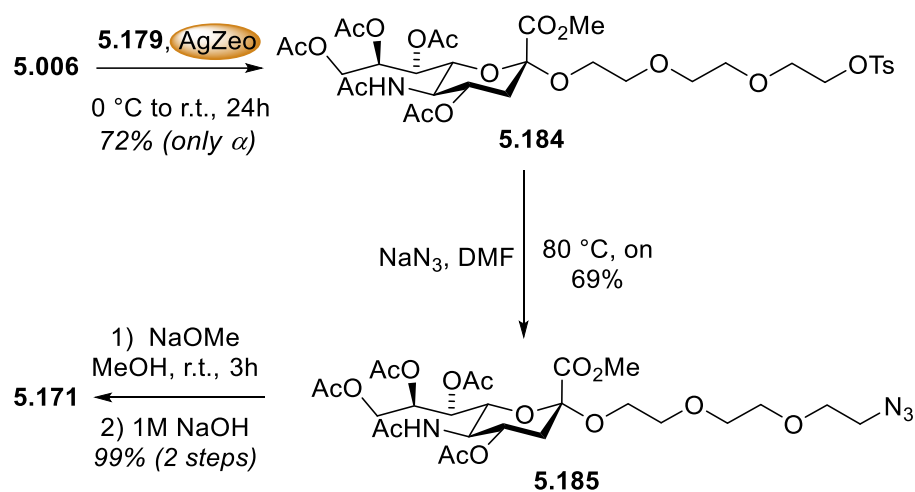


Figure 5.27 ^1H NMR (300 MHz, D_2O) spectrum of compound **5.171**.

An alternative synthetic pathway was next explored to prepare **5.171** through low-cost, atom economical and in stereoselective manner. In 2002 Hindsgaul *et al.* reported treating **5.006** with methyl glycolate in presence of commercially available silver-exchanged zeolite ($\text{Ag}_{84}\text{Na}_2[(\text{AlO}_2)_8(\text{SiO}_2)_{106}] \cdot x\text{H}_2\text{O}$) afforded exclusive α -anomer.⁵⁵⁹ However to our knowledge sialylation with PEGs is not known up to date. In light of Hindsgaul's reported work, **5.183** was successfully synthesized *via* treating **5.006** with **5.179** in presence of insoluble granular mesh of silver-exchanged zeolites

(at room temperature, in dry toluene, 24 h of stirring). After filtration over celite, ^1H NMR analysis of crude product showed only α -anomer formation. Further purification by column chromatography on silica gel afforded **5.184** in 72 % yield as a white solid. All the ^1H (Figure 5.28) and ^{13}C NMR signal assignments were determined by using DEPT (Figure 5.129), 2D COSY (5.130) and HSQC (5.131) experiments. Treatment of tosylate by NaN_3 in DMF at $80\text{ }^\circ\text{C}$ in 8 h gave **5.185** in 69 % yield. Subsequently, total deprotection of **5.185** *via* Zemplén transesterification and basic hydrolysis afforded desired product **5.171** in shortest pathway. Spectroscopic data of obtained product **5.171** by both methods was identical.



Scheme 5.26 Stereoselective sialylation by using insoluble silver zeolite.

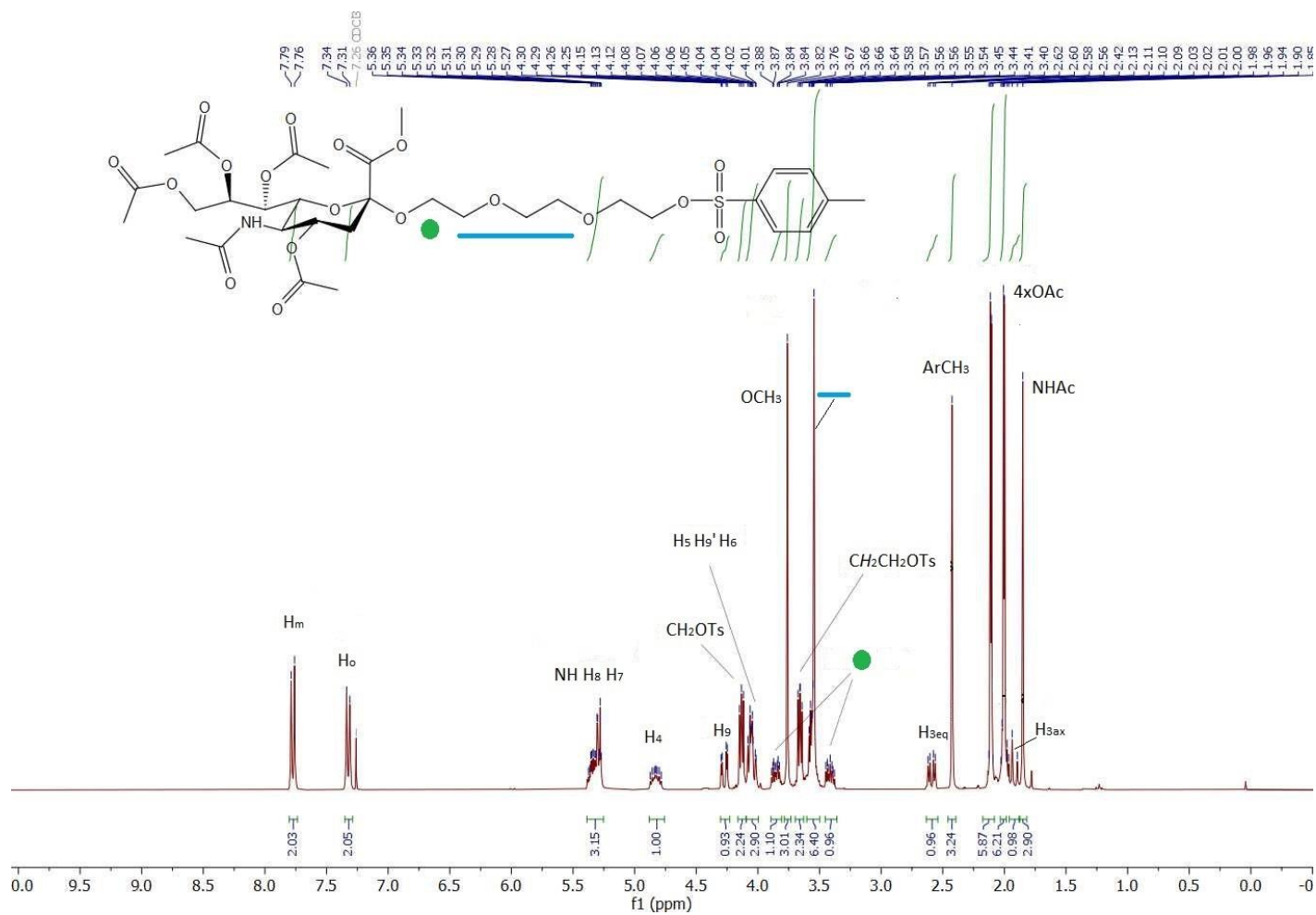


Figure 5.28 $^1\text{H NMR}$ (300 MHz, CDCl_3) spectrum of compound 5.184.

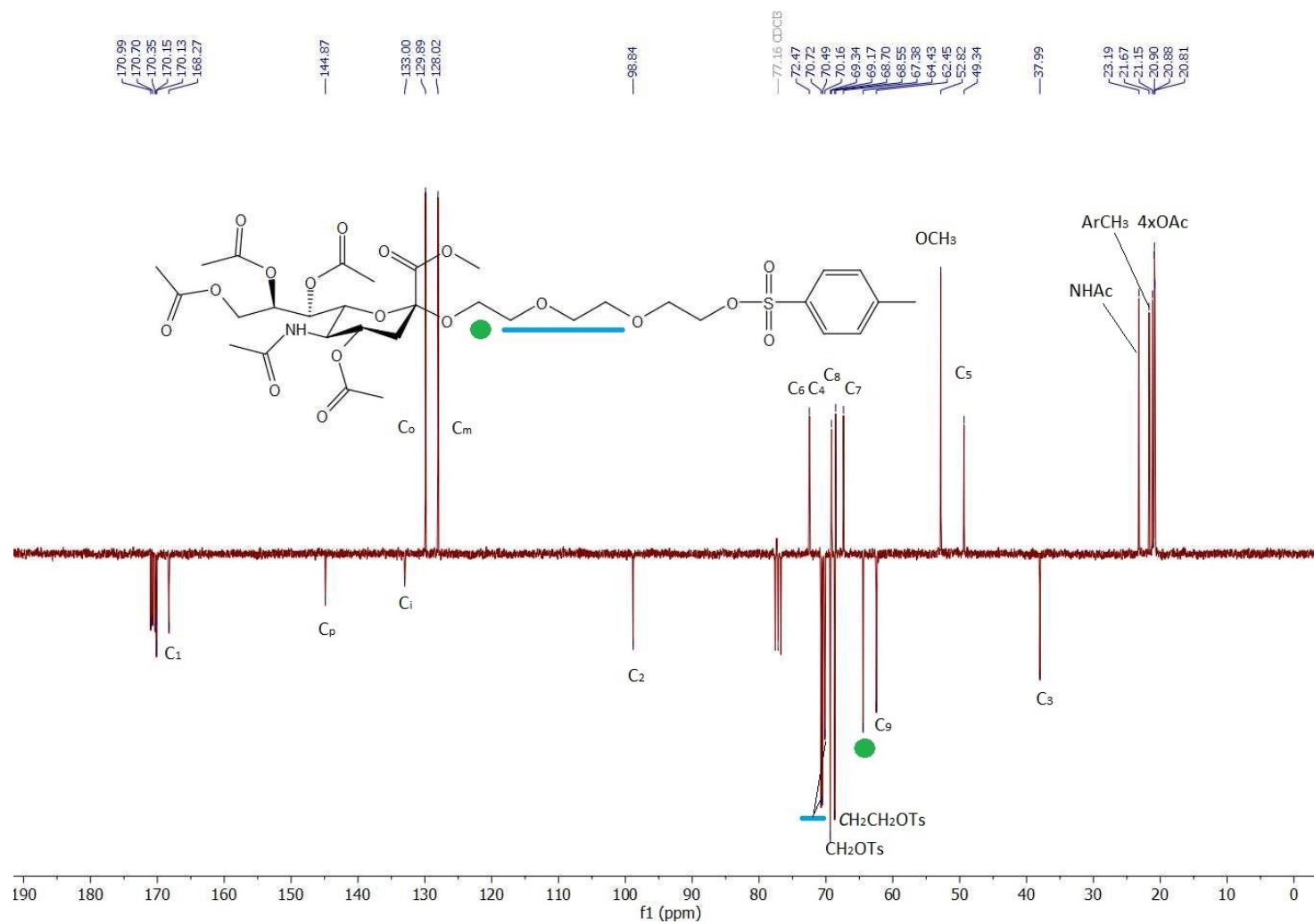


Figure 5.29 DEPT ¹³C NMR (75 MHz, CDCl₃) spectrum of compound 5.184.

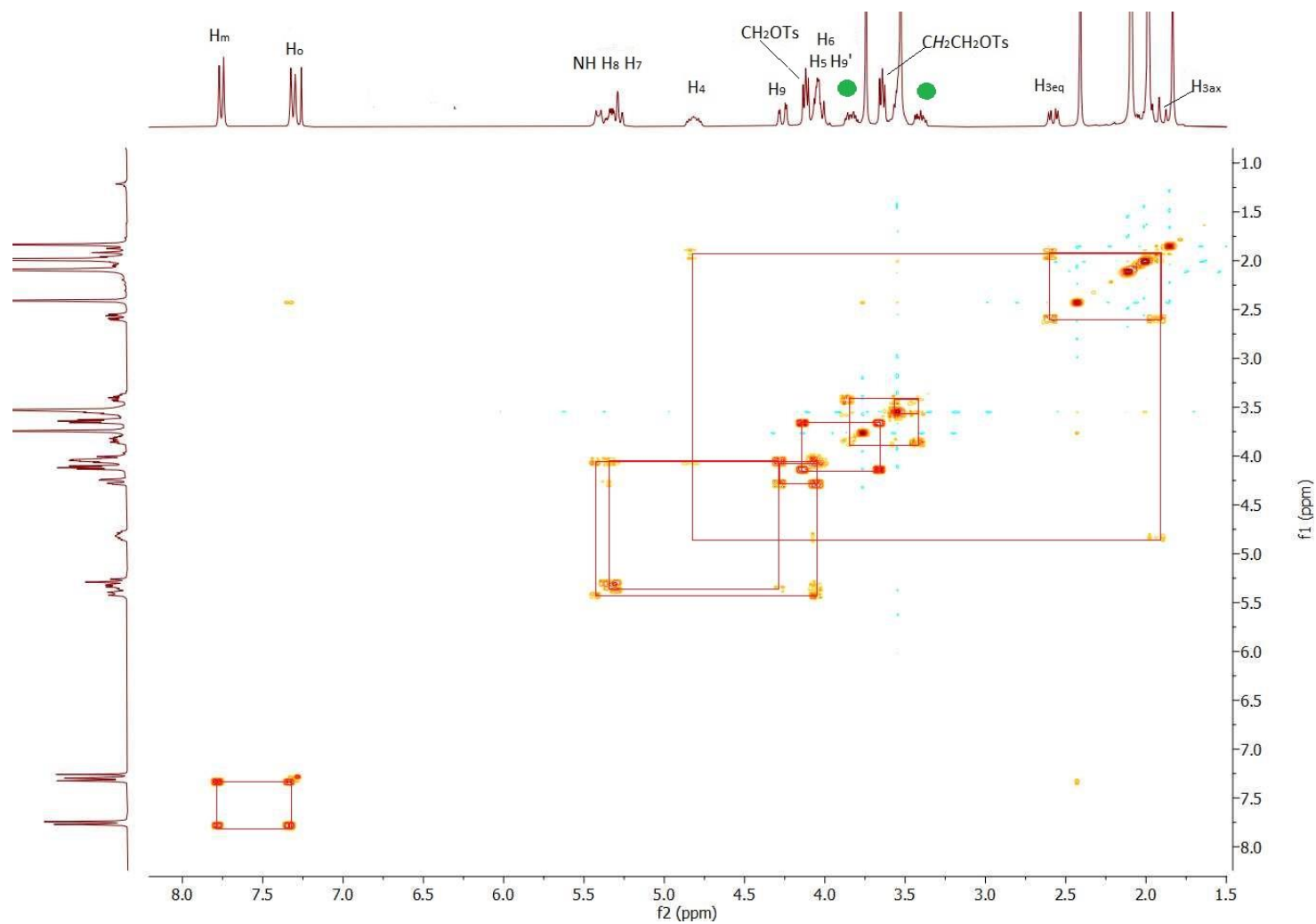


Figure 5.30 2D COSY spectrum of compound 5.184.

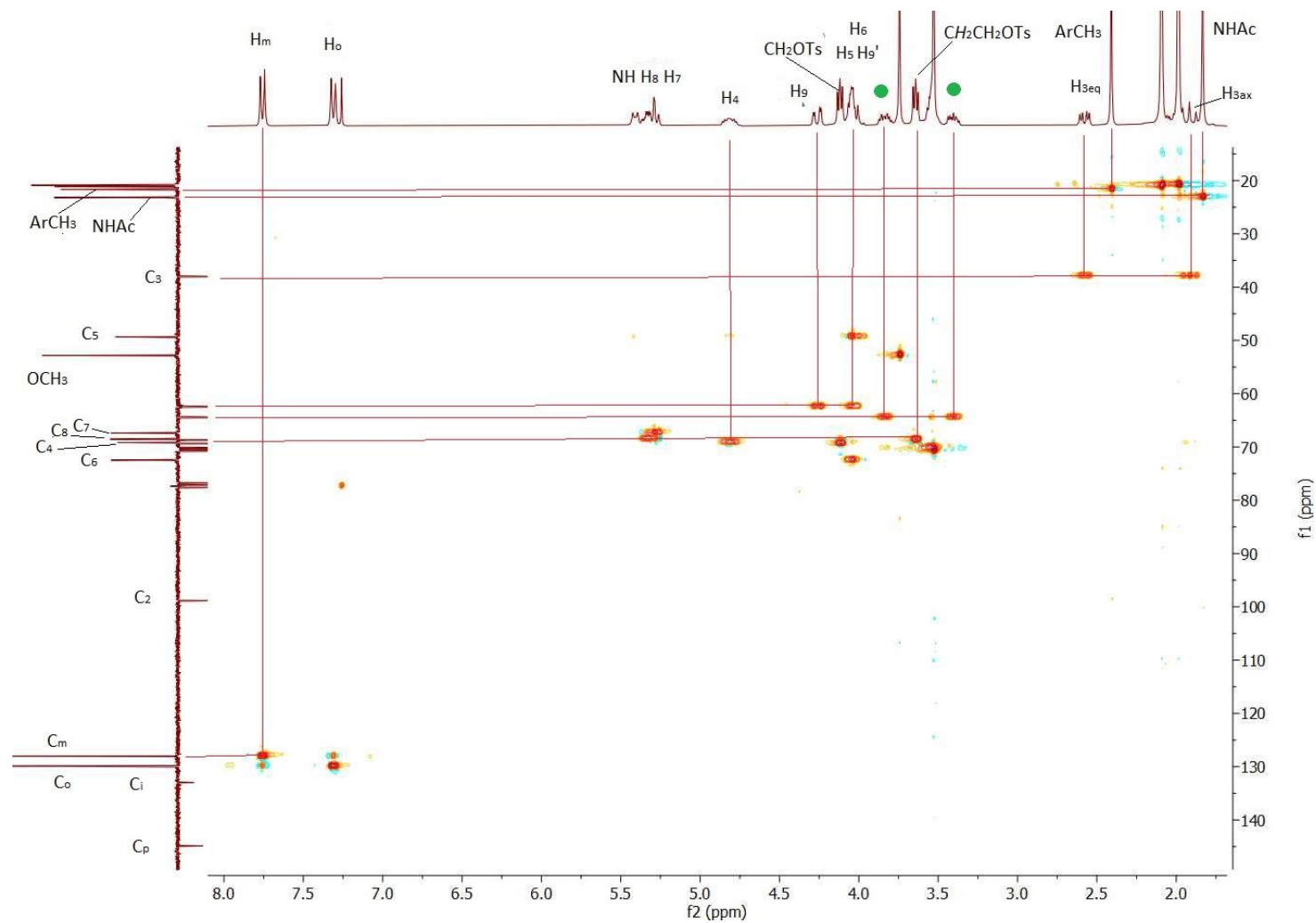
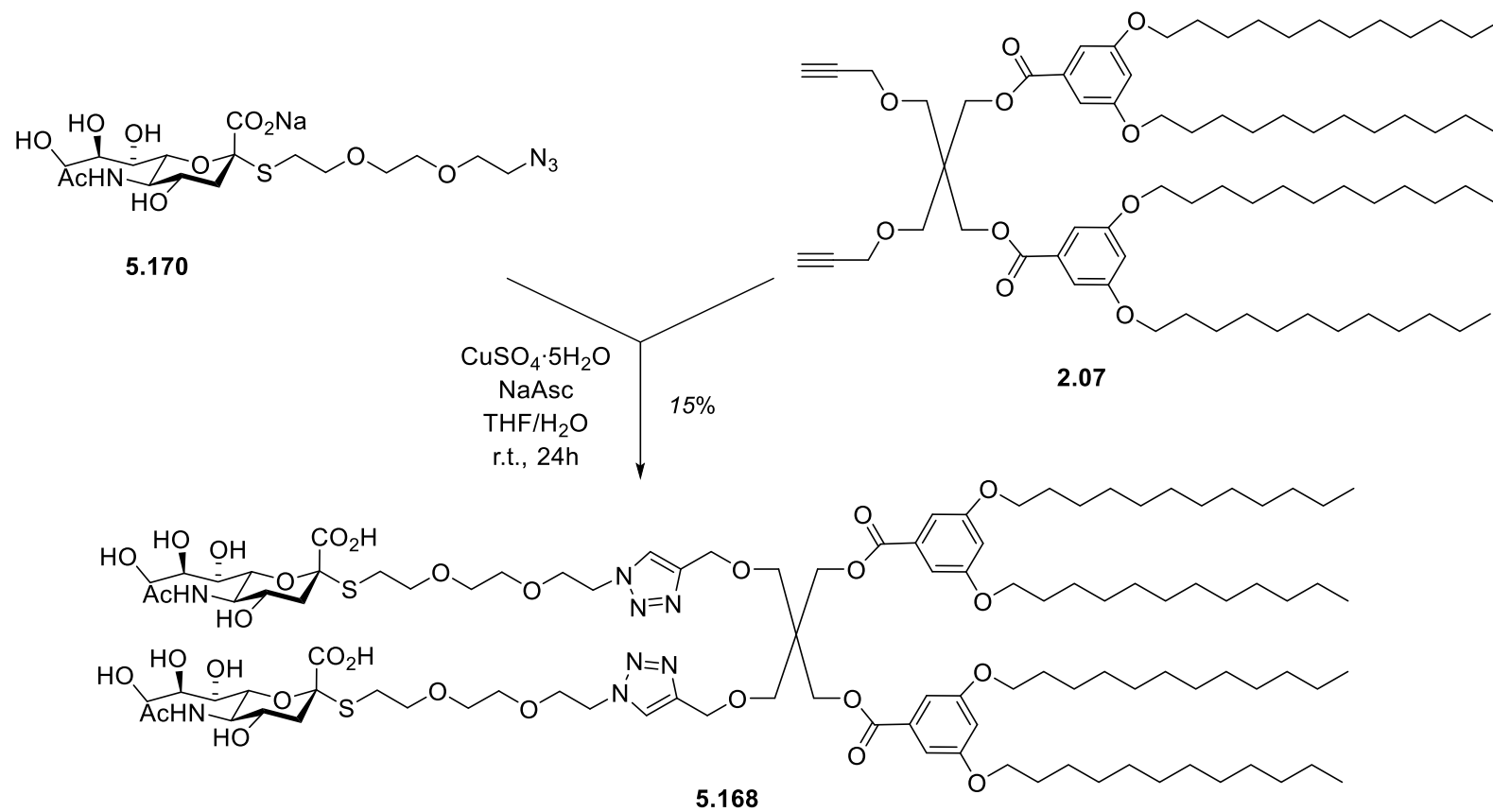


Figure 5.31 HSQC spectrum of compound 5.184.

5.3.4 Synthesis of amphiphilic Janus sialodendrimer and generation of sialodendrimerosomes

After synthesizing both azide and alkyne functionalized intermediates, we turned our efforts to conjugate each other *via* CuAAC-based click reaction. Therefore, treating azido thiosialoside **5.170** with previously prepared hydrophobic lipid tail **2.07** under classical click condition ($\text{CuSO}_4 \cdot 5\text{H}_2\text{O}$, sodium ascorbate (NaAsc) in THF/ H_2O , at room temperature, 24 h of stirring) afforded **5.168**. Unfortunately, purification by silica gel column chromatography did not provide pure product. To address this issue and circumvent the presence of toxic copper, Sephadex[®]-G10 gel filtration was chosen as an alternative. Elution with 0.01M NaN_3 solution afforded desired product as white solid. All the ^1H (Figure 5.32) and ^{13}C (Figure 5.33) signal assignments were unambiguously determined using DEPT- ^{13}C (Figure 5.14) together with 2D-COSY, HSQC and HMBC experiments. Covalent conjugation of the intermediates **5.168** was then confirmed with relative hydrogen ratio between H_{triaz} . (s, 2H, 7.79 ppm), H_{p} (brs, 2H, 6.60 ppm) and $\text{H}_{3\text{ax}}$. (t, 2H, 1.82 ppm) which are 1:1:1. Due to poor yield and difficulty in purification stage, click product **5.169** having *O*-sialoside could not be isolated. In contrast to click reaction between *S*-sialoside **5.170** (0.11 g, 0.23 mmol, 2.5 eq.) and **2.07** (0.11 g, 0.09 mmol, 1 eq.) which led to **5.168** (0.03 g, 0.014 mmol, 15 %), click reaction between *O*-sialoside **5.169** (0.03 g, 0.06 mmol, 2.4 eq.) and **2.07** (0.03 g, 0.025 mmol, 1 eq.) was carried out in smaller scale. To this end, either HPLC purification method or click reaction with increased scale of starting materials could be an alternative solution.



Scheme 5.27 Click reaction between hydrophobic and hydrophilic intermediates.

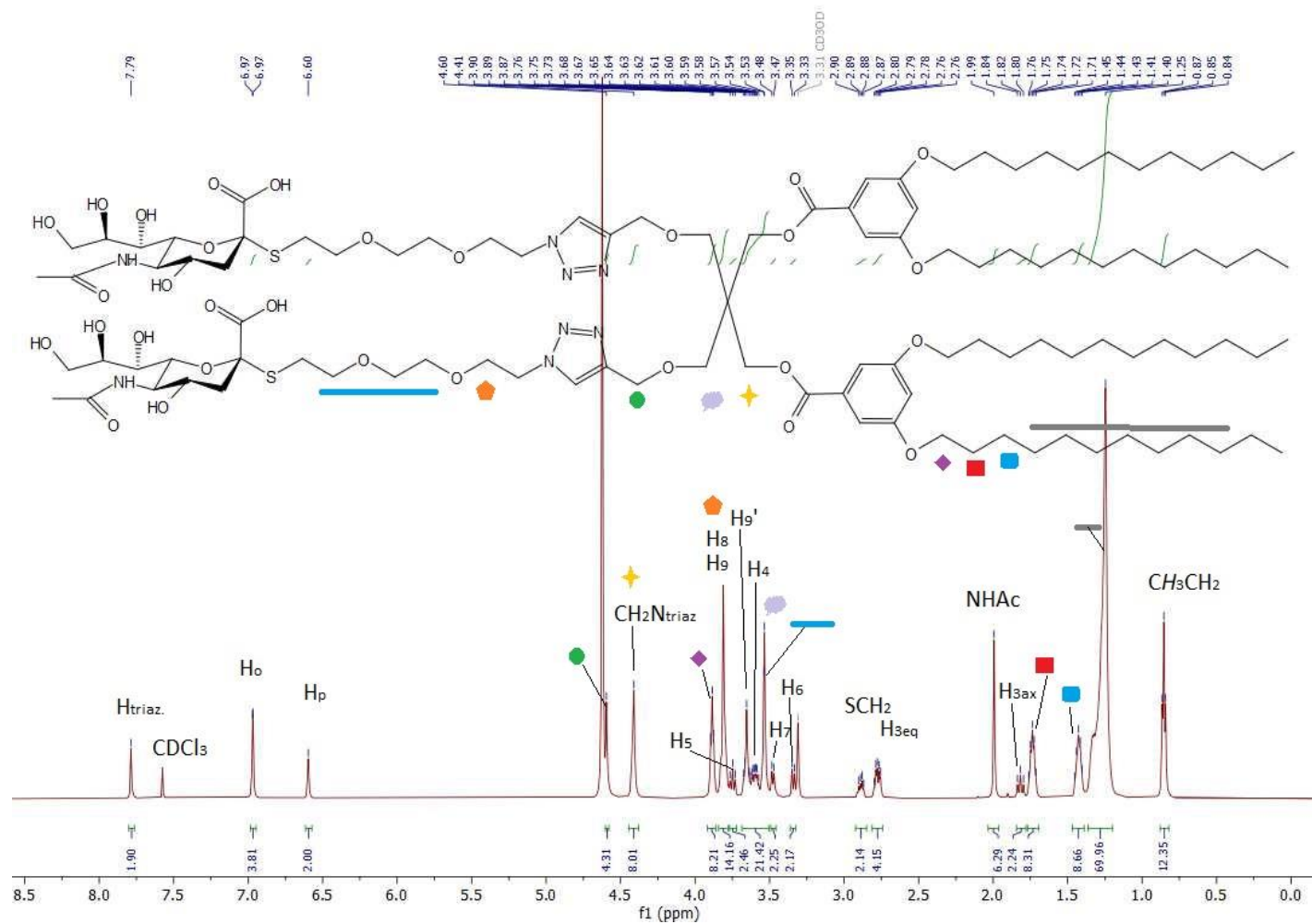


Figure 5.32 ¹H NMR (600 MHz, CD₃OD+CDCl₃ (v/v : 1/1)) spectrum of compound 5.168.

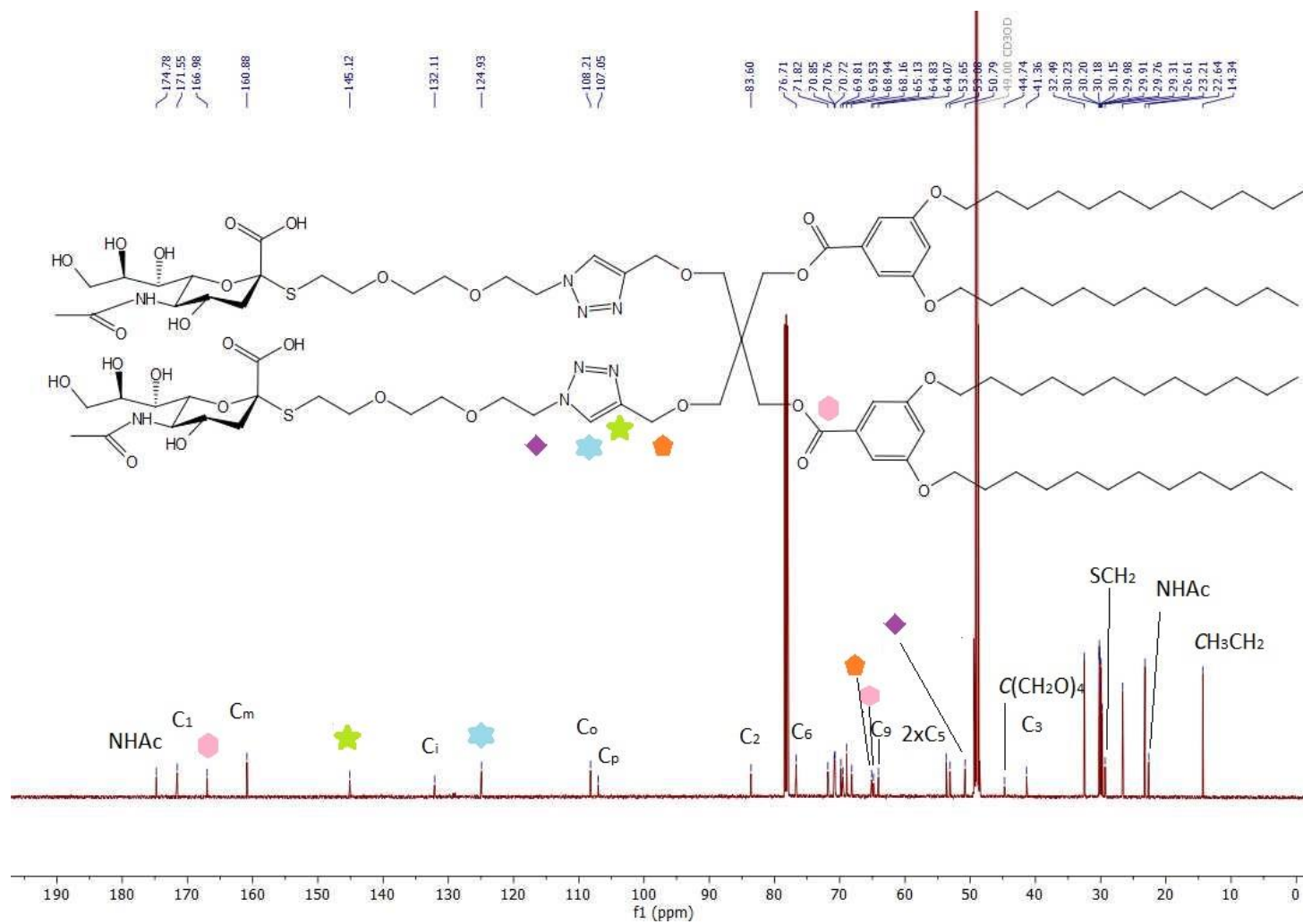


Figure 5.33 ^{13}C NMR (150 MHz, $\text{CD}_3\text{OD}+\text{CDCl}_3$ (v/v : 1/1)) spectrum of compound **5.168**.

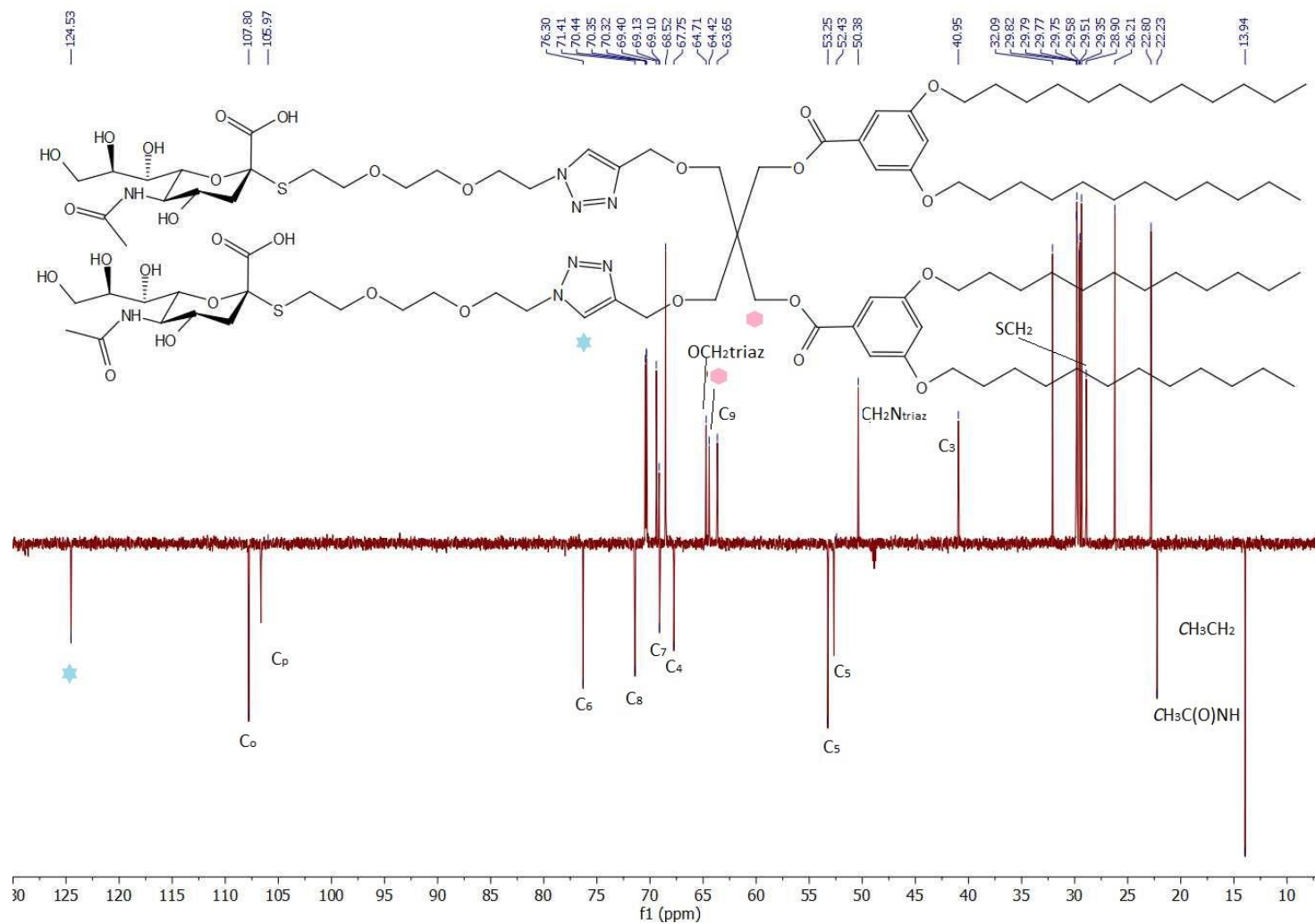
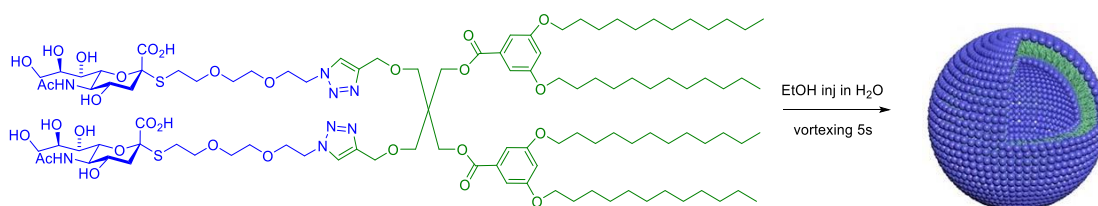


Figure 5.34 DEPT ¹³C NMR (150 MHz, CD₃OD+CDCl₃ (v/v : 1/1)) spectrum of compound 5.109.

Using ethanol injection method, different concentration (0.1mg/mL-5mg/mL) of sialodendrimersomes from **5.168** were prepared and particles size and polydispersity index (PdI) were measured by DLS technique (Scheme 5.29).



Scheme 5.28 Generation of sialodendrimersome via ethanol injection method.

During DLS analysis it was revealed that sialodendrimersomes from **5.168** at 0.1 mg/mL and 0.2 mg/mL in EtOH exhibit higher PdI and as well as LacNAc-based glycodendrimersomes from **4.109** (Figure 5.35). In the context, it was observed that low concentrations (0.1 mg/mL – 0.5 mg/mL) of Glyco-Janus dendrimers in EtOH led to formation of polydisperse suspensions with multiple vesicle size populations. As explained for glycoliposomes, dilute particle concentration affords stable small vesicles with high curvature by virtue of negligible repulsive forces between hydrophilic head group and lipophilic tail.⁵⁶⁰ However, from 0.5mg/mL towards 5mg/mL, Z_{avg} augments in a linear fashion and PdI remains nearly unchanged (Figure 5.36).

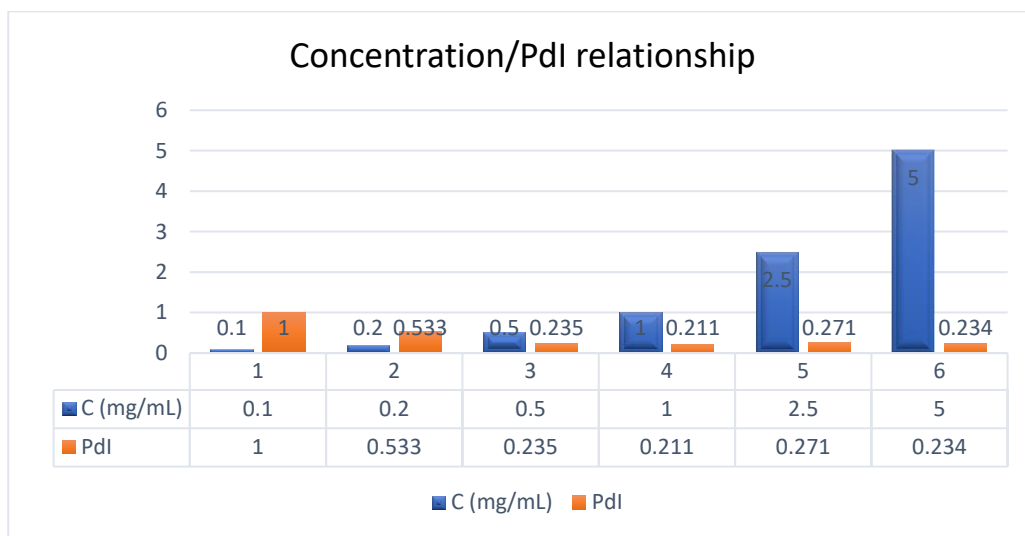


Figure 5.35 Plot of sialodendrimerosome from **5.168**, concentration versus Pdl.

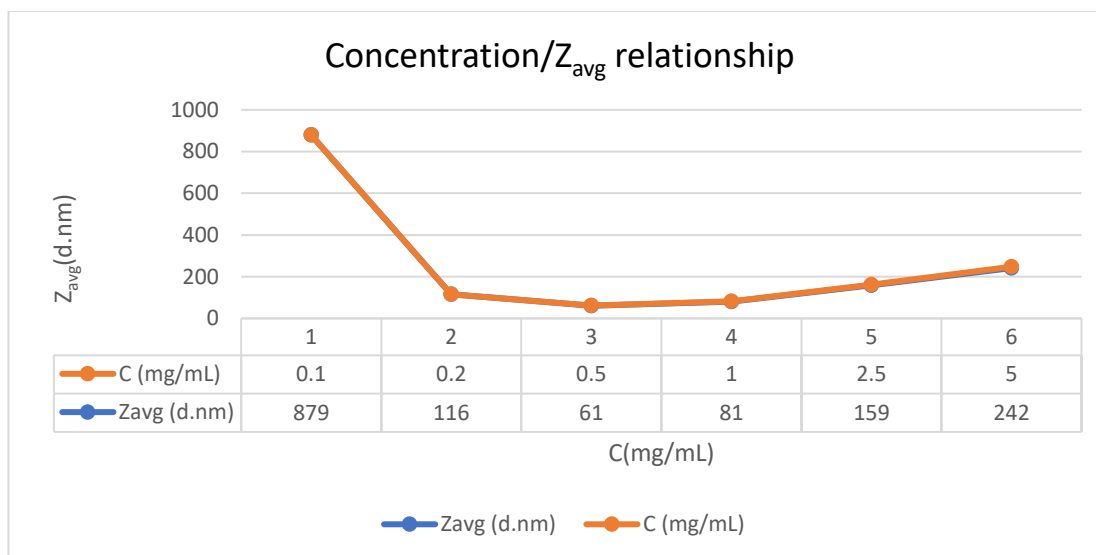


Figure 5.36 Plot of sialodendrimerosome from **5.168**, concentration versus Z_{avg} .

The DLS studies also revealed that the size of nanoparticles is quasi-invariant at first four entries (Figure 5.37).

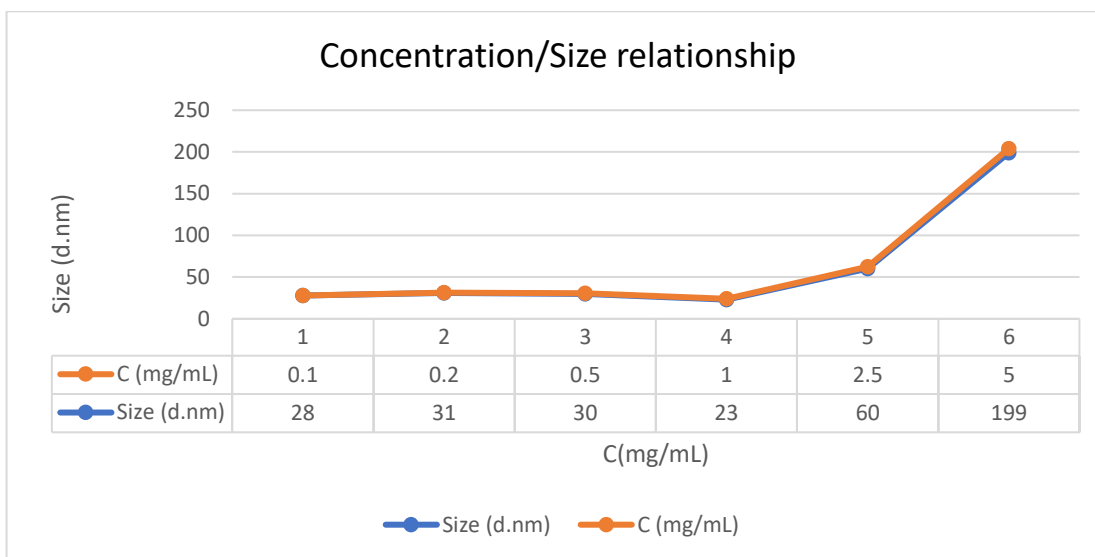
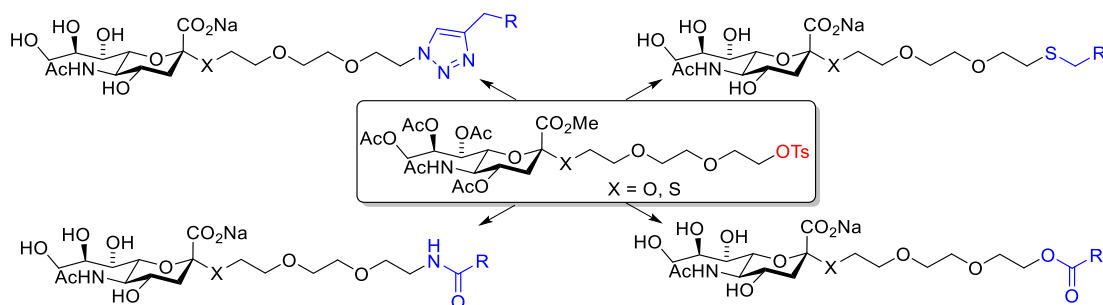


Figure 5.37 Plot of sialodendrimersome from **5.168**, concentration versus size.

The large gap between Z_{avg} and size at 0.1 mg/mL shows the distribution of small and large components in the suspension that corresponds to polydisperse particles. As the PDI value equal to 1, this result is self-explanatory. While increasing concentration up to $C_m = 2.5$ mg/mL, the size of nanoparticle augments from 23 nm to 60 nm. At 5mg/mL the size of nanoparticles is much closer to those of Z_{avg} which is considered sign of monodispersity.

5.4 Conclusion

In summary, the synthesis of Pegylated sialosides with two types of glycosidic linkages were accomplished in low-cost, atom economical and stereoselective manner. Having tosylate group at the focal point is particularly interesting for further coupling with various lipid tails (Scheme 5.29).



Scheme 5.29 Advantage of tosylate activating group at the focal point for further functionalization *via* S_N2 -type substitution.

During *S*-sialoside synthesis replacement of TBAHS by TBATA led to glycal free product. On the other hand, silver-exchanged zeolite was used for the first time with PEG to afford exclusive α -anomer. Conjugation of azido-functionalized *S*-sialoside to Janus dendrimer precursor and formation of first example of sialodendrimerosome was achieved successfully. Size and PDI of generated sialodendrimerosome with various concentration were studied. As the average diameter size of most respiratory viruses including highly pathogenic Influenza vary between 20-200 nm, nanoparticles possessing similar size would be beneficial in the development of nanovaccine.

Moreover, as mentioned earlier, after HA-mediated attachment to host cells (HA binds to sialic acid receptors on the surface of host cells), influenza virus enters host cells by fusion of viral and endosomal membranes. Lee and Gui reported that *via* providing target membrane as synthetic liposome with a diameter between 100-200 nm, viral membrane of Influenza virus-liposome fusion can be achieved.⁵⁶¹

During DLS study of sialodendrimerosomes which were generated from **5.168** by ethanol injection method, it was revealed that increment of concentration of the dendrimers has huge impact on size and dispersity of nanoparticles. We presume at higher particle concentration the enhanced repulsive forces between hydrophilic and

lipophilic segments leads to higher bilayer membrane stiffness and lower curvature that results in coalescence of bilayered membranes to form larger vesicles.

CONCLUSION

During this thesis work, we have synthesized self-assembling Janus dendrimer **2.08** *via* radical initiated thiol-yne coupling (TYC) from previously reported Janus Dendrimer precursor **2.07** (CHAPTER II).¹¹³ Generated dendrimersomes were characterized with various techniques (AFM, TEM, DLS, FTIR) and applied for the first time in dendrimersome formulation of Lidocaine which is widely used as local anesthetic agent in dentistry. Due to poor bioavailability through *Stratum Corneum* the use of lipid-based nanocarrier for the topical delivery of lidocaine is promising for long-lasting and enhanced anesthetic effects. Toward this goal, together with the Lidocaine-loaded dendrimersome and liposomal formulation which is generated from commercially available soybean lecithin phospholipid and cholesterol mixture have been comparatively studied. Although we have found that our colloidal system (dendrimersome formulation) shows similar size and size distribution as well as liposomal formulation, physical and mechanical properties of lidocaine-loaded dendrimersome are superior. Additionally, having higher entrapment efficiency value (97%) of dendrimersomes makes them promising nanocarriers for the delivery of lipophilic drugs including lidocaine (*Int. J. Pharm.*; in preparation).

Knowing that cancer-related galectins bind to LacNAc and Lac residues, a small library of propargyl and *para*-nitrophenyl based lactosides could represent promising candidates for the development of galectin inhibitors. Making series of 3'-*O* derivatives of propargyl and *para*-nitrophenyl based unprotected lactosides requires high regioselectivity (CHAPTER II). Toward this goal, 3'-*O*-sulfation and alkylation have been carried out in regioselective manner by using dibutyltin oxide method.²⁴⁵ In order to obtain desired lactosides derivatives in a short sequence of steps without

unwanted side products synthesis of 6,6'-di-TBDPSi-protected intermediates (**3.34**, **3.50**, **3.59**) is the key strategy of this work. Together with the results of biostudy toward galectins, this work will be published in scientific peer-reviewed journal. Moreover, we have also reported known to date exceptionally short synthesis of trisaccharide – Sialyl (2→3') LacNAc **3.41** in a cost-effective and highly atom-economic fashion (*Carbohydr. Res.*; in preparation).

Propargyl and *para*-nitrophenyl aglycons have been chosen not only for investigation of newly created hydrophobic interactions at carbohydrate binding site of galectins but also for further conjugation to Janus dendrimer precursors (CHAPTER IV). Therefore, glycodendrimersomes have been already reported to show excellent ligand bioactivity *via* selective agglutination in presence of leguminous, bacterial and mammalian lectins. With regard to this matter we have synthesized first example of LacNAc-conjugated Janus dendrimer through CuAAC-mediated click chemistry reaction. During DLS studies it was revealed that depending on concentration the size of lactodendrimersomes generated from **4.109** can be predictable. Together with further biological investigation of lactodendrimersomes toward galectins this thesis work can be published in scientific peer-reviewed journal.

In the latest chapter (CHAPTER V) we have reported first example of sialic acid-attached Janus dendrimer and formation of sialodendrimersomes within ethanol injection method. The size-concentration relation was studied by DLS technique and found that at smaller concentrations ($C_m = 0.1$ mg/mL and 0.2 mg/mL) of sialic acid-attached Janus dendrimer in ethanol, formed colloidal suspensions are polydisperse. However, starting from $C_m = 0.5$ mg/mL toward 5 mg/mL the vesicle sizes augment in linear fashion with narrow size distribution. Moreover during this project we have developed an efficient method to synthesize pegylated *S*-sialosides. Therefore, by using tetrabutylammonium thioacetate (TBATA) as phase transfer agent, incorporation of sulfur atom through nucleophilic substitution reaction under PTC

conditions (β -chloro sialyl donor, KSAc, TBATA, 0.5M Na₂CO₃ in EtOAc) afforded desired thioacetyl derivative of sialic acid without formation of the glycal (Carbohydrate Chemistry: Proven Synthetic Methods Vol. 6; in preparation). The low-cost and atom economical stereoselective synthesis of pegylated *O*-sialoside with tosylate activating group at focal point by using commercially available silver-exchanged zeolite was also reported for the first time in this work (Carbohydrate Chemistry: Proven Synthetic Methods Vol. 6; in preparation).

At the end it worth to note that throughout this thesis work at chromatographic purification stage all products are isolated by using classical silica gel column chromatography.

CHAPTER VI

EXPERIMENTAL PARTS

6.1 Materials and methods

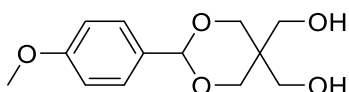
All reactions in organic medium were performed in standard oven dried glassware under an inert atmosphere of nitrogen using freshly distilled solvents. Solvents and reagents were deoxygenated, when necessary, by purging with nitrogen. All reagents were used as supplied without prior purification unless otherwise stated, and obtained from Sigma-Aldrich Chemical Co. Ltd. Reactions were monitored by analytical thin-layer chromatography (TLC) using silica gel 60 F254 precoated plates (E. Merck) and compounds were visualized with a 254 nm UV lamp, potassium permanganate solution (1.5 g KMnO_4 , 10 g K_2CO_3 , 1.5 mL 10 % NaOH in 200 mL H_2O), a mixture of iodine/silica gel and/or mixture of ceric ammonium molybdate solution (100 mL H_2SO_4 , 900 mL H_2O , 25 g $(\text{NH}_4)_6\text{Mo}_7\text{O}_{24}\cdot\text{H}_2\text{O}$, 10 g $\text{Ce}(\text{SO}_4)_2$), and subsequent spots development by gentle warming with a heat-gun. Purifications were performed either by silica gel flash column chromatography using Silica (60 Å, 40-63 μm) with the indicated eluent or Sephadex® G-10 gel filtration method. The optical rotation measurement $[\alpha]_D$ was performed at 589 nm by using Jasco P2000 polarimeter. NMR

spectroscopy was used to record ^1H NMR and ^{13}C NMR spectra at 300 or 600 MHz and at 75 or 150 MHz, respectively, on Bruker (300 MHz) and Bruker Avance III HD 600 MHz spectrometers. Proton and carbon chemical shifts (δ) are reported in ppm relative to the chemical shift of residual CDCl_3 (in ^1H 7.26 ppm, in ^{13}C 77.16 ppm), CD_3OD (in ^1H , 3.31 ppm and in ^{13}C , 49.0 ppm), DMSO-d_6 (in ^1H , 2.50 ppm and in ^{13}C , 39.5 ppm), Acetone-d_6 (in ^1H , 2.05 ppm and in ^{13}C , 206.7, 29.9 ppm), D_2O (in ^1H , 4.79 ppm) which were set respectively. 2D homonuclear correlation spectroscopy ^1H - ^1H (COSY) and ^1H - ^{13}C heteronuclear single quantum coherence (HSQC) experiments were used to confirm NMR peak assignments. Coupling constants (J) are reported in Hertz (Hz), and the following abbreviations are used for peak multiplicities: singlet (s), broad singlet (brs), doublet (d), doublet of doublets (dd), doublet of doublets of doublets (ddd), triplet (t), doublet of triplets (dt), triplet of doublets (td), triplet of triplets (tt), multiplet (m). Analysis and assignments were made using COSY (Correlated SpectroscopY) and HSQC (Heteronuclear Single Quantum Coherence) experiments. High-resolution mass spectrometry (HRMS) data were measured either with a LC-MS-TOF (Liquid Chromatography-Mass Spectrometry-Time of Flight; Agilent Technologies) in positive and/or negative electrospray mode(s) at the analytical platform of UQAM or with MALDI-TOF (matrix-assisted laser desorption/ionization time of flight mass spectrometry) at McGill university. Particle size distribution (DLS) was measured in water with the help of Zetasizer Nano S90 from Malvern Instruments at UQAM.

6.2 Experimental Part of Chapter II

6.2.1 Synthesis and characterization

2-(4-Methoxyphenyl)-5,5-bis(hydroxymethyl)-1,3-dioxane (**2.01**)



Pentaerythritol (5.22 g, 38.3 mol, 1 eq.) was dissolved in water (50 mL) with heating until complete dissolution. The solution was then cooled to room temperature. Into the stirring solution, commercially available concentrated 37 % HCl (0.35 mL) and *para*-anisaldehyde (0.45 mL, 3.7 mmol, 0.1 eq) were added successively. Upon appearance of precipitation, another portion of *para*-anisaldehyde (4.2 mL, 34.47 mmol, 0.9 eq.) was added dropwise and the reaction mixture was stirred at room temperature for 4.5 h. The precipitate was collected, washed with ice-cold Na₂CO₃ solution (10 g of Na₂CO₃ in 500 mL of H₂O), Et₂O (2 x 250 mL), dried over P₂O₅ and concentrated *in-vacuo* to give **2.01** as a white solid (8.2 g, 32.59 mmol, 85 %).

¹H NMR (300 MHz, DMSO-*d*₆) δ (ppm) 7.34 (d, *J* = 8.7 Hz, 2H), 6.90 (d, *J* = 8.8 Hz, 2H), 5.35 (s, 1H), 4.59 (brs, 2H), 3.90 (d, *J* = 11.4 Hz, 2H), 3.84 – 3.57 (m, 7H), 3.26 (s, 2H)

¹³C NMR (75 MHz, DMSO-*d*₆) δ (ppm) 159.4, 131.3, 127.5, 113.3, 100.7, 69.1, 61.1, 59.6, 55.1

The spectroscopic data agreed well with those of the literature.¹¹³

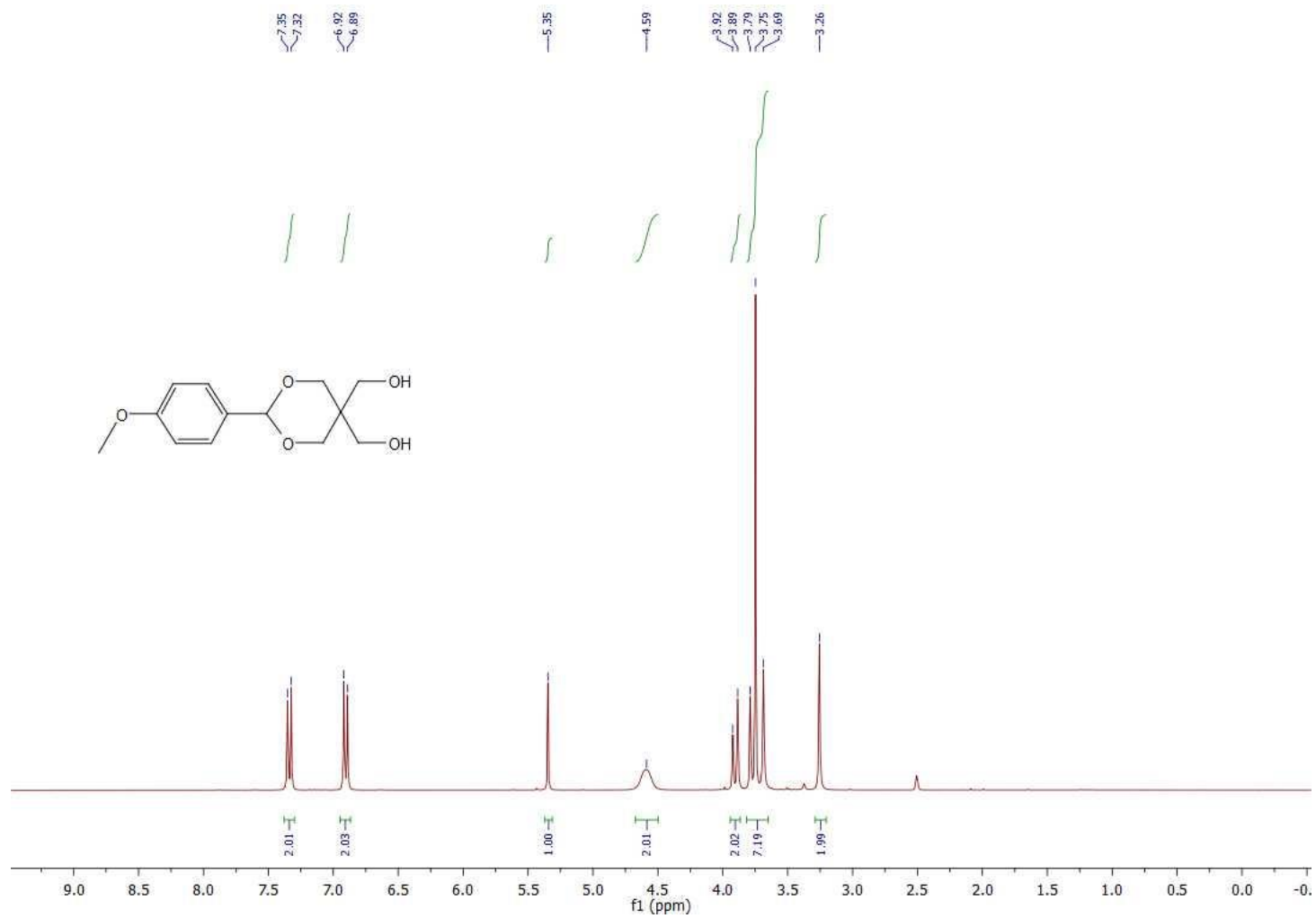


Figure 6.1 ¹H NMR (300 MHz, DMSO-d₆) spectrum of compound **2.01**.

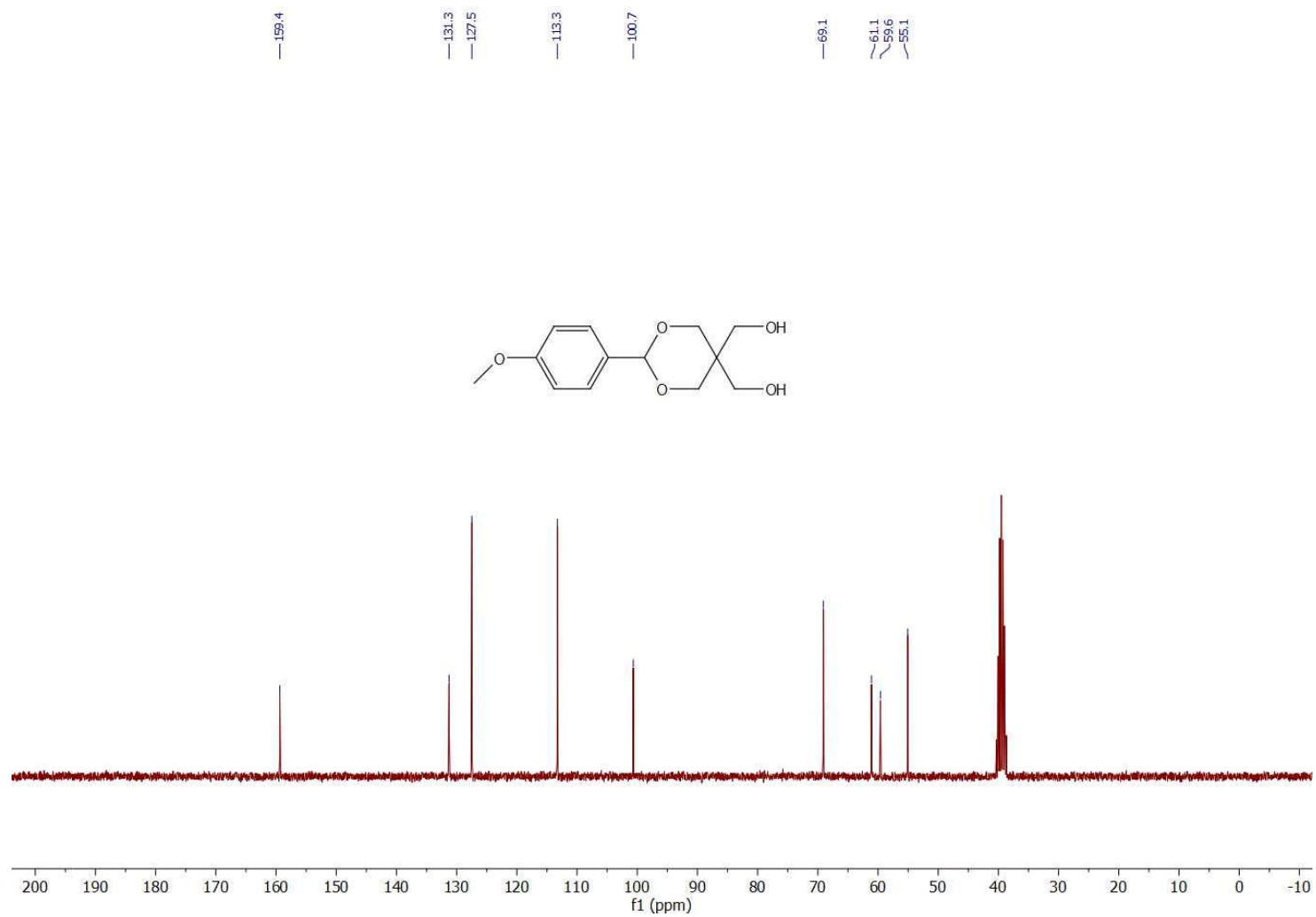
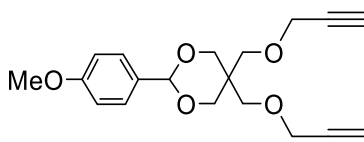


Figure 6.2 ^{13}C NMR (75 MHz, DMSO- d_6) spectrum of compound 2.01.

2-(4-Methoxyphenyl)-5,5-bis((prop-2-yn-1-yloxy)methyl)-1,3-dioxane **2.02**

To a solution of compound **2.01** (5.2 g, 20.47 mmol, 1 eq.) in dry DMF (70 mL) was added NaH (60 % dispersion in mineral oil; 6.45 g, 161.25 mol, 7.9 eq.) in one portion at 0 °C and stirred for 30 min. Then, propargyl bromide (80 % in toluene, 5.25 mL, 47.13 mmol, 2.3 eq.) was added dropwise and the reaction mixture was stirred at room temperature for 12 h. The water was added (100 mL), and the reaction mixture was extracted with Et₂O (3 x 150 mL), washed with water (2 x 100 mL) and dried over Na₂SO₄ and concentrated *in-vacuo*. After chromatographic purification compound **2.02** (5.88 g, 17.81 mmol, 87 %) was obtained as a pale-yellow oil.

R_f = 0.36, (EtOAc/hexane : 1/4)

¹H NMR (300 MHz, CDCl₃) δ (ppm) 7.41 (d, *J* = 8.7 Hz, 2H), 6.89 (d, *J* = 8.8 Hz, 2H), 5.39 (s, 1H), 4.21 (d, *J* = 2.4 Hz, 2H), 4.12 (d, *J* = 2.3 Hz, 2H), 4.08 (s, 2H), 3.92 – 3.84 (m, 4H), 3.80 (s, 3H), 3.37 (s, 2H), 2.48 – 2.40 (m, 2H)

¹³C NMR (75 MHz, CDCl₃) δ (ppm) 160.1, 131.0, 127.5, 113.7, 101.8, 80.0, 79.7, 74.7, 74.3, 69.9, 69.9, 68.8, 58.9, 58.9, 55.4, 38.6

The spectroscopic data agreed well with those of the literature.¹¹³

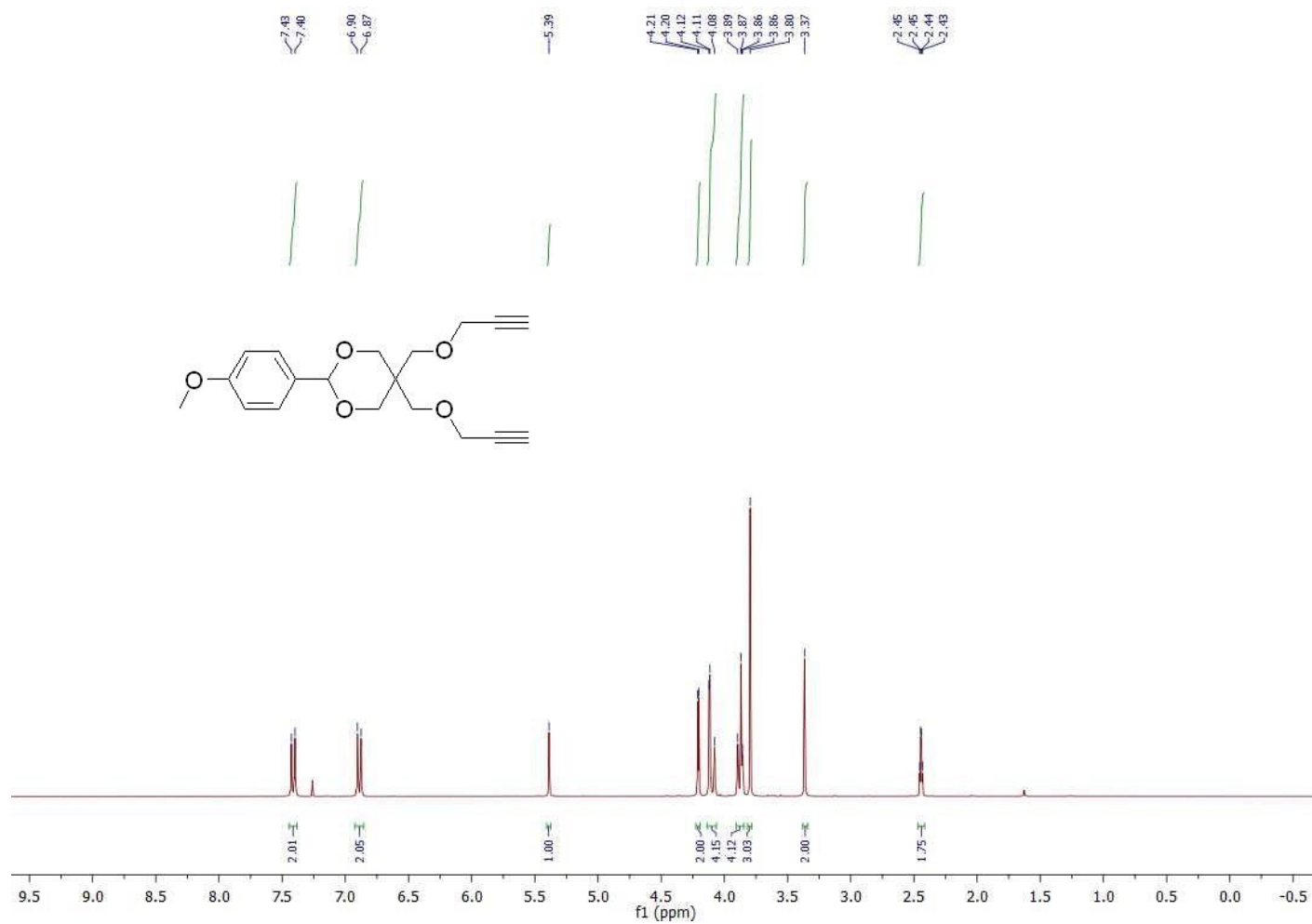


Figure 6.3 ¹H NMR (300 MHz, CDCl₃) spectrum of compound **2.02**.

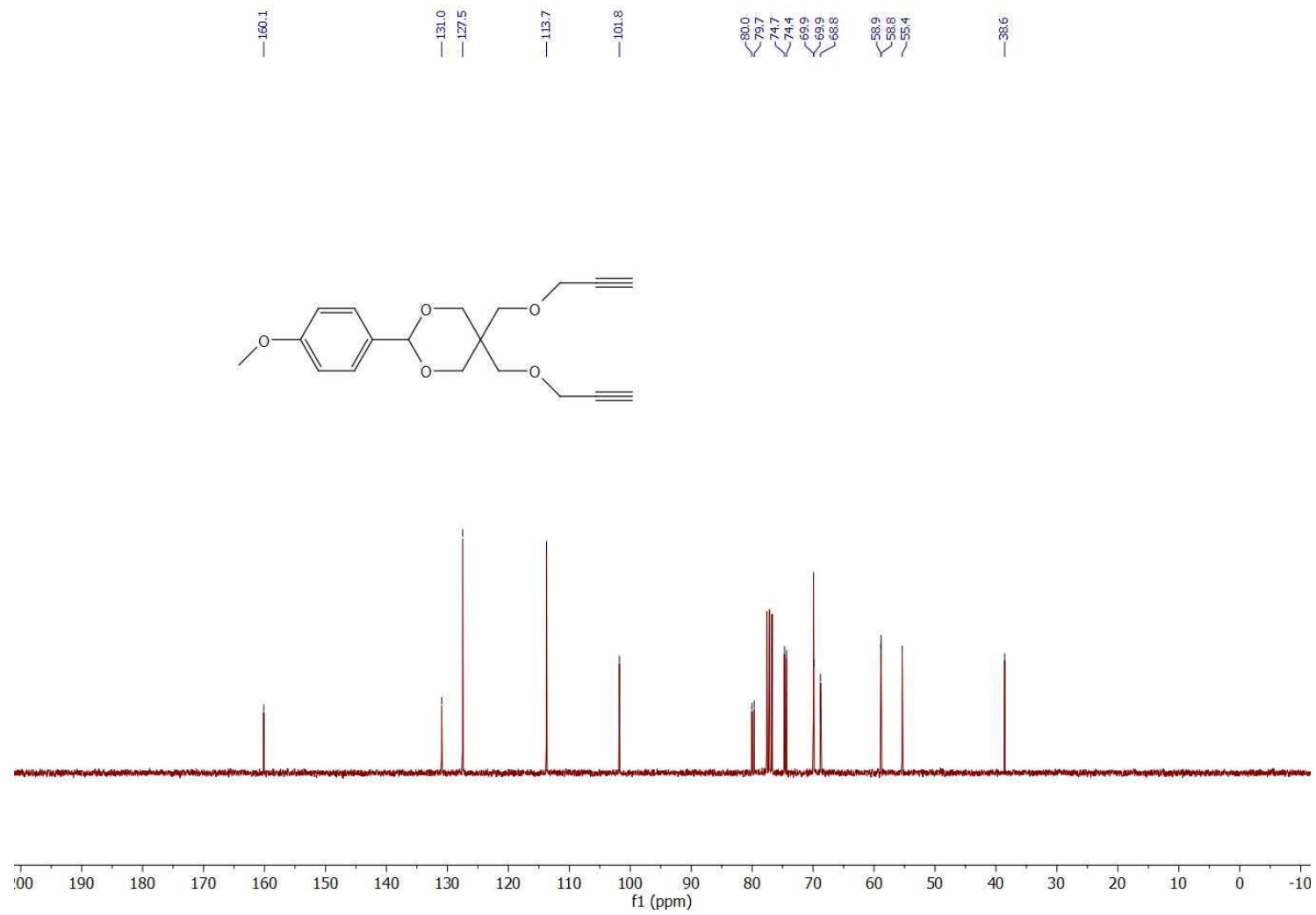
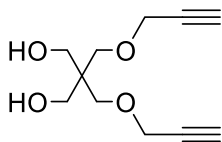


Figure 6.4 ¹³C NMR (75 MHz, CDCl₃) spectrum of compound **2.02**.

2,2-Bis((prop-2-yn-1-yloxy)methyl)propane-1,3-diol **2.03**

The solution of **2.02** (3.64 g, 11.04 mmol) in 60 mL of AcOH:H₂O (7:3) was stirred at 45 °C for 3 h. The reaction mixture was cooled to room temperature, concentrated under reduced pressure. After chromatographic purification compound **2.03** (2.04 g, 9.6 mmol, 87 %) was obtained as a pale-yellow oil.

R_f = 0.26, (EtOAc/hexane : 1/1)

¹H NMR (300 MHz, CDCl₃) δ (ppm) 4.14 – 4.07 (m, 4H), 3.63 (s, 4H), 3.53 (d, 4H), 2.82 (s, 2H), 2.44 (s, 2H)

¹³C NMR (75 MHz, CDCl₃) δ (ppm) 79.5, 74.8, 70.0, 63.3, 58.6, 44.7

The spectroscopic data agreed well with those of the literature.¹¹³

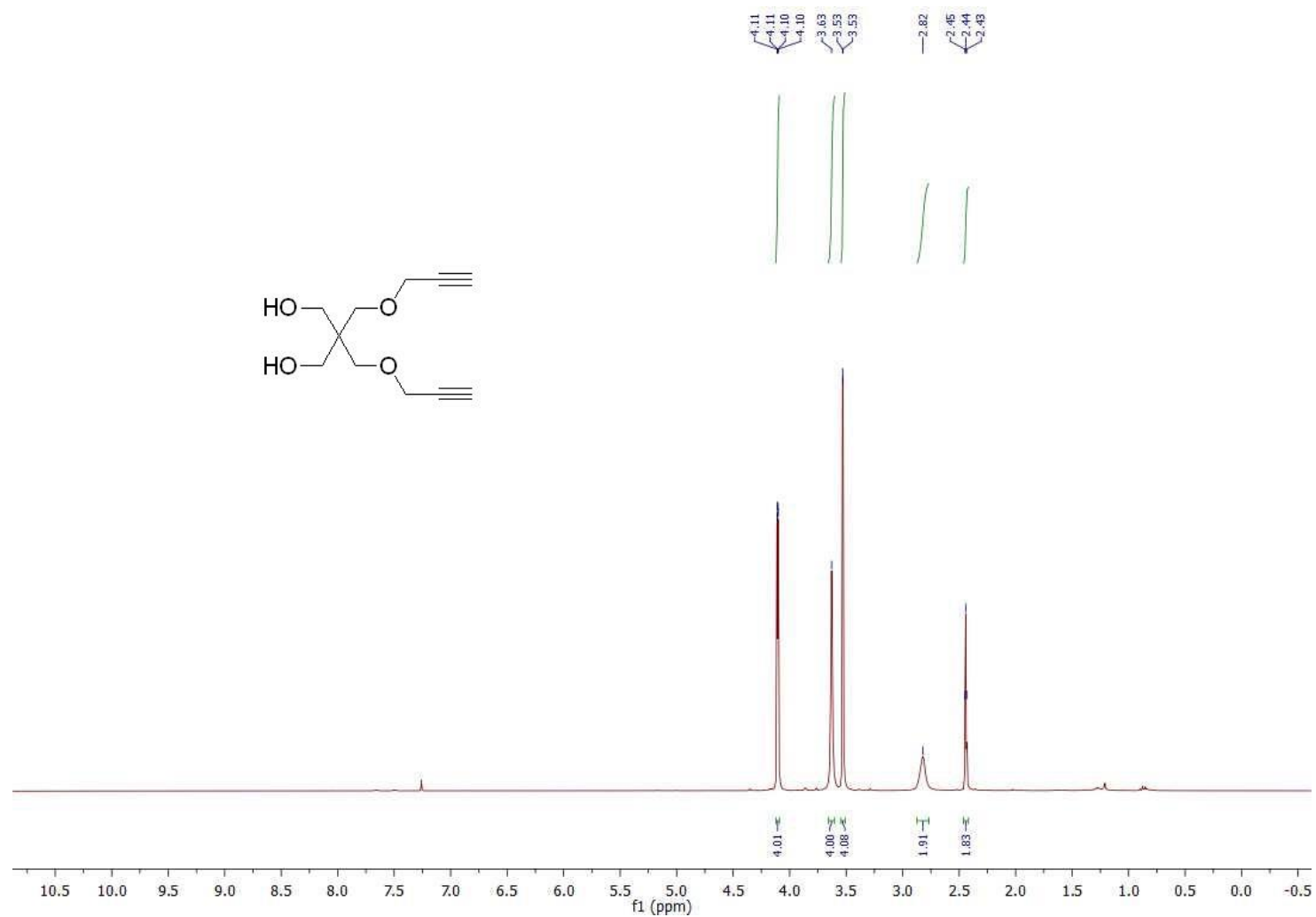


Figure 6.5 ¹H NMR (300 MHz, CDCl₃) spectrum of compound **2.03**.

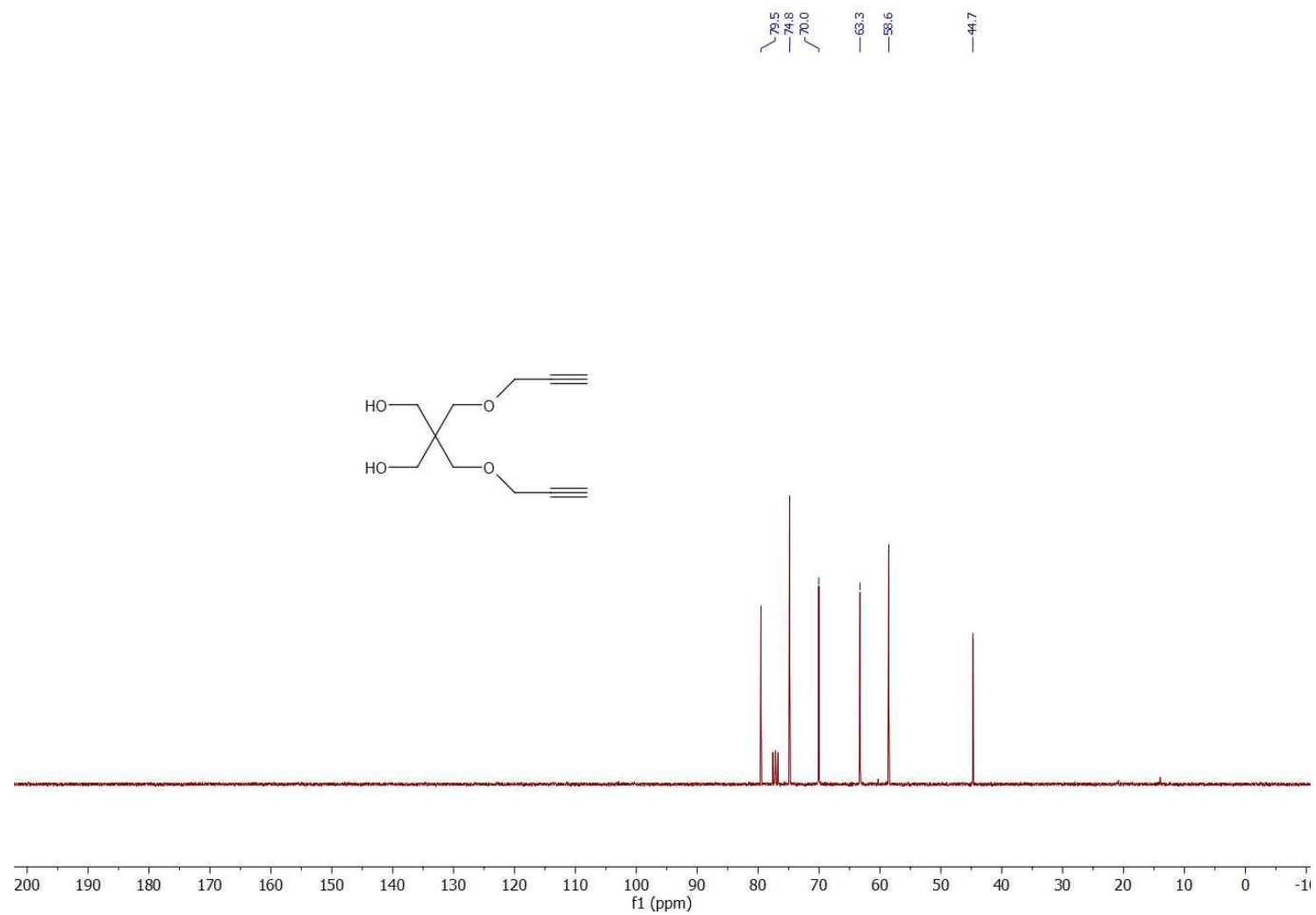
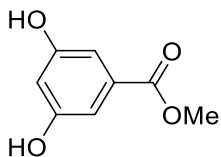


Figure 6.6 ^{13}C NMR (75 MHz, CDCl_3) spectrum of compound **2.03**.

Methyl 3,5-dihydroxybenzoate (**2.04**).



To a solution of 3,5-dihydroxybenzoic acid (2.46 g, 15.96 mmol) in MeOH (30 mL) was added concentrated sulfuric acid (0.3 mL) and resulting mixture was refluxed 9 h. After evaporation of the solvent under vacuum, the reaction mixture was diluted in EtOAc (100 mL), washed multiple times with saturated aqueous NaHCO₃ solution (until neutralization of pH) and dried over Na₂SO₄. The filtrate was concentrated *in vacuo* to give yellow-beige powder (2.66 g, 15.83 mmol, 99 %).

¹H NMR (300 MHz, DMSO-*d*₆) δ (ppm) 9.61 (s, 2H), 6.82 (d, *J* = 2.3 Hz, 2H), 6.45 (t, *J* = 2.3 Hz, 1H), 3.77 (s, 3H)

¹³C NMR (75 MHz, DMSO-*d*₆) δ (ppm) 166.4, 158.7, 131.4, 107.3, 107.2, 52.0

The spectroscopic data agreed well with those of the literature.¹¹³

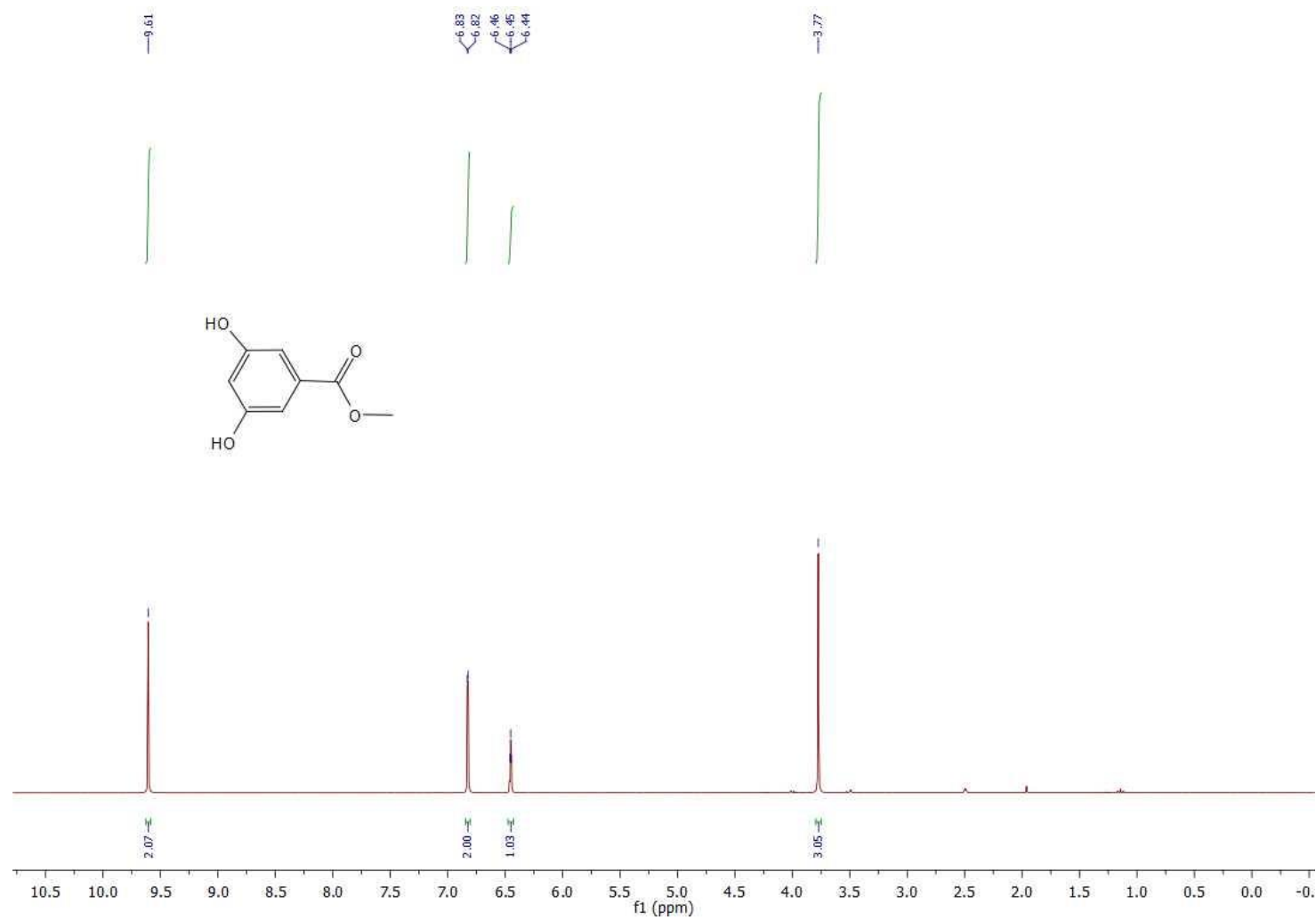


Figure 6.7 ^1H NMR (300 MHz, DMSO- d_6) spectrum of compound **2.04**.

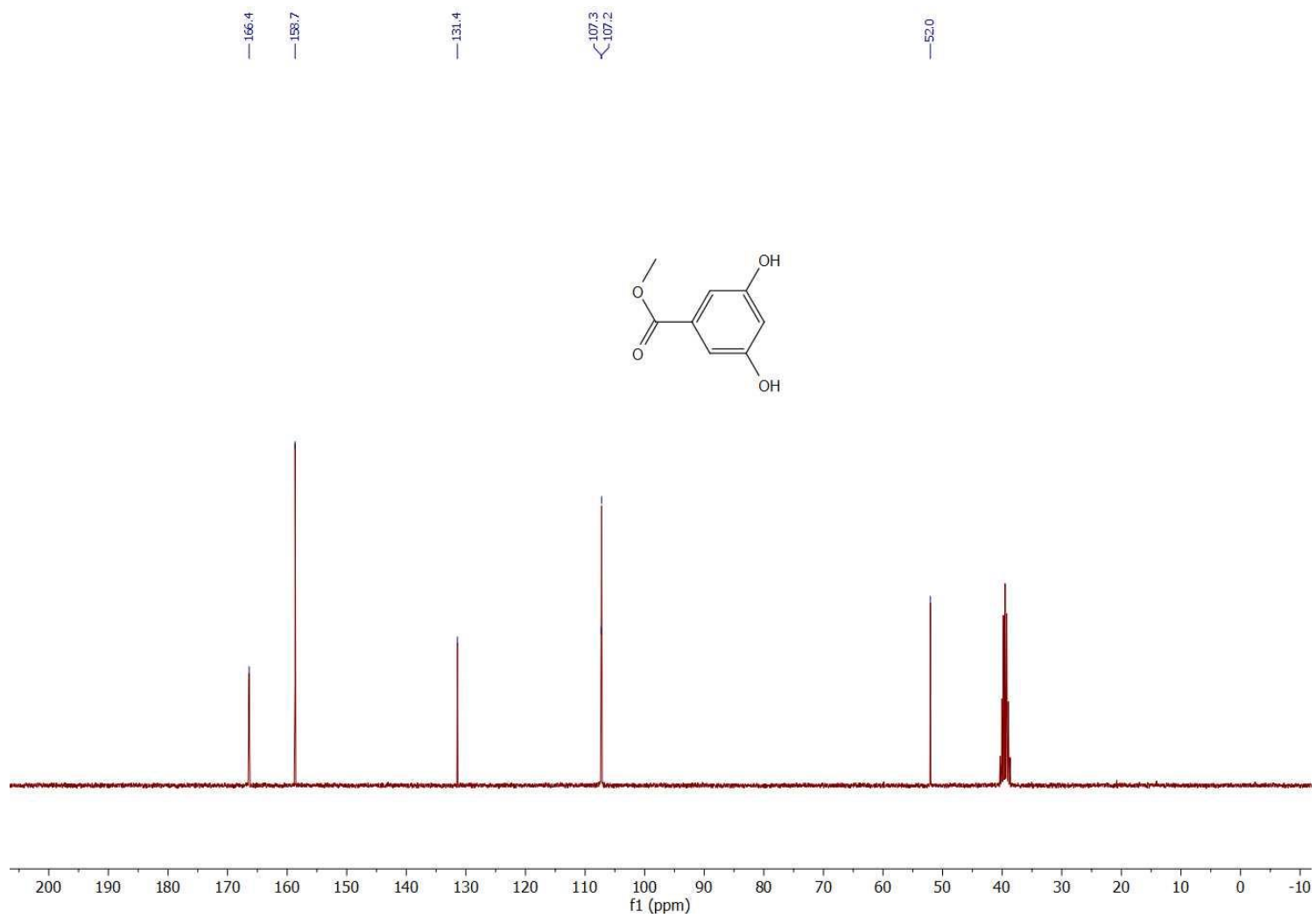
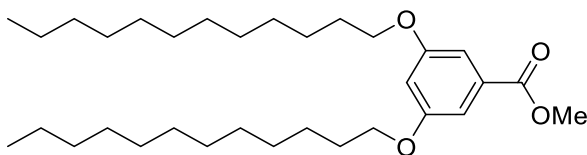


Figure 6.8 ^{13}C NMR (75 MHz, DMSO- d_6) spectrum of compound **2.04**.

Methyl 3,5-bis(dodecyloxy)benzoate (**2.05**)

The mixture of **2.04** (2.61 g, 15.52 mmol, 1 eq.), 1-bromododecane (8.6 mL, 37.2 mmol, 2.39 eq.), K_2CO_3 (12.87 g, 93.15 mmol, 6 eq.), TBAI (0.29 g, 0.77 mmol, 0.05 eq.) in dry DMF (50 mL) was stirred under nitrogen atmosphere at 90 °C for 12 h. The reaction mixture was cooled to room temperature, followed by addition of 170 mL of water. The organic phase was extracted with EtOAc (4 x 100 mL), dried over Na_2SO_4 and concentrated *in-vacuo*. After chromatographic purification compound **2.05** (7.75 g, 15.37 mmol, 99 %) was obtained as a white powder.

$R_f = 0.51$, (EtOAc/hexane : 5/95)

1H NMR (300 MHz, $CDCl_3$) δ (ppm) 7.16 (d, $J = 2.3$ Hz, 2H), 6.63 (t, $J = 2.3$ Hz, 1H), 3.96 (t, $J = 6.5$ Hz, 4H), 3.89 (s, 3H), 1.85 – 1.59 (m, 4H), 1.52 – 1.37 (m, 4H), 1.27 (s, 32H)

^{13}C NMR (75 MHz, $CDCl_3$) δ (ppm) 167.2, 160.3, 132.0, 107.8, 106.7, 68.5, 52.3, 32.1, 29.8, 29.8, 29.8, 29.7, 29.5, 29.5, 29.3, 26.2, 22.8, 14.3

The spectroscopic data agreed well with those of the literature.¹¹³

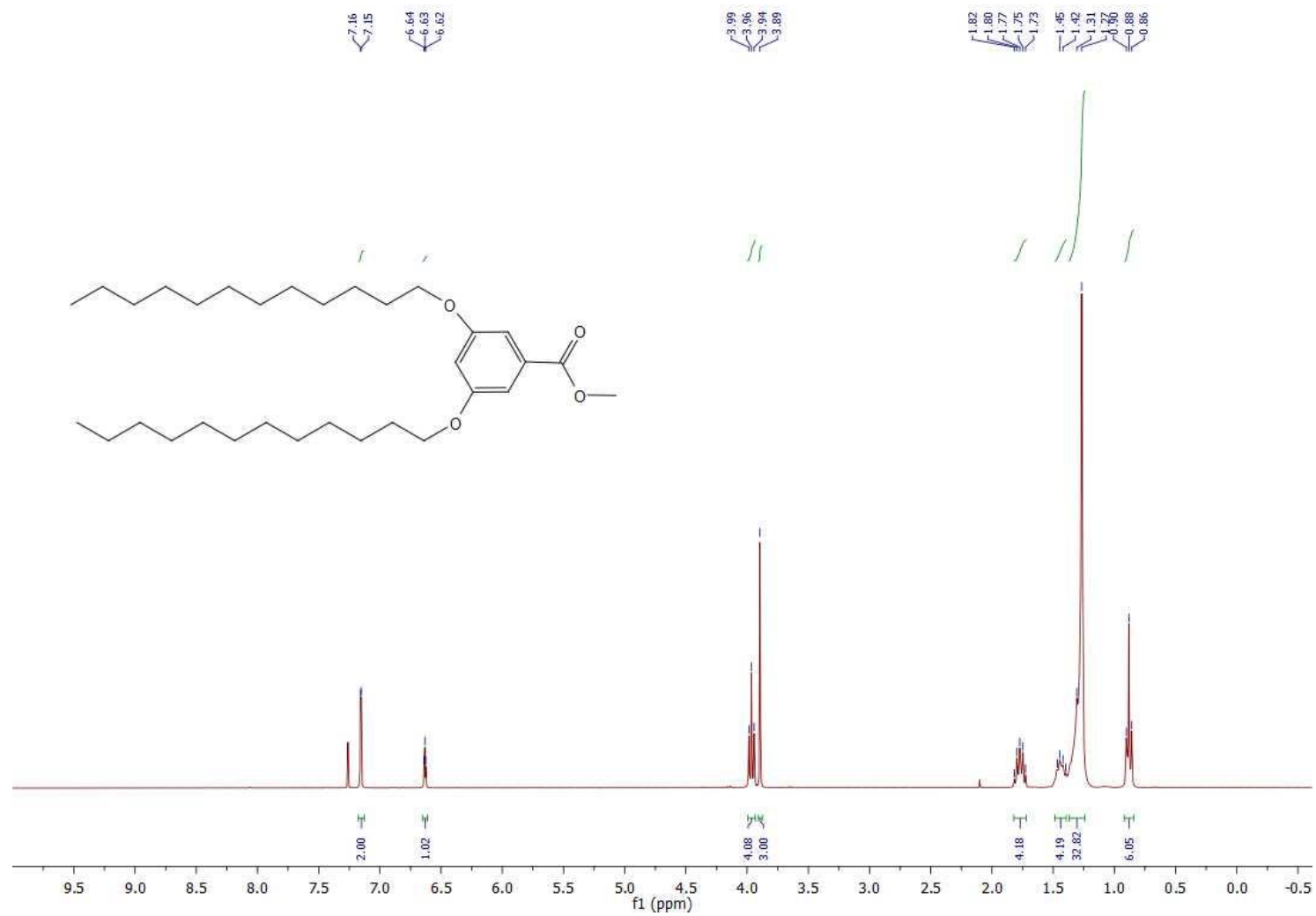


Figure 6.9 ^1H NMR (300 MHz, CDCl_3) spectrum of compound 2.05.

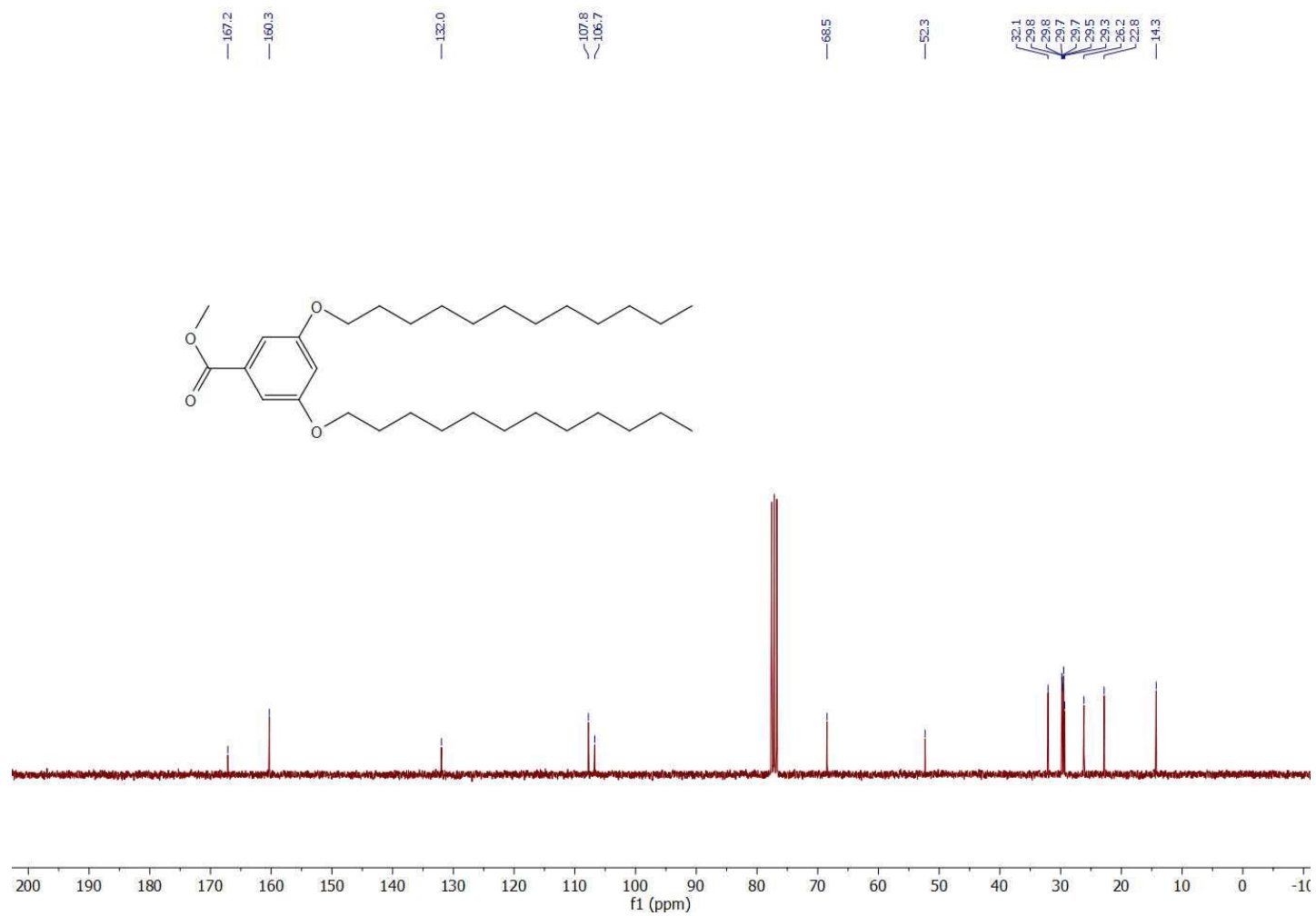
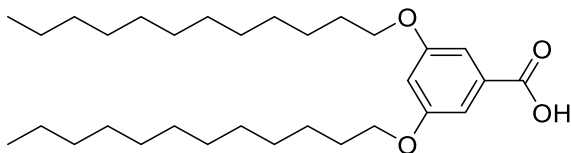


Figure 6.10 ^{13}C NMR (75 MHz, CDCl_3) spectrum of compound 2.05.

3,5-bis(dodecyloxy)benzoic acid (**2.06**)

To a solution of **2.05** (5.98 g, 11.89 mmol) in EtOH (95 mL) was added 10 % KOH solution (15 mL) and the resulting mixture was refluxed for 3.5 h. The reaction mixture was cooled to room temperature, dissolved in DCM (200 mL) washed with 1M HCl (150 mL), brine (200 mL) and dried over Na₂SO₄. The filtrate was concentration *in-vacuo* to give soft white solid (5.7 g, 11.61 mmol, 98 %).

¹H NMR (300 MHz, CDCl₃) δ (ppm) 7.23 (d, *J* = 2.2 Hz, 2H), 6.69 (t, *J* = 2.0 Hz, 1H), 3.98 (t, *J* = 6.5 Hz, 4H), 1.86 – 1.71 (m, 4H), 1.51 – 1.40 (m, 4H), 1.27 (s, 32H), 0.88 (t, *J* = 6.5 Hz, 6H)

¹³C NMR (75 MHz, CDCl₃) δ (ppm) 172.3, 160.4, 131.2, 108.3, 107.6, 68.5, 32.1, 29.8, 29.8, 29.8, 29.7, 29.5, 29.3, 26.2, 22.8, 14.3

The spectroscopic data agreed well with those of the literature.¹¹³

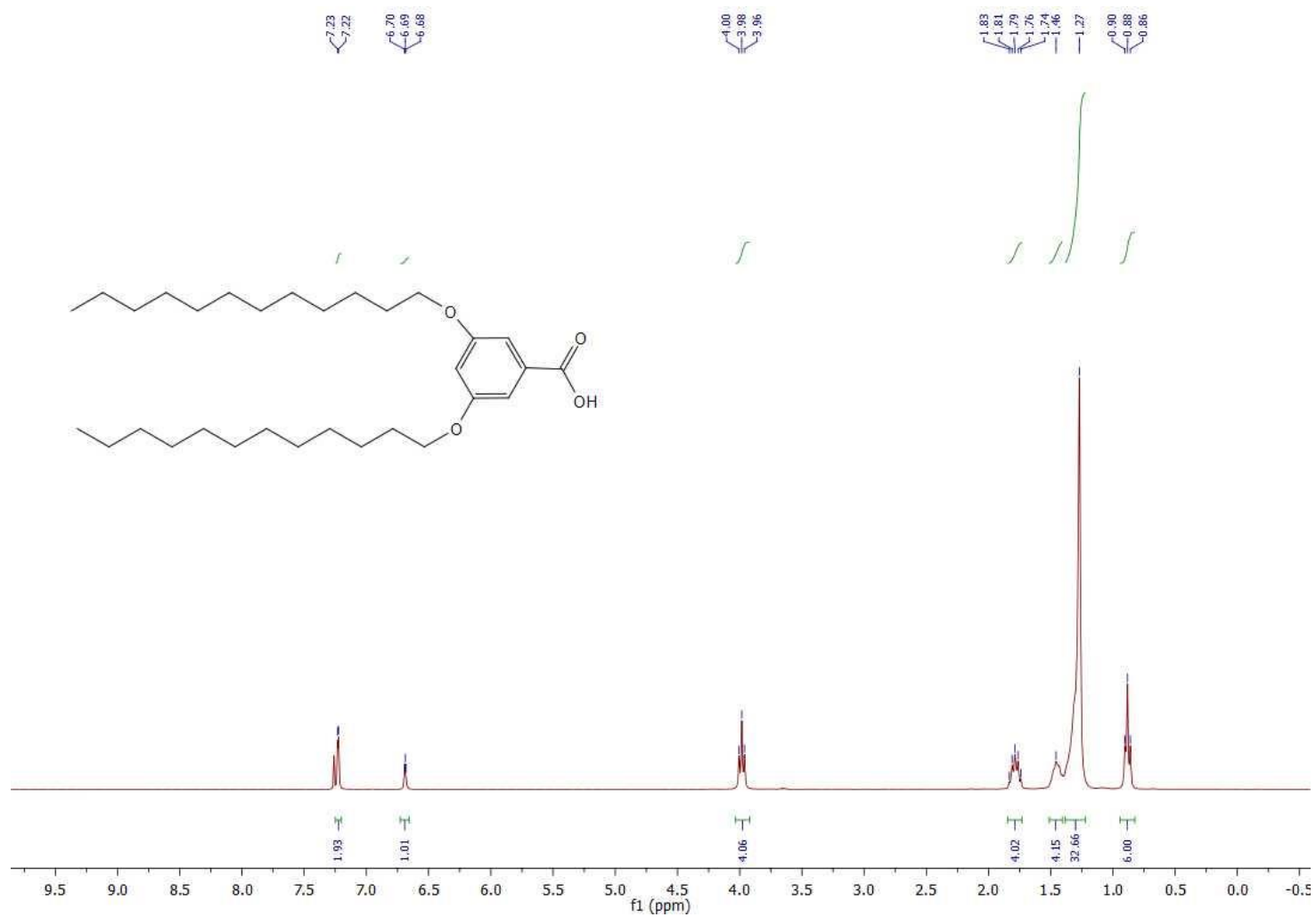


Figure 6.11 ^1H NMR (300 MHz, CDCl_3).spectrum of compound **2.06**.

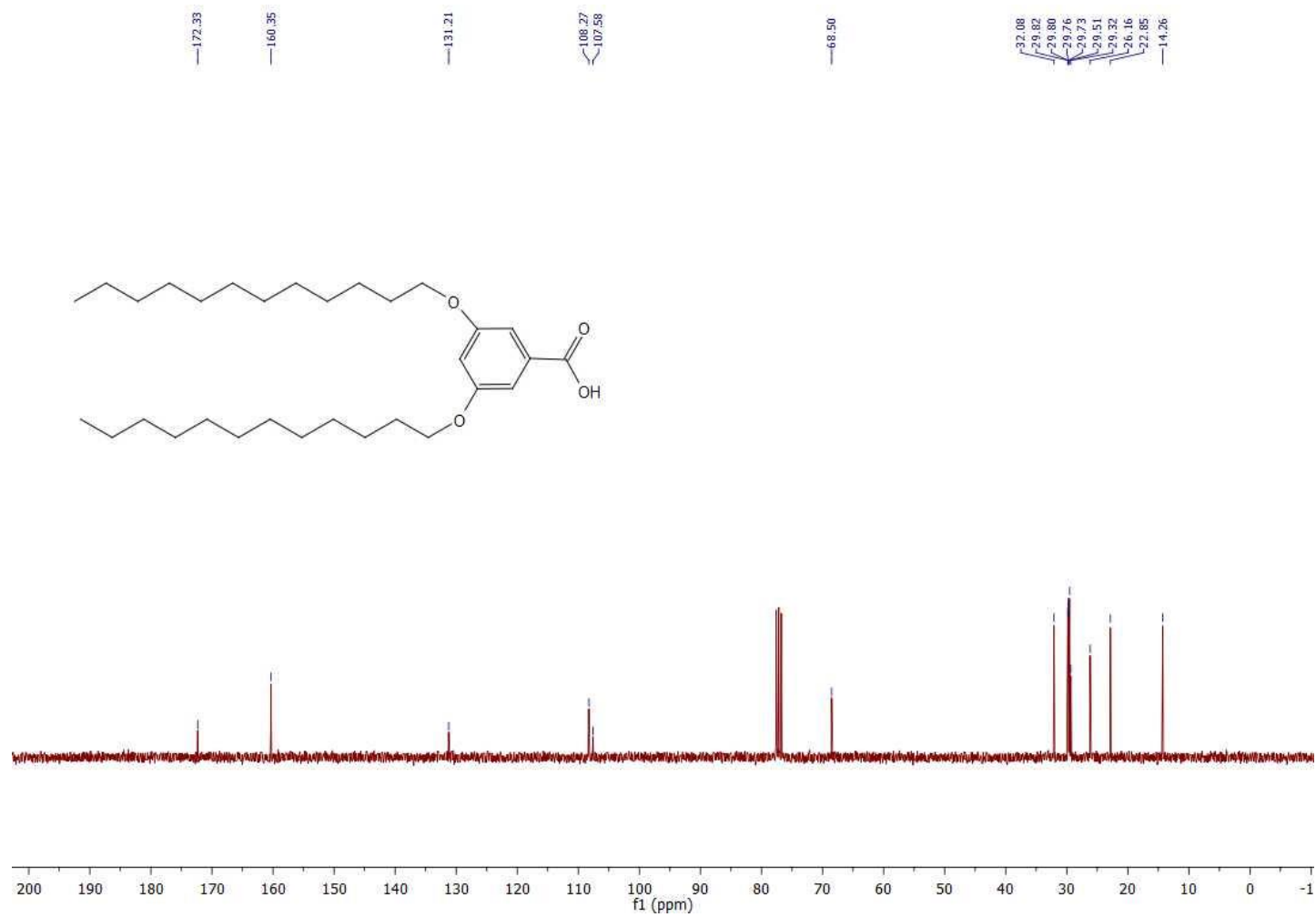
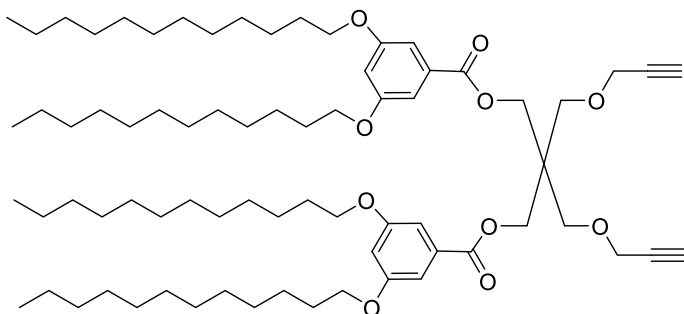


Figure 6.12 ^{13}C NMR (75 MHz, CDCl_3) spectrum of compound 2.06.

Amphiphilic Janus Dendrimer precursor (**2.07**)

To a solution of **2.03** (0.36 g, 1.69 mmol, 1 eq.) **2.06** (2 g, 4.08 mmol, 2.4 eq.), and DMAP (0.26 g, 2.15 mmol, 1.27 eq.) in dry DCM (20 mL) was added a solution of DCC (1.05 g, 5.08 mmol, 3 eq.) in DCM (3 mL) under nitrogen atmosphere at room temperature. The reaction mixture was stirred at room temperature for 18 h. After evaporation of solvent under vacuum, the residue was purified with the help of column chromatography to afford the desired compound **2.11** (1.6 g, 1.39 mmol, 82 %) as a viscous colorless oil.

$R_f = 0.42$, (DCM/hexane : 1/1)

$^1\text{H NMR}$ (300 MHz, CDCl_3) δ (ppm) 7.14 (d, $J = 2.2$ Hz, 2H), 6.61 (t, $J = 2.1$ Hz, 2H), 4.46 (s, 4H), 4.14 (d, $J = 2.2$ Hz, 4H), 3.93 (t, $J = 6.5$ Hz, 8H), 3.72 (s, 4H), 2.36 (t, $J = 2.2$ Hz, 2H), 1.86 – 1.69 (m, 8H), 1.56 – 1.37 (m, 8H), 1.26 (s, 64H), 0.87 (t, $J = 6.6$ Hz, 12H)

$^{13}\text{C NMR}$ (75 MHz, CDCl_3) δ (ppm) 166.0, 160.2, 131.8, 107.8, 106.3, 79.5, 74.8, 68.5, 68.3, 63.8, 58.7, 44.0, 32.0, 29.8, 29.7, 29.7, 29.7, 29.5, 29.4, 29.3, 26.1, 22.8, 14.2

The spectroscopic data agreed well with those of the literature.¹¹³

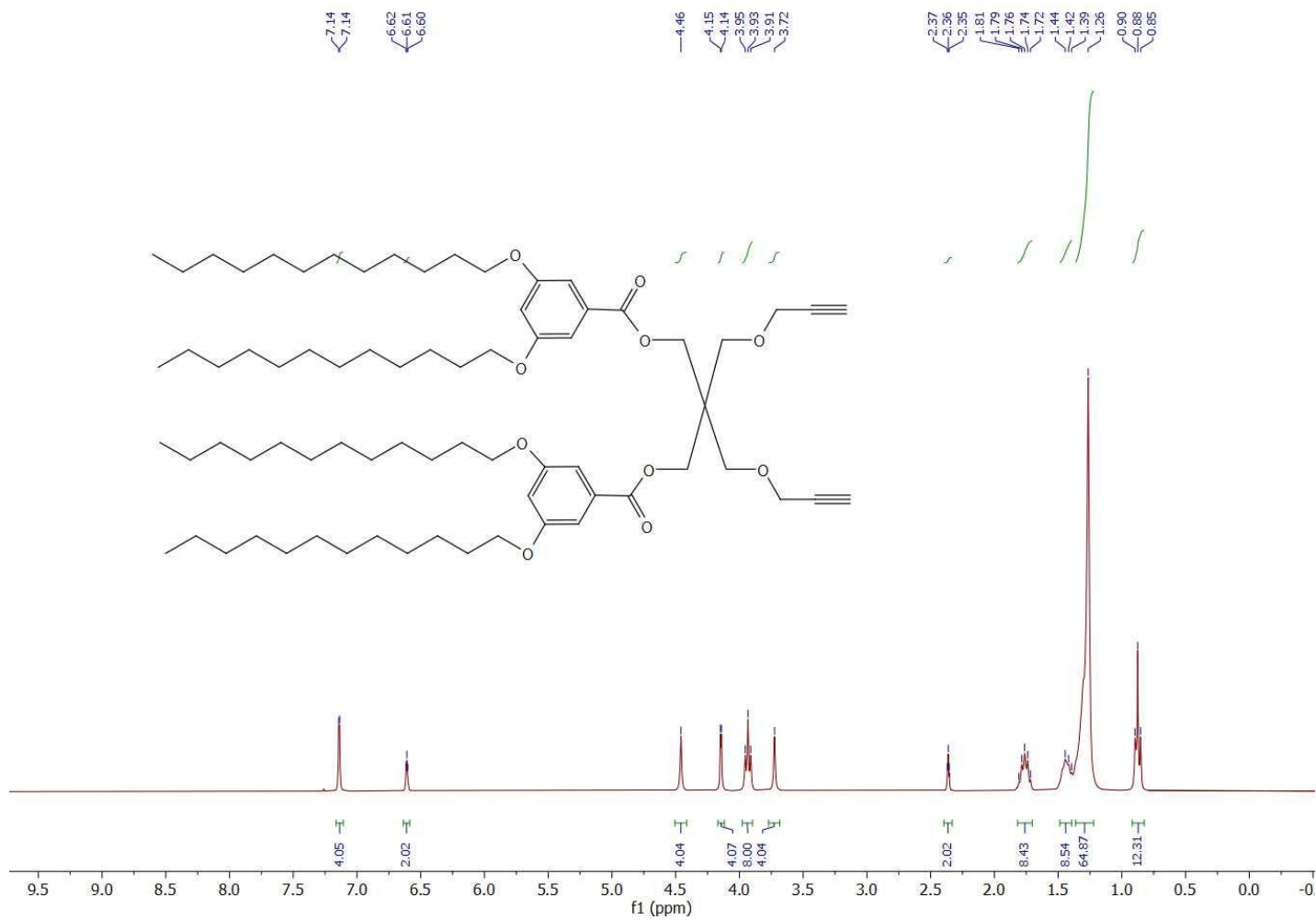


Figure 6.13 ^1H NMR (300 MHz, CDCl_3) spectrum of compound 2.07.

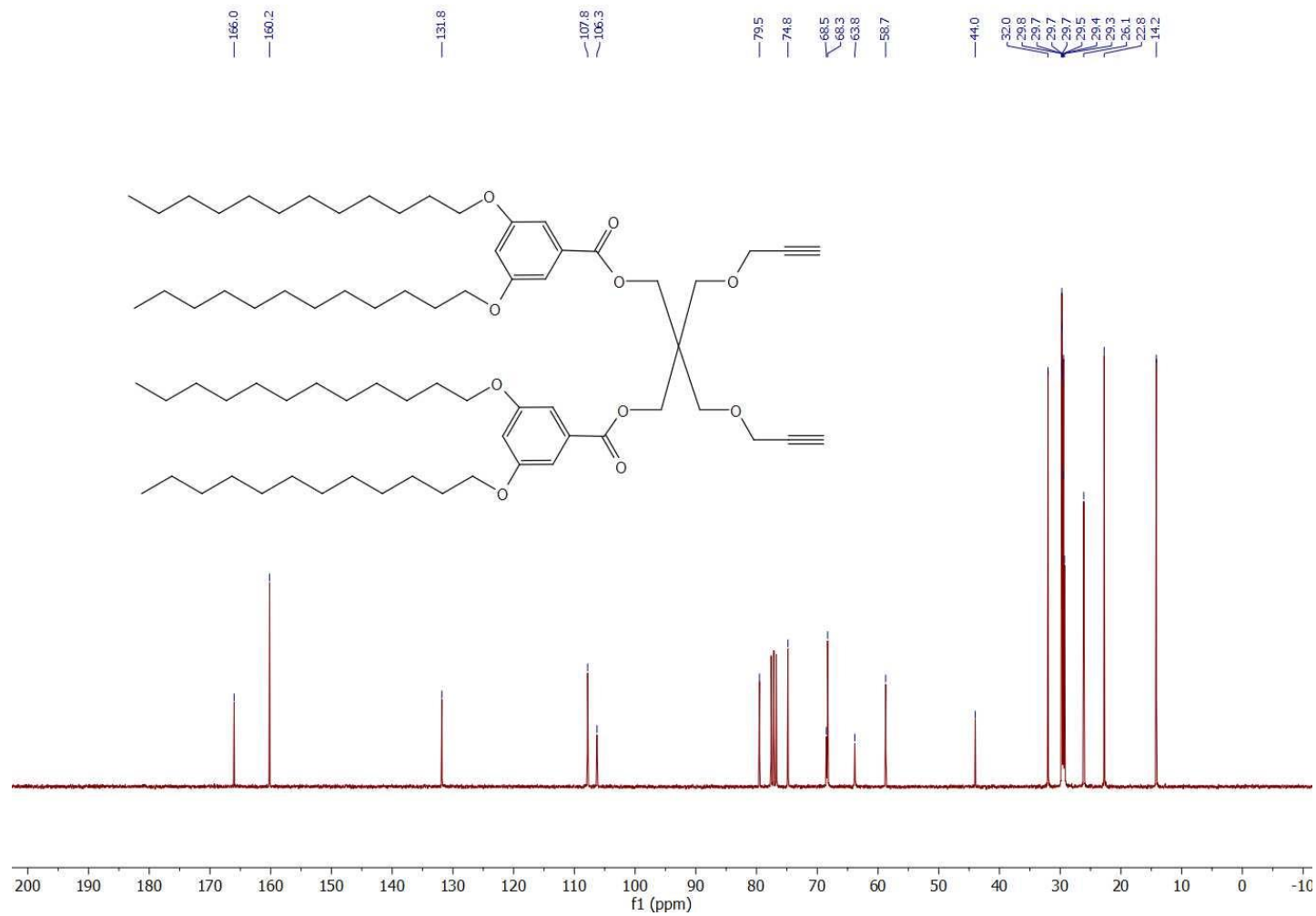
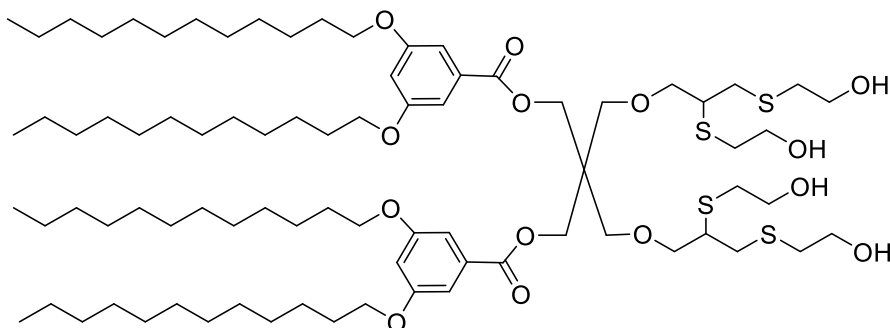


Figure 6.14 ^{13}C NMR (75 MHz, CDCl_3) spectrum of compound 2.07.

Amphiphilic Janus Dendrimer **2.08**

To a solution of **2.07** (0.71 g, 0.617 mmol, 1 eq.) DMPA (2, 2-dimethoxy-2-phenylacetophenone 0.017 g, 0.066 mmol, 0.1 eq.) in DMF (0.7 mL) was added mercaptoethanol (2 mL, 28.51 mmol, 46 eq.) at room temperature under nitrogen. The reaction mixture was stirred under UV light (365 nm) for 12 h in UV quartz cell. The reaction mixture was concentrated *in vacuo*, the residue was dissolved in DCM (5 mL), washed with water (2 x 5 mL) dried over Na₂SO₄. After chromatographic purification compound **2.08** (0.84 g, 0.575 mmol, 93 %) was obtained as yellowish oil.

R_f = 0.61, (MeOH/DCM : 1/9)

¹H NMR (300 MHz, CDCl₃) δ (ppm) 7.04 (d, *J* = 2.1 Hz, 4H), 6.55 (t, *J* = 2.1 Hz, 2H), 4.41 (s, 4H), 3.86 (t, *J* = 5.9 Hz, 8H), 3.69-3.52 (m, 18H), 2.99-2.90 (m, 2H), 2.86-2.77 (m, 2H), 2.74-2.62 (m, 8H), 1.81-1.59 (m, 8H), 1.43-1.33 (m, 8H), 1.20 (s, 64H), 0.81 (t, *J* = 6.5 Hz, 12H)

¹³C NMR (75 MHz, CDCl₃) δ (ppm) 166.1, 160.0, 131.3, 107.6, 106.2, 73.4, 68.1, 61.5, 61.1, 60.2, 45.9, 44.4, 41.2, 35.7, 31.8, 29.6, 29.5, 29.5, 29.3, 29.2, 29.1, 25.9, 22.6, 14.0

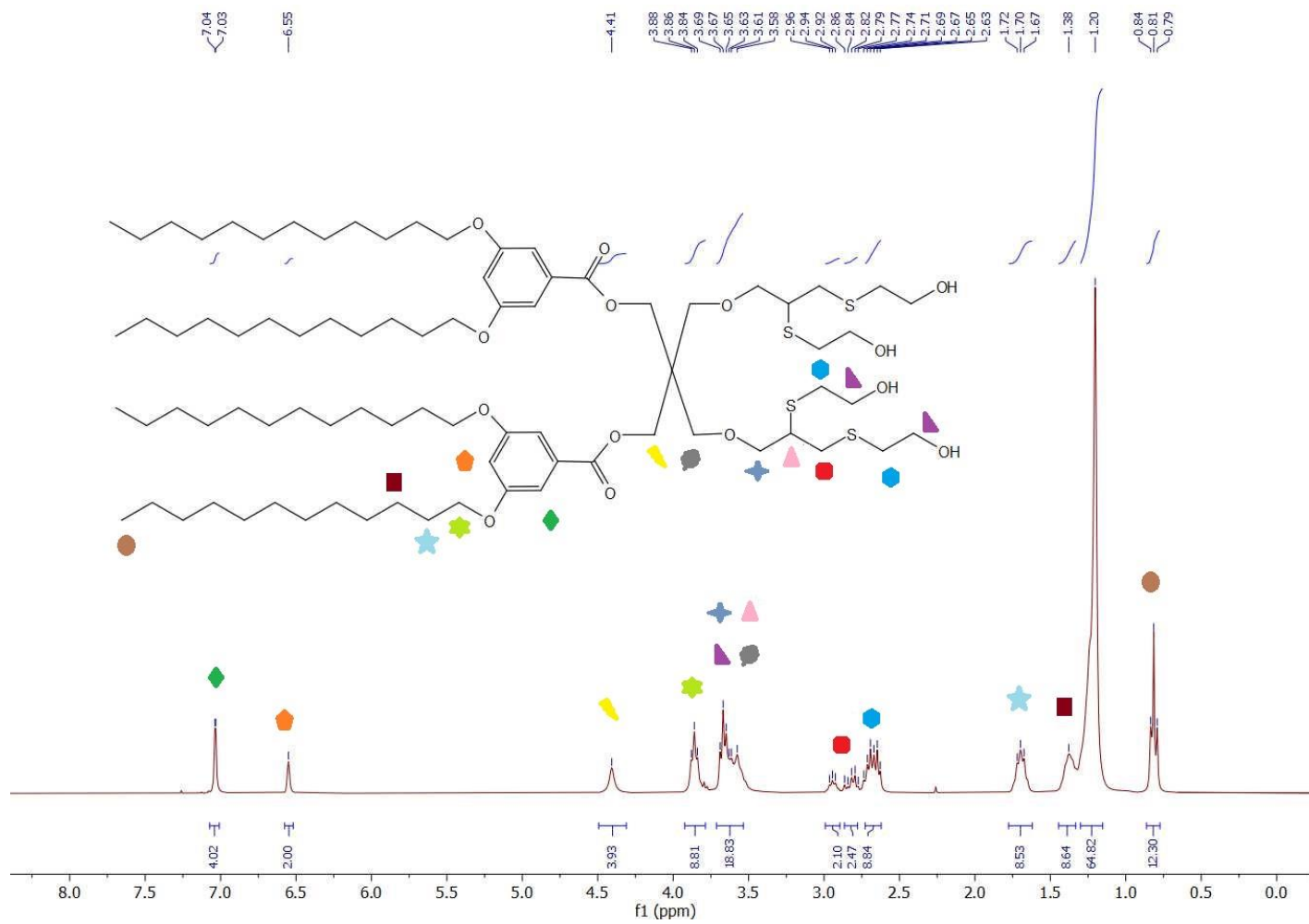


Figure 6.15 ^1H NMR (300 MHz, CDCl_3) spectrum of compound 2.08.

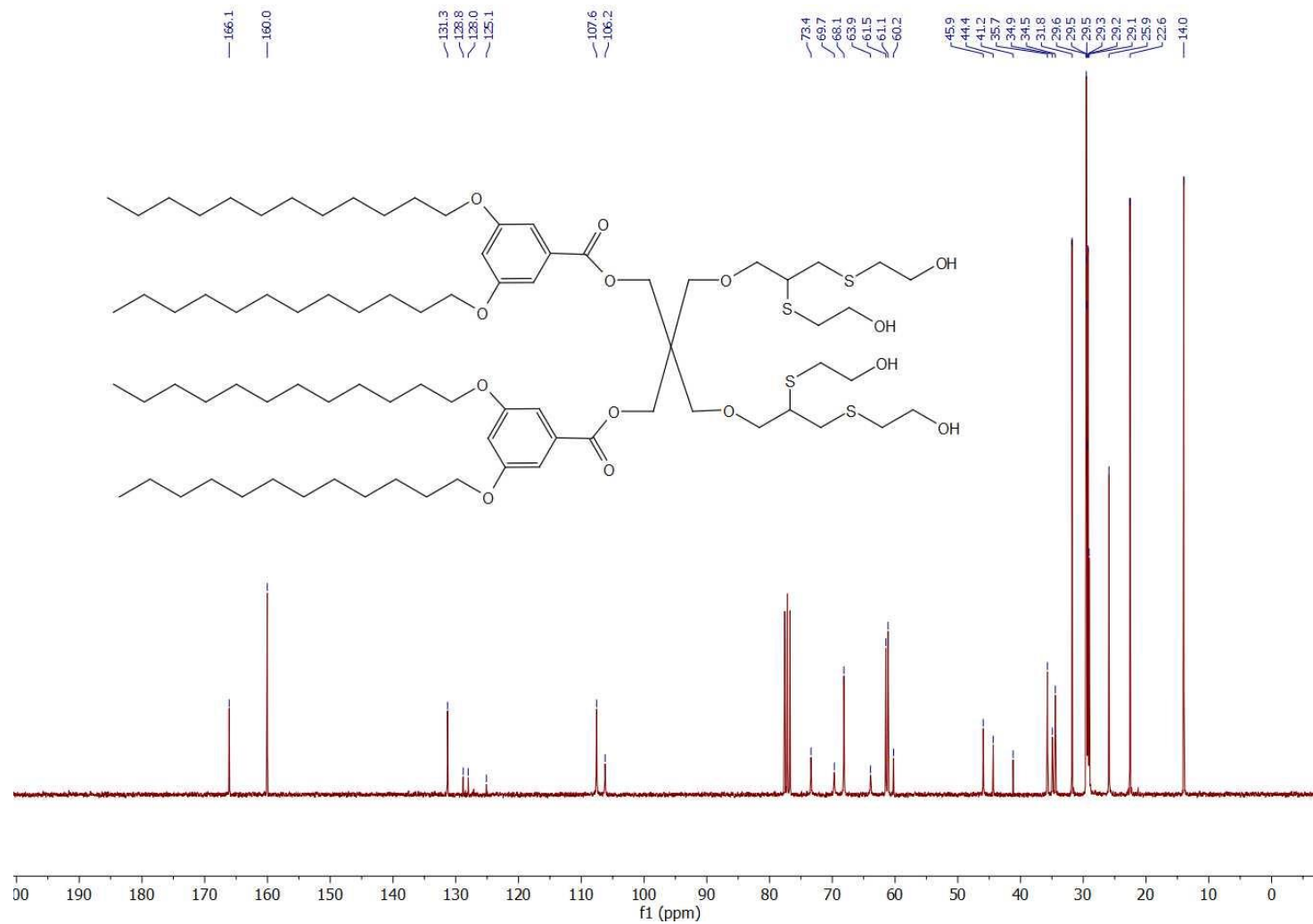
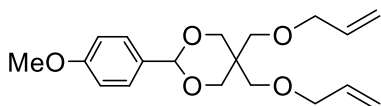


Figure 6.16 ^{13}C NMR (75 MHz, CDCl_3) spectrum of compound 2.08.

2-(4-Methoxyphenyl)-5,5-bis((prop-2-en-1-yloxy)methyl)-1,3-dioxane **2.09**

To a solution of compound **2.01** (5.01 g, 19.72 mmol, 1 eq.) in dry DMF (70 mL) was added NaH (60 % dispersion in mineral oil; 6.54 g, 163.5 mmol, 8.29) in one portion at 0 °C and stirred for 30 min. Then, allyl bromide (5.1 mL, 58.93 mmol 3 eq.) was added dropwise, and the reaction mixture was stirred at room temperature for 12 h. The water was added (100 mL), and the reaction mixture was extracted with Et₂O (3 x 150 mL), washed with water (2 x 100 mL) and dried over Na₂SO₄ and concentrated *in-vacuo*. After chromatographic purification compound **2.09** (6 g, 17.95 mmol, 91 %) was obtained as a pale-yellow oil.

R_f = 0.42, (EtOAc/hexane : 1/4)

¹H NMR (300 MHz, CDCl₃): δ (ppm) 7.43 (d, *J* = 8.7 Hz, 2H), 6.90 (d, *J* = 8.7 Hz, 2H), 5.91 – 5.83 (m, 2H), 5.40 (s, 1H), 5.34 – 5.24 (m, 2H), 5.22 – 5.16 (m, 2H), 4.13 (d, *J* = 11.7 Hz, 2H), 4.06 (dt, *J* = 5.4, 1.4 Hz, 2H), 3.95 (dt, *J* = 5.4, 1.4 Hz, 2H), 3.90 (d, *J* = 11.7 Hz, 2H), 3.80 (s, 5H), 3.30 (s, 2H)

¹³C NMR (75 MHz, CDCl₃): δ (ppm) 160.1, 135.1, 134.7, 131.0, 127.4, 116.7, 116.4, 113.7, 101.7, 72.4, 72.4, 70.3, 70.1, 68.9, 55.3, 38.9

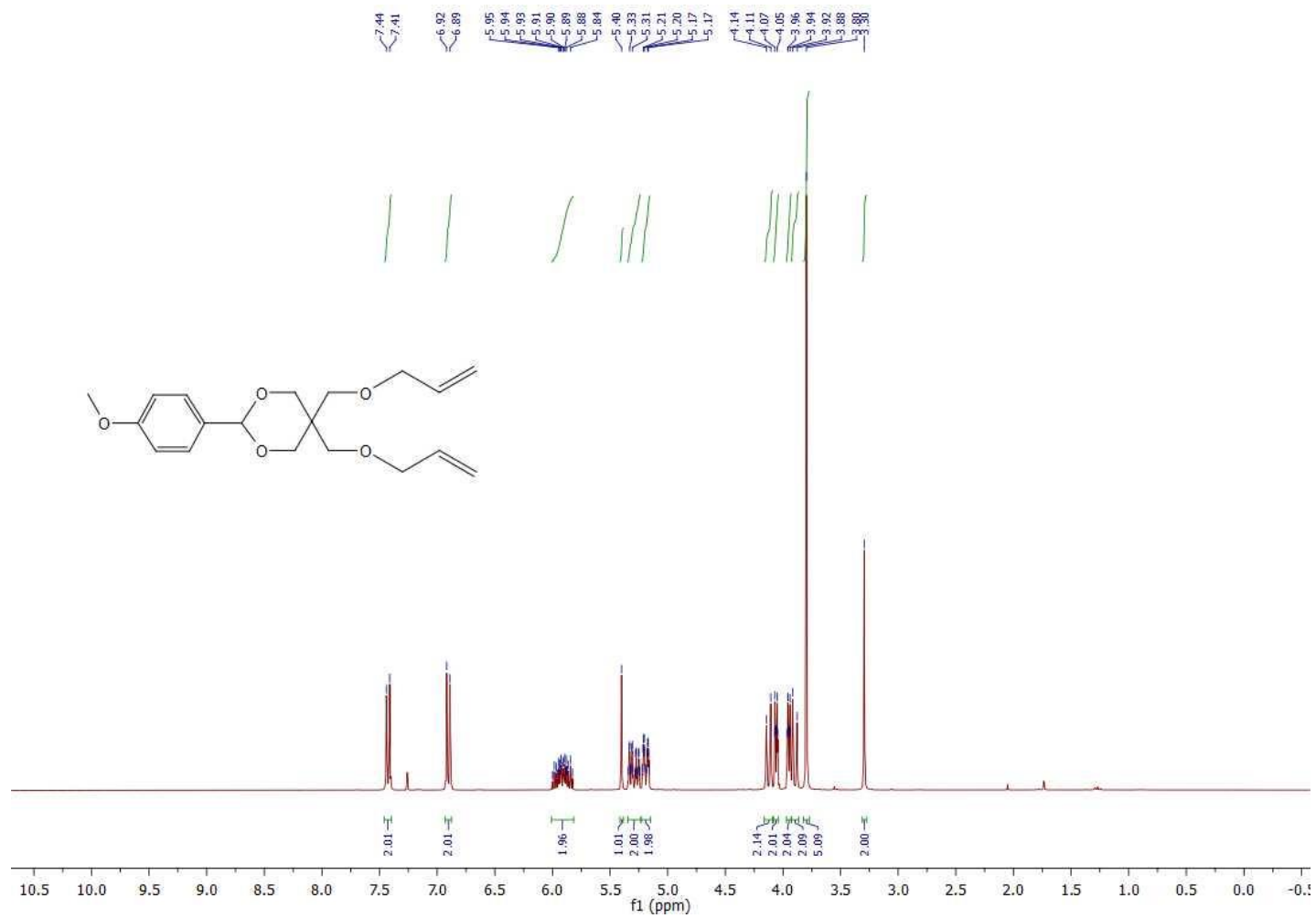


Figure 6.17 ¹H NMR (300 MHz, CDCl₃) spectrum of compound 2.09.

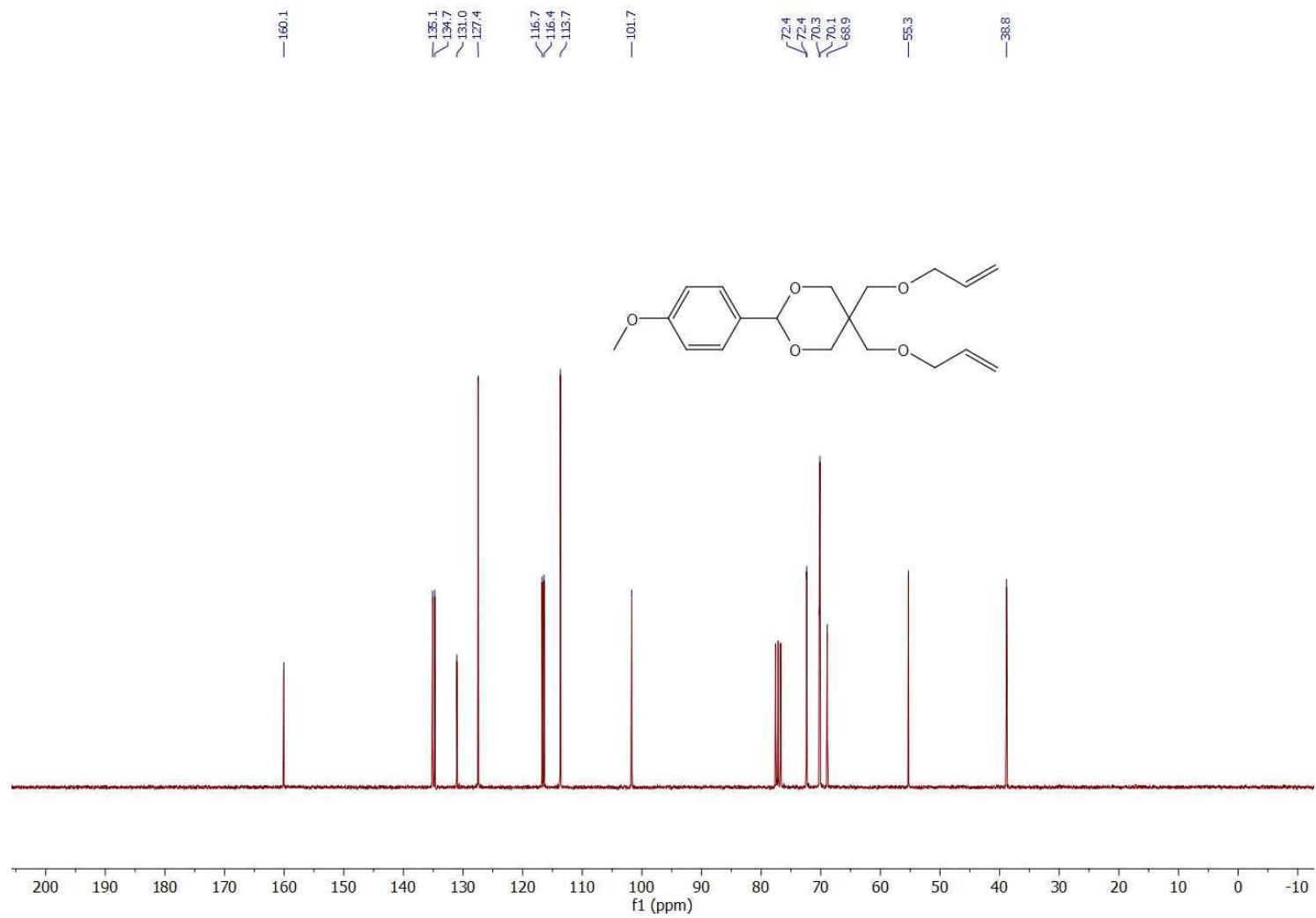
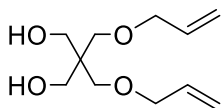


Figure 6.18 ^{13}C NMR (75 MHz, CDCl_3) spectrum of compound **2.09**.

2,2-Bis((prop-2-en-1-yloxy)methyl)propane-1,3-diol 2.10

The solution of **2.09** (4.4 g, 13.16 mmol) in 100 mL of AcOH:H₂O (7:3) was stirred at 45 °C for 3 h. The reaction mixture was cooled to room temperature, concentrated under reduced pressure. After chromatographic purification compound **2.10** (2.47 g, 11.45 mmol, 87 %) was obtained as a pale-yellow oil.

R_f = 0.23, (EtOAc/hexane : 1/1).

¹H NMR (300 MHz, CDCl₃): δ (ppm) 5.81 (ddt, *J* = 17.2, 10.7, 5.5 Hz, 2H), 5.19 (ddd, *J* = 17.3, 3.2, 1.6 Hz, 2H), 5.11 (ddd, *J* = 10.5, 2.8, 1.3 Hz, 2H), 3.91 (dt, *J* = 5.5, 1.4 Hz, 4H), 3.60 (s, 4H), 3.43 (s, 4H), 3.20 (s, 2H)

¹³C NMR (75 MHz, CDCl₃): δ (ppm) 134.4, 117.2, 72.6, 71.9, 64.8, 44.9

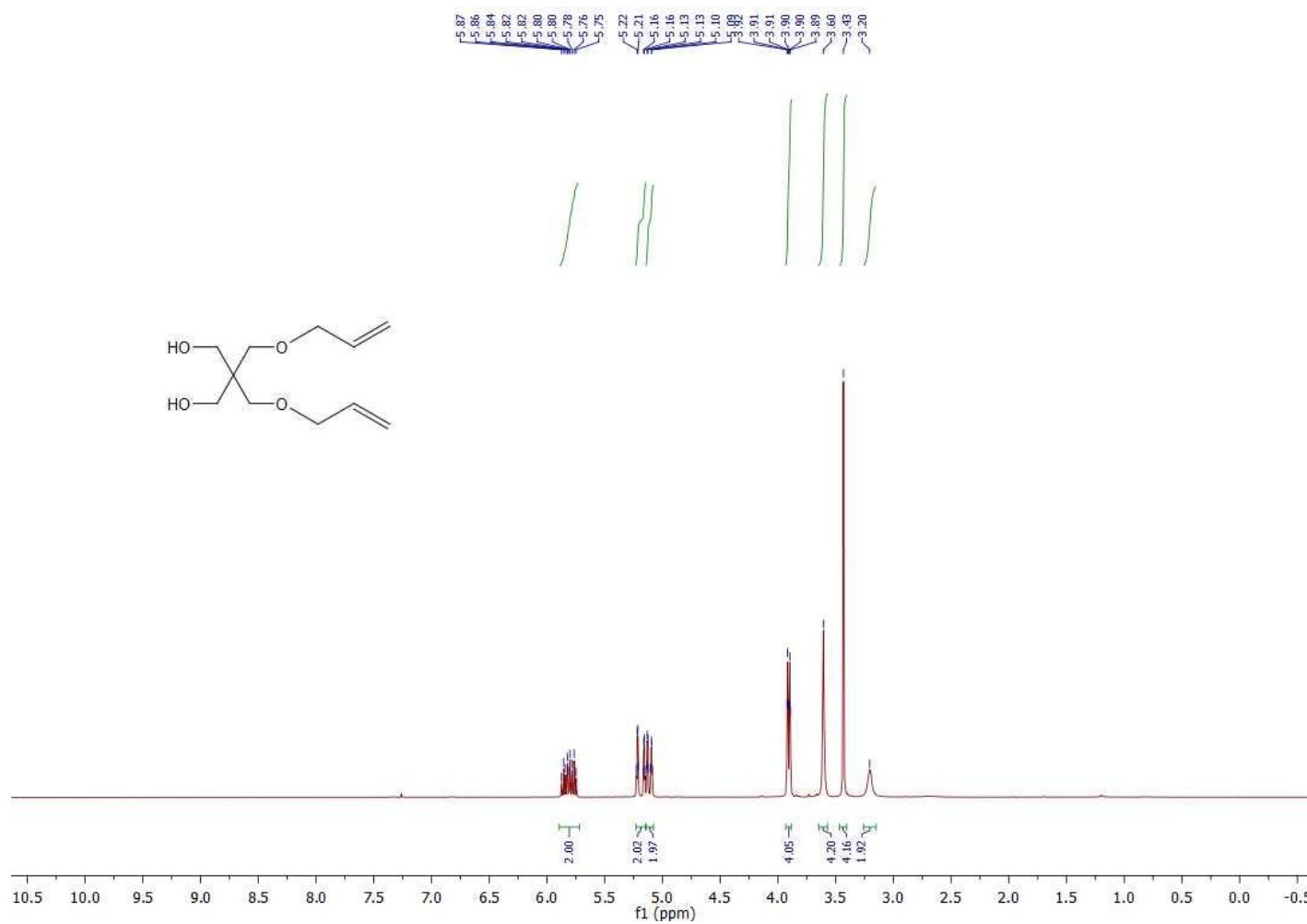


Figure 6.19 ¹H NMR (300 MHz, CDCl₃) spectrum of compound 2.10.

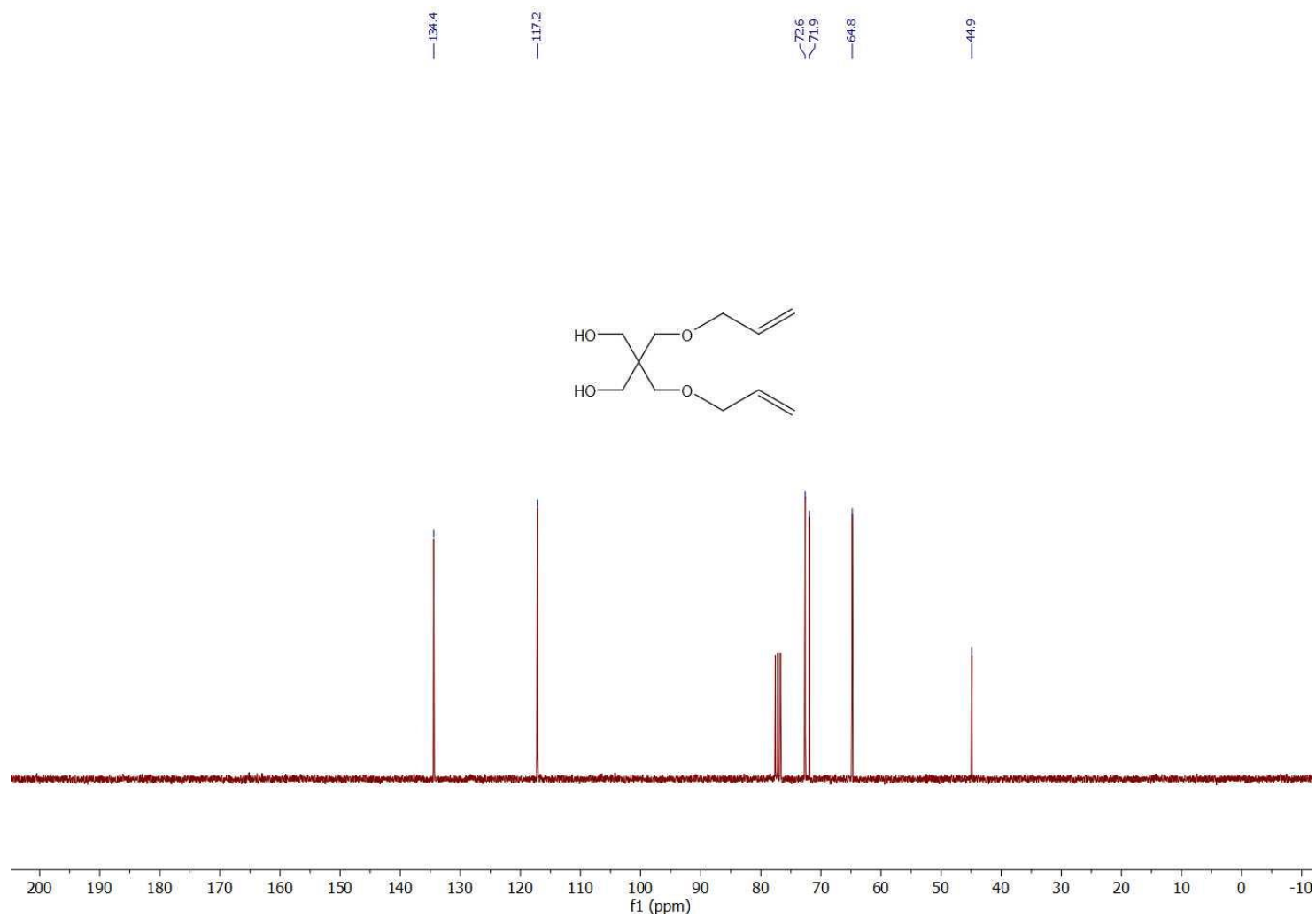
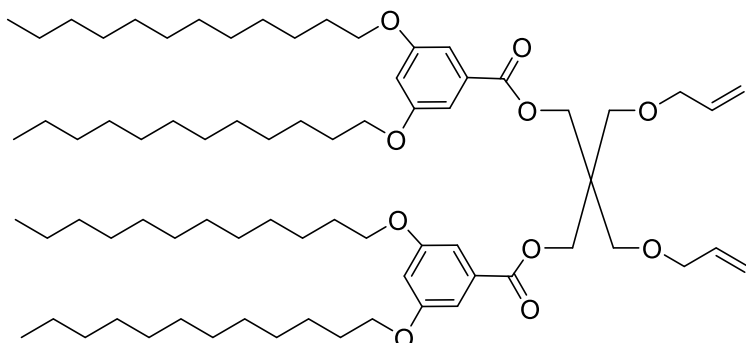


Figure 6.20 ^{13}C NMR (75 MHz, CDCl_3) spectrum of compound 2.10.

Amphiphilic Janus Dendrimer precursor **2.11**

To a solution of **2.06** (1.77 g, 3.61 mmol, 2.44 eq.), **2.10** (0.32 g, 1.48 mmol, 1 eq.) and DMAP (0.27 g, 2.22 mmol, 1.5 eq.) in dry DCM (12 mL) was added a solution of DCC (0.89 g, 4.3 mmol, 2.93 eq.) in dry DCM (5 mL) under nitrogen atmosphere at room temperature. The reaction mixture was stirred at room temperature for 18 h. After evaporation of solvent under vacuum, the residue was purified with the help of column chromatography to afford the desired compound **2.11** (1.54 g, 1.33 mmol, 90 %) as a viscous colorless oil.

$R_f = 0.45$, (DCM/hexane : 1/1)

$^1\text{H NMR}$ (300 MHz, CDCl_3): δ (ppm) 7.11 (d, $J = 2.3$ Hz, 4H), 6.62 (t, $J = 2.3$ Hz, 2H), 5.85 (ddt, $J = 17.1, 10.7, 5.5$ Hz, 2H), 5.24 (dq, $J = 17.2, 1.5$ Hz, 2H), 5.13 (dq, $J = 10.4, 1.5$ Hz, 2H), 4.47 (s, 4H), 3.98 – 3.88 (m, 12H), 3.61 (s, 4H), 1.89 – 1.68 (m, 8H), 1.49 – 1.39 (m, 8H), 1.27 (s, 64H), 0.88 (t, $J = 6.7$ Hz, 12H)

$^{13}\text{C NMR}$ (75 MHz, CDCl_3): δ (ppm) 166.3, 160.3, 134.8, 131.9, 117.0, 107.8, 106.5, 72.6, 69.0, 68.5, 64.3, 44.3, 32.1, 29.8, 29.8, 29.8, 29.7, 29.6, 29.5, 29.3, 26.2, 22.8, 14.3

ESI-HRMS: *m/z* calcd. for $C_{73}H_{124}O_{10}$ $[M+H]^+$, 1161.9273; found 1161.9287
 $[M+H]^+$

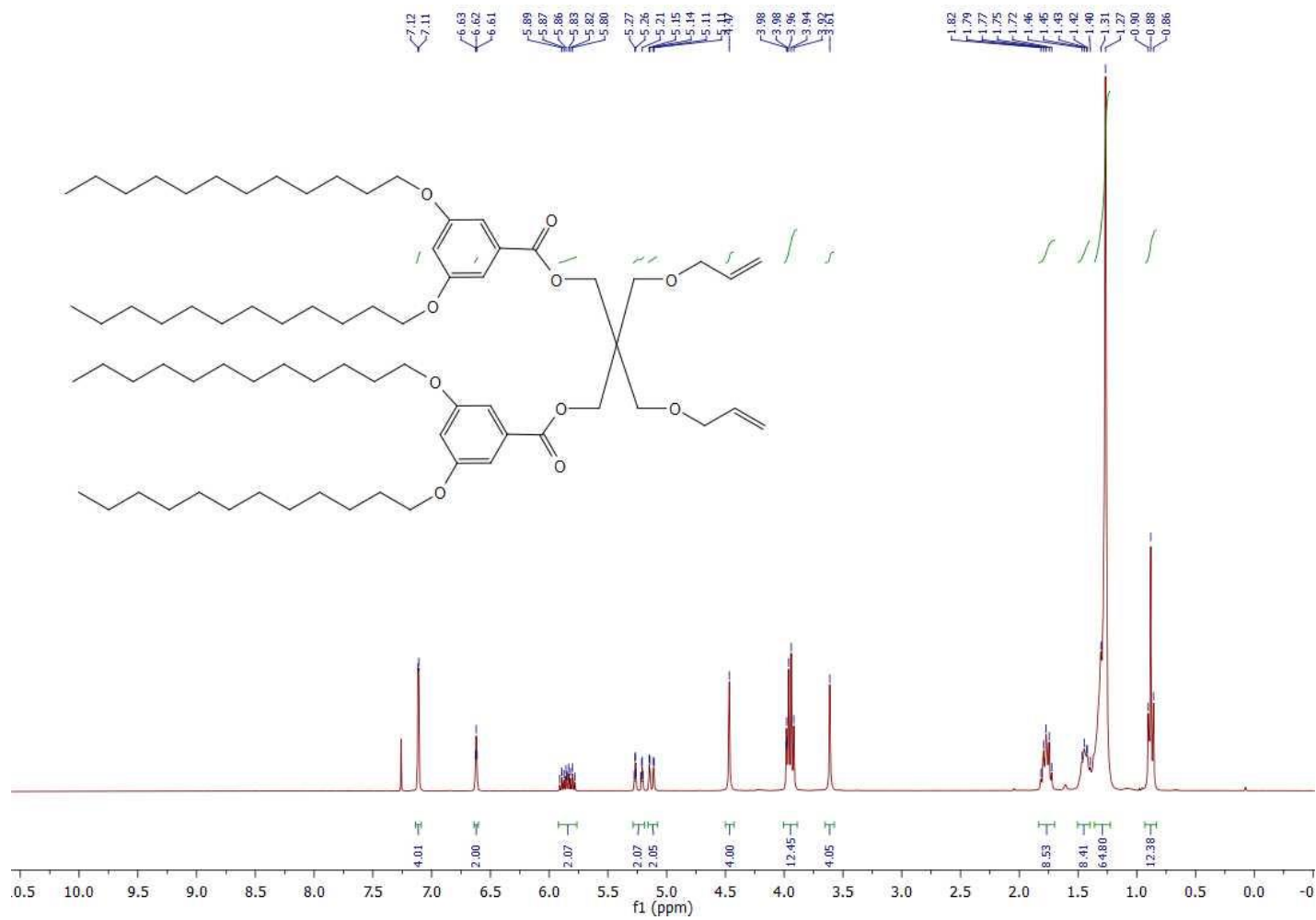


Figure 6.21 ^1H NMR (300 MHz, CDCl_3) spectrum of compound 2.11.

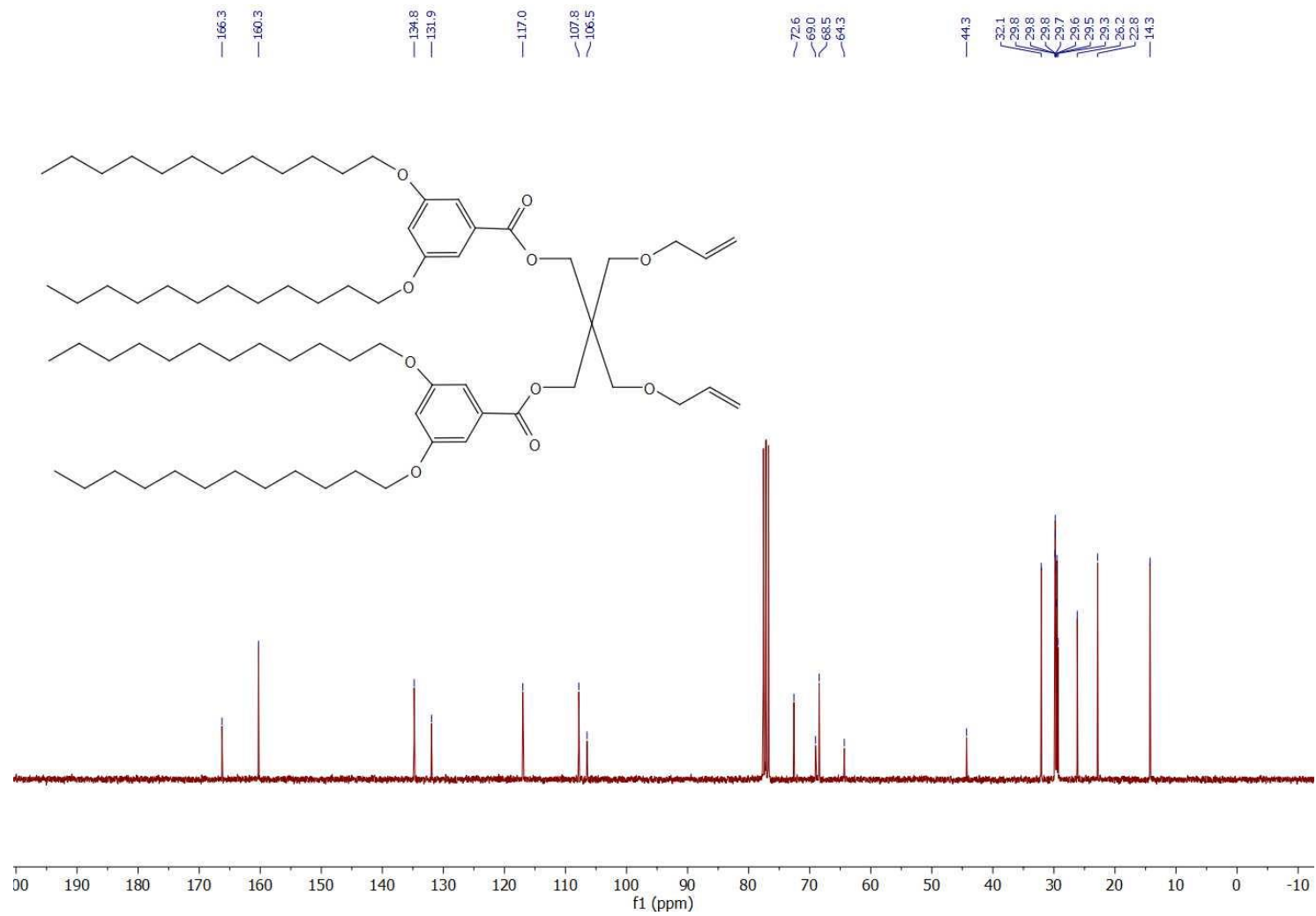


Figure 6.22 ¹³C NMR (75 MHz, CDCl₃) spectrum of compound 2.11.

Compound Table

Compound Label	RT	Mass	Abund	Formula	Tgt Mass	Diff (ppm)
Cpd 1: C73 H124 O10	0.13	1160.9212	8562	C73 H124 O10	1160.9195	1.51

Compound Label	RT	Algorithm	Mass
Cpd 1: C73 H124 O10	0.13	Find By Formula	1160.9212

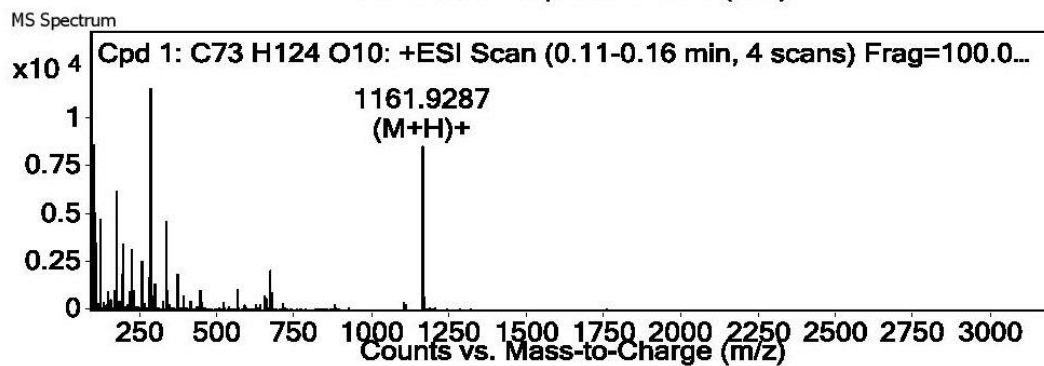
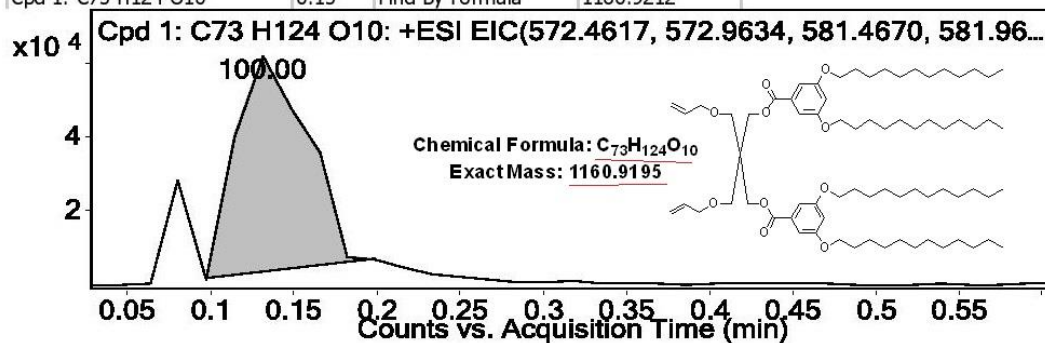
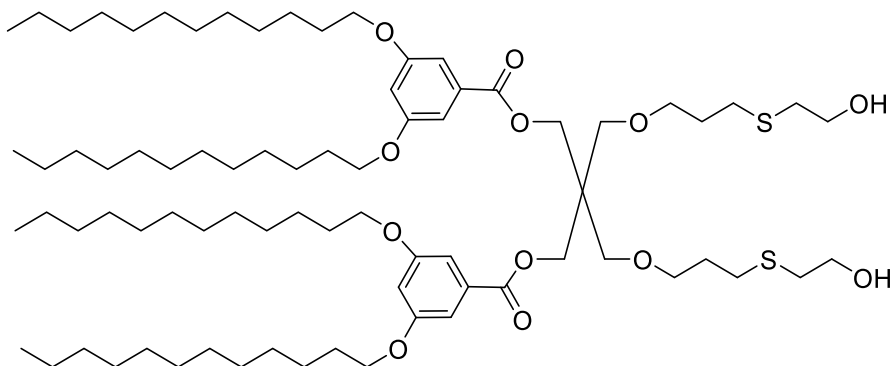


Figure 6.23 HRMS spectrum of compound 2.11.

Amphiphilic Janus Dendrimer **2.12**

To a stirring solution of **2.11** (0.11 g, 0.09 mmol, 1 eq.), 2,2'-dimethoxy-2-phenylacetophenone (DMPAP, 0.003 g, 0.01 mmol, 0.11 eq) in dry DMF (0.2 mL) was added mercaptoethanol (0.2 mL, 2.874 mmol, 29.3 eq.) under nitrogen. The vial was then purged with nitrogen for 5 min and irradiated for 14 h using UV lamp at room temperature (*classical glassware, UV lamp (365 nm, Model UVGL-58 MINERALIGHT® LAMP) in a cardboard box*). The solvent was removed under vacuum and residue was dissolved in DCM (20 mL) washed with water (2 x 15 mL), dried over Na₂SO₄ and concentrated in-vacuo. After chromatographic purification, compound **2.12** (0.12 g, 0.09 mmol, 96 %) was obtained as a viscous colorless oil.

R_f = 0.60, (MeOH/DCM : 1/9)

¹H NMR (300 MHz, CDCl₃): δ (ppm) 7.10 (d, *J* = 2.1 Hz, 4H), 6.62 (t, *J* = 2.1 Hz, 2H), 4.45 (s, 4H), 3.94 (t, *J* = 6.5 Hz, 8H), 3.68 (t, *J* = 6.0 Hz, 4H), 3.56 (s, 4H), 3.49 (t, *J* = 5.8 Hz, 4H), 2.66 (t, *J* = 6.0 Hz, 4H), 2.56 (t, *J* = 7.2 Hz, 4H), 1.89 – 1.65 (m, 12H), 1.47 – 1.39 (m, 8H), 1.26 (s, 64H), 0.87 (t, *J* = 6.6 Hz, 12H)

¹³C NMR (75 MHz, CDCl₃): δ (ppm) 166.3, 160.3, 131.8, 107.8, 106.4, 69.9, 68.5, 64.3, 60.5, 44.4, 35.4, 32.0, 29.9, 29.8, 29.8, 29.7, 29.7, 29.5, 29.5, 29.3, 28.5, 26.2, 22.8, 14.2

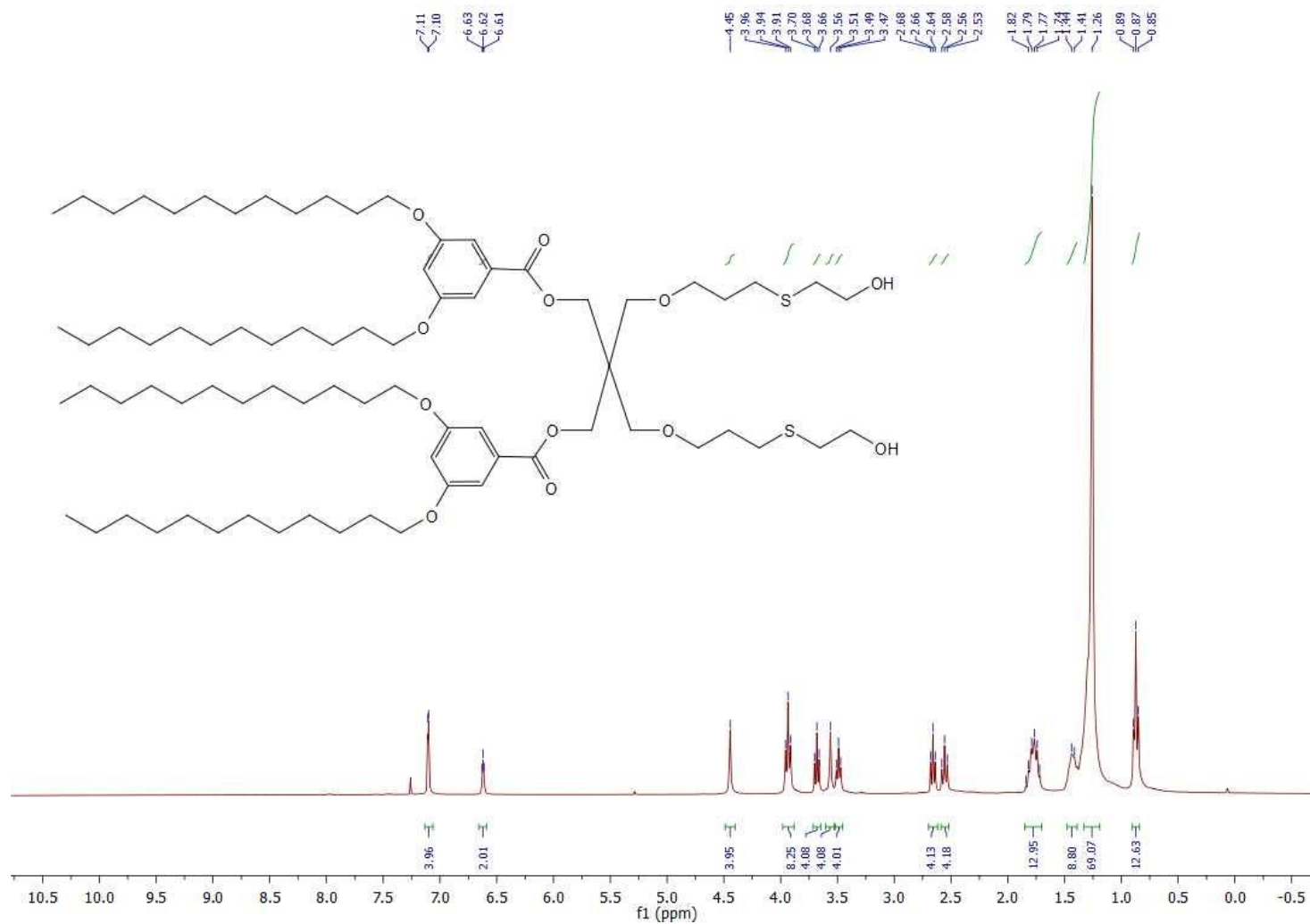


Figure 6.24 ¹H NMR (300 MHz, CDCl₃) spectrum of compound 2.12.

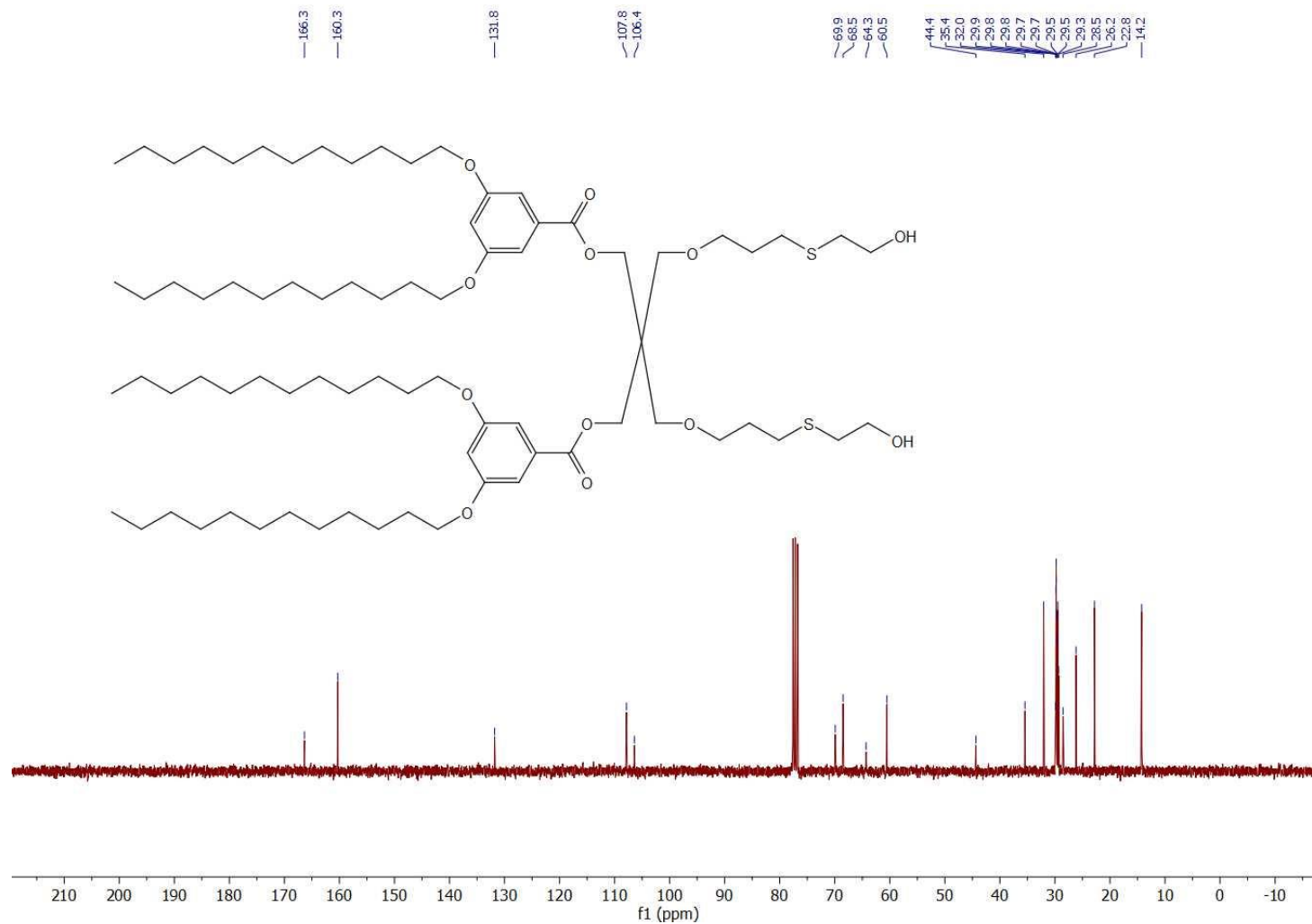


Figure 6.25 ¹³C NMR (75 MHz, CDCl₃) spectrum of compound 2.12.

6.3 Experimental Part of Chapter III

6.3.1 Synthesis and characterization

General synthetic procedure A: preparation of 3'-*O*-sulfated lactosides

A mixture of deacetylated lactosides (1 eq.) and dibutyltin oxide (Bu_2SnO , 1.08 eq.) in MeOH (4 mL per 0.1 mmol of the SM) was stirred at 80 °C for 4h under nitrogen atmosphere. The solution was then concentrated and sulfur trioxide-triethylamine complex ($\text{Et}_3\text{N}\cdot\text{SO}_3$) (1.2 eq.) and dry DMF (4 mL per 0.1 mmol of the SM) were added. After stirring at 60 °C for 17 h, the reaction was quenched with methanol and the reaction mixture was concentrated *in-vacuo*. The residue was purified through a classical column chromatography to give desired compound.

General synthetic procedure B: Zemplén transesterification reaction

To a solution of lactoside (1 eq.) in dry methanol (2 mL per 0.1 mmol of the SM) was added a solution of sodium methoxide (25 % in MeOH, 0.5 eq.). After stirring at room temperature for 3 h, the basic media was neutralized by addition of ion-exchange resin (Amberlite IR 120 H^+). The reaction mixture was filtered through a pad of celite and concentrated *in vacuo* to afford the de-*O*-acetylated lactosides.

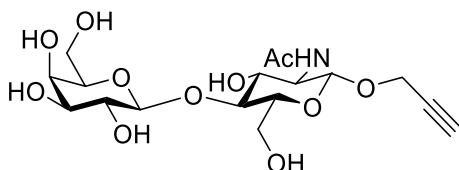
General synthetic procedure C: Protection of primary alcohol with *tert*-butyldiphenyl silyl ether (TBDPS)

To a solution of lactoside (1 eq.) in Pyridine (2 mL per 0.1 mmol of SM) was added TBDPSCl (1.5 eq. per primary alcohol) at room temperature under nitrogen atmosphere. After 8 h of stirring the reaction was quenched with methanol, the reaction mixture was co-evaporated with toluene under vacuum and the residue was purified using column chromatography.

General synthetic procedure D: Deprotection of *tert*-butyldiphenyl silyl ether (TBDPS)

To a solution of silyl ether lactoside (1 eq.) in Pyridine (10 mL per 0.1 mmol of the SM) was added HF·Py (70 % in Py, 0.1 mL per 0.1 mmol) at 0 °C and the resulted mixture was stirred at room temperature for 24 h. The reaction was quenched with solid NaHCO₃ at 0 °C and the solvent was co-evaporated with toluene and the residue was purified using column chromatography.

Propargyl (β -D-galactopyranosyl)-(1 \rightarrow 4)- 2-*N*-acetamido-2-deoxy - β -D-glucopyranoside (**3.32**).



To a solution of compound **3.31** (0.2 g, 0.241 mmol) in dry THF (5mL) was added TBAF (1M in THF, 0.5 mL). The reaction mixture was stirred at room temperature for 14 h, then the reaction mixture was concentrated *in-vacuo* and the residue was dissolved in MeOH/THF (1:1 v/v, 5mL) and NaOMe (25 % in MeOH, 0.05 mL) was added. After 3 h of stirring, the basic media was neutralized using Amberlite 120 H⁺. After chromatographic purification, a white solid (0.08 g, 0.212 mmol, 88 %) was obtained.

$[\alpha]_{\text{D}}^{20} = -26.3$ (c 0.01, H₂O).

$R_f = 0.44$, (EtOAc/*i*PrOH/H₂O : 6/5/2)

¹H NMR (300 MHz, D₂O): δ (ppm) 4.49 (d, $J = 7.7$ Hz, 1H), 4.43 (d, $J = 1.9$ Hz, 2H), 4.01 (d, $J = 11.3$ Hz, 1H), 3.91 (dd, $J = 21.3, 3.8$ Hz, 2H), 3.91 (dd, $J = 21.3, 3.8$ Hz, 2H), 3.89 – 3.51 (m, 9H), 3.61 – 3.45 (m, 1H), 2.94 (brs, 1H), 2.06 (s, 3H)

¹³C NMR (75 MHz, D₂O): δ (ppm) 174.7, 102.9, 99.3, 78.8, 78.3, 76.2, 75.3, 75.3, 72.5, 71.0, 68.5, 61.0, 60.0, 56.7, 54.9, 22.2

ESI-HRMS: m/z calcd. for C₁₇H₂₇NO₁₁ [M+Na]⁺, 444.1482; found 444.1477 [M+Na]⁺

The spectroscopic data agreed well with those of the literature.⁵⁶²

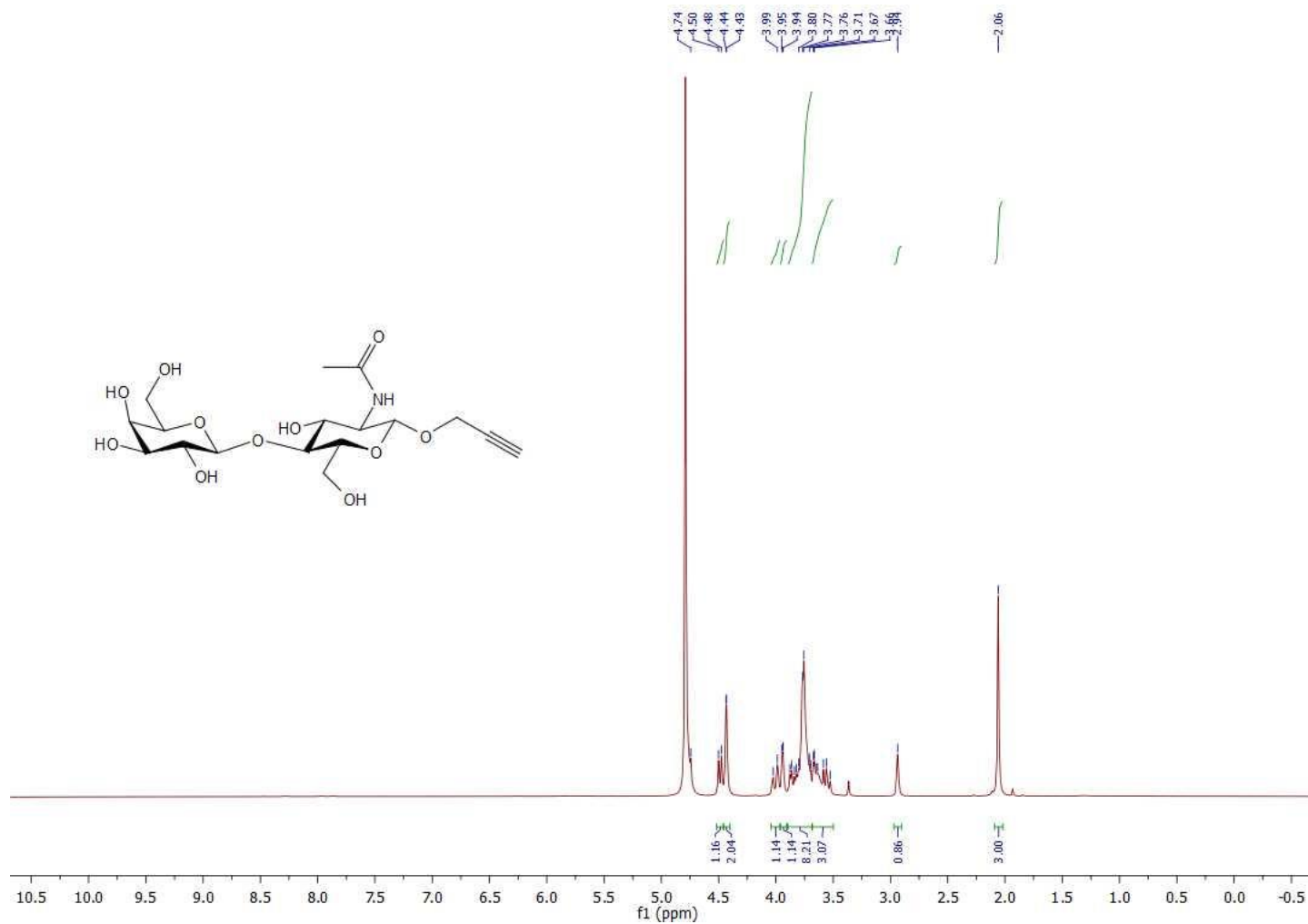


Figure 6.26 ¹H NMR (300 MHz, D₂O) spectrum of compound 3.32.

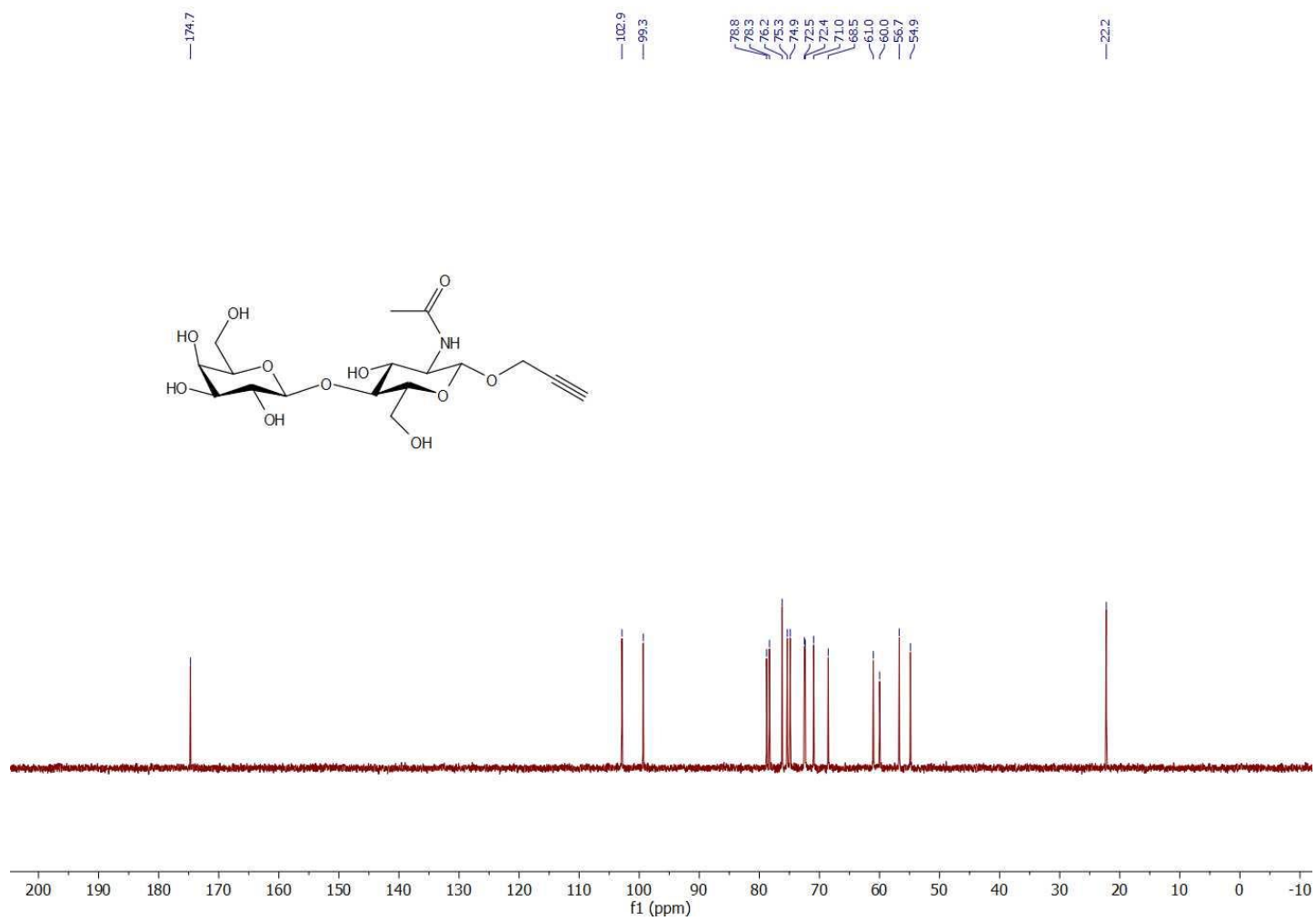


Figure 6.27 ^{13}C NMR (75 MHz, D_2O) spectrum of compound 3.32.

Compound Table

Compound Label	RT	Mass	Abund	Formula	Tgt Mass	Diff (ppm)
Cpd 2: C17 H27 N O11	0.16	421.1585	15515	C17 H27 N O11	421.1584	0.3
Cpd 1: C28 H44 N2 O19	0.16	712.2538	6804	C28 H44 N2 O19	712.2538	-0.06

Compound Label	RT	Algorithm	Mass
Cpd 2: C17 H27 N O11	0.16	Find By Formula	421.1585

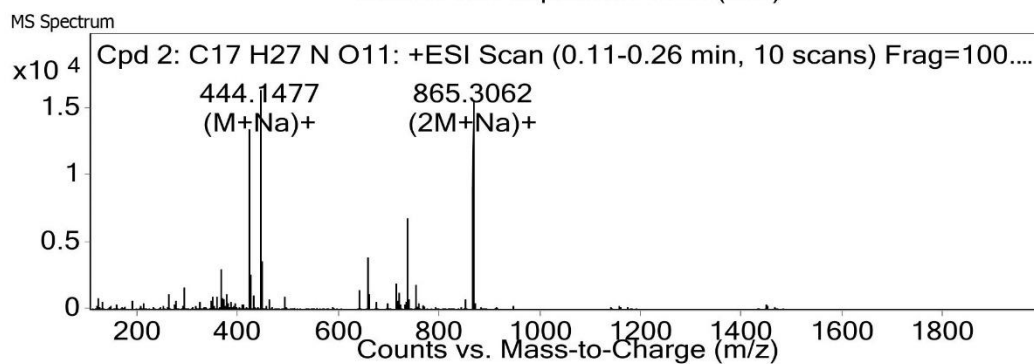
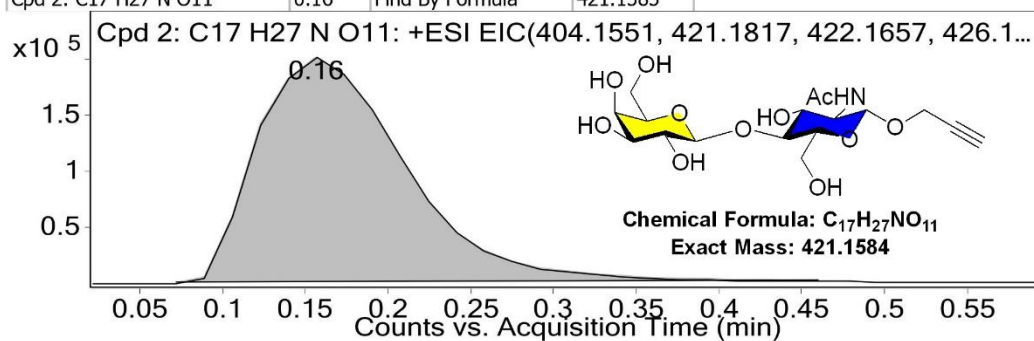
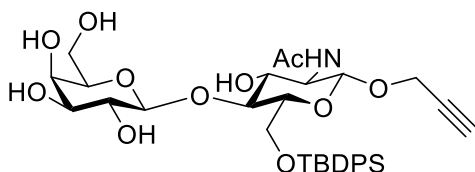


Figure 6.28 HRMS spectrum of compound 3.32.

Propargyl (β -D-galactopyranosyl)-(1 \rightarrow 4)-2-*N*-acetamido-2-deoxy-6-*O*-*tert*-butyldiphenylsilyl- β -D-glucopyranoside (**3.33**).



Following the general procedure B, compound **3.33** was obtained as a white solid (0.32 g, 0.49 mmol, 99 %) without further purification.

$[\alpha]_{\text{D}}^{21} = -12.8$ (c 0.02, MeOH).

^1H NMR (300 MHz, CD_3OD): δ (ppm) 7.65 (d, $J = 7.2$ Hz, 4H), 7.38 – 7.26 (m, 6H), 4.59 (d, $J = 7.4$ Hz, 1H), 4.57 (d, $J = 6.9$ Hz, 1H), 4.29 – 4.09 (m, 3H), 3.99 – 3.86 (m, 2H), 3.82 – 3.60 (m, 5H), 3.57 – 3.39 (m, 4H), 3.27 (brs, 1H), 1.99 (s, 3H), 0.95 (s, 9H)

^{13}C NMR (75 MHz, CD_3OD): δ (ppm) 174.6, 136.7, 136.5, 134.5, 133.9, 130.9, 128.8, 128.6, 103.9, 99.7, 78.0, 76.9, 76.3, 74.4, 73.7, 72.1, 69.9, 62.9, 62.2, 56.2, 56.2, 27.3, 23.1, 19.9

ESI-HRMS: m/z calcd. for $\text{C}_{33}\text{H}_{45}\text{NO}_{11}\text{Si}$ $[\text{M}+\text{Na}]^+$, 682.2654; found 682.2662
 $[\text{M}+\text{Na}]^+$

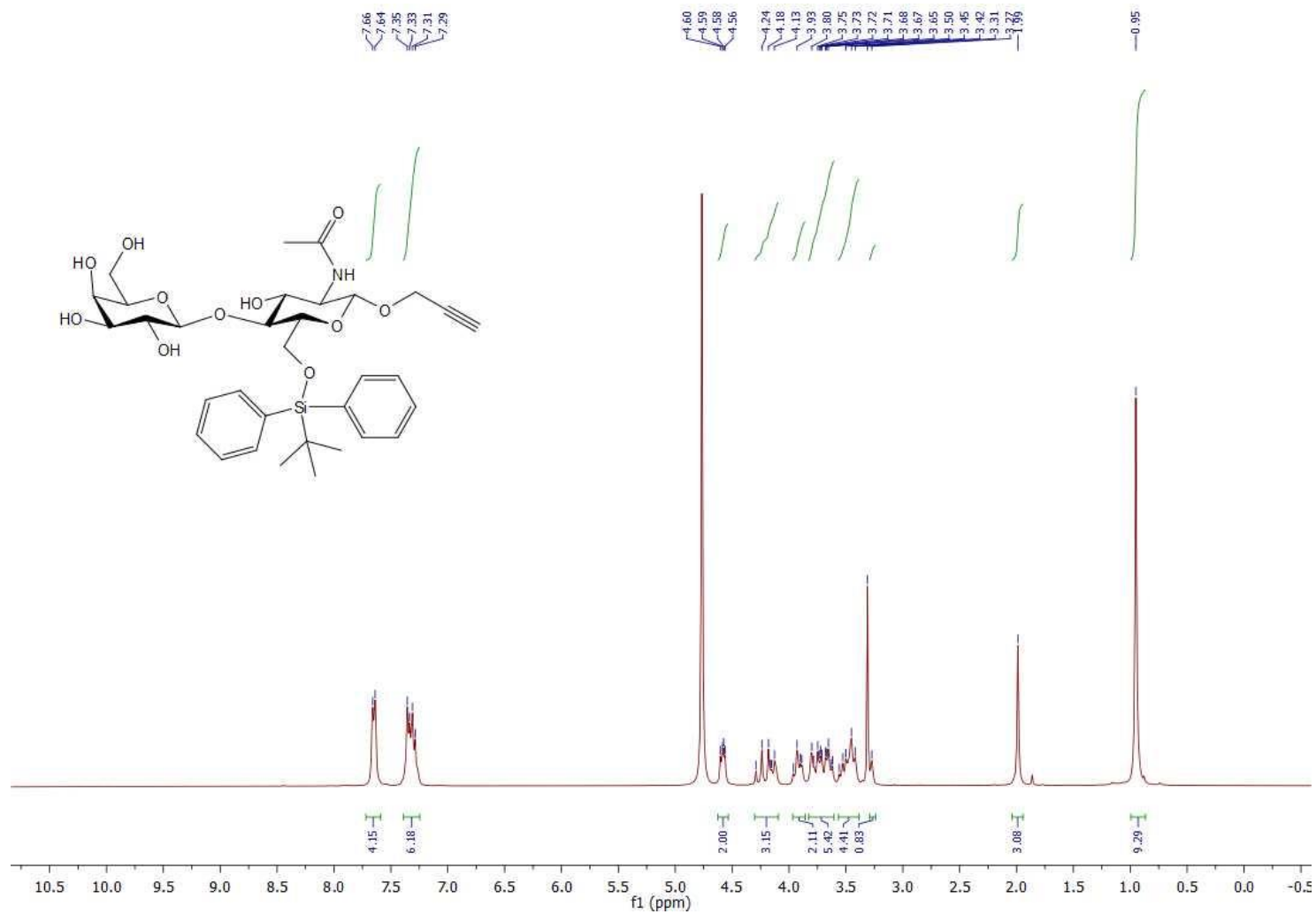


Figure 6.29 ¹H NMR (300 MHz, CD₃OD) spectrum of compound 3.33.

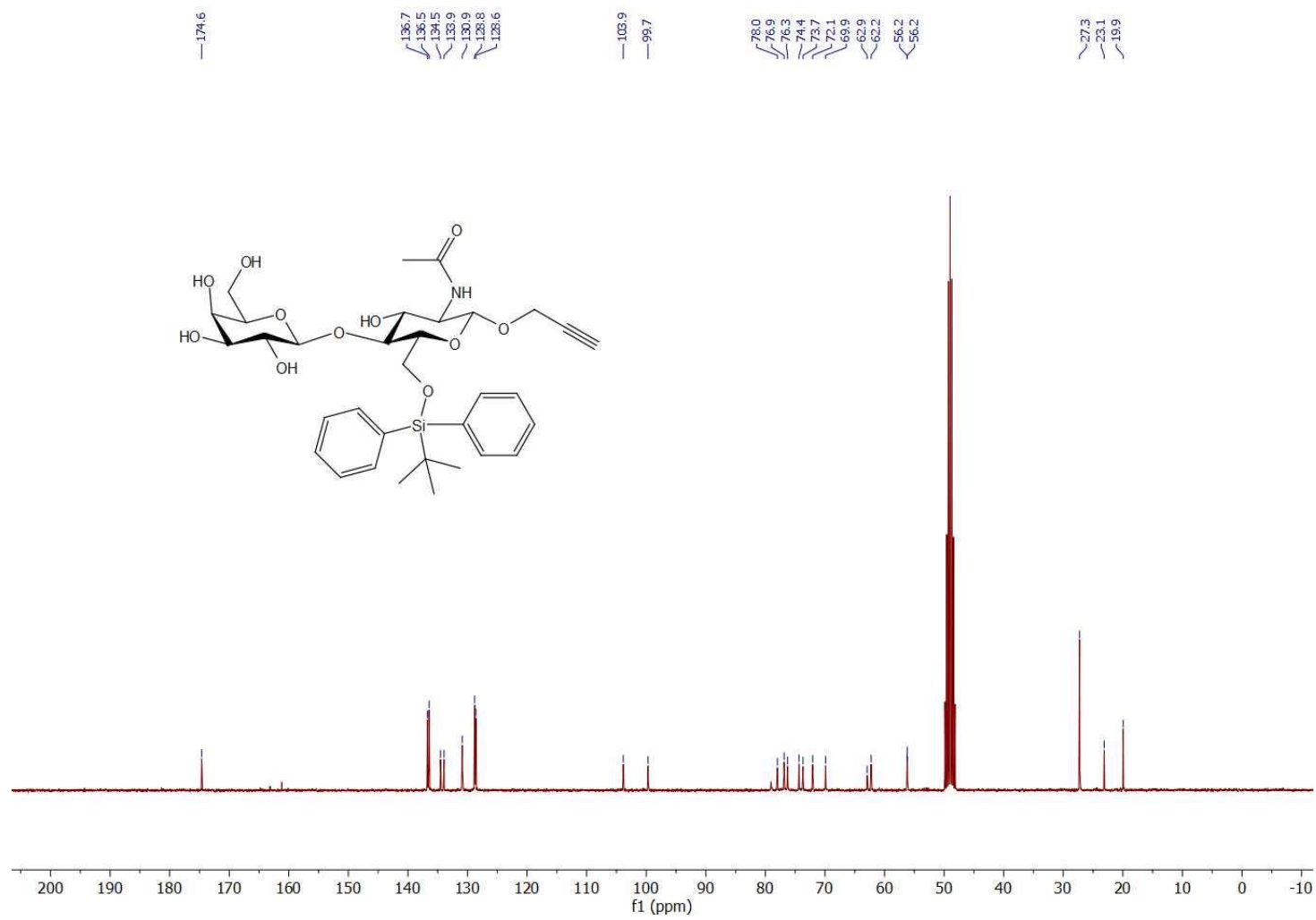
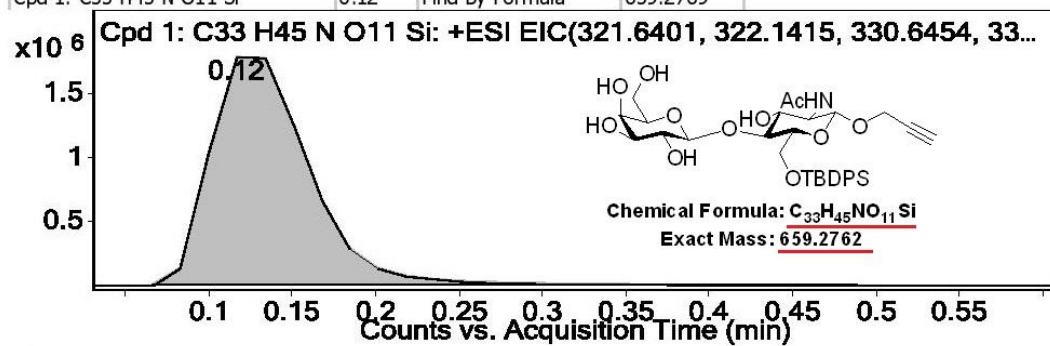


Figure 6.30 ^{13}C NMR (75 MHz, CD_3OD) spectrum of compound 3.33.

Compound Table

Compound Label	RT	Mass	Abund	Formula	Tgt Mass	Diff (ppm)
Cpd 1: C ₃₃ H ₄₅ N O ₁₁ Si	0.12	<u>659.2769</u>	235098	<u>C₃₃ H₄₅ N O₁₁ Si</u>	<u>659.2762</u>	<u>1.01</u>

Compound Label	RT	Algorithm	Mass
Cpd 1: C ₃₃ H ₄₅ N O ₁₁ Si	0.12	Find By Formula	659.2769



MS Spectrum

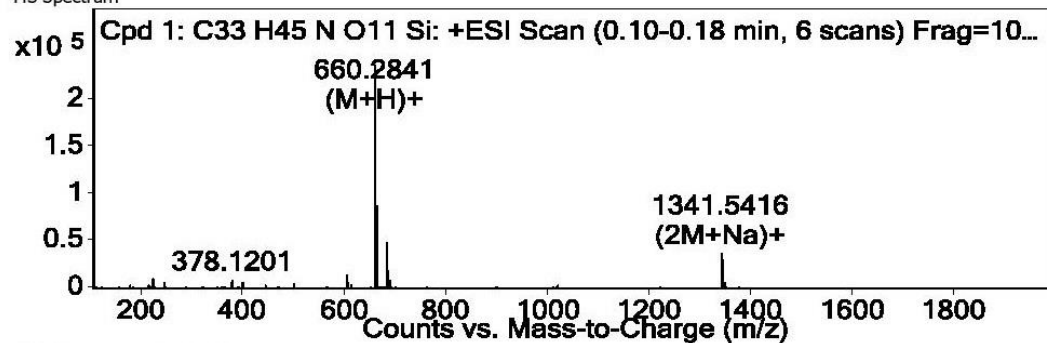
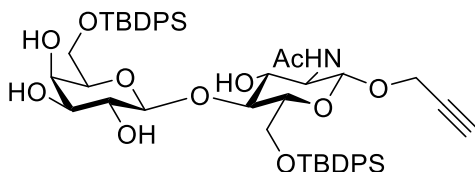


Figure 6.31 HRMS spectrum of compound 3.33.

Propargyl (6-*O*-*tert*-butyldiphenylsilyl- β -D-galactopyranosyl)-(1 \rightarrow 4)-2-*N*-acetamido-2-deoxy-6-*O*-*tert*-butyldiphenylsilyl- β -D-glucopyranoside (**3.34**).



Following the general procedure C, compound **3.34** was obtained as a white solid (0.25 mg, 0.28 mmol, 80 %).

$R_f = 0.54$, (EtOAc/MeOH : 9.5/0.5).

$[\alpha]_D^{21} = -15.8$ (c 0.04, MeOH).

$^1\text{H NMR}$ (300 MHz, CD_3OD): δ (ppm) 7.80 – 7.76 (m, 4H), 7.70 – 7.65 (m, 4H), 7.42 – 7.28 (m, 12H), 4.64 (d, $J = 8.0$ Hz, 1H), 4.59 (d, $J = 7.7$ Hz, 1H), 4.43 – 4.15 (m, 3H), 3.97 (d, $J = 12.1$ Hz, 1H), 3.92 – 3.83 (m, 4H), 3.81 – 3.68 (m, 2H), 3.67 – 3.57 (m, 2H), 3.47 (dd, $J = 9.7, 3.1$ Hz, 2H), 2.84 (t, $J = 2.4$ Hz, 1H), 1.96 (s, 3H), 1.04 (s, 9H), 1.03 (s, 9H)

$^{13}\text{C NMR}$ (75 MHz, CD_3OD): δ (ppm) 173.5, 137.0, 136.7, 136.6, 134.8, 134.3, 134.3, 134.1, 130.9, 130.9, 130.8, 130.7, 128.8, 128.8, 128.6, 104.7, 100.0, 79.7, 79.5, 76.7, 76.5, 76.4, 75.0, 73.6, 72.3, 69.6, 63.5, 63.2, 56.5, 56.0, 27.4, 27.4, 23.0, 20.2, 19.9

ESI-HRMS: m/z calcd. for $\text{C}_{49}\text{H}_{63}\text{NO}_{11}\text{Si}_2$ $[\text{M}+\text{Na}]^+$, 920.3832; found 920.3830 $[\text{M}+\text{Na}]^+$

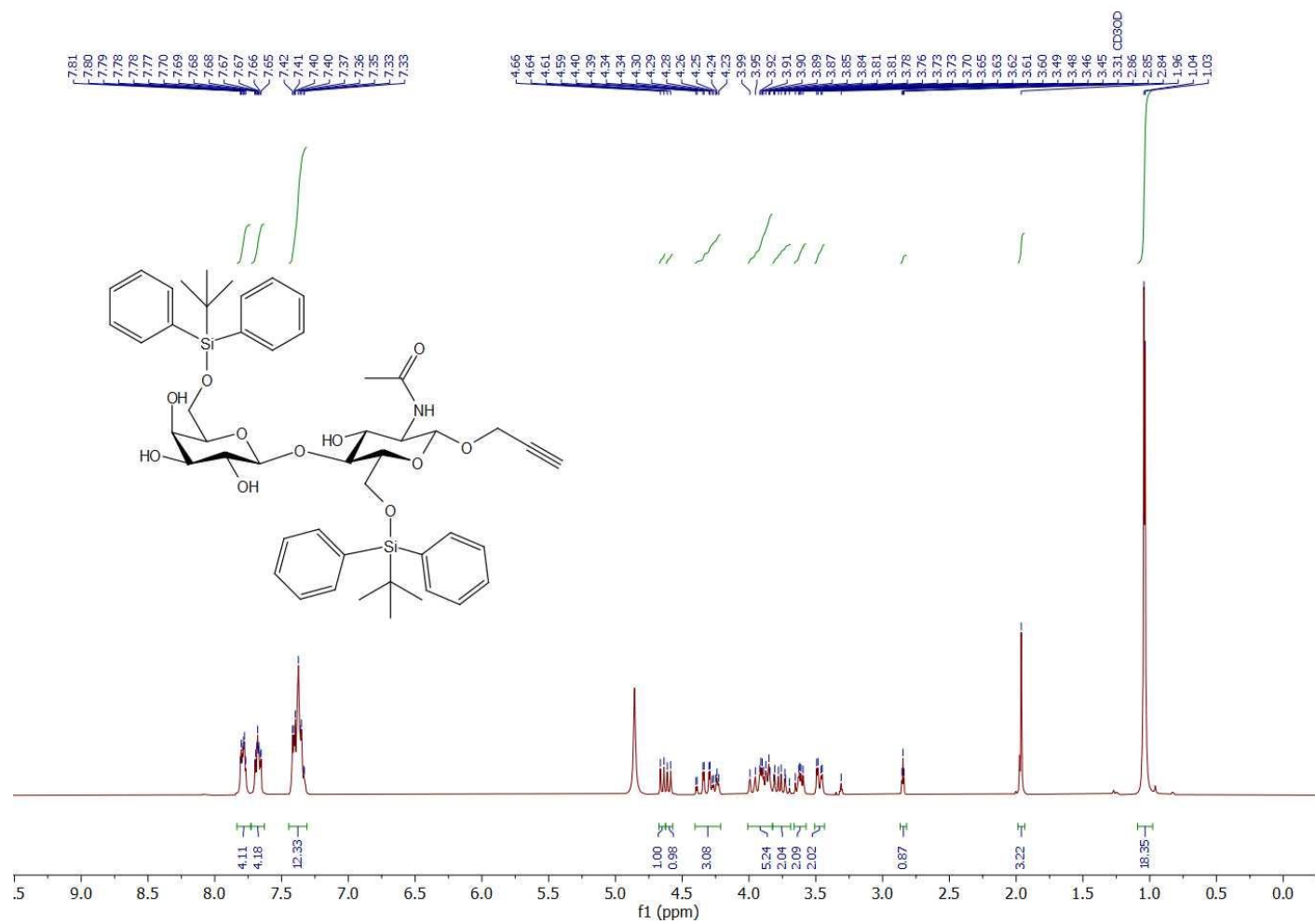


Figure 6.32 ¹H NMR (300 MHz, CD₃OD) spectrum of compound 3.34.

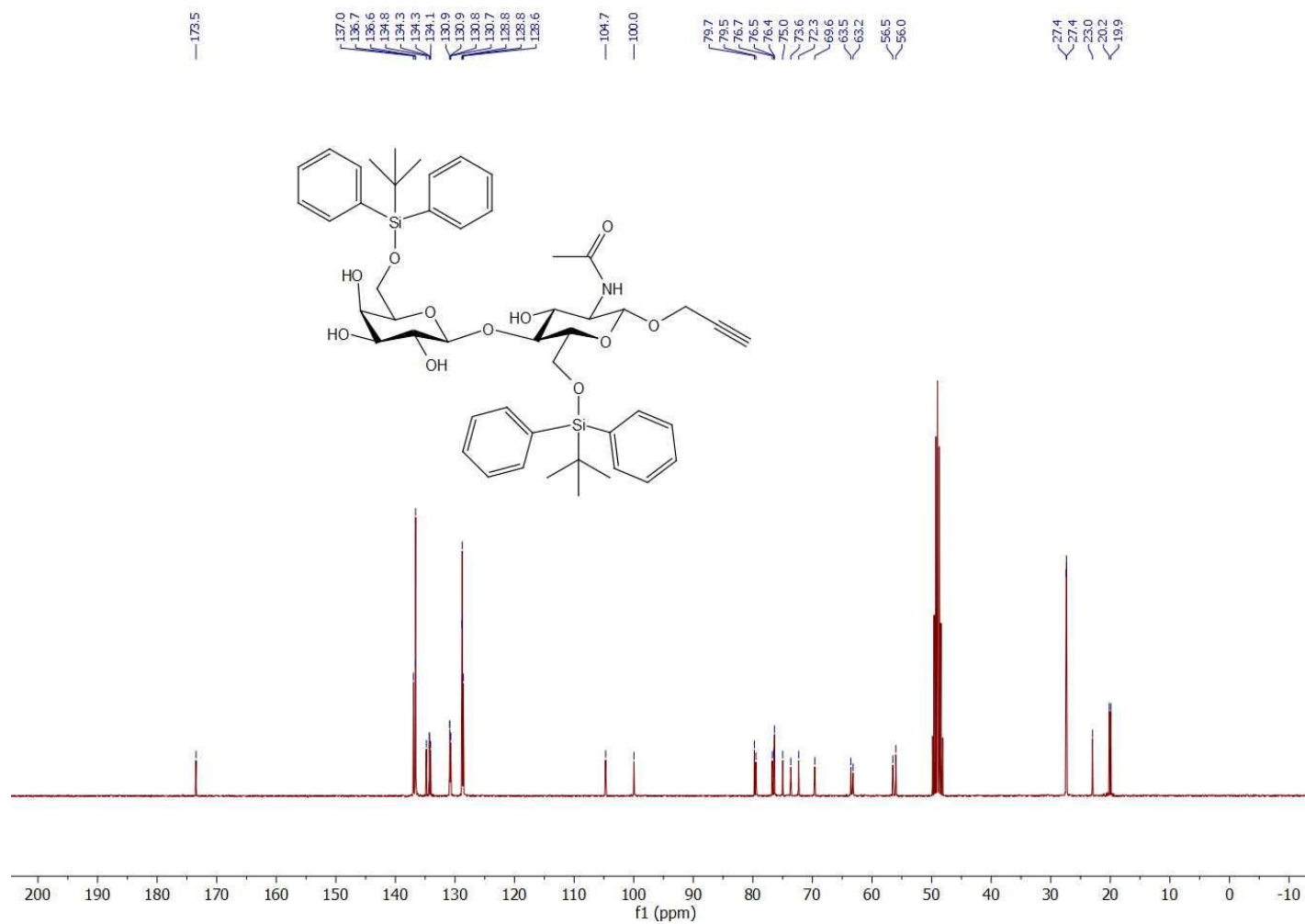


Figure 6.33 ^{13}C NMR (75 MHz, CD_3OD) spectrum of compound 3.34.

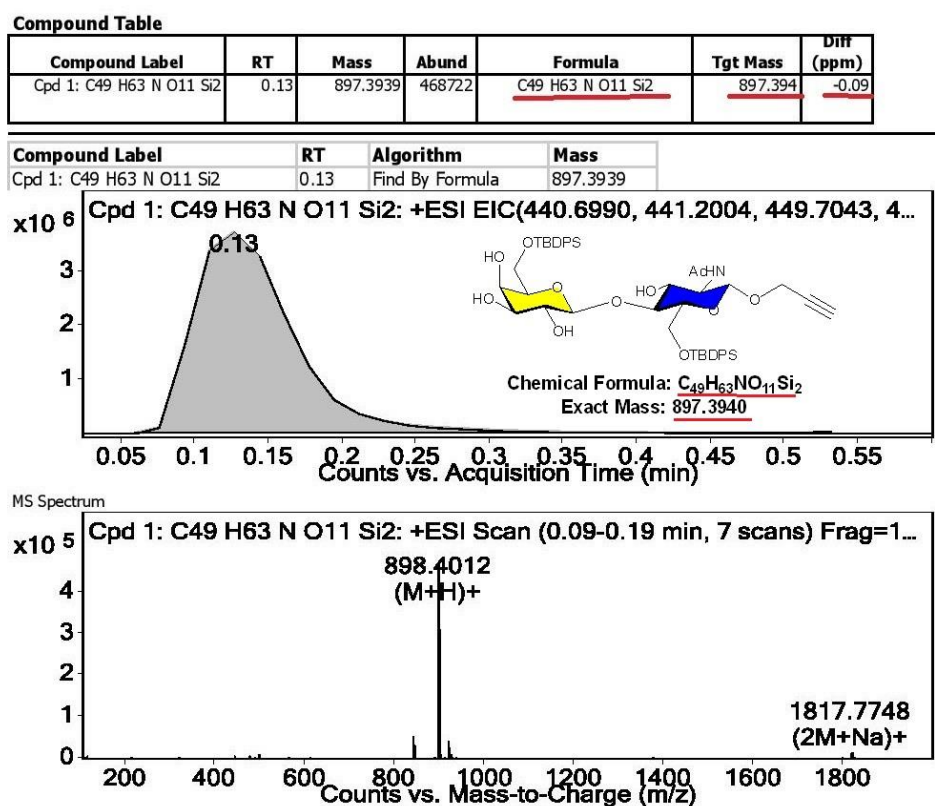
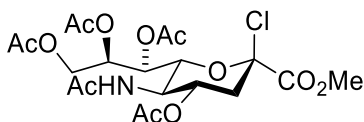


Figure 6.34 HRMS spectrum of compound 3.34.

Methyl (2-Chloro-4,7,8,9-tetra-*O*-acetyl-3,5-dideoxy-5-*N*-acetamido-D-glycero- β -D-galacto-non-2-ulopyranitol)onate (**3.35**)



To a solution of Neu5Ac (0.21 g, 0.68 mmol) in dry methanol (20 mL) was added Amberlite® IR120 H⁺ (0.15 g) and the resulting mixture was stirred for 24 h at room temperature. The reaction mixture was then filtered over a pad of celite and concentrated *in-vacuo*. After recrystallization from methanol/diethyl ether, the white solid was immediately treated with freshly distilled acetyl chloride (20 mL) at -10 °C and the resulting mixture was stirred at room temperature for 72 h, then concentrated *in-vacuo*. After chromatographic purification over silica **3.35** (0.29 mg, 0.56 mmol, 83 %) was obtained as a white foam.

R_f = 0.74, (EtOAc).

¹H NMR (300 MHz, CDCl₃): δ (ppm) 6.46 (d, *J* = 10.0 Hz, 1H), 5.36 (dd, *J* = 6.3, 2.3 Hz, 1H), 5.26 (td, *J* = 10.8, 4.9 Hz, 1H), 5.04 (td, *J* = 6.3, 2.6 Hz, 1H), 4.50 – 4.19 (m, 2H), 4.10 (q, *J* = 10.3 Hz, 1H), 3.96 (dd, *J* = 12.5, 6.3 Hz, 1H), 3.74 (s, 3H), 2.65 (dd, *J* = 13.9, 4.8 Hz, 1H), 2.11 (dd, *J* = 14.0, 11.2 Hz, 1H), 2.00 (s, 3H), 1.94 (s, 3H), 1.92 (s, 6H), 1.77 (s, 3H)

¹³C NMR (75 MHz, CDCl₃): δ (ppm) 170.7, 170.5, 170.5, 169.8, 96.6, 77.4, 73.8, 70.2, 68.7, 66.9, 62.0, 53.6, 48.2, 40.5, 22.9, 20.8, 20.7, 20.6

The spectroscopic data agreed well with those of the literature.⁵⁶³

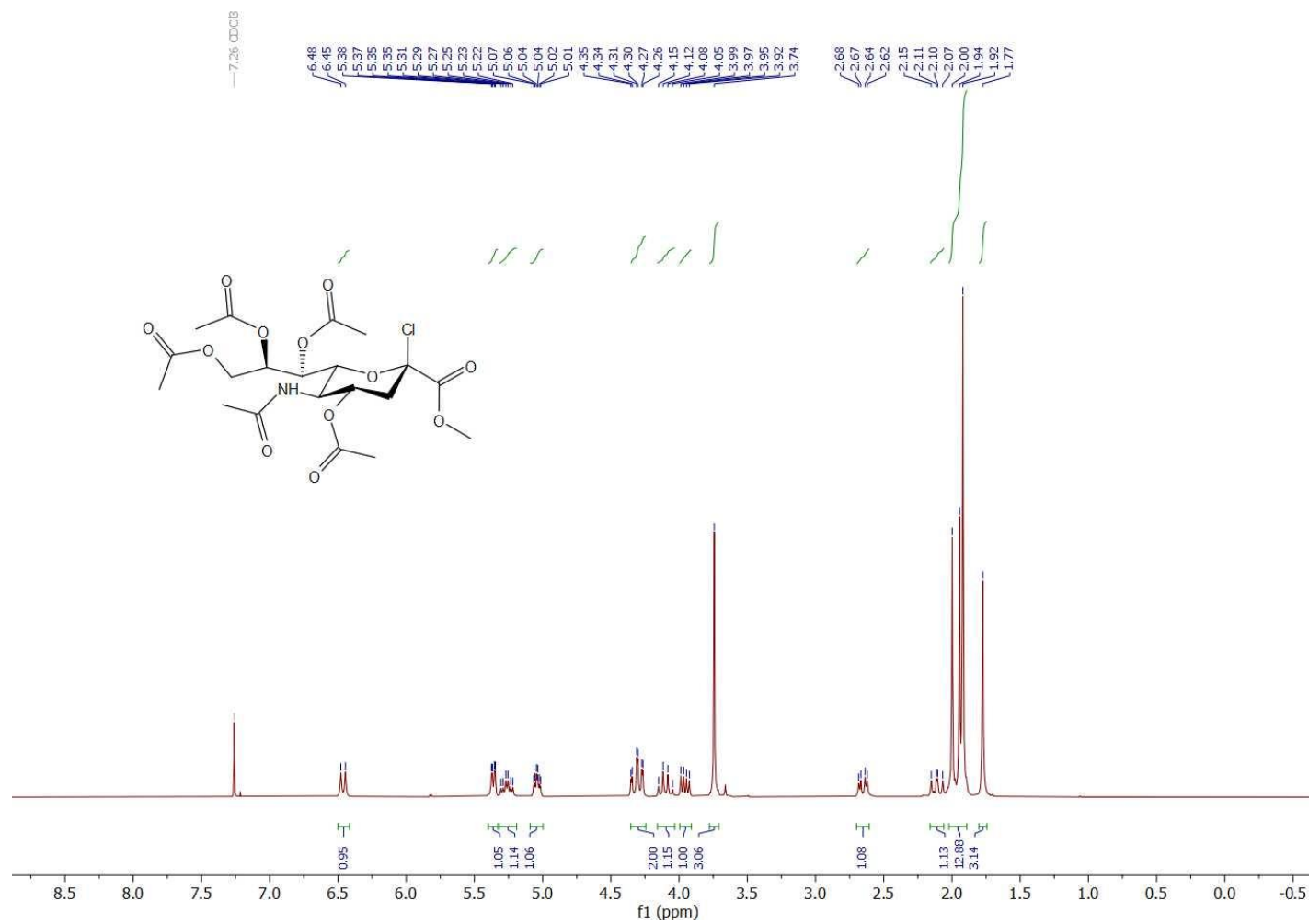


Figure 6.35 ^1H NMR (300 MHz, CDCl_3) spectrum of compound 3.35.

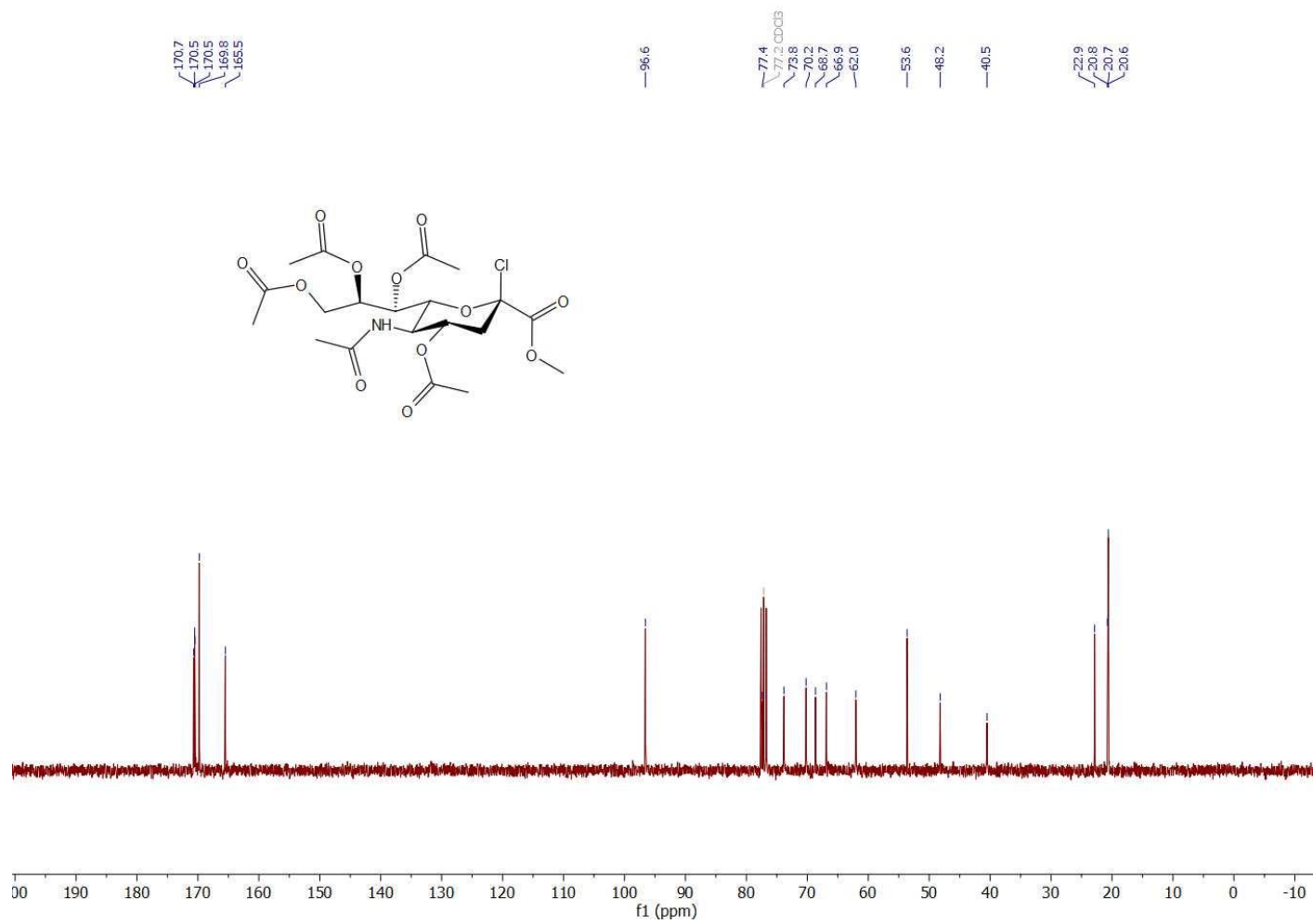
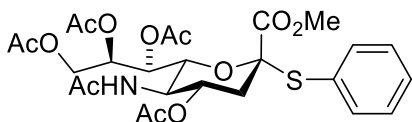


Figure 6.36 ^{13}C NMR (75 MHz, CDCl_3) spectrum of compound 3.35.

Methyl (2-*S*-phenyl-4,7,8,9-tetra-*O*-acetyl-3,5-dideoxy-5-*N*-acetamido-D-glycero- β -D-galacto-non-2-ulopyranitol)onate (**3.36**)



The compounds **3.36** was prepared according to a modified literature procedure.³⁸¹

To a solution of **3.35** (0.28 g, 0.56 mmol 1eq.), TBAHS (0.19 g, 0.56 mmol 1eq.) in EtOAc (4 mL) was added thiophenol (0.18 mg, 1.68 mmol, 3 eq.) in 1M Na₂CO₃ (4 mL). After 3 h stirring at room temperature, reaction mixture was diluted in chloroform (25 mL), washed with 0.5M NaOH (2 x 25 mL), 0.5M HCl (25 mL), brine (25 mL), dried over Na₂SO₄ and concentrated *in-vacuo*. Recrystallization from CHCl₃/hexane afforded **3.36** (0.3 g, 0.52 mmol, 93 %) as a white solid.

¹H NMR (300 MHz, CDCl₃): δ (ppm) 7.67 – 7.46 (m, 2H), 7.44 – 7.29 (m, 3H), 5.34 – 5.21 (m, 2H), 5.12 (d, $J = 9.8$ Hz, 1H), 4.84 (ddd, $J = 11.7, 10.0, 4.7$ Hz, 1H), 4.39 (dd, $J = 12.4, 2.2$ Hz, 1H), 4.19 (dd, $J = 12.4, 4.7$ Hz, 1H), 3.98 (q, $J = 10.2$ Hz, 1H), 3.89 (dd, $J = 10.7, 1.6$ Hz, 1H), 3.57 (s, 3H), 2.81 (dd, $J = 12.9, 4.7$ Hz, 1H), 2.14 (s, 3H), 2.05 (s, 3H), 2.04 (s, 3H), 2.02 (brs, 4H), 1.86 (s, 3H)

¹³C NMR (75 MHz, CDCl₃): δ (ppm) 171.0, 170.7, 170.3, 170.2, 170.1, 168.0, 136.5, 129.9, 128.9, 128.7, 87.6, 74.9, 70.2, 69.8, 67.8, 62.1, 52.8, 49.2, 38.2, 23.2, 21.0, 20.9, 20.8

The spectroscopic data agreed well with those of the literature.⁵⁶³

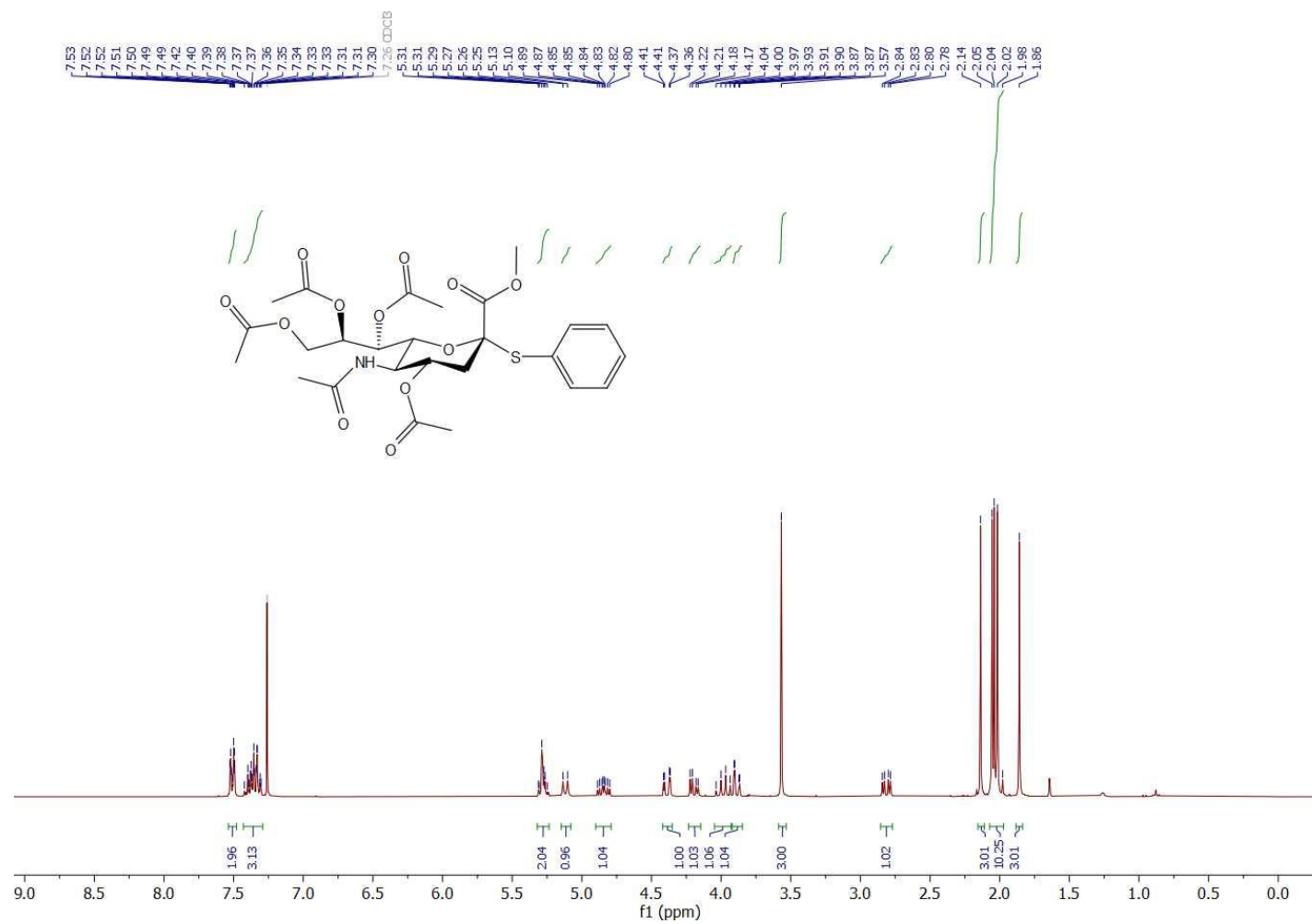


Figure 6.37 ^1H NMR (300 MHz, CDCl_3) spectrum of compound 3.36.

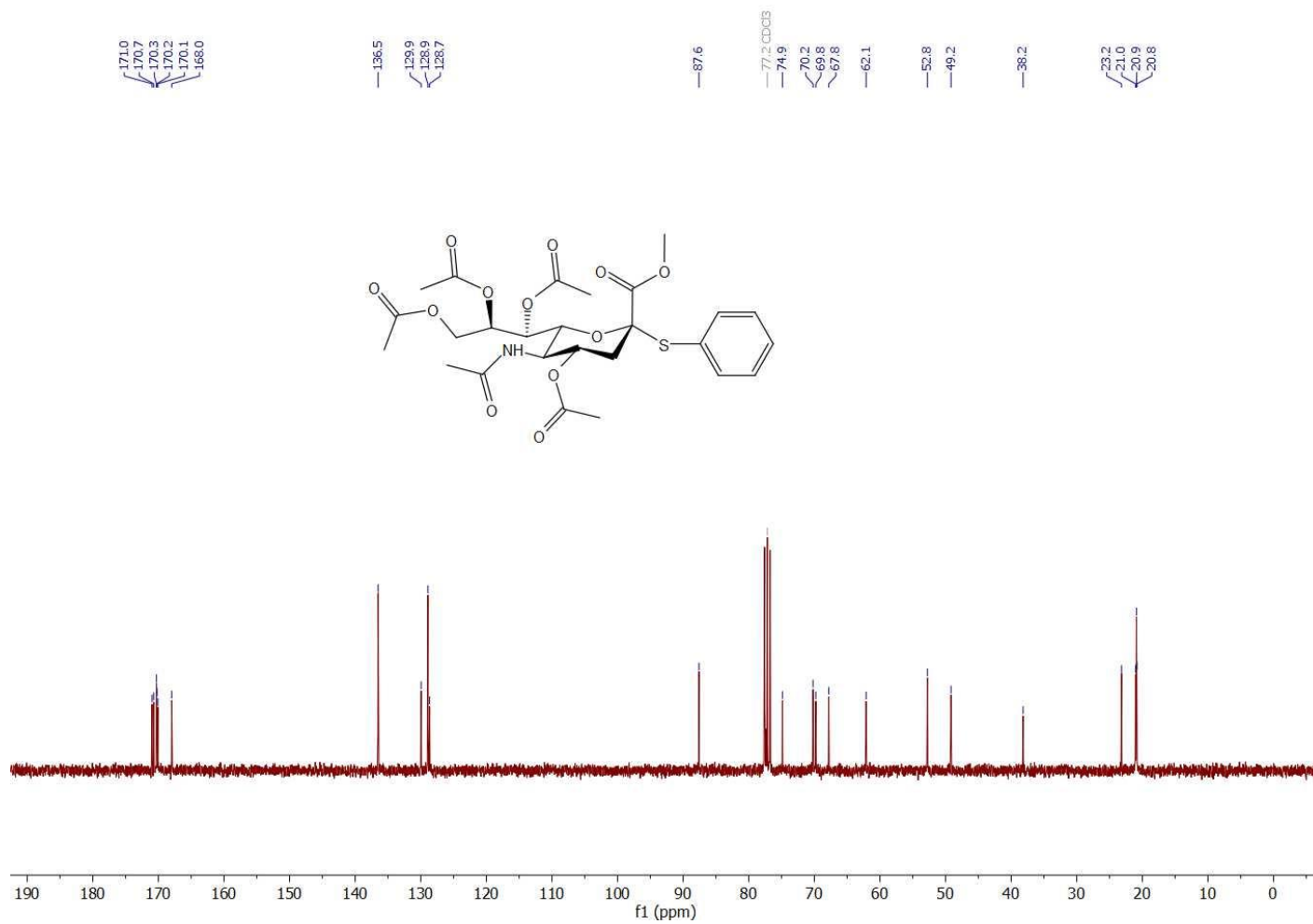
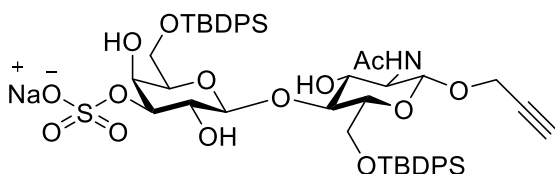


Figure 6.38 ¹³C NMR (75 MHz, CDCl₃) spectrum of compound **3.36**.

Propargyl (3-*O*-sulfo-6-*O*-*tert*-butyldiphenylsilyl)- β -D-galactopyranosyl)-(1 \rightarrow 4)-2-*N*-acetamido-2-deoxy-6-*O*-*tert*-butyldiphenylsilyl)- β -D-glucopyranoside sodium salt (**3.37**).



Following the general procedure, A, compound **3.37** was obtained as a white solid (161 mg, 0.161 mmol, 90 %).

$R_f = 0.08$, (EtOAc/MeOH : 9/1).

$[\alpha]_D^{21} = -10.8$ (c 0.005, MeOH)

$^1\text{H NMR}$ (300 MHz, CD_3OD): δ (ppm) 7.81 – 7.75 (m, 4H), 7.69 – 7.63 (m, 4H), 7.50 – 7.31 (m, 12H), 4.72 (d, $J = 7.7$ Hz, 1H), 4.63 (d, $J = 8.2$ Hz, 1H), 4.42 – 4.19 (m, 5H), 3.96 – 3.62 (m, 8H), 3.46 (d, $J = 9.0$ Hz, 1H), 2.87 (t, $J = 2.7$ Hz, 1H), 1.96 (s, 3H), 1.03 (s, 9H), 1.02 (s, 9H)

$^{13}\text{C NMR}$ (75 MHz, CD_3OD): δ (ppm) 173.6, 137.0, 136.7, 136.6, 134.7, 134.3, 134.3, 134.1, 130.9, 130.9, 130.9, 130.8, 129.0, 128.9, 128.8, 128.7, 104.1, 100.2, 82.0, 79.8, 79.1, 76.4, 76.2, 73.8, 71.1, 67.8, 63.1, 63.0, 56.3, 56.2, 55.1, 27.4, 27.3, 23.0, 20.2, 19.9

ESI-HRMS: m/z calcd. for $\text{C}_{49}\text{H}_{64}\text{NO}_{14}\text{SSi}_2$ $[\text{M}+\text{H}]^+$, 978.3581; found 978.3579 $[\text{M}+\text{H}]^+$

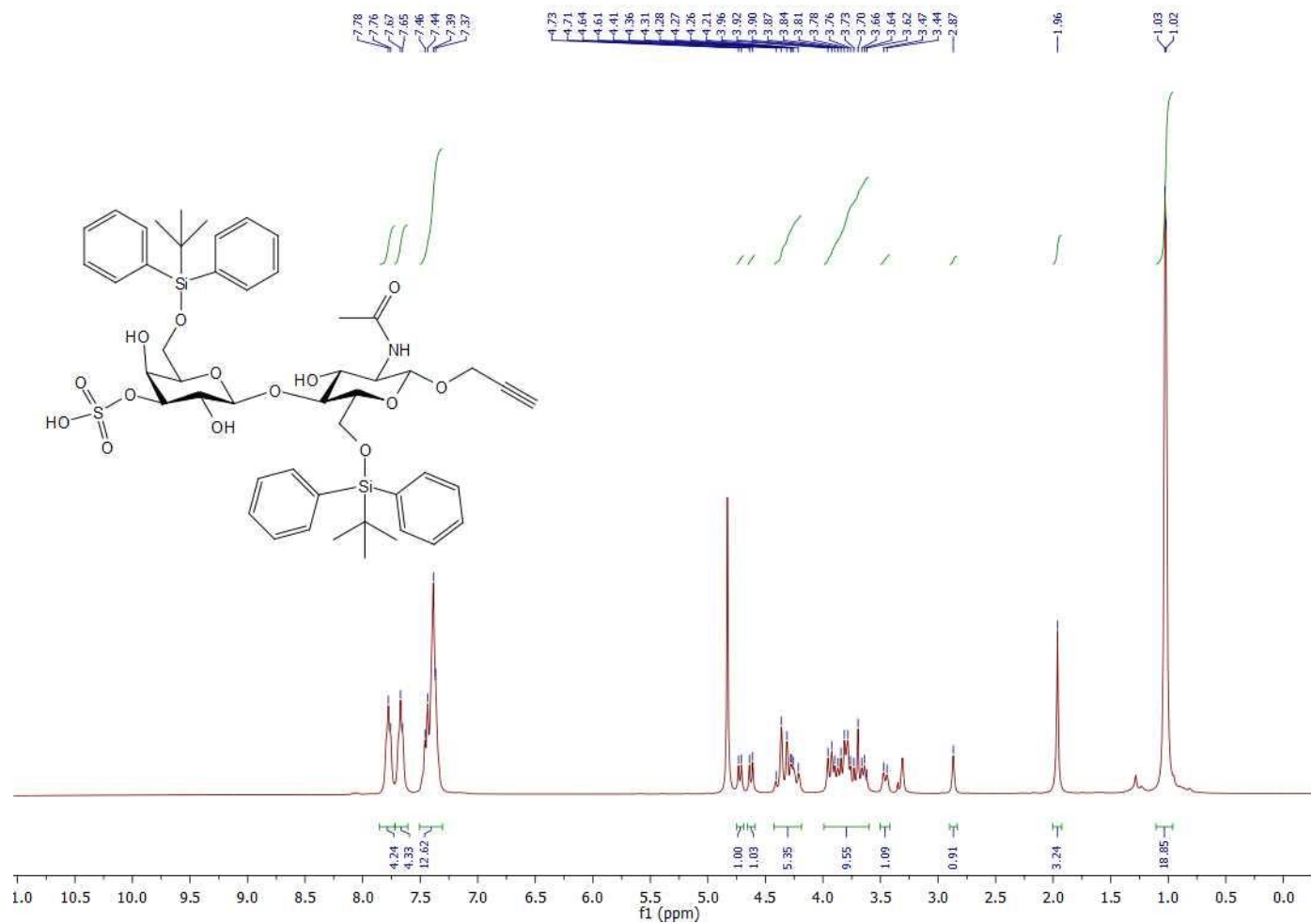


Figure 6.39 ¹H NMR (300 MHz, CD₃OD) spectrum of compound 3.37.

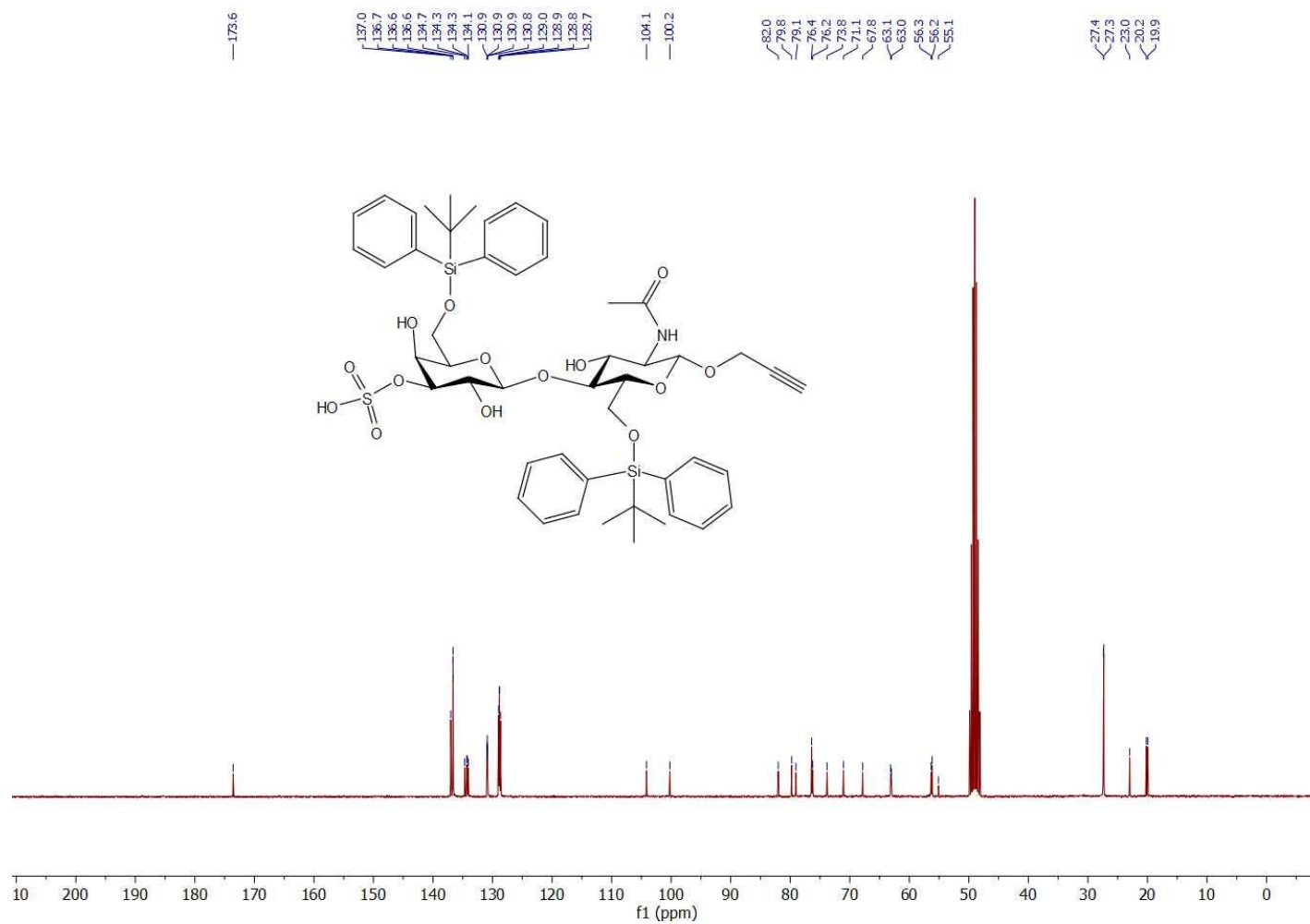
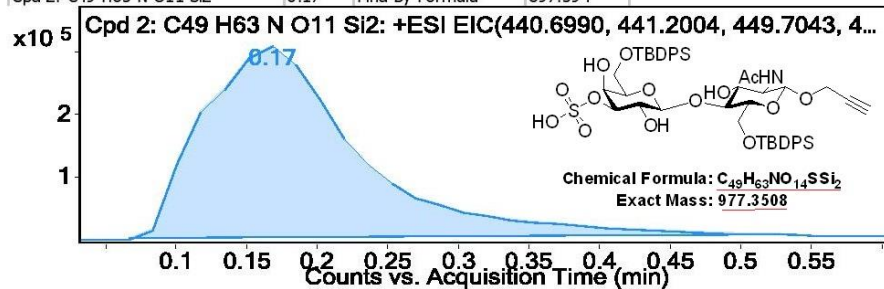


Figure 6.40 ^{13}C NMR (75 MHz, CD_3OD) spectrum of compound 3.37.

Compound Table

Compound Label	RT	Mass	Abund	Formula	Tgt Mass	Diff (ppm)
Cpd 2: C ₄₉ H ₆₃ N O ₁₁ Si ₂	0.17	897.394	26946	C ₄₉ H ₆₃ N O ₁₁ Si ₂	897.394	0
Cpd 1: C ₄₉ H ₆₃ N O ₁₄ S Si ₂	0.17	<u>977.3505</u>	7170	<u>C₄₉H₆₃N O₁₄ S Si₂</u>	<u>977.3508</u>	-0.29

Compound Label	RT	Algorithm	Mass
Cpd 2: C ₄₉ H ₆₃ N O ₁₁ Si ₂	0.17	Find By Formula	897.394



MS Spectrum

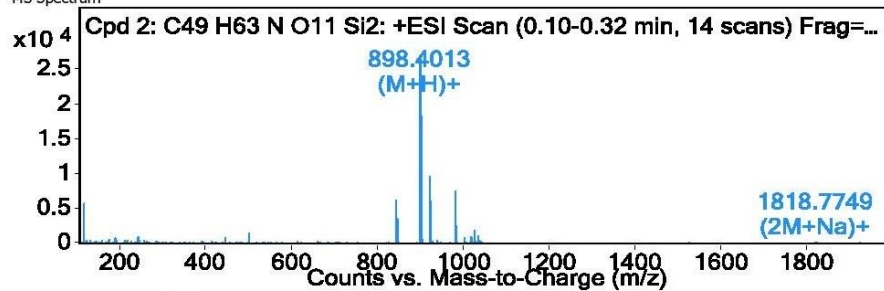
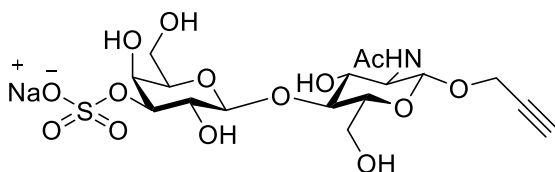


Figure 6.41 HRMS spectrum of compound 3.37.

Propargyl (3-*O*-sulfo- β -D-galactopyranosyl)-(1 \rightarrow 4)-2-*N*-acetamido-2-deoxy- β -D-glucopyranoside sodium salt (**3.38**).



Following the general procedure D, compound **3.38** was obtained as a white solid (0.027 g, 0.051 mmol, 64 %).

$R_f = 0.27$, (EtOAc/*i*PrOH/H₂O : 5/5/2.5)

$[\alpha]_D^{21} = -11.0$ (c 0.002, H₂O).

¹H NMR (300 MHz, D₂O): δ (ppm) 4.61 (d, $J = 7.8$ Hz, 1H), 4.44 (d, $J = 2.3$ Hz, 2H), 4.36 (dd, $J = 9.8, 3.2$ Hz, 1H), 4.31 (d, $J = 3.2$ Hz, 1H), 4.02 (dd, $J = 12.3, 2.0$ Hz, 1H), 3.91 – 3.60 (m, 9H), 2.93 (t, $J = 2.3$ Hz, 1H), 2.06 (s, 3H)

¹³C NMR (75 MHz, D₂O): δ (ppm) 174.8, 102.5, 99.4, 80.0, 78.8, 78.2, 76.2, 74.9, 74.8, 72.3, 69.1, 66.8, 60.9, 59.9, 56.7, 54.9, 22.2

ESI-HRMS: m/z calcd. for C₁₇H₂₈NO₁₄S [M+H]⁺, 502.1225; found 502.1227 [M+H]⁺

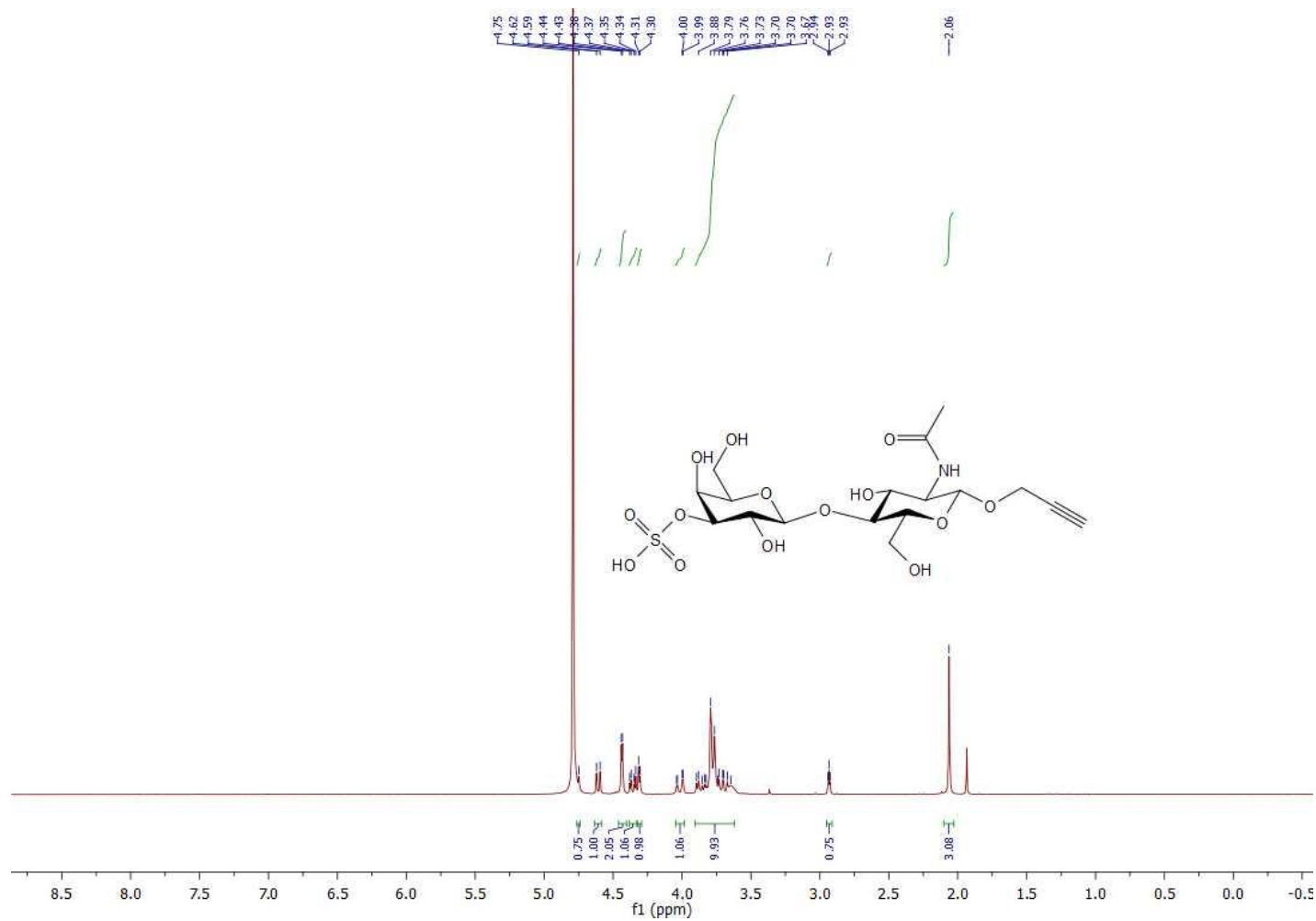


Figure 6.42 ^1H NMR (300 MHz, D_2O) spectrum of compound 3.38.

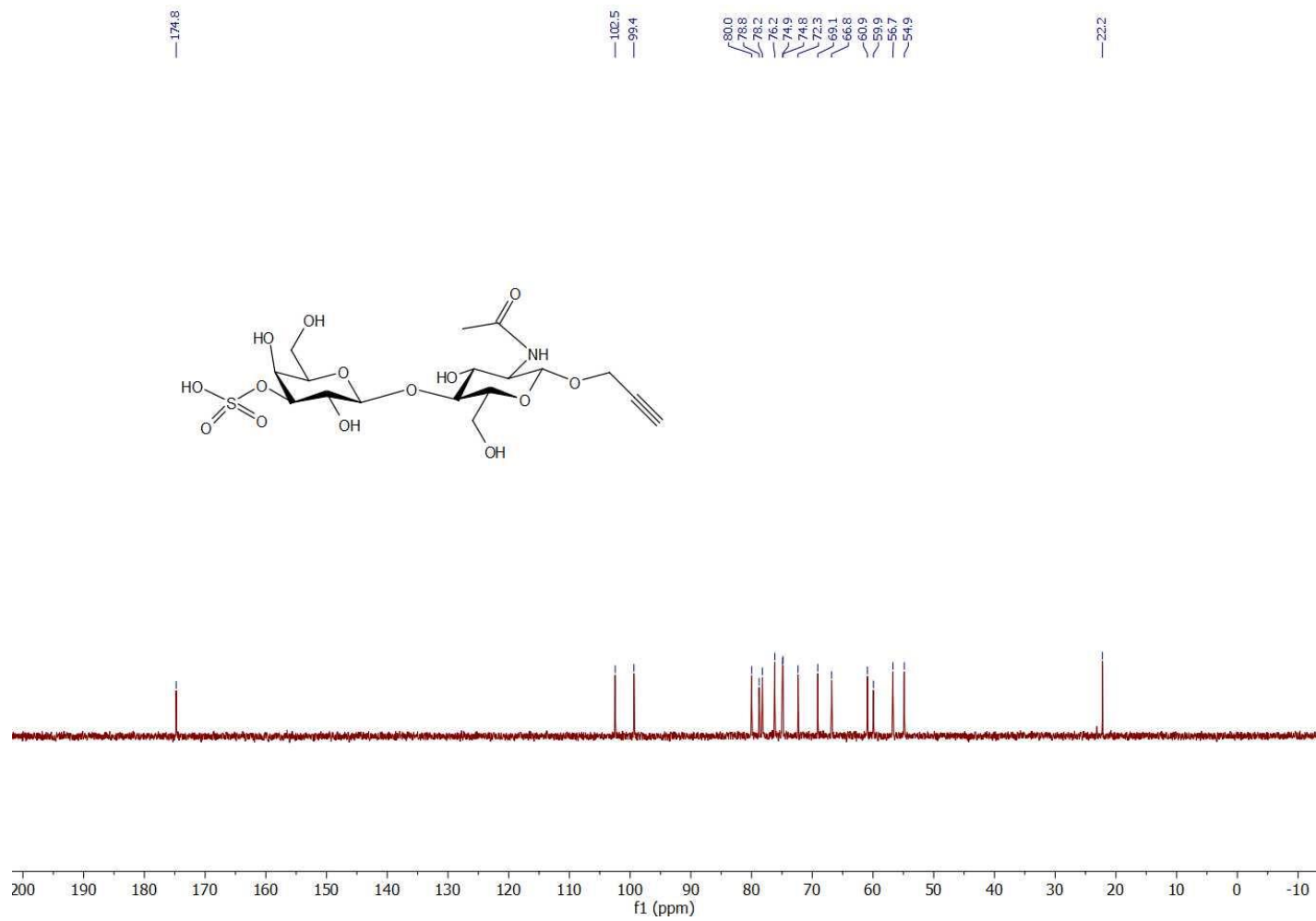
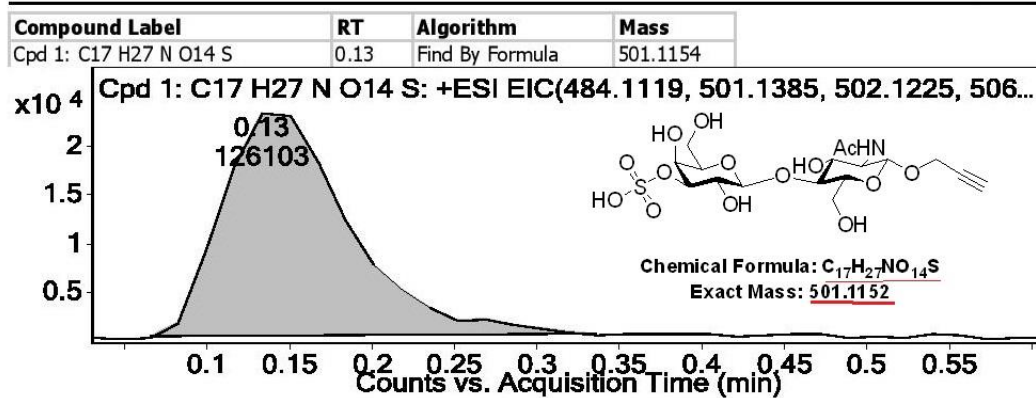


Figure 6.43 ^{13}C NMR (75 MHz, D_2O) spectrum of compound 3.38.

Compound Table

Compound Label	RT	Mass	Abund	Formula	Tgt Mass	Diff (ppm)
Cpd 1: C17 H27 N O14 S	0.13	<u>501.1154</u>	4519	<u>C17 H27 N O14 S</u>	<u>501.1152</u>	<u>0.39</u>



MS Spectrum

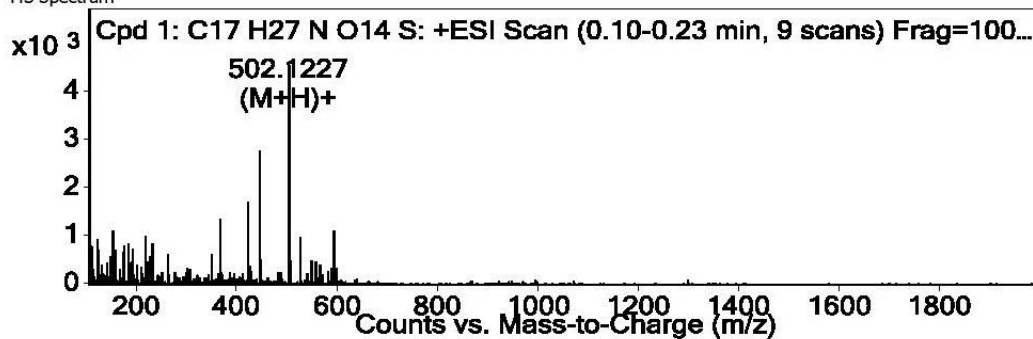
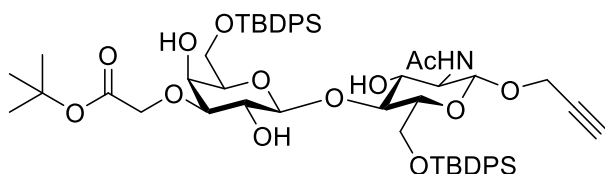


Figure 6.44 HRMS spectrum of compound 3.38.

Propargyl (3-*O*-[2-(1,1-dimethylethoxy)-2-oxoethyl]-6-*O*-*tert*-butyldiphenylsilyl]- β -D-galactopyranosyl)-(1 \rightarrow 4)-2-*N*-acetamido-2-deoxy-6-*O*-*tert*-butyldiphenylsilyl]- β -D-glucopyranoside (**3.39**).



A mixture of compound **3.34** (0.21 mg, 0.23 mmol, 1 eq.) and dibutyltin oxide (0.07 g, 0.28 mmol 1.2 eq.) in THF/Toluene (1/1 : v/v, (4 mL) was stirred using the Dean-Stark trap at 115 °C for 4h under nitrogen atmosphere. The solution was then concentrated and compound **7** (0.3 mL, 1.97 mmol, 8.5 eq.), tetrabutylammonium bromide (TBAB, 0.16 g, 0.49 mmol, 2.1 eq.) and dry THF (6 mL) were added. After stirring at 70 °C for 4 h, the reaction was cooled to room temperature and quenched with methanol and the reaction mixture was concentrated *in-vacuo*. The residue was purified through a classical column chromatography to give white solid (0.19 g, 0.19 mmol, 80 %).

$R_f = 0.27$, (EtOAc)

$[\alpha]_D^{22} = -19.4$ (c 0.01, MeOH)

$^1\text{H NMR}$ (300 MHz, CDCl_3): δ (ppm) 7.79 – 7.77 (m, 4H), 7.66 – 7.65 (m, 4H), 7.40 – 7.37 (m, 12H), 6.03 (d, $J = 8.3$ Hz, 1H), 4.73 (d, $J = 8.3$ Hz, 1H), 4.52 (d, $J = 7.8$ Hz, 1H), 4.43 – 4.10 (m, 5H), 4.05 – 3.77 (m, 7H), 3.67 (d, $J = 8.8$ Hz, 1H), 3.55 (t, $J = 6.6$ Hz, 1H), 3.47 – 3.38 (m, 1H), 3.22 (dd, $J = 9.5, 3.1$ Hz, 1H), 2.42 (t, $J = 2.4$ Hz, 1H), 1.97 (s, 3H), 1.47 (s, 9H), 1.04 (s, 18H)

¹³C NMR (75 MHz, CDCl₃): δ (ppm) 171.6, 170.9, 136.0, 135.7, 135.7, 135.6, 133.8, 133.1, 133.1, 133.0, 129.9, 129.9, 129.7, 129.6, 127.9, 127.8, 127.8, 127.6, 103.9, 98.3, 84.4, 83.1, 80.1, 79.1, 75.0, 74.8, 72.0, 69.9, 67.8, 65.4, 62.4, 62.0, 56.1, 55.1, 28.1, 26.9, 23.7, 19.4, 19.2

ESI-HRMS: *m/z* calcd. for C₅₅H₇₃NO₁₃Si₂ [M+H]⁺., 1012.4693; found 1012.4679
[M+H]⁺

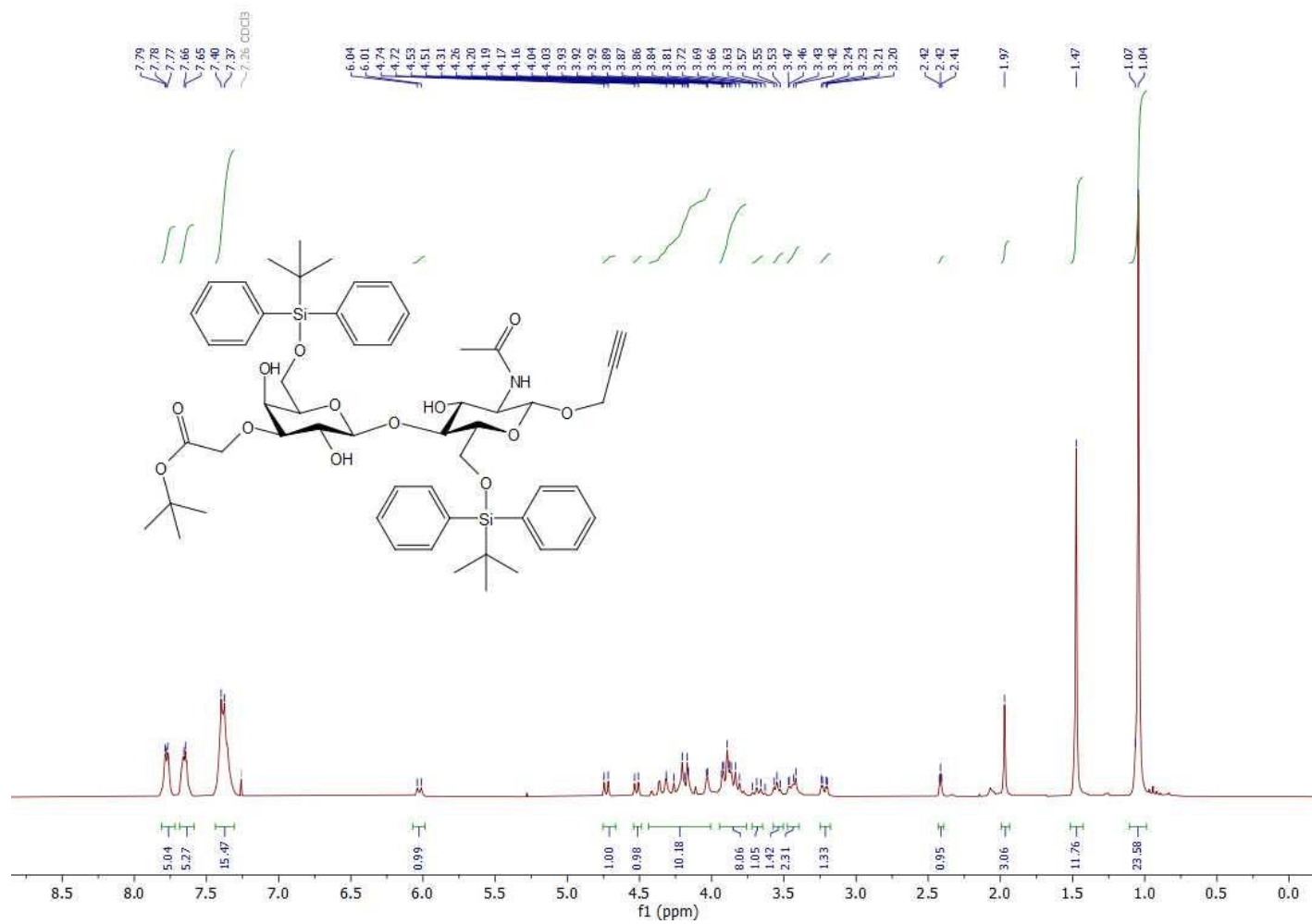


Figure 6.45 ^1H NMR (300 MHz, CDCl_3) spectrum of compound 3.39.

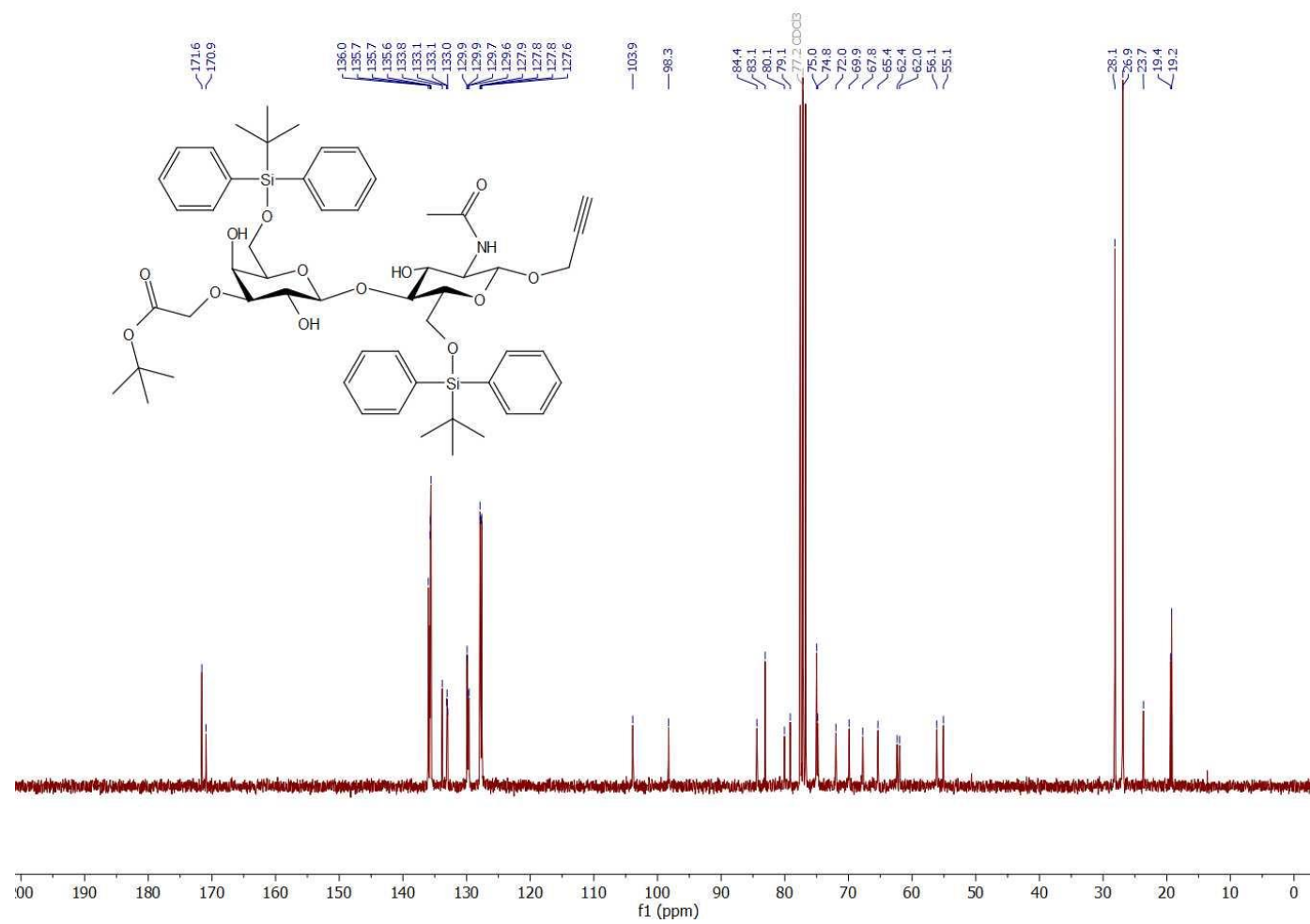
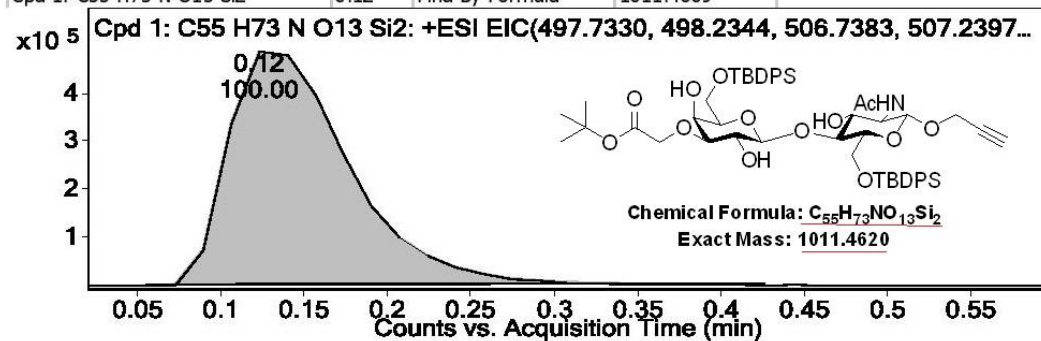


Figure 6.46 ^{13}C NMR (75 MHz, CDCl_3) spectrum of compound 3.39.

Compound Table

Compound Label	RT	Mass	Abund	Formula	Tgt Mass	Diff (ppm)
Cpd 1: C ₅₅ H ₇₃ N O ₁₃ Si ₂	0.12	1011.4609	29823	<u>C₅₅H₇₃N O₁₃Si₂</u>	<u>1011.462</u>	-1.14

Compound Label	RT	Algorithm	Mass
Cpd 1: C ₅₅ H ₇₃ N O ₁₃ Si ₂	0.12	Find By Formula	1011.4609



MS Spectrum

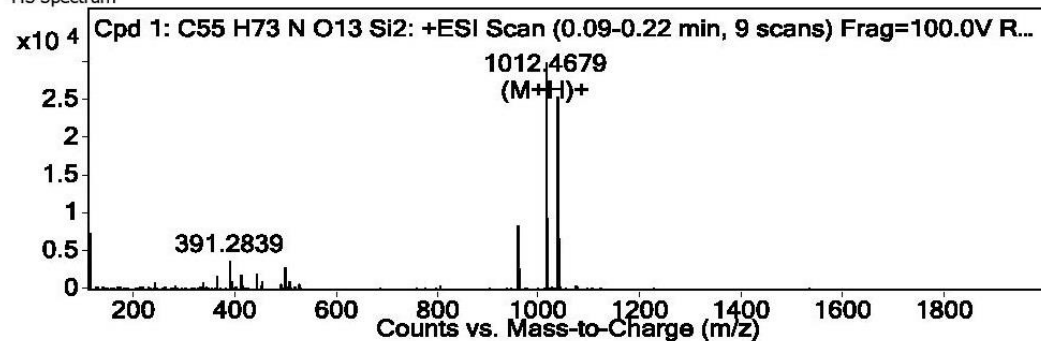
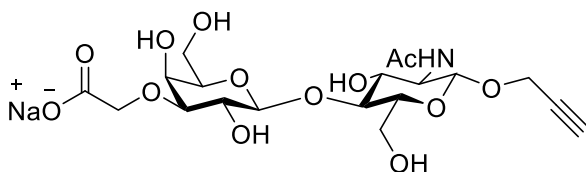


Figure 6.47 HRMS spectrum of compound 3.39.

Propargyl (3-*O*-carboxymethyl- β -D-galactopyranosyl)-(1 \rightarrow 4)-2-*N*-acetamido-2-deoxy- β -D-glucopyranoside sodium salt (**3.40**).



To a solution of compound **3.39** (0.15 g, 0.15 mmol) in DCM (2 mL) was added trifluoroacetic acid (TFA, 2 mL) at 0 °C and the reaction mixture was stirred at room temperature for 30 min. After removal of solvent *in-vacuo*, the general procedure D was applied to give white solid (0.064 g, 0.126 mmol, 85 %).

$R_f = 0.15$, (EtOAc/*i*PrOH/H₂O : 6/5.5/2.5)

$[\alpha]_D^{22} = -9.0$ (c 0.003, H₂O)

¹H NMR (600 MHz, D₂O): δ (ppm) 4.75 (d, $J = 7.7$ Hz, 1H), 4.52 (d, $J = 7.9$ Hz, 1H), 4.42 (s, 2H), 4.10 (d, $J = 3.8$ Hz, 1H), 4.09 (s, 2H), 4.00 (dd, $J = 12.4, 2.3$ Hz, 1H), 3.86 (dd, $J = 12.4, 5.0$ Hz, 1H), 3.83 – 3.73 (m, 5H), 3.71 (dd, $J = 8.1, 3.5$ Hz, 1H), 3.65 (dd, $J = 9.8, 7.9$ Hz, 1H), 3.63 – 3.61 (m, 1H), 3.51 (dd, $J = 9.8, 3.2$ Hz, 1H), 2.05 (s, 3H)

¹³C NMR (150 MHz, D₂O): δ (ppm) 181.5, 174.8, 102.8, 99.5, 81.8, 78.2, 75.1, 74.9, 72.4, 69.9, 68.5, 65.4, 61.1, 60.0, 56.8, 54.9, 23.3

ESI-HRMS: m/z calcd. for C₁₉H₂₉NO₁₃ [M+Na]⁺, 502.1531; found 502.1524 [M+Na]⁺

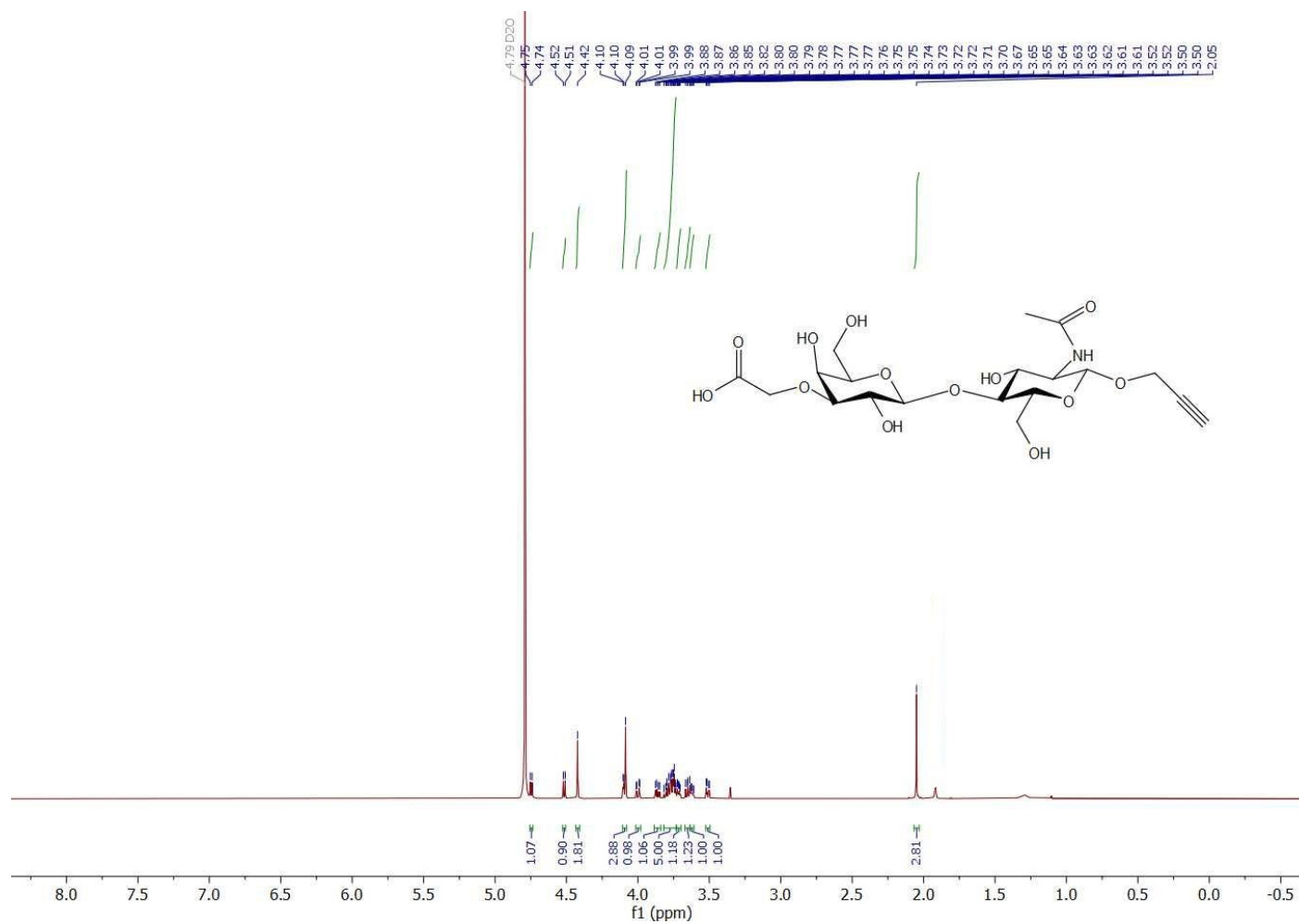


Figure 6.48 ^1H NMR (600 MHz, D_2O) spectrum of compound 3.40.

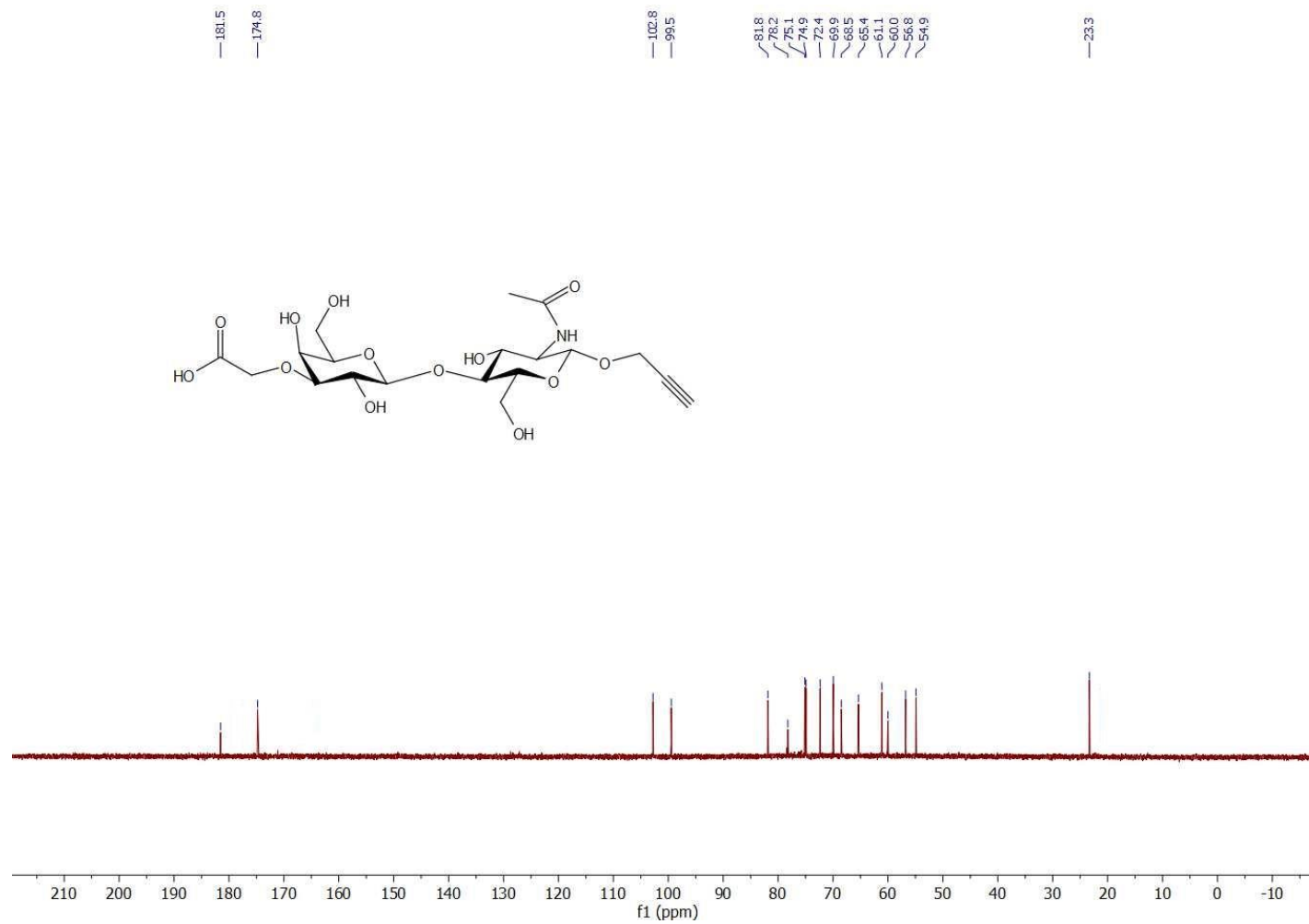
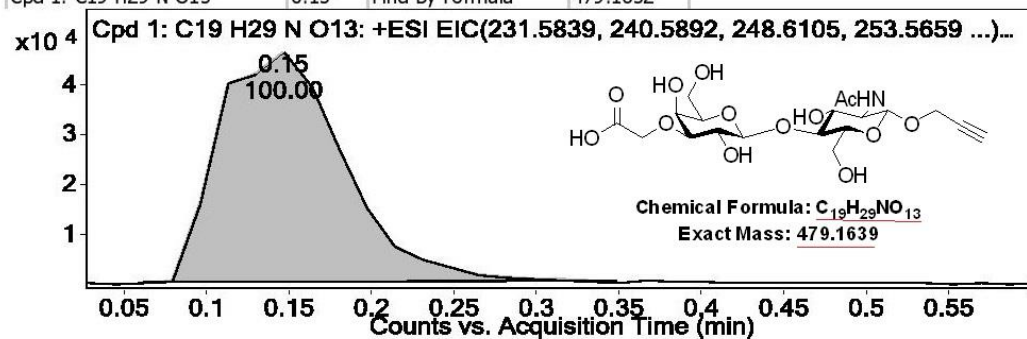


Figure 6.49 ^{13}C NMR (150 MHz, D_2O) spectrum of compound 3.40.

Compound Table

Compound Label	RT	Mass	Abund	Formula	Tgt Mass	Diff (ppm)
Cpd 1: C19 H29 N O13	0.15	479.1632	8937	C19 H29 N O13	479.1639	-1.47

Compound Label	RT	Algorithm	Mass
Cpd 1: C19 H29 N O13	0.15	Find By Formula	479.1632



MS Spectrum

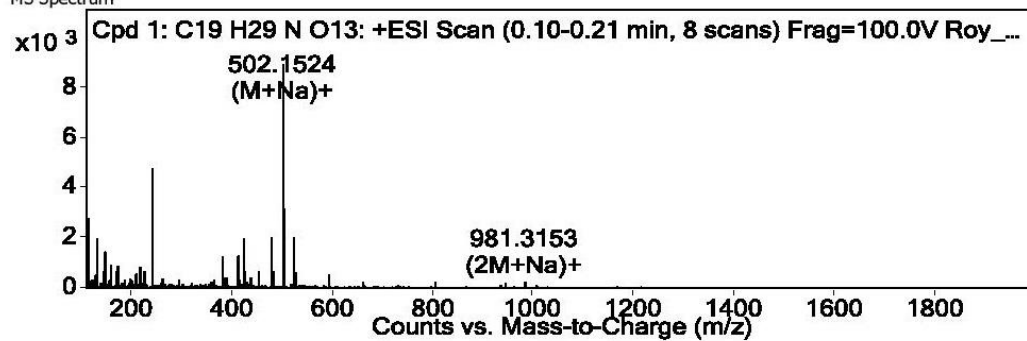
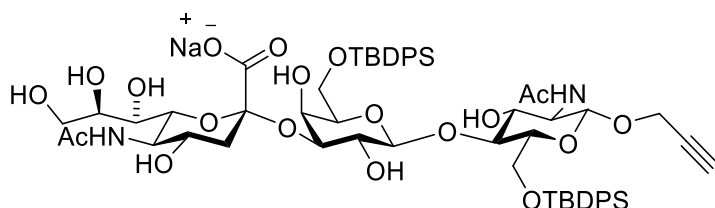


Figure 6.50 HRMS spectrum of compound 3.40.

Propargyl (5-*N*-acetamido-3,5-dideoxy- α -D-galacto-2-nonulopyranosylonic acid)-(2 \rightarrow 3)-(6-*O*-*tert*-butyldiphenylsilyl- β -D-galactopyranosyl)-(1 \rightarrow 4)-2-*N*-acetamido-2-deoxy-6-*O*-*tert*-butyldiphenylsilyl- β -D-glucopyranoside sodium salt (**3.41**).



A solution of lactoside acceptor **3.34** (0.19 g, 0.22 mmol, 1 eq.), sialyl donor **3.36** (0.2 g, 0.41 mmol, 1.8 eq.), and pulverized activated 4Å MS (0.45 g) in dry DCM/MeCN (1.5/1 : v/v, 6 mL) was stirred under nitrogen at room temperature for 0.5 h. The reaction mixture was cooled to -78 °C followed by successive addition of NIS (0.11 g, 0.47 mmol, 2.20 eq.) and TfOH (0.01 mL, 0.09 mmol, 0.41 eq.). After stirring for 7 h at -45 °C, the reaction was quenched by addition of Hunig's base (0.2 mL). The reaction mixture was filtered through a pad of celite, diluted in DCM (25 mL) washed with Na₂S₂O₃ (25 %, 20 mL), Brine solution (20 mL), dried over Na₂SO₄ and concentrated *in-vacuo*. The residue was dissolved in THF/H₂O (3/1 : v/v, 10 mL) and NaOH (1M, 2.5 mL) was added and stirred for 3 h. Amberlite IR 120 H⁺ was added and the reaction mixture was additionally stirred for another 0.5 h. After chromatographic purification compound **3.41** (0.08 g, 0.07 mmol, 32 %) as a white solid.

R_f = 0.1, (EtOAc/MeOH: 8/2)

[α]_D²² = -18.7 (c 0.003, MeOH)

¹H NMR (600 MHz, CD₃OD): δ (ppm) 7.78 – 7.72 (m, 4H), 7.68 – 7.65 (m, 4H), 7.47 – 7.32 (m, 12H), 4.62 (d, *J* = 7.8 Hz, 1H), 4.60 (d, *J* = 8.4 Hz, 1H), 4.32 (dd, *J* = 15.7, 2.5 Hz, 1H), 4.24 (dd, *J* = 15.7, 2.4 Hz, 1H), 4.16 (dd, *J* = 11.5, 3.8 Hz, 1H), 4.08 – 3.96 (m, 3H), 3.87 (t, *J* = 9.2 Hz, 1H), 3.85 – 3.56 (m, 14H), 3.48 (ddd, *J* = 9.7, 3.8, 1.8 Hz, 1H), 2.87 – 2.85 (m, 2H), 2.02 (s, 3H), 1.94 (s, 3H), 1.84 (t, *J* = 11.5 Hz, 1H), 1.04 (s, 9H), 1.02 (s, 9H)

¹³C NMR (150 MHz, CD₃OD): δ (ppm) 175.6, 175.2, 173.5, 137.0, 136.7, 134.8, 134.5, 134.4, 130.8, 130.7, 128.9, 128.8, 128.8, 128.6, 103.8, 100.1, 79.8, 79.5, 77.6, 76.5, 76.5, 76.3, 75.0, 73.6, 72.5, 71.1, 69.4, 69.4, 68.7, 64.1, 63.9, 63.7, 56.3, 56.1, 54.0, 27.5, 27.4, 23.0, 22.7, 20.2, 19.9

ESI-HRMS: *m/z* calcd. for C₆₀H₈₀N₂O₁₉Si₂ [M+Na]⁺., 1211.4786; found 1211.4787
[M+Na]⁺

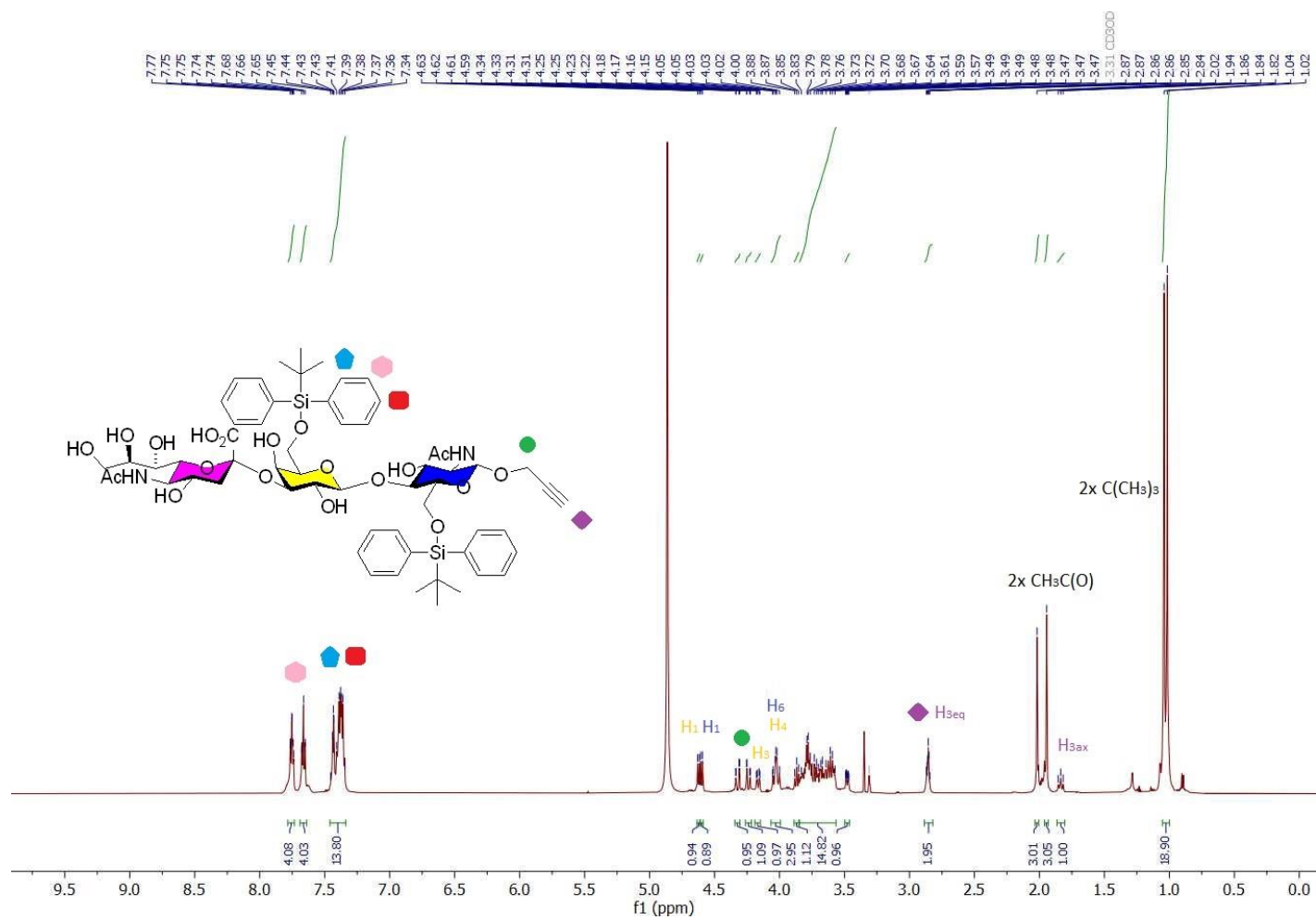


Figure 6.51 ^1H NMR (600 MHz, CD_3OD) spectrum of compound 3.41.

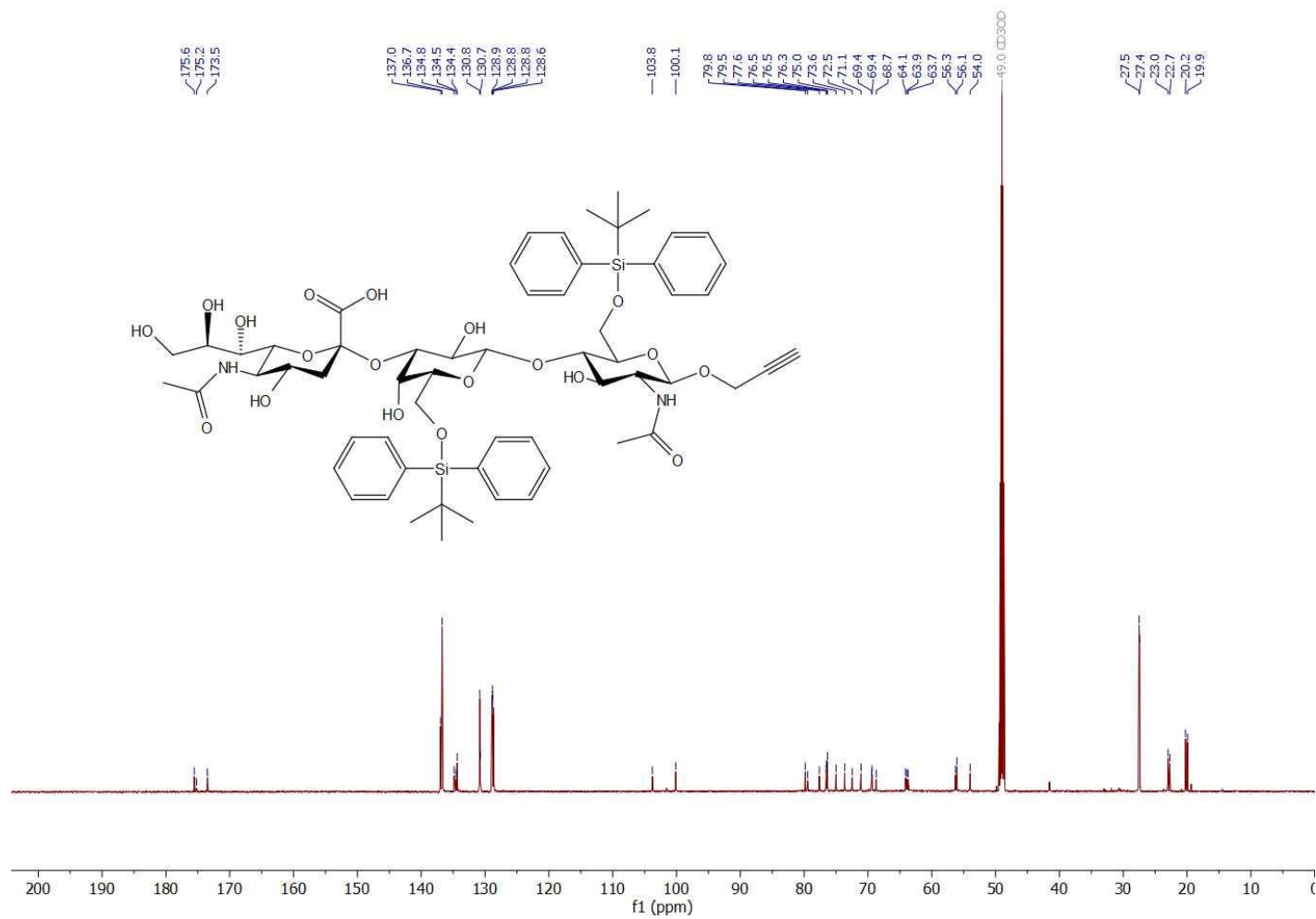
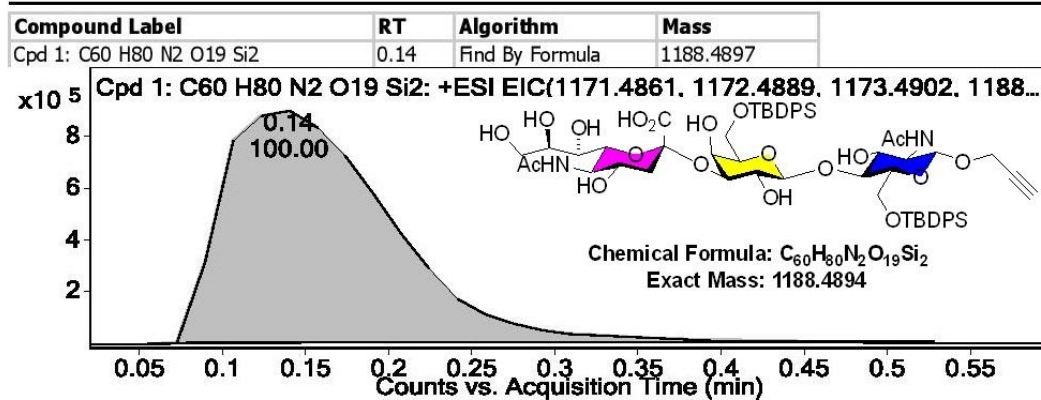


Figure 6.52 ^{13}C NMR (150 MHz, CD_3OD) spectrum of compound 3.41.

Compound Table

Compound Label	RT	Mass	Abund	Formula	Tgt Mass	Diff (ppm)
Cpd 1: C60 H80 N2 O19 Si2	0.14	<u>1188.4897</u>	50099	<u>C60 H80 N2 O19 Si2</u>	<u>1188.4894</u>	0.3



MS Spectrum

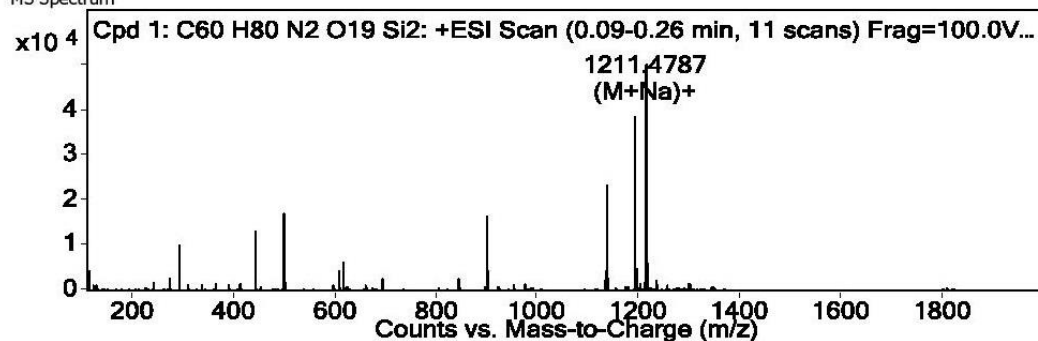
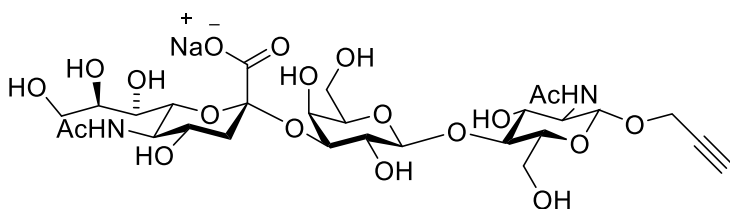


Figure 6.53 HRMS spectrum of compound 3.41.

Propargyl (5-*N*-acetamido-3,5-dideoxy- α -D-galacto-2-nonulopyranosylonic acid)-(2 \rightarrow 3)-(β -D-galactopyranosyl)-(1 \rightarrow 4)-2-*N*-acetamido-2-deoxy- β -D-glucopyranoside sodium salt (**3.42**).



Following the general procedure D, the desilylated residue was dissolved in MeOH/H₂O (1/1 : v/v, 4 mL) and LiOH (2M, 0.1 mL) was added. After 2 h of stirring, silica gel was added and the reaction mixture was subjected to the column chromatography to give white solid (0.03 g, 0.04 mmol, 73 %).

$R_f = 0.59$, (EtOAc/^{*i*}PrOH/H₂O : 5/6/3)

$[\alpha]_D^{22} = -14.6$ (c 0.005, H₂O)

¹H NMR (300 MHz, D₂O): δ (ppm) 4.74 (d, $J = 7.9$ Hz, 1H), 4.56 (d, $J = 7.8$ Hz, 1H), 4.42 (d, $J = 2.4$ Hz, 2H), 4.12 (dd, $J = 9.9, 3.1$ Hz, 1H), 4.06 – 3.93 (m, 2H), 3.96 – 3.80 (m, 4H), 3.78 – 3.49 (m, 12H), 2.92 (t, $J = 2.4$ Hz, 1H), 2.76 (dd, $J = 12.4, 4.6$ Hz, 1H), 2.05 (s, 3H), 2.04 (s, 3H), 1.81 (t, $J = 12.1$ Hz, 1H)

¹³C NMR (75 MHz, D₂O): δ (ppm) 175.0, 174.7, 173.9, 102.5, 99.8, 99.4, 78.7, 78.1, 76.1, 75.4, 75.2, 74.9, 72.9, 72.3, 71.7, 69.4, 68.3, 68.1, 67.5, 62.6, 61.0, 59.9, 56.7, 54.8, 51.7, 39.6, 22.2, 22.0

ESI-HRMS: m/z calcd. for C₁₉H₂₉NO₁₃ [M+Na]⁺, 502.1531; found 502.1524 [M+Na]⁺

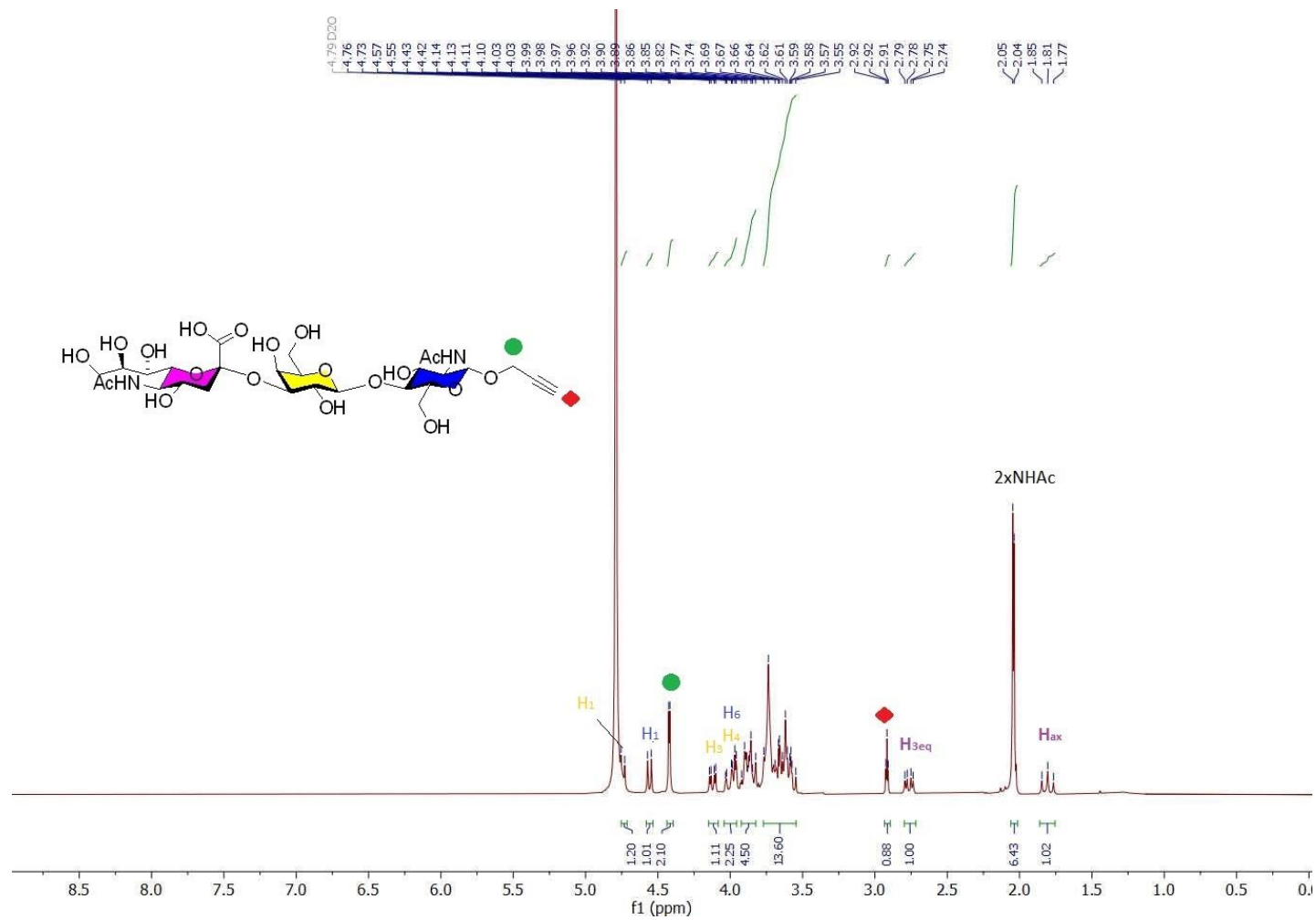


Figure 6.54 ¹H NMR (300 MHz, D₂O) spectrum of compound 3.42.

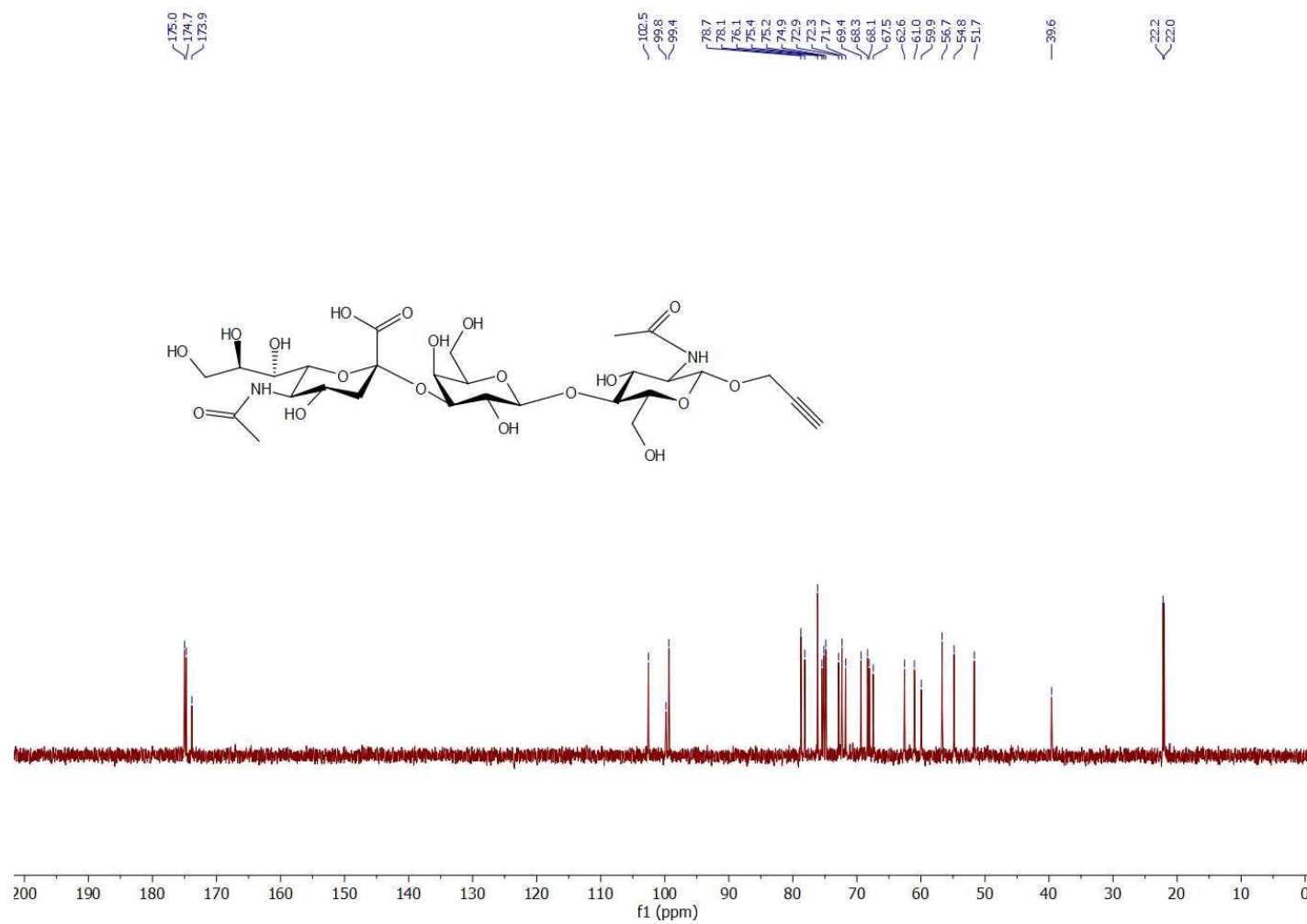


Figure 6.55 ^{13}C NMR (75 MHz, D_2O) spectrum of compound 3.42.

Compound Table

Compound Label	RT	Mass	Abund	Formula	Tgt Mass	Diff (ppm)
Cpd 2: C17 H27 N O11	0.16	421.1585	15515	C17 H27 N O11	421.1584	0.3
Cpd 1: C28 H44 N2 O19	0.16	<u>712.2538</u>	6804	<u>C28 H44 N2 O19</u>	<u>712.2538</u>	-0.06

Compound Label	RT	Algorithm	Mass
Cpd 2: C17 H27 N O11	0.16	Find By Formula	421.1585

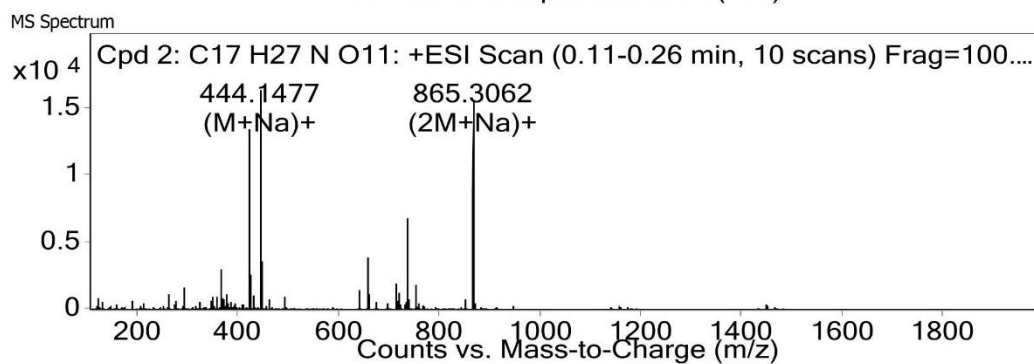
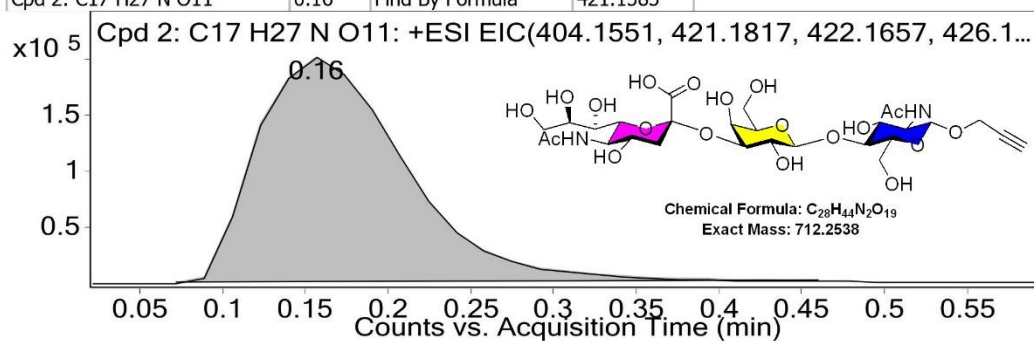
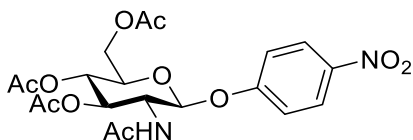


Figure 6.56 HRMS spectrum of compound 3.42.

4-Nitrophenyl-3,4,6-tri-*O*-acetyl-2-*N*-acetamido-2-deoxy- β -D-glucopyranoside (**3.44**).



To a solution of **3.43** (0.98 g, 2.52 mmol 1 eq.) in DCM/AcCl (v/v:1/1; 60 mL) was added dry methanol (6 mL) at -10 °C. The reaction mixture was kept sealed for 36h at room temperature without stirring. After evaporating solvent, the residue and TBAHS (0.85 g, 2.52 mmol, 1eq.) were dissolved in dry DCM (25 mL). A solution of *para*-nitrophenol (0.87 g, 6.29 mmol, 2.5 eq.) in 1M NaOH (25 mL) was added and resulted mixture stirred at room temperature for 5 h. The reaction mixture was then diluted in DCM (50 mL), washed with 1M NaOH (2 x 50 mL), brine (50 mL), dried over Na₂SO₄ and concentrated *in-vacuo*. Recrystallization from EtOAc/hexane afforded **3.44** (0.72 g, 1.53 mmol, 61 %) as white solid.

¹H NMR (300 MHz, CDCl₃): δ (ppm) 8.18 (d, $J = 9.2$ Hz, 2H), 7.06 (d, $J = 9.2$ Hz, 2H), 5.64 (d, $J = 8.5$ Hz, 1H), 5.51 – 5.39 (m, 2H), 5.14 (t, $J = 9.5$ Hz, 1H), 4.28 (dd, $J = 12.3, 5.6$ Hz, 1H), 4.22 – 4.02 (m, 2H), 3.99 – 3.87 (m, 1H), 2.07 (s, 6H), 2.06 (s, 3H), 1.95 (s, 3H)

¹³C NMR (75 MHz, CDCl₃): δ (ppm) 170.9, 170.6, 170.6, 169.5, 161.6, 143.3, 125.9, 116.7, 98.1, 72.6, 71.7, 68.4, 62.2, 55.0, 23.5, 20.8, 20.8, 20.8

The spectroscopic data agreed well with those of the literature.⁵⁶⁴

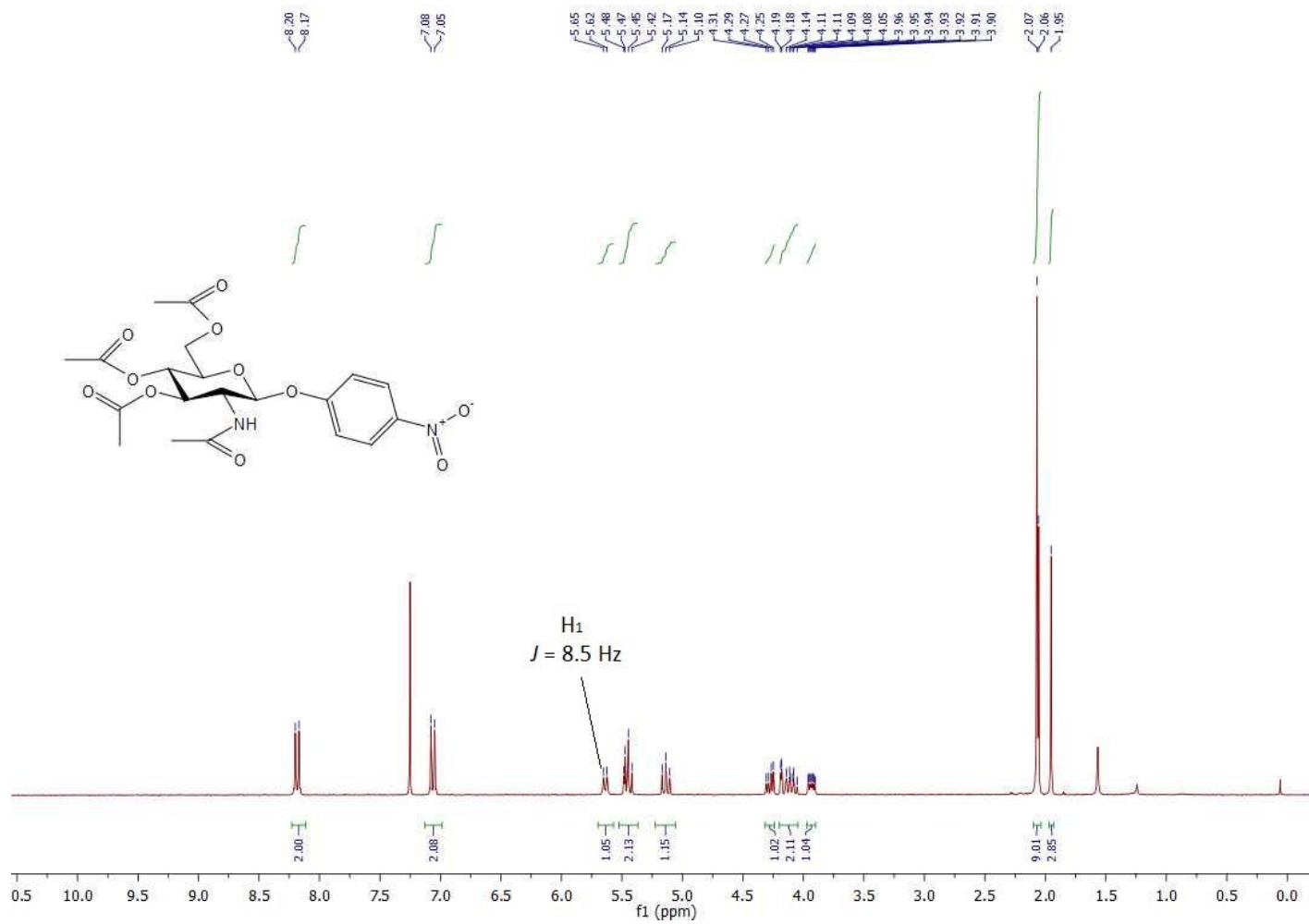


Figure 6.57 ^1H NMR (300 MHz, CDCl_3) spectrum of compound 3.44.

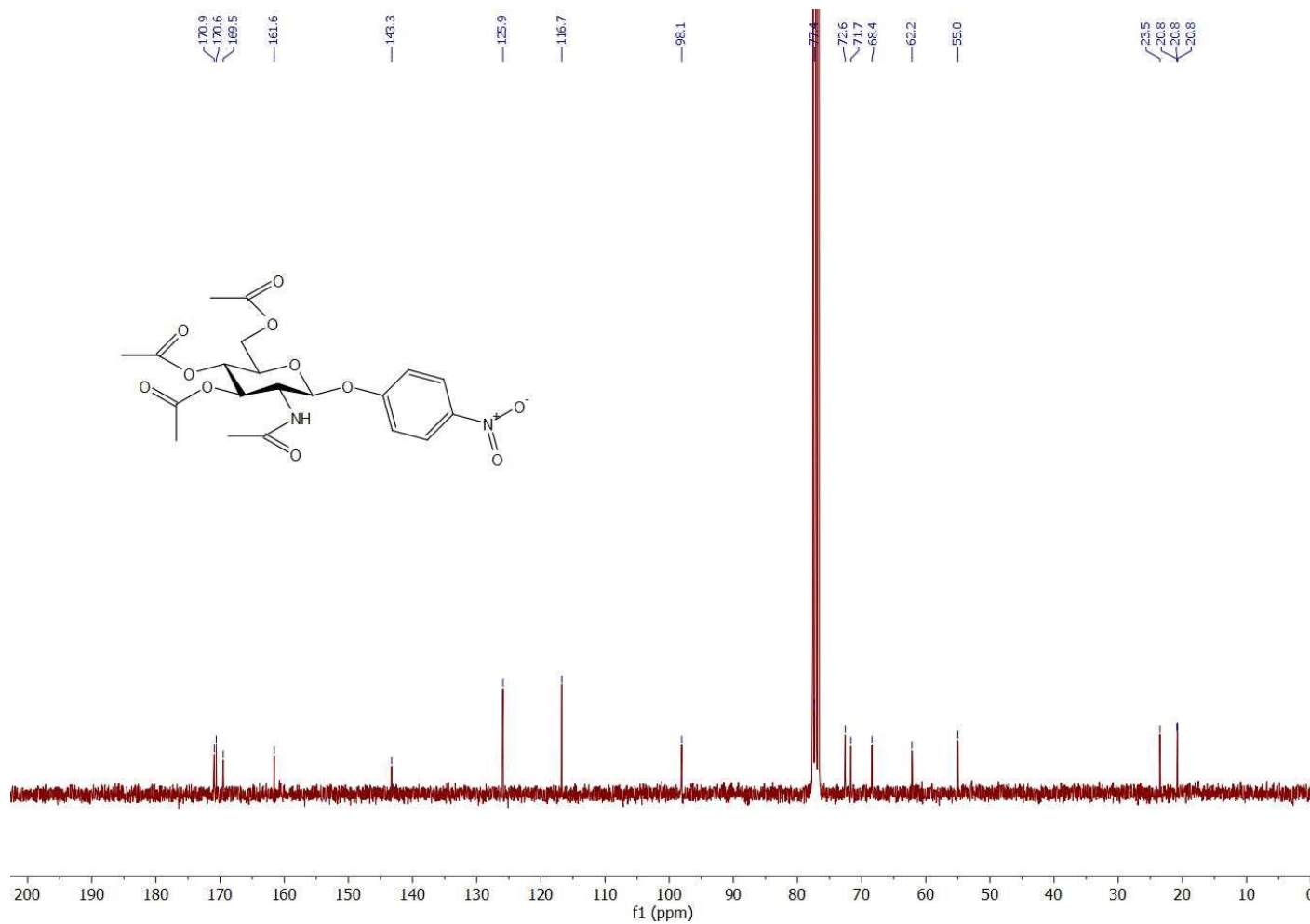
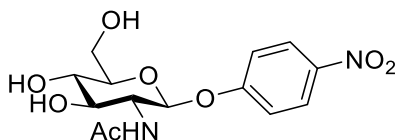


Figure 6.58 ^{13}C NMR (75 MHz, CDCl_3) spectrum of compound 3.44.

4-Nitrophenyl-2-*N*-acetamido-2-deoxy- β -D-glucopyranoside (**3.45**).



Following the general procedure B, compound **3.45** was obtained as a white solid (0.46 g, 1.33 mmol, 97 %) without further purification.

¹H NMR (300 MHz, CD₃OD): δ (ppm) 8.21 (d, $J = 9.2$ Hz, 2H), 7.18 (d, $J = 9.3$ Hz, 2H), 5.21 (d, $J = 8.4$ Hz, 1H), 4.01 – 3.87 (m, 2H), 3.72 (dd, $J = 12.1, 5.6$ Hz, 1H), 3.60 (dd, $J = 10.3, 8.6$ Hz, 1H), 3.56 – 3.46 (m, 1H), 3.49 – 3.37 (m, 1H), 1.98 (s, 3H)

¹³C NMR (75 MHz, CD₃OD): δ (ppm) 173.9, 163.7, 144.0, 126.6, 117.7, 100.0, 78.5, 75.7, 71.7, 62.5, 57.1, 22.9

The spectroscopic data agreed well with those of the literature.⁵⁶⁴

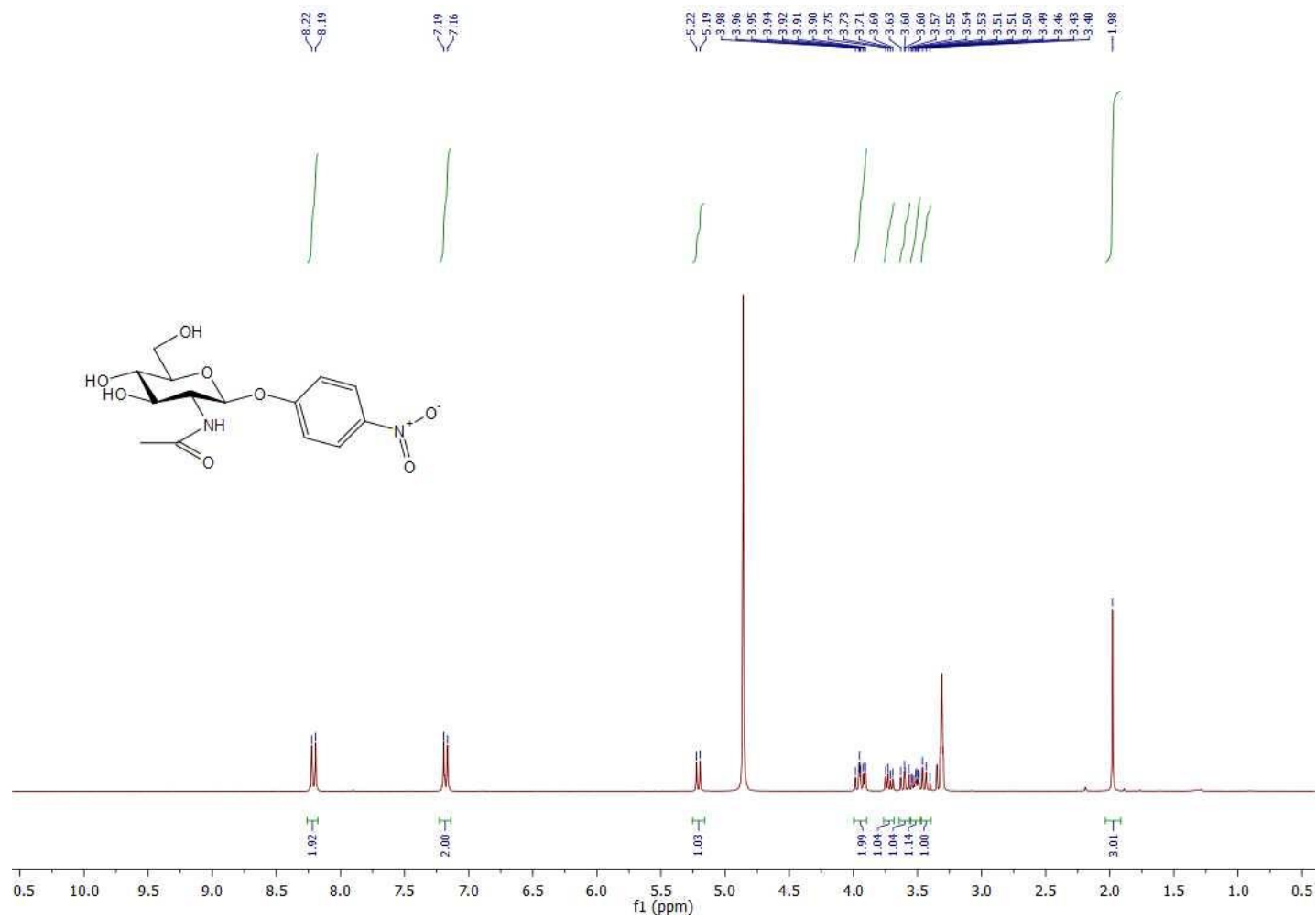


Figure 6.59 ¹H NMR (300 MHz, CD₃OD) spectrum of compound 3.45.

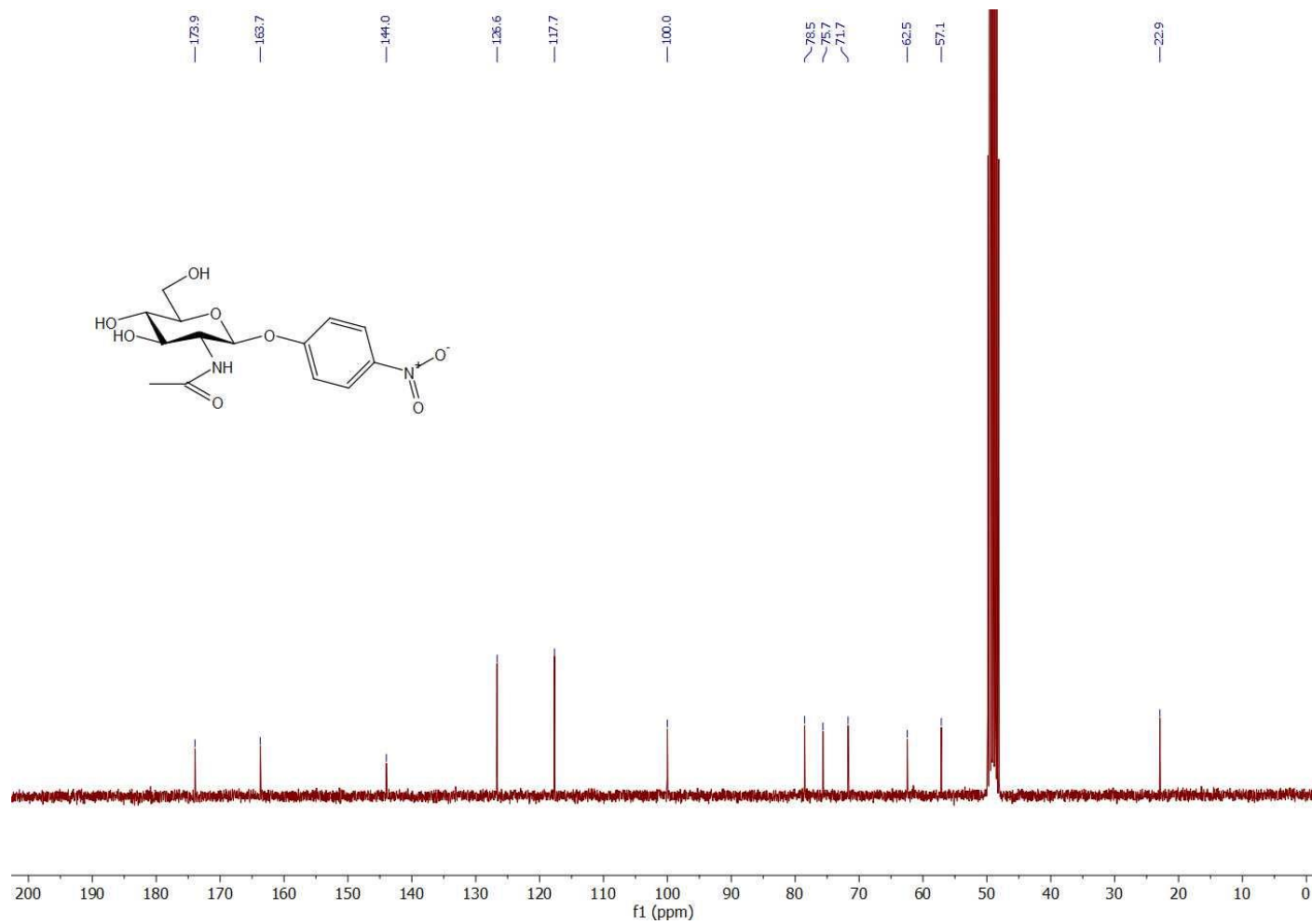
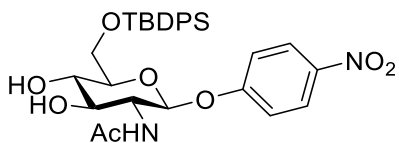


Figure 6.60 ^{13}C NMR (75 MHz, CD_3OD) spectrum of compound 3.45.

4-Nitrophenyl 2-*N*-acetamido-2-deoxy-6-*O*-*tert*-butyldiphenylsilyl- β -D-glucopyranoside (**3.46**).



Following the general procedure C, compound **3.46** was obtained as a white solid (0.73 g, 1.25 mmol, 91 %).

$R_f = 0.50$, (EtOAc).

$^1\text{H NMR}$ (300 MHz, CDCl_3): δ (ppm) 7.98 (d, $J = 9.1$ Hz, 2H), 7.66 – 7.55 (m, 4H), 7.44 – 7.28 (m, 2H), 7.31 – 7.18 (m, 4H), 7.03 (d, $J = 9.2$ Hz, 1H), 6.49 (brs, 1H), 5.20 (d, $J = 7.8$ Hz, 1H), 4.08 – 3.98 (m, 1H), 3.97 – 3.76 (m, 3H), 3.71 – 3.60 (m, 1H), 3.60 – 3.50 (m, 1H), 2.03 (s, 3H), 1.02 (s, 9H)

$^{13}\text{C NMR}$ (75 MHz, CDCl_3): δ (ppm) 172.9, 161.8, 142.7, 135.7, 135.6, 133.1, 132.9, 130.0, 130.0, 127.9, 127.8, 125.9, 116.6, 98.0, 76.9, 75.2, 71.6, 63.9, 56.8, 26.9, 23.6, 19.4

The spectroscopic data agreed well with those of the literature.⁵⁶⁵

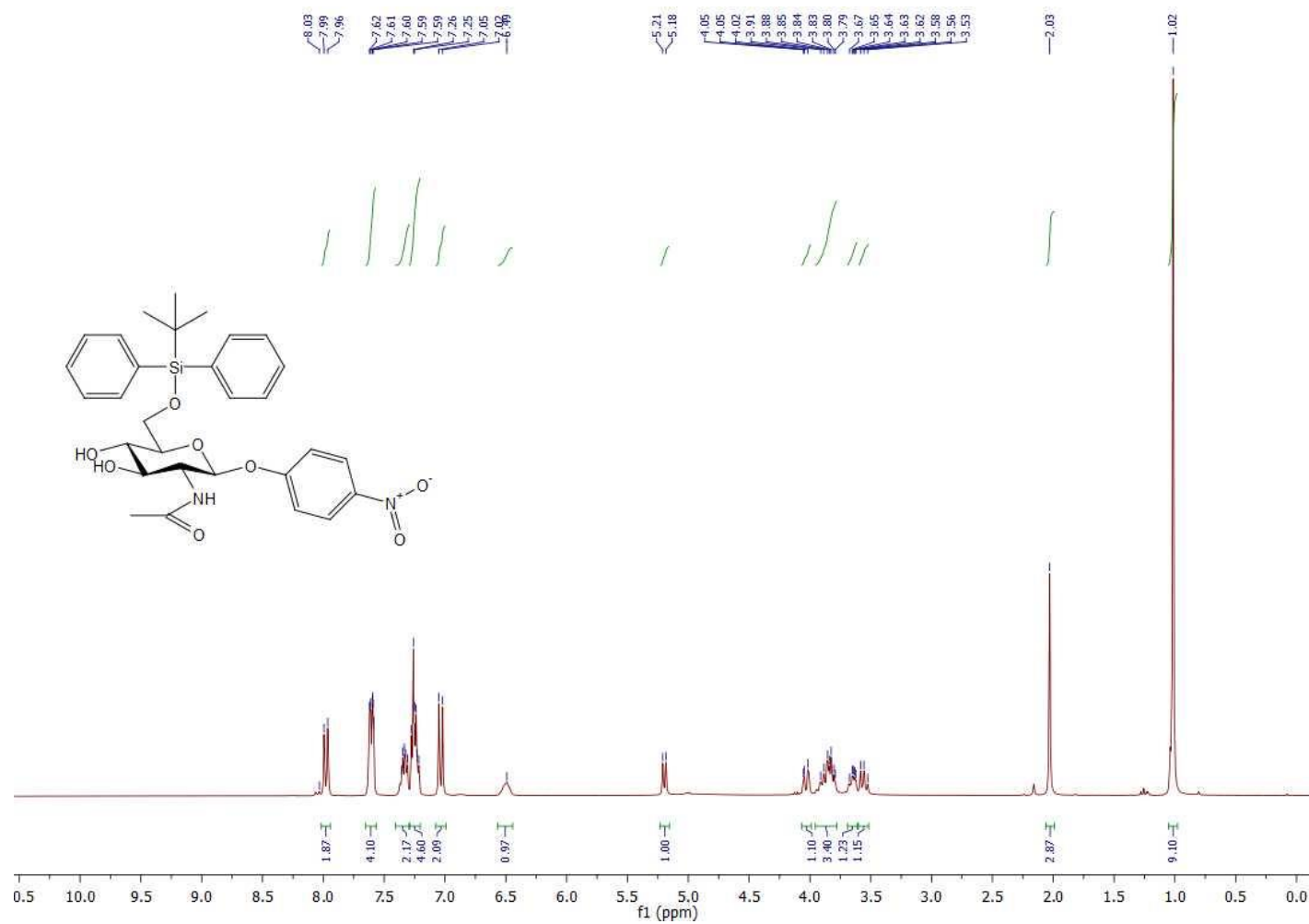


Figure 6.61 ^1H NMR (300 MHz, CDCl_3) spectrum of compound 3.46.

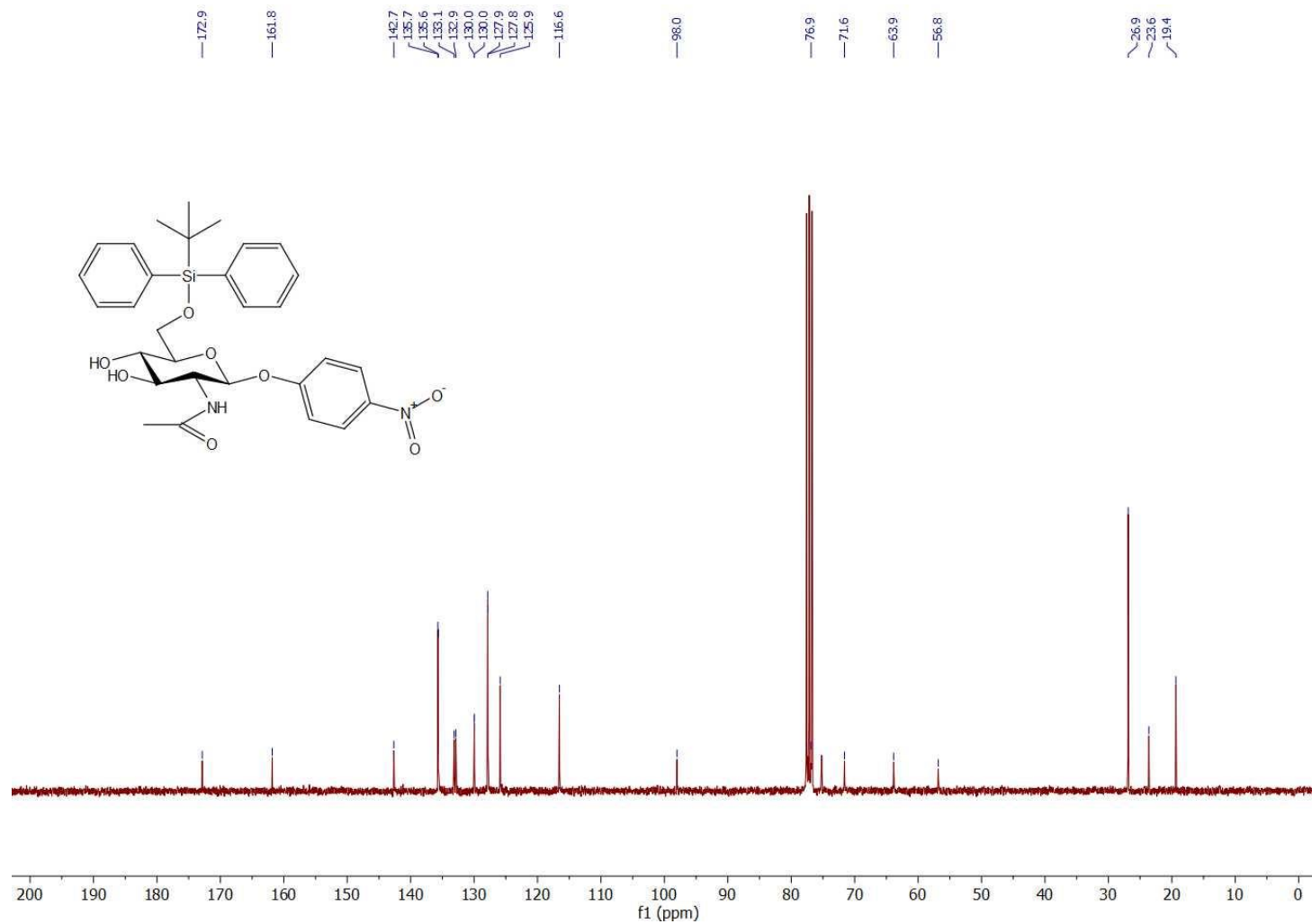
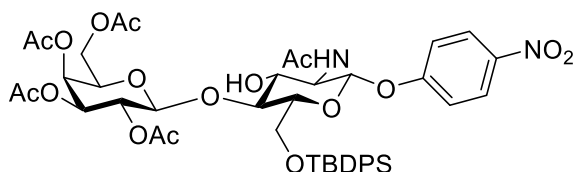


Figure 6.62 ^{13}C NMR (75 MHz, CDCl_3) spectrum of compound 3.46.

4-Nitrophenyl (2,3,4,6-tetra-*O*-acetyl- β -D-galactopyranosyl)-(1 \rightarrow 4)-2-*N*-acetamido-2-deoxy-6-*O*-*tert*-butyldiphenylsilyl- β -D-glucopyranoside (**3.48**).



A solution of glucoside acceptor **3.47** (1.46 g, 2.51 mmol, 1 eq.), galactoside donor **3.46** (2.22 g, 4.5 mmol, 1.79 eq.), and pulverized activated 4Å MS (750 mg) in dry DCM/THF (4/1 : v/v, 75 mL) was stirred under nitrogen at room temperature for 0.5 h. The reaction mixture was cooled to -35 °C followed by addition of BF₃·OEt₂ (0.49 mL, 3.97 mmol, 1.58 eq.). After stirring of 5 h, the reaction was quenched by addition of triethylamine (0.5 mL). The reaction mixture was filtered through a pad of celite and concentrated *in-vacuo*. After chromatographic purification compound **3.48** (0.87 g, 0.96 mmol, 38 %) was obtained as white solid.

R_f = 0.57, (EtOAc).

[α]_D²³ = -18.3 (c 0.01, Acetone)

¹H NMR (600 MHz, CDCl₃): δ (ppm) 8.10 (d, *J* = 9.2 Hz, 2H), 7.68 – 7.52 (m, 4H), 7.45 – 7.28 (m, 4H), 7.09 (t, *J* = 7.5 Hz, 2H), 7.05 (d, *J* = 9.2 Hz, 2H), 5.95 (d, *J* = 8.0 Hz, 1H), 5.53 (d, *J* = 8.1 Hz, 1H), 5.38 (dd, *J* = 3.4, 1.0 Hz, 1H), 5.20 (dd, *J* = 10.5, 8.0 Hz, 1H), 4.98 (dd, *J* = 10.5, 3.4 Hz, 1H), 4.71 (d, *J* = 8.0 Hz, 1H), 4.20 – 4.03 (m, 3H), 4.03 – 3.90 (m, 2H), 3.92 – 3.72 (m, 3H), 3.65 (d, *J* = 11.2 Hz, 1H), 2.15 (s, 3H), 2.06 (s, 3H), 2.01 (s, 3H), 1.98 (s, 3H), 1.69 (s, 3H), 1.02 (s, 9H)

¹³C NMR (150 MHz, CDCl₃): δ (ppm) 170.9, 170.5, 170.2, 170.0, 169.2, 162.0, 142.8, 135.8, 135.5, 133.2, 132.2, 130.1, 130.0, 127.9, 127.7, 125.8, 116.7, 101.2,

97.5, 79.9, 75.0, 71.5, 71.2, 70.8, 68.9, 67.0, 61.8, 61.4, 56.8, 26.9, 23.7, 20.7, 20.7,
20.6, 20.4, 19.4

ESI-HRMS: m/z calcd. for $C_{44}H_{55}N_2O_{17}Si$ $[M+Na]^+$, 933.3084; found 933.3085
 $[M+Na]^+$

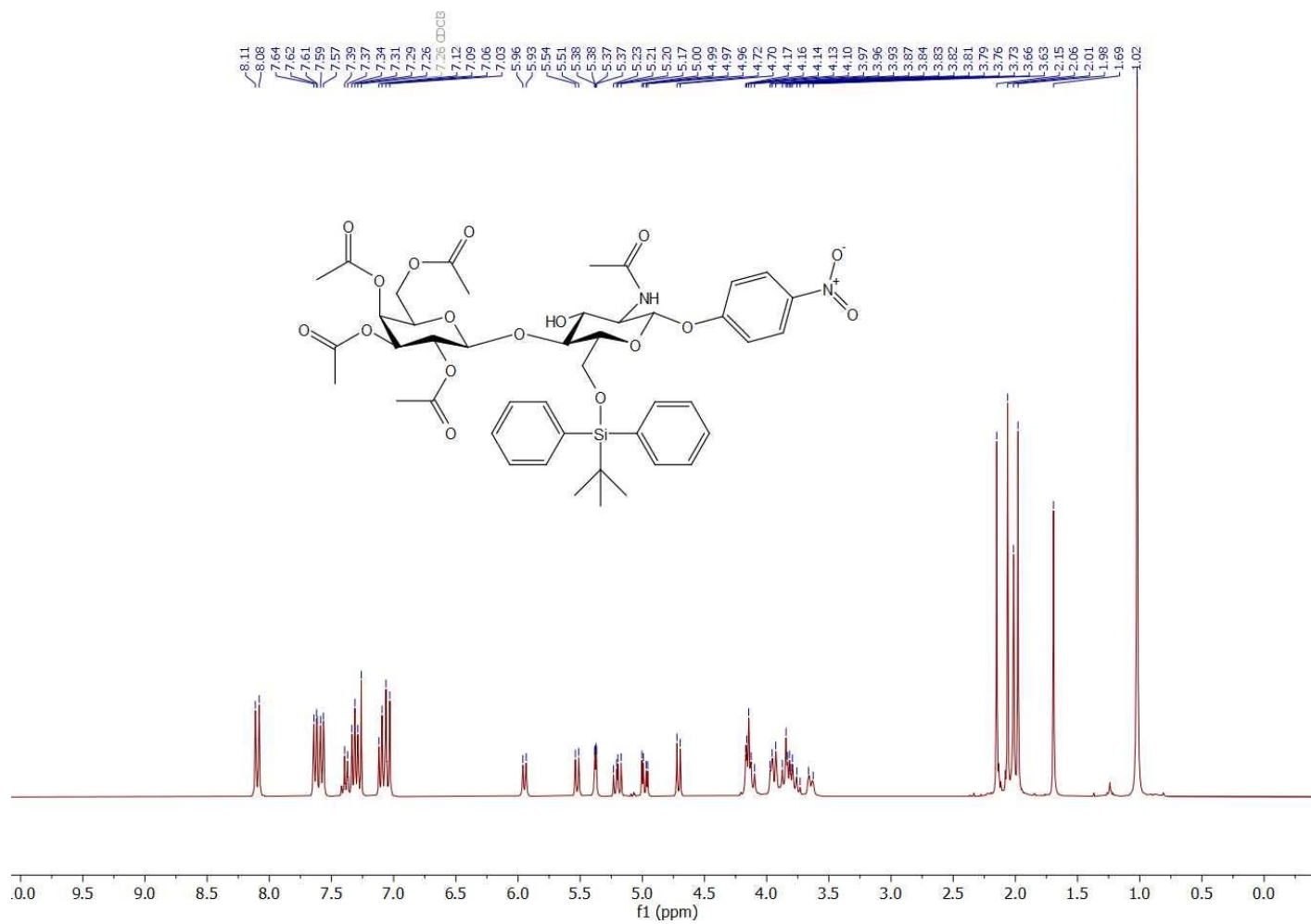


Figure 6.63 ¹H NMR (600 MHz, CDCl₃) spectrum of compound 3.48.

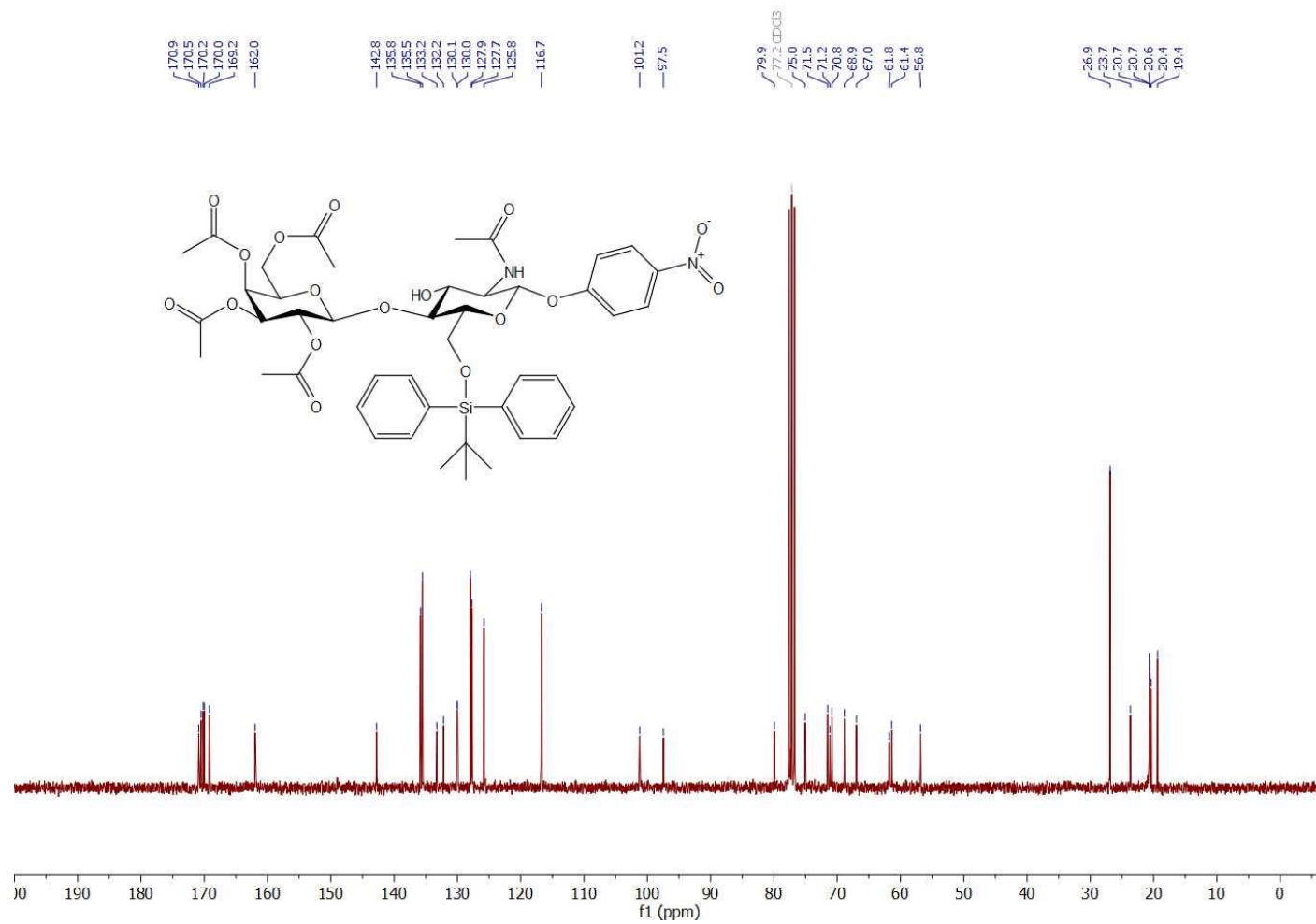
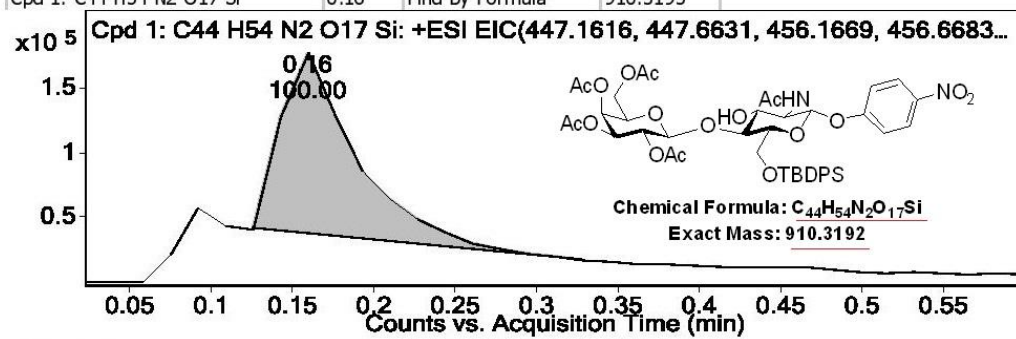


Figure 6.64 ¹³C NMR (150 MHz, CDCl₃) spectrum of compound 3.48.

Compound Table

Compound Label	RT	Mass	Abund	Formula	Tgt Mass	Diff (ppm)
Cpd 1: C ₄₄ H ₅₄ N ₂ O ₁₇ Si	0.16	<u>910.3193</u>	19801	<u>C₄₄ H₅₄ N₂ O₁₇ Si</u>	<u>910.3192</u>	0.09

Compound Label	RT	Algorithm	Mass
Cpd 1: C ₄₄ H ₅₄ N ₂ O ₁₇ Si	0.16	Find By Formula	910.3193



MS Spectrum

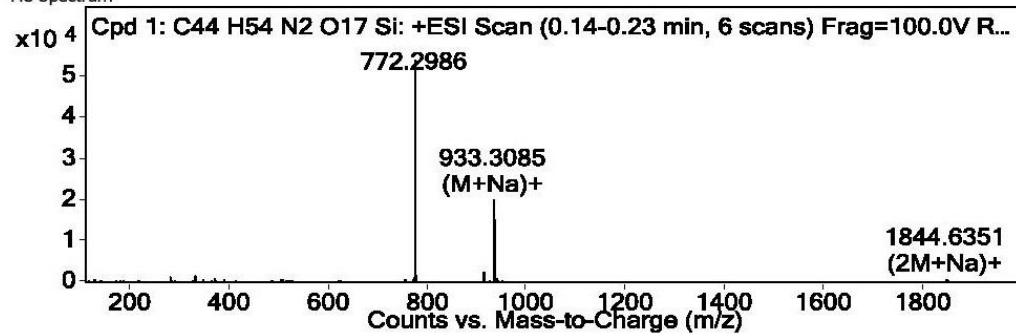
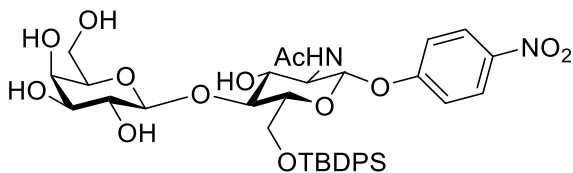


Figure 6.65 HRMS spectrum of compound 3.48.

4-Nitrophenyl (β -D-galactopyranosyl)-(1 \rightarrow 4)-2-*N*-acetamido-2-deoxy-6-*O*-*tert*-butyldiphenylsilyl- β -D-glucopyranoside (**3.49**).



Following the general procedure B, compound **3.49** was obtained as a white solid (0.34 g, 0.47 mmol, 97 %) without further purification.

$[\alpha]_{\text{D}}^{23} = -23.67$ (c 0.011, MeOH)

^1H NMR (300 MHz, CD_3OD): δ (ppm) 8.17 (d, $J = 8.9$ Hz, 2H), 7.73 (d, $J = 8.1$ Hz, 2H), 7.66 (d, $J = 7.4$ Hz, 2H), 7.42 – 7.23 (m, 4H), 7.19 (d, $J = 9.0$ Hz, 2H), 7.07 (t, $J = 7.5$ Hz, 2H), 5.29 (d, $J = 8.3$ Hz, 1H), 4.65 (d, $J = 7.6$ Hz, 1H), 4.30 (dd, $J = 11.7$, 3.3 Hz, 1H), 4.22 – 3.98 (m, 3H), 3.90 – 3.45 (m, 8H), 2.03 (s, 3H), 1.04 (s, 9H)

^{13}C NMR (75 MHz, CD_3OD): δ (ppm) 173.8, 163.5, 143.9, 136.9, 136.7, 134.9, 134.0, 130.7, 130.6, 128.7, 128.5, 126.7, 117.7, 104.8, 99.4, 78.9, 77.4, 77.0, 75.1, 73.8, 72.5, 70.4, 63.1, 62.7, 56.6, 27.3, 23.0, 20.2

ESI-HRMS: m/z calcd. for $\text{C}_{36}\text{H}_{46}\text{N}_2\text{O}_{13}\text{Si}$ $[\text{M}+\text{Na}]^+$, 765.2661; found 765.2646 $[\text{M}+\text{Na}]^+$

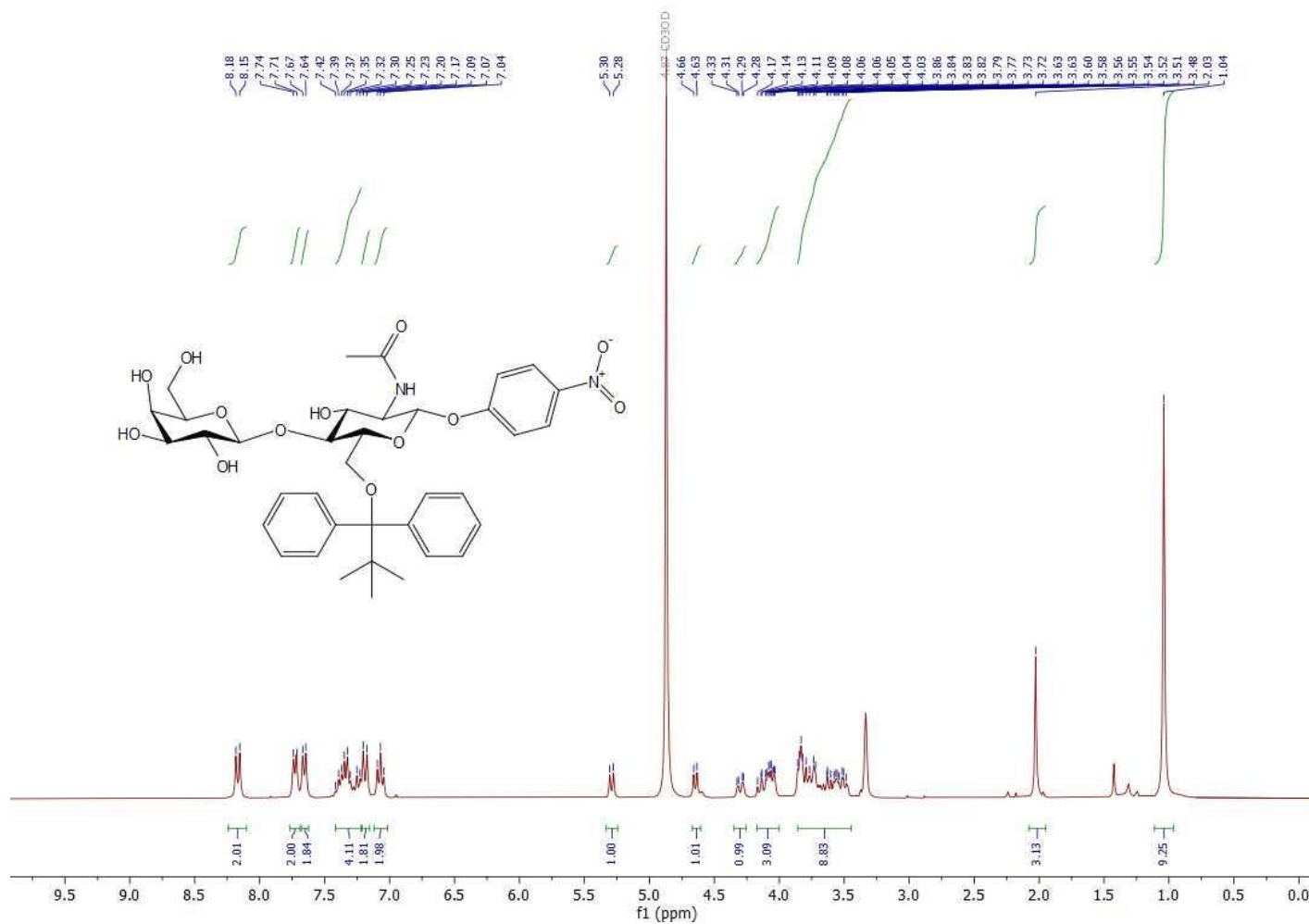


Figure 6.66 ^1H NMR (300 MHz, CD_3OD) spectrum of compound 3.49.

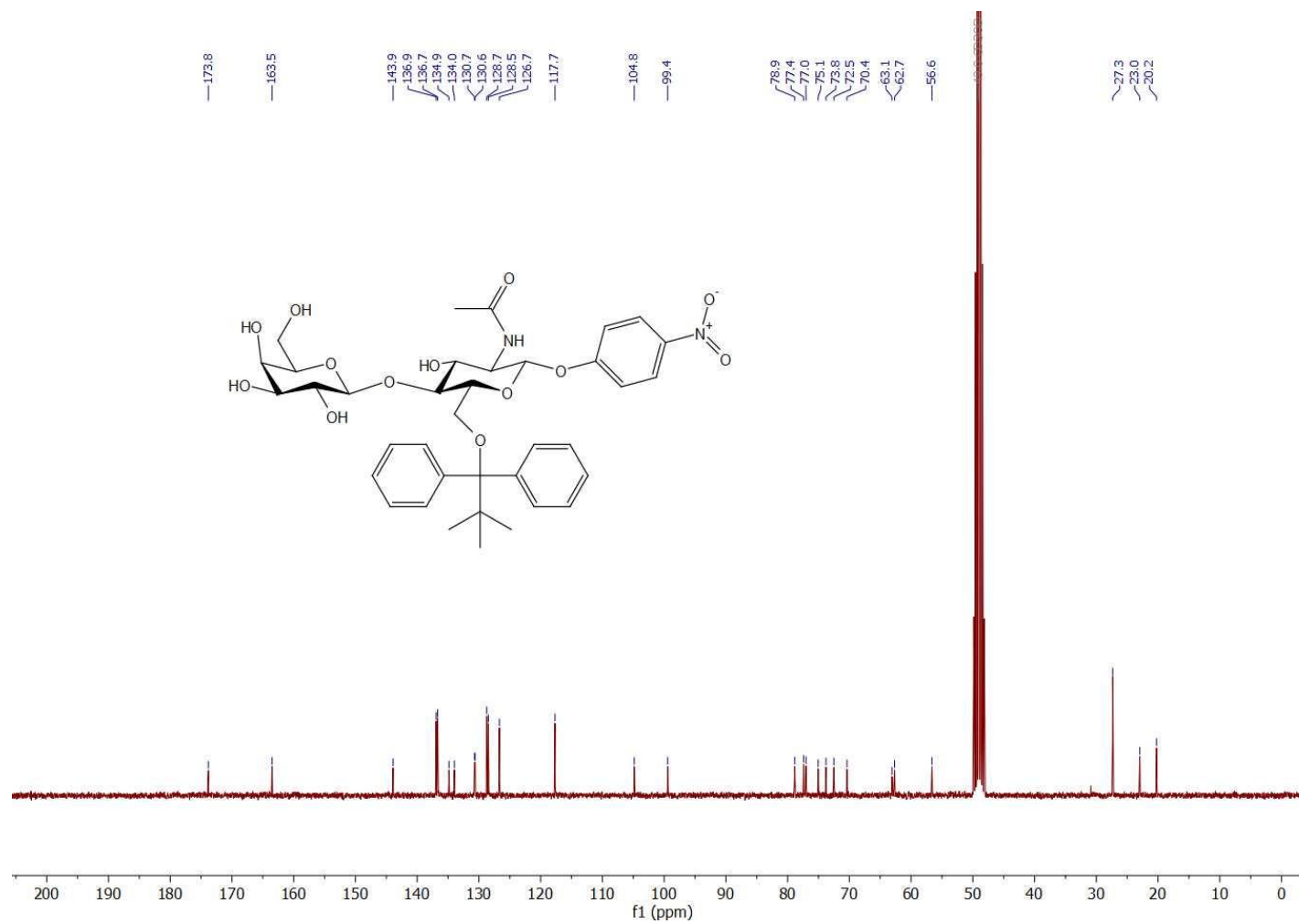
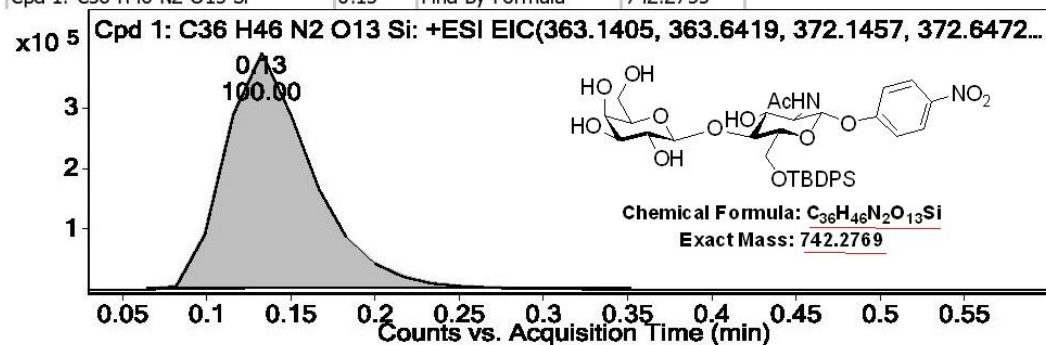


Figure 6.67 ¹³C NMR (75 MHz, CD₃OD) spectrum of compound 3.49.

Compound Table

Compound Label	RT	Mass	Abund	Formula	Tgt Mass	Diff (ppm)
Cpd 1: C ₃₆ H ₄₆ N ₂ O ₁₃ Si	0.13	<u>742.2753</u>	33146	<u>C₃₆ H₄₆ N₂ O₁₃ Si</u>	<u>742.2769</u>	-2.12

Compound Label	RT	Algorithm	Mass
Cpd 1: C ₃₆ H ₄₆ N ₂ O ₁₃ Si	0.13	Find By Formula	742.2753



MS Spectrum

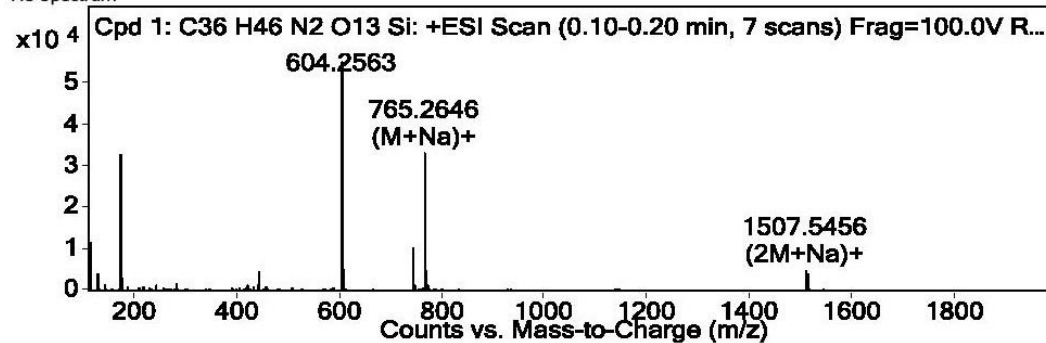
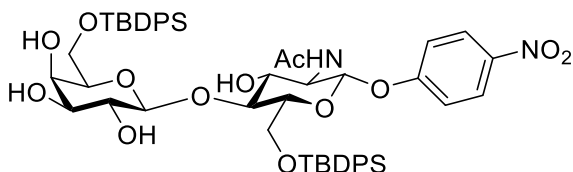


Figure 6.68 HRMS spectrum of compound 3.49.

4-Nitrophenyl (6-*O*-*tert*-butyldiphenylsilyl- β -D-galactopyranosyl)-(1 \rightarrow 4)-2-*N*-acetamido-2-deoxy-6-*O*-*tert*-butyldiphenylsilyl- β -D-glucopyranoside (**3.50**).



Following the general procedure C, compound **3.50** was obtained as a white solid (253 mg, 0.258 mmol, 86 %).

$R_f = 0.34$, (EtOAc)

$[\alpha]_D^{23} = -7.45$ (c 0.004, MeOH)

$^1\text{H NMR}$ (300 MHz, CD_3OD): δ (ppm) 8.14 (d, $J = 9.3$ Hz, 2H), 7.74 – 7.57 (m, 8H), 7.46 – 7.27 (m, 9H), 7.22 (t, $J = 7.5$ Hz, 1H), 7.16 (d, $J = 9.3$ Hz, 2H), 7.03 (t, $J = 7.6$ Hz, 2H), 5.27 (d, $J = 8.4$ Hz, 1H), 4.58 (d, $J = 7.7$ Hz, 1H), 4.23 (dd, $J = 11.5, 3.6$ Hz, 1H), 4.09 – 4.00 (m, 2H), 3.99 – 3.78 (m, 5H), 3.74 (d, $J = 9.7$ Hz, 1H), 3.66 – 3.55 (m, 2H), 3.47 (dd, $J = 9.7, 3.2$ Hz, 1H), 1.96 (s, 3H), 1.05 (s, 9H), 0.99 (s, 9H)

$^{13}\text{C NMR}$ (75 MHz, CD_3OD): δ (ppm) 173.7, 163.5, 143.9, 136.9, 136.7, 136.7, 134.8, 134.4, 134.4, 133.9, 130.9, 130.7, 130.6, 128.9, 128.9, 128.8, 128.5, 126.7, 117.7, 105.0, 99.4, 79.5, 77.0, 76.9, 75.1, 73.5, 72.4, 69.8, 63.8, 63.2, 56.7, 27.4, 27.4, 23.0, 20.2, 20.0

ESI-HRMS: m/z calcd. for $\text{C}_{52}\text{H}_{64}\text{N}_2\text{O}_{13}\text{Si}_2$ $[\text{M}+\text{Na}]^+$, 1003.3839; found 1003.3835 $[\text{M}+\text{Na}]^+$

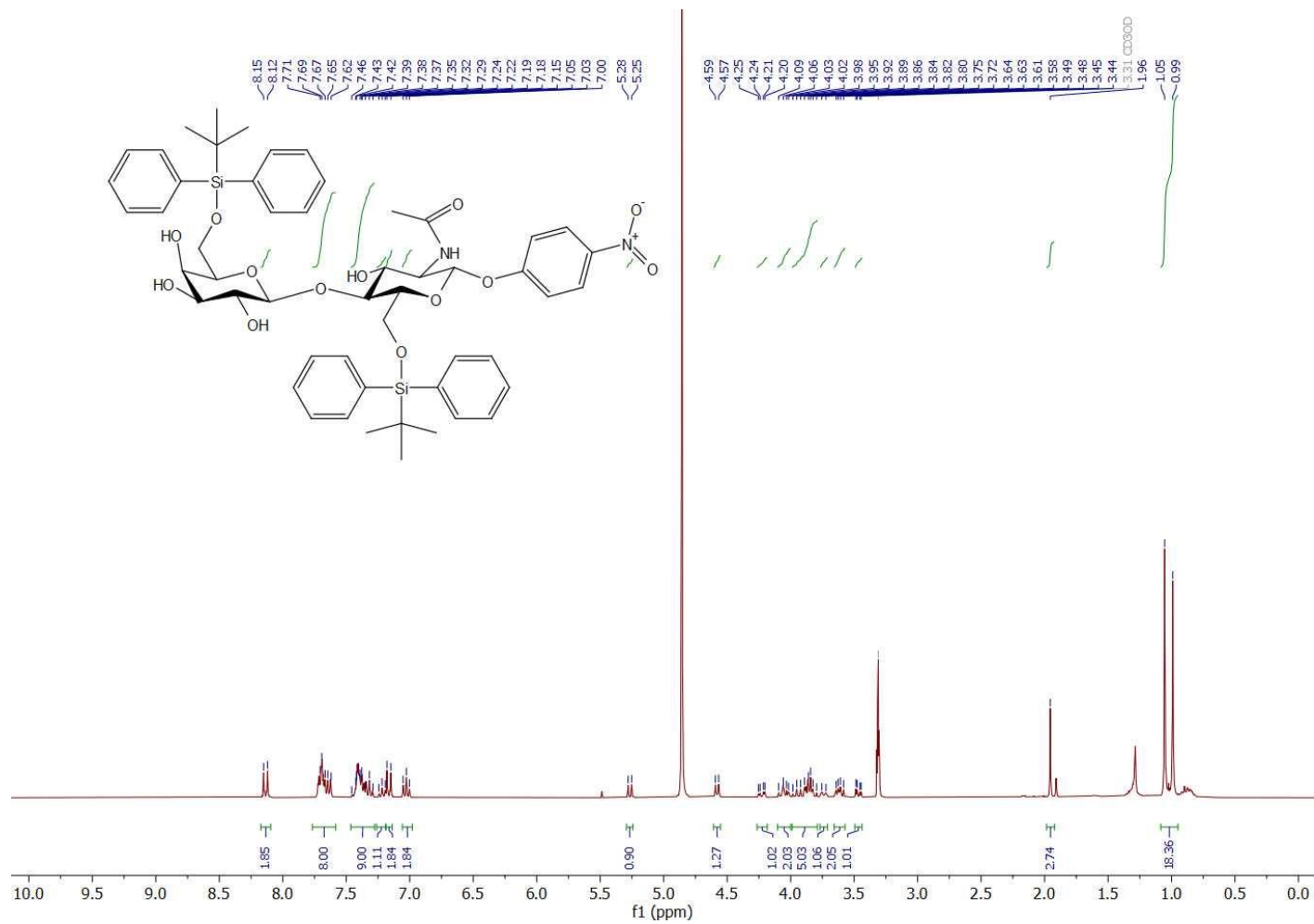


Figure 6.69 ¹H NMR (300 MHz, CD₃OD) spectrum of compound 3.50.

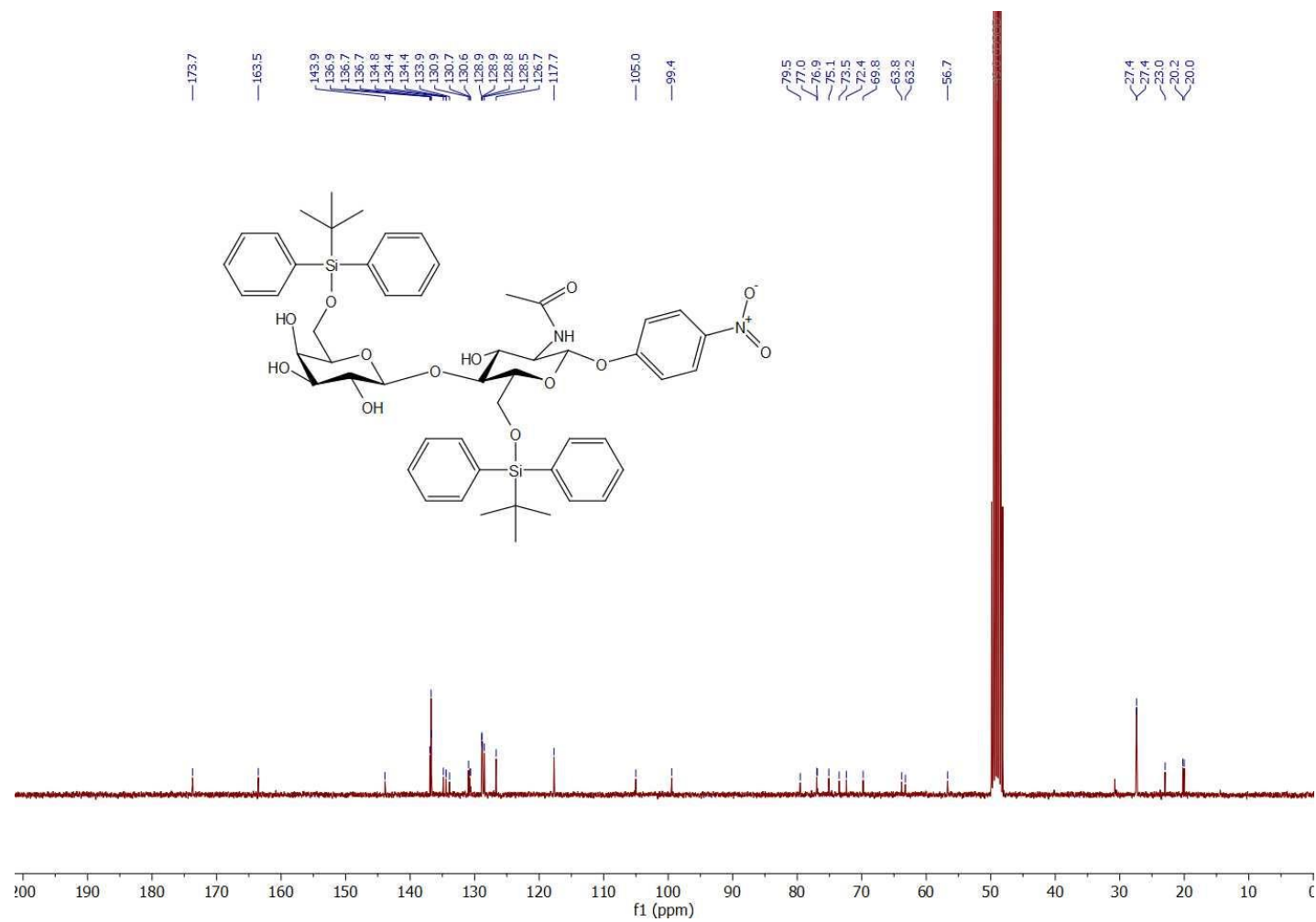
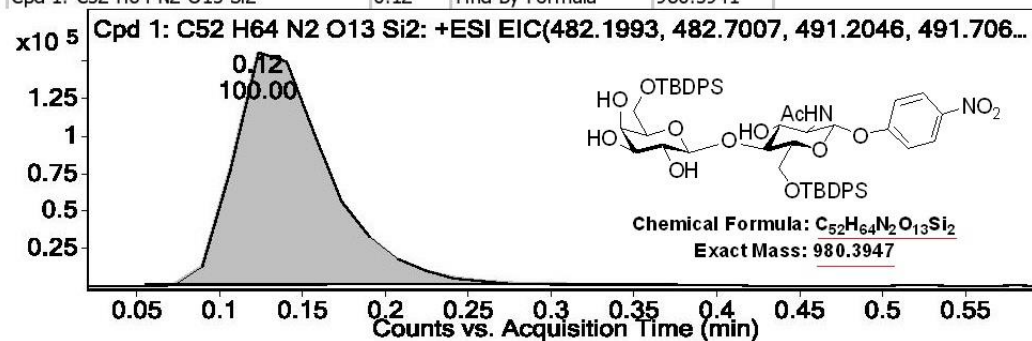


Figure 6.70 ^{13}C NMR (75 MHz, CD_3OD) spectrum of compound 3.50.

Compound Table

Compound Label	RT	Mass	Abund	Formula	Tgt Mass	Diff (ppm)
Cpd 1: C ₅₂ H ₆₄ N ₂ O ₁₃ Si ₂	0.12	<u>980.3941</u>	16047	<u>C₅₂H₆₄N₂O₁₃Si₂</u>	980.3947	-0.61

Compound Label	RT	Algorithm	Mass
Cpd 1: C ₅₂ H ₆₄ N ₂ O ₁₃ Si ₂	0.12	Find By Formula	980.3941



MS Spectrum

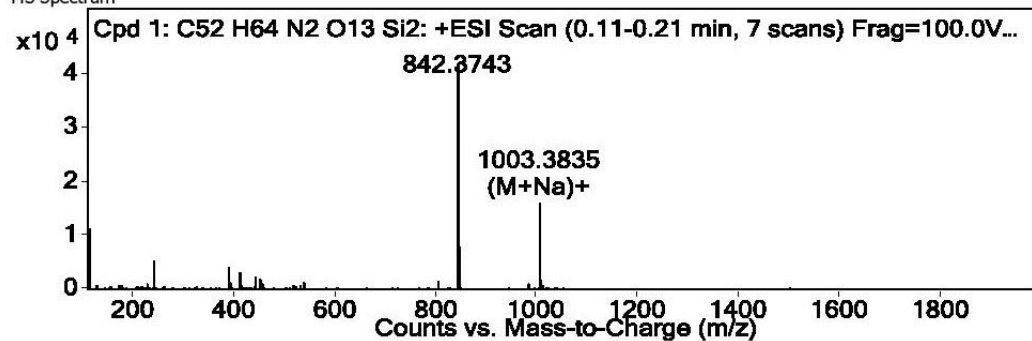
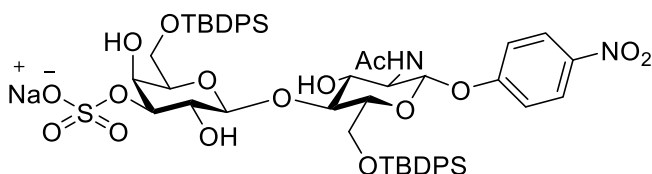


Figure 6.71 HRMS spectrum of compound 3.50.

4-Nitrophenyl (3-*O*-sulfo-6-*O*-*tert*-butyldiphenylsilyl- β -D-galactopyranosyl)-(1 \rightarrow 4)-2-*N*-acetamido-2-deoxy-6-*O*-*tert*-butyldiphenylsilyl- β -D-glucopyranoside sodium salt (**3.51**).



Following the general procedure A, compound 3.51 was obtained as a white solid (0.12 mg, 0.11 mmol, 83 %).

$R_f = 0.09$, (EtOAc/MeOH : 9/1)

$[\alpha]_D^{22} = -23.7$ (c 0.011, MeOH)

$^1\text{H NMR}$ (300 MHz, CD_3OD): δ (ppm) 8.16 (d, $J = 9.3$ Hz, 2H), 7.81 – 7.50 (m, 8H), 7.49 – 7.25 (m, 9H), 7.26 – 7.10 (m, 3H), 6.98 (t, $J = 7.6$ Hz, 2H), 5.36 (d, $J = 8.4$ Hz, 1H), 4.74 (d, $J = 7.8$ Hz, 1H), 4.37 – 4.29 (m, 2H), 4.22 (dd, $J = 11.7, 3.1$ Hz, 1H), 4.13 (dd, $J = 10.3, 8.4$ Hz, 1H), 4.05 – 3.77 (m, 7H), 3.68 (t, $J = 6.6$ Hz, 1H), 1.97 (s, 3H), 1.04 (s, 9H), 0.97 (s, 9H)

$^{13}\text{C NMR}$ (75 MHz, CD_3OD): δ (ppm) 173.7, 163.5, 143.8, 136.9, 136.7, 136.6, 134.6, 134.3, 133.7, 130.9, 130.8, 130.6, 128.9, 128.9, 128.8, 128.4, 126.6, 117.7, 104.4, 99.4, 82.0, 79.0, 76.6, 76.4, 73.5, 71.0, 68.0, 63.4, 62.9, 56.4, 27.4, 27.3, 23.0, 20.2, 20.0

ESI-HRMS: m/z calcd. for $\text{C}_{52}\text{H}_{64}\text{N}_2\text{O}_{16}\text{SSi}_2$ $[\text{M}+\text{Na}]^+$, 1083.3407; found 1083.3358 $[\text{M}+\text{Na}]^+$

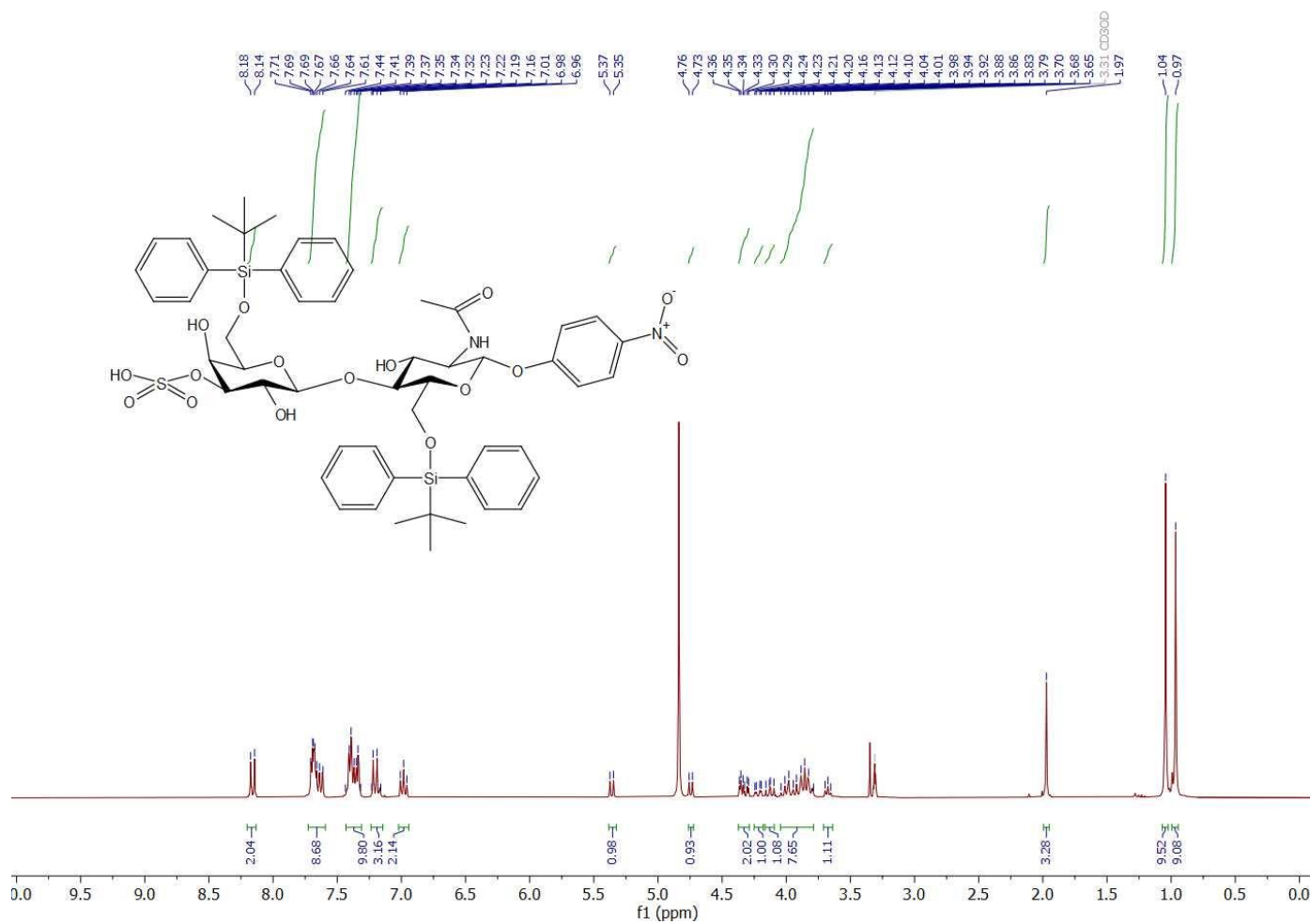


Figure 6.72 ^1H NMR (300 MHz, CD_3OD) spectrum of compound 3.51.

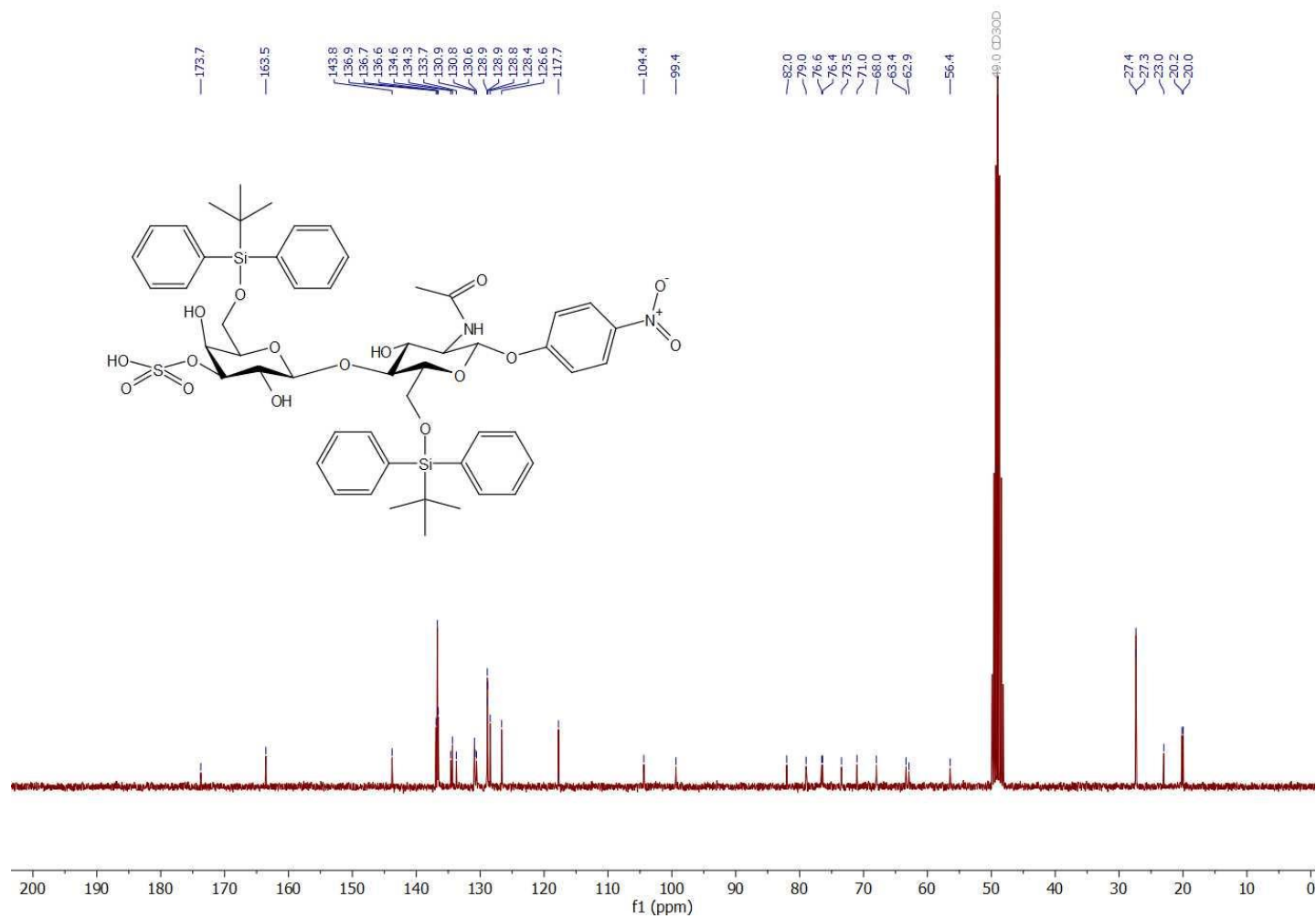
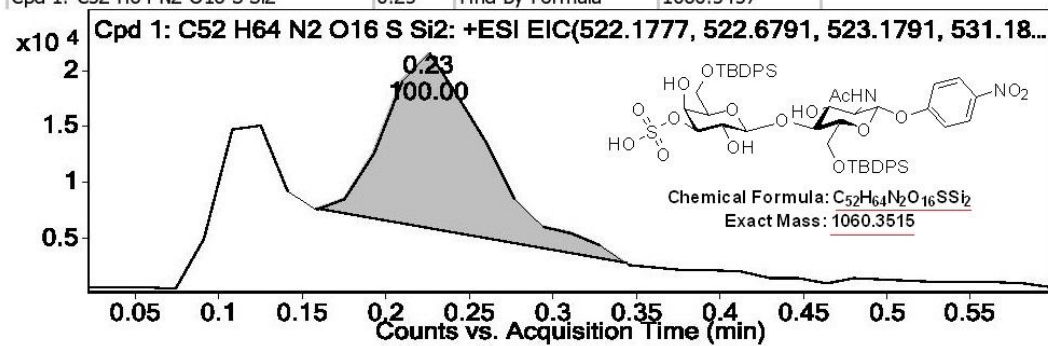


Figure 6.73 ^{13}C NMR (75 MHz, CD_3OD) spectrum of compound 3.51.

Compound Table

Compound Label	RT	Mass	Abund	Formula	Tgt Mass	Diff (ppm)
Cpd 1: C ₅₂ H ₆₄ N ₂ O ₁₆ S Si ₂	0.23	<u>1060.3457</u>	1099	<u>C₅₂ H₆₄ N₂ O₁₆ S Si₂</u>	<u>1060.3515</u>	-5.46

Compound Label	RT	Algorithm	Mass
Cpd 1: C ₅₂ H ₆₄ N ₂ O ₁₆ S Si ₂	0.23	Find By Formula	1060.3457



MS Spectrum

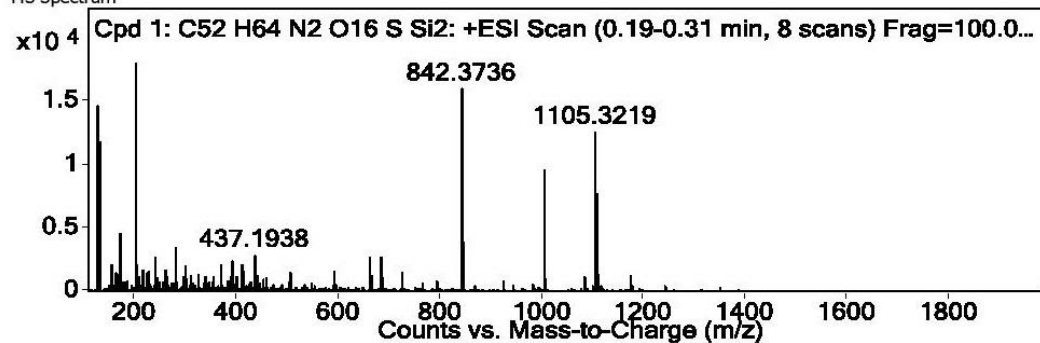
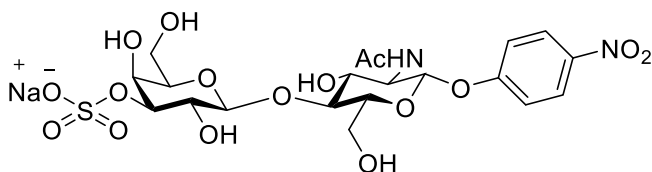


Figure 6.74 HRMS spectrum of compound 3.51.

4-Nitrophenyl (3-*O*-sulfo- β -D-galactopyranosyl)-(1 \rightarrow 4)-2-*N*-acetamido-2-deoxy- β -D-glucopyranoside sodium salt (**3.52**).



Following the general procedure D, compound **3.52** was obtained as a white solid (43 mg, 0.071 mmol, 72 %).

$R_f = 0.54$, (EtOAc/*i*PrOH/H₂O : 6/5/3)

$[\alpha]_D^{23} = -10.8$ (c 0.003, H₂O)

¹H NMR (600 MHz, D₂O): δ (ppm) 8.35 (d, $J = 9.0$ Hz, 2H), 7.30 (d, $J = 9.1$ Hz, 2H), 5.48 (d, $J = 8.4$ Hz, 1H), 4.73 (d, $J = 7.9$ Hz, 1H), 4.47 (dd, $J = 10.0, 3.3$ Hz, 1H), 4.40 (d, $J = 3.3$ Hz, 1H), 4.19 (t, $J = 9.0$ Hz, 1H), 4.12 (d, $J = 11.8$ Hz, 1H), 4.06 – 3.95 (m, 3H), 3.92 – 3.84 (m, 4H), 3.81 (dd, $J = 9.9, 8.0$ Hz, 1H), 2.12 (s, 3H)

¹³C NMR (75 MHz, D₂O): δ (ppm) 175.0, 161.7, 142.7, 126.8, 116.7, 102.6, 98.6, 79.9, 77.9, 75.1, 75.0, 72.0, 69.2, 66.9, 61.0, 59.9, 54.9, 22.3

ESI-HRMS: m/z calcd. for C₂₀H₂₉N₂O₁₆S [M+H]⁺, 585.1232; found 585.1222 [M+H]⁺

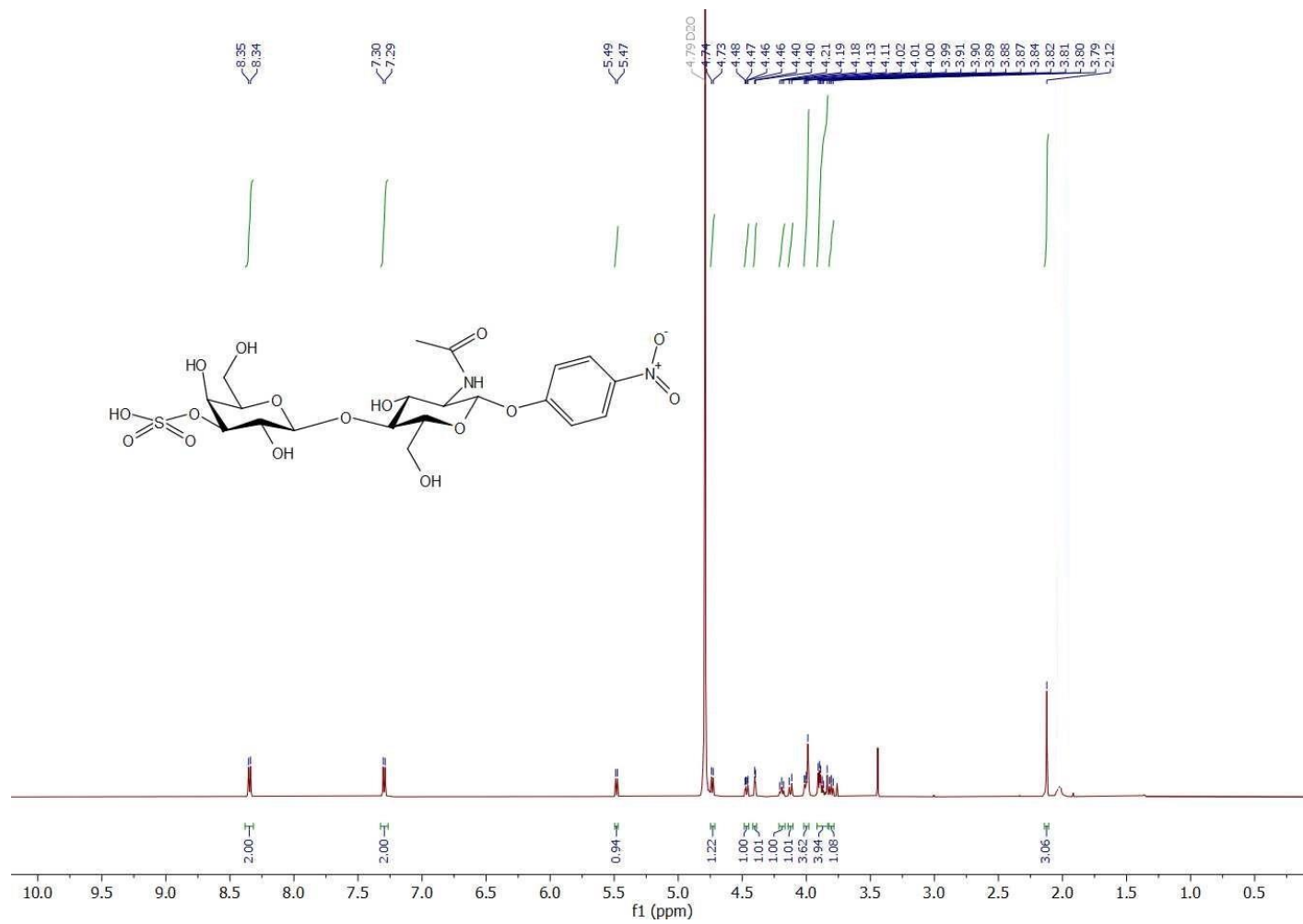


Figure 6.75 ¹H NMR (600 MHz, D₂O) spectrum of compound 3.52.

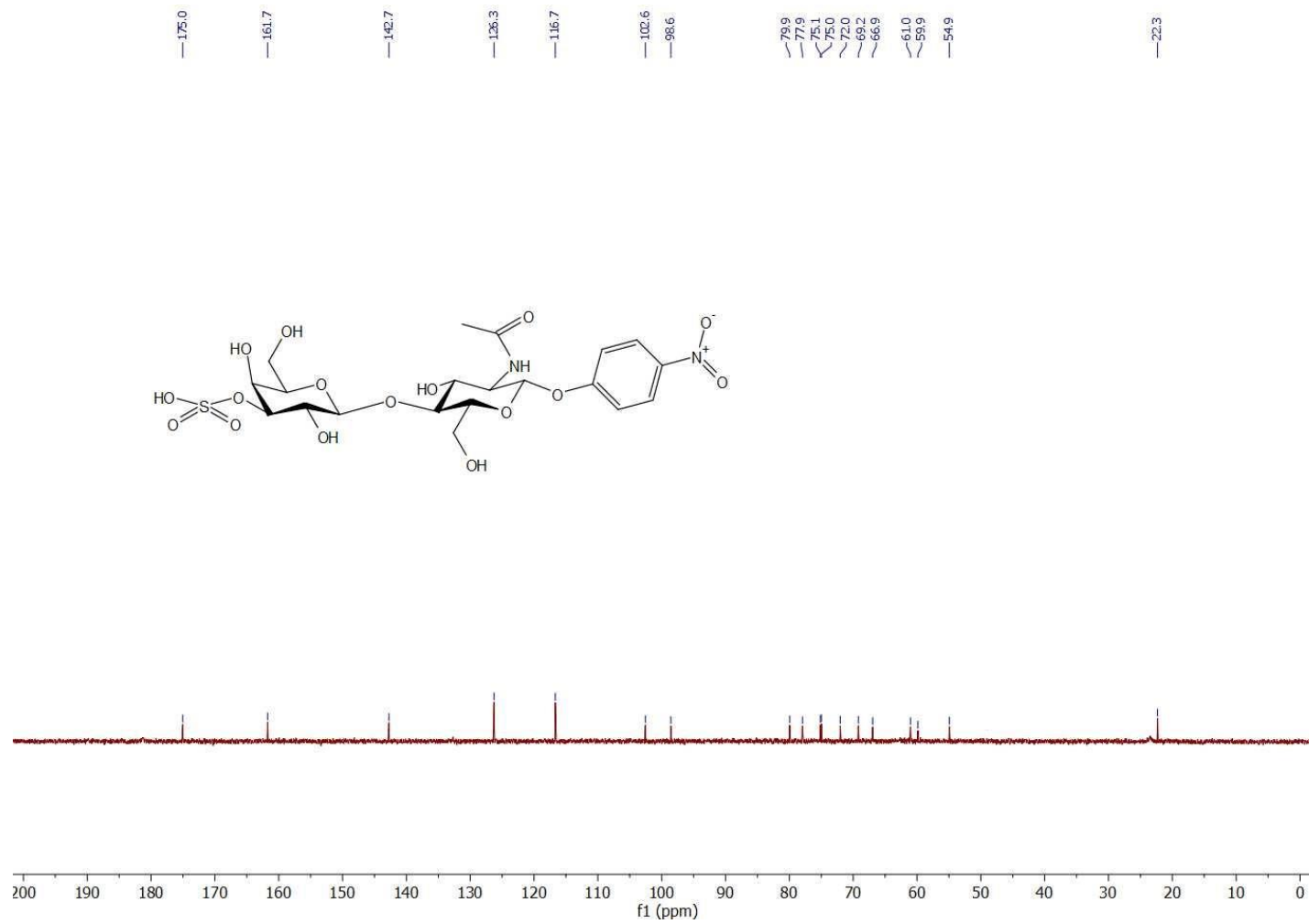


Figure 6.76 ¹³C NMR (75 MHz, D₂O) spectrum of compound **3.52**.

Compound Table

Compound Label	RT	Mass	Abund	Formula	Tgt Mass	Diff (ppm)
Cpd 1: C ₂₀ H ₂₈ N ₂ O ₁₆ S	4.4	<u>584.1148</u>	1674	<u>C₂₀ H₂₈ N₂ O₁₆ S</u>	<u>584.116</u>	-1.95

Compound Label	RT	Algorithm	Mass
Cpd 1: C ₂₀ H ₂₈ N ₂ O ₁₆ S	4.4	Find By Formula	584.1148

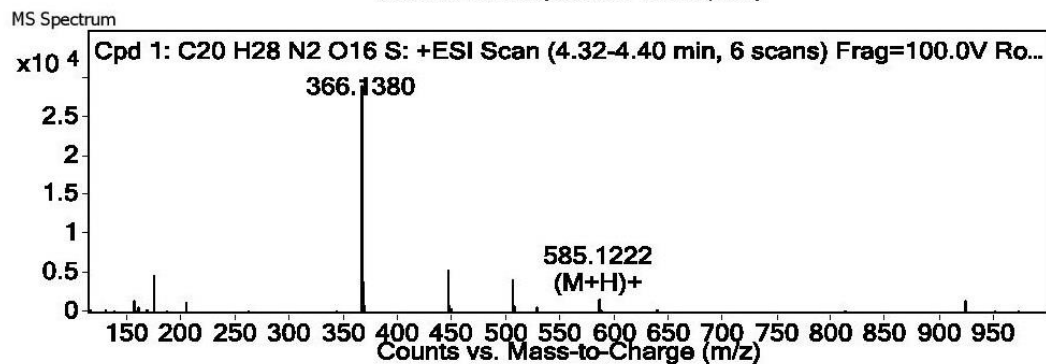
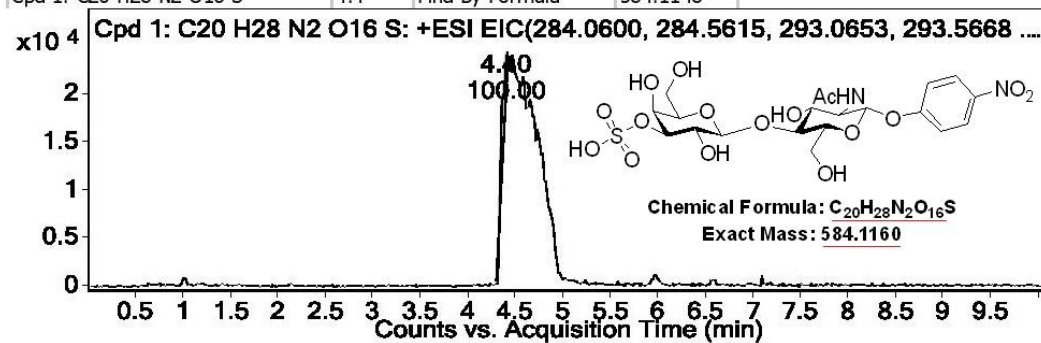
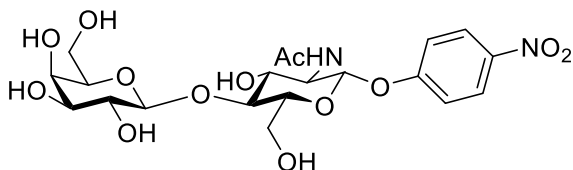


Figure 6.77 HRMS spectrum of compound 3.52.

4-Nitrophenyl (β -D-galactopyranosyl)-(1 \rightarrow 4)-2-*N*-acetamido-2-deoxy- β -D-glucopyranoside (**3.53**).



Following the general procedure D, compound **3.53** was obtained as a white solid (71 mg, 0.14 mmol, 91 %).

$R_f = 0.14$, (EtOAc/*i*PrOH/H₂O : 6/5/2)

$[\alpha]_D^{22} = -17.8$ (c 0.01, H₂O)

¹H NMR (300 MHz, D₂O): δ (ppm) 8.26 (d, $J = 9.2$ Hz, 2H), 7.21 (d, $J = 9.3$ Hz, 2H), 5.37 (d, $J = 8.3$ Hz, 1H), 4.54 (d, $J = 7.7$ Hz, 1H), 4.12 – 3.79 (m, 10H), 3.71 (dd, $J = 10.1, 3.3$ Hz, 1H), 3.59 (dd, $J = 10.0, 7.6$ Hz, 1H), 2.05 (s, 3H)

¹³C NMR (75 MHz, D₂O): δ (ppm) 174.9, 161.7, 142.7, 126.1, 116.5, 102.9, 98.5, 78.1, 75.4, 75.2, 72.5, 72.0, 71.0, 68.6, 61.1, 59.8, 55.5, 54.9, 22.1

ESI-HRMS: m/z calcd. for C₂₀H₂₈N₂O₁₃ [M+Na]⁺, 527.1489; found 527.1478 [M+Na]⁺

The spectroscopic data agreed well with those of the literature.⁵⁶⁵

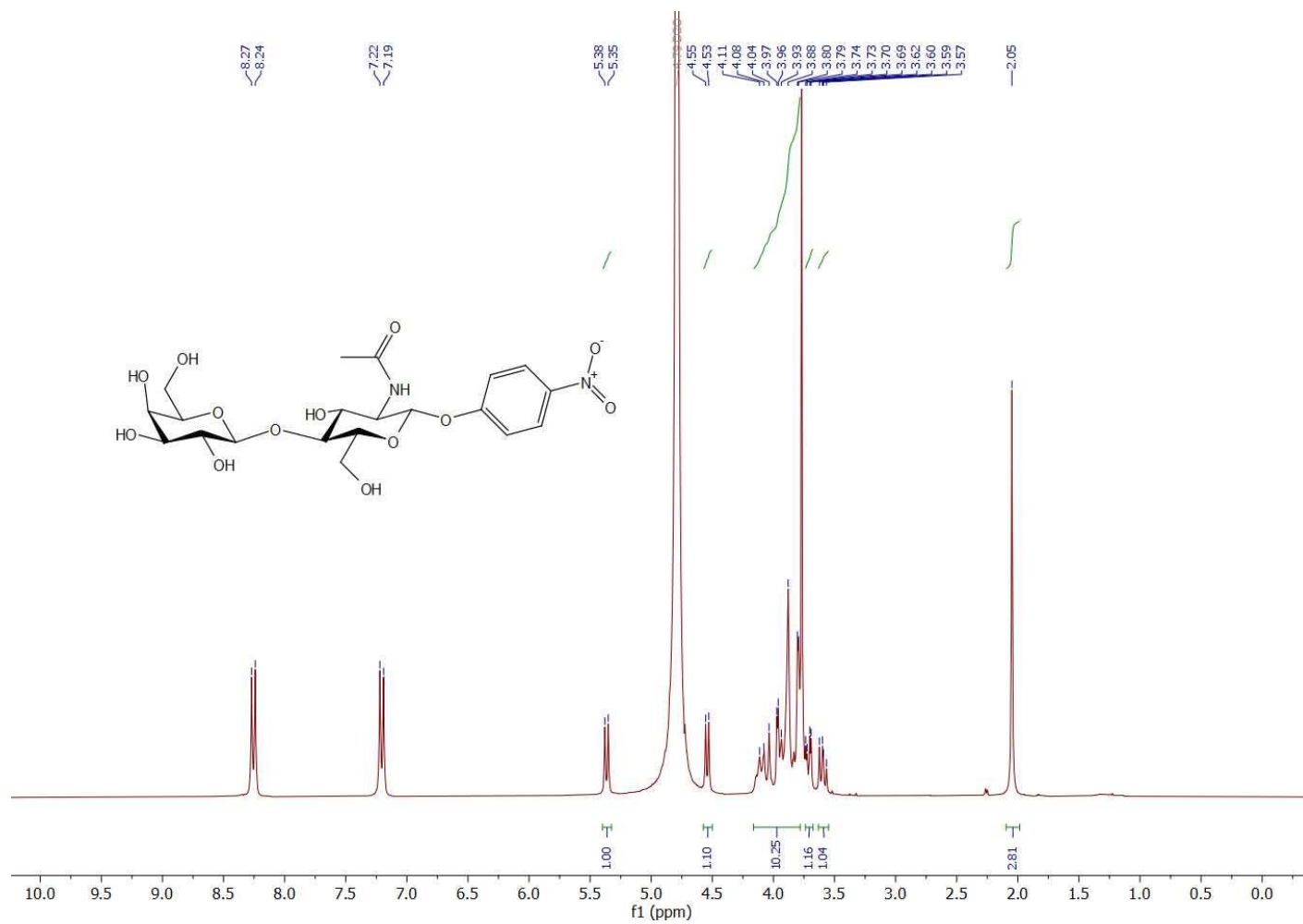


Figure 6.78 ^1H NMR (300 MHz, D_2O) spectrum of compound 3.53.

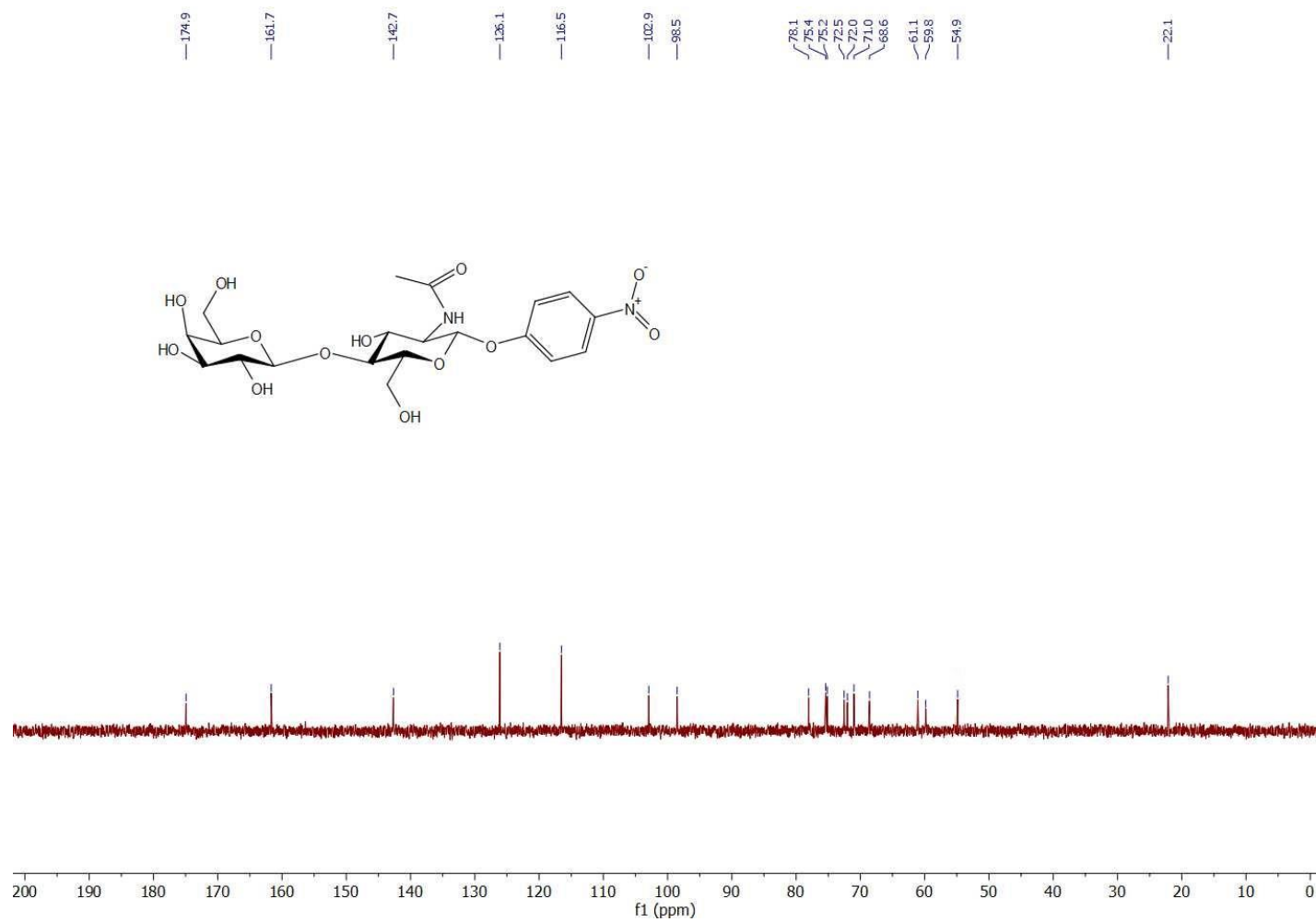
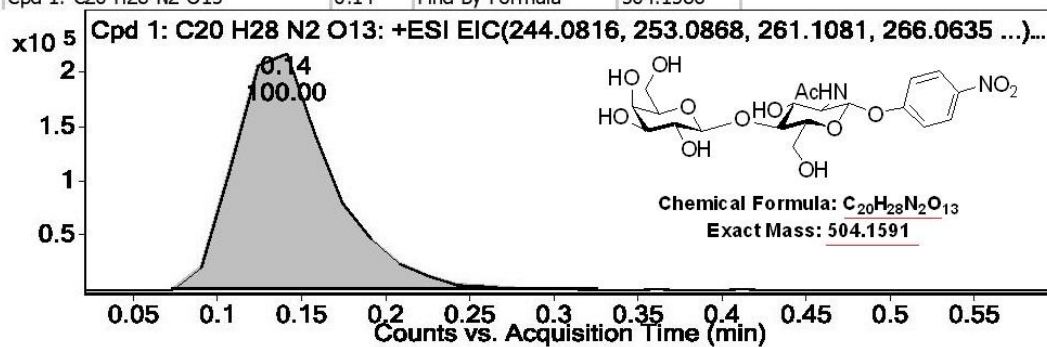


Figure 6.79 ¹³C NMR (75 MHz, D₂O) spectrum of compound **3.53**.

Compound Table

Compound Label	RT	Mass	Abund	Formula	Tgt Mass	Diff (ppm)
Cpd 1: C ₂₀ H ₂₈ N ₂ O ₁₃	0.14	<u>504.1586</u>	30086	<u>C₂₀ H₂₈ N₂ O₁₃</u>	<u>504.1591</u>	-1.12

Compound Label	RT	Algorithm	Mass
Cpd 1: C ₂₀ H ₂₈ N ₂ O ₁₃	0.14	Find By Formula	504.1586



MS Spectrum

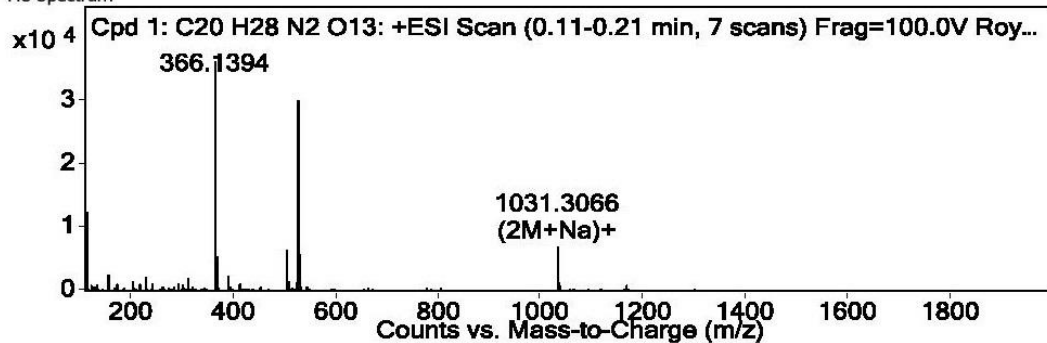
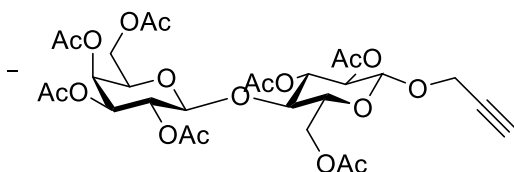


Figure 6.80 HRMS spectrum of compound 3.53.

Propargyl (2,3,4,6-tetra-*O*-acetyl- β -D-galactopyranosyl)-(1 \rightarrow 4)-2,3,6-tri-*O*-acetyl- β -D-glucopyranoside (**3.55**).



A solution of compound **3.54** (1.19 g, 1.76 mmol, 1 eq.), propargyl alcohol (0.140 mL, 2.34 mmol, 1.32 eq.), and pulverized activated 4Å MS (1.05 g) in dry DCM (15 mL) was stirred under nitrogen at room temperature for 0.5 h. The reaction mixture was cooled to 0 °C followed by addition of $\text{BF}_3 \cdot \text{OEt}_2$ (0.32 mL, 2.59 mmol, 1.47 eq.). After stirring of 9 h, the reaction was quenched by addition of triethylamine (0.5 mL). The reaction mixture was filtered through a pad of celite and concentrated *in-vacuo*. After chromatographic purification compound **3.55** (0.94 g, 1.39 mmol, 79 %) was obtained as white solid.

$R_f = 0.24$, (EtOAc/Hex : 1/1)

$[\alpha]_D^{23} = -28.9$ (c 0.06, CHCl_3)

^1H NMR (300 MHz, CDCl_3): δ (ppm) 5.33 (dd, $J = 3.4, 1.2$ Hz, 1H), 5.22 (t, $J = 9.2$ Hz, 1H), 5.10 (dd, $J = 10.4, 7.8$ Hz, 1H), 4.99 – 4.84 (m, 2H), 4.73 (d, $J = 7.9$ Hz, 1H), 4.55 – 4.41 (m, 2H), 4.32 (d, $J = 2.4$ Hz, 2H), 4.18 – 4.00 (m, 3H), 3.92 – 3.74 (m, 2H), 3.62 (ddd, $J = 9.9, 4.9, 2.1$ Hz, 1H), 2.45 (t, $J = 2.4$ Hz, 1H), 2.14 (s, 3H), 2.11 (s, 3H), 2.05 (s, 3H), 2.04 (s, 3H), 2.03 (s, 6H), 1.95 (s, 3H)

^{13}C NMR (75 MHz, CDCl_3): δ (ppm) 170.5, 170.3, 170.2, 169.9, 169.2, 101.2, 98.0, 78.2, 76.2, 75.6, 71.4, 71.1, 70.8, 69.2, 66.7, 61.9, 60.9, 56.0, 21.0, 20.9, 20.8, 20.8, 20.6

The spectroscopic data agreed well with those of the literature.⁵⁶⁶

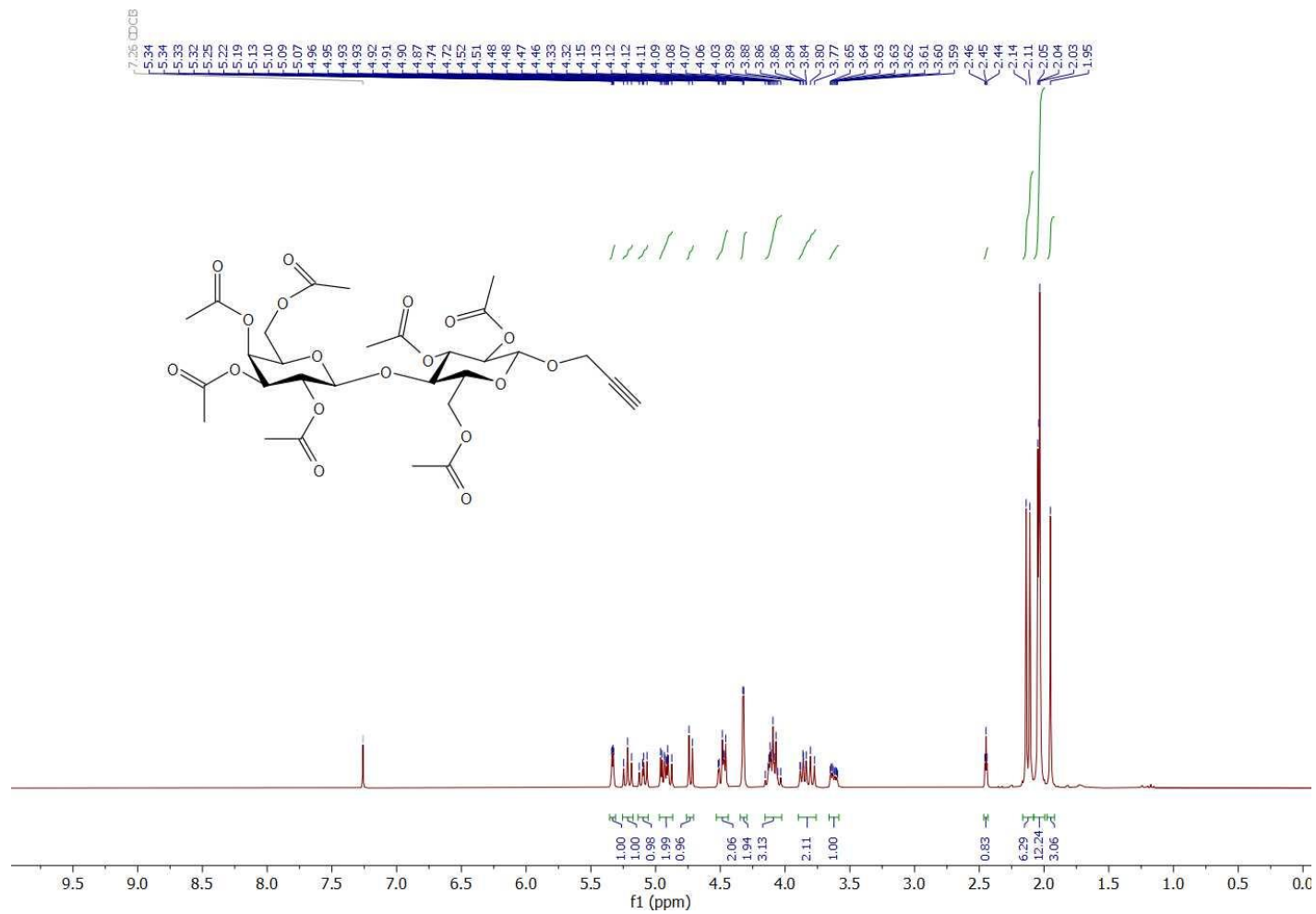


Figure 6.81 ¹H NMR (300 MHz, CDCl₃) spectrum of compound 3.55.

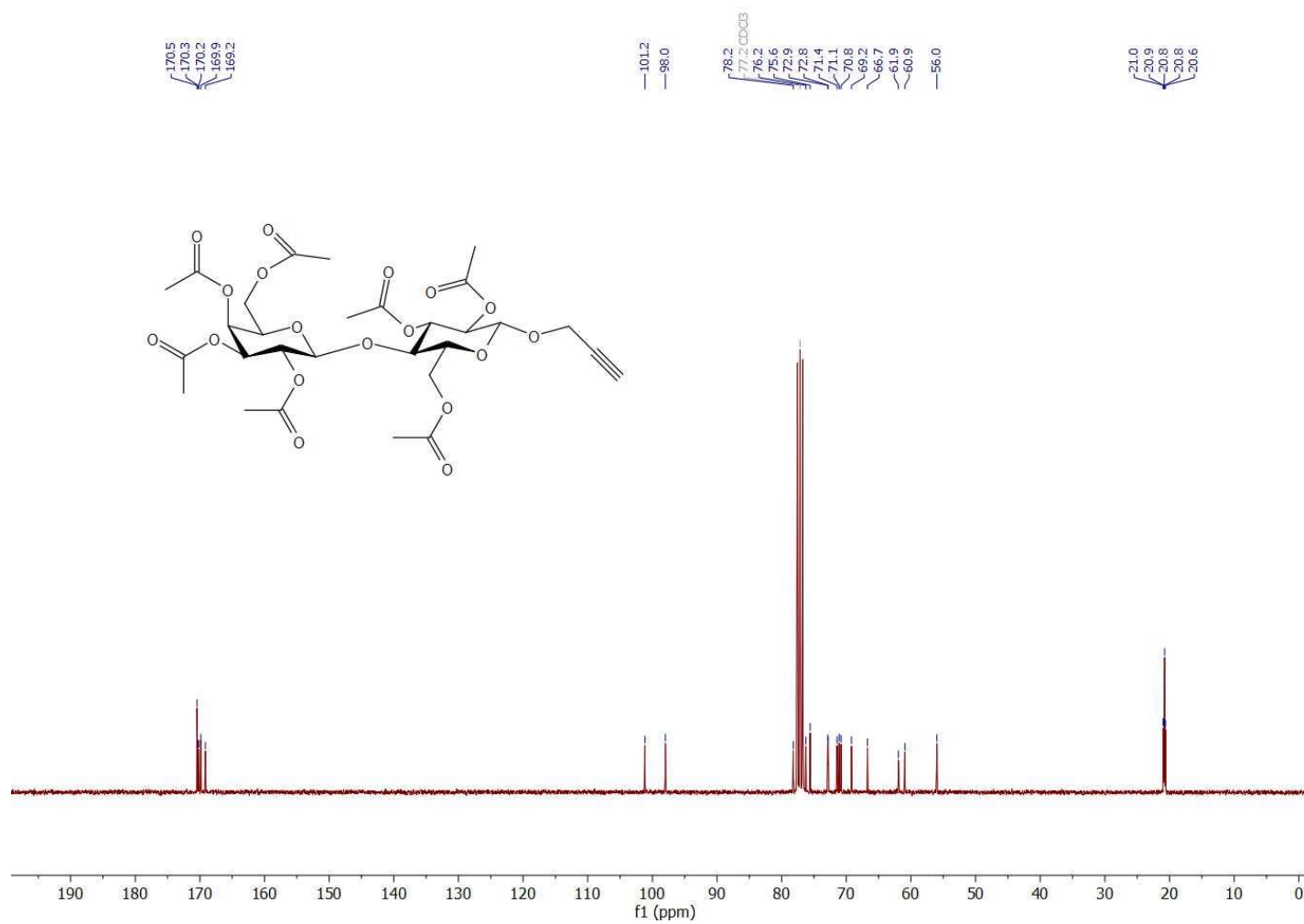
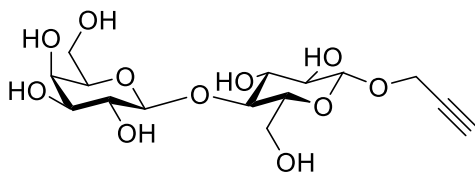


Figure 6.82 ^{13}C NMR (75 MHz, CDCl_3) spectrum of compound 3.55.

Propargyl (β -D-galactopyranosyl)-(1 \rightarrow 4)- β -D-glucopyranoside (**3.56**).



Following the general procedure B, compound **3.56** was obtained as a white solid (0.28 g, 0.75 mmol, 99 %).

$[\alpha]_{\text{D}}^{23} = -33.9$ (c 0.05, D₂O)

¹H NMR (300 MHz, CDCl₃): δ (ppm) 4.65 (d, $J = 7.9$ Hz, 1H), 4.47 – 4.42 (m, 2H), 4.09 – 3.86 (m, 2H), 3.82 – 3.44 (m, 8H) 3.33 (t, $J = 6.3$ Hz, 1H),

¹³C NMR (75 MHz, CDCl₃): δ (ppm) 102.9, 100.4, 78.3, 75.3, 74.8, 74.3, 72.6, 72.5, 70.9, 68.5, 61.0, 60.0, 56.6

The spectroscopic data agreed well with those of the literature.⁵⁶⁷

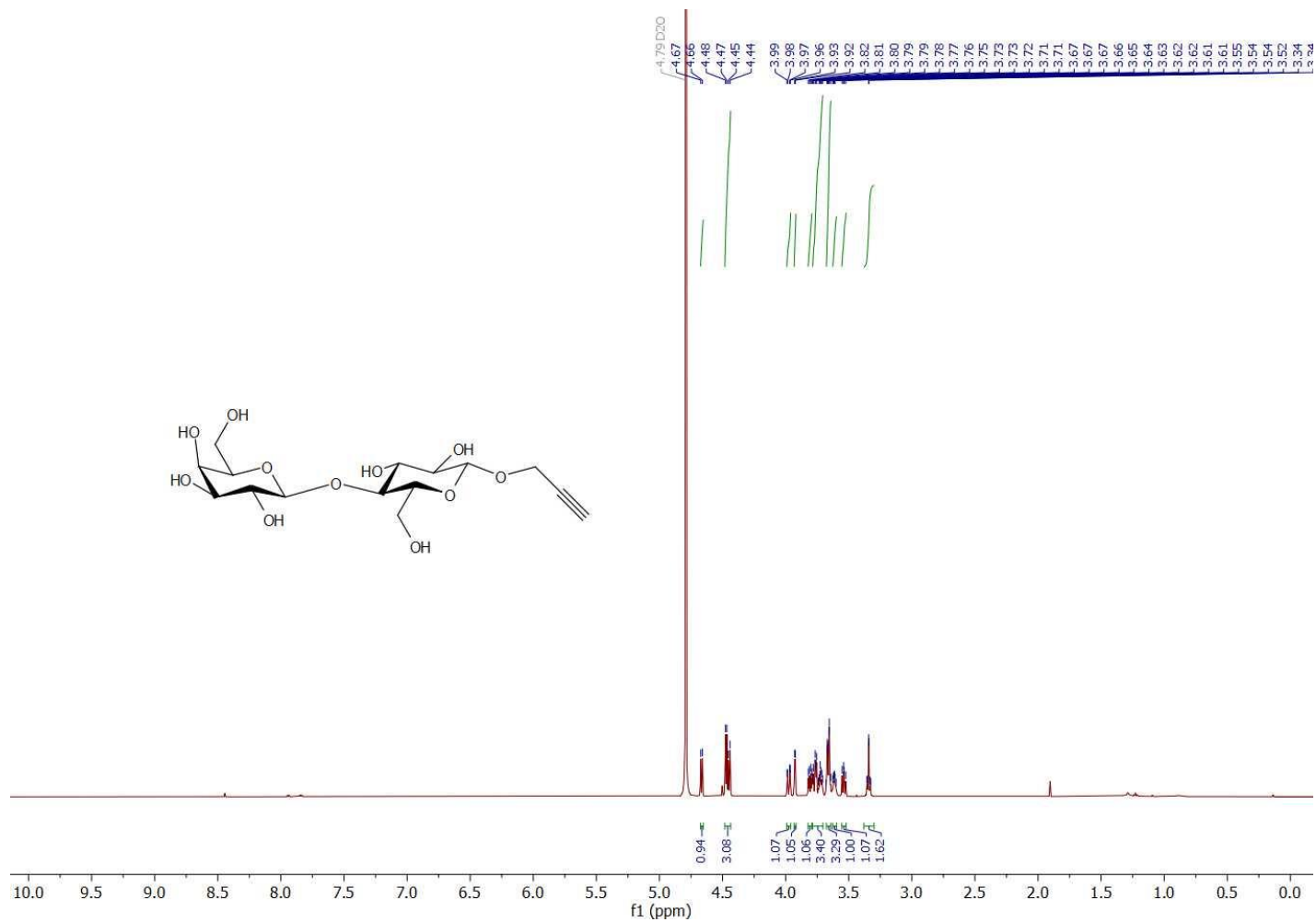


Figure 6.83 ^1H NMR (600 MHz, D_2O) spectrum of compound 3.56.

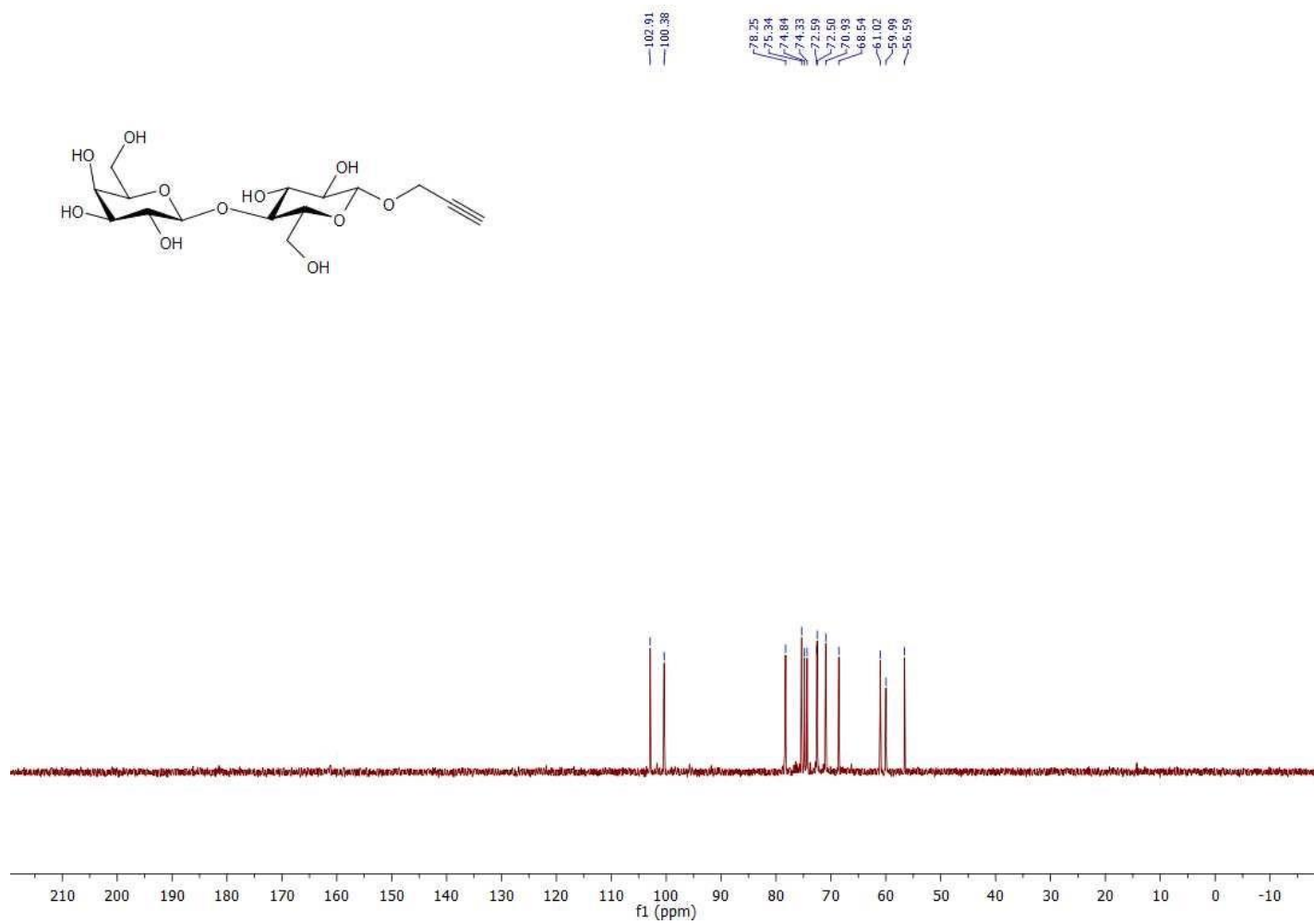
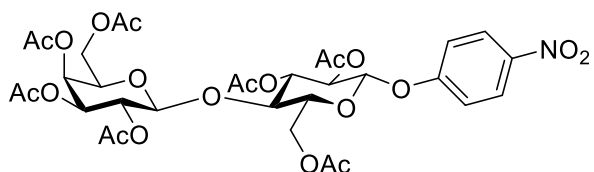


Figure 6.84 ^{13}C NMR (75 MHz, D_2O) spectrum of compound 3.56.

4-Nitrophenyl (2,3,4,6-tetra-*O*-acetyl- β -D-galactopyranosyl)-(1 \rightarrow 4)-2,3,6-tri-*O*-acetyl- β -D-glucopyranoside (**3.57**).



In light of previously reported protocols²¹⁰, to a solution of compound **3.54** (3.05 g, 4.5 mmol, 1 eq.) in DCM (50 mL) was added HBr (33 % in AcOH, 12 mL) over 0.5 h at 0 °C. After 3.5 h of stirring the yellow mixture was poured into ice-cold water (80 mL), extracted with DCM (3 x 90 mL), washed with water (5 x 60 mL), saturated solution of NaHCO₃ (until pH=7), dried over Na₂SO₄ and concentrated *in-vacuo*. The residue was dissolved in DCM (45 mL) and mixed with separately prepared solution of 4-nitrophenol (1.38 g, 9.9 mmol 2 eq.), tetrabutylammonium hydrogen sulfate (TBAHS, 1.53 g, 4.5 mmol 1 eq.) in NaOH (1M, 45 mL). The mixture was stirred at room temperature for 3 h and then diluted in DCM (100 mL) washed successively with NaOH (1M, 2 x 50 mL), saturated solution of ammonium chloride (2 x 50 mL) and brine solution (50 mL), dried over Na₂SO₄ and concentrated under reduced pressure. After chromatographic purification compound **3.57** (2.08 g, 2.74 mmol, 61 %) as a white solid.

R_f = 0.56, (EtOAc/Hex : 6/4)

[α]_D²³ = -28.9 (c 0.06, CHCl₃)

¹H NMR (300 MHz, CDCl₃): δ (ppm) 8.18 (d, *J* = 9.0 Hz, 2H), 7.04 (d, *J* = 9.2 Hz, 1H), 5.34 (d, *J* = 3.1 Hz, 1H), 5.32 – 5.24 (m, 1H), 5.22 – 5.05 (m, 3H), 4.96 (dd, *J* = 10.4, 3.3 Hz, 1H), 4.55 – 4.44 (m, 2H), 4.19 – 4.00 (m, 3H), 3.96 – 3.79 (m, 3H), 2.13 (s, 3H), 2.06 (s, 3H), 2.05 (s, 6H), 2.04 (s, 6H), 1.95 (s, 3H)

¹³C NMR (75 MHz, CDCl₃): δ (ppm) 170.4, 170.2, 170.2, 170.1, 169.7, 169.5, 169.2, 161.3, 143.3, 125.8, 116.7, 101.2, 97.8, 76.0, 73.2, 72.7, 71.3, 71.0, 70.9, 69.2, 66.7, 62.0, 60.9, 20.8, 20.8, 20.7, 20.6

The spectroscopic data agreed well with those of the literature.²¹⁰

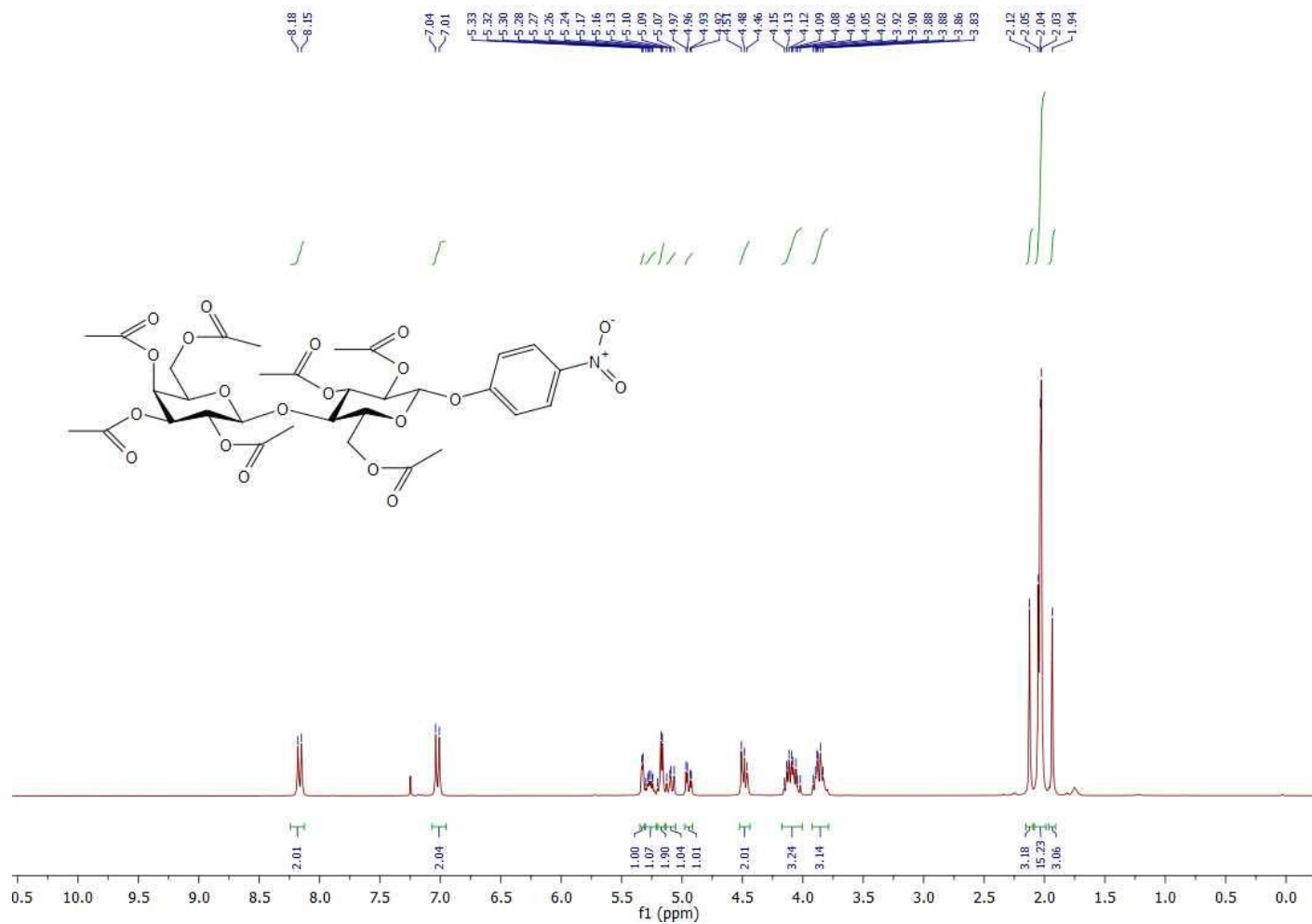


Figure 6.85 ^1H NMR (300 MHz, CDCl_3) spectrum of compound 3.57.

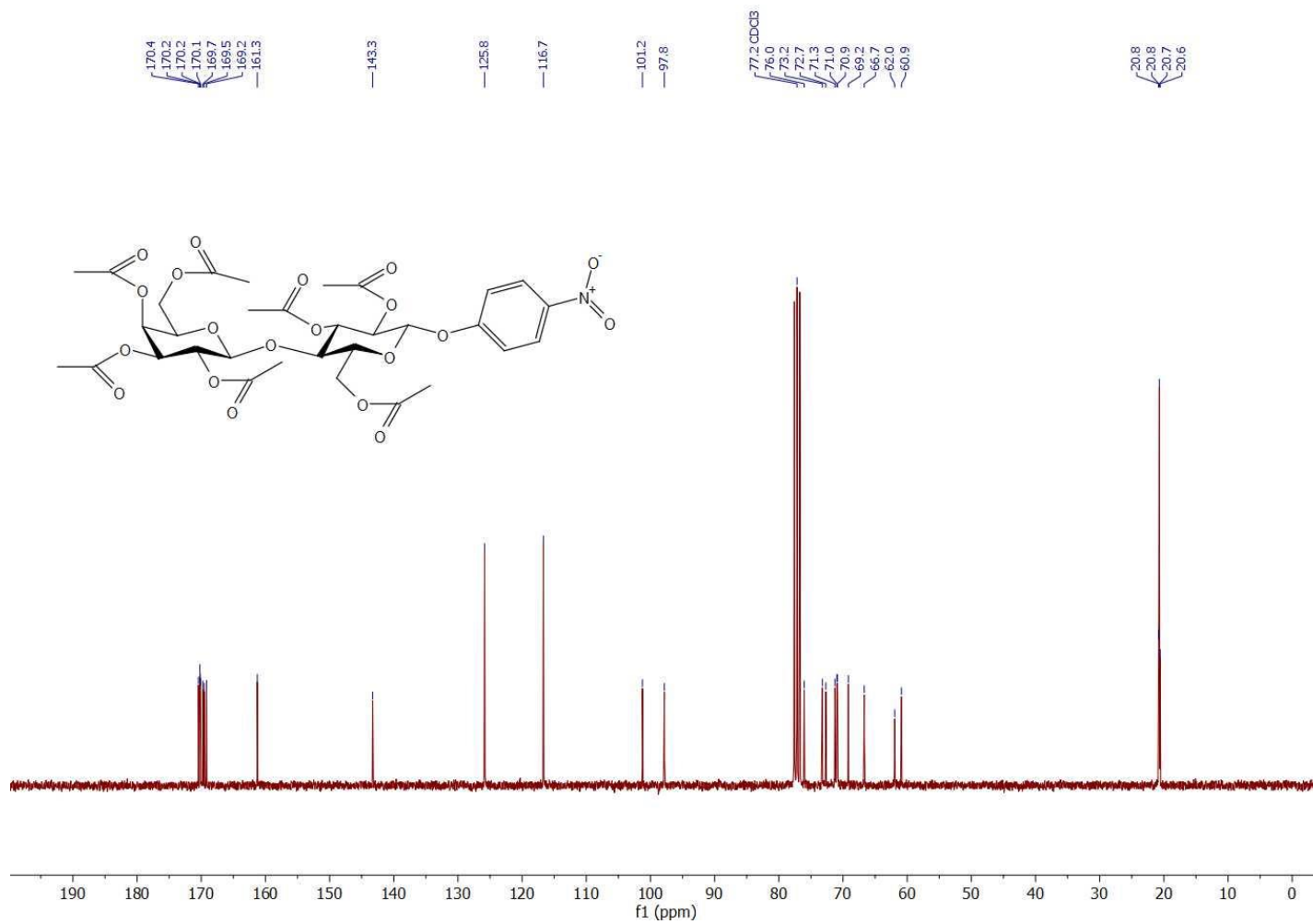
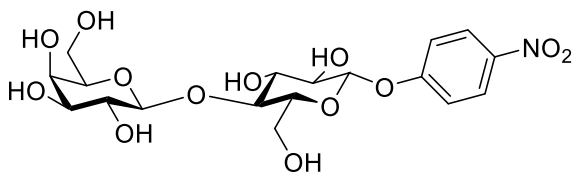


Figure 6.86 ^{13}C NMR (75 MHz, CDCl_3) spectrum of compound 3.57.

4-Nitrophenyl (β -D-galactopyranosyl)-(1 \rightarrow 4)- β -D-glucopyranoside (**3.58**).



Following the general procedure B, compound **3.58** was obtained as a white solid (0.29 g, 0.64 mmol, 97 %).

$[\alpha]_{\text{D}}^{23} = -4.7$ (c 0.002, H₂O)

¹H NMR (600 MHz, D₂O): δ (ppm) 8.29 (d, $J = 9.2$ Hz, 2H), 7.27 (d, $J = 9.2$ Hz, 2H), 5.32 (d, $J = 7.8$ Hz, 1H), 4.50 (d, $J = 7.8$ Hz, 1H), 4.02 (d, $J = 10.1$ Hz, 1H), 3.95 (brs, 1H), 3.88 – 3.84 (m, 2H), 3.81 – 3.75 (m, 5H), 3.73 – 3.65 (m, 2H), 3.58 (t, $J = 8.8$ Hz, 1H)

¹³C NMR (150 MHz, DMSO-*d*₆): δ (ppm) 162.3, 141.7, 125.7, 116.5, 103.8, 99.3, 79.9, 75.6, 75.1, 74.7, 73.3, 72.8, 70.6, 68.1, 60.4, 59.9

The spectroscopic data agreed well with those of the literature.²¹⁰

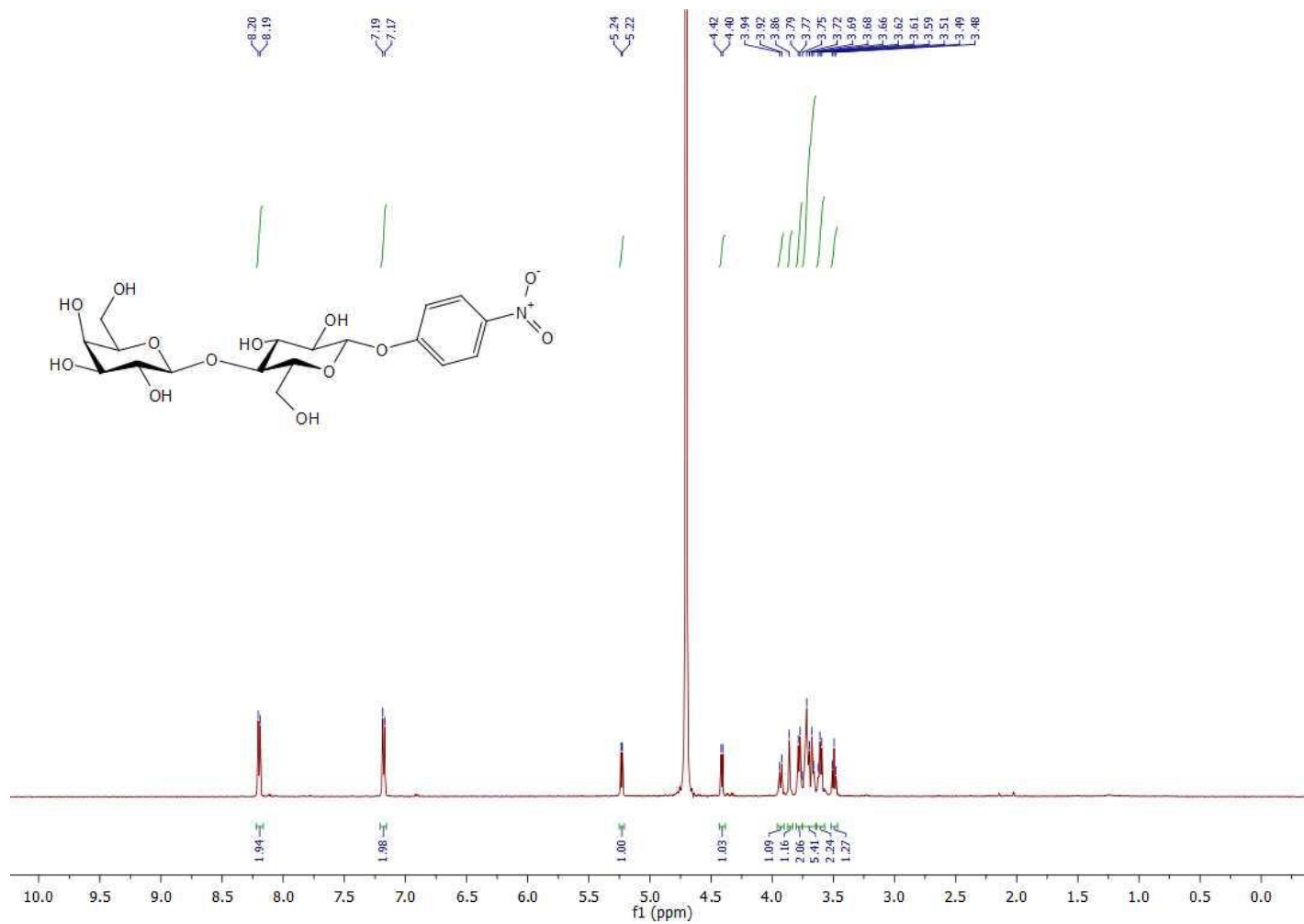


Figure 6.87 ^1H NMR (600 MHz, D_2O) spectrum of compound 3.58.

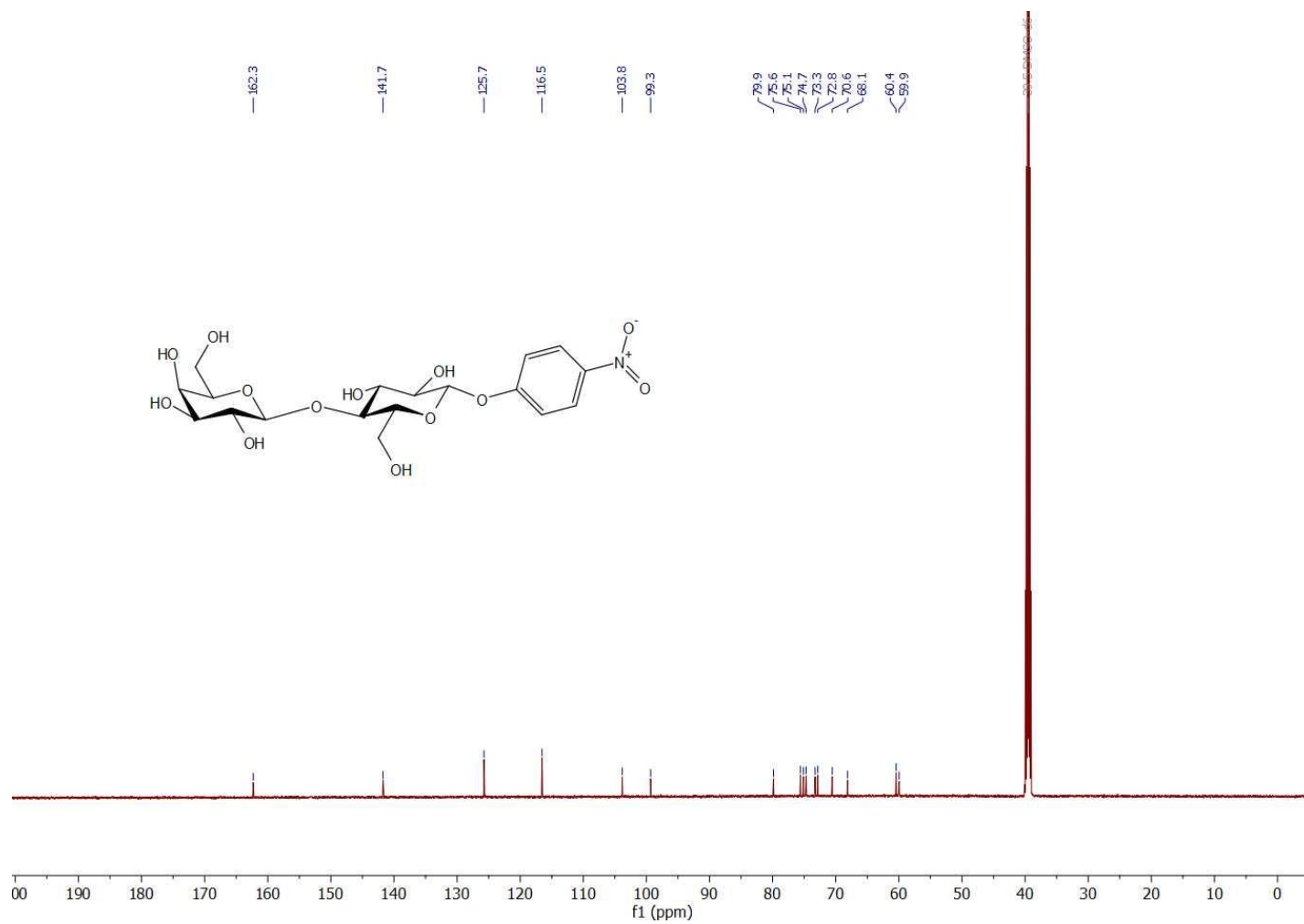
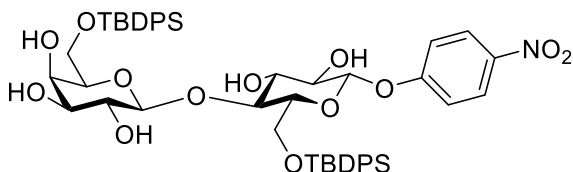


Figure 6.88 ¹³C NMR (150 MHz, DMSO-d₆) spectrum of compound **3.58**.

4-Nitrophenyl (6-*O*-*tert*-butyldiphenylsilyl- β -D-galactopyranosyl)-(1 \rightarrow 4)-6-*O*-*tert*-butyldiphenylsilyl- β -D-glucopyranoside (**3.59**).



Following the general procedure C, compound **3.59** was obtained as a white solid (0.74 g, 0.79 mmol, 84 %).

$R_f = 0.66$, (EtOAc/MeOH : 9.9/0.1)

$[\alpha]_D^{21} = -11.67$ (c 0.011, MeOH)

$^1\text{H NMR}$ (300 MHz, CDCl_3): δ (ppm) 8.06 (d, $J = 8.9$ Hz, 2H), 7.72 – 7.54 (m, 8H), 7.41 – 7.19 (m, 10H), 7.08 (t, $J = 7.5$ Hz, 2H), 7.02 (d, $J = 9.0$ Hz, 2H), 4.95 (d, $J = 7.2$ Hz, 1H), 4.52 (d, $J = 7.5$ Hz, 1H), 4.04 (d, $J = 12.2$ Hz, 1H), 3.98 (d, $J = 3.0$ Hz, 1H), 3.95 – 3.67 (m, 7H), 3.67 – 3.21 (m, 3H), 1.03 (s, 9H), 1.01 (s, 9H)

$^{13}\text{C NMR}$ (75 MHz, CDCl_3): δ (ppm) 161.9, 142.8, 135.8, 135.6, 135.5, 133.4, 132.9, 132.4, 130.1, 129.9, 128.0, 128.0, 127.9, 127.6, 125.8, 116.8, 103.2, 99.6, 77.8, 75.7, 75.3, 74.5, 73.9, 73.7, 71.4, 68.5, 62.3, 62.2, 26.9, 26.8, 19.4, 19.2

ESI-HRMS: m/z calcd. for $\text{C}_{50}\text{H}_{61}\text{NO}_{13}\text{Si}_2$ $[\text{M}+\text{Na}]^+$, 962.3574; found 962.3565
 $[\text{M}+\text{Na}]^+$

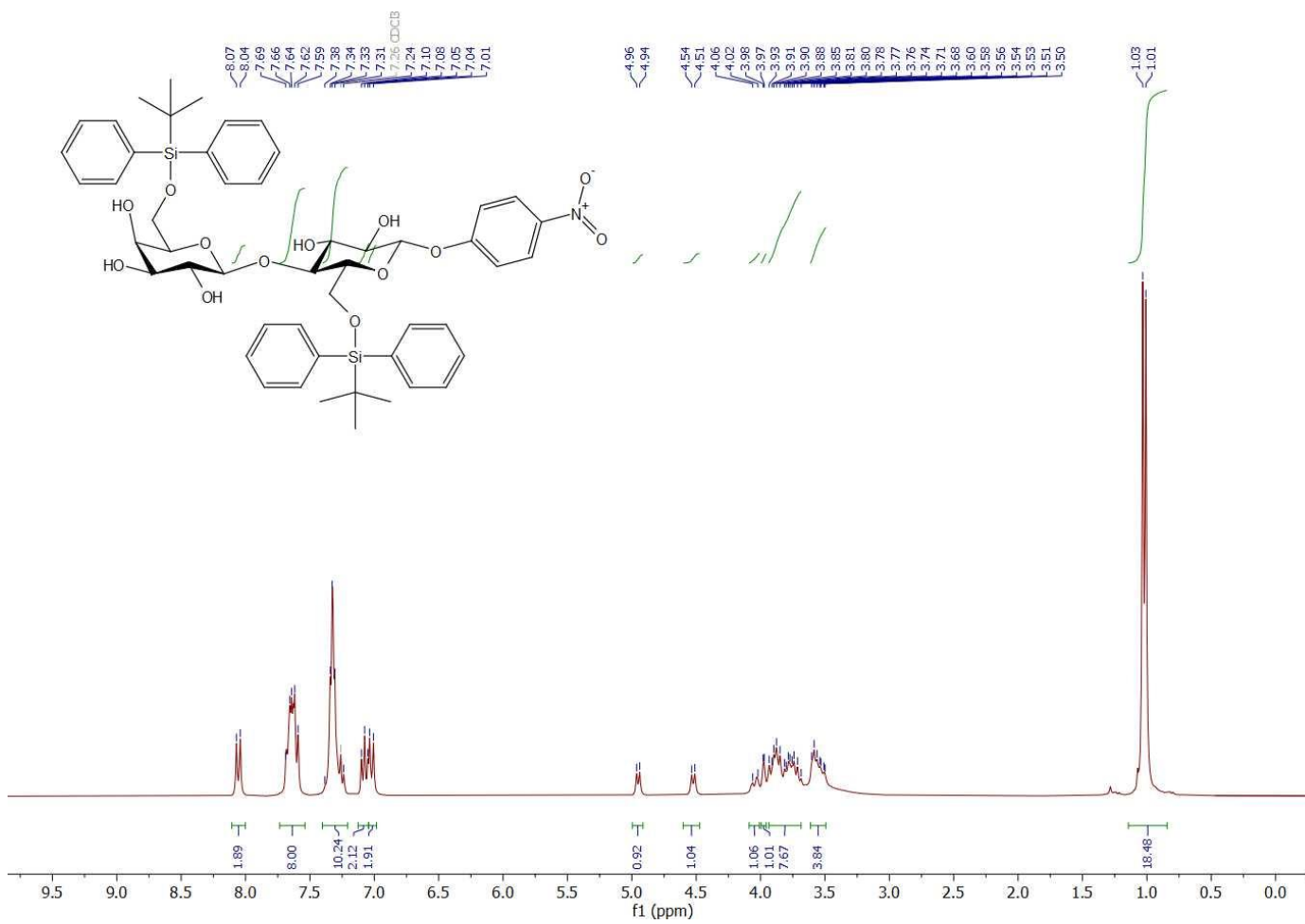


Figure 6.89 ^1H NMR (300 MHz, CDCl_3) spectrum of compound **3.59**.

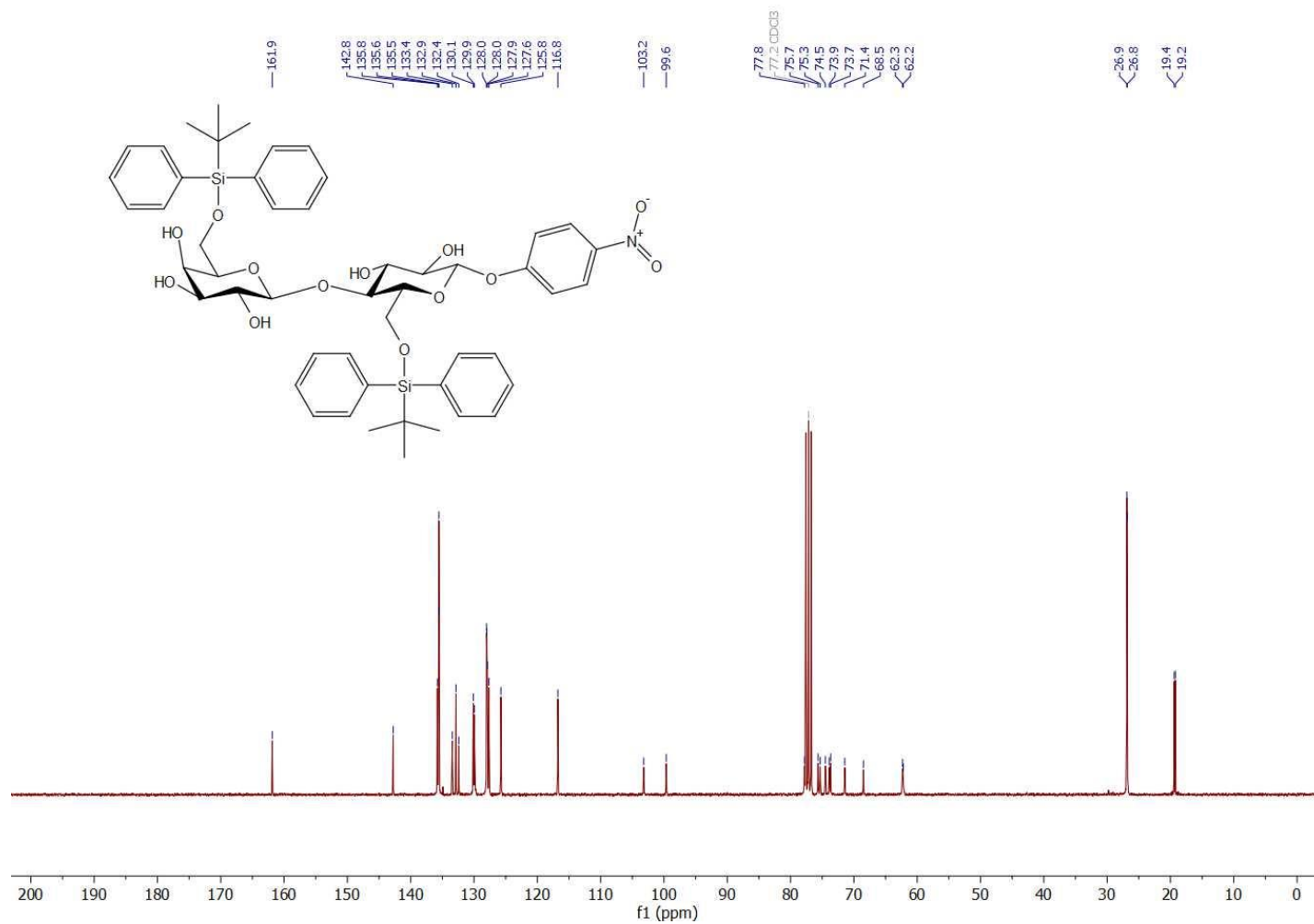
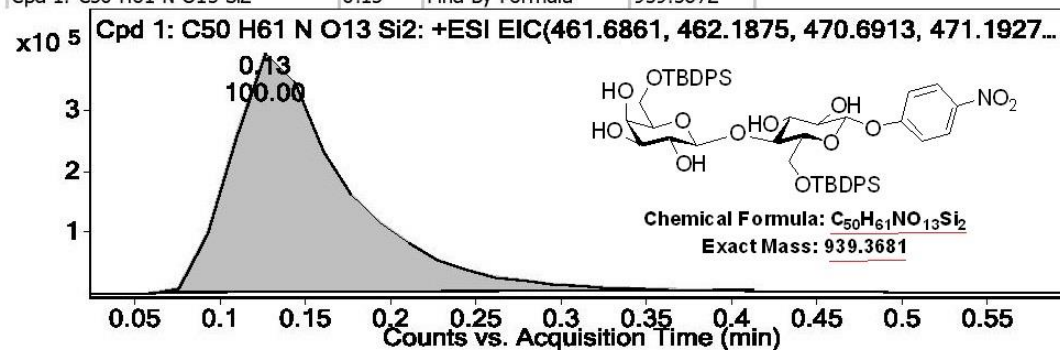


Figure 6.90 ^{13}C NMR (75 MHz, CDCl₃) spectrum of compound **3.59**.

Compound Table

Compound Label	RT	Mass	Abund	Formula	Tgt Mass	Diff (ppm)
Cpd 1: C ₅₀ H ₆₁ N O ₁₃ Si ₂	0.13	939.3672	36688	C ₅₀ H ₆₁ N O ₁₃ Si ₂	939.3681	-1.03

Compound Label	RT	Algorithm	Mass
Cpd 1: C ₅₀ H ₆₁ N O ₁₃ Si ₂	0.13	Find By Formula	939.3672



MS Spectrum

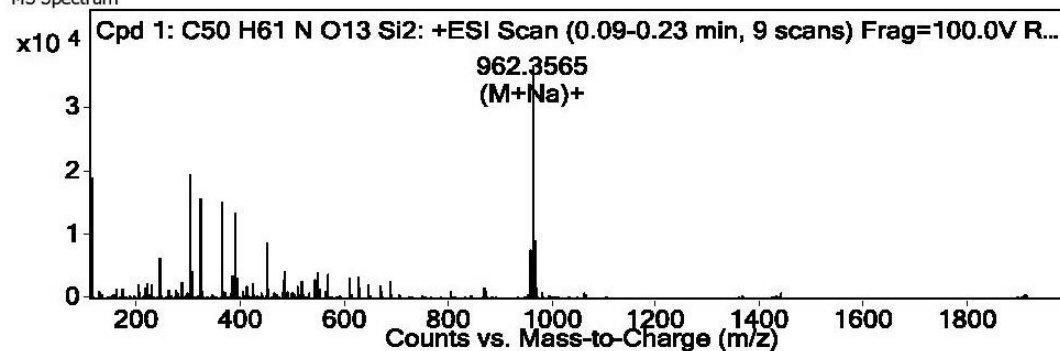
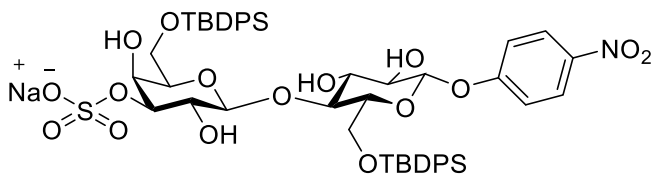


Figure 6.91 HRMS spectrum of compound 3.59.

4-Nitrophenyl (3-*O*-sulfo-6-*O*-*tert*-butyldiphenylsilyl- β -D-galactopyranosyl)-(1 \rightarrow 4)-6-*O*-*tert*-butyldiphenylsilyl- β -D-glucopyranoside sodium salt (**3.60**).



Following the general procedure A, compound **3.60** was obtained as a white solid (0.2 g, 0.19 mmol, 86 %).

$R_f = 0.50$, (EtOAc/MeOH : 9/1)

$[\alpha]_D^{21} = -10.47$ (c 0.006, MeOH)

$^1\text{H NMR}$ (600 MHz, CD_3OD): δ (ppm) 8.15 (d, $J = 9.2$ Hz, 2H), 7.74 – 7.64 (m, 6H), 7.62 (d, $J = 7.1$ Hz, 2H), 7.42 – 7.32 (m, 9H), 7.24 (d, $J = 9.2$ Hz, 2H), 7.17 (t, $J = 7.5$ Hz, 1H), 6.97 (t, $J = 7.5$ Hz, 2H), 5.21 (d, $J = 7.7$ Hz, 1H), 4.78 (d, $J = 7.8$ Hz, 1H), 4.41 (d, $J = 2.6$ Hz, 1H), 4.34 (dd, $J = 9.8, 2.9$ Hz, 1H), 4.25 (dd, $J = 11.7, 2.5$ Hz, 1H), 4.02 (t, $J = 9.5$ Hz, 1H), 3.99 (d, $J = 11.5$ Hz, 1H), 3.97 – 3.85 (m, 2H), 3.84 (dd, $J = 9.9, 6.2$ Hz, 1H), 3.82 – 3.74 (m, 2H), 3.68 (t, $J = 6.6$ Hz, 1H), 3.63 (t, $J = 8.0$ Hz, 1H), 1.04 (s, 9H), 0.95 (s, 9H)

$^{13}\text{C NMR}$ (150 MHz, CD_3OD): δ (ppm) 163.6, 143.6, 136.8, 136.6, 136.6, 136.5, 134.6, 134.3, 134.3, 133.6, 130.9, 130.9, 130.8, 130.5, 128.9, 128.8, 128.8, 128.4, 126.6, 117.7, 104.0, 100.8, 82.0, 77.8, 76.5, 76.3, 75.4, 74.7, 70.9, 67.9, 63.2, 62.9, 27.4, 27.3, 20.2, 19.9

ESI-HRMS: m/z calcd. for $\text{C}_{50}\text{H}_{61}\text{NO}_{16}\text{SSi}_2$ $[\text{M}+\text{Na}]^+$, 1042.3142; found 1042.3140 $[\text{M}+\text{Na}]^+$

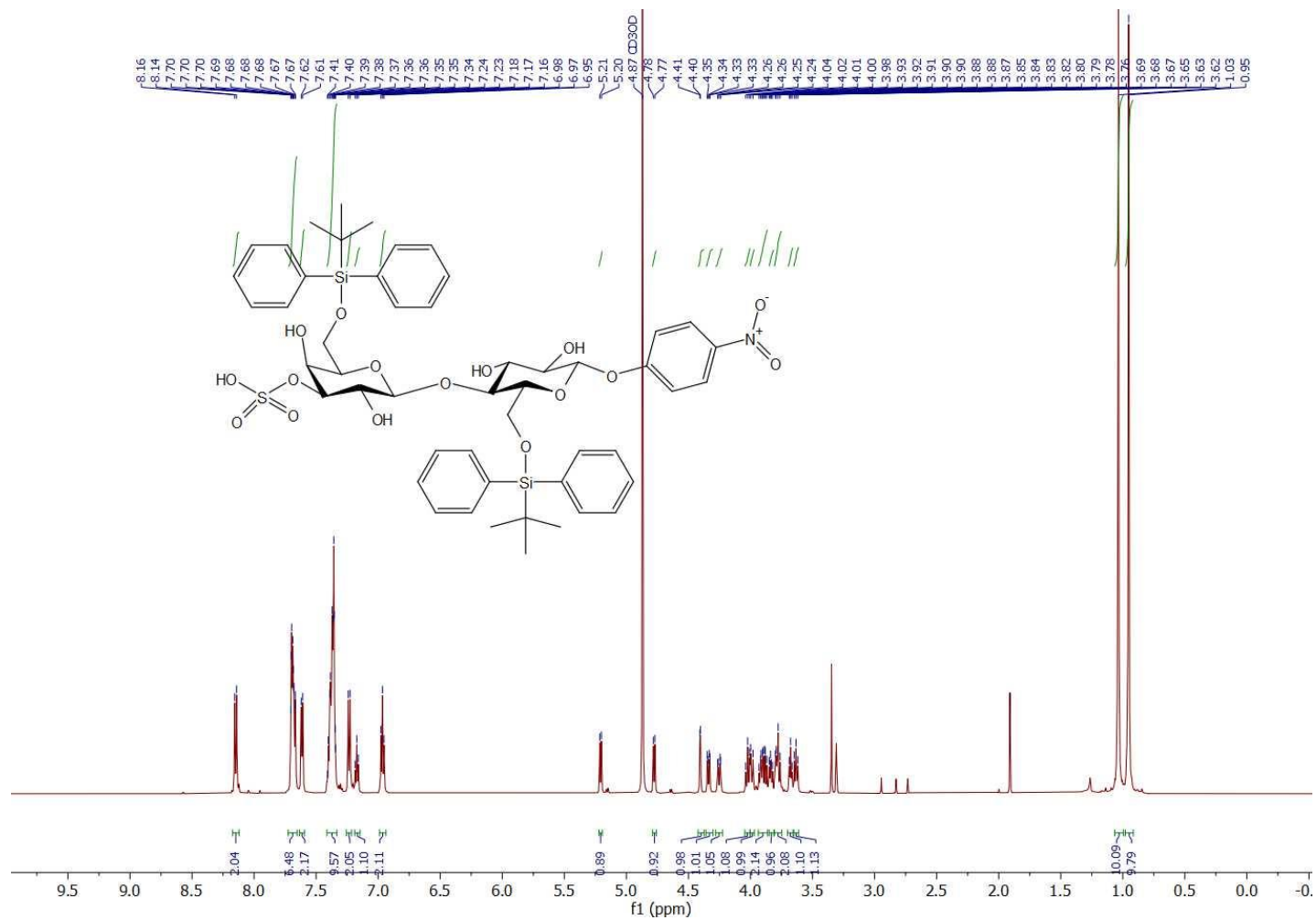


Figure 6.92 ^1H NMR (600 MHz, CD_3OD) spectrum of compound 3.60.

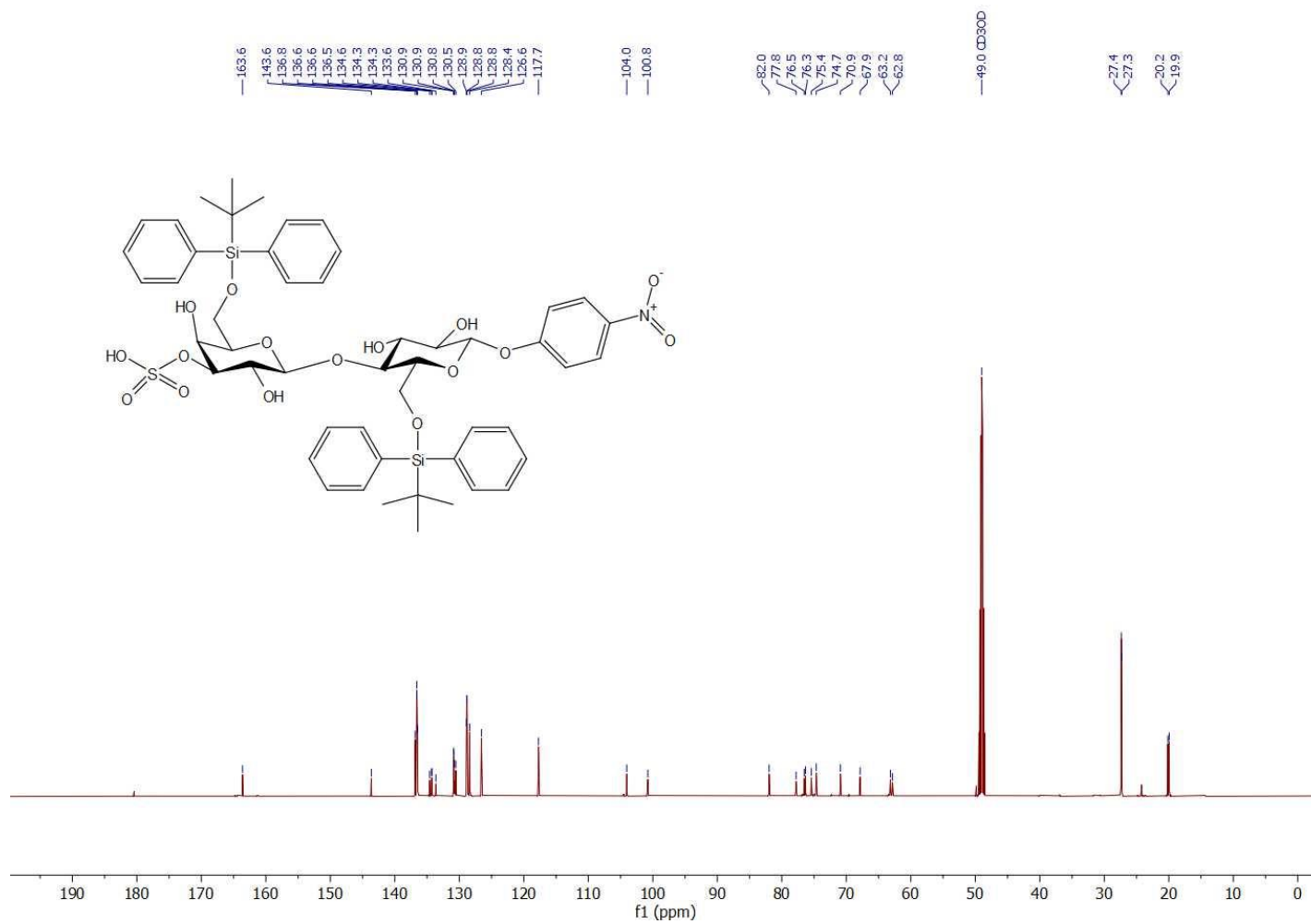


Figure 6.93 ^{13}C NMR (150 MHz, CD_3OD) spectrum of compound 3.60.

Compound Table

Compound Label	RT	Mass	Abund	Formula	Tgt Mass	Diff (ppm)
Cpd 1: C ₅₀ H ₆₁ N O ₁₆ S Si ₂	0.11	<u>1019.325</u>	4751	<u>C₅₀H₆₁N O₁₆S Si₂</u>	<u>1019.325</u>	0.09

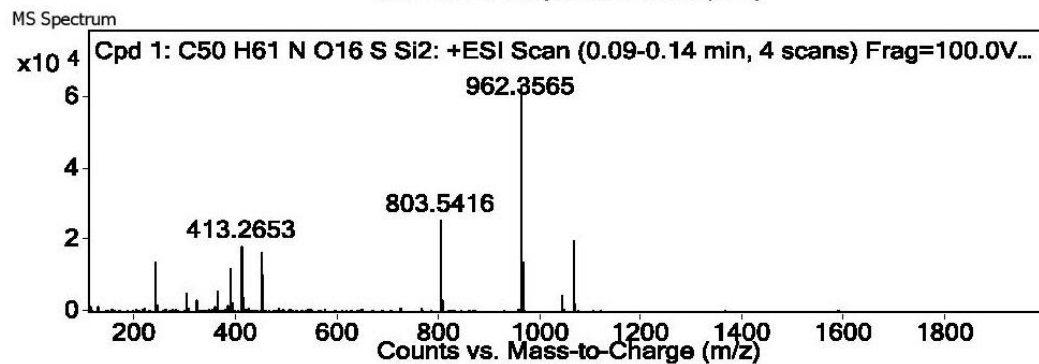
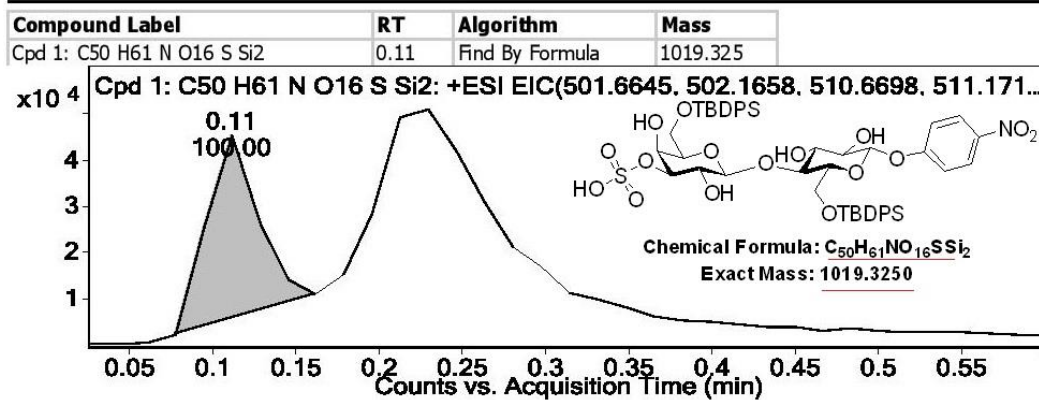
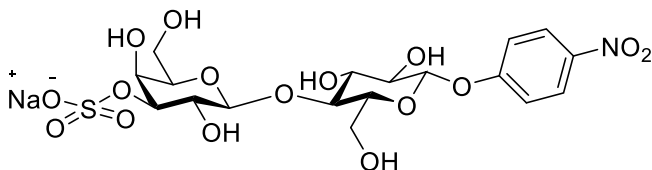


Figure 6.94 HRMS spectrum of compound 3.60.

4-Nitrophenyl (3-*O*-sulfo- β -D-galactopyranosyl)-(1 \rightarrow 4) - β -D-glucopyranoside sodium salt (**3.61**).



Following the general procedure D, compound **3.61** was obtained as a white solid (0.04 g, 0.067 mmol, 74 %).

$R_f = 0.38$, (EtOAc/*i*PrOH/H₂O : 5/6/2.5)

$[\alpha]_D^{22} = -12.7$ (c 0.005, H₂O)

¹H NMR (600 MHz, D₂O): δ (ppm) 8.26 (d, $J = 9.2$ Hz, 2H), 7.26 (d, $J = 9.3$ Hz, 2H), 5.31 (d, $J = 7.8$ Hz, 1H), 4.63 (d, $J = 7.8$ Hz, 1H), 4.38 (dd, $J = 9.9, 3.2$ Hz, 1H), 4.33 (d, $J = 3.1$ Hz, 1H), 4.04 (d, $J = 10.6$ Hz, 1H), 3.92 – 3.78 (m, 7H), 3.76 – 3.69 (m, 2H)

¹³C NMR (150 MHz, D₂O): δ (ppm) 161.7, 142.6, 126.1, 116.5, 102.6, 99.3, 80.0, 77.9, 75.1, 75.0, 74.1, 72.5, 69.1, 66.9, 61.0, 59.8

ESI-HRMS: m/z calcd. for C₁₈H₂₅NO₁₆S [M+Na]⁺, 566.0786; found 566.0784 [M+Na]⁺

The spectroscopic data agreed well with those of the literature.²³⁶

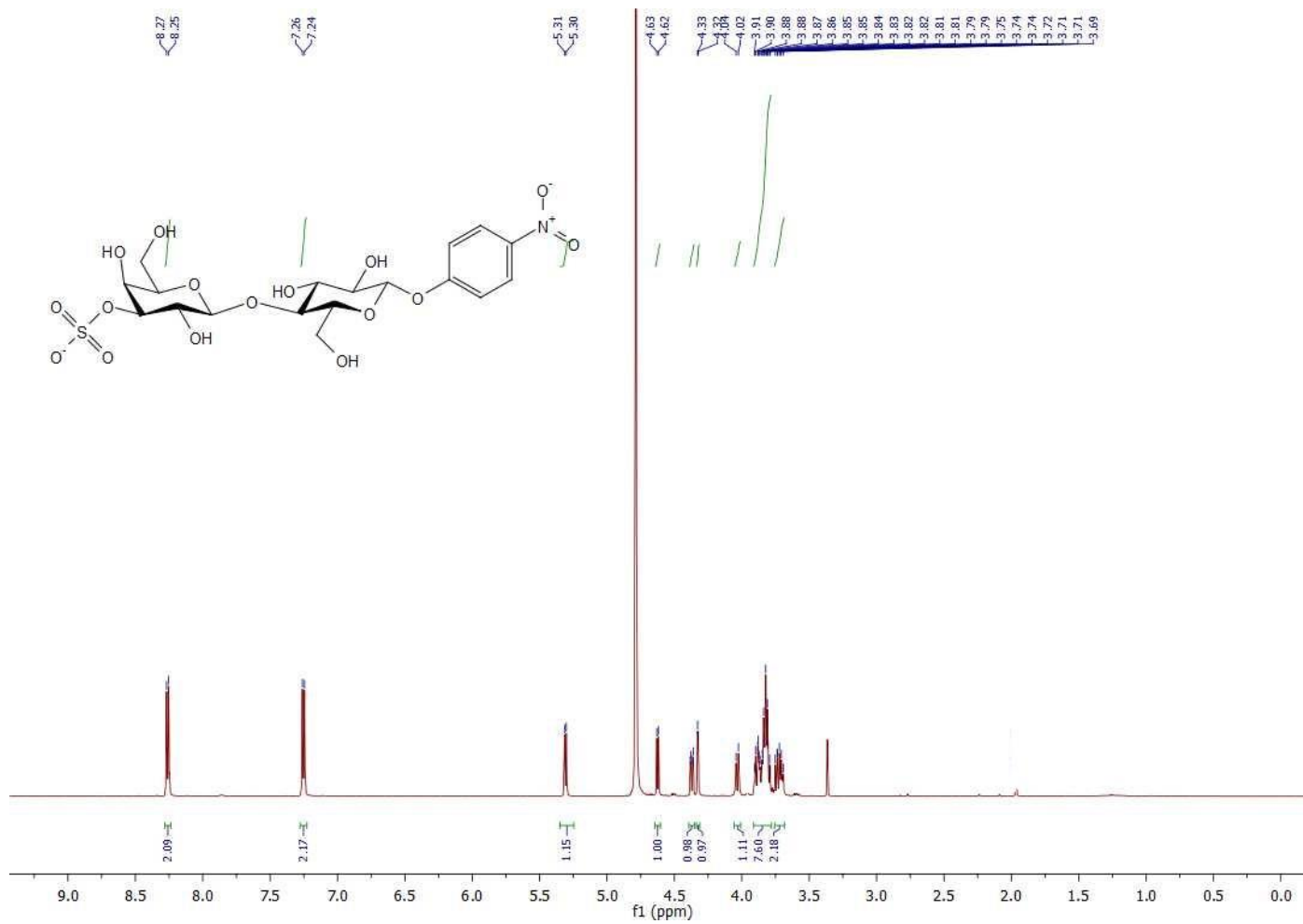


Figure 6.95 ¹H NMR (600 MHz, D₂O) spectrum of compound 3.61.

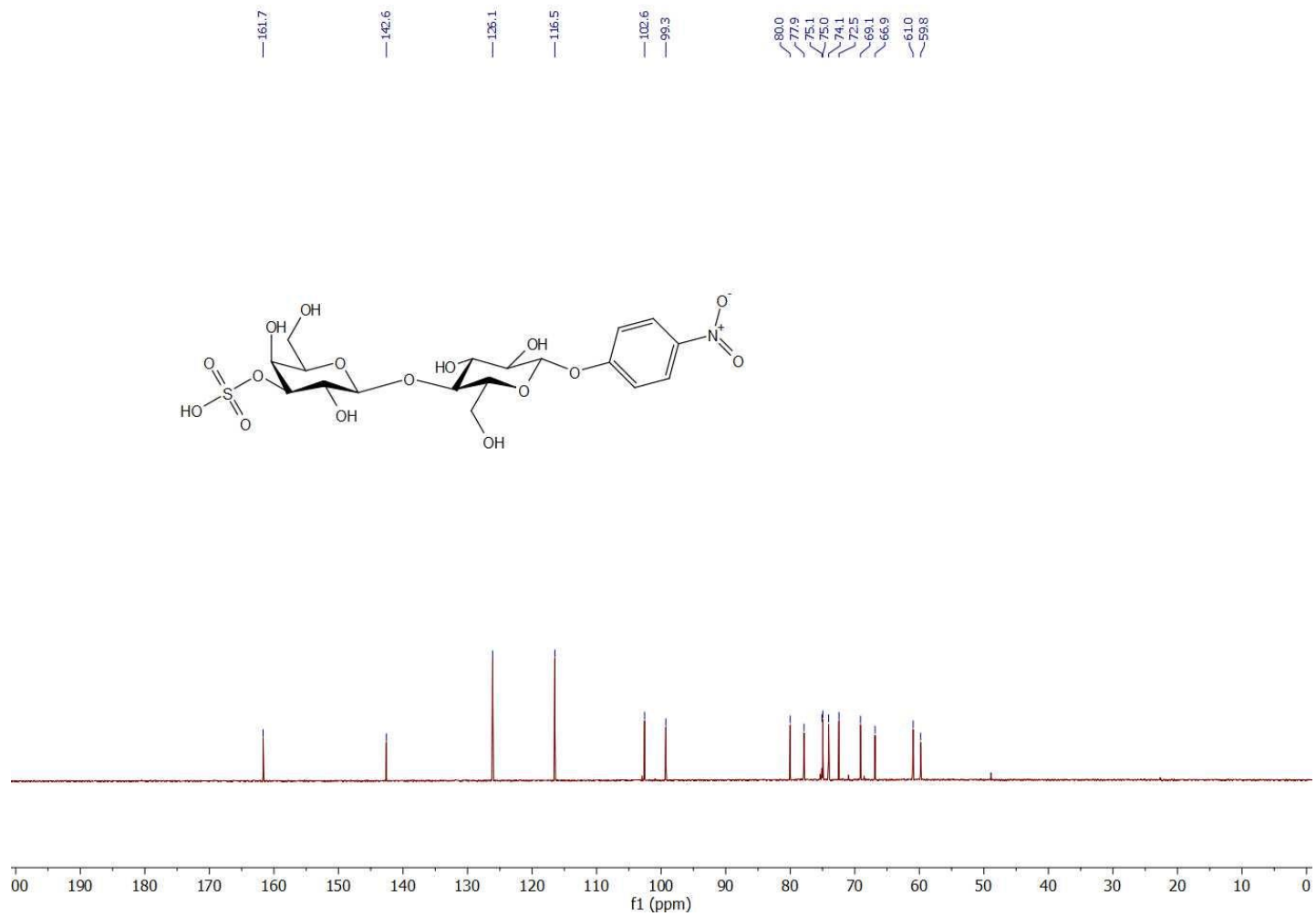
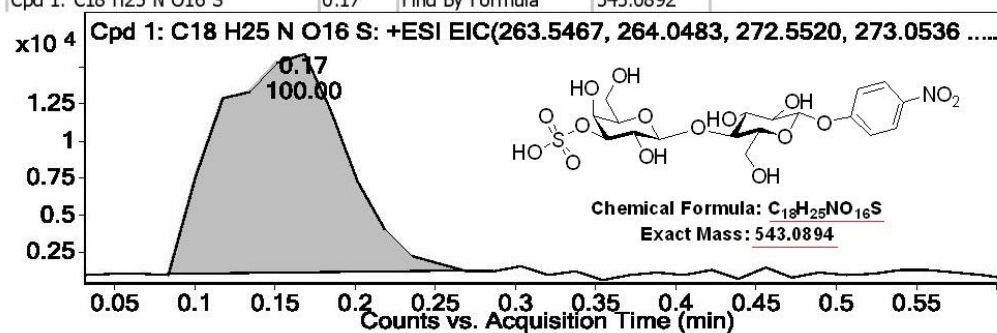


Figure 6.96 ^{13}C NMR (150 MHz, D_2O) spectrum of compound 3.61.

Compound Table

Compound Label	RT	Mass	Abund	Formula	Tgt Mass	Diff (ppm)
Cpd 1: C18 H25 N O16 S	0.17	<u>543.0892</u>	2782	<u>C18 H25 N O16 S</u>	<u>543.0894</u>	-0.35

Compound Label	RT	Algorithm	Mass
Cpd 1: C18 H25 N O16 S	0.17	Find By Formula	543.0892



MS Spectrum

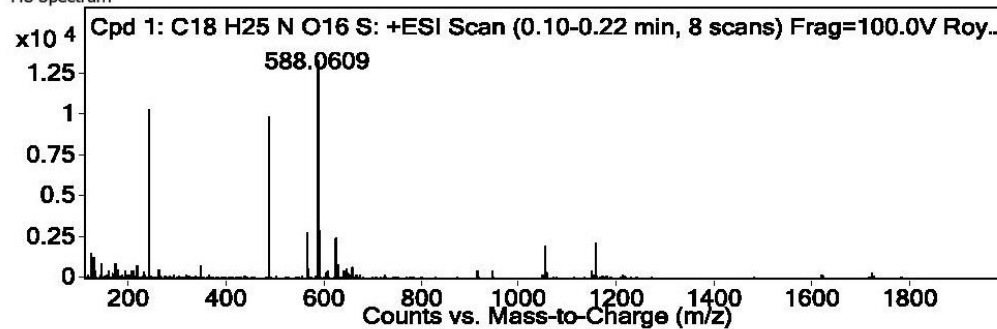
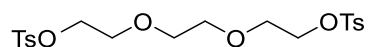


Figure 6.97 HRMS spectrum of compound 3.61.

6.4 Experimental Part of Chapter IV

6.4.1 Synthesis and characterization

2-[2-[2-[[[4-Methylphenyl)sulfonyl]oxy]ethoxy]ethoxy]ethyl
methylbenzenesulfonate (**4.117**) 4-



To a solution of triethylene glycol (PEG₃; 3.06 g, 20.4 mmol, 1 eq.) and TsCl (7.78 g, 40.8 mmol, 2 eq.) in DCM (35 mL) was added portionwise powdered KOH (9.16 g, 163.3 mmol, 8 eq.) at 0 °C and resulted mixture was stirred at the same temperature for 3 h. After addition of water (30 mL), organic phase was extracted with DCM (2 x 50 mL), dried over Na₂SO₄ and concentrated *in-vacuo*. Recrystallization from MeOH afforded **4.117** (8.97 g, 19.56, 96 %) as white solid.

¹H NMR (300 MHz, CDCl₃): δ (ppm) 7.77 (d, *J* = 8.3 Hz, 4H), 7.33 (d, *J* = 8.0 Hz, 4H), 44.16 – 4.05 (m, 4H), 3.69 – 3.59 (m, 4H), 3.50 (s, 4H), 2.43 (s, 6H)

¹³C NMR (75 MHz, CDCl₃): δ (ppm) 145.0, 133.0, 129.9, 128.0, 70.7, 69.3, 68.8, 21.7

The spectroscopic data agreed well with those of the literature.⁵⁶⁸

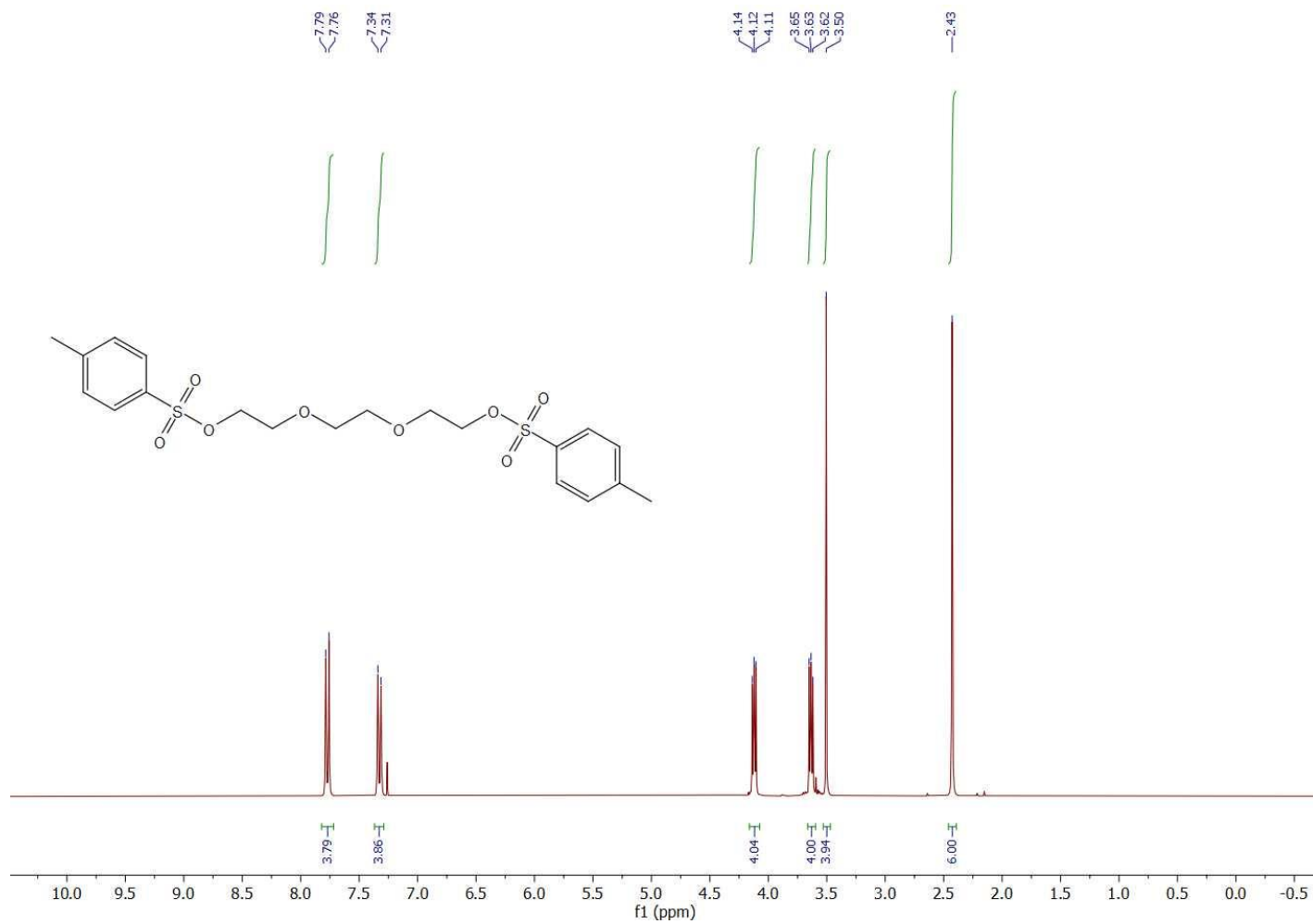


Figure 6.98 ^1H NMR (300 MHz, CDCl_3) spectrum of compound 4.117.

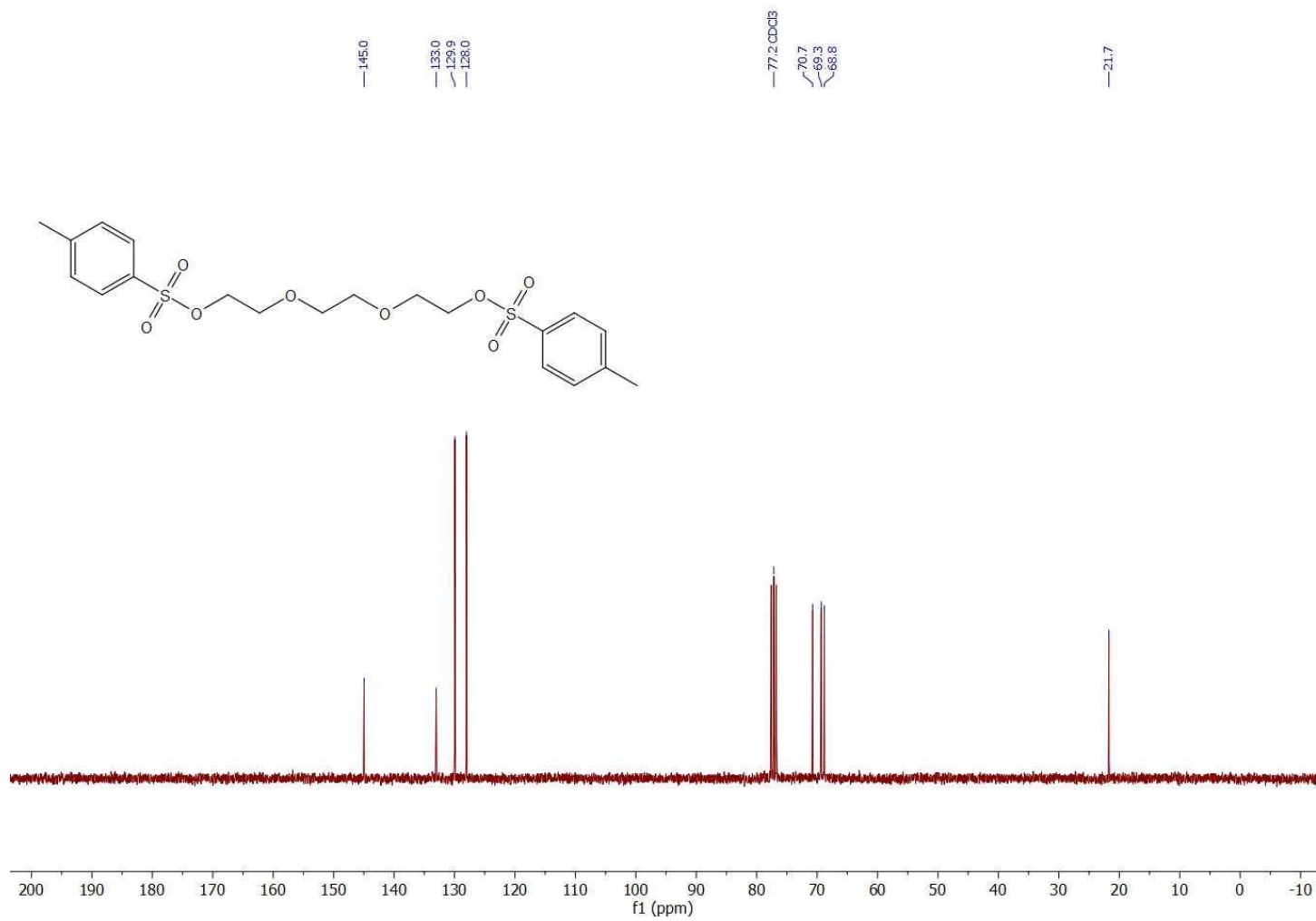
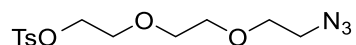


Figure 6.99. ¹³C NMR (75 MHz, CDCl₃) spectrum of compound 4.117.

2-[2-(2-Azidoethoxy)ethoxy]ethyl 4-methylbenzenesulfonate (**4.118**)

To a solution of **4.117** (4.56 g, 9.94 mmol, 1 eq.) in dry DMF (70 mL) was added NaN₃ (0.71 g, 10.87 mmol, 1.09 eq.) added at room temperature under nitrogen atmosphere and resulted mixture was stirred at 80 °C overnight. The reaction was cooled down to room temperature, quenched by addition of water (40 mL), and organic phase was extracted with DCM (4 x 100 mL), dried over Na₂SO₄ and concentrated *in-vacuo*. After chromatographic purification compound **4.118** (2.42 g, 7.36 mmol, 74 %) as colorless oil.

R_f = 0.37, (EtOAc/heptane : 4/6)

¹H NMR (300 MHz, CDCl₃): δ (ppm) 7.71 (d, *J* = 8.3 Hz, 2H), 7.27 (d, *J* = 8.0 Hz, 2H), 4.07 (dd, *J* = 5.4, 4.1 Hz, 2H), 3.64 – 3.57 (m, 2H), 3.55 (dd, *J* = 5.5, 4.5 Hz, 2H), 3.50 (s, 4H), 3.32 – 3.23 (m, 2H), 2.36 (s, 3H)

¹³C NMR (75 MHz, CDCl₃): δ (ppm) 144.7, 132.7, 129.7, 127.7, 70.5, 70.3, 69.8, 69.2, 68.5, 50.4, 21.4

The spectroscopic data agreed well with those of the literature.⁵⁶⁷

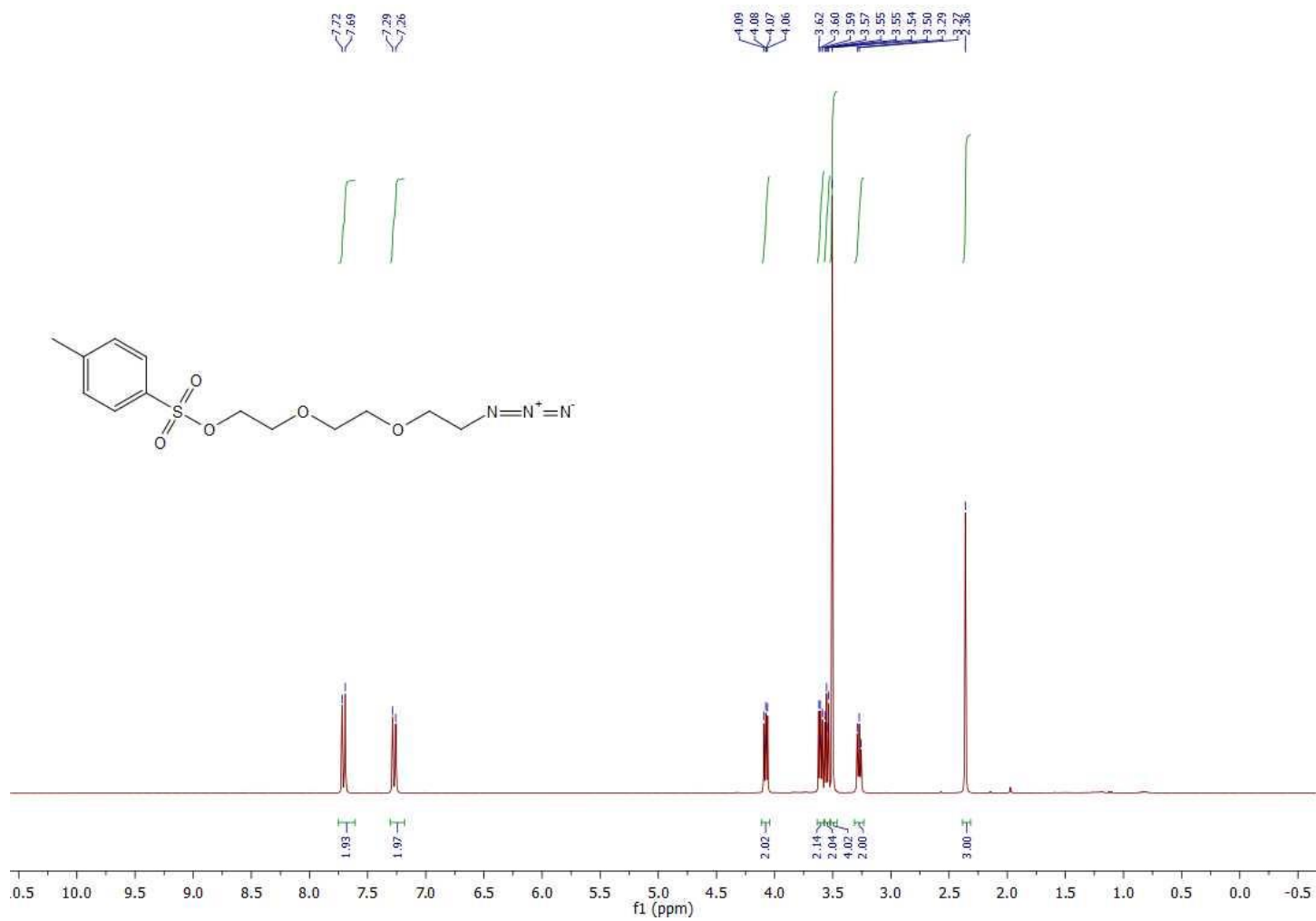


Figure 6.100 ^1H NMR (300 MHz, CDCl_3) spectrum of compound 4.118.

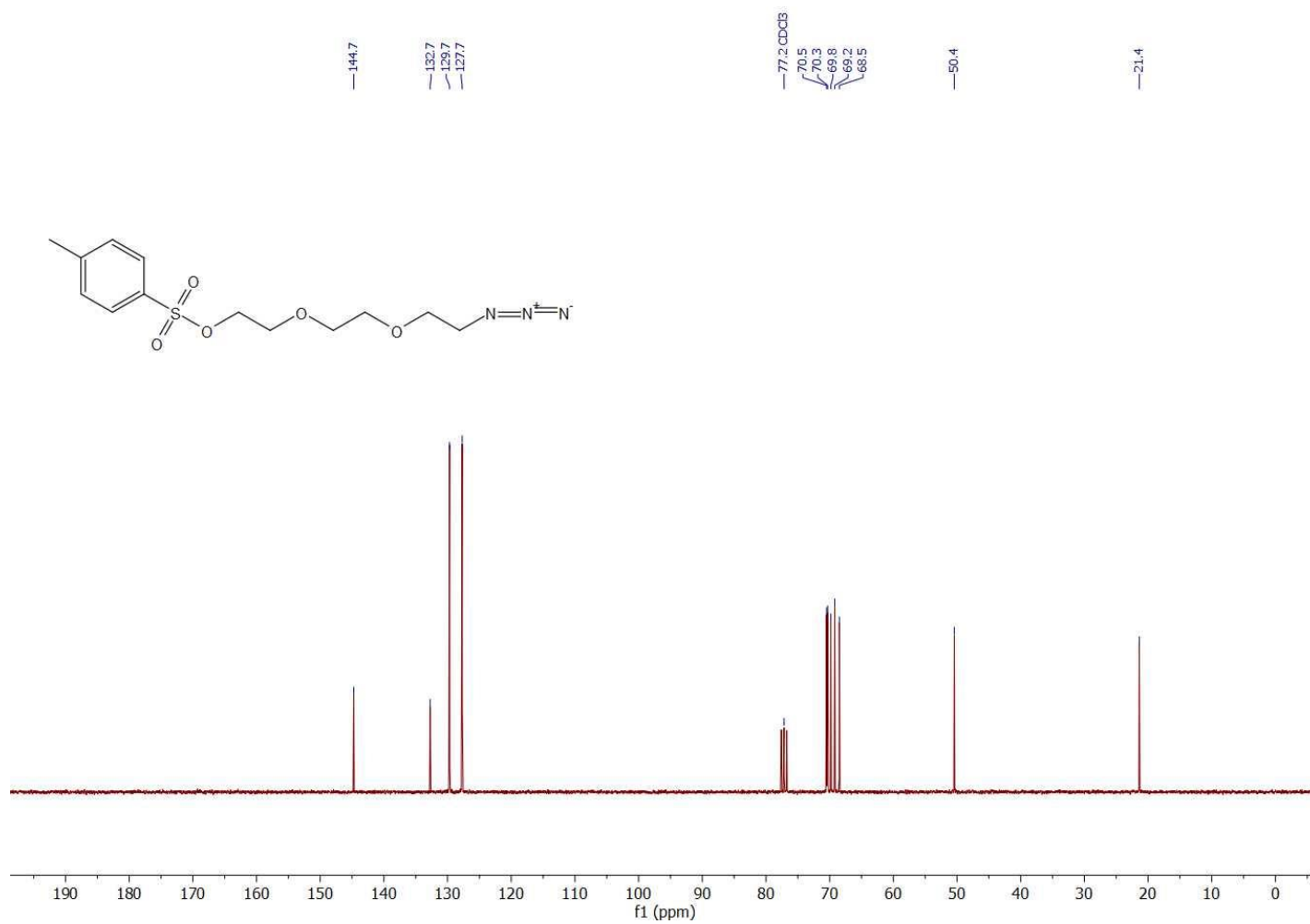
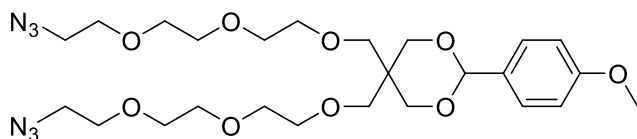


Figure 6.101 ¹³C NMR (75 MHz, CDCl₃) spectrum of compound 4.118.

5,5-bis((2-(2-(2-azidoethoxy)ethoxy)ethoxy)methyl)-2-(4-methoxyphenyl)-1,3-dioxane (**4.119**)



To a solution of **2.01** (0.34 g, 1.33 mmol, 1 eq.) in DMF (5 mL) was added NaH (60 % dispersion in mineral oil, 0.46 mg, 11.57 mmol, 8.7 eq.) at 0 °C under nitrogen atmosphere. After 30 minutes, a solution of **4.118** (1.09 g, 3.32 mmol, 2.5 eq.) in DMF (2.5 mL) was added dropwise and resulted reaction mixture was stirred at room temperature for 12 h. The reaction was quenched with water, organic phase was extracted with Et₂O (3 x 20 mL), washed with brine solution (20 mL), dried over Na₂SO₄, and concentrated *in-vacuo*. After chromatographic purification **4.119** (0.71 g, 1.25 mmol, 94 %) was obtained as colorless oil.

R_f = 0.29, (EtOAc/Hex : 7/3)

¹H NMR (300 MHz, CDCl₃): δ (ppm) 7.39 (d, *J* = 8.7 Hz, 2H), 6.88 (d, *J* = 8.7 Hz, 2H), 5.37 (s, 1H), 4.07 (d, *J* = 11.7 Hz, 2H), 3.87 (d, *J* = 11.7 Hz, 2H), 3.79 (s, 3H), 3.77 (s, 2H), 3.73 – 3.59 (m, 18H), 3.60 – 3.50 (m, 2H), 3.44 – 3.31 (m, 4H), 3.30 (s, 2H)

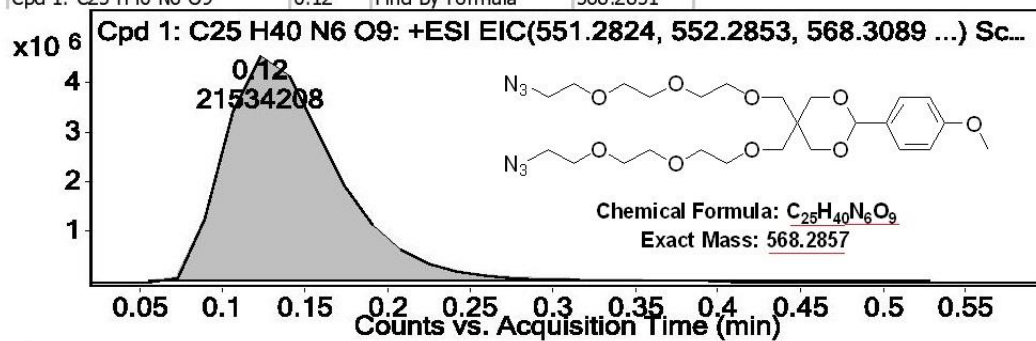
¹³C NMR (75 MHz, CDCl₃): δ (ppm) 160.1, 131.1, 127.5, 113.7, 101.7, 71.3, 71.1, 70.9, 70.8, 70.8, 70.8, 70.6, 70.6, 70.2, 70.1, 70.0, 69.9, 55.4, 50.8, 39.0

ESI-HRMS: *m/z* calcd. for C₂₅H₄₀N₆O₉ [M+Na]⁺, 591.2749; found 591.2744 [M+Na]⁺

Compound Table

Compound Label	RT	Mass	Abund	Formula	Tgt Mass	Diff (ppm)
Cpd 1: C ₂₅ H ₄₀ N ₆ O ₉	0.12	568.2851	283348	C ₂₅ H ₄₀ N ₆ O ₉	568.2857	-1.07

Compound Label	RT	Algorithm	Mass
Cpd 1: C ₂₅ H ₄₀ N ₆ O ₉	0.12	Find By Formula	568.2851



MS Spectrum

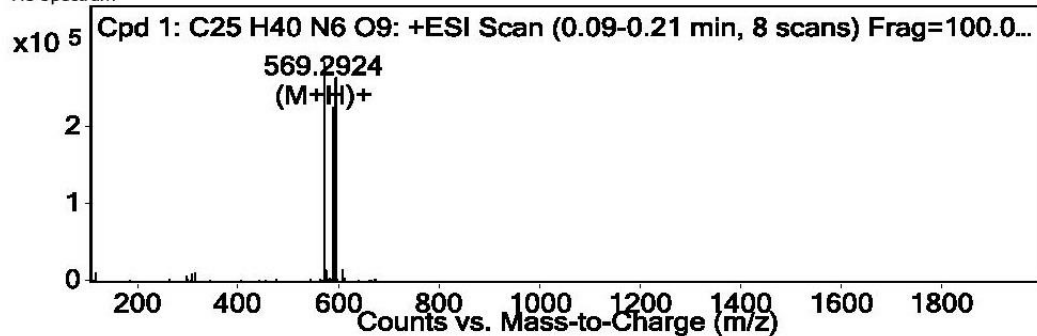
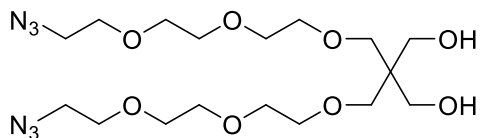


Figure 6.104 HRMS spectrum of compound 4.119.

2,2-bis((2-(2-(2-azidoethoxy)ethoxy)ethoxy)methyl)propane-1,3-diol (**4.120**)

4.119 (0.32 g, 0.57 mmol) was dissolved in AcOH/H₂O (v/v : 8/2; 10 mL) and the reaction mixture was stirred at 50 °C for 3.5 h until TLC revealed complete conversion of the starting material. After concentration in-vacuo, the residue was subjected to column chromatography and **4.120** (0.22 g, 0.5 mmol, 88 %) was obtained as colorless oil.

$R_f = 0.45$, (EtOAc/MeOH : 9.5/0.5)

¹H NMR (300 MHz, CDCl₃): δ (ppm) 3.67 – 3.51 (m, 24H), 3.48 (s, 4H), 3.39 – 3.30 (m, 4H), 3.06 (s, 2H)

¹³C NMR (75 MHz, CDCl₃): δ (ppm) 72.3, 70.7, 70.6, 70.5, 70.3, 70.0, 64.4, 50.6, 45.2

ESI-HRMS: m/z calcd. for C₁₇H₃₄N₆O₈ [M+H]⁺, 451.2511; found 451.2512 [M+H]⁺

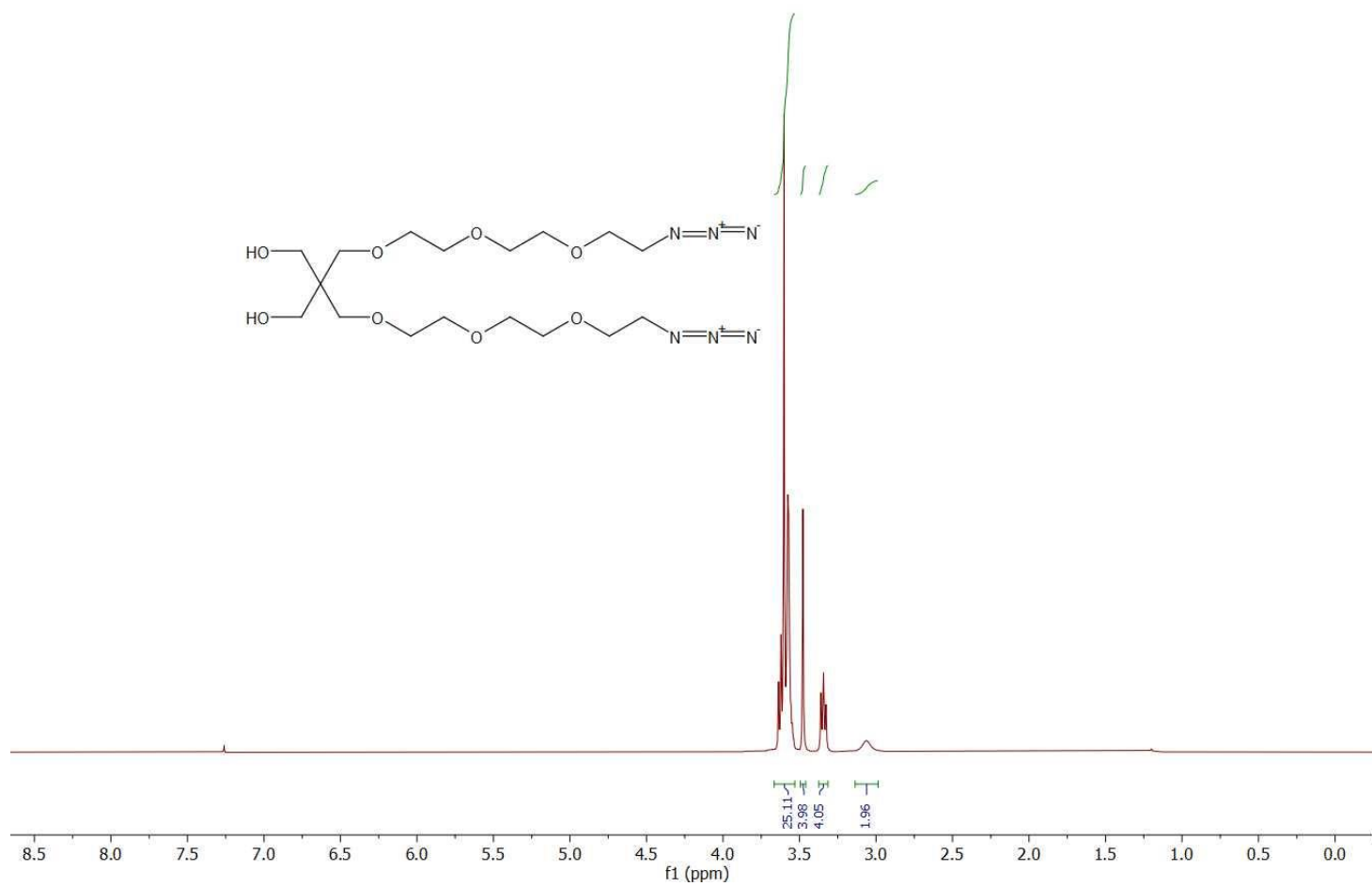


Figure 6.105 ^1H NMR (300 MHz, CDCl_3) spectrum of compound 4.120.

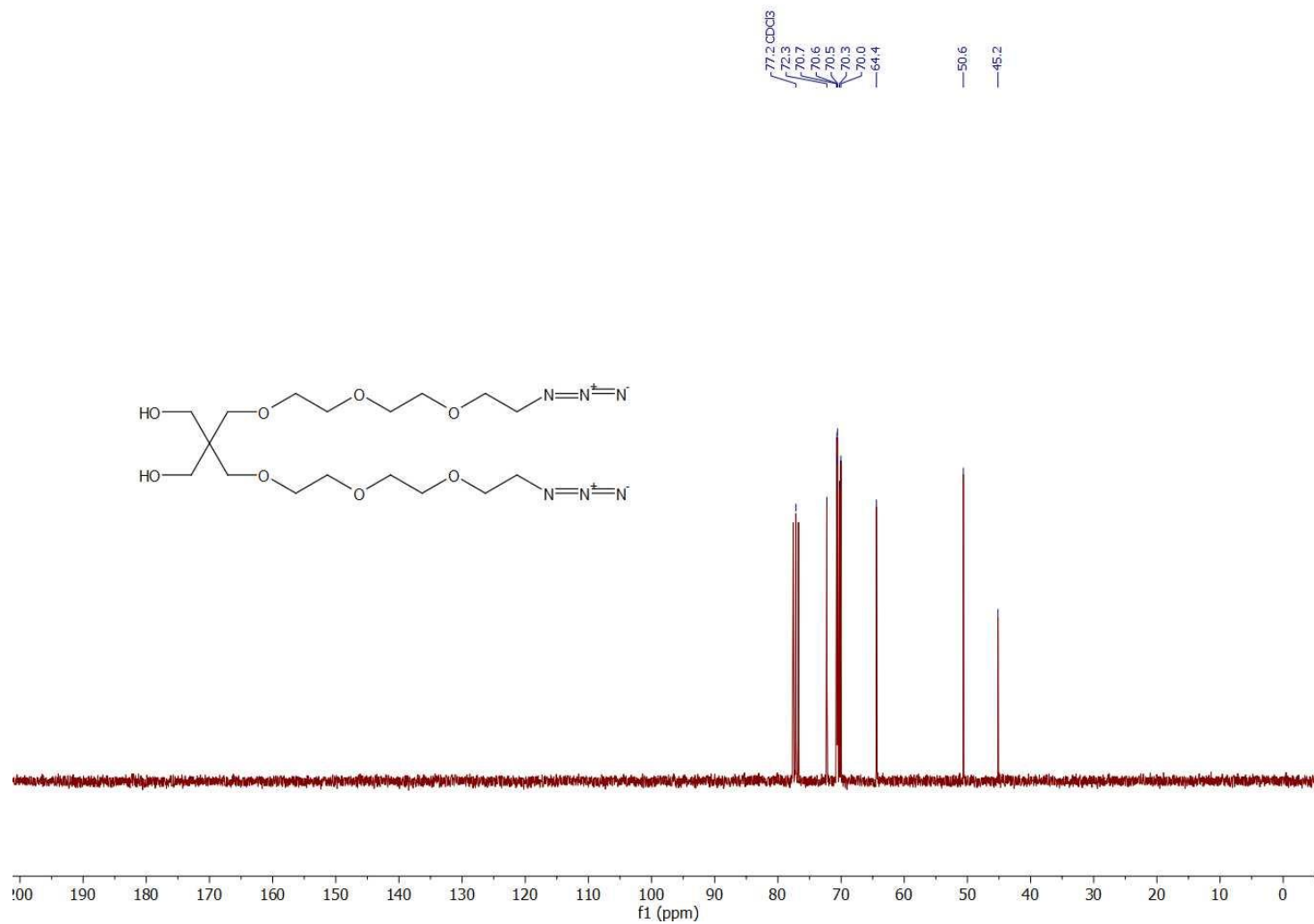
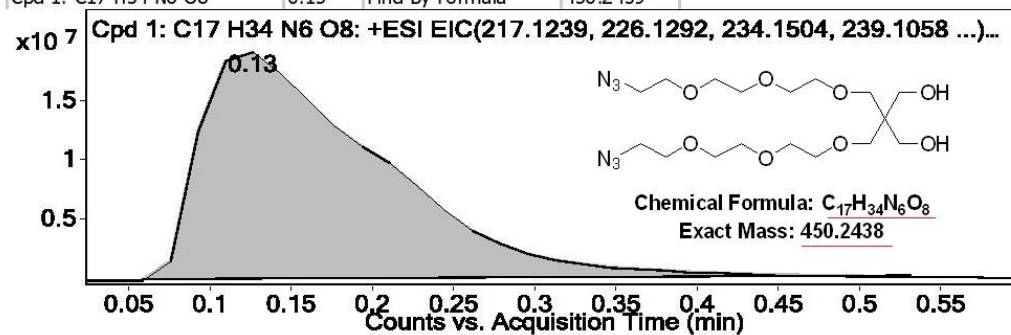


Figure 6.106 ^{13}C NMR (75 MHz, CDCl_3) spectrum of compound 4.120.

Compound Table

Compound Label	RT	Mass	Abund	Formula	Tgt Mass	Diff (ppm)
Cpd 1: C ₁₇ H ₃₄ N ₆ O ₈	0.13	<u>450.2439</u>	721306	<u>C₁₇H₃₄N₆O₈</u>	<u>450.2438</u>	0.13

Compound Label	RT	Algorithm	Mass
Cpd 1: C ₁₇ H ₃₄ N ₆ O ₈	0.13	Find By Formula	450.2439



MS Spectrum

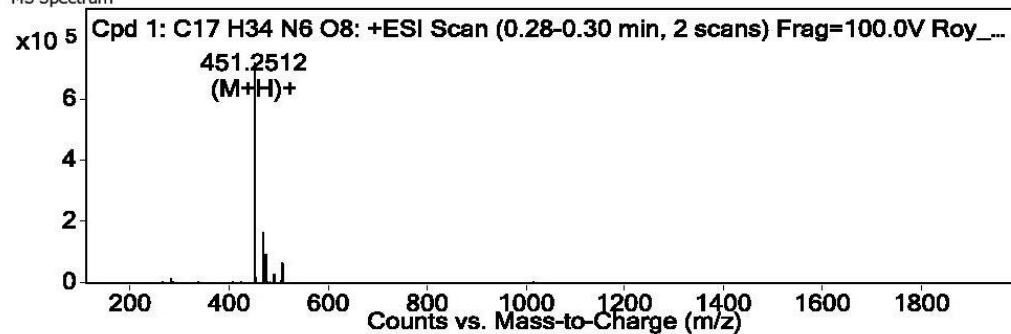
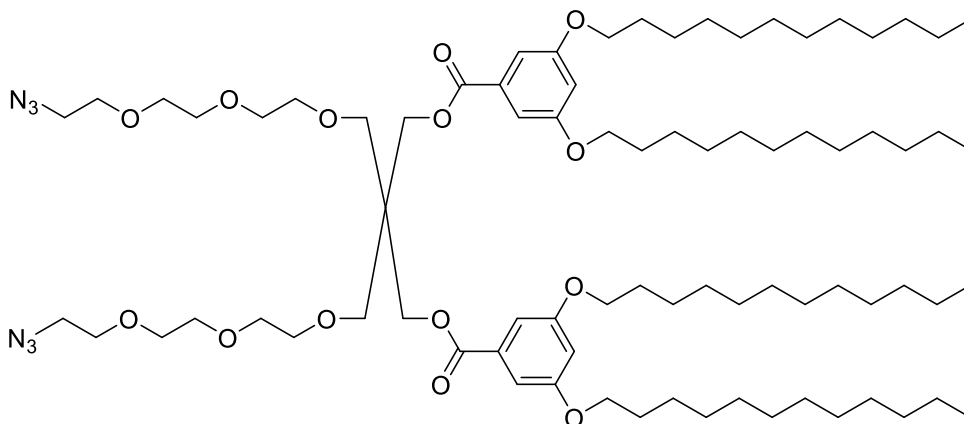


Figure 6.107 HRMS spectrum of compound 4.120.

2,2-bis((2-(2-(2-azidoethoxy)ethoxy)ethoxy)methyl)propane-1,3-diyl bis(3,5-bis(dodecyloxy)benzoate) (**4.121**)



To a solution of **4.120** (0.12 g, 0.27 mmol 1 eq.), **2.06** (0.33 g, 0.67 mmol, 2.5 eq.) and DMAP (0.05 g, 0.4 mmol, 1.5 eq.) in DCM (3.5 mL) was added dropwise a solution of DCC (0.16 g, 0.78 mmol, 2.9 eq.) in DCM (1.5 mL) under nitrogen atmosphere. After 18 h of stirring at room temperature, the reaction mixture was diluted in DCM (20 mL), washed with water (10 mL), dried over Na₂SO₄ and concentrated *in-vacuo*. After chromatographic purification **4.121** (0.35 g, 0.25 mmol, 92 %) was obtained as colorless oil.

R_f = 0.39, (EtOAc/Hex : 7.5/2.5)

¹H NMR (300 MHz, CDCl₃): δ (ppm) 7.10 (d, *J* = 2.3 Hz, 4H), 6.62 (t, *J* = 2.3 Hz, 2H), 4.45 (s, 4H), 3.93 (t, *J* = 6.3 Hz, 8H), 3.64 – 3.60 (m, 24H), 3.35 (t, *J* = 4.8 Hz, 4H), 1.84 – 1.69 (m, 8H), 1.52 – 1.34 (m, 8H), 1.26 (s, 64H), 0.88 (t, *J* = 6.1 Hz, 12H)

¹³C NMR (75 MHz, CDCl₃): δ (ppm) 166.1, 160.2, 131.8, 107.7, 106.2, 71.3, 70.8, 70.7, 70.5, 70.1, 70.0, 68.3, 64.2, 50.6, 44.3, 31.9, 29.7, 29.7, 29.6, 29.6, 29.4, 29.4, 29.2, 26.1, 22.7, 14.1

ESI-HRMS: m/z calcd. for $C_{79}H_{138}N_6O_{14}$ $[M+H]^+$, 1396.0344; found 1396.0370
 $[M+H]^+$

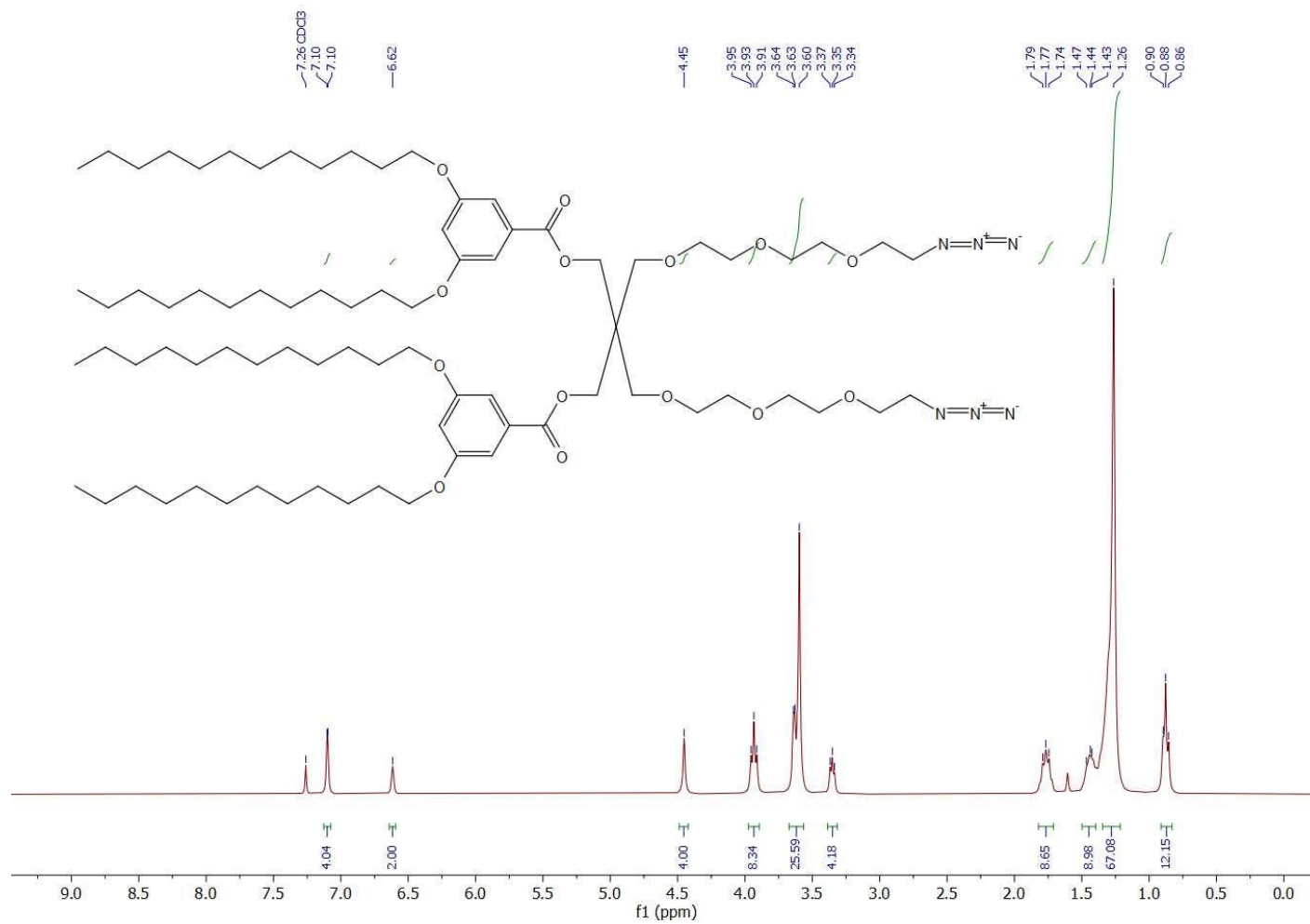


Figure 6.108 ^1H NMR (300 MHz, CDCl_3) spectrum of compound 4.121.

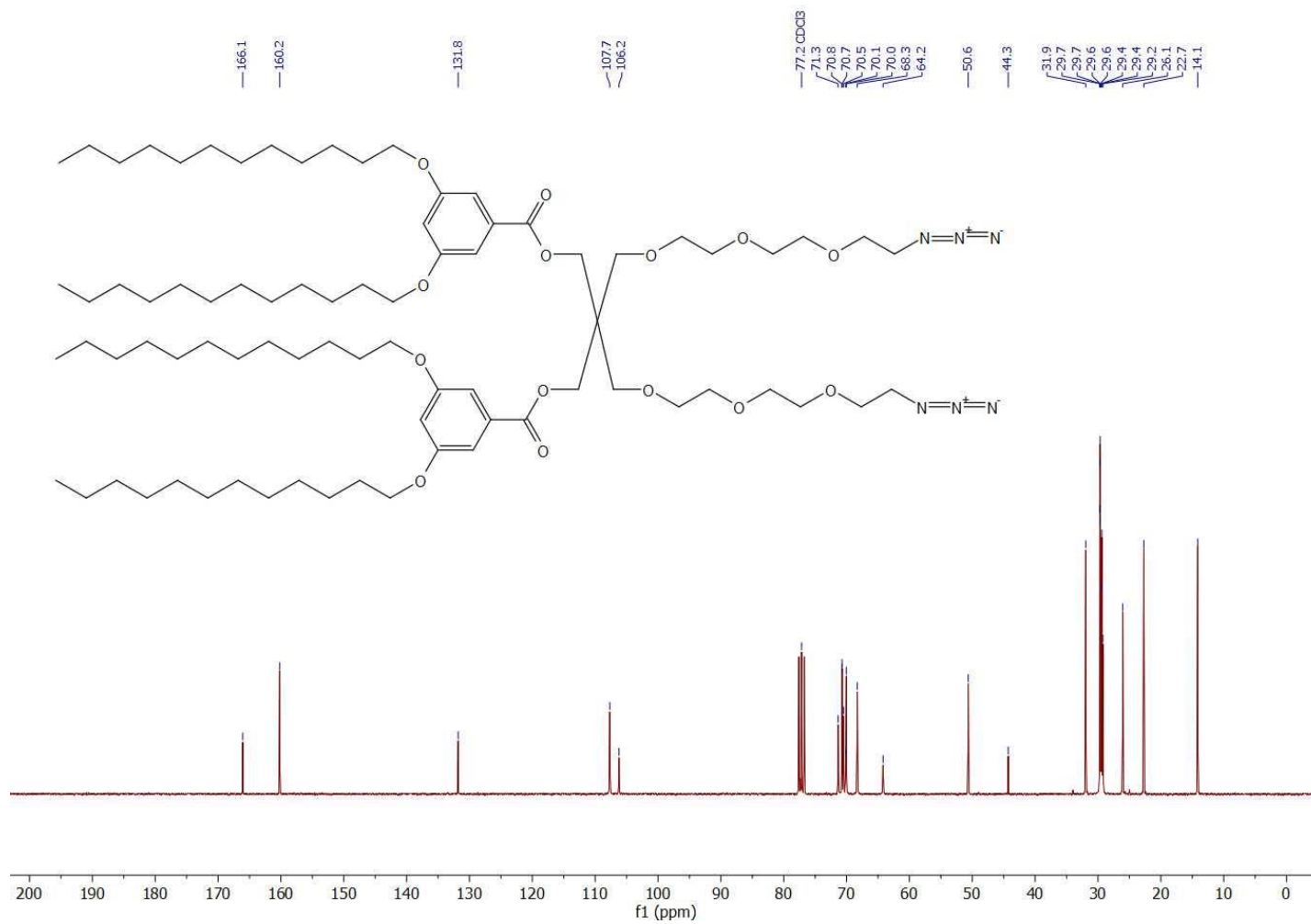


Figure 6.109 ¹³C NMR (75 MHz, CDCl₃) spectrum of compound **4.121**.

Compound Table

Compound Label	RT	Mass	Abund	Formula	Tgt Mass	Diff (ppm)
Cpd 1: C ₇₉ H ₁₃₈ N ₆ O ₁₄	0.13	<u>1395.0294</u>	1087	<u>C₇₉ H₁₃₈ N₆ O₁₄</u>	<u>1395.0271</u>	<u>1.66</u>

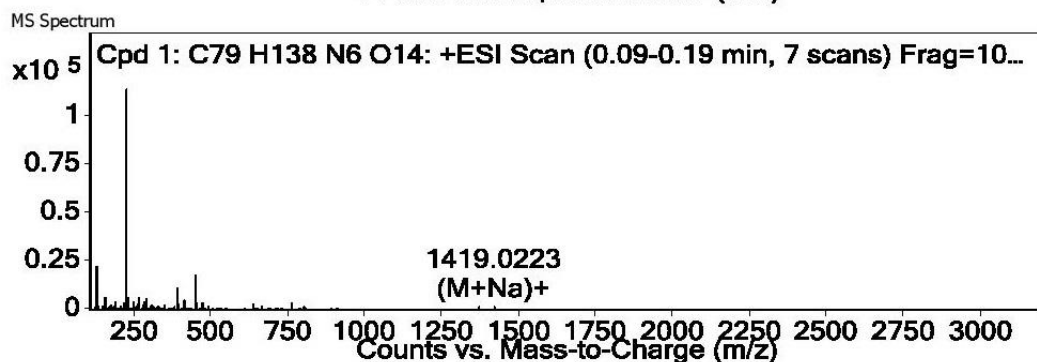
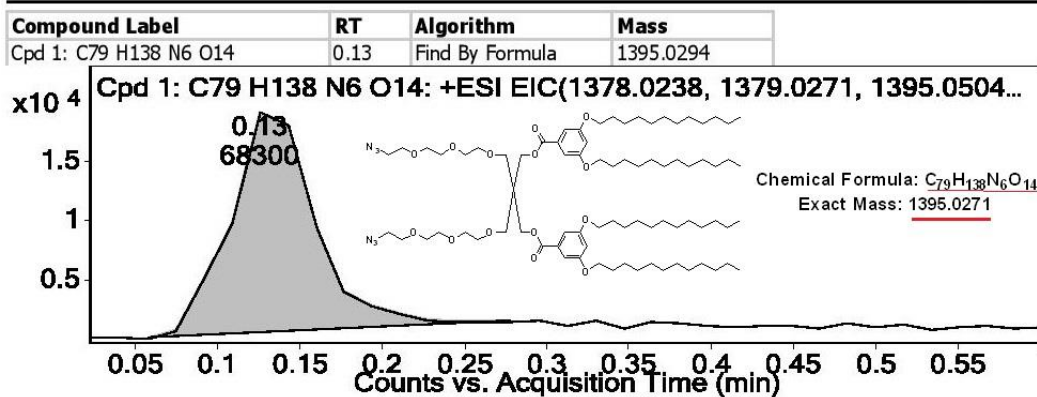
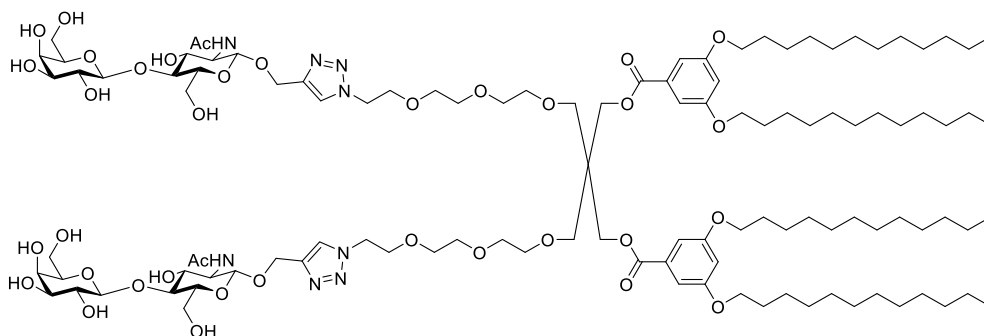


Figure 6.110 HRMS spectrum of compound 4.121.

LacNAc-JD (bislicked) (**4.109**)

To a solution of **4.121** (0.032mg, 0.023 mmol, 1 eq.) and **3.32** (21 mg, 0.050 mmol, 2.2 eq.) in THF/H₂O (3.5/0.5 mL) were added separately CuSO₄·5H₂O (10 mg, 0.040 mmol, 1.7 eq.) and sodium ascorbate (12 mg, 0.060 mmol, 2.6 eq.) in H₂O (0.1 mL each) at room temperature, under nitrogen atmosphere. After 48 h of stirring, the reaction mixture was concentrated *in-vacuo* and subjected to column chromatography (dry loading). Eluting with DCM/MeOH (10/1 to 6/4) afforded **4.113** (6.5 mg, 0.0036 mmol, 15 %) and **4.109** (10 mg, 0.0044 mmol, 19 %) as white solids.

¹H NMR (600 MHz, CDCl₃-CD₃OD): δ (ppm) 7.86 (s, 1H), 7.03 (d, *J* = 2.3 Hz, 4H), 6.60 (d, *J* = 2.3 Hz, 2H), 4.87 (d, *J* = 12.4 Hz, 2H), 4.57 – 4.46 (m, 4H), 4.45 (s, 4H), 4.41 – 4.26 (m, 5H), 3.92 – 3.38 (m, 48H), 1.92 (s, 6H), 1.85 – 1.64 (m, 6H), 1.48 – 1.34 (m, 8H), 1.24 (s, 64H), 0.85 (t, *J* = 6.6 Hz, 12H)

¹³C NMR (150 MHz, CDCl₃-CD₃OD): δ (ppm) 173.2, 167.2, 161.0, 132.3, 125.4, 108.4, 107.0, 104.4, 101.2, 80.3, 76.4, 75.9, 74.2, 73.7, 71.9, 71.1, 71.0, 70.9, 69.9, 69.8, 69.0, 65.4, 62.5, 62.1, 61.4, 56.0, 45.0, 32.6, 30.3, 30.3, 30.2, 30.2, 30.0, 30.0, 29.8, 26.7, 23.3, 23.0, 14.4

MALDI-HRMS: *m/z* calcd. for C₁₁₃H₁₉₂N₈O₃₆ [M+Na]⁺, 2260.3337; found 2260.3331 [M+Na]⁺

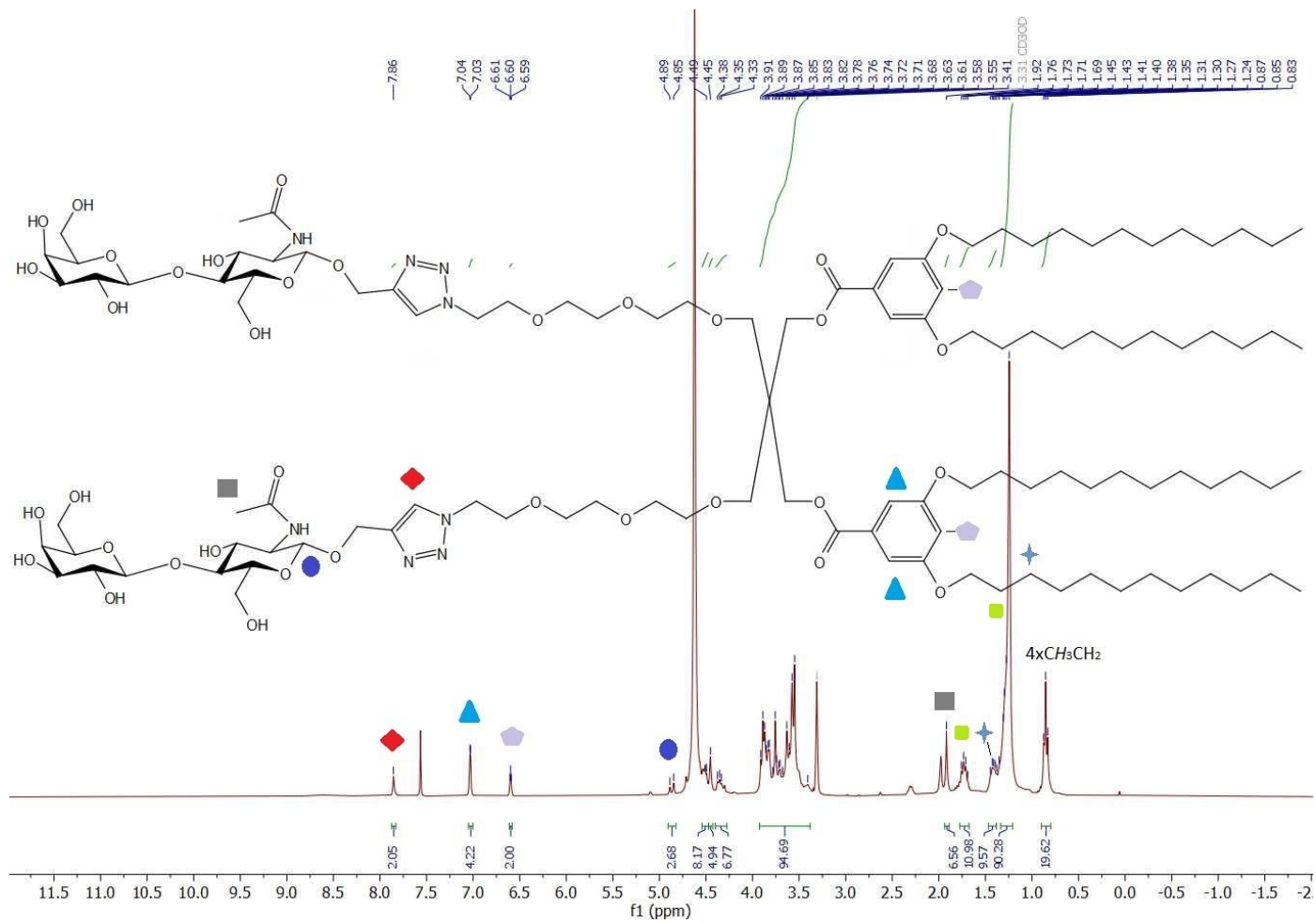


Figure 6.111 ¹H NMR (300 MHz, CD₃OD+CDCl₃ (v/v : 1/1)) spectrum of compound 4.109.

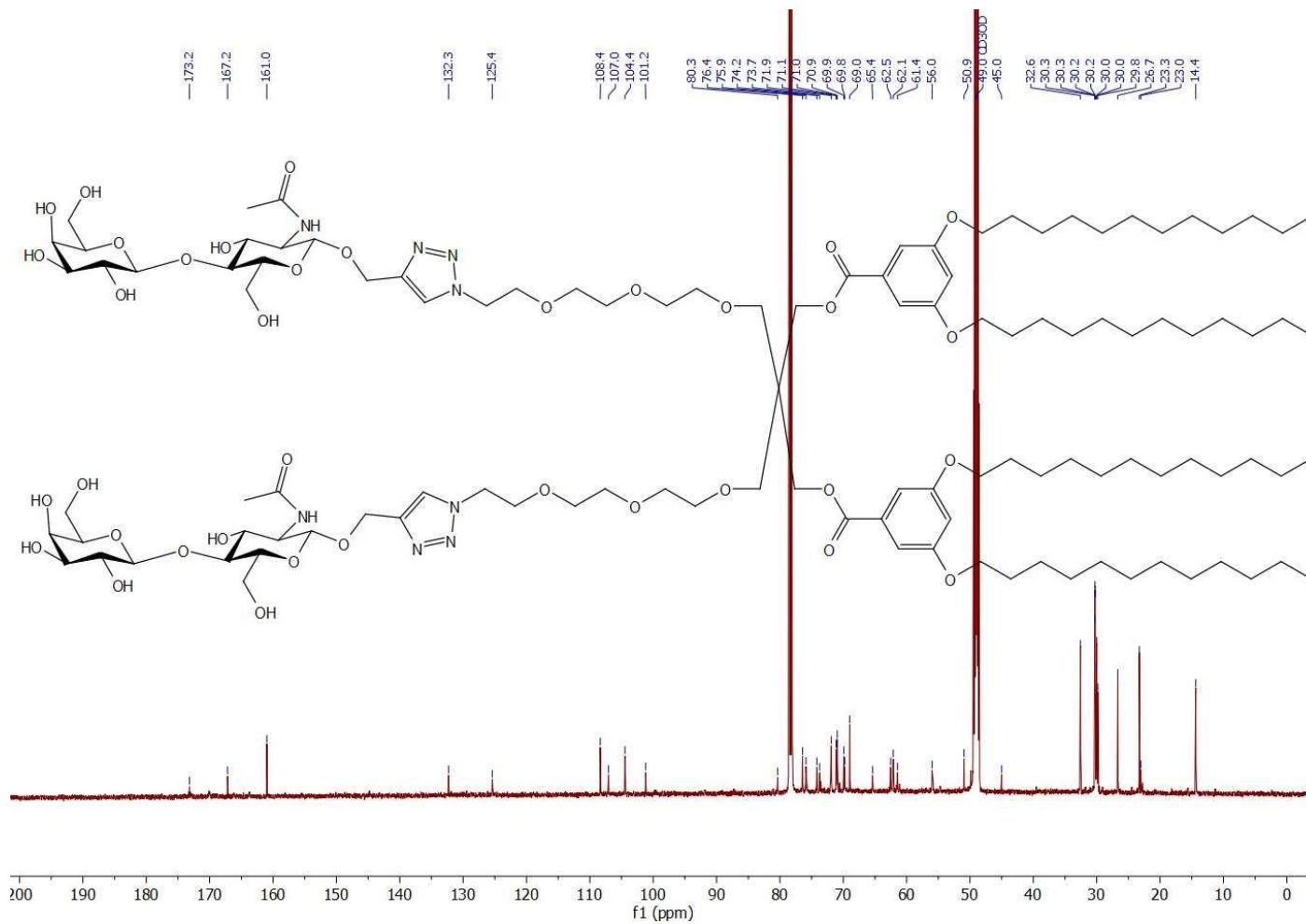


Figure 6.112 ¹³C NMR (150 MHz, CD₃OD+CDCl₃ (v/v : 1/1)) spectrum of compound 4.109.

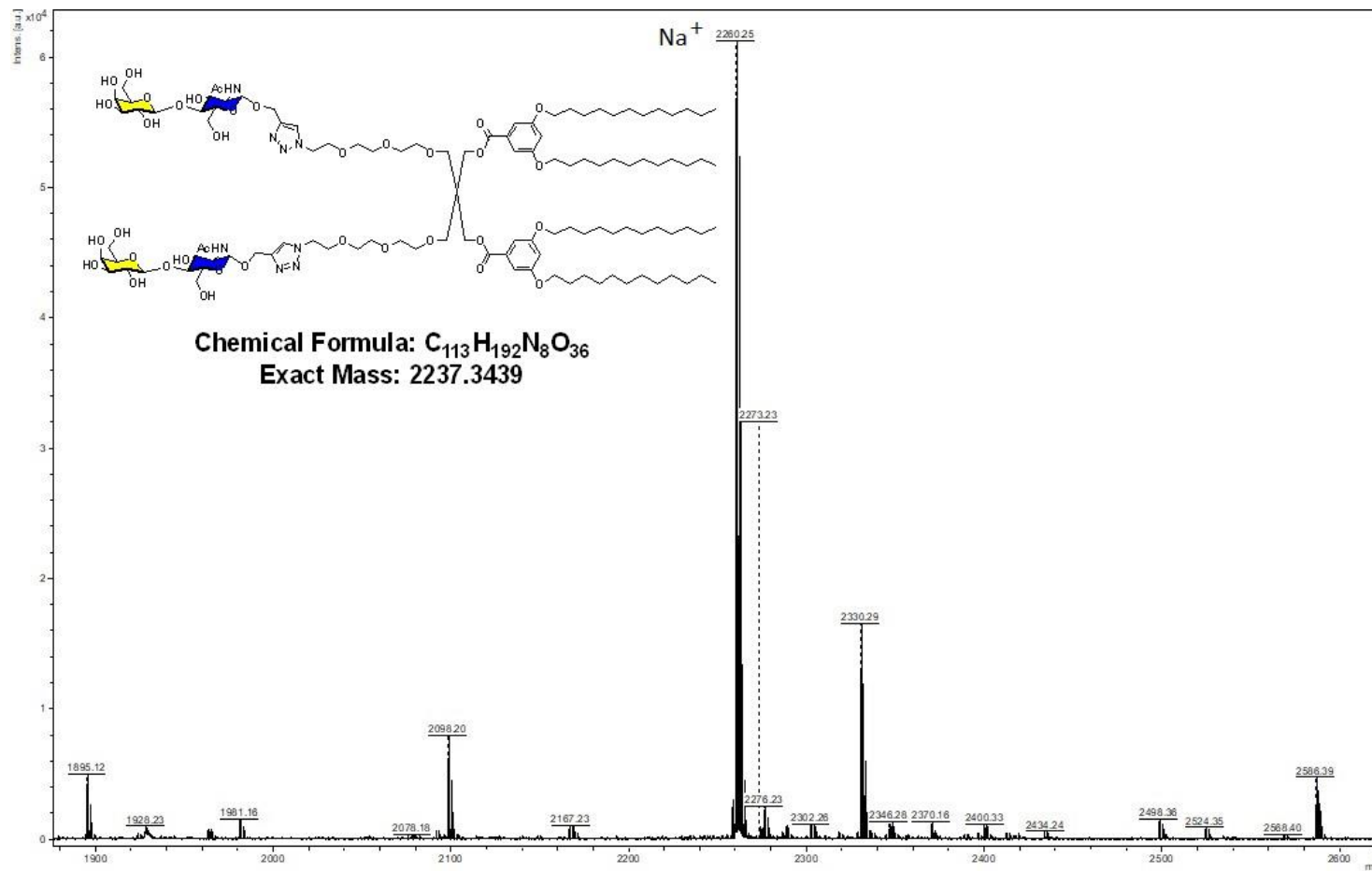


Figure 6.113 MALDI-TOF MS spectrum of compound 4.109.

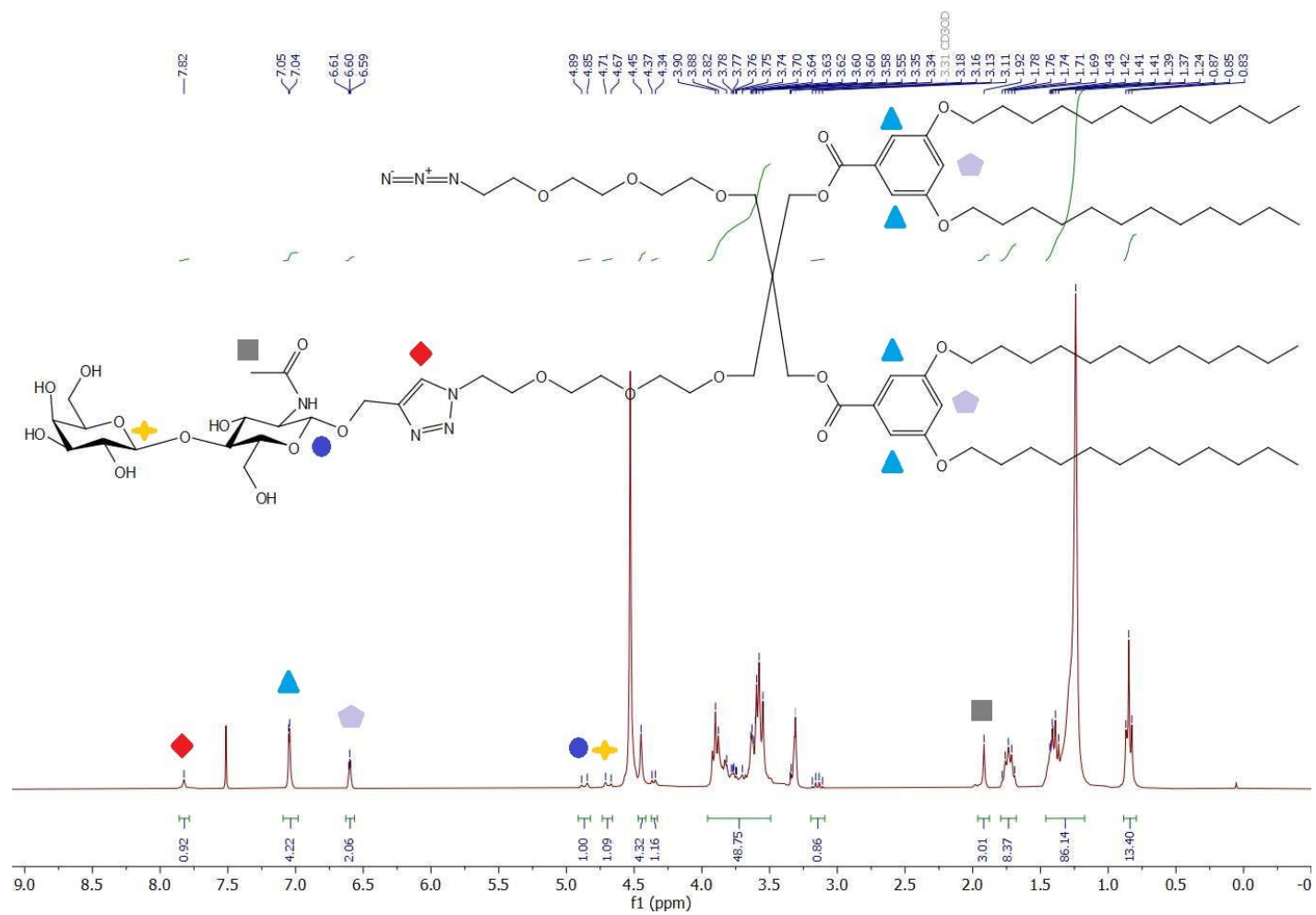


Figure 6.114 ^1H NMR (300 MHz, $\text{CD}_3\text{OD}+\text{CDCl}_3$ (v/v : 1/1)) spectrum of compound 4.113.

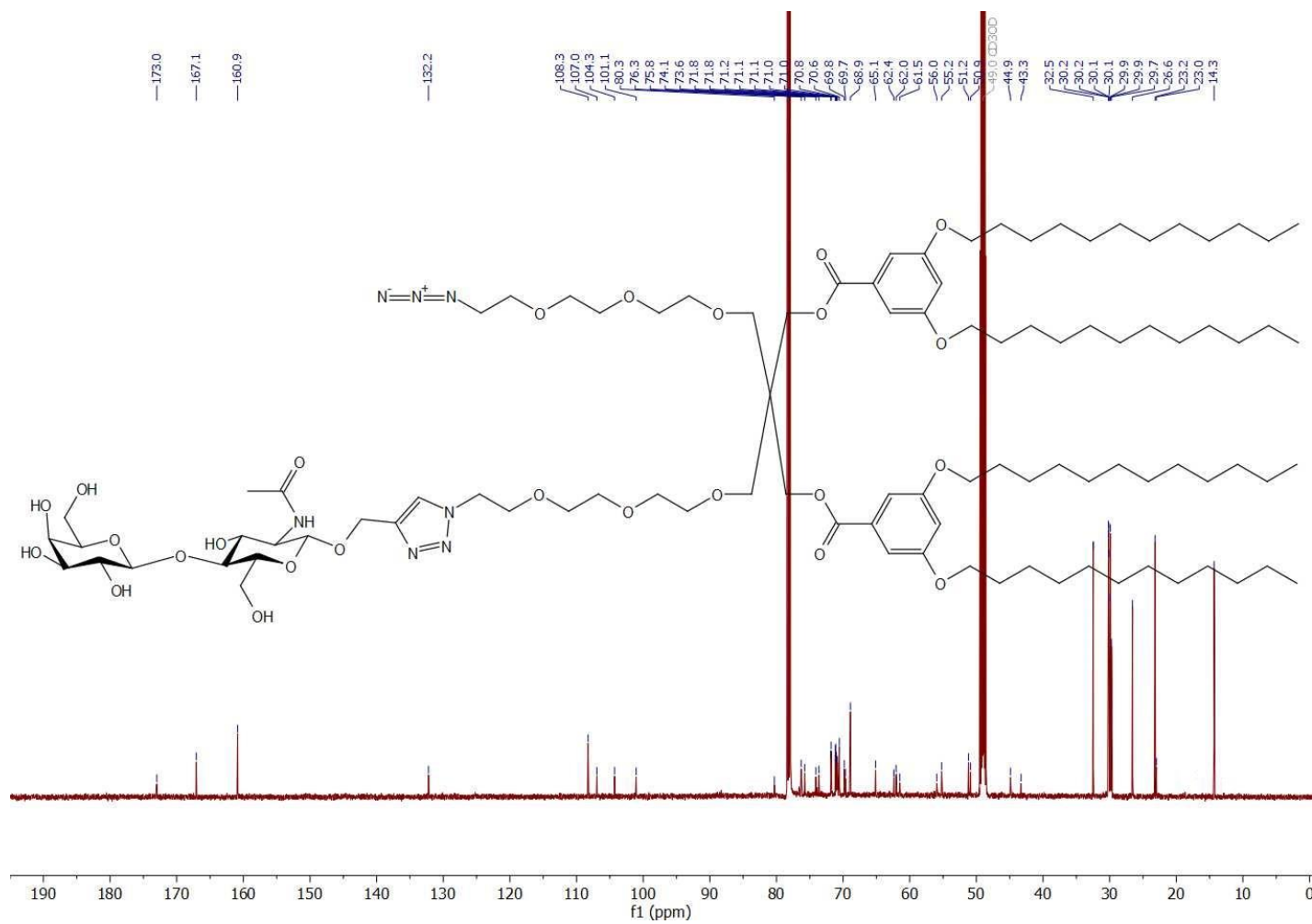


Figure 6.115 ¹³C NMR (150 MHz, CD₃OD+CDCl₃ (v/v : 1/1)) spectrum of compound 4.113.

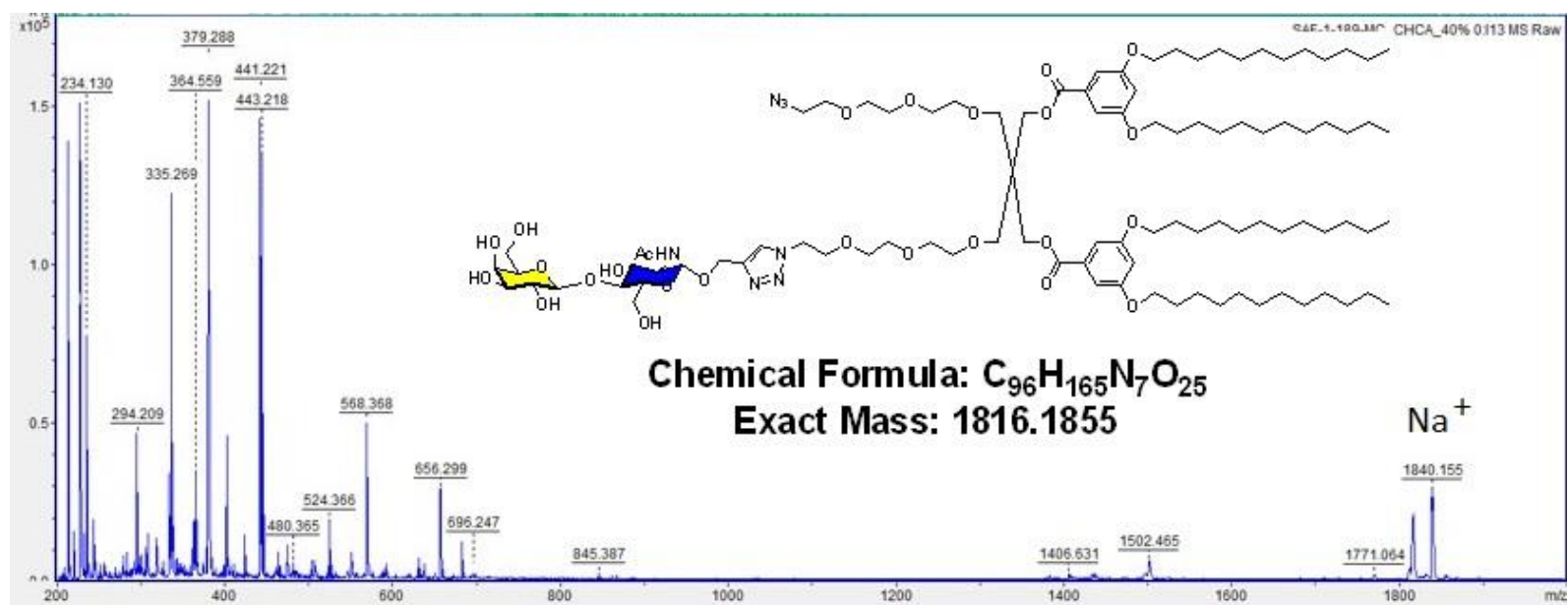


Figure 6.116 MALDI-TOF MS spectrum of compound 4.113.

Formation of Dendrimerosomes from LacNAc-JDs

Different solutions (0.2 mg/mL, 0.5 mg/mL, 1.0 mg/mL, 5.0 mg/mL) of **4.109** and **4.113** in EtOH were prepared by dissolving required amounts.

200 μ L from each solution was injected into 1 mL of milli-Q water followed by 5 s vortexing.

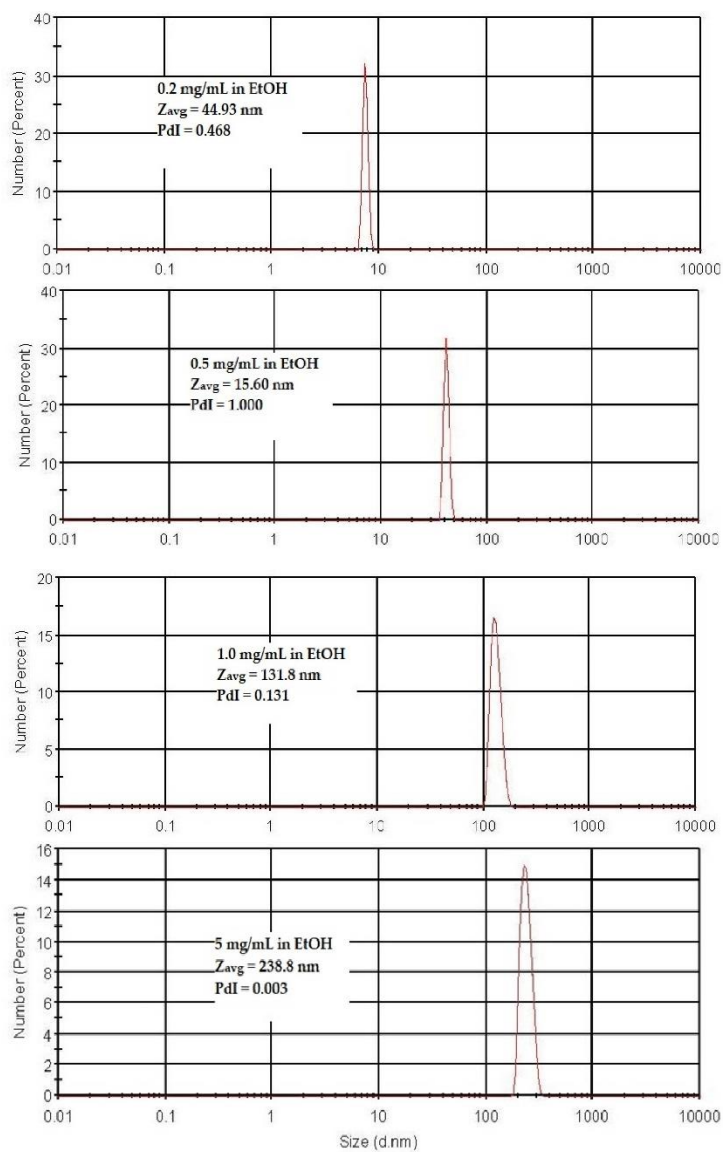


Figure 6.117 DLS analysis of glycodendrimerosomes of **4.109** with different concentration in EtOH.

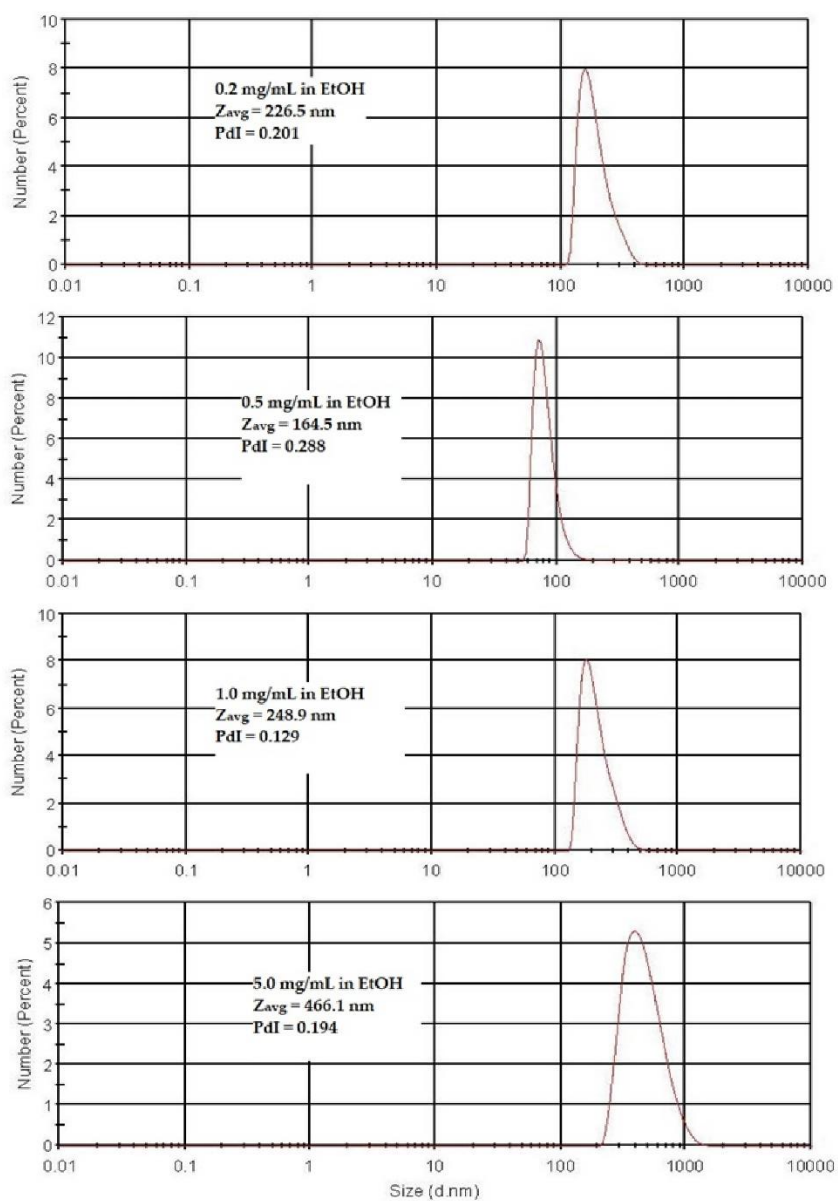


Figure 6.118 DLS analysis of glycodendrimersomes of **4.113** with different concentration in EtOH.

6.5 Experimental Part of Chapter V

6.5.1 Synthesis and characterization

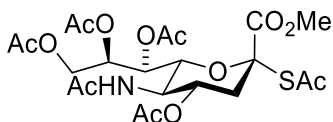
General synthetic procedure A: Phase Transfer Catalyst-mediated sialylation

To a solution of β -chloro sialoside donor **5.006** (1 eq.) and tetrabutylammonium hydrogensulfate (TBAHS, 1 eq.) in EtOAc (6 mL per 1 mmol of the SM) was added corresponding thiol or their potassium salt (3 eq.) in 1M Na₂CO₃ (6 mL per 1 mmol of the SM) at room temperature and resulted mixture was stirred for 3 h. After diluting in CHCl₃ organic phase was washed twice with 1M NaOH, 1M HCl and brine solutions, dried over Na₂SO₄ and concentrated *in-vacuo*. The residue was purified either *via* recrystallization from CHCl₃/hexane or through a classical column chromatography to give desired compound.

General synthetic procedure B: Zemplén transesterification reaction

To a solution of lactoside (1 eq.) in dry methanol (2 mL per 0.1 mmol of the SM) was added a solution of sodium methoxide (25 % in MeOH, 0.5 eq.). After stirring at room temperature for 3 h, the basic media was neutralized by addition of ion-exchange resin (Amberlite IR 120 H⁺). The reaction mixture was filtered through a pad of celite and concentrated *in vacuo* to afford the de-*O*-acetylated product.

Methyl (2-*S*-acetyl-4,7,8,9-tetra-*O*-acetyl-3,5-dideoxy-5-*N*-acetamido-D-glycero- α -D-galacto-non-2-ulopyranitol)onate (**5.126**)



Method A. Following the general procedure A, compound **5.126** (0.48 g, 0.88 mmol, 67 %) was obtained as a white foam.

Method B. To a solution of pure (crystallized from Et₂O/Petroleum ether/benzene) **5.006** (0.79 g, 1.55 mmol, 1 eq.) and freshly prepared TBATA (0.49 g, 1.55 mmol, 1 eq.) in EtOAc (8 mL) was added potassium thioacetate (531 mg, 4.647 mmol, 3 eq.) in 0.5 M Na₂CO₃ (8 mL) at 15 °C and resulted mixture was stirred for 3 h. The reaction mixture was diluted in CHCl₃ (30 mL), washed with saturated solution of NaHCO₃ (2 x 25 mL), dried over Na₂SO₄ and concentrated under reduced pressure. After chromatographic purification, compound **5.126** (0.66 g, 1.21 mmol, 78 %) was obtained as a white foam.

R_f = 0.48, (EtOAc)

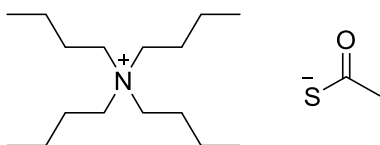
R_f = 0.45, (EtOAc/MeOH : 9.5/0.5)

¹H NMR (300 MHz, CDCl₃): δ (ppm) 5.66 (d, J = 10.2 Hz, 1H), 5.33 (d, J = 5.9 Hz, 1H), 5.17 (d, J = 6.7 Hz, 1H), 4.86 (dt, J = 11.1, 5.5 Hz, 1H), 4.63 (d, J = 10.9 Hz, 1H), 4.38 (d, J = 12.0 Hz, 1H), 4.16 – 3.92 (m, 2H), 3.75 (s, 3H), 2.58 (dd, J = 13.0, 4.6 Hz, 1H), 2.24 (s, 3H), 2.10 (s, 3H), 2.08 (s, 3H), 1.99 (brs, 7H), 1.84 (s, 3H)

¹³C NMR (75 MHz, CDCl₃): δ (ppm) 191.6, 170.9, 170.8, 170.5, 170.4, 170.2, 169.4, 84.5, 75.3, 70.9, 69.0, 68.0, 62.6, 53.5, 48.9, 37.5, 30.1, 23.2, 21.0, 20.9, 20.9, 20.8

The spectroscopic data agreed well with those of the literature.⁵⁵⁵

Preparation of tetrabutylammonium thioacetate (TBATA)



To a solution of tetrabutylammonium bromide (TBAB, 2.02 g, 6.27 mmol, 1 eq.) in MeOH was added potassium thioacetate (0.73 g, 6.27 mmol, 1 eq.) and resulted mixture was stirred at room temperature for 3 h. The reaction mixture was then filtered over Buchner and concentrated under reduced pressure. The residue was dissolved in acetonitrile and formed white precipitate was removed by filtration through a pad of celite and filtrate was concentrated *in-vacuo*. Recrystallization from THF/hexane afforded desired compound (1.87 g, 5.9 mmol, 94 %) as yellow crystal.

M.p. = 74.9 °C

¹H NMR (300 MHz, CDCl₃): δ (ppm) 3.36 – 3.04 (m, 8H), 2.44 (s, 3H), 1.74 – 1.57 (m, 8H), 1.46 – 1.28 (m, 8H), 0.96 (t, *J* = 7.4 Hz, 12H)

¹³C NMR (75 MHz, CDCl₃): δ (ppm) 58.2, 58.1, 58.1, 37.7, 23.2, 19.2, 19.2, 19.2, 12.9

The spectroscopic data agreed well with those of the literature.⁵⁶⁹

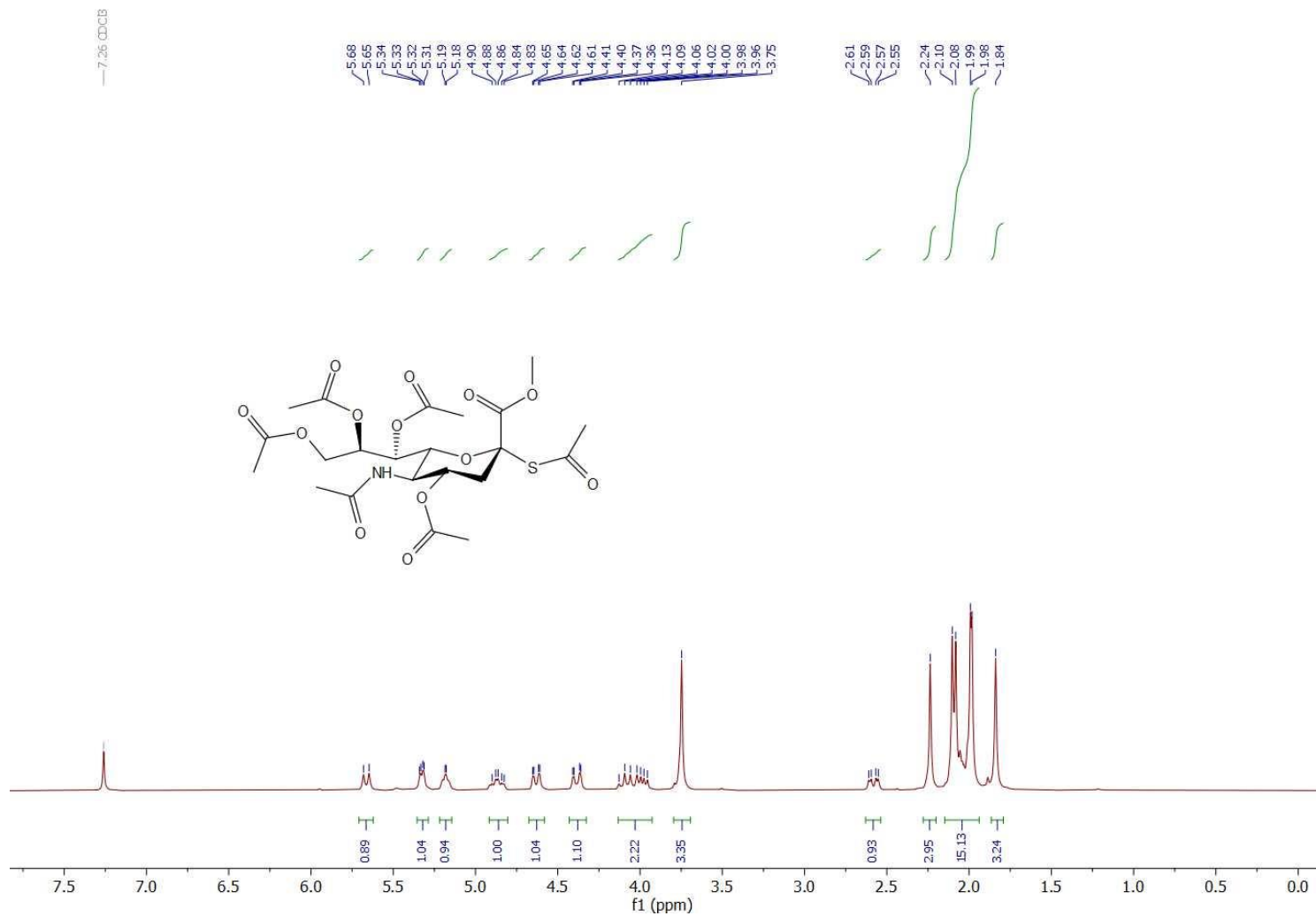


Figure 6.119 ¹H NMR (300 MHz, CDCl₃) spectrum of compound 5.126.

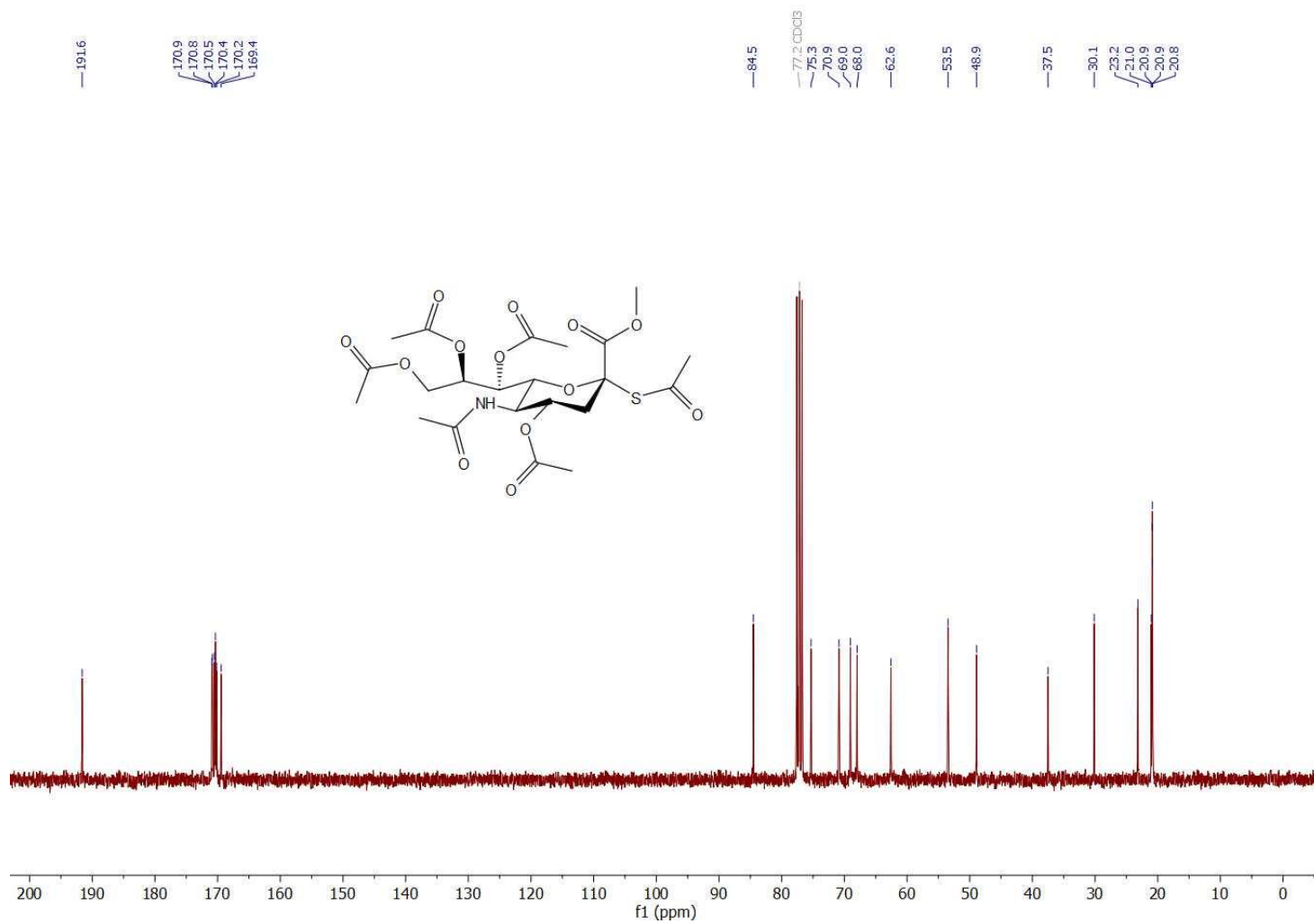


Figure 6.120 ^{13}C NMR (75 MHz, CDCl₃) spectrum of compound 5.126.

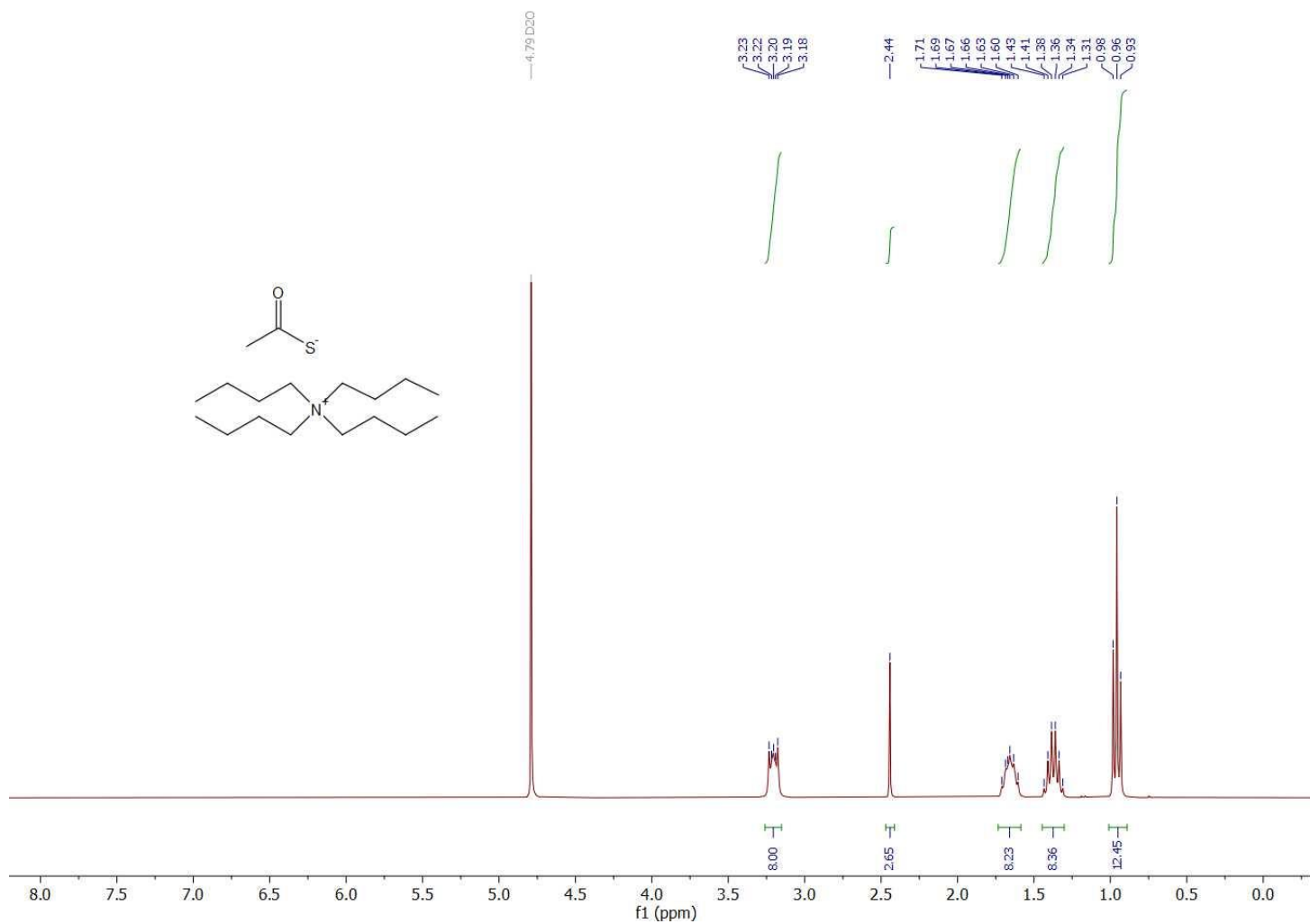


Figure 6.121 ^1H NMR (300 MHz, D_2O) spectrum of compound TBATA.

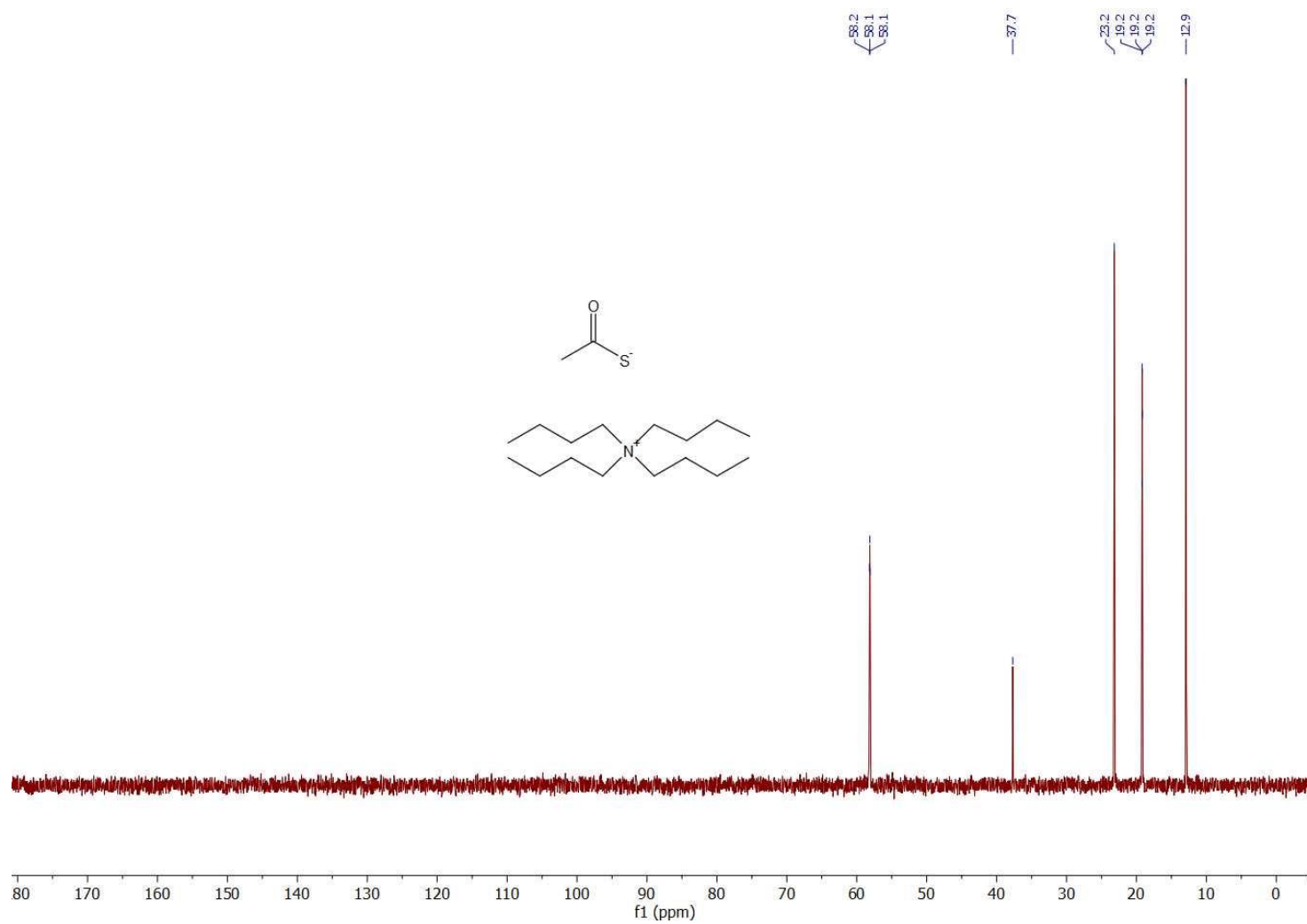
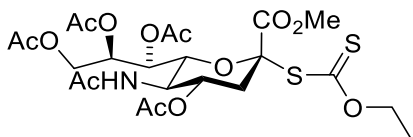


Figure 6.122 ^{13}C NMR (75 MHz, D_2O) spectrum of compound TBATA.

Methyl (2-*S*-(*O*-ethylcarbonodithionato)-4,7,8,9-tetra-*O*-acetyl-3,5-dideoxy-5-*N*-acetamido-*D*-glycero- α -*D*-galacto-non-2-ulopyranitol)onate (**5.174**)



Following the general procedure A, compound **5.174** (0.72 g, 1.2 mmol, 82 %) was obtained as a white foam.

$R_f = 0.47$, (EtOAc)

$^1\text{H NMR}$ (300 MHz, CDCl_3): δ (ppm) 5.36 (d, $J = 10.1$ Hz, 1H), 5.34 – 5.22 (m, 2H), 4.95 – 4.71 (m, 2H), 4.61 – 4.45 (m, 2H), 4.32 (dd, $J = 12.5, 2.4$ Hz, 1H), 4.18 (dd, $J = 12.4, 5.2$ Hz, 1H), 4.02 (q, $J = 10.4$ Hz, 1H), 3.79 (s, 3H), 2.61 (dd, $J = 12.9, 4.7$ Hz, 1H), 2.13 (s, 3H), 2.11 (s, 3H), 2.02 (brs, 7H), 1.88 (s, 3H), 1.36 (t, $J = 7.1$ Hz, 3H)

$^{13}\text{C NMR}$ (75 MHz, CDCl_3): δ (ppm) 207.3, 171.0, 170.7, 170.4, 170.3, 170.2, 168.8, 86.6, 75.2, 70.6, 70.3, 68.9, 67.3, 62.1, 53.4, 49.3, 37.2, 23.3, 21.2, 20.9, 20.9, 20.9, 13.5

The spectroscopic data agreed well with those of the literature.⁵⁶³

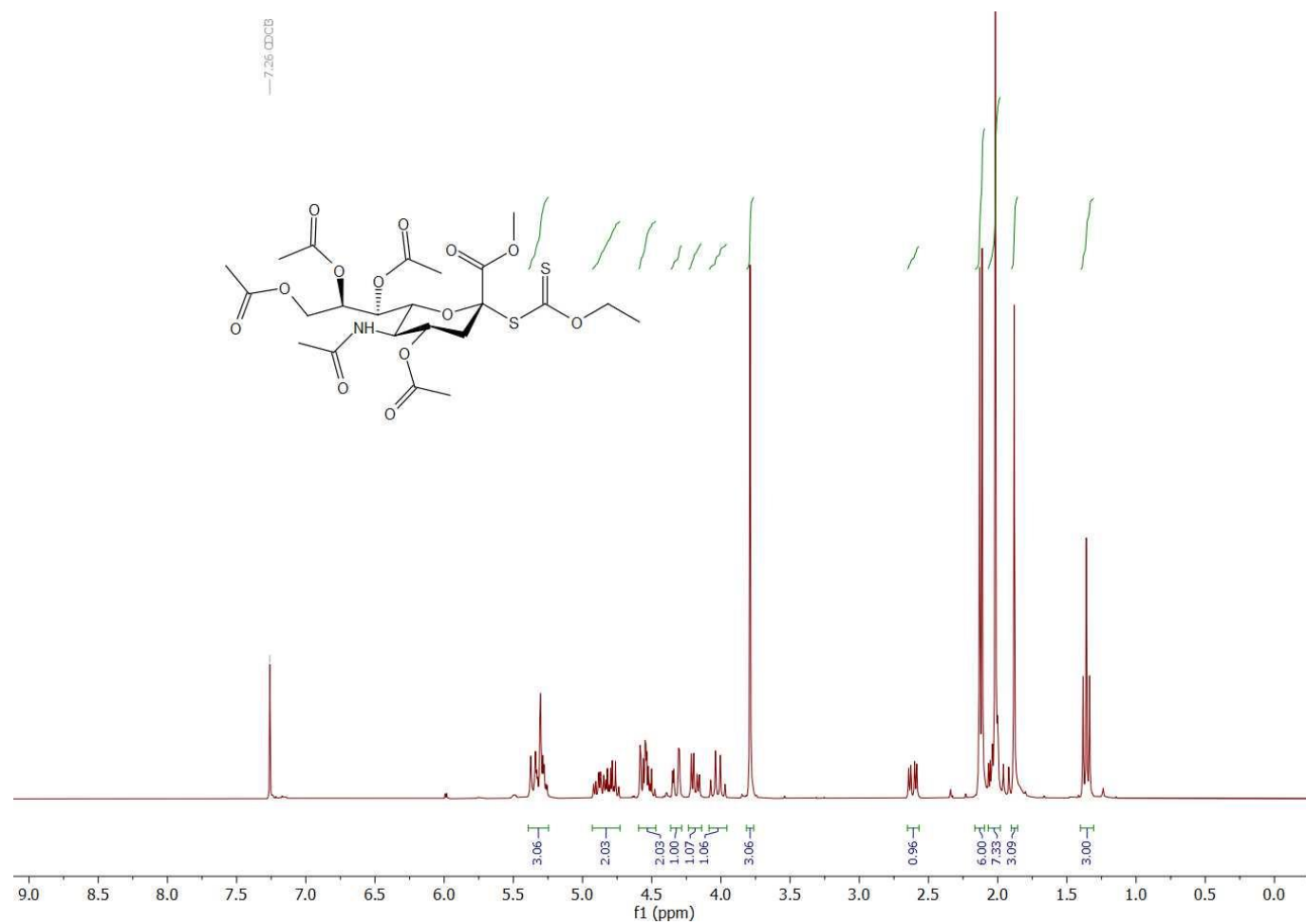


Figure 6.123 ¹H NMR (300 MHz, CDCl₃) spectrum of compound **5.174**.

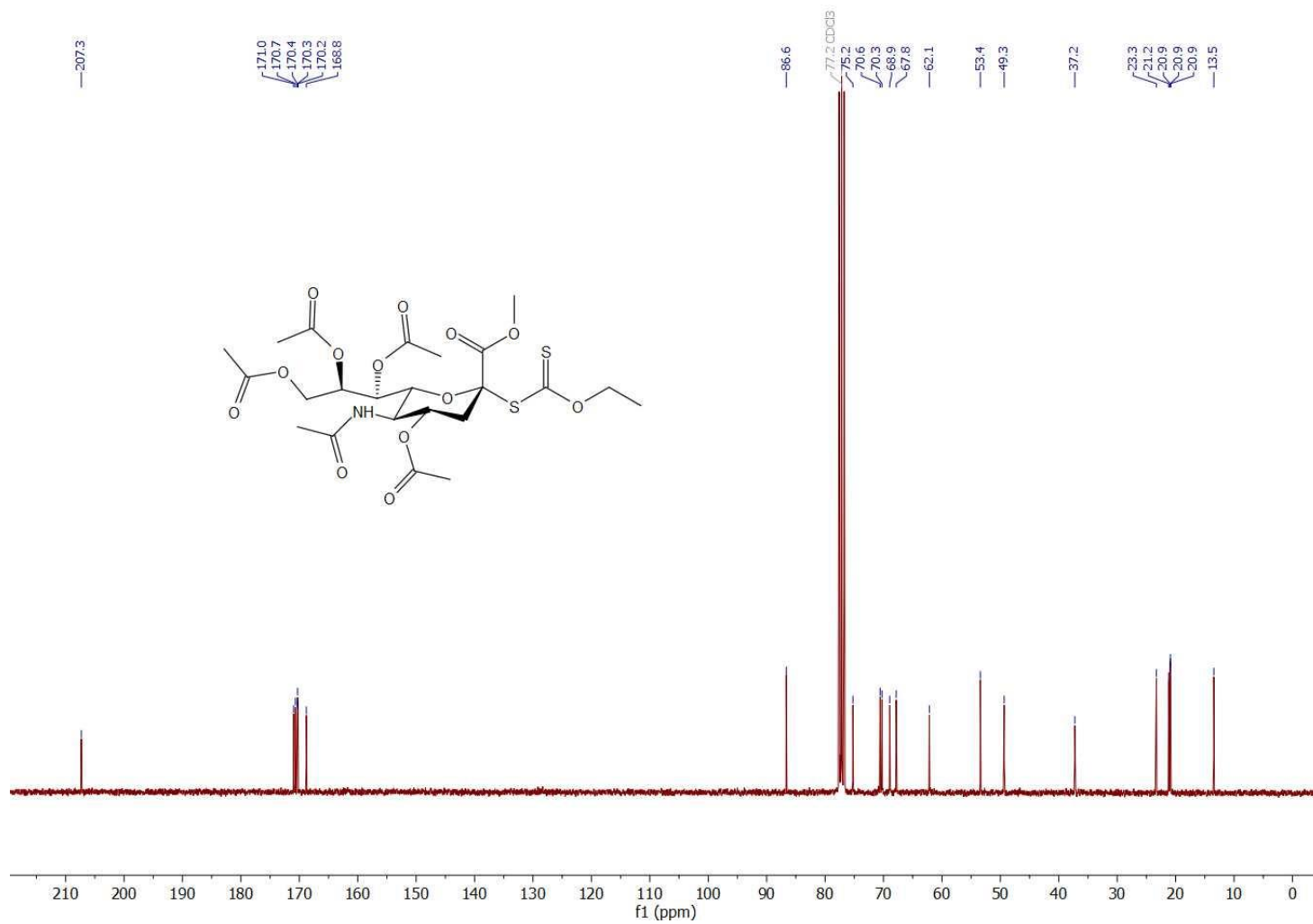


Figure 6.124 ^{13}C NMR (75 MHz, CDCl₃) spectrum of compound 5.174.

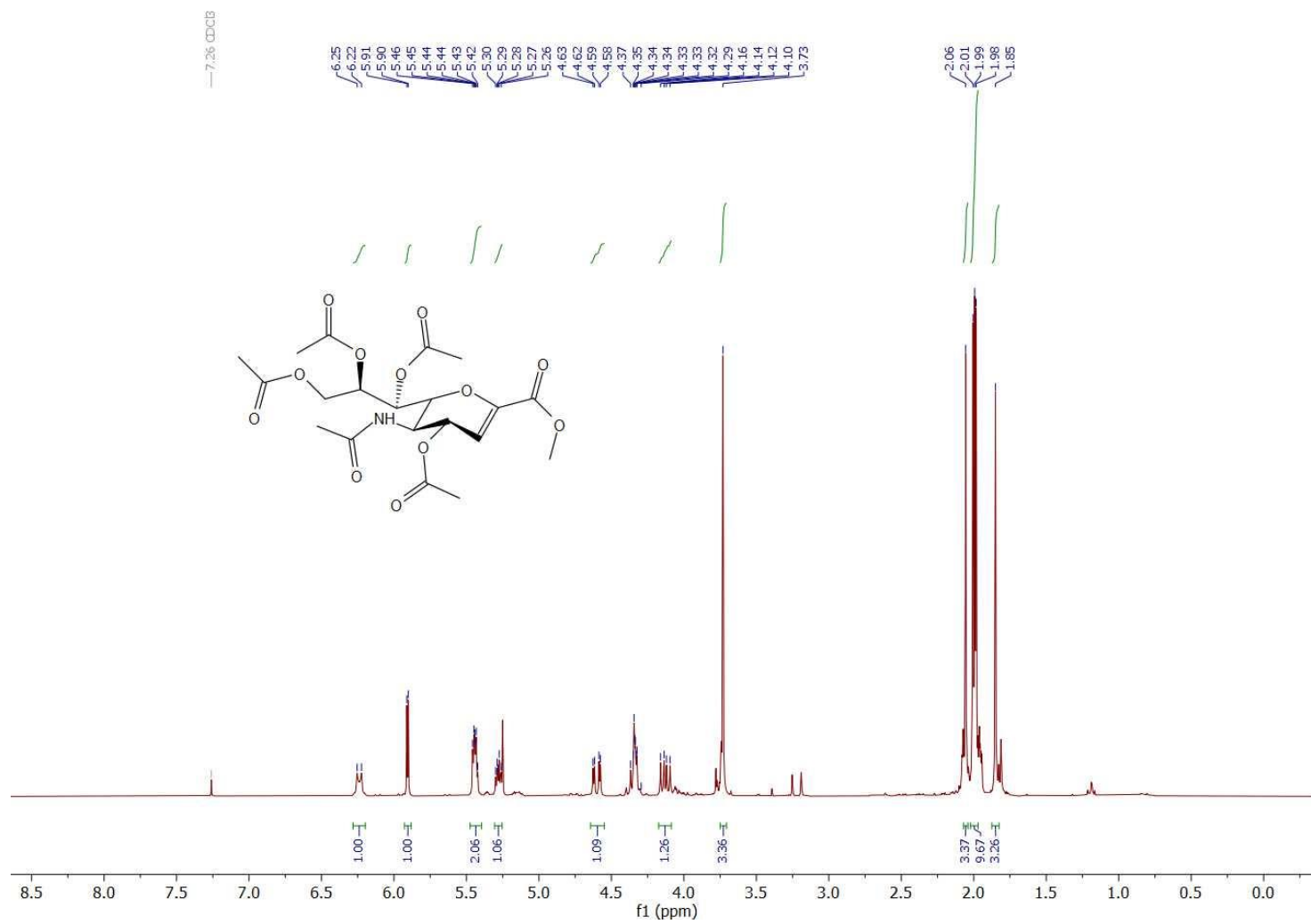


Figure 6.125 ¹H NMR (300 MHz, CDCl₃) spectrum of compound 5.175.

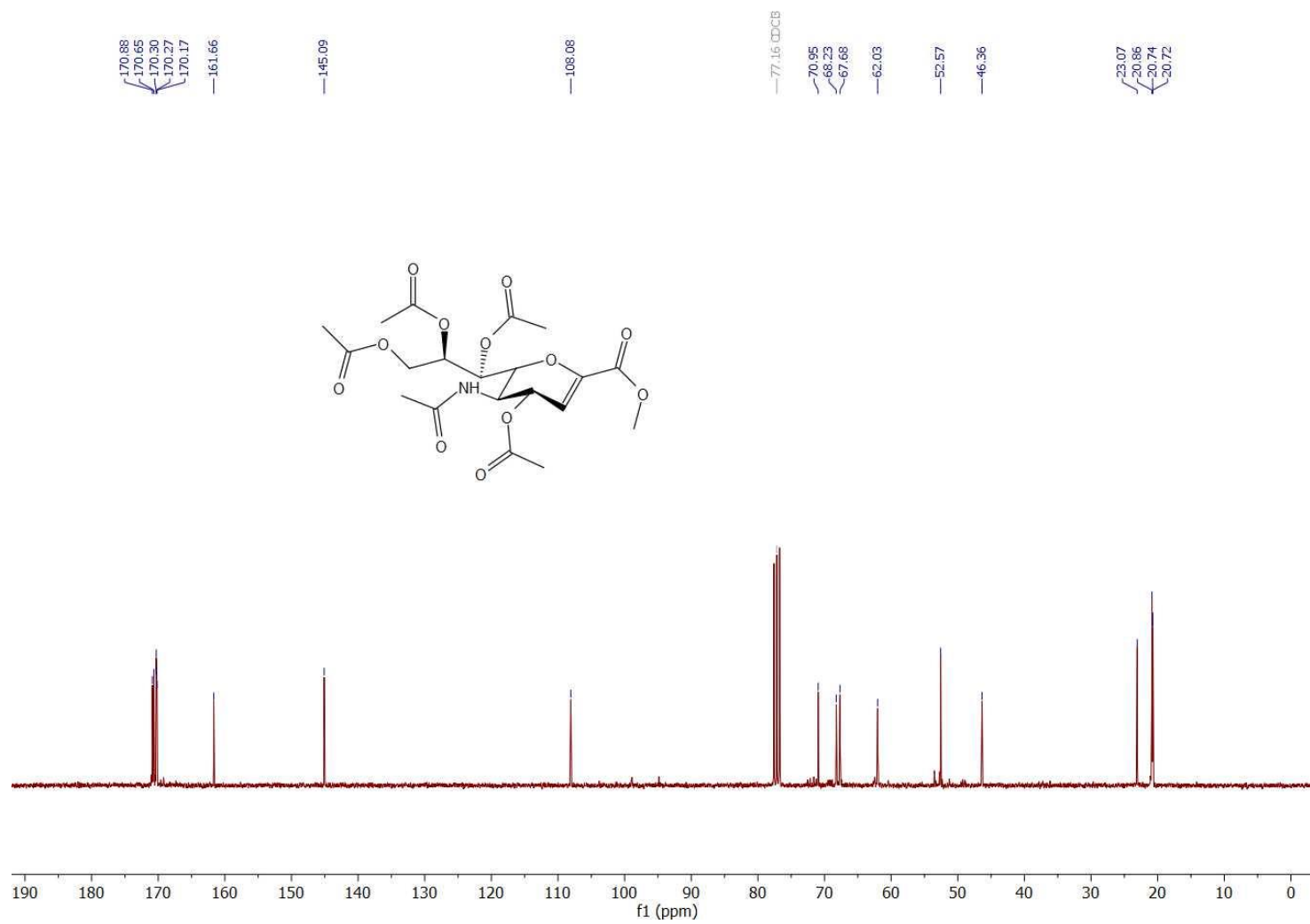
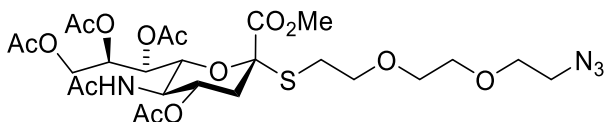


Figure 6.126 ¹³C NMR (75 MHz, CDCl₃) spectrum of compound 5.175.

Methyl (2-*S*-[2-[2-(2-azidoethoxy)ethoxy]ethyl]-4,7,8,9-tetra-*O*-acetyl-3,5-dideoxy-5-*N*-acetamido-*D*-glycero- α -*D*-galacto-non-2-ulopyranitol)onate (**5.128**)



To a solution of **5.126** (0.34 g, 0.62 mmol, 1 eq.) and **4.118** (0.41 g, 1.25 mmol 2 eq.) in MeOH was added K_2CO_3 (0.09 g, 0.62 mmol, 1 eq.) at 0 °C under nitrogen atmosphere. After 10 h stirring at the same temperature, the reaction was quenched by addition of acetic acid (0.11 mL, 1.91 mmol, 3.1 eq.) and concentrated *in-vacuo*. The residue was dissolved in Ac_2O (3 mL) and after successive addition of Pyridine (5 mL) and catalytic amount of DMAP (0.01 g, 0.08 mmol, 0.13 eq.) at 0 °C, the reaction mixture was stirred at room temperature overnight. The reaction mixture was diluted in $CHCl_3$ (30 mL), washed with ice cold water (2 x 25 mL), 0.2 M HCl (2 x 30 mL), brine (30 mL) and concentrated *in-vacuo*. After chromatographic purification **5.176** (0.29 mg, 0.44 mmol, 72 %) was obtained as white foam.

$R_f = 0.2$, (EtOAc)

1H NMR (300 MHz, $CDCl_3$): δ (ppm) 5.55 – 5.25 (m, 2H), 5.18 (d, $J = 10.0$ Hz, 1H), 4.86 (ddd, $J = 11.6, 10.2, 4.6$ Hz, 1H), 4.29 (dd, $J = 12.5, 2.4$ Hz, 1H), 4.15 – 3.94 (m, 2H), 3.82 – 3.79 (m, 4H), 3.72 – 3.56 (m, 8H), 3.38 (t, $J = 5.1$ Hz, 2H), 3.06 – 2.75 (m, 2H), 2.72 (dd, $J = 12.7, 4.6$ Hz, 1H), 2.15 (s, 2H), 2.13 (s, 2H), 2.03 (s, 2H), 2.02 (s, 1H), 1.99 (t, $J = 12.4$ Hz, 1H), 1.87 (s, 3H)

^{13}C NMR (75 MHz, $CDCl_3$): δ (ppm) 171.1, 170.8, 170.3, 170.3, 170.2, 168.6, 83.1, 74.2, 70.7, 70.4, 70.2, 69.7, 68.6, 67.4, 62.3, 53.1, 50.8, 49.5, 38.1, 29.1, 23.3, 21.3, 21.0, 20.9

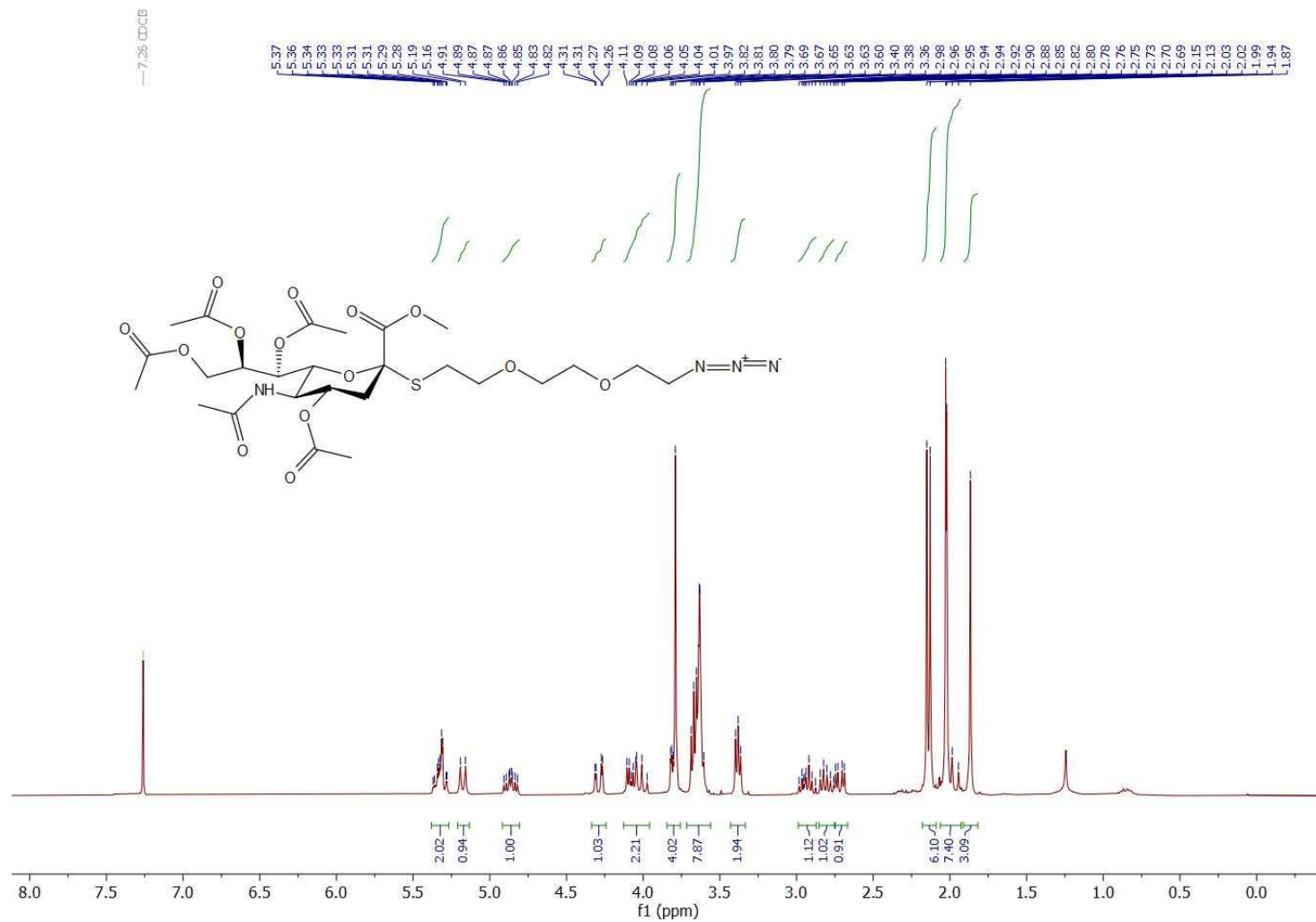


Figure 6.127 ¹H NMR (300 MHz, CDCl₃) spectrum of compound 5.176.

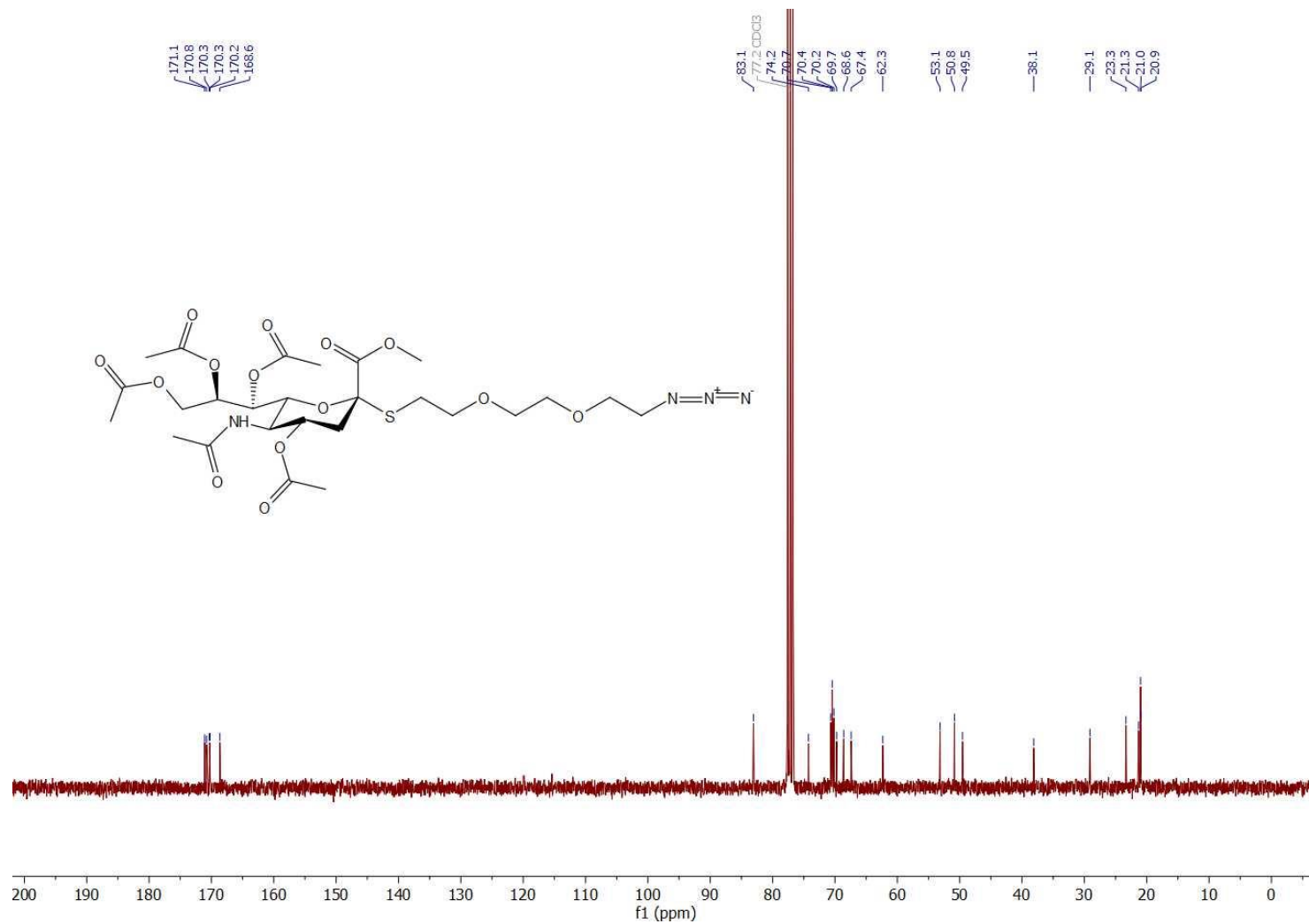
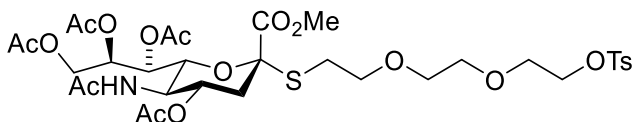


Figure 6.128 ^{13}C NMR (75 MHz, CDCl_3) spectrum of compound 5.176.

Methyl (2-*S*-[2-[2-[2-[(4-methylphenyl)sulfonyl]ethoxy]ethoxy]ethyl]-3,5-dideoxy-5-*N*-acetamido-*D*-glycero- α -*D*-galacto-non-2-ulopyranitol)onate (**5.177**)



Method A. To a solution of **5.126** (1.14 g, 2.07 mmol, 1 eq.) and **4.117** (4.76 g, 10.39 mmol, 5 eq.) in DMF (70 mL) was added Et₂NH (1.4 mL, 13.53 mmol, 6.5 eq.) at room temperature under nitrogen. After stirring for additional 17 h, reaction mixture was concentrated *in-vacuo* and subjected to column chromatography to afford **5.177** (1.13 g, 1.8 mmol, 87 %). was obtained as a white foam

Method B. To a solution of **5.174** (0.36 g, 0.6 mmol, 1 eq.) in dry THF (3.5 mL) was added butylamine (0.07 mL, 0.71 mmol, 1.18 eq) at room temperature under nitrogen. After stirring for 4 h the reaction mixture was diluted in DCM (20 mL), washed with saturated solution of NH₄Cl (20 mL), dried over Na₂SO₄ and concentrated *in-vacuo*. To a solution of residue and **4.117** (0.69 g, 1.51 mmol, 2.5 eq) in DMF (5 mL) was added Na₂CO₃ (0.13 g, 1.21 mmol, 2 eq.) and resulted mixture was stirred at room temperature overnight. The reaction mixture was diluted in CHCl₃ (20 mL), washed with water (2 x 10 mL), dried over Na₂SO₄ and concentrated under reduced pressure. After chromatographic purification **5.177** (0.25 g, 0.4 mmol, 67 %) as white foam.

Method C. To a solution of **5.006** (0.45 g, 0.88 mmol, 1 eq.) in dry MeOH (4 mL) was added sodium thiophosphate (0.56 g, 1.41 mmol, 1.6 eq) at room temperature under nitrogen. After stirring for 6 h the reaction mixture was poured in cold water (20 mL), extracted with DCM (3 x 20 mL), dried over Na₂SO₄ and concentrated *in-vacuo*. To a solution of residue and **4.117** (1.01 g, 2.2 mmol, 2.5 eq) in DMF (5 mL) was added Na₂CO₃ (0.19 g, 1.76 mmol, 2 eq.) and resulted mixture was stirred at

room temperature overnight. Following work-up and purification procedure from *Method B 5.177* (0.31 g, 0.49 mmol, 56 %) was obtained as white foam.

$R_f = 0.36$, (EtOAc)

$[\alpha]_D^{19} = 17$ (c 0.006, CHCl₃)

¹H NMR (300 MHz, CDCl₃): δ (ppm) 7.76 (d, $J = 8.5$ Hz, 2H), 7.31 (d, $J = 8.0$ Hz, 2H), 5.41 (d, $J = 10.0$ Hz, 1H), 5.36 – 5.22 (m, 2H), 4.83 (td, $J = 11.0, 4.5$ Hz, 1H), 4.26 (dd, $J = 12.4, 2.2$ Hz, 1H), 4.13 – 4.10 (m, 2H), 4.09 – 3.92 (m, 2H), 3.38 – 3.75 (m, 4H), 3.70 – 3.59 (m, 2H), 3.62 – 3.48 (m, 6H), 2.95 – 2.81 (m, 1H), 2.82 – 2.63 (m, 2H), 2.41 (s, 3H), 2.11 (s, 3H), 2.09 (s, 3H), 1.98 – 1.89 (m, 7H), 1.83 (s, 3H)

¹³C NMR (75 MHz, CDCl₃): δ (ppm) 170.9, 170.7, 170.3, 170.2, 170.1, 168.5, 144.9, 133.0, 129.9, 128.0, 82.9, 74.1, 70.6, 70.3, 70.2, 69.3, 68.7, 68.6, 67.4, 62.3, 53.0, 49.3, 38.2, 23.2, 21.7, 21.2, 20.9, 20.8

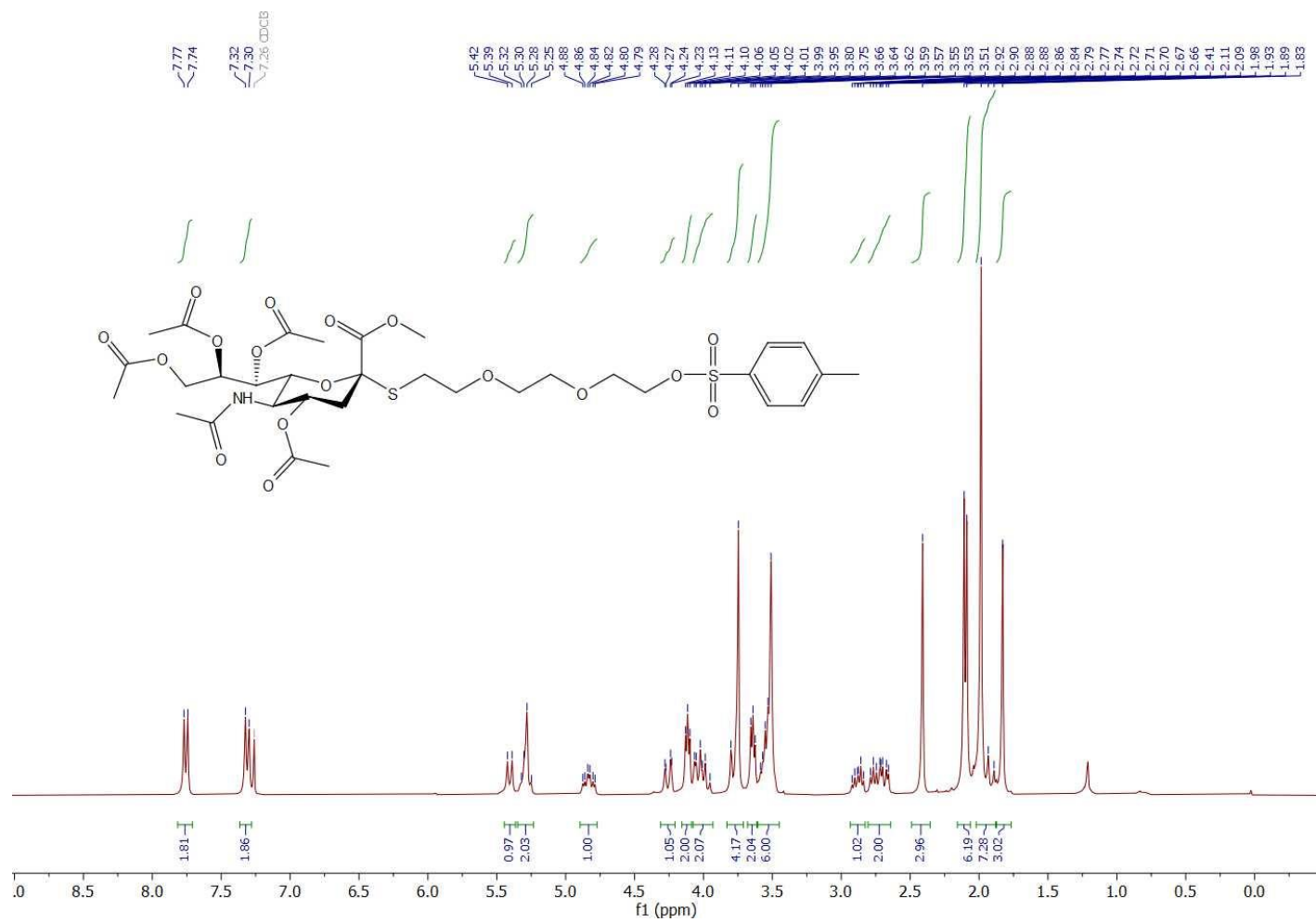


Figure 6.129 ¹H NMR (300 MHz, CDCl₃) spectrum of compound **5.177**.

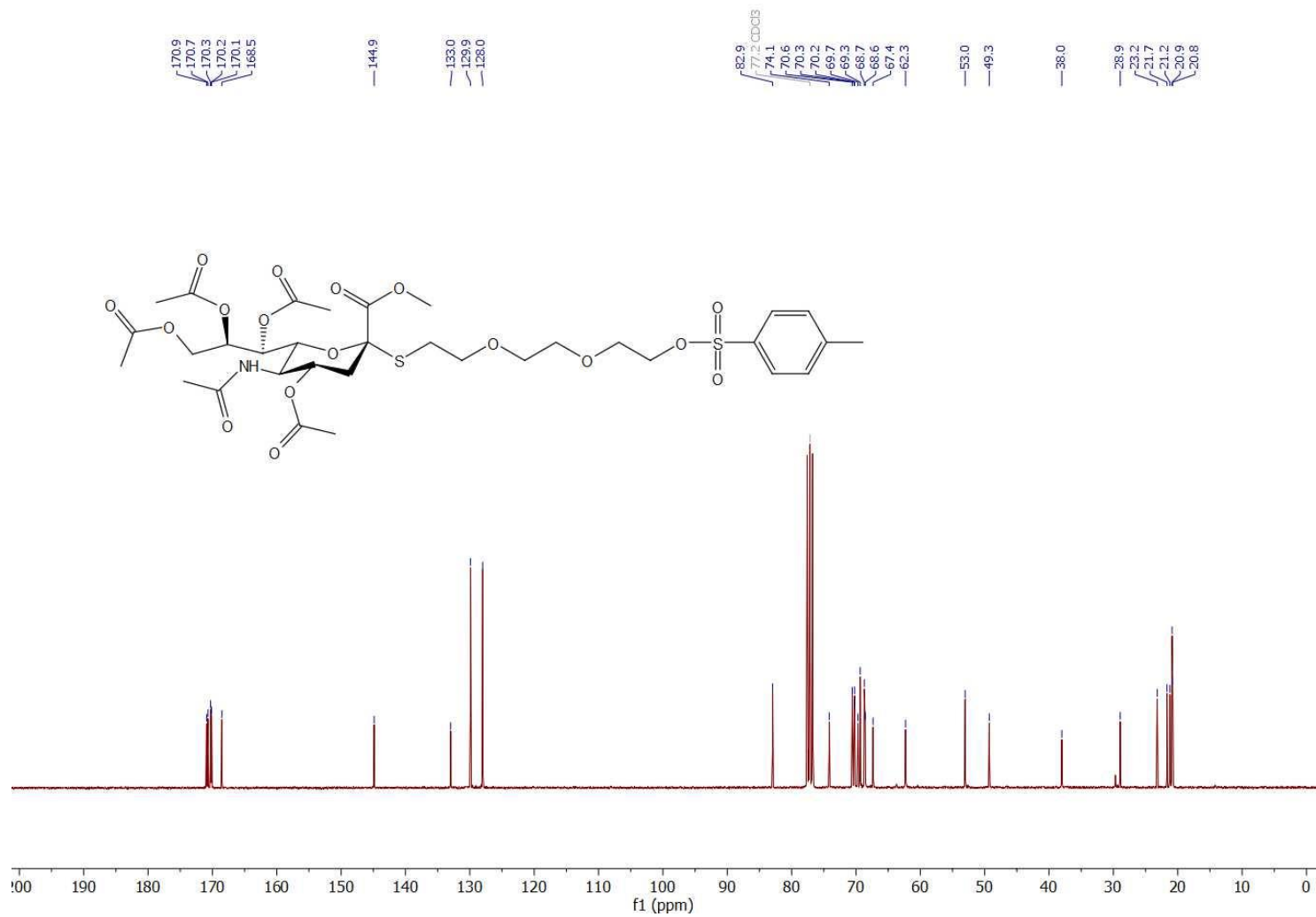
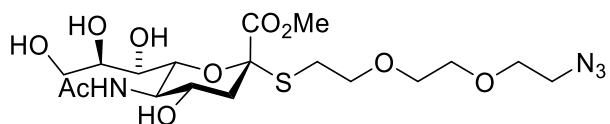


Figure 6.130 ¹³C NMR (75 MHz, CDCl₃) spectrum of compound 5.177.

Methyl (2-*S*-[2-[2-(2-azidoethoxy)ethoxy]ethyl]-3,5-dideoxy-5-*N*-acetamido-*D*-glycero- α -*D*-galacto-non-2-ulopyranitol)onate (**5.178**)



Following the general procedure B, compound **5.178** (0.48 g, 0.88 mmol, 67 %) was obtained as a white solid.

$[\alpha]_{\text{D}}^{19} = -8.7$ (c 0.003, H_2O)

^1H NMR (300 MHz, CD_3OD): δ (ppm) 3.84 (s, 3H), 3.83 – 3.72 (m, 3H), 3.71 – 3.59 (m, 9H), 3.49 (dd, $J = 8.8, 1.7$ Hz, 1H), 3.44 (dd, $J = 10.3, 1.7$ Hz, 1H), 3.37 (t, $J = 5.0$ Hz, 2H), 2.96 (dt, $J = 13.0, 6.4$ Hz, 1H), 2.85 (dt, $J = 13.6, 6.9$ Hz, 1H), 2.76 (dd, $J = 12.8, 4.6$ Hz, 1H), 2.00 (s, 3H), 1.79 (dd, $J = 12.9, 11.2$ Hz, 1H)

^{13}C NMR (75 MHz, CD_3OD): δ (ppm) 175.2, 172.2, 84.2, 77.2, 72.6, 71.5, 71.4, 71.4, 71.2, 70.2, 68.9, 64.7, 53.7, 51.8, 42.1, 29.8, 22.6

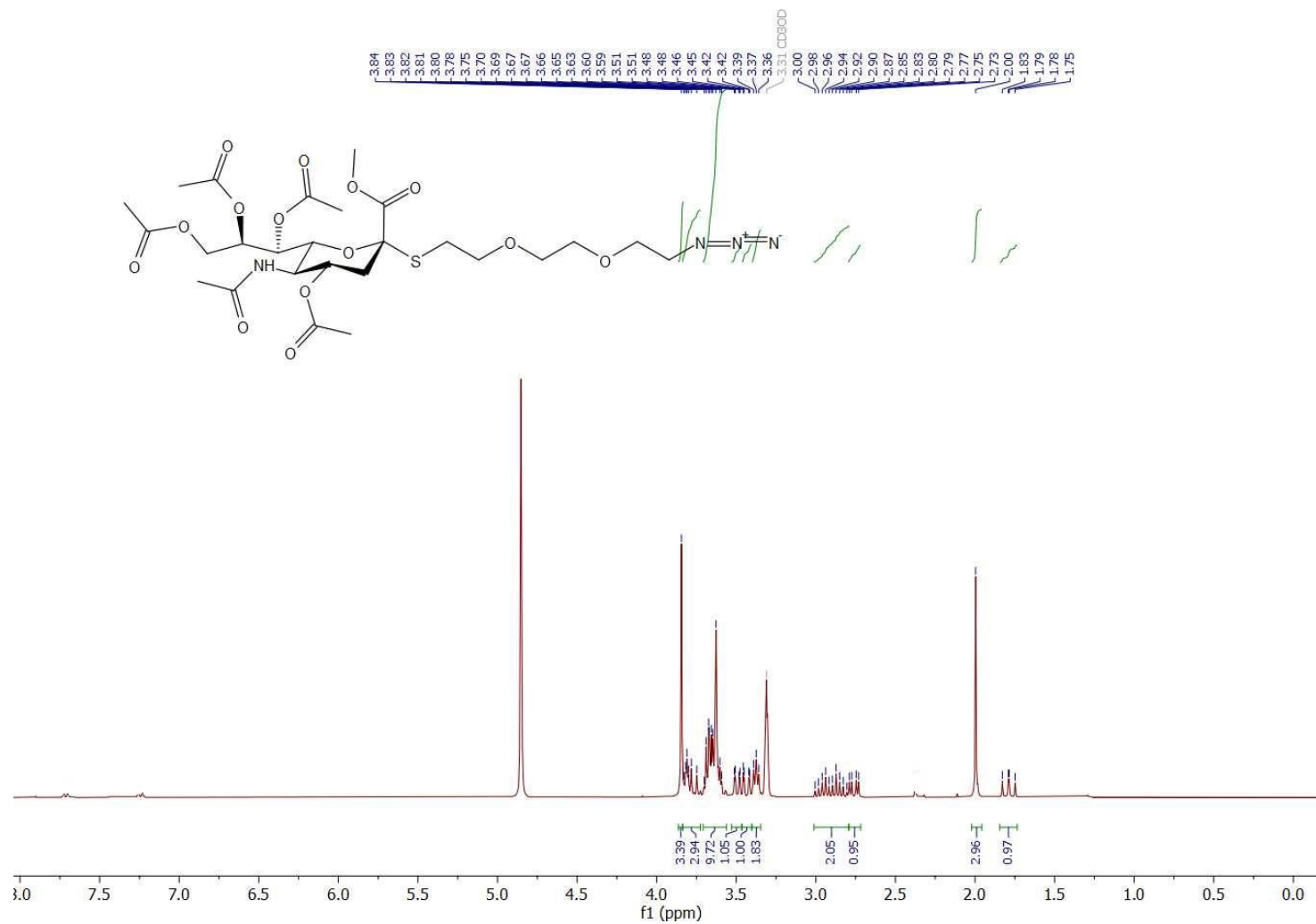


Figure 6.131 ^1H NMR (300 MHz, CD_3OD) spectrum of compound 5.178.

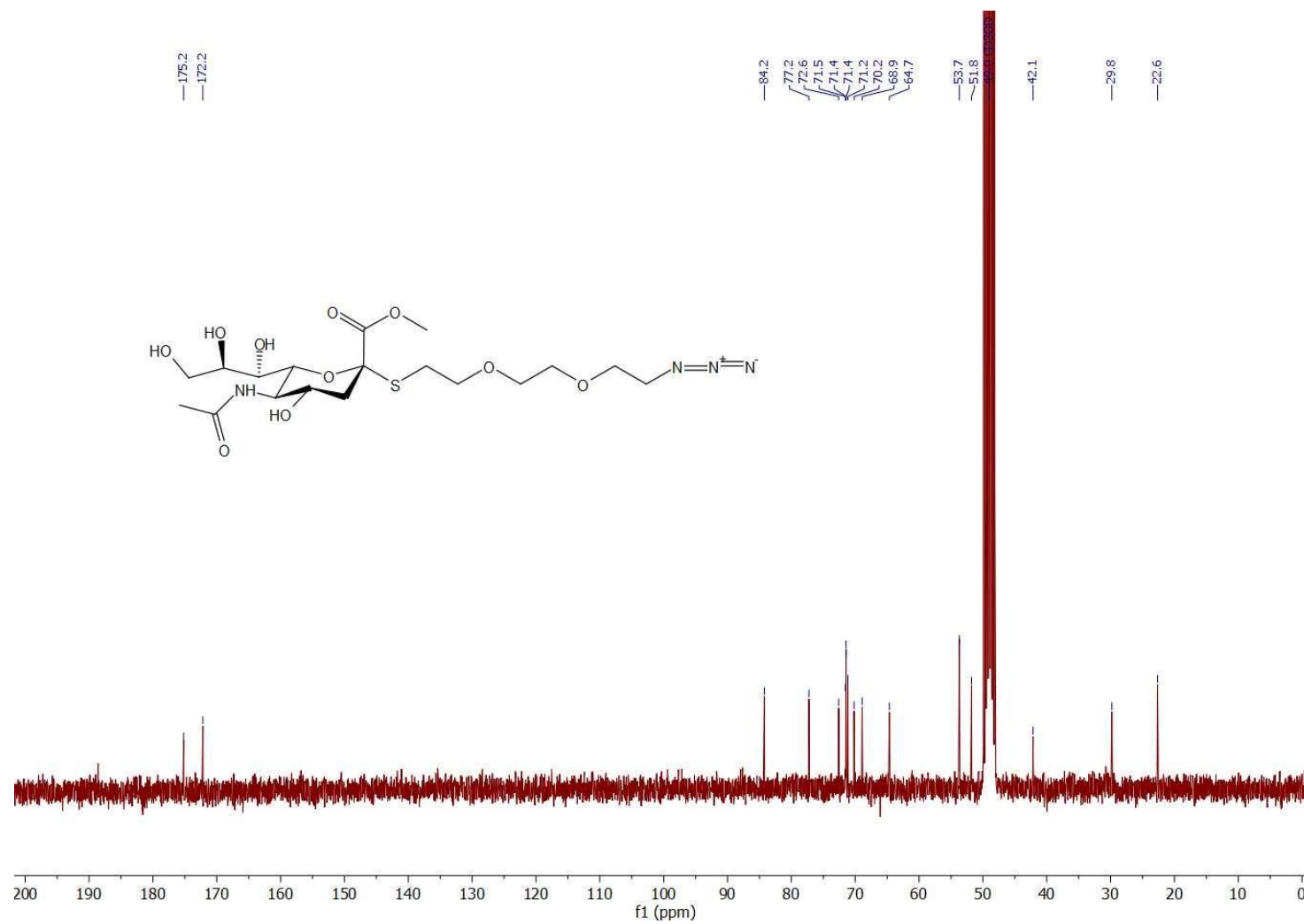
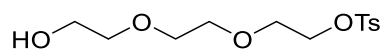


Figure 6.132 ^{13}C NMR (75 MHz, CDCl_3) spectrum of compound **5.178**.

2-(2-(2-hydroxyethoxy)ethoxy)ethyl 4-methylbenzenesulfonate (**5.179**)

To a solution of PEG₃ (16.24 g, 108.15 mmol, 10 eq.) in THF (45 mL) was added 6 mL of 4 M aqueous solution of NaOH at 0 °C and resulted reaction mixture was stirred for 1 h. Using a dropping funnel, a solution of TsCl (2.11 g, 10.82 mmol, 1 eq.) in THF (25 mL) added dropwise over 30 min and the reaction mixture was stirred at 0 °C for additional 3 h. Then the reaction mixture was poured into ice-cold water (200 mL) and extracted with DCM (3 x 200 mL), dried over Na₂SO₄ and concentrated *in-vacuo*. After chromatographic purification compound **5.179** (3.29 g, 10.82 mmol, 99 %) was obtained as a colorless oil.

R_f = 0.47, (DCM/Acetone : 7/3)

¹H NMR (300 MHz, CDCl₃): δ (ppm) 7.73 (d, *J* = 8.3 Hz, 2H), 7.29 (d, *J* = 8.1 Hz, 2H), 4.14 – 4.05 (m, 2H), 3.71 – 3.58 (m, 5H), 3.56 – 3.42 (m, 6H), 2.84 (brs, 1H), 2.38 (s, 3H)

¹³C NMR (75 MHz, CDCl₃): δ (ppm) 144.7, 132.5, 129.6, 127.6, 72.2, 70.3, 69.8, 69.1, 68.2, 61.2, 21.2

The spectroscopic data agreed well with those of the literature.⁵⁷⁰

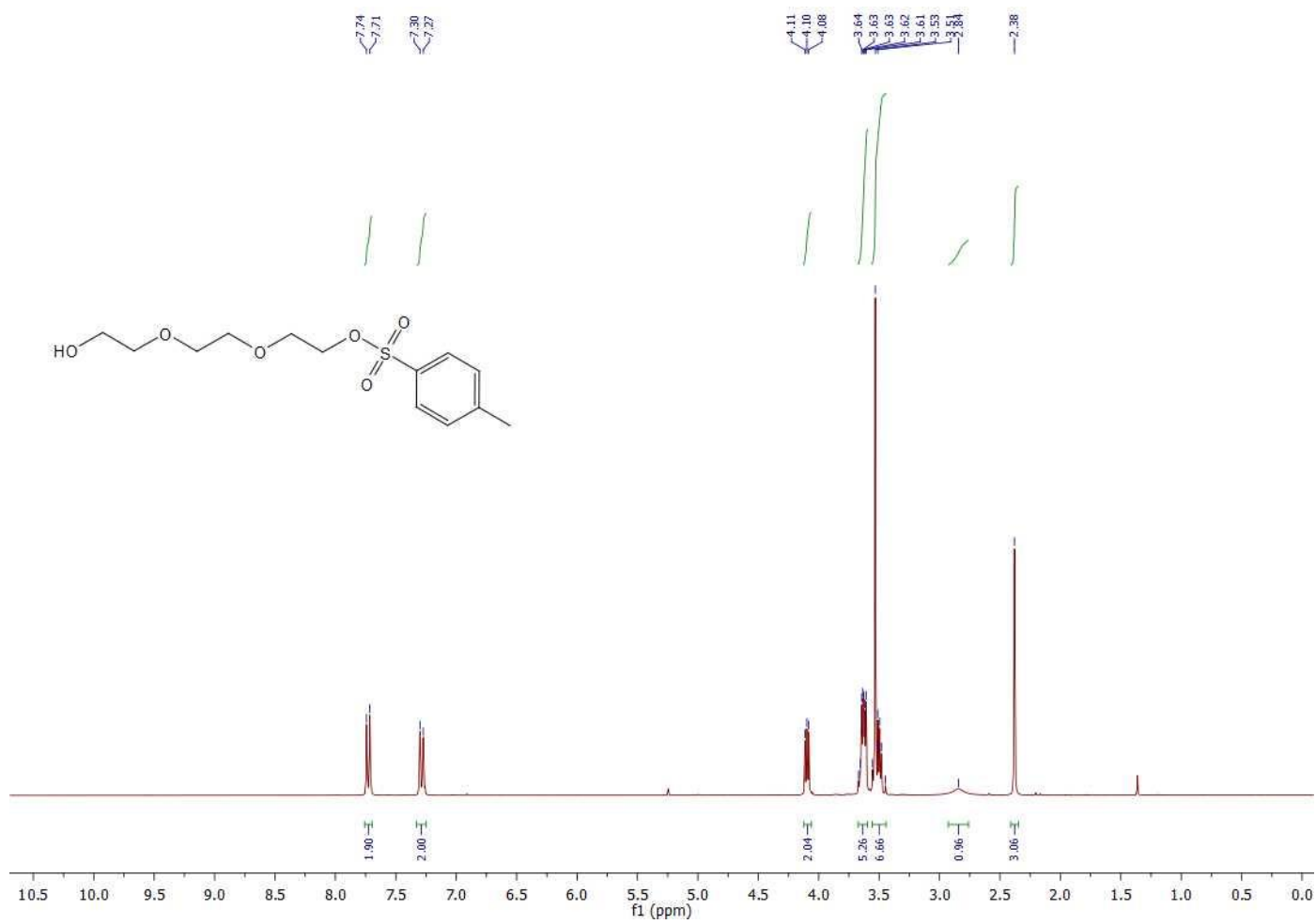


Figure 6.133 ^1H NMR (300 MHz, CDCl_3) spectrum of compound 5.179.

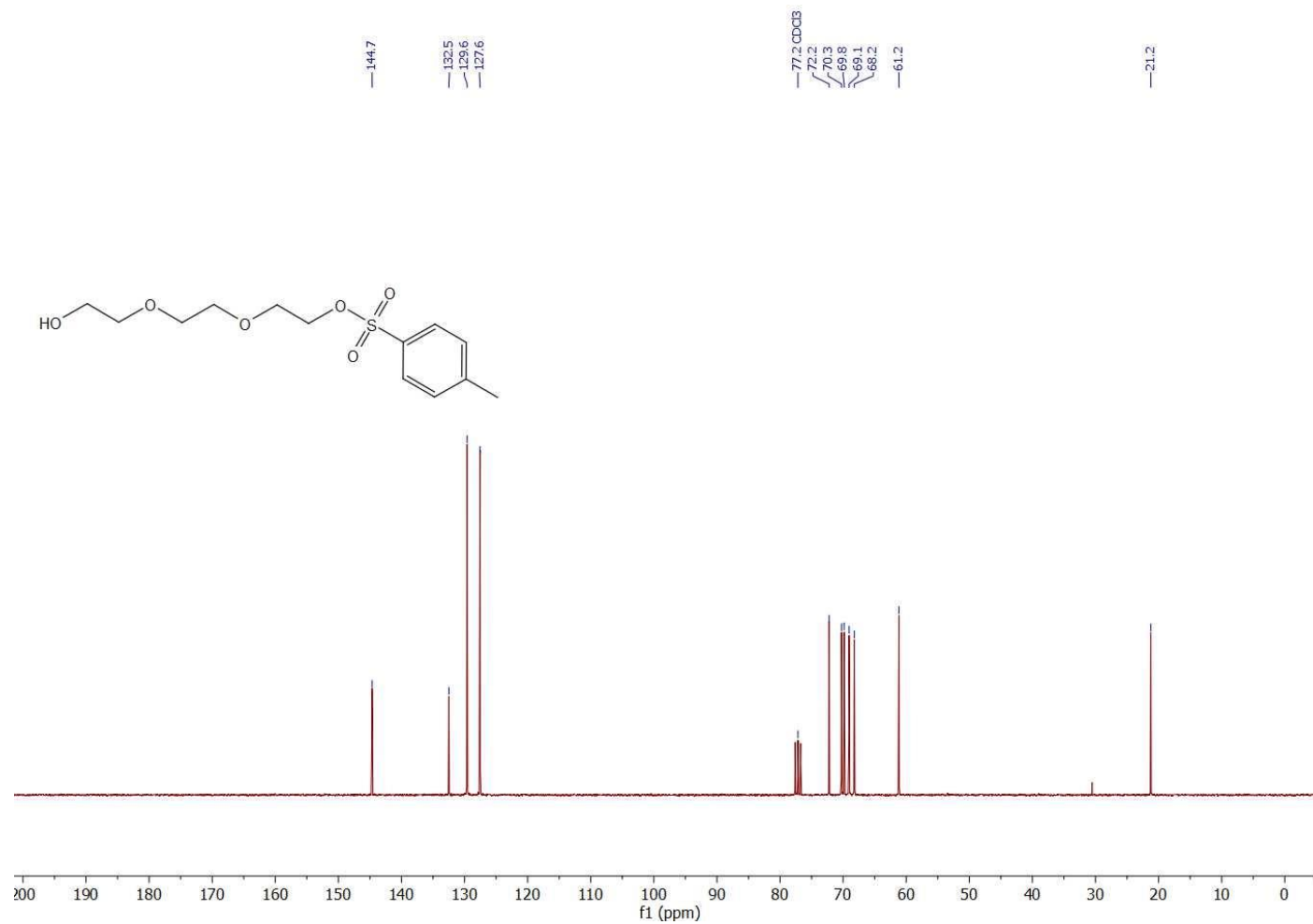
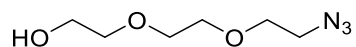


Figure 6.134 ¹³C NMR (75 MHz, CDCl₃) spectrum of compound 5.179.

2-(2-(2-hydroxyethoxy)ethoxy)ethyl 4-methylbenzenesulfonate (**5.179**)

To a solution of **5.179** (1.1 g, 3.62 mmol, 1 eq.) in dry DMF (11 mL) was added NaN₃ (0.72 g, 11.1 mmol, 3 eq.) added at room temperature under nitrogen atmosphere and resulted mixture was stirred at 80 °C overnight. The reaction was cooled down to room temperature, quenched by addition of water (20 mL), and organic phase was extracted with DCM (4 x 50 mL), dried over Na₂SO₄ and concentrated *in-vacuo*. After short filtration through a pad of silica gel compound **5.180** (0.57 g, 3.26 mmol, 90 %) was obtained as yellowish oil.

¹H NMR (300 MHz, CDCl₃): δ (ppm) 3.62 – 3.46 (m, 8H), 3.48 – 3.41 (m, 2H), 3.28 – 3.19 (m, 2H), 3.16 (brs, 1H)

¹³C NMR (75 MHz, CDCl₃): δ (ppm) 72.3, 70.2, 70.0, 69.6, 61.2, 50.3

The spectroscopic data agreed well with those of the literature.⁵⁷⁰

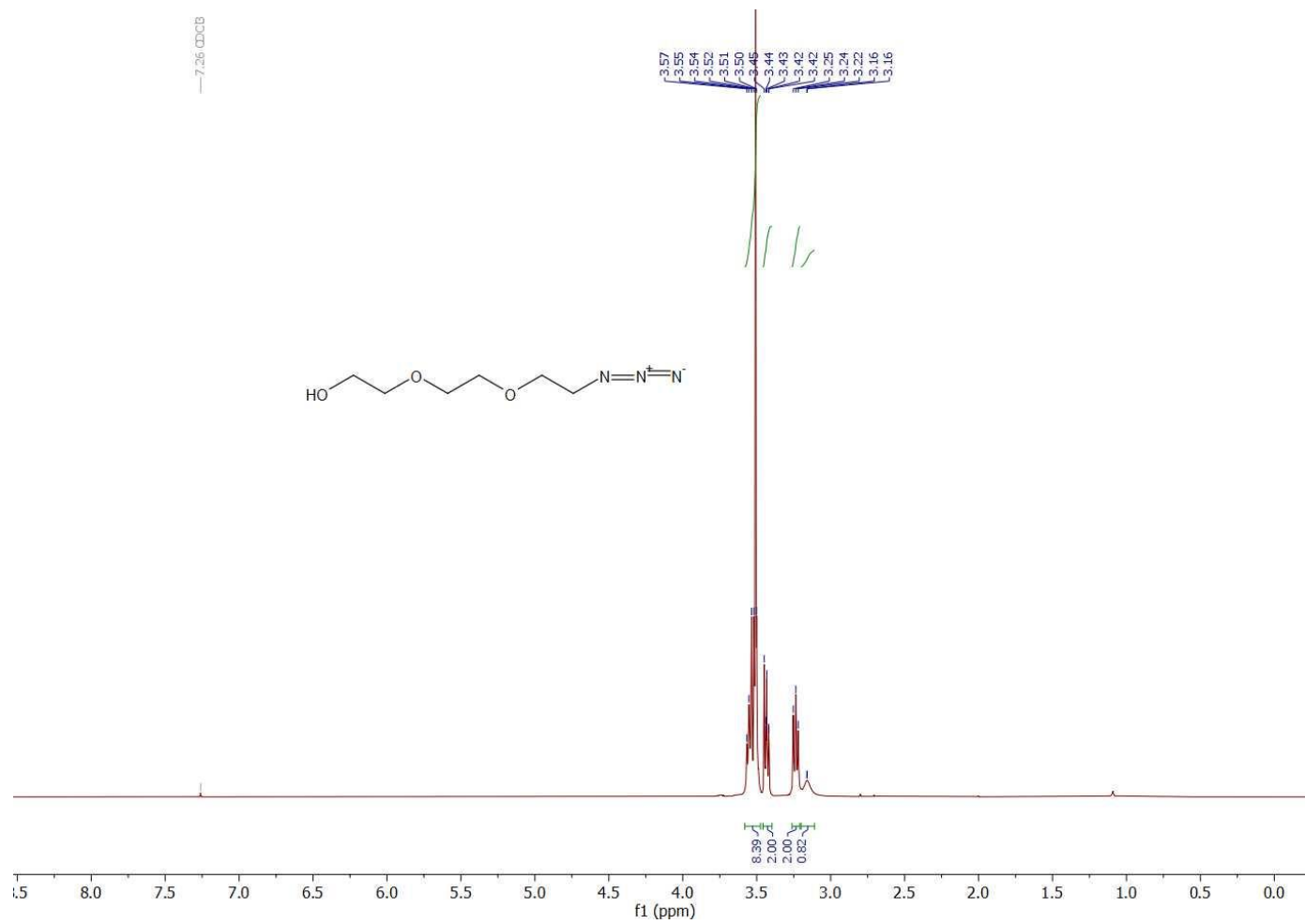


Figure 6.135 ^1H NMR (300 MHz, CDCl_3) spectrum of compound **5.180**.

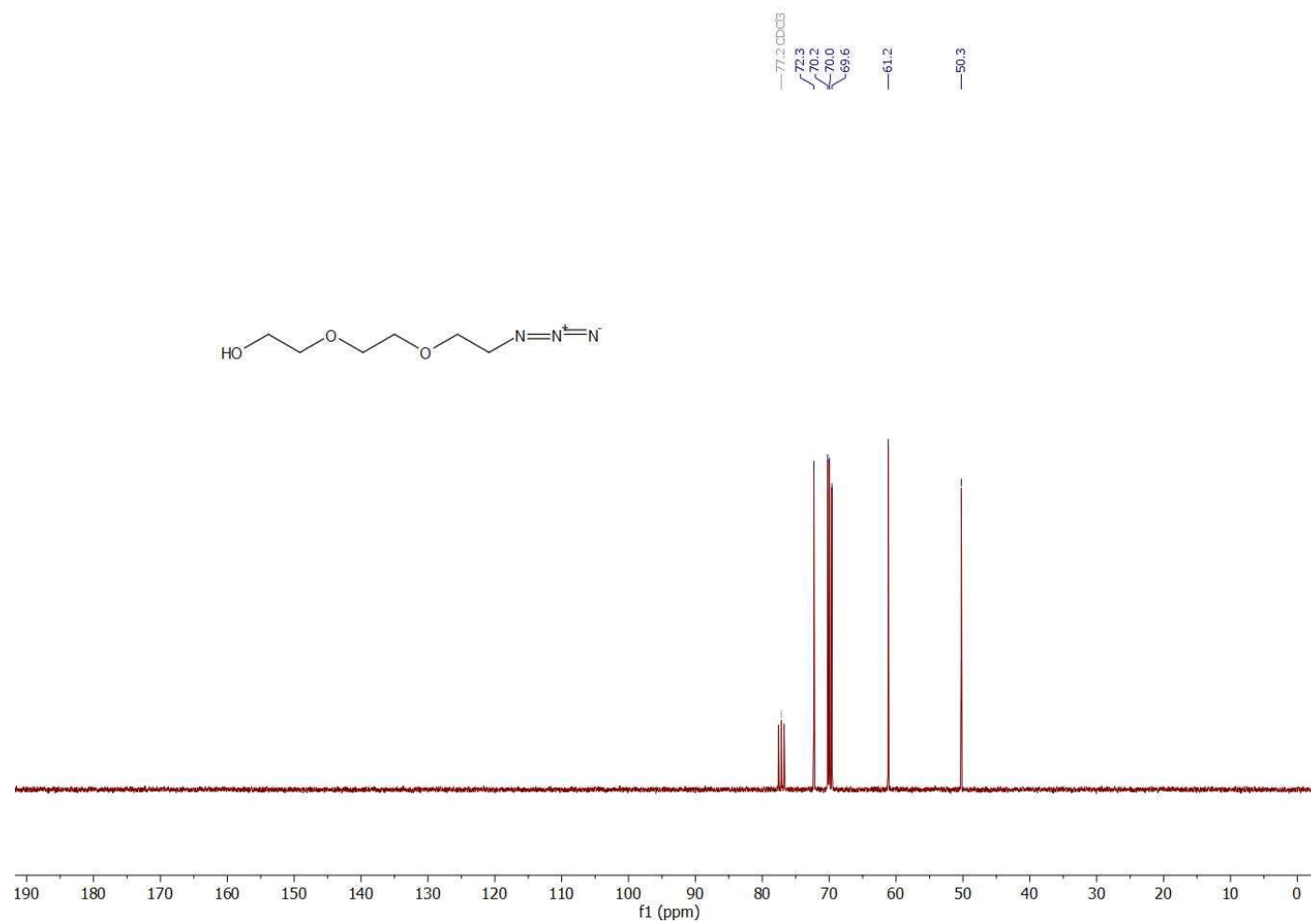
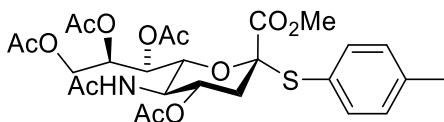


Figure 6.136 ^{13}C NMR (75 MHz, CDCl_3) spectrum of compound **5.180**.

Methyl (2-*S*-(4-methylphenyl)-4,7,8,9-tetra-*O*-acetyl-3,5-dideoxy-5-*N*-acetamido-D-glycero- β -D-galacto-non-2-ulopyranitol)onate (**5.181**)



Following the general procedure A, compound **5.181** (1.25 g, 2.09 mmol, 70 %) was obtained as a white solid.

¹H NMR (300 MHz, CDCl₃): δ (ppm) 7.38 (d, $J = 8.1$ Hz, 2H), 7.13 (d, $J = 7.6$ Hz, 2H), 5.35 – 5.21 (m, 2H), 5.17 (d, $J = 9.8$ Hz, 1H), 4.83 (ddd, $J = 11.7, 9.9, 4.7$ Hz, 1H), 4.40 (dd, $J = 12.4, 2.4$ Hz, 1H), 4.20 (dd, $J = 12.4, 5.3$ Hz, 1H), 3.97 (q, $J = 10.1$ Hz, 1H), 3.87 (dd, $J = 10.7, 1.7$ Hz, 1H), 3.59 (s, 3H), 2.77 (dd, $J = 12.9, 4.7$ Hz, 1H), 2.36 (s, 3H), 2.13 (s, 3H), 2.05 (s, 3H), 2.04 (s, 3H), 2.01 (brs, 4H), 1.85 (s, 3H)

¹³C NMR (75 MHz, CDCl₃): δ (ppm) 171.1, 170.8, 170.3, 170.2, 170.2, 168.2, 140.4, 136.7, 129.8, 125.1, 87.6, 75.0, 70.3, 69.9, 67.9, 62.2, 52.9, 49.4, 38.2, 23.3, 21.5, 21.1, 21.0, 21.0, 20.9

The spectroscopic data agreed well with those of the literature.⁴⁴⁹

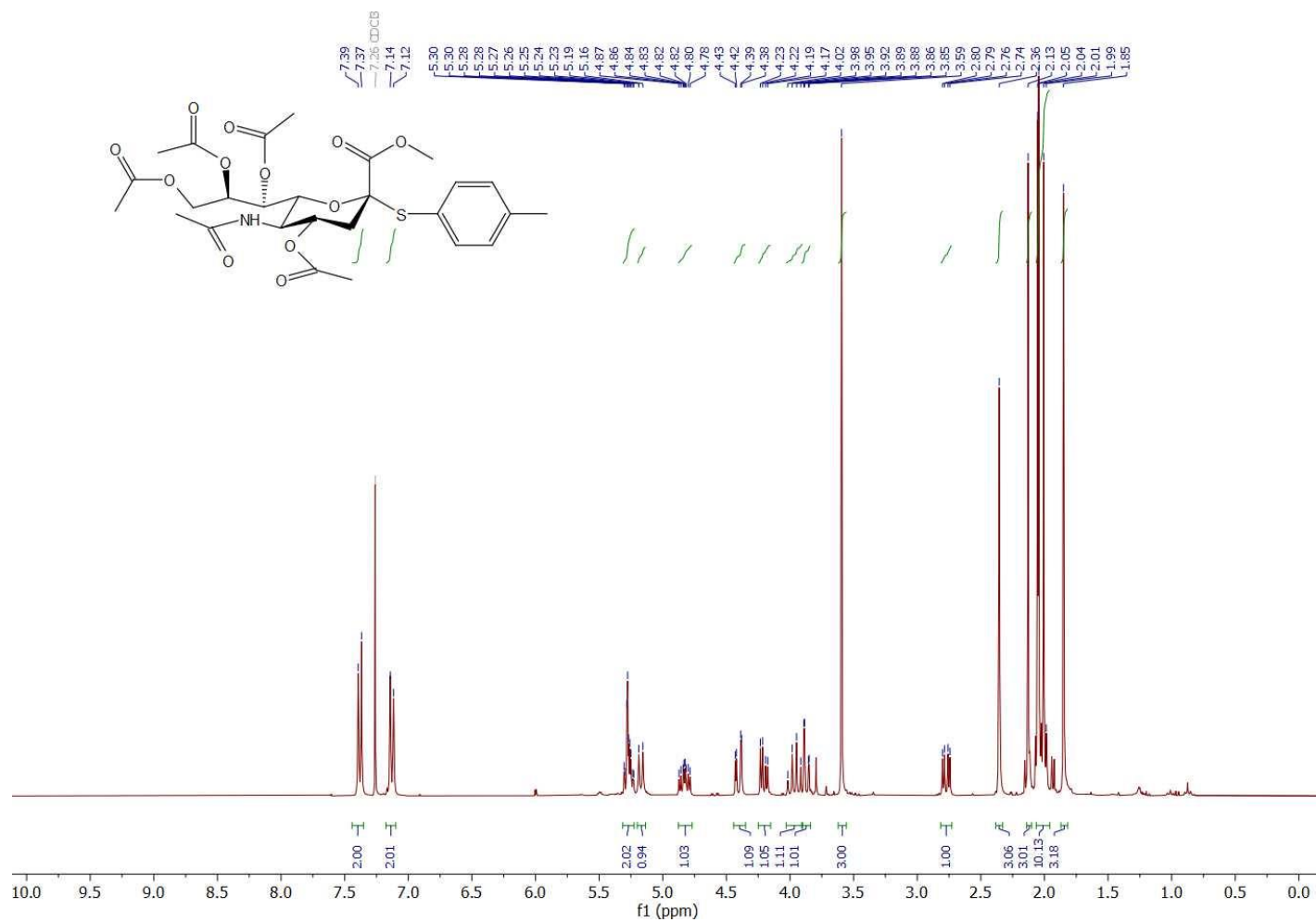


Figure 6.137 ^1H NMR (300 MHz, CDCl_3) spectrum of compound 5.181.

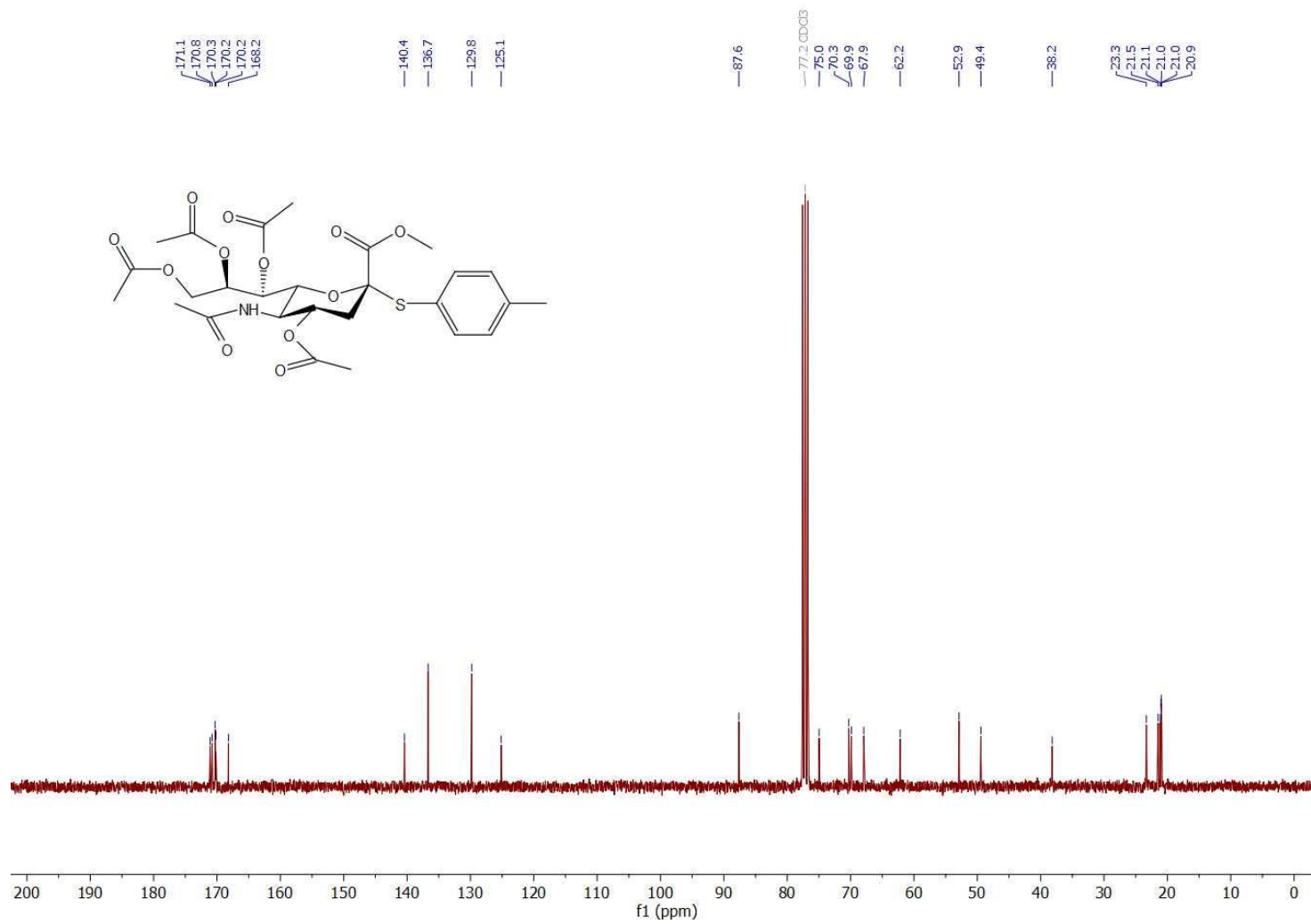
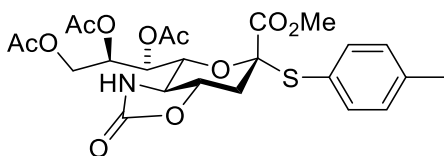


Figure 6.138 ^{13}C NMR (75 MHz, CDCl_3) spectrum of compound 5.181.

Methyl (2-*S*-(4-methylphenyl)-7,8,9-tri-*O*-acetyl-3,5-dideoxy-5-amino-5-*N*, 4-*O*-carbonyl-D-glycero- β -D-galacto-non-2-ulopyranitol)onate (**5.182**)



The compounds **5.182** was prepared according to a modified literature procedure.⁵⁷¹

To a solution of **5.181** (0.8 g, 1.34 mmol 1eq.), in MeOH (5 mL) was added methanesulfonic acid (MsOH, 0.09 mL, 1.38 mmol, 1.03 eq.) at room temperature under nitrogen. After stirring at 65 °C for 17 h, the reaction mixture was cooled to room temperature and quenched by excess amount of Et₃N (0.15 mL) and concentrated *in-vacuo*. The residue was dissolved in MeCN/H₂O (v/v : 4/1; 10 mL) and in presence of NaHCO₃ (0.62 g, 7.43 mmol, 5.55 eq.) a solution of 4-nitrophenyl chloroformate (0.97 g, 4.68 mmol, 3.5 eq.) in MeCN (2 mL) was added at 0 °C. After 3 h stirring, the reaction mixture was poured into ice cold saturated solution of NaHCO₃ (20 mL), extracted with EtOAc (3 x 50mL), dried over Na₂SO₄ and concentrated under reduced pressure. After short filtration over a pad of silica gel, and concentration *in-vacuo*, the residue was dissolved in Ac₂O (3 mL) and Pyridine (5 mL) the reaction mixture was stirred at room temperature overnight. The reaction mixture was diluted in CHCl₃ (30 mL), washed with ice cold water (2 x 25 mL), 0.2 M HCl (2 x 30 mL), brine (30 mL) and concentrated *in-vacuo*. After chromatographic purification **5.182** (0.32 g, 0.59 mmol, 44 %) was obtained as white solid.

R_f = 0.12, (EtOAc/hexane : 1/3)

¹H NMR (300 MHz, CDCl₃): δ (ppm) 7.33 (d, *J* = 7.9 Hz, 2H), 7.12 (d, *J* = 7.8 Hz, 2H), 5.47 – 5.23 (m, 2H), 5.07 (dd, *J* = 9.3, 1.7 Hz, 1H), 4.45 – 4.28 (m, 2H), 4.00

(dd, $J = 9.9, 1.7$ Hz, 1H), 3.90 (ddd, $J = 12.6, 10.8, 3.6$ Hz, 1H), 3.53 (s, 3H), 3.07 (dd, $J = 12.0, 3.7$ Hz, 1H), 3.02 – 2.88 (m, 1H), 2.34 (s, 3H), 2.16 (s, 3H), 2.09 (d, $J = 12.3$ Hz, 1H), 2.04 (s, 3H), 2.03 (s, 3H)

^{13}C NMR (75 MHz, CDCl_3): δ (ppm) 171.5, 170.6, 169.5, 167.9, 159.1, 140.4, 136.2, 129.7, 125.0, 88.4, 77.4, 75.2, 69.0, 68.1, 61.4, 57.8, 52.9, 37.6, 21.4, 20.9, 20.8, 20.7

The spectroscopic data agreed well with those of the literature.⁵⁷¹

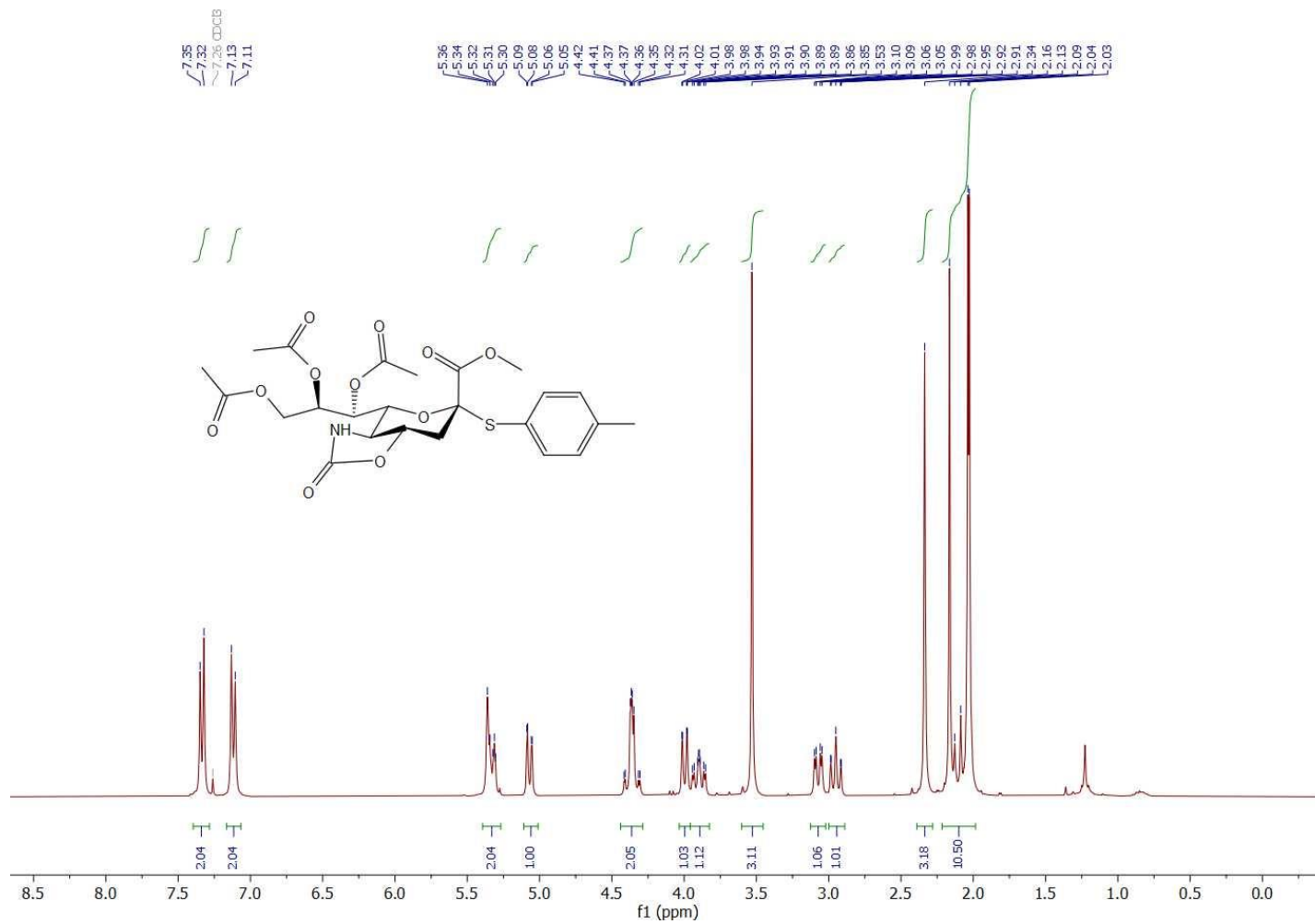


Figure 6.139 ^1H NMR (300 MHz, CDCl_3) spectrum of compound 5.182.

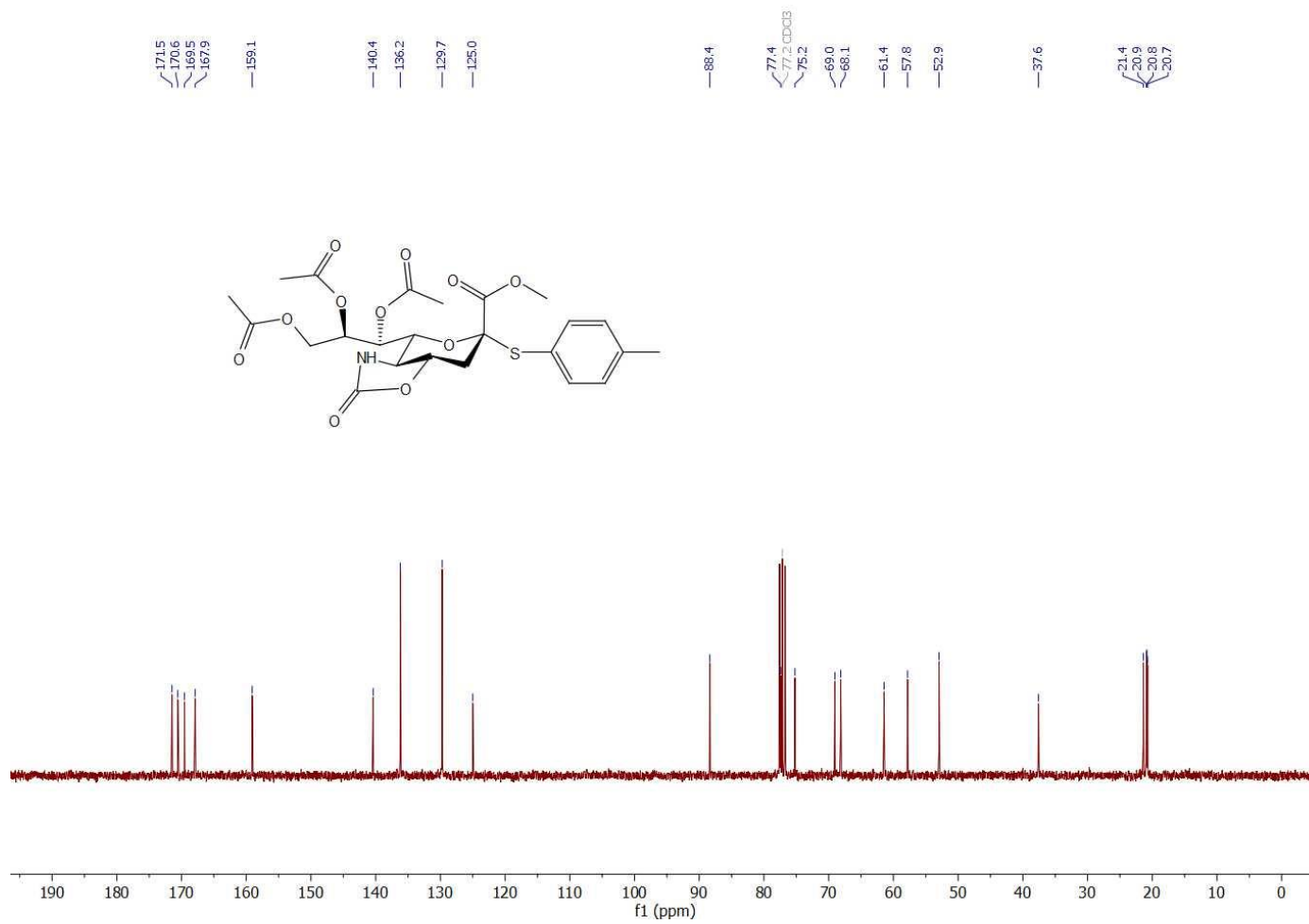
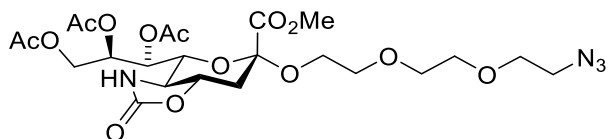


Figure 6.140 ^{13}C NMR (75 MHz, CDCl_3) spectrum of compound **5.182**.

Methyl (2-[2-[2-(2-azidoethoxy)ethoxy]ethyl]-7,8,9-tri-*O*-acetyl-3,5-dideoxy-5-amino-5-*N*, 4-*O*-carbonyl- β -D-glycero- β -D-galacto-non-2-ulopyranitol)onate (**5.183**)



A solution of sialyl donor **5.182** (0.09 g, 0.16 mmol, 1 eq.), acceptor **5.180** (0.06 g, 0.35 mmol, 2.22 eq.) and pulverized activated 4Å MS (0.06 g) in dry DCM/MeCN (0.6/0.4 mL) was stirred under nitrogen at room temperature for 0.5 h. The reaction mixture was cooled to -78 °C followed by successive addition of NIS (0.08 g, 0.35 mmol, 2.2 eq.) and TfOH (6 µL, 0.07 mmol, 0.42 eq.). After stirring for 7 h at the same temperature, the reaction mixture was quenched by excess amount of Hunig's base (0.02 mL), filtered through a pad of celite and concentrated under reduced pressure. After chromatographic purification compound **5.183** (0.07 g, 0.12 mmol, 77 %) was obtained as a brownish oil.

$R_f = 0.15$, (EtOAc/heptane : 1/1)

$[\alpha]_D^{21} = -20$ (c 0.004, CHCl₃)

¹H NMR (300 MHz, CD₃OD): δ (ppm) 5.43 (dt, $J = 9.8, 2.7$ Hz, 1H), 5.35 (s, 1H), 5.09 (dd, $J = 9.8, 1.9$ Hz, 1H), 4.26 (d, $J = 2.8$ Hz, 2H), 4.22 (dd, $J = 9.9, 1.9$ Hz, 1H), 3.98 – 3.79 (m, 2H), 3.76 (s, 3H), 3.73 – 3.46 (m, 8H), 3.46 – 3.31 (m, 3H), 3.02 (dd, $J = 15.3, 5.5$ Hz, 1H), 2.88 (dd, $J = 12.1, 3.5$ Hz, 1H), 2.15 (s, 3H), 2.14 (s, 3H), 2.08 – 2.00 (m, 4H)

¹³C NMR (750 MHz, CD₃OD): δ (ppm) 171.6, 170.6, 169.9, 168.5, 159.4, 100.3, 76.8, 73.6, 70.8, 70.6, 70.2, 70.1, 68.9, 67.0, 65.0, 61.8, 57.9, 53.0, 50.7, 37.5, 21.1, 20.8, 20.7

ESI-HRMS: *m/z* calcd. for C₂₃H₃₄N₄O₁₄ [M+Na]⁺, 613.1969; found 613.1932
[M+Na]⁺

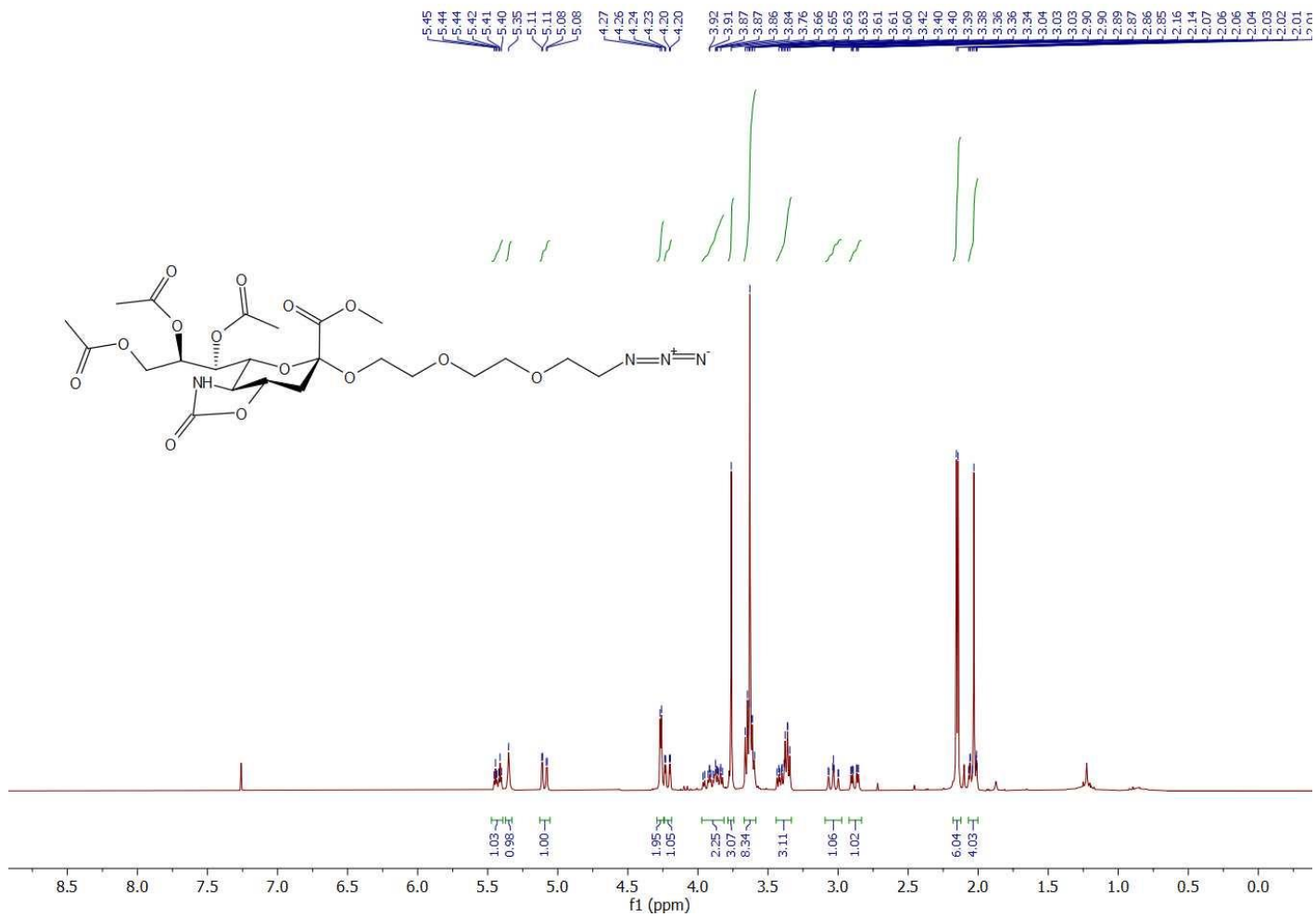


Figure 6.141 ^1H NMR (300 MHz, CDCl_3) spectrum of compound 5.183.

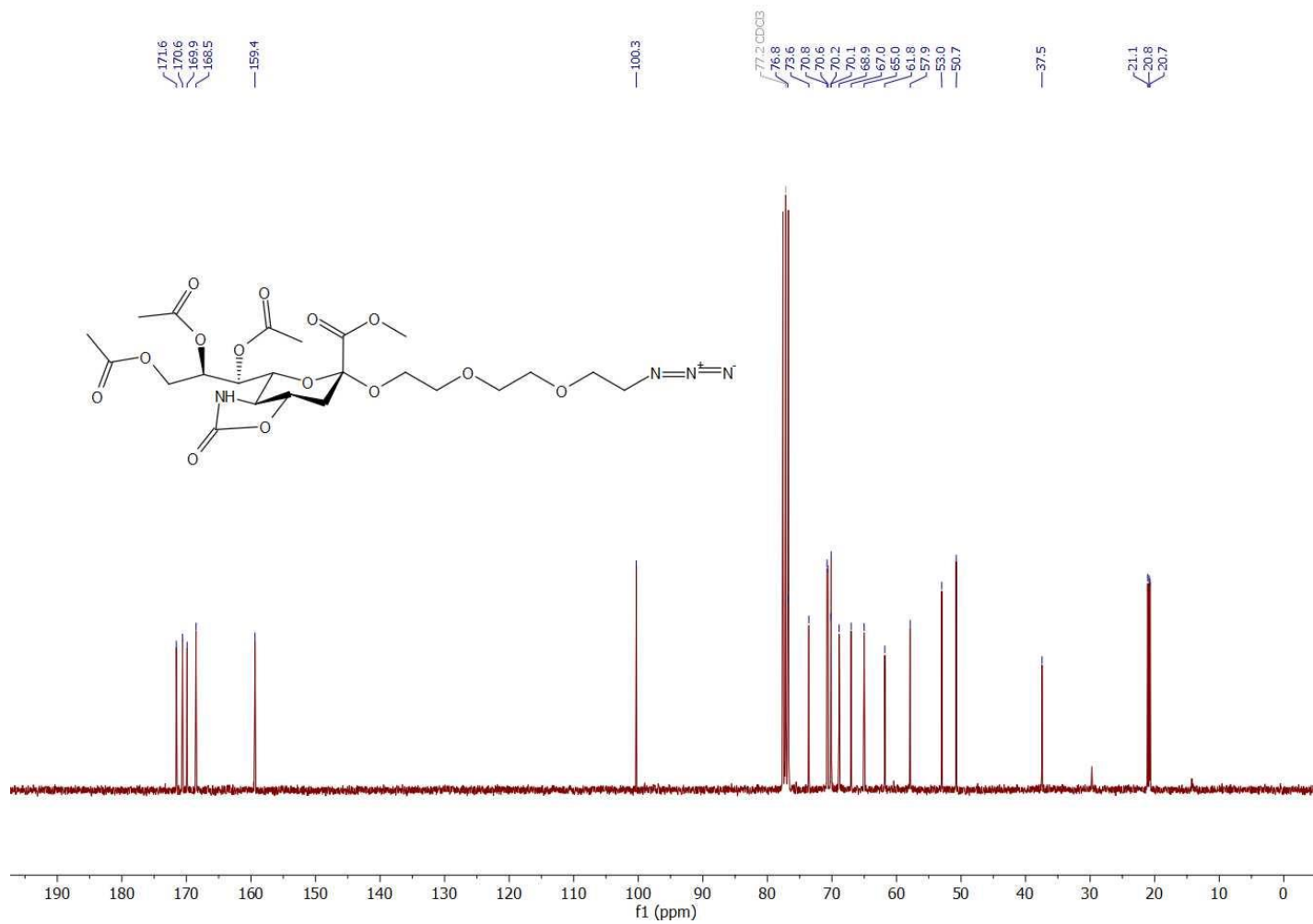
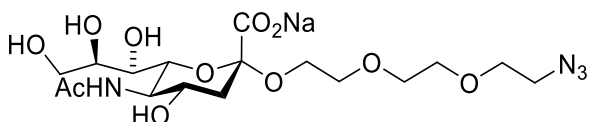


Figure 6.142 ^{13}C NMR (75 MHz, CDCl_3) spectrum of compound 5.183.

2-[2-[2-(2-azidoethoxy)ethoxy]ethyl]-3,5-dideoxy-5-*N*-acetamido-D-glycero- β -D-galacto-non-2-ulopyranosylonic acid (**5.171**)



To a solution of **5.183** (46 mg, 0.078 mmol, 1 eq.) in EtOH (0.3 mL), was added LiOH·H₂O (72 mg, 1.716 mmol, 22 eq.) in H₂O (0.3 mL). After stirring at 80 °C for 12 h, the reaction mixture was cooled down to room temperature, quenched with Amberlite[®] IR120 H⁺ and concentrated under reduced pressure. The residue was dissolved in H₂O (1.5 mL) and in presence of NaHCO₃ (197 mL, 2.344 mmol, 30 eq.) Ac₂O (0.6 mL) was added and resulted mixture was stirred for 12 h. After concentration *in-vacuo* the residue was dissolved in H₂O/MeOH and NaOMe was added dropwise until (pH = 9) and resulted mixture was stirred for additional 0.5 h. The reaction was quenched by aforementioned acidic resin, filtered through a pad of celite and concentrated under reduced pressure to crude **5.171** (36 mg, 0.077 mmol, 99 %) was as a white solid.

¹H NMR (300 MHz, D₂O): δ (ppm) 3.92 – 3.35 (m, 19H), 2.74 (dd, $J = 12.4, 4.4$ Hz, 1H), 2.03 (s, 3H), 1.68 (t, $J = 12.2$ Hz, 1H)

¹³C NMR (750 MHz, D₂O): δ (ppm) 174.9, 173.3, 100.4, 72.4, 71.6, 69.5, 69.4, 69.3, 69.1, 68.1, 67.9, 63.2, 62.4, 51.8, 50.0, 40.0, 22.2

ESI-HRMS: m/z calcd. for C₁₇H₃₀N₄O₁₁ [M+Na]⁺, 489.1809; found 489.1798 [M+Na]⁺

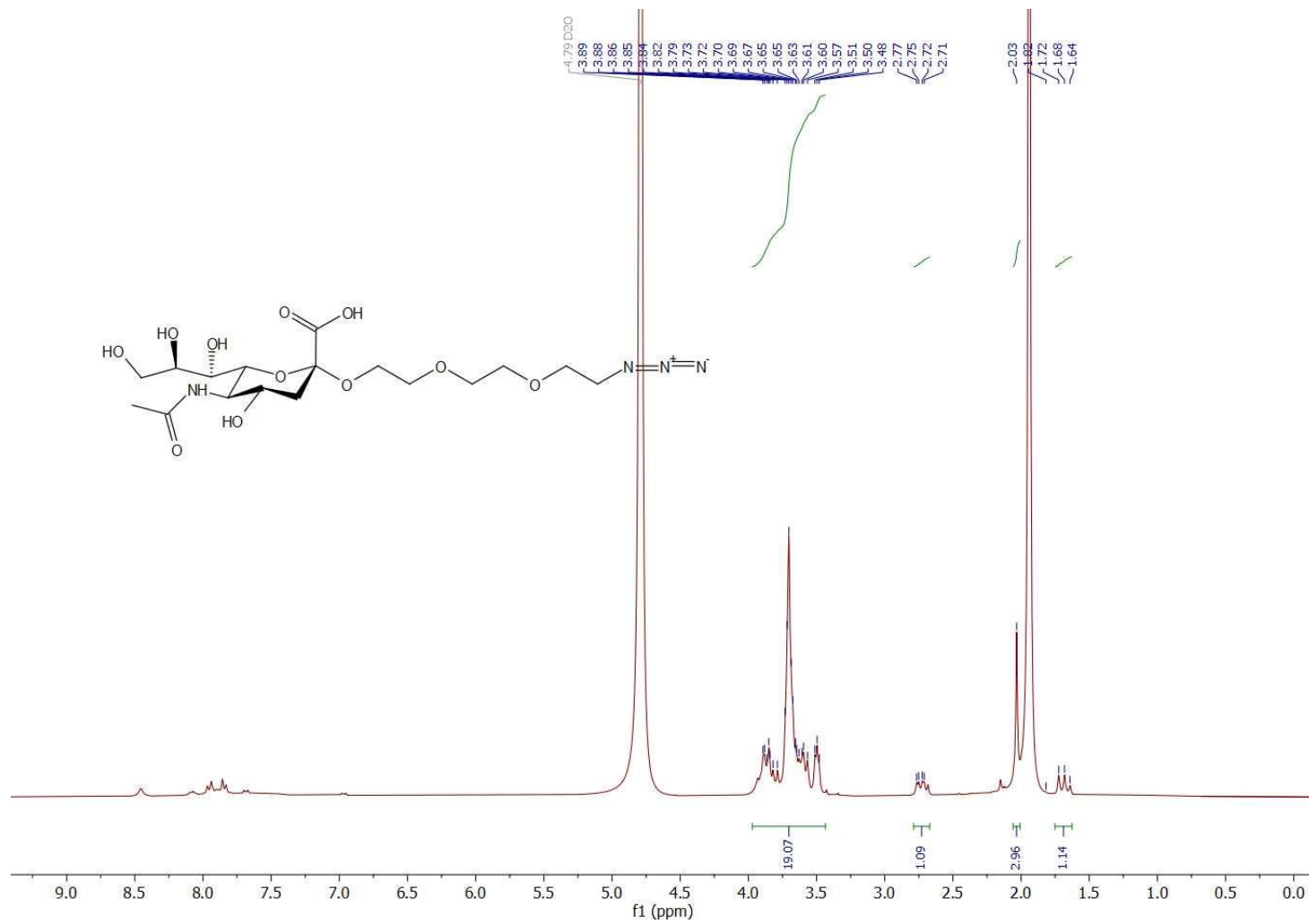
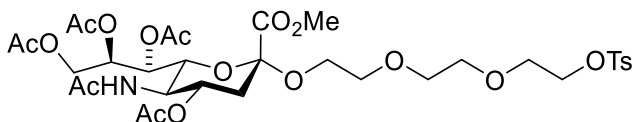


Figure 6.143 ¹H NMR (300 MHz, D₂O) spectrum of compound 5.171.

Methyl (2-[2-[2-[2-[(4-methylphenyl)sulfonyl]ethoxy]ethoxy]ethyl]-3,5-dideoxy-5-*N*-acetamido-D-glycero- α -D-galacto-non-2-ulopyranitol)onate (**5.184**)



To a mixture of silver-exchanged zeolite (2.04 g), **5.179** (1.23 g, 4031 μ mol, 2.25 eq.) in toluene (11 mL) was added dropwise a solution of **5.006** (0.91 g, 1.79 μ mol, 1 eq.) in toluene (6 mL) at 0 °C under nitrogen atmosphere. After 24 h of stirring, the reaction mixture was filtered through a pad of celite, concentrated under pressure and subjected to column chromatography to give **5.184** (1 g, 1.29 μ mol, 72 %) as a white solid.

$R_f = 0.54$, (EtOAc)

$[\alpha]_D^{21} = 6.1$ (c 0.003, CHCl_3)

$^1\text{H NMR}$ (300 MHz, CDCl_3): δ (ppm) 7.77 (d, $J = 8.3$ Hz, 2H), 7.32 (d, $J = 7.8$ Hz, 2H), 5.45 – 5.20 (m, 3H), 4.83 (ddd, $J = 12.3, 9.7, 4.7$ Hz, 1H), 4.27 (dd, $J = 12.4, 2.6$ Hz, 1H), 4.19 – 4.09 (m, 2H), 4.11 – 3.97 (m, 3H), 3.86 (ddd, $J = 10.7, 5.0, 3.5$ Hz, 1H), 3.76 (s, 3H), 3.71 – 3.61 (m, 2H), 3.61 – 3.51 (m, 6H), 3.41 (ddd, $J = 10.4, 6.4, 3.7$ Hz, 1H), 2.59 (dd, $J = 12.8, 4.6$ Hz, 1H), 2.42 (s, 3H), 2.11 (s, 3H), 2.10 (s, 3H), 2.01 (s, 3H), 2.00 (s, 3H), 1.94 (t, $J = 12.6$ Hz, 1H), 1.85 (s, 3H)

$^{13}\text{C NMR}$ (75 MHz, CDCl_3): δ (ppm) 171.1, 170.7, 170.4, 170.2, 170.2, 168.3, 144.9, 133.1, 129.9, 128.1, 98.9, 72.5, 70.8, 70.5, 70.2, 69.4, 69.2, 68.7, 68.5, 67.4, 64.5, 62.5, 52.9, 49.4, 38.1, 23.3, 21.7, 21.2, 20.9, 20.9, 20.8

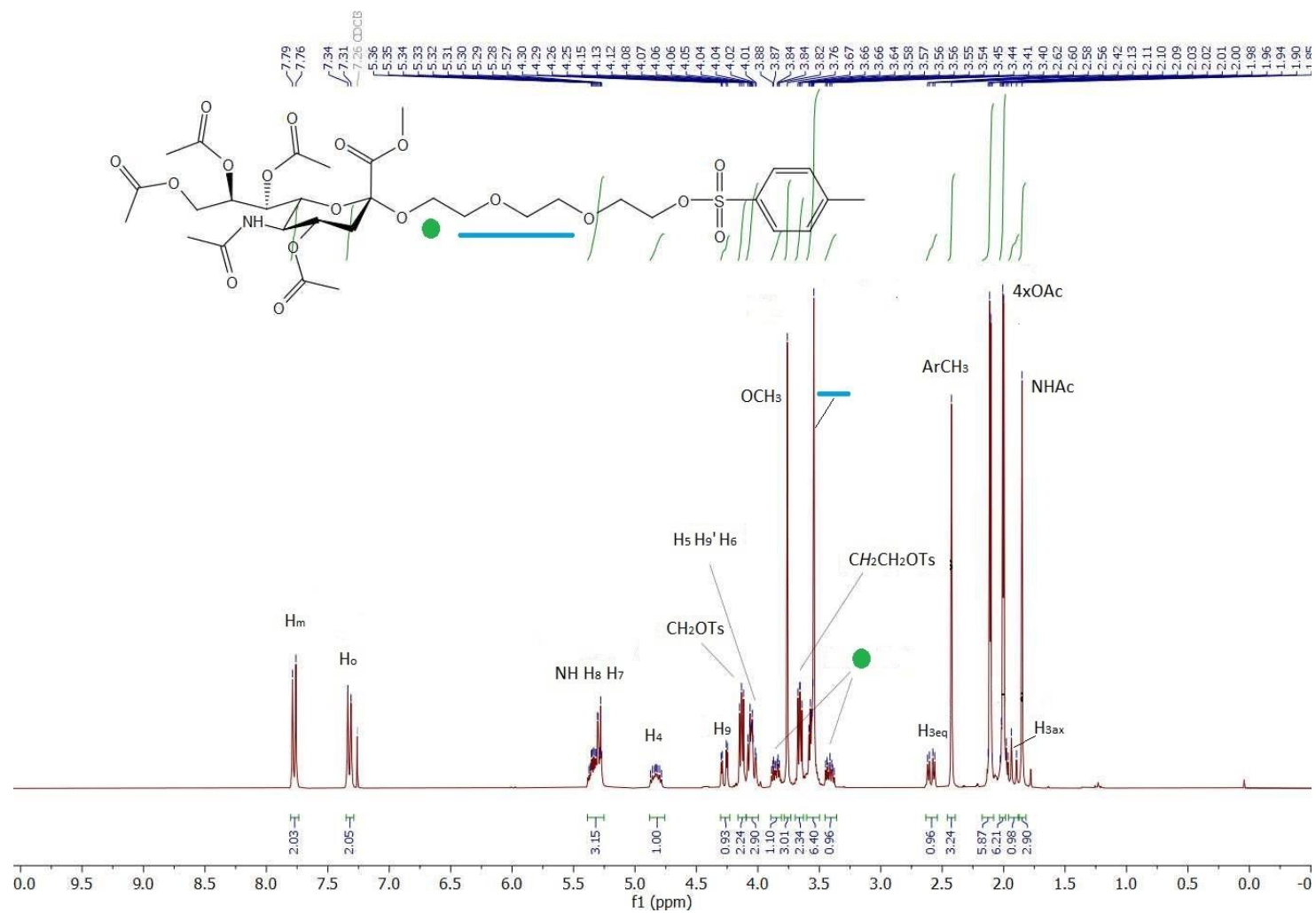


Figure 6.145 ^1H NMR (300 MHz, CDCl_3) spectrum of compound 5.184.

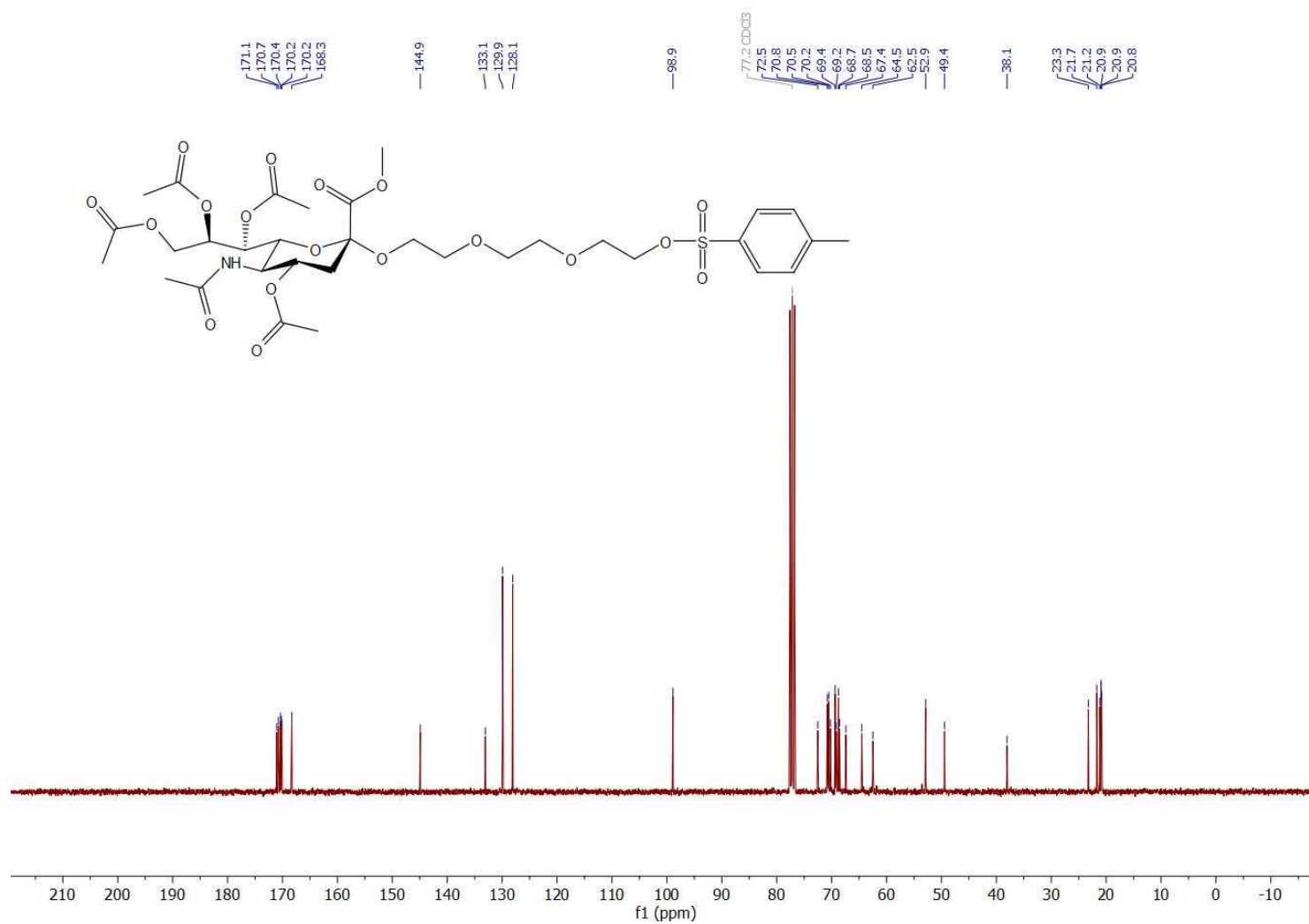
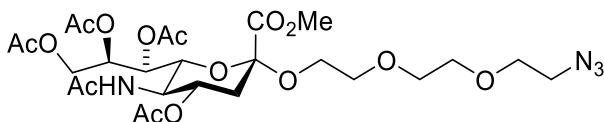


Figure 6.146 ^{13}C NMR (75 MHz, CDCl_3) spectrum of compound 5.184.

Methyl (2-[2-[2-(2-azidoethoxy)ethoxy]ethyl]-4,7,8,9-tetra-*O*-acetyl-3,5-dideoxy-5-*N*-acetamido-*D*-glycero- α -*D*-galacto-non-2-ulopyranitol)onate (**5.185**)



To a solution of **5.184** (0.45 g, 0.58 mmol, 1 eq.) and in DMF (12 mL) was added NaN₃ (0.11 g, 1.75 mmol, 3 eq.) at room temperature under nitrogen atmosphere and resulted mixture was stirred at 80 °C for 8 h. The reaction mixture was diluted in CHCl₃ (30 mL), washed with H₂O (3 x 20 mL), dried over Na₂SO₄ and concentrated under reduced pressure. After chromatographic purification **5.185** (0.26 g, 0.4 mmol, 69 %) was obtained as a brownish oil.

R_f = 0.31, (EtOAc)

[α]_D²¹ = -10.89.1 (c 0.018, CH₂Cl₂)

¹H NMR (300 MHz, CDCl₃): δ (ppm) 5.52 – 5.49 (m, 1H), 5.38 – 5.13 (m, 2H), 4.97 – 4.59 (m, 2H), 4.25 (dd, *J* = 12.4, 2.6 Hz, 1H), 4.10 – 3.90 (m, 3H), 3.90 – 3.78 (m, 1H), 3.73 (s, 3H), 3.66 – 3.52 (m, 8H), 3.44 – 3.29 (m, 4H), 2.55 (dd, *J* = 12.8, 4.6 Hz, 1H), 2.08 (s, 3H), 2.07 (s, 3H), 1.97 – 1.91 (m, 7H), 1.81 (s, 3H)

¹³C NMR (75 MHz, CDCl₃): δ (ppm) 171.0, 170.7, 170.3, 170.1, 168.3, 98.8, 72.5, 70.6, 70.6, 70.1, 70.0, 69.2, 68.7, 67.4, 64.4, 62.4, 52.7, 50.7, 49.2, 37.9, 23.1, 21.1, 20.8, 20.8, 20.8

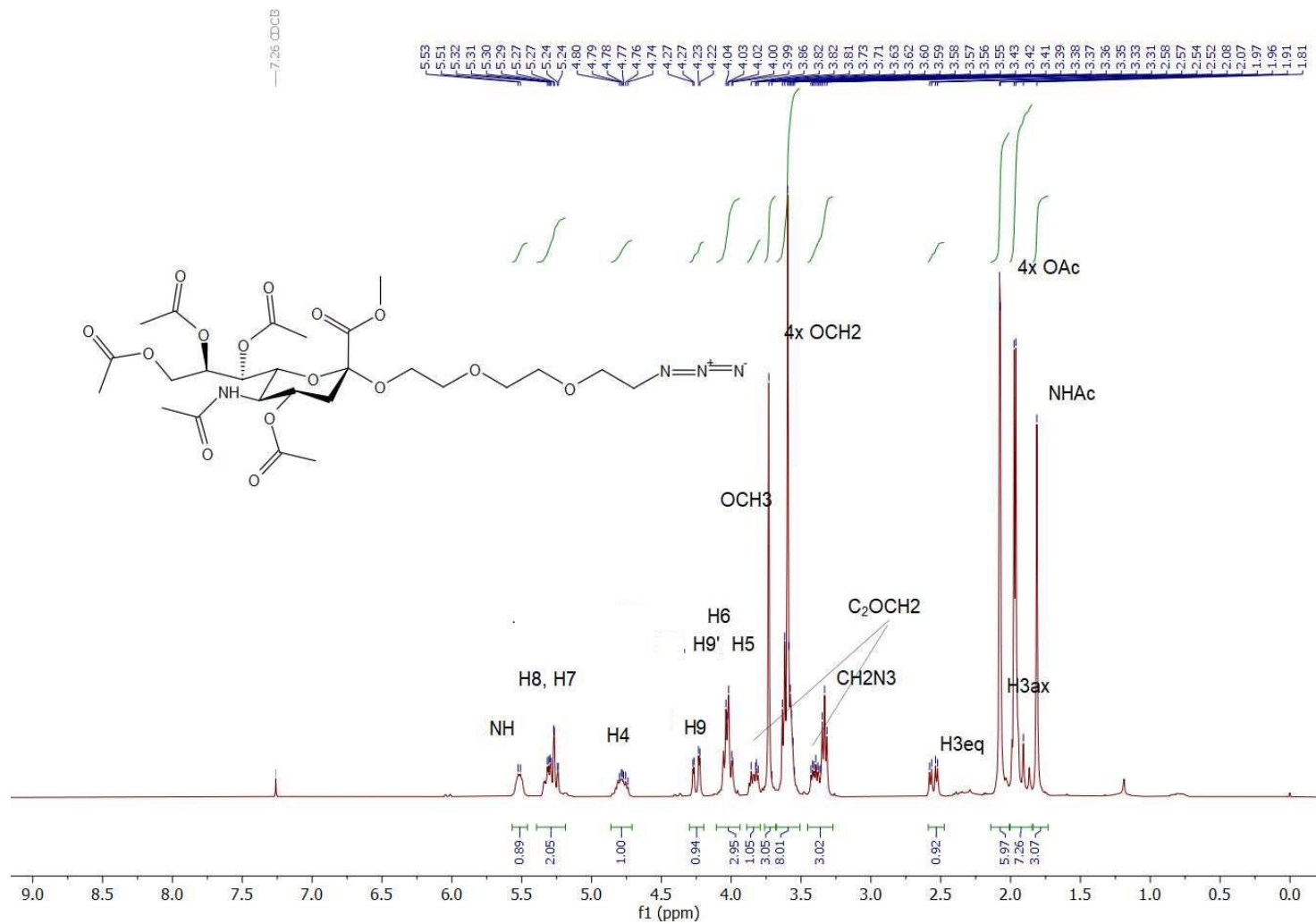


Figure 6.147 ^1H NMR (300 MHz, CDCl_3) spectrum of compound 5.185.

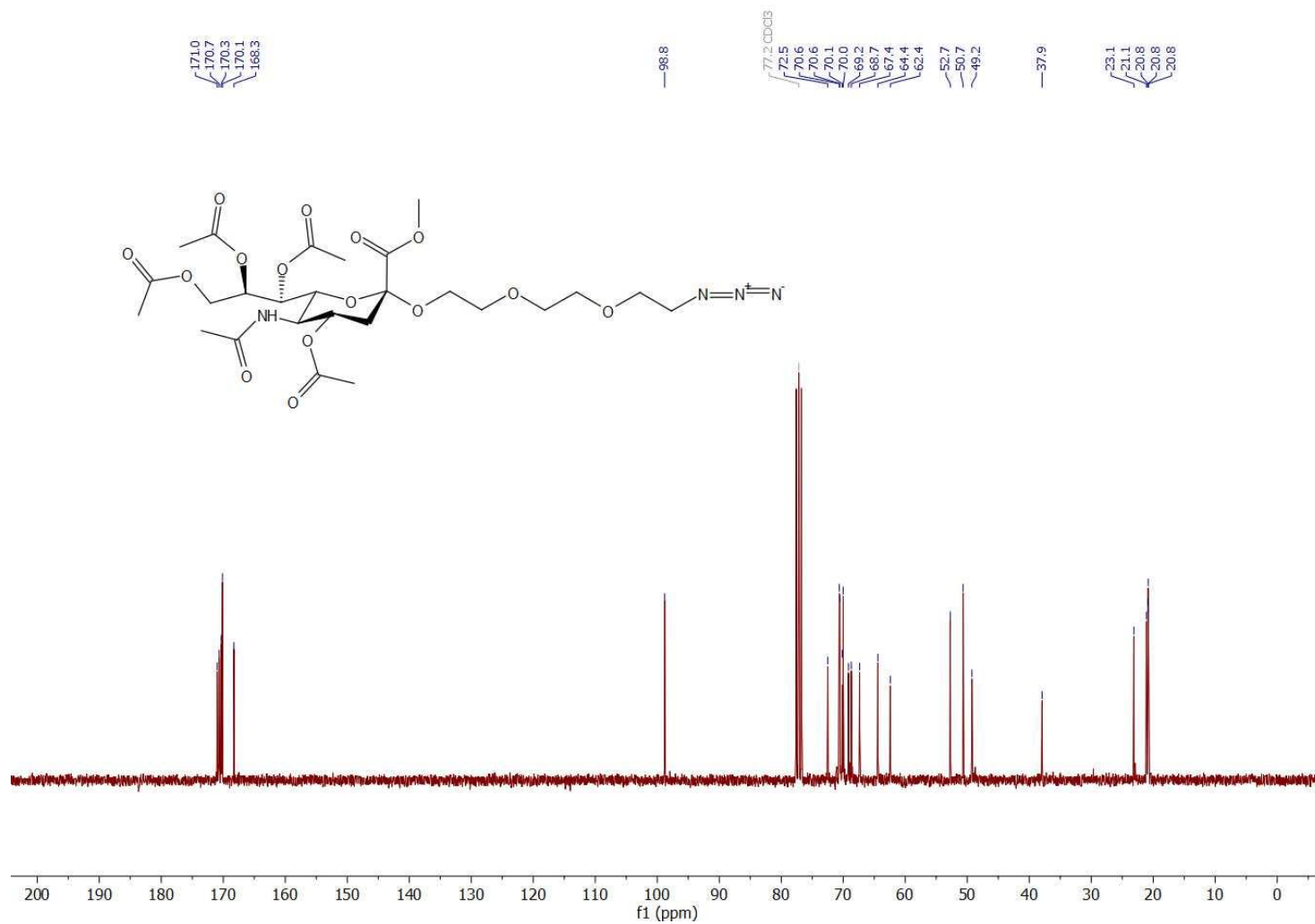


Figure 6.148 ^{13}C NMR (75 MHz, CDCl_3) spectrum of compound 5.185.

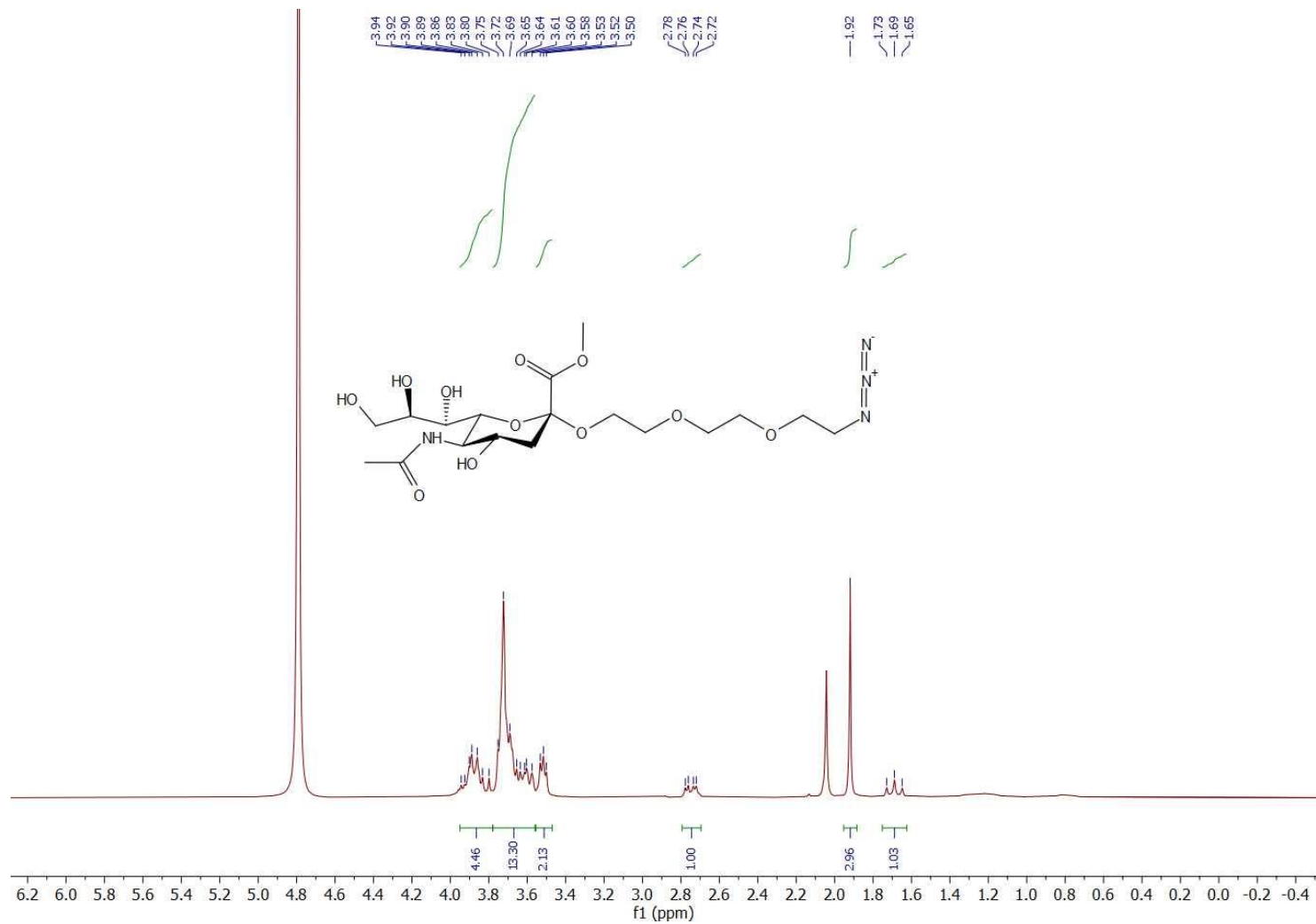


Figure 6.149 ^1H NMR (300 MHz, D_2O) spectrum of compound 5.185b.

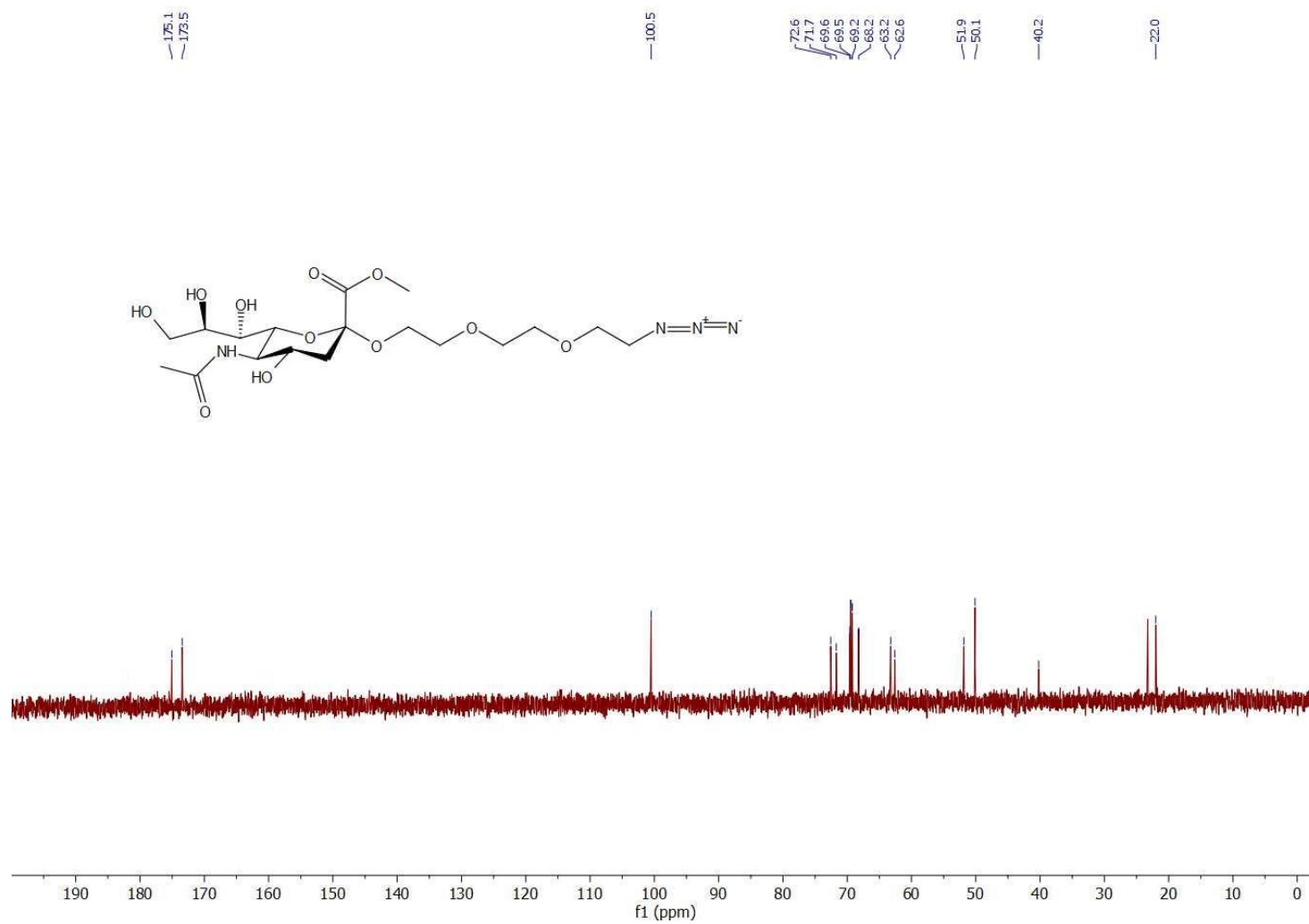
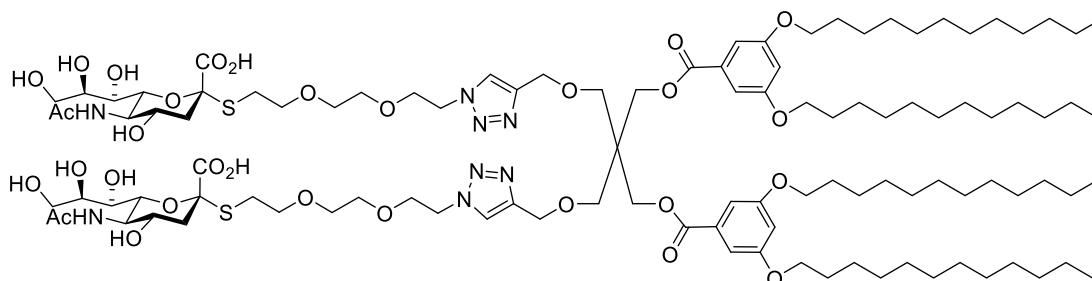


Figure 6.150 ¹³C NMR (75 MHz, D₂O) spectrum of compound 5.185b.

Sia-JD (bisclicked) (**5.109**)

To a solution of **5.170** (0.11 g, 0.23 mmol, 2.5 eq.) and **2.07** (0.11 g, 0.09 mmol, 1 eq.) in THF/H₂O (3.5/0.5 mL) were added separately CuSO₄·5H₂O (0.05 g, 0.19 mmol, 2 eq.) and sodium ascorbate (0.06 g, 0.28 mmol, 3 eq.) in H₂O (0.1 mL each) at room temperature, under nitrogen atmosphere. After 48 h of stirring, the reaction mixture was concentrated *in-vacuo* and subjected to filtration through a short column of silica gel (dry loading). The filtrate was then concentrated under reduced pressure and residue was purified using Sephadex® G10 and eluting with 0.01 M NaN₃ to give afforded **5.168** (0.03 g, 0.014 mmol, 15 %) as white solid.

¹H NMR (600 MHz, CDCl₃-CD₃OD): δ (ppm) 7.79 (s, 2H), 6.97 (d, *J* = 2.3 Hz, 4H), 6.60 (brs, 2H), 4.60 (s, 4H), 4.41 (s, 8H), 3.89 (t, *J* = 6.5 Hz, 8H), 3.83 – 3.79 (m, 14H), 3.75 (t, *J* = 10.3 Hz, 2H), 3.70 – 3.51 (m, 20H), 3.48 (d, *J* = 8.8 Hz, 2H), 3.34 (d, *J* = 10.3 Hz, 2H), 3.31 (s, 2H), 2.95 – 2.85 (m, 2H), 2.80 – 2.76 (m, 4H), 1.99 (s, 6H), 1.82 (t, *J* = 12.1 Hz, 2H), 1.74 (p, *J* = 6.9 Hz, 8H), 1.42 (p, *J* = 7.5 Hz, 8H), 1.34 – 1.25 (m, 64H), 0.85 (t, *J* = 6.9 Hz, 12H)

¹³C NMR (150 MHz, CDCl₃-CD₃OD): δ (ppm) 174.8, 171.6, 167.0, 160.9, 145.1, 132.1, 124.9, 108.2, 107.1, 83.6, 76.7, 71.8, 70.8, 70.8, 70.7, 69.8, 69.5, 68.9, 68.2, 65.1, 64.8, 64.1, 53.7, 53.1, 50.8, 44.7, 41.4, 32.5, 30.2, 30.2, 30.2, 30.2, 30.0, 29.9, 29.8, 29.3, 26.6, 23.2, 22.6, 14.3

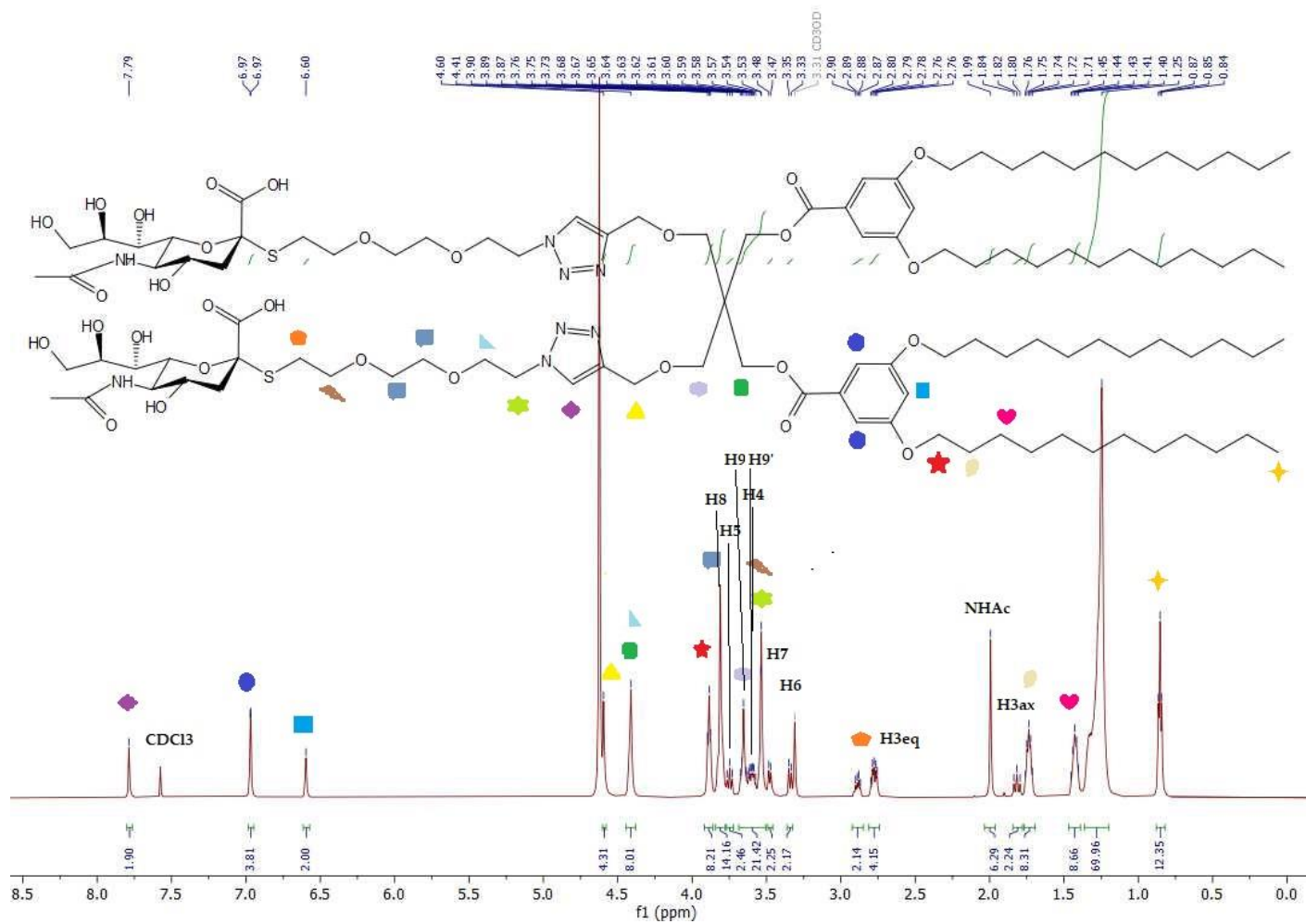


Figure 6.151 ^1H NMR (600 MHz, $\text{CD}_3\text{OD}+\text{CDCl}_3$ (v/v : 1/1)) spectrum of compound **5.109**.

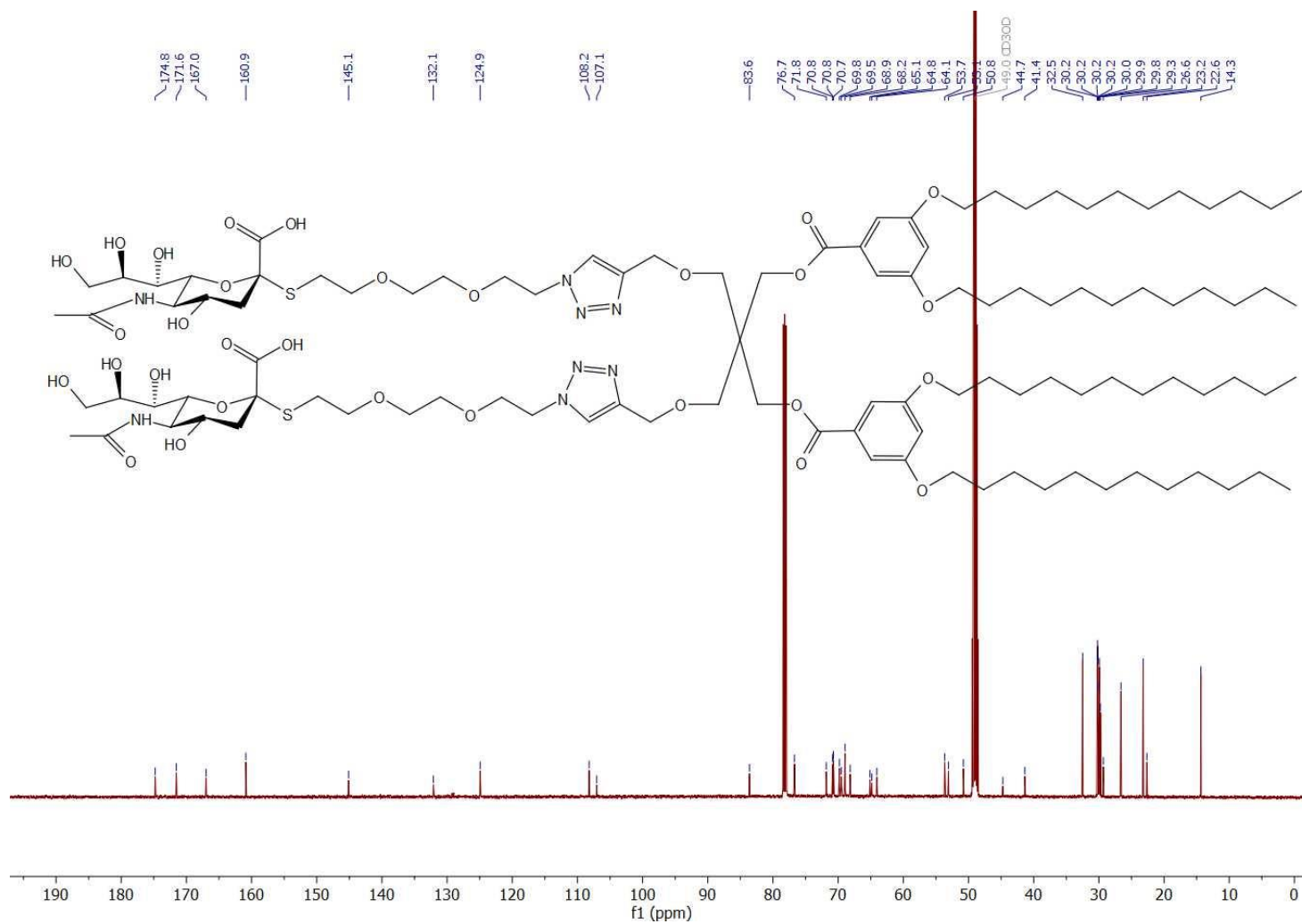


Figure 6.152 ¹³C NMR (150 MHz, CD₃OD+CDCl₃ (v/v : 1/1)) spectrum of compound **5.109**.

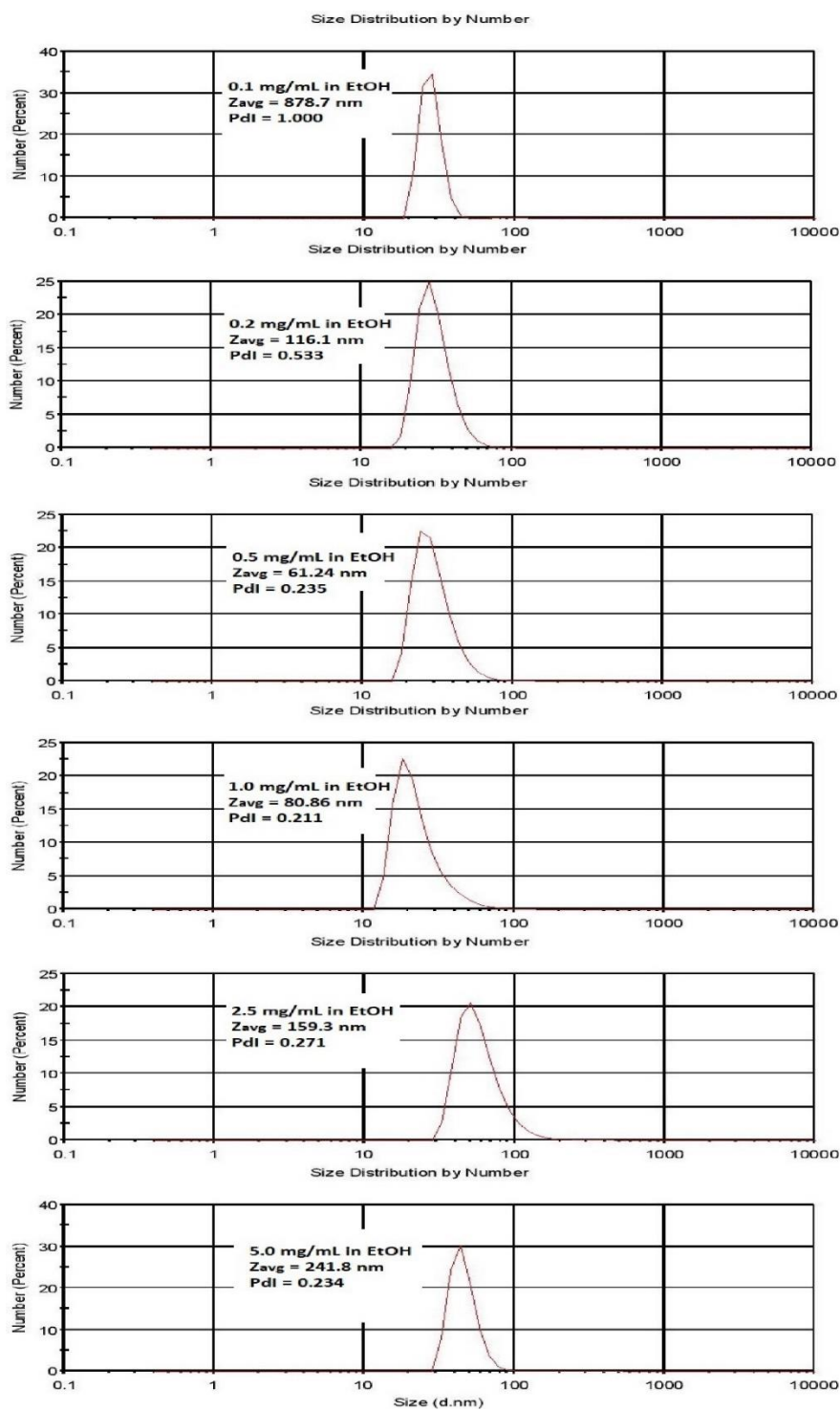


Figure 6.153 DLS analysis of sialodendrimerosomes of **5.168** with different concentration in EtOH.

REFERENCES

1. De Souza, G. A.; Oliveira, P. S.; Trapani, S.; Santos, A. C. O.; Rosa, J. C.; Laure, H. J.; Faça, V. M.; Correia, M. T.; Tavares, G. A.; Oliva, G., Amino acid sequence and tertiary structure of Cratylia mollis seed lectin. *Glycobiology* **2003**, *13* (12), 961-972.
2. Pauling, L., *The Nature of the Chemical Bond*. Cornell university press Ithaca, NY: 1960; Vol. 260.
3. Abel, R.; Young, T.; Farid, R.; Berne, B. J.; Friesner, R. A., Role of the active-site solvent in the thermodynamics of factor Xa ligand binding. *J. Am. Chem. Soc.* **2008**, *130* (9), 2817-2831.
4. Chodera, J. D.; Mobley, D. L., Entropy-enthalpy compensation: role and ramifications in biomolecular ligand recognition and design. *Annu. Rev. Biophys.* **2013**, *42*, 121-142.
5. Leigh, D. A., Summing up ligand binding interactions. *Chem. Biol.* **2003**, *10* (12), 1143-1144.
6. Wang, R.; Lai, L.; Wang, S., Further development and validation of empirical scoring functions for structure-based binding affinity prediction. *J. Comput. Aided Mol. Des.* **2002**, *16* (1), 11-26.
7. Toone, E. J., Structure and energetics of protein-carbohydrate complexes. *Curr. Opin. Struct. Biol.* **1994**, *4* (5), 719-728.

8. Lemieux, R. U., How water provides the impetus for molecular recognition in aqueous solution. *Acc. Chem. Res* **1996**, *29* (8), 373-380.
9. Leonidas, D. D.; Vatzaki, E. H.; Vorum, H.; Celis, J. E.; Madsen, P.; Acharya, K. R., Structural basis for the recognition of carbohydrates by human galectin-7. *Biochemistry* **1998**, *37* (40), 13930-13940.
10. Huyskens, P. L., Factors governing the influence of a first hydrogen bond on the formation of a second one by the same molecule or ion. *J. Am. Chem. Soc.* **1977**, *99* (8), 2578-2582.
11. Asensio, J. L.; Cañada, F. J.; Siebert, H.-C.; Laynez, J.; Poveda, A.; Nieto, P. M.; Soedjanaamadja, U.; Gabius, H.-J.; Jiménez-Barbero, J., Structural basis for chitin recognition by defense proteins: GlcNAc residues are bound in a multivalent fashion by extended binding sites in hevein domains. *Chem. Biol.* **2000**, *7* (7), 529-543.
12. Kauzmann, W., Some factors in the interpretation of protein denaturation. In *Advances in protein chemistry*, Elsevier: 1959; Vol. 14, pp 1-63.
13. Hildebrand, J. H., A criticism of the term "hydrophobic bond". *J. Phys. Chem.* **1968**, *72* (5), 1841-1842.
14. Frank, H. S.; Evans, M. W., Free volume and entropy in condensed systems III. Entropy in binary liquid mixtures; partial molal entropy in dilute solutions; structure and thermodynamics in aqueous electrolytes. *J. Chem. Phys.* **1945**, *13* (11), 507-532.
15. Abraham, M. H., Free energies, enthalpies, and entropies of solution of gaseous nonpolar nonelectrolytes in water and nonaqueous solvents. The hydrophobic effect. *J. Am. Chem. Soc.* **1982**, *104* (8), 2085-2094.
16. Vyas, N. K., Atomic features of protein-carbohydrate interactions. *Curr. Opin. Struct. Biol.* **1991**, *1* (5), 732-740.
17. Weis, W. I.; Drickamer, K., Structural basis of lectin-carbohydrate recognition. *Annu. Rev. Biochem* **1996**, *65* (1), 441-473.

18. Fujimoto, Z.; Jackson, A.; Michikawa, M.; Maehara, T.; Momma, M.; Henrissat, B.; Gilbert, H. J.; Kaneko, S., The structure of a *Streptomyces avermitilis* α -L-rhamnosidase reveals a novel carbohydrate-binding module CBM67 within the six-domain arrangement. *J. Biol. Chem.* **2013**, *288* (17), 12376-12385.
19. Loukachevitch, L. V.; Bensing, B. A.; Yu, H.; Zeng, J.; Chen, X.; Sullam, P. M.; Iverson, T. M., Structures of the *Streptococcus sanguinis* SrpA binding region with human sialoglycans suggest features of the physiological ligand. *Biochemistry* **2016**, *55* (42), 5927-5937.
20. Sears, P.; Wong, C. H., Carbohydrate mimetics: a new strategy for tackling the problem of carbohydrate - mediated biological recognition. *Angew. Chem. Int. Ed.* **1999**, *38* (16), 2300-2324.
21. Sharon, N.; Lis, H., Lectins: cell-agglutinating and sugar-specific proteins. *Science* **1972**, *177* (4053), 949-959.
22. Gabius, H. J.; Siebert, H. C.; André, S.; Jiménez - Barbero, J.; Rüdiger, H., Chemical biology of the sugar code. *ChemBioChem* **2004**, *5* (6), 740-764.
23. Gabius, H.-J.; André, S.; Kaltner, H.; Siebert, H.-C., The sugar code: functional lectinomics. *Biochim. Biophys. Acta Gen. Subj.* **2002**, *1572* (2-3), 165-177.
24. Loris, R., Principles of structures of animal and plant lectins. *Biochim. Biophys. Acta Gen. Subj.* **2002**, *1572* (2-3), 198-208.
25. Halverson, L. J.; Stacey, G., Host recognition in the *Rhizobium*-soybean symbiosis: evidence for the involvement of lectin in nodulation. *Plant Physiol.* **1985**, *77* (3), 621-625.
26. Hirsch, A. M., Role of lectins (and rhizobial exopolysaccharides) in legume nodulation. *Curr. Opin. Plant Biol.* **1999**, *2* (4), 320-326.
27. Etzler, M. E., Plant lectins: molecular and biological aspects. *Annu. Rev. Plant Physiol.* **1985**, *36* (1), 209-234.
28. Bouckaert, J.; Loris, R.; Poortmans, F.; Wyns, L., Crystallographic structure of metal - free concanavalin A at 2.5 Å resolution. *Proteins* **1995**, *23* (4), 510-524.

29. Bouckaert, J.; Hamelryck, T.; Wyns, L.; Loris, R., Novel structures of plant lectins and their complexes with carbohydrates. *Curr. Opin. Struct. Biol.* **1999**, *9* (5), 572-577.
30. Sharon, N., Lectins: carbohydrate-specific reagents and biological recognition molecules. *J. Biol. Chem.* **2007**, *282* (5), 2753-2764.
31. Ivatt, R. J.; Harnett, P. B.; Reeder, J. W., Isolated erythroglucans have a high-affinity interaction with wheat germ agglutinin but are poorly accessible in situ. *Biochim. Biophys. Acta Gen. Subj.* **1986**, *881* (1), 124-134.
32. Karlsson, A., Wheat germ agglutinin induces NADPH-oxidase activity in human neutrophils by interaction with mobilizable receptors. *Infect. Immun.* **1999**, *67* (7), 3461-3468.
33. Sharon, N., Surface carbohydrates and surface lectins are recognition determinants in phagocytosis. *Immunol. Today* **1984**, *5* (5), 143-147.
34. Park, Y. R.; Kim, D. S.; Lee, D.-H.; Kang, H. G.; Park, J. H.; Lee, S. J., Cadmium-substituted concanavalin A and its trimeric complexation. *J. Microbiol. Biotechnol.* **2018**, *28* (12), 2106-2112.
35. Banerjee, R.; Das, K.; Ravishankar, R.; Suguna, K.; Surolia, A.; Vijayan, M., Conformation, protein-carbohydrate interactions and a novel subunit association in the refined structure of peanut lectin-lactose complex. *J. Mol. Biol.* **1996**, *259* (2), 281-296.
36. Harata, K.; Nagahora, H.; Jigami, Y., X-ray structure of wheat germ agglutinin isolectin 3. *Acta Crystallogr., Sec. D: Biol. Crystallogr.* **1995**, *51* (6), 1013-1019.
37. Imberty, A.; Varrot, A., Microbial recognition of human cell surface glycoconjugates. *Curr. Opin. Struct. Biol.* **2008**, *18* (5), 567-576.
38. Karlsson, K.-A., Microbial recognition of target-cell glycoconjugates. *Curr. Opin. Struct. Biol.* **1995**, *5* (5), 622-635.

39. Nizet, V.; Varki, A.; Aebi, M., Microbial lectins: hemagglutinins, adhesins, and toxins. Editors, T. C. o. G., Ed. Cold Spring Harbor Laboratory Press: La Jolla, California, 2017.
40. Imberty, A.; Mitchell, E. P.; Wimmerová, M., Structural basis of high-affinity glycan recognition by bacterial and fungal lectins. *Curr. Opin. Struct. Biol.* **2005**, *15* (5), 525-534.
41. Schauer, R., Chemistry, Metabolism, and Biological Functions of Sialic Acids. *Adv. Carbohydr. Chem. Biochem.* **1982**, *40*, 131-234.
42. Gamblin, S. J.; Skehel, J. J., Influenza hemagglutinin and neuraminidase membrane glycoproteins. *J. Biol. Chem.* **2010**, *285* (37), 28403-28409.
43. Weis, W.; Brown, J.; Cusack, S.; Paulson, J.; Skehel, J.; Wiley, D., Structure of the influenza virus haemagglutinin complexed with its receptor, sialic acid. *Nature* **1988**, *333* (6172), 426-431.
44. Drickamer, K.; Taylor, M. E., Biology of animal lectins. *Annu. Rev. Cell Biol.* **1993**, *9* (1), 237-264.
45. Drickamer, K.; Dell, A.; Fadden, A. J. In *Genomic analysis of C-type lectins*, Biochemical Society Symposia, Portland Press: 2002; pp 59-72.
46. Bevilacqua, M. P.; Nelson, R. M., Selectins. *J. Clin. Invest.* **1993**, *91* (2), 379-387.
47. Powell, L. D.; Varki, A., I-type lectins. *J. Biol. Chem.* **1995**, *270* (24), 14243-14246.
48. Varki, A.; Crocker, P. R., I-type lectins. In *Essentials of Glycobiology. 2nd edition*, Cold Spring Harbor Laboratory Press: 2009.
49. Pillai, S.; Netravali, I. A.; Cariappa, A.; Mattoo, H., Siglecs and immune regulation. *Annu. Rev. Immunol.* **2012**, *30*, 357-392.
50. Crocker, P. R.; Clark, E.; Filbin, M.; Gordon, S.; Jones, Y.; Kehrl, J.; Kelm, S.; Le Douarin, N.; Powell, L.; Roder, J., Siglecs: a family of sialic-acid binding lectins. *Glycobiology* **1998**, *8* (2), v.

51. Kiriyaama, K.; Itoh, K., Glycan Recognition and Application of P-Type Lectins. In *Lectin Purification and Analysis*, Springer: 2020; pp 267-276.
52. Dahms, N. M.; Hancock, M. K., P-type lectins. *Biochim. Biophys. Acta Gen. Subj.* **2002**, *1572* (2-3), 317-340.
53. Hirabayashi, J.; Kasai, K.-i., The family of metazoan metal-independent β -galactoside-binding lectins: structure, function and molecular evolution. *Glycobiology* **1993**, *3* (4), 297-304.
54. Arnoys, E. J.; Wang, J. L., Dual localization: proteins in extracellular and intracellular compartments. *Acta Histochem.* **2007**, *109* (2), 89-110.
55. Gloster, T. M., Development of inhibitors as research tools for carbohydrate-processing enzymes. Portland Press Ltd.: 2012.
56. Colman, P. M., Neuraminidase. In *The influenza viruses*, Springer: 1989; pp 175-218.
57. Kitaoka, M.; Hayashi, K., Carbohydrate-processing phosphorolytic enzymes. *Trends Glycosci. Glycotechnol.* **2002**, *14* (75), 35-50.
58. Kiessling, L. L.; Young, T.; Mortell, K. H., Multivalency in protein-carbohydrate recognition. In *Glycoscience: Chemistry and Chemical Biology I-III*, Springer: 2001; pp 1817-1861.
59. Mammen, M.; Choi, S. K.; Whitesides, G. M., Polyvalent interactions in biological systems: implications for design and use of multivalent ligands and inhibitors. *Angew. Chem. Int. Ed.* **1998**, *37* (20), 2754-2794.
60. Schug, K. A.; Joshi, M. D.; Fryčák, P.; Maier, N. M.; Lindner, W., Investigation of monovalent and bivalent enantioselective molecular recognition by electrospray ionization-mass spectrometry and tandem mass spectrometry. *J. Am. Soc. Mass Spectrom.* **2011**, *19* (11), 1629-1642.
61. Lee, Y. C.; Lee, R. T., Carbohydrate-protein interactions: basis of glycobiology. *Acc. Chem. Res.* **1995**, *28* (8), 321-327.

62. Lundquist, J. J.; Toone, E. J., The Cluster Glycoside Effect. *Chem. Rev.* **2002**, *102*, 555-578.
63. Kiessling, L. L.; Gestwicki, J. E.; Strong, L. E., Synthetic multivalent ligands in the exploration of cell-surface interactions. *Curr. Opin. Struct. Biol.* **2000**, *4* (6), 696-703.
64. Howorka, S.; Nam, J.; Bayley, H.; Kahne, D., Stochastic detection of monovalent and bivalent protein–ligand interactions. *Angew. Chem.* **2004**, *116* (7), 860-864.
65. Kiessling, L. L.; Gestwicki, J. E.; Strong, L. E., Synthetic multivalent ligands in the exploration of cell-surface interactions. *Curr. Opin. Chem. Biol.* **2000**, *4*, 696 - 703.
66. Roy, R., Syntheses and some applications of chemically defined multivalent glycoconjugates. *Curr. Opin. Struct. Biol.* **1996**, *6* (5), 692-702.
67. Roy, R., Recent developments in the rational design of multivalent glycoconjugates. In *Glycoscience Synthesis of Substrate Analogs and Mimetics*, Springer: 1997; pp 241-274.
68. Gestwicki, J. E.; Cairo, C. W.; Strong, L. E.; Oetjen, K. A.; Kiessling, L. L., Influencing Receptor-Ligand Binding Mechanisms with Multivalent Ligand Architecture. *J. Am. Chem. Soc.* **2002**, *124*, 14922-14933-14933.
69. Chabre, Y. M.; Roy, R., Design and Creativity in Synthesis of Multivalent Neoglycoconjugates. *Adv. Carbohydr. Chem. Biochem.* **2010**, *63*, 165-393.
70. Roy, R.; Murphy, P. V.; Gabius, H. J., Multivalent Carbohydrate-Lectin Interactions: How Synthetic Chemistry Enables Insights into Nanometric Recognition. *Molecules* **2016**, *21* (5).
71. Bernardi, A.; Jiménez-Barbero, J.; Casnati, A.; De Castro, C.; Darbre, T.; Fieschi, F.; Finne, J.; Funken, H.; Jaeger, K.-E.; Lahmann, M., Multivalent glycoconjugates as anti-pathogenic agents. *Chem. Soc. Rev.* **2013**, *42* (11), 4709-4727.

72. Bhatia, S.; Dimde, M.; Haag, R., Multivalent glycoconjugates as vaccines and potential drug candidates. *MedChemComm* **2014**, *5* (7), 862-878.
73. Davis, B. G., Synthesis of glycoproteins. *Chem. Rev.* **2002**, *102* (2), 579-602.
74. Payne, R. J.; Wong, C.-H., Advances in chemical ligation strategies for the synthesis of glycopeptides and glycoproteins. *Chem. Commun.* **2010**, *46* (1), 21-43.
75. Rendle, P. M.; Seger, A.; Rodrigues, J.; Oldham, N. J.; Bott, R. R.; Jones, J. B.; Cowan, M. M.; Davis, B. G., Glycodendriproteins: a synthetic glycoprotein mimic enzyme with branched sugar-display potentially inhibits bacterial aggregation. *J. Am. Chem. Soc.* **2004**, *126* (15), 4750-4751.
76. Lin, J. D.; Liu, X. W., Recent Development in Ligation Methods for Glycopeptide and Glycoprotein Synthesis. *Chem. Asian J.* **2020**, *15* (17), 2548-2557.
77. Roy, R., A decade of glycodendrimer chemistry. *Trends Glycosci. Glycotechnol.* **2003**, *15* (85), 291-310.
78. Imberty, A.; Chabre, Y. M.; Roy, R., Glycomimetics and glycodendrimers as high affinity microbial anti-adhesins. *Chemistry* **2008**, *14* (25), 7490-9.
79. Shiao, T. C.; Roy, R., Glycodendrimers as functional antigens and antitumor vaccines. *New J. Chem.* **2012**, *36* (2), 324-339.
80. Cousin, J. M.; Cloninger, M. J., Glycodendrimers: tools to explore multivalent galectin-1 interactions. *Beilstein J. Org. Chem.* **2015**, *11* (1), 739-747.
81. Abbassi, L.; Chabre, Y. M.; Kottari, N.; Arnold, A. A.; André, S.; Josserand, J.; Gabius, H.-J.; Roy, R., Multifaceted glycodendrimers with programmable bioactivity through convergent, divergent, and accelerated approaches using polyfunctional cyclotriphosphazenes. *Polym. Chem.* **2015**, *6* (44), 7666-7683.
82. Bes, L.; Angot, S.; Limer, A.; Haddleton, D. M., Sugar-coated amphiphilic block copolymer micelles from living radical polymerization: recognition by immobilized lectins. *Macromolecules* **2003**, *36* (7), 2493-2499.

83. Ponader, D.; Wojcik, F.; Beceren-Braun, F.; Dervede, J.; Hartmann, L., Sequence-defined glycopolymer segments presenting mannose: synthesis and lectin binding affinity. *Biomacromolecules* **2012**, *13* (6), 1845-1852.
84. Roy, R., Blue-prints, synthesis and applications of glycopolymers. *Trends Glycosci. Glycotechnol.* **1996**, *8* (40), 79-99.
85. Meunier, S. J.; Roy, R., Polysialosides scaffolded on p-Tert-butylcalix [4] arene. *Tetrahedron Lett.* **1996**, *37* (31), 5469-5472.
86. Marradi, M.; Martin-Lomas, M.; Penades, S., Glyconanoparticles: polyvalent tools to study carbohydrate-based interactions. In *Advances in carbohydrate chemistry and biochemistry*, Elsevier: 2010; Vol. 64, pp 211-290.
87. Reichardt, N. C.; Martín-Lomas, M.; Penadés, S., Glyconanotechnology. *Chem. Soc. Rev.* **2013**, *42* (10), 4358-4376.
88. Kikkeri, R.; Laurino, P.; Odedra, A.; Seeberger, P. H., Synthesis of carbohydrate - functionalized quantum dots in microreactors. *Angew. Chem. Int. Ed.* **2010**, *49* (11), 2054-2057.
89. Wang, X.; Matei, E.; Deng, L.; Ramström, O.; Gronenborn, A. M.; Yan, M., Multivalent glyconanoparticles with enhanced affinity to the anti-viral lectin Cyanovirin-N. *Chem. Commun.* **2011**, *47* (30), 8620-8622.
90. Compostella, F.; Pitirollo, O.; Silvestri, A.; Polito, L., Glyco-gold nanoparticles: synthesis and applications. *Beilstein J. Org. Chem.* **2017**, *13* (1), 1008-1021.
91. Sangabathuni, S.; Murthy, R. V.; Chaudhary, P. M.; Surve, M.; Banerjee, A.; Kikkeri, R., Glyco-gold nanoparticle shapes enhance carbohydrate-protein interactions in mammalian cells. *Nanoscale* **2016**, *8* (25), 12729-12735.
92. Zhu, J.; Xue, J.; Guo, Z.; Zhang, L.; Marchant, R. E., Biomimetic glycoliposomes as nanocarriers for targeting P-selectin on activated platelets. *Bioconjug. Chem.* **2007**, *18* (5), 1366-1369.

93. Jayaraman, N.; Maiti, K.; Naresh, K., Multivalent glycoliposomes and micelles to study carbohydrate–protein and carbohydrate–carbohydrate interactions. *Chem. Soc. Rev.* **2013**, *42* (11), 4640-4656.
94. AlSawaftah, N. M.; Abusamra, R. H.; Husseini, G., Carbohydrate-Functionalized Liposomes In Cancer Therapy. *Curr. Cancer Therapy Rev.* **2020**.
95. Stahn, R.; Schäfer, H.; Schreiber, J.; Brudel, M., Glycoliposomes-simple preparation and specific binding to lectin. *J. Liposome Res.* **1995**, *5* (1), 61-73.
96. Geissner, A.; Pereira, C. L.; Leddermann, M.; Anish, C.; Seeberger, P. H., Deciphering antigenic determinants of *Streptococcus pneumoniae* serotype 4 capsular polysaccharide using synthetic oligosaccharides. *ACS Chem. Biol.* **2016**, *11* (2), 335-344.
97. Wang, C. H.; Li, S. T.; Lin, T. L.; Cheng, Y. Y.; Sun, T. H.; Wang, J. T.; Cheng, T. J. R.; Mong, K. K. T.; Wong, C. H.; Wu, C. Y., Synthesis of *Neisseria meningitidis* serogroup W135 capsular oligosaccharides for immunogenicity comparison and vaccine development. *Angew. Chem. Int. Ed.* **2013**, *52* (35), 9157-9161.
98. Van Der Put, R. M.; Kim, T. H.; Guerreiro, C.; Thouron, F.; Hoogerhout, P.; Sansonetti, P. J.; Westdijk, J.; Stork, M.; Phalipon, A.; Mulard, L. A., A synthetic carbohydrate conjugate vaccine candidate against shigellosis: improved bioconjugation and impact of alum on immunogenicity. *Bioconjug. Chem.* **2016**, *27* (4), 883-892.
99. Edelman, R.; Talor, D. N.; Wasserman, S. S.; McClain, J. B.; Cross, A. S.; Sadoff, J. C.; Que, J. U.; Cryz, S. J., Phase 1 trial of a 24-valent *Klebsiella* capsular polysaccharide vaccine and an eight-valent *Pseudomonas* O-polysaccharide conjugate vaccine administered simultaneously. *Vaccine* **1994**, *12* (14), 1288-1294.
100. Armstrong, G. D.; Fodor, E.; Vanmaele, R., Investigation of Shiga-like toxin binding to chemically synthesized oligosaccharide sequences. *J. Infect. Dis.* **1991**, *164* (6), 1160-1167.

101. Kaper, J. B.; O'Brien, A. D., *Escherichia coli* 0157: H7 and other shiga toxin-producing *E. coli* strains. ASM Press: 1998.
102. Rowe, P. C.; Milner, R.; Orrbine, E.; Klassen, T. P.; Goodyer, P. G.; MacKenzie, A. M.; Wells, G. A.; Auclair, F.; Blanchard, C.; Lior, H., A Phase II Randomized Controlled Trial of Synsorb-PK for the Prevention of Hemolytic Uremic Syndrome in Children with Verotoxin-Producing *E. Coli* (VTEC) Gastroenteritis. *Pediatr. Res.* **1997**, *41* (4), 283-283.
103. Zuercher, A. W.; Horn, M. P.; Que, J. U.; Ruedeberg, A.; Schoeni, M. H.; Schaad, U. B.; Marcus, P.; Lang, A. B., Antibody responses induced by long-term vaccination with an octovalent conjugate *Pseudomonas aeruginosa* vaccine in children with cystic fibrosis. *FEMS Microbiol. Immunol.* **2006**, *47* (2), 302-308.
104. Verez-Bencomo, V.; Fernandez-Santana, V.; Hardy, E.; Toledo, M. E.; Rodriguez, M. C.; Heynngnezz, L.; Rodriguez, A.; Baly, A.; Herrera, L.; Izquierdo, M.; Villar, A.; Valdes, Y.; Cosme, K.; Deler, M. L.; Montane, M.; Garcia, E.; Ramos, A.; Aguilar, A.; Medina, E.; Torano, G.; Sosa, I.; Hernandez, I.; Martinez, R.; Muzachio, A.; Carmenates, A.; Costa, L.; Cardoso, F.; Campa, C.; Diaz, M.; Roy, R., A synthetic conjugate polysaccharide vaccine against *Haemophilus influenzae* type b. *Science* **2004**, *305* (5683), 522-5.
105. Renaudet, O.; Roy, R., Multivalent scaffolds in glycoscience: an overview. *Chem. Soc. Rev.* **2013**, *42* (11), 4515-7.
106. Chabre, Y. M.; Roy, R., Multivalent glycoconjugate syntheses and applications using aromatic scaffolds. *Chem. Soc. Rev.* **2013**, *42* (11), 4657-708.
107. Cecioni, S.; Praly, J. P.; Matthews, S. E.; Wimmerova, M.; Imberty, A.; Vidal, S., Rational design and synthesis of optimized glycoclusters for multivalent lectin-carbohydrate interactions: influence of the linker arm. *Chemistry* **2012**, *18* (20), 6250-63.
108. Chabre, Y. M.; Giguere, D.; Blanchard, B.; Rodrigue, J.; Rocheleau, S.; Neault, M.; Rauthu, S.; Papadopoulos, A.; Arnold, A. A.; Imberty, A.; Roy, R.,

Combining glycomimetic and multivalent strategies toward designing potent bacterial lectin inhibitors. *Chemistry* **2011**, *17* (23), 6545-62.

109. Imberty, A.; Chabre, Y. M.; Roy, R., Glycomimetics and glycodendrimers as high affinity microbial anti - adhesins. *Chem. Eur. J.* **2008**, *14* (25), 7490-7499.

110. Boltje, T. J.; Buskas, T.; Boons, G.-J., Opportunities and challenges in synthetic oligosaccharide and glycoconjugate research. *Nature Chem.* **2009**, *1* (8), 611-622.

111. Follador, R.; Heinz, E.; Wyres, K. L.; Ellington, M. J.; Kowarik, M.; Holt, K. E.; Thomson, N. R., The diversity of *Klebsiella pneumoniae* surface polysaccharides. *Microb. Genom.* **2016**, *2* (8).

112. Moffett, S.; Shiao, T. C.; Mousavifar, L.; Mignani, S.; Roy, R., Aberrant glycosylation patterns on cancer cells: Therapeutic opportunities for glycodendrimers/metallo dendrimers oncology. *Wiley Interdiscip. Rev. Nanomed. Nanobiotechnol.* **2021**, *13* (1), e1659.

113. Percec, V.; Leowanawat, P.; Sun, H. J.; Kulikov, O.; Nusbaum, C. D.; Tran, T. M.; Bertin, A.; Wilson, D. A.; Peterca, M.; Zhang, S.; Kamat, N. P.; Vargo, K.; Moock, D.; Johnston, E. D.; Hammer, D. A.; Pochan, D. J.; Chen, Y.; Chabre, Y. M.; Shiao, T. C.; Bergeron-Brlek, M.; Andre, S.; Roy, R.; Gabius, H. J.; Heiney, P. A., Modular synthesis of amphiphilic Janus glycodendrimers and their self-assembly into glycodendrimersomes and other complex architectures with bioactivity to biomedically relevant lectins. *J. Am. Chem. Soc.* **2013**, *135* (24), 9055-77.

114. Zhang, S.; Moussodia, R. O.; Sun, H. J.; Leowanawat, P.; Muncan, A.; Nusbaum, C. D.; Chelling, K. M.; Heiney, P. A.; Klein, M. L.; Andre, S.; Roy, R.; Gabius, H. J.; Percec, V., Mimicking biological membranes with programmable glycan ligands self-assembled from amphiphilic Janus glycodendrimers. *Angew. Chem. Int. Ed. Engl.* **2014**, *53* (41), 10899-903.

115. Zhang, S.; Moussodia, R. O.; Murzeau, C.; Sun, H. J.; Klein, M. L.; Vertesy, S.; Andre, S.; Roy, R.; Gabius, H. J.; Percec, V., Dissecting molecular

aspects of cell interactions using glycodendrimersomes with programmable glycan presentation and engineered human lectins. *Angew. Chem. Int. Ed. Engl.* **2015**, *54* (13), 4036-40.

116. Xiao, Q.; Zhanga, S.; Wang, Z.; Sherman, S. E.; Moussodia, R.-O.; Peterca, M.; Muncan, A.; Williams, D. R.; Hammer, D. A.; Vértesy, S.; André, S.; Hans-Joachim Gabius; Klein, M. L.; Percec, V., Onion-like glycodendrimersomes from sequence-defined Janus glycodendrimers and influence of architecture on reactivity to a lectin. *Proc. Natl. Acad. Sci. U.S.A.* **2016**, *113* (5), 1162-1167.

117. Rodriguez-Emmenegger, C.; Xiao, Q.; Kostina, N. Y.; Sherman, S. E.; Rahimi, K.; Partridge, B. E.; Li, S.; Sahoo, D.; Perez, A. M. R.; Buzzacchera, I., Encoding biological recognition in a bicomponent cell-membrane mimic. *Proc. Natl. Acad. Sci. U.S.A.* **2019**, *116* (12), 5376-5382.

118. Kostina, N. Y.; Rahimi, K.; Xiao, Q.; Haraszti, T.; Dedisch, S.; Spatz, J. P.; Schwaneberg, U.; Klein, M. L.; Percec, V.; Möller, M., Membrane-mimetic dendrimersomes engulf living bacteria via endocytosis. *Nano Lett.* **2019**, *19* (8), 5732-5738.

119. Xiao, Q.; Ludwig, A.-K.; Romanò, C.; Buzzacchera, I.; Sherman, S. E.; Vetro, M.; Vértesy, S.; Kaltner, H.; Reed, E. H.; Möller, M., Exploring functional pairing between surface glycoconjugates and human galectins using programmable glycodendrimersomes. *Proc. Natl. Acad. Sci. U.S.A.* **2018**, *115* (11), E2509-E2518.

120. Zhang, S.; Xiao, Q.; Sherman, S. E.; Muncan, A.; Ramos Vicente, A. D.; Wang, Z.; Hammer, D. A.; Williams, D.; Chen, Y.; Pochan, D. J., Glycodendrimersomes from sequence-defined Janus glycodendrimers reveal high activity and sensor capacity for the agglutination by natural variants of human lectins. *J. Am. Chem. Soc.* **2015**, *137* (41), 13334-13344.

121. Zhang, S.; Moussodia, R.-O.; Vértesy, S.; André, S.; Klein, M. L.; Gabius, H.-J.; Percec, V., Unraveling functional significance of natural variations of a human

- galectin by glycodendrimersomes with programmable glycan surface. *Proc. Natl. Acad. Sci. U.S.A.* **2015**, *112* (18), 5585-5590.
122. Caldorera-Moore, M.; Guimard, N.; Shi, L.; Roy, K., Designer nanoparticles: incorporating size, shape and triggered release into nanoscale drug carriers. *Expert Opin. Drug Deliv.* **2010**, *7* (4), 479-495.
123. Shi, J.; Votruba, A. R.; Farokhzad, O. C.; Langer, R., Nanotechnology in drug delivery and tissue engineering: from discovery to applications. *Nano Lett.* **2010**, *10* (9), 3223-3230.
124. Ferrari, M., Beyond drug delivery. *Nature Nanotechnol.* **2008**, *3* (3), 131-132.
125. Koo, O. M.; Rubinstein, I.; Onyuksel, H., Role of nanotechnology in targeted drug delivery and imaging: a concise review. *Nanomedicine* **2005**, *1* (3), 193-212.
126. Sharma, A. K.; Keservani, R. K.; Kesharwani, R. K., *Nanobiomaterials: applications in drug delivery*. CRC Press: 2018.
127. Love, S. A.; Maurer-Jones, M. A.; Thompson, J. W.; Lin, Y.-S.; Haynes, C. L., Assessing nanoparticle toxicity. *Annu. Rev. Anal. Chem.* **2012**, *5*, 181-205.
128. Hogan, D. J.; Maibach, H. I., Adverse dermatologic reactions to transdermal drug delivery systems. *J. Am. Acad. Dermatol.* **1990**, *22* (5), 811-814.
129. Murphy, M.; Carmichael, A. J., Transdermal drug delivery systems and skin sensitivity reactions. *Am. J. Clin. Dermatol.* **2000**, *1* (6), 361-368.
130. Sharma, A.; Kakkar, A., Designing dendrimer and miktoarm polymer based multi-tasking nanocarriers for efficient medical therapy. *Molecules* **2015**, *20* (9), 16987-17015.
131. Bangham, A.; Standish, M. M.; Watkins, J. C., Diffusion of univalent ions across the lamellae of swollen phospholipids. *J. Mol. Biol.* **1965**, *13* (1), 238-IN27.
132. Torchilin, V. P., Multifunctional, stimuli-sensitive nanoparticulate systems for drug delivery. *Nat. Rev. Drug Discov.* **2014**, *13* (11), 813-827.

133. Mozafari, M. R.; Khosravi-Darani, K., An overview of liposome-derived nanocarrier technologies. In *Nanomaterials and nanosystems for biomedical applications*, Springer: 2007; pp 113-123.
134. Immordino, M. L.; Dosio, F.; Cattell, L., Stealth liposomes: review of the basic science, rationale, and clinical applications, existing and potential. *Int. J. Nanomed.* **2006**, *1* (3), 297.
135. Bozzuto, G.; Molinari, A., Liposomes as nanomedical devices. *Int. J. Nanomed.* **2015**, *10*, 975.
136. Kataria, S.; Sandhu, P.; Bilandi, A.; Akanksha, M.; Kapoor, B., Stealth liposomes: a review. *Int. J. Res. Ayurveda Pharm.* **2011**, *2* (5).
137. Allen, T. M.; Cullis, P. R., Liposomal drug delivery systems: from concept to clinical applications. *Adv. Drug Deliv. Rev.* **2013**, *65* (1), 36-48.
138. de Araujo, D. R.; Ribeiro, L. N. d. M.; de Paula, E., Lipid-based carriers for the delivery of local anesthetics. *Expert Opin. Drug Deliv.* **2019**, *16* (7), 701-714.
139. de Paula, E.; Cereda, C. M.; Fraceto, L. F.; de Araujo, D. R.; Franz-Montan, M.; Tofoli, G. R.; Ranali, J.; Volpato, M. C.; Groppo, F. C., Micro and nanosystems for delivering local anesthetics. *Expert Opin. Drug Deliv.* **2012**, *9* (12), 1505-1524.
140. Luo, D.; Carter, K. A.; Razi, A.; Geng, J.; Shao, S.; Giraldo, D.; Sunar, U.; Ortega, J.; Lovell, J. F., Doxorubicin encapsulated in stealth liposomes conferred with light-triggered drug release. *Biomaterials* **2016**, *75*, 193-202.
141. Paliwal, S. R.; Paliwal, R.; Mishra, N.; Mehta, A.; Vyas, S., A novel cancer targeting approach based on estrone anchored stealth liposome for site-specific breast cancer therapy. *Curr. Cancer Drug Targets* **2010**, *10* (3), 343-353.
142. Cattell, L.; Ceruti, M.; Dosio, F., From conventional to stealth liposomes: a new frontier in cancer chemotherapy. *J. Chemother.* **2004**, *16* (sup4), 94-97.
143. Barenholz, Y., Liposome application: problems and prospects. *Curr. Opin. Colloid Interface Sci.* **2001**, *6* (1), 66-77.

144. Tomalia, D. A.; Naylor, A. M.; Goddard III, W. A., Starburst dendrimers: molecular - level control of size, shape, surface chemistry, topology, and flexibility from atoms to macroscopic matter. *Angew. Chem. Int. Ed. Engl.* **1990**, *29* (2), 138-175.
145. Discher, B. M.; Won, Y.-Y.; Ege, D. S.; Lee, J. C.; Bates, F. S.; Discher, D. E.; Hammer, D. A., Polymersomes: tough vesicles made from diblock copolymers. *Science* **1999**, *284* (5417), 1143-1146.
146. Percec, V.; Wilson, D. A.; Leowanawat, P.; Wilson, C. J.; Hughes, A. D.; Kaucher, M. S.; Hammer, D. A.; Levine, D. H.; Kim, A. J.; Bates, F. S.; Davis, K. P.; Lodge, T. P.; Klein, M. L.; DeVane, R. H.; Aqad, E.; Rosen, B. M.; Argintaru, A. O.; Sienkowska, M. J.; Rissanen, K.; Nummelin, S.; Ropponen, J., Self-assembly of Janus dendrimers into uniform dendrimersomes and other complex architectures. *Science* **2010**, *328* (5981), 1009-14.
147. Zhang, S.; Sun, H.-J.; Hughes, A. D.; Draghici, B.; Lejnicks, J.; Leowanawat, P.; Bertin, A.; Leon, L. O. D.; Kulikov, O. V.; Chen, Y.; Pochan, D. J.; Heiney, P. A.; Percec, V., "Single-Single" Amphiphilic Janus Dendrimers Self-Assemble into Uniform Dendrimersomes with Predictable Size. *ACS Nano* **2014**, *8* (2), 1554-1565.
148. Sikwal, D. R.; Kalhapure, R. S.; Govender, T., An emerging class of amphiphilic dendrimers for pharmaceutical and biomedical applications: Janus amphiphilic dendrimers. *Eur J Pharm Sci* **2017**, *97*, 113-134.
149. Bouwstra, J. A.; Honeywell-Nguyen, P. L.; Gooris, G. S.; Ponec, M., Structure of the skin barrier and its modulation by vesicular formulations. *Prog. Lipid Res.* **2003**, *42* (1), 1-36.
150. Boogaerts, J. G.; Lafont, N. D.; Declercq, A. G.; Luo, H. C.; Gravet, E. T.; Bianchi, J. A.; Legros, F. J., Epidural administration of liposome associated bupivacaine for the management of postsurgical pain: a first study. *J. Clin. Anesth.* **1994**, *6* (4), 315-320.

151. Becker, D. E.; Reed, K. L., Essentials of local anesthetic pharmacology. *Anesth. Prog.* **2006**, *53* (3), 98-109.
152. Meechan, J., Intra-oral topical anaesthetics: a review. *J. Dent.* **2000**, *28* (1), 3-14.
153. Meechan, J. G., Effective topical anesthetic agents and techniques. *Dent. Clin. North Am.* **2002**, *46* (4), 759-766.
154. Bhalla, J.; Meechan, J. G.; Lawrence, H. P.; Grad, H. A.; Haas, D. A., Effect of time on clinical efficacy of topical anesthesia. *Anesth. Prog.* **2009**, *56* (2), 36-41.
155. Hutchins Jr, H. S.; Young, F. A.; Lackland, D. T.; Fishburne, C. P., The effectiveness of topical anesthesia and vibration in alleviating the pain of oral injections. *Anesth. Prog.* **1997**, *44* (3), 87.
156. Meechan, J.; Thomason, J., A comparison of 2 topical anesthetics on the discomfort of intraligamentary injectionsA double-blind, split-mouth volunteer clinical trial. *Oral Surg. Oral Med. Oral Pathol. Oral Radiol. Endod.* **1999**, *87* (3), 362-365.
157. Donaldson, D.; Meechan, J. G., A comparison of the effects of EMLA cream and topical 5% lidocaine on discomfort during gingival probing. *Anesth. Prog.* **1995**, *42* (1), 7.
158. Nummelin, S.; Selin, M.; Legrand, S.; Ropponen, J.; Seitsonen, J.; Nykänen, A.; Koivisto, J.; Hirvonen, J.; Kostiainen, M. A.; Bimbo, L. M., Modular synthesis of self-assembling Janus-dendrimers and facile preparation of drug-loaded dendrimersomes. *Nanoscale* **2017**, *9* (21), 7189-7198.
159. Batzri, S.; Korn, E. D., Single bilayer liposomes prepared without sonication. *Biochim. Biophys. Acta Gen. Subj.* **1973**, *298* (4), 1015-1019.
160. Peterca, M.; Percec, V.; Leowanawat, P.; Bertin, A., Predicting the size and properties of dendrimersomes from the lamellar structure of their amphiphilic Janus dendrimers. *J. Am. Chem. Soc.* **2011**, *133* (50), 20507-20520.

161. Bader, H.; Cross, L.; Heilbron, I.; Jones, E., Researches on acetylenic compounds. Part XVIII. The addition of thiolacetic acid to acetylenic hydrocarbons. The conversion of monosubstituted acetylenes into aldehydes and 1: 2-dithiols. *J. Chem. Soc.* **1949**, 619-623.
162. Wang, Y.; Bruno, B. J.; Cornillie, S.; Nogueira, J. M.; Chen, D.; Cheatham III, T. E.; Lim, C. S.; Chou, D. H. C., Application of thiol-yne/thiol-ene reactions for peptide and protein macrocyclizations. *Chem. Eur. J.* **2017**, *23* (29), 7087-7092.
163. Goyard, D.; Shiao, T. C.; Fraleigh, N. L.; Vu, H. Y.; Lee, H.; Diaz-Mitoma, F.; Le, H. T.; Roy, R., Expedient synthesis of functional single-component glycoliposomes using thiol-yne chemistry. *J. Mater. Chem. B* **2016**, *4* (23), 4227-4233.
164. Roy, R.; Shiao, T. C., Glyconanosynthons as powerful scaffolds and building blocks for the rapid construction of multifaceted, dense and chiral dendrimers. *Chem. Soc. Rev.* **2015**, *44* (12), 3924-41.
165. Hoyle, C. E.; Lowe, A. B.; Bowman, C. N., Thiol-click chemistry: a multifaceted toolbox for small molecule and polymer synthesis. *Chem. Soc. Rev.* **2010**, *39* (4), 1355-87.
166. Lowe, A. B.; Chan, J. W., Thiol-yne Chemistry in Polymer and Materials Science. In *Design and Synthesis of Conjugated Polymers*, Wiley - VCH Verlag GmbH & Co. KGaA: 2013.
167. Franz-Montan, M.; Baroni, D.; Brunetto, G.; Sobral, V. R. V.; da Silva, C. M. G.; Venâncio, P.; Zago, P. W.; Cereda, C. M. S.; Volpato, M. C.; de Araújo, D. R., Liposomal lidocaine gel for topical use at the oral mucosa: characterization, in vitro assays and in vivo anesthetic efficacy in humans. *J. Liposome Res.* **2015**, *25* (1), 11-19.
168. Gabius, H. J., Animal lectins. *Eur. J. Biochem.* **1997**, *243* (3), 543-576.

169. Barondes, S. H.; Castronovo, V.; Cooper, D.; Cummings, R. D.; Drickamer, K.; Feizi, T.; Gitt, M. A.; Hirabayashi, J.; Hughes, C.; Kasai, K.-i., Galectins: a family of animal beta-galactoside-binding lectins. *Cell* **1994**, *76* (4), 597-8.
170. Barondes, S. H.; Cooper, D.; Gitt, M. A.; Leffler, H., Galectins. Structure and function of a large family of animal lectins. *J. Biol. Chem.* **1994**, *269* (33), 20807-20810.
171. Girotti, M. R.; Salatino, M.; Dalotto-Moreno, T.; Rabinovich, G. A., Sweetening the hallmarks of cancer: Galectins as multifunctional mediators of tumor progression. *J. Exp. Med.* **2020**, *217* (2).
172. Rabinovich, G. A.; Gabrilovich, D.; Sotomayor, E. M., Immunosuppressive strategies that are mediated by tumor cells. *Annu. Rev. Immunol.* **2007**, *25*, 267-296.
173. Elola, M.; Wolfenstein-Todel, C.; Troncoso, M.; Vasta, G.; Rabinovich, G., Galectins: matricellular glycan-binding proteins linking cell adhesion, migration, and survival. *Cell. Mol. Life Sci.* **2007**, *64* (13), 1679-1700.
174. Oka, T.; Murakami, S.; Arata, Y.; Hirabayashi, J.; Kasai, K.-I.; Wada, Y.; Futai, M., Identification and cloning of rat galectin-2: expression is predominantly in epithelial cells of the stomach. *Arch. Biochem. Biophys.* **1999**, *361* (2), 195-201.
175. Jung, J.-H.; Kim, H.-J.; Yeom, J.; Yoo, C.; Shin, J.; Yoo, J.; Kang, C. S.; Lee, C., Lowered expression of galectin-2 is associated with lymph node metastasis in gastric cancer. *J. Gastroenterol.* **2012**, *47* (1), 37-48.
176. Huflejt, M.; Turck, C.; Lindstedt, R.; Barondes, S.; Leffler, H., L-29, a soluble lactose-binding lectin, is phosphorylated on serine 6 and serine 12 in vivo and by casein kinase I. *J. Biol. Chem.* **1993**, *268* (35), 26712-26718.
177. Menon, R. P.; Hughes, R. C., Determinants in the N - terminal domains of galectin - 3 for secretion by a novel pathway circumventing the endoplasmic reticulum–Golgi complex. *Eur. J. Biochem.* **1999**, *264* (2), 569-576.
178. Ahmad, N.; Gabius, H.-J.; André, S.; Kaltner, H.; Sabesan, S.; Roy, R.; Liu, B.; Macaluso, F.; Brewer, C. F., Galectin-3 precipitates as a pentamer with

- synthetic multivalent carbohydrates and forms heterogeneous cross-linked complexes. *J. Biol. Chem.* **2004**, *279* (12), 10841-10847.
179. Ochieng, J.; Green, B.; Evans, S.; James, O.; Warfield, P., Modulation of the biological functions of galectin-3 by matrix metalloproteinases. *Biochim. Biophys. Acta Gen. Subj.* **1998**, *1379* (1), 97-106.
180. Mirandola, L.; Yu, Y.; Chui, K.; Jenkins, M. R.; Cobos, E.; John, C. M.; Chiriva-Internati, M., Galectin-3C inhibits tumor growth and increases the anticancer activity of bortezomib in a murine model of human multiple myeloma. *PloS one* **2011**, *6* (7), e21811.
181. Cao, Z.-Q.; Guo, X.-L., The role of galectin-4 in physiology and diseases. *Protein Cell* **2016**, *7* (5), 314-324.
182. Huflejt, M. E.; Leffler, H., Galectin-4 in normal tissues and cancer. *Glycoconjug. J.* **2003**, *20* (4), 247-255.
183. Tsai, C.-H.; Tzeng, S.-F.; Chao, T.-K.; Tsai, C.-Y.; Yang, Y.-C.; Lee, M.-T.; Hwang, J.-J.; Chou, Y.-C.; Tsai, M.-H.; Cha, T.-L., Metastatic progression of prostate cancer is mediated by autonomous binding of galectin-4-O-glycan to cancer cells. *Cancer Res.* **2016**, *76* (19), 5756-5767.
184. Saussez, S.; Kiss, R., Galectin-7. *Cell. Mol. Life Sci.* **2006**, *63* (6), 686-697.
185. Labrie, M.; Vladoiu, M. C.; Grosset, A.-A.; Gaboury, L.; St-Pierre, Y., Expression and functions of galectin-7 in ovarian cancer. *Oncotarget* **2014**, *5* (17), 7705.
186. Kopitz, J.; Andre, S.; Von Reitzenstein, C.; Versluis, K.; Kaltner, H.; Pieters, R. J.; Wasano, K.; Kuwabara, I.; Liu, F.-T.; Cantz, M., Homodimeric galectin-7 (p53-induced gene 1) is a negative growth regulator for human neuroblastoma cells. *Oncogene* **2003**, *22* (40), 6277-6288.
187. Brewer, C. F., Thermodynamic binding studies of galectin-1,-3 and-7. *Glycoconjug. J.* **2002**, *19* (7), 459-465.

188. Bidon-Wagner, N.; Le Penec, J.-P., Human galectin-8 isoforms and cancer. *Glycoconjug. J.* **2002**, *19* (7), 557-563.
189. Zick, Y.; Eisenstein, M.; Goren, R. A.; Hadari, Y. R.; Levy, Y.; Ronen, D., Role of galectin-8 as a modulator of cell adhesion and cell growth. *Glycoconjug. J.* **2002**, *19* (7), 517-526.
190. Carabelli, J.; Quattrocchi, V.; D' Antuono, A.; Zamorano, P.; Tribulatti, M. V.; Campetella, O., Galectin - 8 activates dendritic cells and stimulates antigen - specific immune response elicitation. *J. Leukoc. Biol.* **2017**, *102* (5), 1237-1247.
191. Carabelli, J.; Prato, C. A.; Sanmarco, L. M.; Aoki, M. P.; Campetella, O.; Tribulatti, M. V., Interleukin - 6 signalling mediates Galectin - 8 co - stimulatory activity of antigen - specific CD 4 T - cell response. *Immunology* **2018**, *155* (3), 379-386.
192. Tribulatti, M. V.; Cattaneo, V.; Hellman, U.; Mucci, J.; Campetella, O., Galectin - 8 provides costimulatory and proliferative signals to T lymphocytes. *J. Leukoc. Biol.* **2009**, *86* (2), 371-380.
193. Prato, C. A.; Carabelli, J.; Campetella, O.; Tribulatti, M. V., Galectin-8 Enhances T cell Response by Promotion of Antigen Internalization and Processing. *Iscience* **2020**, *23* (7), 101278.
194. Rabinovich, G. A., Galectins: an evolutionarily conserved family of animal lectins with multifunctional properties; a trip from the gene to clinical therapy. *Cell Death Differ.* **1999**, *6* (8), 711-721.
195. Kaltner, H.; Toegel, S.; Caballero, G. G.; Manning, J. C.; Ledeen, R. W.; Gabius, H.-J., Galectins: their network and roles in immunity/tumor growth control. *Histochem. Cell Biol.* **2017**, *147* (2), 239-256.
196. Vasta, G. R., Roles of galectins in infection. *Nat. Rev. Microbiol.* **2009**, *7* (6), 424-438.
197. Danguy, A.; Camby, I.; Kiss, R., Galectins and cancer. *Biochim. Biophys. Acta Gen. Subj.* **2002**, *1572* (2-3), 285-293.

198. Almkvist, J.; Karlsson, A., Galectins as inflammatory mediators. *Glycoconjug. J.* **2002**, *19* (7), 575-581.
199. Liu, F. T.; Rabinovich, G. A., Galectins as modulators of tumour progression. *Nat. Rev. Cancer* **2005**, *5* (1), 29-41.
200. Rabinovich, G. A.; Baum, L. G.; Tinari, N.; Paganelli, R.; Natoli, C.; Liu, F.-T.; Iacobelli, S., Galectins and their ligands: amplifiers, silencers or tuners of the inflammatory response? *Trends Immunol.* **2002**, *23* (6), 313-320.
201. Chou, F.-C.; Chen, H.-Y.; Kuo, C.-C.; Sytwu, H.-K., Role of galectins in tumors and in clinical immunotherapy. *Int. J. Mol. Sci.* **2018**, *19* (2), 430.
202. Yang, R.-Y.; Rabinovich, G. A.; Liu, F.-T., Galectins: structure, function and therapeutic potential. *Expert. Rev. Mol. Med.* **2008**, *10*.
203. Giguère, D.; Patnam, R.; Bellefleur, M.-A.; St-Pierre, C.; Sato, S.; Roy, R., Carbohydrate triazoles and isoxazoles as inhibitors of galectins-1 and-3. *Chem. Commun.* **2006**, (22), 2379-2381.
204. Giguere, D.; Bonin, M. A.; Cloutier, P.; Patnam, R.; St-Pierre, C.; Sato, S.; Roy, R., Synthesis of stable and selective inhibitors of human galectins-1 and -3. *Bioorg. Med. Chem.* **2008**, *16* (16), 7811-23.
205. Dahlqvist, A.; Leffler, H.; Nilsson, U. J., C1-Galactopyranosyl Heterocycle Structure Guides Selectivity: Triazoles Prefer Galectin-1 and Oxazoles Prefer Galectin-3. *ACS Omega* **2019**, *4* (4), 7047-7053.
206. Peterson, K.; Kumar, R.; Stenström, O.; Verma, P.; Verma, P. R.; Hakansson, M.; Kahl-Knutsson, B.; Zetterberg, F.; Leffler, H.; Akke, M., Systematic tuning of fluoro-galectin-3 interactions provides thiodigalactoside derivatives with single-digit nM affinity and high selectivity. *J. Mater. Chem.* **2018**, *61* (3), 1164-1175.
207. Giguere, D.; Patnam, R.; Bellefleur, M. A.; St-Pierre, C.; Sato, S.; Roy, R., Carbohydrate triazoles and isoxazoles as inhibitors of galectins-1 and -3. *Chem. Commun.* **2006**, (22), 2379-81.

208. Zetterberg, F. R.; Peterson, K.; Johnsson, R. E.; Brimert, T.; Håkansson, M.; Logan, D. T.; Leffler, H.; Nilsson, U. J., Monosaccharide derivatives with low-nanomolar lectin affinity and high selectivity based on combined fluorine-amide, phenyl-arginine, sulfur- π , and halogen bond interactions. *ChemMedChem* **2018**, *13* (2), 133-137.
209. Vrasidas, I.; André, S.; Valentini, P.; Böck, C.; Lensch, M.; Kaltner, H.; Liskamp, R. M.; Gabius, H.-J.; Pieters, R. J., Rigidified multivalent lactose molecules and their interactions with mammalian galectins: a route to selective inhibitors. *Org. Biomol. Chem.* **2003**, *1* (5), 803-810.
210. Giguere, D.; Sato, S.; St-Pierre, C.; Sirois, S.; Roy, R., Aryl O- and S-galactosides and lactosides as specific inhibitors of human galectins-1 and -3: role of electrostatic potential at O-3. *Bioorg. Med. Chem. Lett.* **2006**, *16* (6), 1668-72.
211. Sörme, P.; Arnoux, P.; Kahl-Knutsson, B.; Leffler, H.; Rini, J. M.; Nilsson, U. J., Structural and thermodynamic studies on cation- π interactions in lectin-ligand complexes: high-affinity galectin-3 inhibitors through fine-tuning of an arginine-arene interaction. *J. Am. Chem. Soc.* **2005**, *127* (6), 1737-1743.
212. Atmanene, C.; Ronin, C.; Téletchéa, S.; Gautier, F.-M.; Djedaïni-Pilard, F.; Ciesielski, F.; Vivat, V.; Grandjean, C., Biophysical and structural characterization of mono/di-arylated lactosamine derivatives interaction with human galectin-3. *Biochem. Biophys. Res. Commun.* **2017**, *489* (3), 281-286.
213. Cumpstey, I.; Salomonsson, E.; Sundin, A.; Leffler, H.; Nilsson, U. J., Studies of arginine - arene interactions through synthesis and evaluation of a series of galectin - binding aromatic lactose esters. *ChemBioChem* **2007**, *8* (12), 1389-1398.
214. van Hattum, H.; Branderhorst, H. M.; Moret, E. E.; Nilsson, U. J.; Leffler, H.; Pieters, R. J., Tuning the preference of thiodigalactoside-and lactosamine-based ligands to galectin-3 over galectin-1. *J. Med. Chem.* **2013**, *56* (3), 1350-1354.
215. Noresson, A.-L.; Aurelius, O.; Öberg, C.; Engström, O.; Sundin, A.; Håkansson, M.; Stenström, O.; Akke, M.; Logan, D.; Leffler, H., Designing

interactions by control of protein–ligand complex conformation: tuning arginine–arene interaction geometry for enhanced electrostatic protein–ligand interactions. *Chem. Sci.* **2018**, *9* (4), 1014-1021.

216. Hsieh, T.-J.; Lin, H.-Y.; Tu, Z.; Lin, T.-C.; Wu, S.-C.; Tseng, Y.-Y.; Liu, F.-T.; Hsu, S.-T. D.; Lin, C.-H., Dual thio-digalactoside-binding modes of human galectins as the structural basis for the design of potent and selective inhibitors. *Sci. Rep.* **2016**, *6* (1), 1-9.

217. Delaine, T.; Collins, P.; MacKinnon, A.; Sharma, G.; Stegmayr, J.; Rajput, V. K.; Mandal, S.; Cumpstey, I.; Larumbe, A.; Salameh, B. A., Galectin-3-binding glycomimetics that strongly reduce bleomycin-induced lung fibrosis and modulate intracellular glycan recognition. *ChemBioChem* **2016**, *17* (18), 1759-1770.

218. Roy, R.; Cao, Y.; Kaltner, H.; Kottari, N.; Shiao, T. C.; Belkhadem, K.; Andre, S.; Manning, J. C.; Murphy, P. V.; Gabius, H. J., Teaming up synthetic chemistry and histochemistry for activity screening in galectin-directed inhibitor design. *Histochem. Cell Biol.* **2017**, *147* (2), 285-301.

219. Allen, H. J.; Ahmed, H.; Matta, K. L., Binding of synthetic sulfated ligands by human splenic galectin 1, a β -galactoside-binding lectin. *Glycoconj. J.* **1998**, *15* (7), 691-695.

220. Bum-Erdene, K.; Leffler, H.; Nilsson, U. J.; Blanchard, H., Structural characterisation of human galectin-4 N-terminal carbohydrate recognition domain in complex with glycerol, lactose, 3' -sulfo-lactose, and 2' -fucosyllactose. *Sci. Rep.* **2016**, *6*, 20289.

221. Carlsson, S.; Öberg, C. T.; Carlsson, M. C.; Sundin, A.; Nilsson, U. J.; Smith, D.; Cummings, R. D.; Almkvist, J.; Karlsson, A.; Leffler, H., Affinity of galectin-8 and its carbohydrate recognition domains for ligands in solution and at the cell surface. *Glycobiology* **2007**, *17* (6), 663-676.

222. Iurisci, I.; Cumashi, A.; Sherman, A. A.; Tsvetkov, Y. E.; Tinari, N.; Piccolo, E.; D'Egidio, M.; Adamo, V.; Natoli, C.; Rabinovich, G. A., Synthetic

inhibitors of galectin-1 and-3 selectively modulate homotypic cell aggregation and tumor cell apoptosis. *Anticancer Res.* **2009**, *29* (1), 403-410.

223. López-Lucendo, M. F.; Solís, D.; André, S.; Hirabayashi, J.; Kasai, K.-i.; Kaltner, H.; Gabius, H.-J.; Romero, A., Growth-regulatory human galectin-1: crystallographic characterisation of the structural changes induced by single-site mutations and their impact on the thermodynamics of ligand binding. *J. Mol. Biol.* **2004**, *343* (4), 957-970.

224. Peterson, K.; Collins, P. M.; Huang, X.; Kahl-Knutsson, B.; Essén, S.; Zetterberg, F. R.; Oredsson, S.; Leffler, H.; Blanchard, H.; Nilsson, U. J., Aromatic heterocycle galectin-1 interactions for selective single-digit nM affinity ligands. *RSC Adv.* **2018**, *8* (44), 24913-24922.

225. Su, J.; Zhang, T.; Wang, P.; Liu, F.; Tai, G.; Zhou, Y., The water network in galectin-3 ligand binding site guides inhibitor design. *Acta biochimica et biophysica Sinica* **2015**, *47* (3), 192-198.

226. Ideo, H.; Seko, A.; Ohkura, T.; Matta, K. L.; Yamashita, K., High-affinity binding of recombinant human galectin-4 to SO₃ - → 3Gal β 1 → 3GalNAc pyranoside. *Glycobiology* **2002**, *12* (3), 199-208.

227. Ideo, H.; Seko, A.; Yamashita, K., Galectin-4 binds to sulfated glycosphingolipids and carcinoembryonic antigen in patches on the cell surface of human colon adenocarcinoma cells. *J. Biol. Chem.* **2005**, *280* (6), 4730-4737.

228. Ideo, H.; Matsuzaka, T.; Nonaka, T.; Seko, A.; Yamashita, K., Galectin-8-N-domain recognition mechanism for sialylated and sulfated glycans. *J. Biol. Chem.* **2011**, *286* (13), 11346-11355.

229. Pal, K. B.; Mahanti, M.; Huang, X.; Persson, S.; Sundin, A. P.; Zetterberg, F. R.; Oredsson, S.; Leffler, H.; Nilsson, U. J., Quinoline-galactose hybrids bind selectively with high affinity to a galectin-8 N-terminal domain. *Org. Biomol. Chem.* **2018**, *16* (34), 6295-6305.

230. Salameh, B.; Sundin, A.; Leffler, H.; Nilsson, U., Thioureido N-acetyllactosamine derivatives as potent galectin-7 and 9N inhibitors. *Bioorg. Med. Chem.* **2006**, *14* (4), 1215-1220.
231. Bum - Erdene, K.; Leffler, H.; Nilsson, U. J.; Blanchard, H., Structural characterization of human galectin - 4 C - terminal domain: elucidating the molecular basis for recognition of glycosphingolipids, sulfated saccharides and blood group antigens. *FEBS J.* **2015**, *282* (17), 3348-3367.
232. Wang, L.-X.; Pavlova, N. V.; Yang, M.; Li, S.-C.; Li, Y.-T.; Lee, Y. C., Synthesis of aryl 3' -sulfo- β -lactosides as fluorogenic and chromogenic substrates for ceramide glycanases. *Carbohydr. Res.* **1998**, *306* (3), 341-348.
233. Belkhadem, K.; Cao, Y.; Roy, R., Synthesis of Galectin Inhibitors by Regioselective 3' -O-Sulfation of Vanillin Lactosides Obtained under Phase Transfer Catalysis. *Molecules* **2021**, *26* (1), 115.
234. Jung, K. H.; Hoch, M.; Schmidt, R. R., Glycosyl Imidates, 42 Selectively Protected Lactose and 2 - Azido Lactose, Building Blocks for Glycolipid Synthesis. *Liebigs Ann. Chem.* **1989**, *1989* (11), 1099-1106.
235. Chervin, S. M.; Lowe, J. B.; Koreeda, M., Synthesis and biological evaluation of a new sialyl Lewis X mimetic derived from lactose. *J. Org. Chem.* **2002**, *67* (16), 5654-5662.
236. Uzawa, H.; Nishida, Y.; Sasaki, K.; Minoura, N.; Kobayashi, K., Synthetic potential of molluscan Sulfatases for the library synthesis of regioselectively O - sulfonated d - Galacto - sugars. *ChemBioChem* **2003**, *4* (7), 640-647.
237. Guilbert, B.; Davis, N. J.; Pearce, M.; Aplin, R. T.; Flitsch, S. L., Dibutylstannylene acetals: Useful intermediates for the regioselective sulfation of glycosides. *Tetrahedron: Asymmetry* **1994**, *5* (11), 2163-2178.
238. Yoshida, H.; Yamashita, S.; Teraoka, M.; Itoh, A.; Nakakita, S. i.; Nishi, N.; Kamitori, S., X - ray structure of a protease - resistant mutant form of human

- galectin - 8 with two carbohydrate recognition domains. *FEBS J.* **2012**, *279* (20), 3937-3951.
239. Misra, A. K.; Agnihotri, G.; Madhusudan, S. K.; Tiwari, P., Practical synthesis of sulfated analogs of lactosamine and sialylated lactosamine derivatives. *J. Carbohydr. Chem.* **2004**, *23* (4), 191-199.
240. Nagorny, P.; Fasching, B.; Li, X.; Chen, G.; Aussedat, B.; Danishefsky, S. J., Toward fully synthetic homogeneous β -human follicle-stimulating hormone (β -hFSH) with a biantennary N-linked dodecasaccharide. Synthesis of β -hFSH with chitobiose units at the natural linkage sites. *J. Am. Chem. Soc.* **2009**, *131* (16), 5792-5799.
241. Xia, J.; Alderfer, J. L.; Piskorz, C. F.; Locke, R. D.; Matta, K. L., A convergent synthesis of trisaccharides with α -Neu5Ac-(2 \rightarrow 3)- β -d-gal-(1 \rightarrow 4)- β -d-GlcNAc and α -Neu5Ac-(2 \rightarrow 3)- β -d-gal-(1 \rightarrow 3)- α -d-GalNAc sequences. *Carbohydr. Res.* **2000**, *328* (2), 147-163.
242. Zhang, Y.; Zhao, F. L.; Luo, T.; Pei, Z.; Dong, H., Regio/Stereoselective Glycosylation of Diol and Polyol Acceptors in Efficient Synthesis of Neu5Ac- α -2,3-LacNPhth Trisaccharide. *Chem. Asian J.* **2019**, *14* (1), 223-234.
243. Rauthu, S. R.; Shiao, T. C.; Andre, S.; Miller, M. C.; Madej, E.; Mayo, K. H.; Gabius, H. J.; Roy, R., Defining the potential of aglycone modifications for affinity/selectivity enhancement against medically relevant lectins: synthesis, activity screening, and HSQC-based NMR analysis. *Chembiochem* **2015**, *16* (1), 126-39.
244. Haque, M. E.; KIKUCHI, T.; YOSHIMOTO, K.; TSUDA, Y., Regioselective monoalkylation of non-protected glycopyranosides by the dibutyltin oxide method. *Chem. Pharm. Bull.* **1985**, *33* (6), 2243-2255.
245. David, S.; Hanessian, S., Regioselective manipulation of hydroxyl groups via organotin derivatives. *Tetrahedron* **1985**, *41* (4), 643-663.
246. Grindley, T. B., Applications of Tin-containing Intermediates. *Advances in carbohydrate chemistry and biochemistry* **1998**, 17.

247. Haller, M.; Boons, G.-J., Towards a modular approach for heparin synthesis. *J. Chem. Soc. Perkin Trans. I* **2001**, (8), 814-822.
248. Roy, R., Phase transfer catalysis in carbohydrate chemistry. In *Handbook of Phase Transfer Catalysis*, Springer: 1997; pp 244-275.
249. Roy, R.; Tropper, F.; Cao, S.; Kim, J., Anomeric Group Transformations Under Phase-Transfer Catalysis. ACS Publications: 1997.
250. Tropper, F. D.; Andersson, F. O.; Grand-Maître, C.; Roy, R., Phase transfer catalyzed synthesis of 4-nitrophenyl 1-thio- β -D-glycobiosides. *Carbohydr. Res.* **1992**, 229 (1), 149-154.
251. Carriere, D.; Meunier, S.; Tropper, F.; Cao, S.; Roy, R., Phase transfer catalysis toward the synthesis of O-, S-, Se- and C-glycosides. *J. Mol. Catal. A Chem.* **2000**, 154 (1-2), 9-22.
252. Dabrowski, U.; Friebolin, H.; Brossmer, R.; Supp, M., ¹H-NMR studies at N-acetyl-D-neuraminic acid ketosides for the determination of the anomeric configuration II. *Tetrahedron Lett.* **1979**, 20 (48), 4637-4640.
253. Paulsen, H.; Tietz, H., Synthese eines trisaccharides aus N-acetylneuraminsäure und N-acetyllactosamin. *Carbohydr. Res.* **1984**, 125 (1), 47-64.
254. Okamoto, K.; Kondo, T.; Goto, T., Syntheses of (α 2-9) and (α 2-8) linked neuraminylnneuraminic acid derivatives. *Tetrahedron Lett.* **1986**, 27 (43), 5229-5232.
255. Okamoto, K.; Kondo, T.; Goto, T., An effective synthesis of α -glycosides of N-acetylneuraminic acid derivatives by use of 2-deoxy-2 β -halo-3 β -hydroxy-4, 7, 8, 9-tetra-O-acetyl-N-acetylneuraminic acid methyl ester. *Tetrahedron* **1987**, 43 (24), 5919-5928.
256. Hori, H.; Nakajima, T.; Nishida, Y.; Ohru, H.; Meguro, H., A simple method to determine the anomeric configuration of sialic acid and its derivatives by ¹³C-NMR. *Tetrahedron Lett.* **1988**, 29 (48), 6317-6320.
257. Liu, B.; Roy, R., Comparative studies of galactoside-containing clusters. In *Methods in enzymology*, Elsevier: 2003; Vol. 362, pp 226-239.

258. Vuong, L.; Kouverianou, E.; Rooney, C. M.; McHugh, B. J.; Howie, S. E.; Gregory, C. D.; Forbes, S. J.; Henderson, N. C.; Zetterberg, F. R.; Nilsson, U. J., An orally active galectin-3 antagonist inhibits lung adenocarcinoma growth and augments response to PD-L1 blockade. *Cancer Res.* **2019**, *79* (7), 1480-1492.
259. Bratteby, K.; Torkelsson, E.; L'Estrade, E. T.; Peterson, K.; Shalgunov, V.; Xiong, M.; Leffler, H.; Zetterberg, F. R.; Olsson, T. G.; Gillings, N., In Vivo Veritas: ¹⁸F-Radiolabeled Glycomimetics Allow Insights into the Pharmacological Fate of Galectin-3 Inhibitors. *J. Med. Chem.* **2019**, *63* (2), 747-755.
260. André, S.; Pieters, R. J.; Vrasidas, I.; Kaltner, H.; Kuwabara, I.; Liu, F. T.; Liskamp, R. M.; Gabius, H. J., Wedgelike glycodendrimers as inhibitors of binding of mammalian galectins to glycoproteins, lactose maxiclusters, and cell surface glycoconjugates. *ChemBioChem* **2001**, *2* (11), 822-830.
261. André, S.; Sansone, F.; Kaltner, H.; Casnati, A.; Kopitz, J.; Gabius, H. J.; Ungaro, R., Calix [n] arene - based glycoclusters: bioactivity of thiourea - linked galactose/lactose moieties as inhibitors of binding of medically relevant lectins to a glycoprotein and cell - surface glycoconjugates and selectivity among human adhesion/growth - regulatory galectins. *ChemBioChem* **2008**, *9* (10), 1649-1661.
262. Leyden, R.; Velasco-Torrijos, T.; Andre, S.; Gouin, S.; Gabius, H.-J.; Murphy, P. V., Synthesis of bivalent lactosides based on terephthalamide, N, N' - diglucosylterephthalamide, and glycophane scaffolds and assessment of their inhibitory capacity on medically relevant lectins. *J. Org. Chem.* **2009**, *74* (23), 9010-9026.
263. Tejler, J.; Tullberg, E.; Frejd, T.; Leffler, H.; Nilsson, U. J., Synthesis of multivalent lactose derivatives by 1, 3-dipolar cycloadditions: selective galectin-1 inhibition. *Carbohydr. Res.* **2006**, *341* (10), 1353-1362.
264. André, S.; Jarikote, D. V.; Yan, D.; Vincenz, L.; Wang, G.-N.; Kaltner, H.; Murphy, P. V.; Gabius, H.-J., Synthesis of bivalent lactosides and their activity as

- sensors for differences between lectins in inter-and intrafamily comparisons. *Bioorg. Med. Chem. Lett.* **2012**, *22* (1), 313-318.
265. Wang, G.-N.; André, S.; Gabius, H.-J.; Murphy, P. V., Bi-to tetravalent glycoclusters: synthesis, structure–activity profiles as lectin inhibitors and impact of combining both valency and headgroup tailoring on selectivity. *Org. Biomol. Chem.* **2012**, *10* (34), 6893-6907.
266. Andre, S.; Wang, G.-N.; Gabius, H.-J.; Murphy, P. V., Combining glycocluster synthesis with protein engineering: an approach to probe into the significance of linker length in a tandem-repeat-type lectin (galectin-4). *Carbohydr. Res.* **2014**, *389*, 25-38.
267. Marchiori, M. F.; Souto, D. E. P.; Bortot, L. O.; Pereira, J. F.; Kubota, L. T.; Cummings, R. D.; Dias-Baruffi, M.; Carvalho, I.; Campo, V. L., Synthetic 1, 2, 3-triazole-linked glycoconjugates bind with high affinity to human galectin-3. *Bioorg. Med. Chem.* **2015**, *23* (13), 3414-3425.
268. Rabinovich, G. A.; Cumashi, A.; Bianco, G. A.; Ciavardelli, D.; Iurisci, I.; D'Egidio, M.; Piccolo, E.; Tinari, N.; Nifantiev, N.; Iacobelli, S., Synthetic lactulose amines: novel class of anticancer agents that induce tumor-cell apoptosis and inhibit galectin-mediated homotypic cell aggregation and endothelial cell morphogenesis. *Glycobiology* **2006**, *16* (3), 210-220.
269. Yao, W.; Xia, M.-j.; Meng, X.-b.; Li, Q.; Li, Z.-j., Adaptable synthesis of C-lactosyl glycoclusters and their binding properties with galectin-3. *Org. Biomol. Chem.* **2014**, *12* (41), 8180-8195.
270. Van Scherpenzeel, M.; Moret, E. E.; Ballell, L.; Liskamp, R. M.; Nilsson, U. J.; Leffler, H.; Pieters, R. J., Synthesis and Evaluation of New Thiodigalactoside - Based Chemical Probes to Label Galectin - 3. *ChemBioChem* **2009**, *10* (10), 1724-1733.
271. MacKinnon, A. C.; Gibbons, M. A.; Farnworth, S. L.; Leffler, H.; Nilsson, U. J.; Delaine, T.; Simpson, A. J.; Forbes, S. J.; Hirani, N.; Gauldie, J., Regulation

- of transforming growth factor- β 1-driven lung fibrosis by galectin-3. *Am. J. Respir. Crit. Care Med.* **2012**, *185* (5), 537-546.
272. Nilsson, U.; Leffler, H.; Cumpstey, I., Galactoside inhibitors of galectins. Google Patents: 2009.
273. Salameh, B. A.; Cumpstey, I.; Sundin, A.; Leffler, H.; Nilsson, U. J., 1H-1, 2, 3-triazol-1-yl thiodigalactoside derivatives as high affinity galectin-3 inhibitors. *Bioorg. Med. Chem.* **2010**, *18* (14), 5367-5378.
274. Nilsson, U.; Leffler, H.; Cumpstey, I., Novel galactoside inhibitors of galectins. Google Patents: 2005.
275. André, S.; Kövér, K. E.; Gabius, H.-J.; Szilágyi, L., Thio- and selenoglycosides as ligands for biomedically relevant lectins: Valency-activity correlations for benzene-based dithiogalactoside clusters and first assessment for (di) selenodigalactosides. *Bioorg. Med. Chem. Lett.* **2015**, *25* (4), 931-935.
276. André, S.; O'Sullivan, S.; Koller, C.; Murphy, P. V.; Gabius, H.-J., Bi- to tetravalent glycoclusters presenting GlcNAc/GalNAc as inhibitors: from plant agglutinins to human macrophage galactose-type lectin (CD301) and galectins. *Org. Biomol. Chem.* **2015**, *13* (14), 4190-4203.
277. André, S.; Liu, B.; Gabius, H.-J.; Roy, R., First demonstration of differential inhibition of lectin binding by synthetic tri- and tetravalent glycoclusters from cross-coupling of rigidified 2-propynyl lactoside. *Org. Biomol. Chem.* **2003**, *1* (22), 3909-3916.
278. Nelson, A.; Belitsky, J. M.; Vidal, S.; Joiner, C. S.; Baum, L. G.; Stoddart, J. F., A self-assembled multivalent pseudopolyrotaxane for binding galectin-1. *J. Am. Chem. Soc.* **2004**, *126* (38), 11914-11922.
279. André, S.; Specker, D.; Bovin, N. V.; Lensch, M.; Kaltner, H.; Gabius, H.-J.; Wittmann, V., Carbamate-linked lactose: design of clusters and evidence for selectivity to block binding of human lectins to (neo) glycoproteins with increasing degree of branching and to tumor cells. *Bioconjug. Chem.* **2009**, *20* (9), 1716-1728.

280. André, S.; Liu, B.; Gabius, H.-J.; Roy, R., First demonstration of differential inhibition of lectin binding by synthetic tri- and tetravalent glycoclusters from cross-coupling of rigidified 2-propynyl lactoside. *Org. Biomol. Chem.* **2003**, *1* (22), 3909-3916.
281. André, S.; Renaudet, O.; Bossu, I.; Dumy, P.; Gabius, H. J., Cyclic neoglycodecapeptides: how to increase their inhibitory activity and selectivity on lectin/toxin binding to a glycoprotein and cells. *J. Pept. Sci.* **2011**, *17* (6), 427-437.
282. Gouin, S. G.; Fernández, J. M. G.; Vanquelef, E.; Dupradeau, F. Y.; Salomonsson, E.; Leffler, H.; Ortega - Muñoz, M.; Nilsson, U. J.; Kovensky, J., Multimeric Lactoside “Click Clusters” as Tools to Investigate the Effect of Linker Length in Specific Interactions with Peanut Lectin, Galectin - 1, and - 3. *ChemBioChem* **2010**, *11* (10), 1430-1442.
283. Chuo, W.-H.; Tsai, T.-R.; Hsu, S.-H.; Cham, T.-M., Preparation and in-vitro evaluation of nifedipine loaded albumin microspheres cross-linked by different glutaraldehyde concentrations. *I. J. Pharm.* **1996**, *144* (2), 241-245.
284. Park, H.-Y.; Song, I.-H.; Kim, J.-H.; Kim, W.-S., Preparation of thermally denatured albumin gel and its pH-sensitive swelling. *I. J. Pharm.* **1998**, *175* (2), 231-236.
285. Lin, W.; Coombes, A.; Davies, M.; Davis, S.; Illum, L., Preparation of sub-100 nm human serum albumin nanospheres using a pH-coacervation method. *J. Drug Target.* **1993**, *1* (3), 237-243.
286. Böcker, S.; Laaf, D.; Elling, L., Galectin binding to neo-glycoproteins: LacDiNAc conjugated BSA as ligand for human galectin-3. *Biomolecules* **2015**, *5* (3), 1671-1696.
287. Fischöder, T.; Laaf, D.; Dey, C.; Elling, L., Enzymatic synthesis of N-acetyllactosamine (LacNAc) type 1 oligomers and characterization as multivalent galectin ligands. *Molecules* **2017**, *22* (8), 1320.

288. Zhang, H.; Laaf, D.; Elling, L.; Pieters, R. J., Thiodigalactoside–Bovine Serum Albumin Conjugates as High-Potency Inhibitors of Galectin-3: An Outstanding Example of Multivalent Presentation of Small Molecule Inhibitors. *Bioconjug. Chem.* **2018**, *29* (4), 1266-1275.
289. Collier, J. H.; Messersmith, P. B., Enzymatic modification of self-assembled peptide structures with tissue transglutaminase. *Bioconjug. Chem.* **2003**, *14* (4), 748-755.
290. Restuccia, A.; Tian, Y. F.; Collier, J. H.; Hudalla, G. A., Self-assembled glycopeptide nanofibers as modulators of galectin-1 bioactivity. *Cell. Mol. Bioeng.* **2015**, *8* (3), 471-487.
291. Zhang, X., Gold nanoparticles: recent advances in the biomedical applications. *Cell Biochem. Biophys.* **2015**, *72* (3), 771-775.
292. Grzelczak, M.; Pérez-Juste, J.; Mulvaney, P.; Liz-Marzán, L. M., Shape control in gold nanoparticle synthesis. *Chem. Soc. Rev.* **2008**, *37* (9), 1783-1791.
293. Bastús, N. G.; Comenge, J.; Puentes, V., Kinetically controlled seeded growth synthesis of citrate-stabilized gold nanoparticles of up to 200 nm: size focusing versus Ostwald ripening. *Langmuir* **2011**, *27* (17), 11098-11105.
294. Zuber, A.; Purdey, M.; Schartner, E.; Forbes, C.; Van der Hoek, B.; Giles, D.; Abell, A.; Monro, T.; Ebdorff-Heidepriem, H., Detection of gold nanoparticles with different sizes using absorption and fluorescence based method. *Sensor. Actuat. B-Chem.* **2016**, *227*, 117-127.
295. Marradi, M.; Chiodo, F.; García, I.; Penadés, S., Glyconanoparticles as multifunctional and multimodal carbohydrate systems. *Chem. Soc. Rev.* **2013**, *42* (11), 4728-4745.
296. Yoshioka, K.; Sato, Y.; Murakami, T.; Tanaka, M.; Niwa, O., One-step detection of galectins on hybrid monolayer surface with protruding lactoside. *Anal. Chem.* **2010**, *82* (4), 1175-1178.

297. Amendola, V.; Saija, R.; Maragò, O. M.; Iatì, M. A., Superior plasmon absorption in iron-doped gold nanoparticles. *Nanoscale* **2015**, *7* (19), 8782-8792.
298. Tang, Z.; He, J.; Chen, J.; Niu, Y.; Zhao, Y.; Zhang, Y.; Yu, C., A sensitive sandwich-type immunosensor for the detection of galectin-3 based on N-GNRs-Fe-MOFs@ AuNPs nanocomposites and a novel AuPt-methylene blue nanorod. *Biosens. Bioelectron.* **2018**, *101*, 253-259.
299. Martos-Maldonado, M. C.; Quesada-Soriano, I.; García-Fuentes, L.; Vargas-Berenguel, A., Multivalent Lactose–Ferrocene Conjugates Based on Poly (Amido Amine) Dendrimers and Gold Nanoparticles as Electrochemical Probes for Sensing Galectin-3. *Nanomaterials* **2020**, *10* (2), 203.
300. Miura, Y.; Hoshino, Y.; Seto, H., Glycopolymer nanobiotechnology. *Chem. Rev.* **2016**, *116* (4), 1673-1692.
301. Li, X.; Chen, G., Glycopolymer-based nanoparticles: synthesis and application. *Polym. Chem.* **2015**, *6* (9), 1417-1430.
302. Pramudya, I.; Chung, H., Recent progress of glycopolymer synthesis for biomedical applications. *Biomater. Sci.* **2019**, *7* (12), 4848-4872.
303. Rosencrantz, S.; Tang, J. S. J.; Schulte - Osseili, C.; Böker, A.; Rosencrantz, R. R., Glycopolymers by RAFT Polymerization as Functional Surfaces for Galectin - 3. *Macromol. Chem. Phys.* **2019**, *220* (20), 1900293.
304. Filipová, M.; Bojarová, P.; Rodrigues Tavares, M.; Bumba, L.; Elling, L.; Chytil, P.; Gunár, K. n.; Křen, V. r.; Etrych, T. s.; Janoušková, O., Glycopolymers for Efficient Inhibition of Galectin-3: In Vitro Proof of Efficacy Using Suppression of T Lymphocyte Apoptosis and Tumor Cell Migration. *Biomacromolecules* **2020**, *21* (8), 3122-3133.
305. Zhou, C.; Reesink, H. L.; Putnam, D. A., Selective and Tunable Galectin Binding of Glycopolymers Synthesized by a Generalizable Conjugation Method. *Biomacromolecules* **2019**, *20* (10), 3704-3712.

306. Tavares, M. R.; Bláhová, M.; Sedláková, L.; Elling, L.; Pelantová, H.; Konefał, R.; Etrych, T. s.; Křen, V. r.; Bojarová, P.; Chytil, P., High-Affinity N-(2-Hydroxypropyl) methacrylamide Copolymers with Tailored N-Acetyllactosamine Presentation Discriminate between Galectins. *Biomacromolecules* **2020**, *21* (2), 641-652.
307. Wolfenden, M.; Cousin, J.; Nangia-Makker, P.; Raz, A.; Cloninger, M., Glycodendrimers and modified ELISAs: Tools to elucidate multivalent interactions of galectins 1 and 3. *Molecules* **2015**, *20* (4), 7059-7096.
308. Xiao, Q.; Ludwig, A.-K.; Romanò, C.; Buzzacchera, I.; Sherman, S. E.; Vetro, M.; Vértesy, S.; Kaltner, H.; Reed, E. H.; Möller, M., Exploring functional pairing between surface glycoconjugates and human galectins using programmable glycodendrimersomes. *Proc. Natl. Acad. Sci. U. S. A.* **2018**, *115* (11), E2509-E2518.
309. Singh, S.; Vardhan, H.; Kotla, N. G.; Maddiboyina, B.; Sharma, D.; Webster, T. J., The role of surfactants in the formulation of elastic liposomal gels containing a synthetic opioid analgesic. *Int. J. Nanomedicine* **2016**, *11*, 1475.
310. Barbosa, R.; Severino, P.; Preté, P.; Santana, M., Influence of different surfactants on the physicochemical properties of elastic liposomes. *Pharma. Dev. Technol.* **2017**, *22* (3), 360-369.
311. Duangjit, S.; Pamornpathomkul, B.; Opanasopit, P.; Rojanarata, T.; Obata, Y.; Takayama, K.; Ngawhirunpat, T., Role of the charge, carbon chain length, and content of surfactant on the skin penetration of meloxicam-loaded liposomes. *Int. J. Nanomedicine* **2014**, *9*, 2005.
312. Gupta, M.; Vaidya, B.; Mishra, N.; Vyas, S. P., Effect of surfactants on the characteristics of fluconazole niosomes for enhanced cutaneous delivery. *Artif. Cells Blood Sub. Biotechnol.* **2011**, *39* (6), 376-384.
313. Varki, A., Glycan-based interactions involving vertebrate sialic-acid-recognizing proteins. *Nature* **2007**, *446* (7139), 1023.

314. Klenk, E., Neuraminsäure, das Spaltprodukt eines neuen Gehirnlipoids. *Z. Physiol. Chem.* **1941**, 268 (1-2), 50-58.
315. Schauer, R.; Kelm, S.; Reuter, G.; Roggentin, P.; Shaw, L., Biochemistry and role of sialic acids. In *Biology of the sialic acids*, Springer: 1995; pp 7-67.
316. Schauer, R., *Sialic acids: chemistry, metabolism, and function*. Springer Science & Business Media: 2012; Vol. 10.
317. Wright, P.; Neumann, G.; Kawaoka, Y., Orthomyxoviruses. Fields Virology. In *Fields Virology*, Lippincott-Williams & Wilkins: Philadelphia, 2007; pp 1691-1740.
318. Salomon, R.; Webster, R. G., The influenza virus enigma. *Cell* **2009**, 136 (3), 402-410.
319. Zhirnov, O. P.; Ikizler, M. R.; Wright, P. F., Cleavage of influenza a virus hemagglutinin in human respiratory epithelium is cell associated and sensitive to exogenous antiproteases. *J. Virol.* **2002**, 76 (17), 8682-8689.
320. Sriwilajaroen, N.; Suzuki, Y., Molecular basis of the structure and function of H1 hemagglutinin of influenza virus. *Proc. Jpn. Acad. Ser. B* **2012**, 88 (6), 226-249.
321. Matrosovich, M.; Gambaryan, A.; Teneberg, S.; Piskarev, V.; Yamnikova, S.; Lvov, D.; Robertson, J.; Karlsson, K.-A., Avian influenza A viruses differ from human viruses by recognition of sialyloligosaccharides and gangliosides and by a higher conservation of the HA receptor-binding site. *Virology* **1997**, 233 (1), 224-234.
322. Rogers, G.; Paulson, J.; Daniels, R.; Skehel, J.; Wilson, I.; Wiley, D., Single amino acid substitutions in influenza haemagglutinin change receptor binding specificity. *Nature* **1983**, 304 (5921), 76-78.
323. Stevens, J.; Blixt, O.; Glaser, L.; Taubenberger, J. K.; Palese, P.; Paulson, J. C.; Wilson, I. A., Glycan microarray analysis of the hemagglutinins from modern and pandemic influenza viruses reveals different receptor specificities. *J. Mol. Biol.* **2006**, 355 (5), 1143-1155.

324. Wiley, D. C.; Skehel, J. J., The structure and function of the hemagglutinin membrane glycoprotein of influenza virus. *Annu. Rev. Biochem.* **1987**, *56* (1), 365-394.
325. Stencel-Baerenwald, J. E.; Reiss, K.; Reiter, D. M.; Stehle, T.; Dermody, T. S., The sweet spot: defining virus-sialic acid interactions. *Nat. Rev. Microbiol.* **2014**, *12* (11), 739-749.
326. Matrosovich, M. N.; Matrosovich, T. Y.; Gray, T.; Roberts, N. A.; Klenk, H.-D., Neuraminidase is important for the initiation of influenza virus infection in human airway epithelium. *J. Virol.* **2004**, *78* (22), 12665-12667.
327. McAuley, J. L.; Gilbertson, B. P.; Trifkovic, S.; Brown, L. E.; McKimm-Breschkin, J. L., Influenza virus neuraminidase structure and functions. *Front. Microbiol.* **2019**, *10*, 39.
328. Colman, P. M.; Hoyne, P. A.; Lawrence, M. C., Sequence and structure alignment of paramyxovirus hemagglutinin-neuraminidase with influenza virus neuraminidase. *J. Virol.* **1993**, *67* (6), 2972-2980.
329. Varghese, J. N.; McKimm - Breschkin, J. L.; Caldwell, J. B.; Kortt, A. A.; Colman, P. M., The structure of the complex between influenza virus neuraminidase and sialic acid, the viral receptor. *Proteins: Struct. Funct. Bioinf.* **1992**, *14* (3), 327-332.
330. Ward, C. W.; Colman, P. M.; Laver, W. G., The disulphide bonds of an Asian influenza virus neuraminidase. *FEBS Lett.* **1983**, *153* (1), 29-33.
331. Lenza, M. P.; Atxabal, U.; Oyenarte, I.; Jiménez-Barbero, J.; Ereño-Orbea, J., Current Status on Therapeutic Molecules Targeting Siglec Receptors. *Cells* **2020**, *9* (12), 2691.
332. Meezan, E.; Wu, H. C.; Black, P. H.; Robbins, P. W., Comparative studies on the carbohydrate-containing membrane components of normal and virus-transformed mouse fibroblasts. II. Separation of glycoproteins and glycopeptides by sephadex chromatography. *Biochemistry* **1969**, *8* (6), 2518-2524.

333. Pinho, S. S.; Reis, C. A., Glycosylation in cancer: mechanisms and clinical implications. *Nat. Rev. Cancer* **2015**, *15* (9), 540-555.
334. Adams, O. J.; Stanczak, M. A.; von Gunten, S.; Läubli, H., Targeting sialic acid–Siglec interactions to reverse immune suppression in cancer. *Glycobiology* **2018**, *28* (9), 640-647.
335. Pearce, O. M.; Läubli, H., Sialic acids in cancer biology and immunity. *Glycobiology* **2016**, *26* (2), 111-128.
336. Varki, A.; Schauer, R., Sialic acids. In *Essentials of Glycobiology. 2nd edition*, Cold Spring Harbor Laboratory Press: La Jolla, California, 2009.
337. Severi, E.; Hood, D. W.; Thomas, G. H., Sialic acid utilization by bacterial pathogens. *Microbiology* **2007**, *153* (9), 2817-2822.
338. Varki, A., Glycan-based interactions involving vertebrate sialic-acid-recognizing proteins. *Nature* **2007**, *446* (7139), 1023-1029.
339. Zhou, X.; Yang, G.; Guan, F., Biological functions and analytical strategies of sialic acids in tumor. *Cells* **2020**, *9* (2), 273.
340. Läubli, H.; Kawanishi, K.; George Vazhappilly, C.; Matar, R.; Merheb, M.; Sarwar Siddiqui, S., Tools to study and target the Siglec–sialic acid axis in cancer. *FEBS J.* **2020**.
341. Yu, C. C.; Withers, S. G., Recent developments in enzymatic synthesis of modified sialic acid derivatives. *Adv. Synth. Catal.* **2015**, *357* (8), 1633-1654.
342. Li, W.; McArthur, J. B.; Chen, X., Strategies for chemoenzymatic synthesis of carbohydrates. *Carbohydr. Res.* **2019**, *472*, 86-97.
343. Muthana, S.; Cao, H.; Chen, X., Recent progress in chemical and chemoenzymatic synthesis of carbohydrates. *Curr. Opin. Chem. Biol.* **2009**, *13* (5-6), 573-581.
344. Boons, G.-J.; Demchenko, A. V., Recent advances in O-sialylation. *Chem. Rev.* **2000**, *100* (12), 4539-4566.

345. Ress, D. K.; Linhardt, R. J., Sialic acid donors: chemical synthesis and glycosylation. *Curr. Org. Synth.* **2004**, *1* (1), 31-46.
346. Ando, H.; Imamura, A., Proceedings in synthetic chemistry of sialo-glycoside. *Trends Glycosci. Glycotechnol.* **2004**, *16* (91), 293-303.
347. Lih, Y. H.; Wu, C. Y., Chemical Synthesis of Sialosides. In *Selective Glycosylations: Synthetic Methods and Catalysts*, Wiley Online Library: 2017; pp 353-370.
348. Meo, C. D.; Demchenko, A. V.; Boons, G.-J., A stereoselective approach for the synthesis of α -sialosides. *J. Org. Chem.* **2001**, *66* (16), 5490-5497.
349. Navuluri, C.; Crich, D., Stereocontrolled synthesis of sialosides. *Glycochem. Sci.* **2016**, 131-154.
350. Wang, P. G.; Bertozzi, C. R., *Glycochemistry: principles, synthesis, and applications*. Marcel Dekker, Inc.: 2001.
351. Hasegawa, A.; Kiso, M., *Chemical synthesis of sialyl glycosides*. Marcel Dekker, Inc New York: 1997; Vol. 357.
352. Kiso, M.; Ishida, H.; Ito, H., Special problems in glycosylation reactions: sialidations. *Carbohydr. Chem. Biol.* **2000**, 345-365.
353. Okamoto, K.; Goto, T., Glycosidation of sialic acid. *Tetrahedron* **1990**, *46* (17), 5835-5857.
354. Ogawa, T.; Sugimoto, M., Synthesis of α -Neu5acp-(2 \rightarrow 3)-d-Gal and α -Neu5acp-(2 \rightarrow 3)- β -d-Galp-(1 \rightarrow 4)-d-Glc. *Carbohydr. Res.* **1985**, *135* (2), C5-C9.
355. DeNinno, M. P., The Synthesis and Glycosidation of-Acetylneuraminic Acid. *Synthesis* **1991**, *1991* (8), 583-593.
356. Danishefsky, S. J.; DeNinno, M. P.; Chen, S. H., Stereoselective total syntheses of the naturally occurring enantiomers of N-acetylneuraminic acid and 3-deoxy-D-manno-2-octulosonic acid. A new and stereospecific approach to sialo and 3-deoxy-D-manno-2-octulosonic acid conjugates. *J. Am. Chem. Soc.* **1988**, *110* (12), 3929-3940.

357. Takahashi, T.; Tsukamoto, H.; Yamada, H., A new method for the formation of the α -glycoside bond of sialyl conjugates based on long-range participation. *Tetrahedron Lett.* **1997**, *38* (47), 8223-8226.
358. Haberman, J. M.; Gin, D. Y., A new C (1)-auxiliary for anomeric stereocontrol in the synthesis of α -sialyl glycosides. *Org. Lett.* **2001**, *3* (11), 1665-1668.
359. Chen, J.; Hansen, T.; Zhang, Q. J.; Liu, D. Y.; Sun, Y.; Yan, H.; Codée, J. D.; Schmidt, R. R.; Sun, J. S., 1 - Picolinyl - 5 - azido Thiosialosides: Versatile Donors for the Stereoselective Construction of Sialyl Linkages. *Angew. Chem.* **2019**, *131* (47), 17156-17164.
360. Zhang, Y.; Yang, M.; Wang, X.; Gu, G.; Cai, F., Improved α -Sialylation through the Synergy of 5-N, 4-O-Oxazolidinone Protection and Exocyclic C-1 Neighboring Group Participation. *J. Org. Chem.* **2020**, *85* (21), 13589-13601.
361. Haberman, J. M.; Gin, D. Y., Dehydrative sialylation with C2-hemiketal sialyl donors. *Org. Lett.* **2003**, *5* (14), 2539-2541.
362. Hanashima, S.; Akai, S.; Sato, K.-i., Thioester-assisted α -sialylation reaction. *Tetrahedron Lett.* **2008**, *49* (34), 5111-5114.
363. Okamoto, K.; Kondo, T.; Goto, T., A stereospecific β -glycosylation of 2 β , 3 α -dibromo-n-acetylneuraminic acid. *Tetrahedron* **1987**, *43* (24), 5909-5918.
364. Ito, Y.; Ogawa, T., Highly stereoselective glycosylation of N-acetylneuraminic acid aided by a phenylthio substituent as a stereocontrolling auxiliary. *Tetrahedron Lett.* **1988**, *29* (32), 3987-3990.
365. Ito, Y.; Ogawa, T., Highly stereoselective glycosylation of sialic acid aided by stereocontrolling auxiliaries. *Tetrahedron* **1990**, *46* (1), 89-102.
366. Ercegovic, T.; Magnusson, G., Highly Stereoselective. α -Sialylation. Synthesis of GM3-Saccharide and a Bis-Sialic Acid Unit. *J. Org. Chem.* **1995**, *60* (11), 3378-3384.

367. Martichonok, V.; Whitesides, G. M., A practical method for the synthesis of sialyl α -glycosides. *J. Am. Chem. Soc.* **1996**, *118* (35), 8187-8191.
368. Ercégovic, T.; Magnusson, G., Synthesis of a Bis (sialic acid) 8, 9-Lactam. *J. Org. Chem.* **1996**, *61* (1), 179-184.
369. Castro-Palomino, J. C.; Tsvetkov, Y. E.; Schmidt, R. R., 8-O-Sialylation of neuraminic acid. *J. Am. Chem. Soc.* **1998**, *120* (22), 5434-5440.
370. Hossain, N.; Magnusson, G., A novel donor for stereoselective α -sialylation; efficient synthesis of an α (2–8)-linked bis-sialic acid unit. *Tetrahedron Lett.* **1999**, *40* (11), 2217-2220.
371. Christensen, H. M.; Oscarson, S.; Jensen, H. H., Common side reactions of the glycosyl donor in chemical glycosylation. *Carbohydr. Res.* **2015**, *408*, 51-95.
372. Marra, A.; Sinaÿ, P., A novel stereoselective synthesis of N-acetyl- α -neuraminosyl-galactose di-saccharide derivatives, using anomeric S-glycosyl xanthates. *Carbohydr. Res.* **1990**, *195* (2), 303-308.
373. Martichonok, V.; Whitesides, G. M., Stereoselective α -sialylation with sialyl xanthate and phenylsulfenyl triflate as a promotor. *J. Org. Chem.* **1996**, *61* (5), 1702-1706.
374. Dziadek, S.; Brocke, C.; Kunz, H., Biomimetic Synthesis of the Tumor - Associated (2, 3) - Sialyl - T Antigen and Its Incorporation into Glycopeptide Antigens from the Mucins MUC1 and MUC4. *Chem. Eur. J.* **2004**, *10* (17), 4150-4162.
375. Qu, H.; Liu, J.-M.; Wdzieczak-Bakala, J.; Lu, D.; He, X.; Sun, W.; Sollogoub, M.; Zhang, Y., Synthesis and cytotoxicity assay of four ganglioside GM3 analogues. *Eur. J. Med. Chem.* **2014**, *75*, 247-257.
376. Zheng, C.; Qu, H.; Liao, W.; Bavaro, T.; Terreni, M.; Sollogoub, M.; Ding, K.; Zhang, Y., Chemoenzymatically synthesized GM3 analogues as potential therapeutic agents to recover nervous functionality after injury by inducing neurite outgrowth. *Eur. J. Med. Chem.* **2018**, *146*, 613-620.

377. Tropper, F. D.; Andersson, F. O.; Cao, S.; Roy, R., Synthesis of S-glycosyl xanthates by phase transfer catalyzed substitution of glycosyl halides. *J. Carbohydr. Chem.* **1992**, *11* (6), 741-750.
378. Hasegawa, A.; Nagahama, T.; Ohki, H.; Hotta, K.; Ishida, H.; Kiso, M., Communication: Synthetic Studies on Sialoglycoconjugates 25: Reactivity of Glycosyl Promoters in α -Glycosylation of N-Acetyl-Neuraminic Acid with the Primary and Secondary Hydroxyl Groups in the Suitably Protected Galactose and Lactose Derivatives. *J. Carbohydr. Chem.* **1991**, *10* (3), 493-498.
379. Hasegawa, A.; Ohki, H.; Nagahama, T.; Ishida, H.; Kiso, M., A facile, large-scale preparation of the methyl 2-thioglycoside of N-acetylneuraminic acid, and its usefulness for the α -stereoselective synthesis of sialoglycosides. *Carbohydr. Res.* **1991**, *212*, 277-281.
380. Roy, R.; Andersson, F. O.; Letellier, M., "Active" and "Latent" Thioglycosyl Donors in Oligosaccharide Synthesis. Application to the synthesis of α -sialosides. *Tetrahedron Lett.* **1992**, *33* (41), 6053-6056.
381. Cao, S.; Meunier, S. J.; Andersson, F. O.; Letellier, M.; Roy, R., Mild stereoselective syntheses of thioglycosides under PTC conditions and their use as active and latent glycosyl donors. *Tetrahedron: Asymmetry* **1994**, *5* (11), 2303-2312.
382. Shiao, T. C.; Roy, R., "Active-Latent" Thioglycosyl Donors and Acceptors in Oligosaccharide Syntheses. In *Reactivity Tuning in Oligosaccharide Assembly*, Springer: 2010; pp 69-108.
383. Garegg, P. J., Thioglycosides as glycosyl donors in oligosaccharide synthesis. *Adv. Carbohydr. Chem. Biochem.* **1997**, *52*, 179-205.
384. Crich, D.; Li, W., α -Selective sialylations at -78 C in nitrile solvents with a 1-adamantanyl thiosialoside. *J. Org. Chem.* **2007**, *72* (20), 7794-7797.
385. Roy, R.; Zanini, D.; Meunier, S.; Romanowska, A., Synthesis and antigenic properties of sialic acid based dendrimers. Series, A. S., Ed. ACS Publications: 1994; Vol. 560, pp 104-119.

386. Zhang, Z.; Ollmann, I. R.; Ye, X.-S.; Wischnat, R.; Baasov, T.; Wong, C.-H., Programmable one-pot oligosaccharide synthesis. *J. Am. Chem. Soc.* **1999**, *121* (4), 734-753.
387. Nicolaou, K.; Ueno, H., *Preparative Carbohydrate Chemistry*. 1996; p 313-338.
388. Crich, D.; Li, W., Efficient glycosidation of a phenyl thiosialoside donor with diphenyl sulfoxide and triflic anhydride in dichloromethane. *Org. Lett.* **2006**, *8* (5), 959-962.
389. Gu, Z. y.; Zhang, J. x.; Xing, G. w., N - Acetyl - 5 - N, 4 - O - oxazolidinone - Protected Sialyl Sulfoxide: An α - Selective Sialyl Donor with Tf₂O/(Tol) ₂SO in Dichloromethane. *Chem. Asian J.* **2012**, *7* (7), 1524-1528.
390. Zeng, J.; Liu, Y.; Chen, W.; Zhao, X.; Meng, L.; Wan, Q., Glycosyl Sulfoxides in Glycosylation Reactions. *Sulphur Chem.* **2019**, 367-398.
391. Liu, G.-J.; Li, C.-Y.; Zhang, X.-T.; Du, W.; Gu, Z.-Y.; Xing, G.-W., Modulation of the stereoselectivity and reactivity of glycosylation via (p-Tol) ₂SO/Tf₂O preactivation strategy: From O-, C-sialylation to general O-, N-glycosylation. *Chin. Chem. Lett.* **2018**, *29* (1), 1-10.
392. De Meo, C.; Parker, O., Thiomidoyl approach to the synthesis of α -sialosides. *Tetrahedron: Asymmetry* **2005**, *16* (2), 303-307.
393. Tanaka, H.; Tatenno, Y.; Nishiura, Y.; Takahashi, T., Efficient synthesis of an α (2, 9) trisialic acid by one-pot glycosylation and polymer-assisted deprotection. *Org. Lett.* **2008**, *10* (24), 5597-5600.
394. Harris, B. N.; Patel, P. P.; Gobble, C. P.; Stark, M. J.; De Meo, C., C - 5 Modified S - Benzoxazolyl Sialyl Donors: Towards More Efficient Selective Sialylations. Wiley Online Library: 2011.
395. Roy, R.; Andersson, F. O.; Letellier, M., "Active" and "Latent" Thioglycosyl Donors in Oligosaccharide Synthesis. Application to the Synthesis of α -Sialosides. *Tetrahedron Lett.* **1992**, *33* (41), 6053-6056.

396. Crich, D.; Li, W., α -Selective sialylations at -78°C in nitrile solvents with a 1-adamantanyl thiosialoside. *J. Org. Chem.* **2007**, *72* (20), 7794-7797.
397. Kondo, H.; Ichikawa, Y.; Wong, C. H., . beta.-Sialyl phosphite and phosphoramidite: synthesis and application to the chemoenzymic synthesis of CMP-sialic acid and sialyl oligosaccharides. *J. Am. Chem. Soc.* **1992**, *114* (22), 8748-8750.
398. Sim, M. M.; Kondo, H.; Wong, C. H., Synthesis and use of glycosyl phosphites: an effective route to glycosyl phosphates, sugar nucleotides, and glycosides. *J. Am. Chem. Soc.* **1993**, *115* (6), 2260-2267.
399. Martin, T. J., Efficient sialylation with phosphite as leaving group. *Tetrahedron Lett.* **1992**, *33* (41), 6123-6126.
400. Martin, T. J.; Brescello, R.; Toepfer, A.; Schmidt, R. R., Synthesis of phosphites and phosphates of neuraminic acid and their glycosyl donor properties—convenient synthesis of GM 3. *Glycoconjug. J.* **1993**, *10* (1), 16-25.
401. Singh, K.; Fernández-Mayoralas, A.; Martín-Lomas, M., Synthesis of oligosaccharides structurally related to E-selection ligands. *J. Chem. Soc. Chem. Commun.* **1994**, (6), 775-776.
402. Tsvetkov, Y. E.; Schmidt, R. R., 8-O-Sialylation of derivatives of neuraminic acid 1, 7-lactone unusual stereoselectivity. *Tetrahedron Lett.* **1994**, *35* (46), 8583-8586.
403. Qiu, D.; Gandhi, S. S.; Koganty, R. R., β Gal (1–3) GalNAc block donor for the synthesis of TF and α Sialy (2–6) TF as glycopeptide building blocks. *Tetrahedron Lett.* **1996**, *37* (5), 595-598.
404. Schwarz, J. B.; Kuduk, S. D.; Chen, X.-T.; Sames, D.; Glunz, P. W.; Danishefsky, S. J., A broadly applicable method for the efficient synthesis of α -O-linked glycopeptides and clustered sialic acid residues. *J. Am. Chem. Soc.* **1999**, *121* (12), 2662-2673.

405. Hsu, C. H.; Chu, K. C.; Lin, Y. S.; Han, J. L.; Peng, Y. S.; Ren, C. T.; Wu, C. Y.; Wong, C. H., Highly α - selective sialyl phosphate donors for efficient preparation of natural sialosides. *Chem. Eur. J.* **2010**, *16* (6), 1754-1760.
406. Bernardi, A.; Boschin, G.; Checchia, A.; Lattanzio, M.; Manzoni, L.; Potenza, D.; Scolastico, C., Synthesis of a Pseudo Tetrasaccharide Mimic of Ganglioside GM 1. *Eur. J. Org. Chem.* **1999**, *1999* (6), 1311-1317.
407. Winterfeld, G. A.; Schmidt, R. R., Nitroglycal Concatenation: A Broadly Applicable and Efficient Approach to the Synthesis of Complex O - Glycans. *Angew. Chem. Int. Ed.* **2001**, *40* (14), 2654-2657.
408. Mong, T. K.-K.; Lee, H.-K.; Durón, S. G.; Wong, C.-H., Reactivity-based one-pot total synthesis of fucose GM1 oligosaccharide: a sialylated antigenic epitope of small-cell lung cancer. *Proc. Natl. Acad. Sci. U. S. A.* **2003**, *100* (3), 797-802.
409. Tanaka, H.; Nishiura, Y.; Adachi, M.; Takahashi, T., Synthetic study of α (2, 8) oligosialoside using N-Troc sialyl N-phenyltrifluoroimidate. *Heterocycles* **2006**, *67* (1), 107-112.
410. Wu, B.; Hua, Z.; Warren, J. D.; Ranganathan, K.; Wan, Q.; Chen, G.; Tan, Z.; Chen, J.; Endo, A.; Danishefsky, S. J., Synthesis of the fucosylated biantennary N-glycan of erythropoietin. *Tetrahedron Lett.* **2006**, *47* (31), 5577-5579.
411. Chuang, H.-Y.; Ren, C.-T.; Chao, C.-A.; Wu, C.-Y.; Shivatare, S. S.; Cheng, T.-J. R.; Wu, C.-Y.; Wong, C.-H., Synthesis and vaccine evaluation of the tumor-associated carbohydrate antigen RM2 from prostate cancer. *J. Am. Chem. Soc.* **2013**, *135* (30), 11140-11150.
412. Cai, S.; Yu, B., Efficient sialylation with phenyltrifluoroacetimidates as leaving groups. *Org. Lett.* **2003**, *5* (21), 3827-3830.
413. Tanaka, S. i.; Goi, T.; Tanaka, K.; Fukase, K., Highly Efficient α - Sialylation by Virtue of Fixed Dipole Effects of N - Phthalyl Group: Application to Continuous Flow Synthesis of α (2 - 3) - and α (2 - 6) - Neu5Ac - Gal Motifs by Microreactor. *J. Carbohydr. Chem.* **2007**, *26* (7), 369-394.

414. Liu, Y.; Ruan, X.; Li, X.; Li, Y., Efficient synthesis of a sialic acid α (2 \rightarrow 3) galactose building block and its application to the synthesis of ganglioside GM3. *J. Org. Chem.* **2008**, *73* (11), 4287-4290.
415. Demchenko, A. V.; Boons, G.-J., A novel and versatile glycosyl donor for the preparation of glycosides of N-acetylneuraminic acid. *Tetrahedron Lett.* **1998**, *39* (19), 3065-3068.
416. Demchenko, A. V.; Boons, G. J., A Novel Direct Glycosylation Approach for the Synthesis of Dimers of N - Acetylneuraminic Acid. *Chem. Eur. J.* **1999**, *5* (4), 1278-1283.
417. Gong, J.; Liu, H.; Nicholls, J. M.; Li, X., Studies on the sialylation of galactoses with different C-5 modified sialyl donors. *Carbohydr. Res.* **2012**, *361*, 91-99.
418. Meijer, A.; Ellervik, U., Interhalogens (ICl/IBr) and AgOTf in thioglycoside activation; synthesis of bislactam analogues of ganglioside GD3. *J. Org. Chem.* **2004**, *69* (19), 6249-6256.
419. Tanaka, H.; Ando, H.; Ishida, H.; Kiso, M.; Ishihara, H.; Koketsu, M., Synthetic study on α (2 \rightarrow 8)-linked oligosialic acid employing 1, 5-lactamization as a key step. *Tetrahedron Lett.* **2009**, *50* (31), 4478-4481.
420. De Meo, C.; Farris, M.; Ginder, N.; Gulley, B.; Priyadarshani, U.; Woods, M., Solvent effect in the synthesis of sialosyl α (2-6) galactosides: is acetonitrile the only choice? Wiley Online Library: 2008.
421. Wu, J.; Guo, Z., Improving the antigenicity of sTn antigen by modification of its sialic acid residue for development of glycoconjugate cancer vaccines. *Bioconjug. Chem.* **2006**, *17* (6), 1537-1544.
422. Ando, H.; Koike, Y.; Koizumi, S.; Ishida, H.; Kiso, M., 1, 5 - Lactamized Sialyl Acceptors for Various Disialoside Syntheses: Novel Method for the Synthesis of Glycan Portions of Hp - s6 and HLG - 2 Gangliosides. *Angew. Chem.* **2005**, *117* (41), 6917-6921.

423. Lin, C.-C.; Adak, A. K.; Horng, J.-C.; Lin, C.-C., Phosphite-based sialic acid donors in the synthesis of α (2 \rightarrow 9) oligosialic acids. *Tetrahedron* **2009**, *65* (24), 4714-4725.
424. Mondal, P. K.; Liao, G.; Mondal, M. A.; Guo, Z., Chemical synthesis of the repeating unit of type ia group b streptococcus capsular polysaccharide. *Org. Lett.* **2015**, *17* (5), 1102-1105.
425. Ren, C. T.; Chen, C. S.; Yu, Y. P.; Tsai, Y. F.; Lin, P. Y.; Chen, Y. J.; Zou, W.; Wu, S. H., Synthesis of α - (2 \rightarrow 5) Neu5Gc Oligomers. *Chem. Eur. J.* **2003**, *9* (5), 1085-1095.
426. Ando, H.; Koike, Y.; Ishida, H.; Kiso, M., Extending the possibility of an N-Troc-protected sialic acid donor toward variant sialo-glycoside synthesis. *Tetrahedron Lett.* **2003**, *44* (36), 6883-6886.
427. Tanaka, H.; Adachi, M.; Takahashi, T., One - Pot Synthesis of Sialo - Containing Glycosyl Amino Acids by Use of an N - Trichloroethoxycarbonyl - β - thiophenyl Sialoside. *Chem. Eur. J.* **2005**, *11* (3), 849-862.
428. Fuse, T.; Ando, H.; Imamura, A.; Sawada, N.; Ishida, H.; Kiso, M.; Ando, T.; Li, S.-C.; Li, Y.-T., Synthesis and enzymatic susceptibility of a series of novel GM2 analogs. *Glycoconjug. J.* **2006**, *23* (5), 329-343.
429. Imamura, A.; Kimura, A.; Ando, H.; Ishida, H.; Kiso, M., Extended Applications of Di - tert - butylsilylene - Directed α - Predominant Galactosylation Compatible with C2 - Participating Groups toward the Assembly of Various Glycosides. *Chem. Eur. J.* **2006**, *12* (34), 8862-8870.
430. Hanashima, S.; Seeberger, P. H., Total synthesis of sialylated glycans related to avian and human influenza virus infection. *Chem. Asian J.* **2007**, *2* (11), 1447-1459.
431. Komori, T.; Ando, T.; Imamura, A.; Li, Y.-T.; Ishida, H.; Kiso, M., Design and efficient synthesis of novel GM2 analogues with respect to the elucidation of the function of GM2 activator. *Glycoconjug. J.* **2008**, *25* (7), 647-661.

432. Sahabuddin, S.; Chang, T.-C.; Lin, C.-C.; Jan, F.-D.; Hsiao, H.-Y.; Huang, K.-T.; Chen, J.-H.; Horng, J.-C.; Ho, J.-a. A.; Lin, C.-C., Synthesis of N-modified sTn analogs and evaluation of their immunogenicities by microarray-based immunoassay. *Tetrahedron* **2010**, *66* (38), 7510-7519.
433. Kurimoto, K.; Yamamura, H.; Miyagawa, A., Sialylation with systematically protected allyl galactoside acceptors using sialyl phosphate donors. *Tetrahedron Lett.* **2016**, *57* (13), 1442-1445.
434. Johansson, S.; Nilsson, E.; Qian, W.; Guilligay, D.; Crepin, T.; Cusack, S.; Arnberg, N.; Elofsson, M., Design, synthesis, and evaluation of N-acyl modified sialic acids as inhibitors of adenoviruses causing epidemic keratoconjunctivitis. *J. Med. Chem.* **2009**, *52* (12), 3666-3678.
435. Adachi, M.; Tanaka, H.; Takahashi, T., An effective sialylation method using N-Troc-and N-Fmoc-protected β -thiophenyl sialosides and application to the one-pot two-step synthesis of 2, 6-sialyl-T antigen. *Synlett* **2004**, *2004* (04), 609-614.
436. Sherman, A. A.; Yudina, O. N.; Shashkov, A. S.; Menshov, V. M.; Nifant'ev, N. E., Synthesis of Neu5Ac-and Neu5Gc- α -(2 \rightarrow 6')-lactosamine 3-aminopropyl glycosides. *Carbohydr. Res.* **2001**, *330* (4), 445-458.
437. Ikeda, K.; Miyamoto, K.; Sato, M., Synthesis of N, N-Ac, Boc laurylthio sialoside and its application to O-sialylation. *Tetrahedron Lett.* **2007**, *48* (42), 7431-7435.
438. Chen, W.-S.; Sawant, R. C.; Yang, S.-A.; Liao, Y.-J.; Liao, J.-W.; Badsara, S. S.; Luo, S.-Y., Synthesis of ganglioside Hp-s1. *RSC Adv.* **2014**, *4* (88), 47752-47761.
439. Sun, B.; Jiang, H., Pre-activation based, highly alpha-selective O-sialylation with N-acetyl-5-N, 4-O-carbonyl-protected p-tolyl thiosialoside donor. *Tetrahedron Lett.* **2011**, *52* (45), 6035-6038.
440. Takeda, Y.; Horito, S., Synthesis of α -series ganglioside GM1 α containing C20-sphingosine. *Carbohydr. res.* **2005**, *340* (2), 211-220.

441. Sun, B.; Jiang, H., An efficient approach for total synthesis of aminopropyl functionalized ganglioside GM1b. *Tetrahedron Lett.* **2012**, *53* (42), 5711-5715.
442. Fujita, S.; Numata, M.; Sugimoto, M.; Tomita, K.; Ogawa, T., Total synthesis of a modified ganglioside, de-N-acetyl GM2. *Carbohydr. Res.* **1994**, *263* (2), 181-196.
443. Hsu, Y.; Ma, H. H.; Lico, L. S.; Jan, J. T.; Fukase, K.; Uchinashi, Y.; Zulueta, M. M. L.; Hung, S. C., One - pot synthesis of N - acetyl - and N - glycolylneuraminic acid capped trisaccharides and evaluation of their influenza A (H1 N1) inhibition. *Angew. Chem.* **2014**, *126* (9), 2445-2448.
444. Tanaka, K.; Goi, T.; Fukase, K., Highly efficient sialylation towards α (2-3)- and α (2-6)-Neu5Ac-Gal synthesis: significant 'fixed dipole effect' of N-phthalyl group on α -selectivity. *Synlett* **2005**, *2005* (19), 2958-2962.
445. Salmasan, R. M.; Manabe, Y.; Kitawaki, Y.; Chang, T.-C.; Fukase, K., Efficient Glycosylation Using In (OTf) 3 as a Lewis Acid: Activation of N-Phenyltrifluoroacetimidate or Thioglycosides with Halogenated Reagents or PhIO. *Chem. Lett.* **2014**, *43* (6), 956-958.
446. Iwayama, Y.; Ando, H.; Tanaka, H.-N.; Ishida, H.; Kiso, M., Synthesis of the glycan moiety of ganglioside HPG-7 with an unusual trimer of sialic acid as the inner sugar residue. *Chem. Commun.* **2011**, *47* (34), 9726-9728.
447. Takeda, N.; Takei, T.; Asahina, Y.; Hojo, H., Sialyl Tn Unit with TFA - Labile Protection Realizes Efficient Synthesis of Sialyl Glycoprotein. *Chem. Eur. J.* **2018**, *24* (11), 2593-2597.
448. Lu, K.-C.; Tseng, S.-Y.; Lin, C.-C., 5-Azido neuraminic acid thioglycoside as sialylation donor. *Carbohydr. Res.* **2002**, *337* (8), 755-760.
449. Yu, C. S.; Niikura, K.; Lin, C. C.; Wong, C. H., The thioglycoside and glycosyl phosphite of 5 - azido sialic acid: excellent donors for the α - glycosylation of primary hydroxy groups. *Angew. Chem.* **2001**, *113* (15), 2984-2987.

450. Dhakal, B.; Buda, S.; Crich, D., Stereoselective synthesis of 5-epi- α -sialosides related to the pseudaminic acid glycosides. Reassessment of the stereoselectivity of the 5-azido-5-deacetamidodialyl thioglycosides and use of triflate as nucleophile in the zbiral deamination of sialic acids. *J. Org. Chem.* **2016**, *81* (22), 10617-10630.
451. Ogasahara, R.; Abdullayev, S.; Sarpe, V. A.; Mandhapati, A. R.; Crich, D., Influence of protecting groups on O- and C-glycosylation with neuraminyl and ulosonyl dibutylphosphates. *Carbohydr. Res.* **2020**, *496*, 108100.
452. Schneider, R.; Freyhardt, C. C.; Schmidt, R. R., 5 - Azido Derivatives of Neuraminic Acid— Synthesis and Structure. *Eur. J. Org. Chem.* **2001**, *2001* (9), 1655-1661.
453. Mandhapati, A. R.; Rajender, S.; Shaw, J.; Crich, D., The isothiocyanato moiety: an ideal protecting group for the stereoselective synthesis of sialic acid glycosides and subsequent diversification. *Angew. Chem. Int. Ed.* **2015**, *54* (4), 1275-1278.
454. Tanaka, H.; Nishiura, Y.; Takahashi, T., Stereoselective Synthesis of Oligo- α -(2,8)-Sialic Acids. *J. Am. Chem. Soc.* **2006**, *128*, 7124-7125.
455. Farris, M. D.; De Meo, C., Application of 4,5-O,N-oxazolidinone protected thiophenyl sialosyl donor to the synthesis of α -sialosides. *Tetrahedron Lett.* **2007**, *48* (7), 1225-1227.
456. Crich, D.; Li, W., O-Sialylation with N-acetyl-5-N, 4-O-carbonyl-protected thiosialoside donors in dichloromethane: facile and selective cleavage of the oxazolidinone ring. *J. Org. Chem.* **2007**, *72* (7), 2387-2391.
457. Noel, A.; Delpech, B.; Crich, D., Stereoselective, electrophilic α -C-sialidation. *Org. Lett.* **2012**, *14* (5), 1342-1345.
458. Noel, A.; Delpech, B.; Crich, D., Highly stereoselective synthesis of primary, secondary, and tertiary α -S-sialosides under Lewis acidic conditions. *Org. Lett.* **2012**, *14* (16), 4138-4141.

459. Kancharla, P. K.; Navuluri, C.; Crich, D., Dissecting the influence of oxazolidinones and cyclic carbonates in sialic acid chemistry. *Angew. Chem.* **2012**, *124* (44), 11267-11271.
460. De Meo, C.; Jones, B. T., Chemical Synthesis of Glycosides of N-Acetylneuraminic Acid. *Adv. Carbohydr. Chem. Biochem.* **2018**, *75*, 215-316.
461. Kancharla, P. K.; Crich, D., Influence of side chain conformation and configuration on glycosyl donor reactivity and selectivity as illustrated by sialic acid donors epimeric at the 7-position. *J. Am. Chem. Soc.* **2013**, *135* (50), 18999-19007.
462. Kancharla, P. K.; Kato, T.; Crich, D., Probing the Influence of Protecting Groups on the Anomeric Equilibrium in Sialic Acid Glycosides with the Persistent Radical Effect. *J. Am. Chem. Soc.* **2014**, *136* (14), 5472-5480.
463. Kononov, L.; Malysheva, N.; Kononova, E.; Garkusha, O., The first example of synergism in glycosylation. Possible reasons and consequences. *Russ. Chem. Bull.* **2006**, *55* (7), 1311-1313.
464. Amarasekara, H.; Buda, S.; Mandhapaty, A. R.; Crich, D., Protecting Group Strategies for Sialic Acid Derivatives. In *Protecting Groups: Strategies and Applications in Carbohydrate Chemistry*, Vidal, S., Ed. 2019; pp 283-306.
465. Amarasekara, H.; Crich, D., Synthesis and intramolecular glycosylation of sialyl mono-esters of o-xylylene glycol. The importance of donor configuration and nitrogen protecting groups on cyclization yield and selectivity; isolation and characterization of a N-sialyl acetamide indicative of participation by acetonitrile. *Carbohydr. Res.* **2016**, *435*, 113-120.
466. De Meo, C.; Priyadarshani, U., C-5 Modifications in N-acetyl-neuraminic acid: scope and limitations. *Carbohydr. Res.* **2008**, *343* (10-11), 1540-1552.
467. Cohen, S. B.; Halcomb, R. L., Synthesis and characterization of an anomeric sulfur analogue of CMP-sialic acid. *J. Org. Chem.* **2000**, *65* (19), 6145-6152.

468. Montero, E.; Vallmitjana, M.; Pérez-Pons, J. A.; Querol, E.; Jiménez-Barbero, J.; Cañada, F. J., NMR studies of the conformation of thiocellobiose bound to a β - glucosidase from *Streptomyces* sp. *FEBS Lett.* **1998**, *421* (3), 243-248.
469. Huo, C.-X.; Zheng, X.-J.; Xiao, A.; Liu, C.-C.; Sun, S.; Lv, Z.; Ye, X.-S., Synthetic and immunological studies of N-acyl modified S-linked STn derivatives as anticancer vaccine candidates. *Org. Biomol. Chem.* **2015**, *13* (12), 3677-3690.
470. Kuan, T. C.; Wu, H. R.; Adak, A. K.; Li, B. Y.; Liang, C. F.; Hung, J. T.; Chiou, S. P.; Yu, A. L.; Hwu, J. R.; Lin, C. C., Synthesis of an S - Linked α (2 \rightarrow 8) GD3 Antigen and Evaluation of the Immunogenicity of Its Glycoconjugate. *Chem. Eur. J.* **2017**, *23* (28), 6876-6887.
471. Rich, J. R.; Wakarchuk, W. W.; Bundle, D. R., Chemical and Chemoenzymatic Synthesis of S - Linked Ganglioside Analogues and Their Protein Conjugates for Use as Immunogens. *Chem. Eur. J.* **2006**, *12* (3), 845-858.
472. Kuan, T. C.; Wu, H. R.; Adak, A. K.; Li, B. Y.; Liang, C. F.; Hung, J. T.; Chiou, S. P.; Yu, A. L.; Hwu, J. R.; Lin, C. C., Synthesis of an S-Linked α (2 \rightarrow 8) GD3 Antigen and Evaluation of the Immunogenicity of Its Glycoconjugate. *Chem. Eur. J.* **2017**, *23* (28), 6876-6887.
473. Dam, T. K.; Roy, R.; Pagé, D.; Brewer, C. F., Thermodynamic binding parameters of individual epitopes of multivalent carbohydrates to concanavalin A as determined by “reverse” isothermal titration microcalorimetry. *Biochemistry* **2002**, *41* (4), 1359-1363.
474. Roy, R.; Laferrière, C. A.; Gamian, A.; Jennings, H. J., N-acetylneuraminic acid: Neoglycoproteins and pseudopolysaccharides. *J. Carbohydr. Chem.* **1987**, *6* (1), 161-165.
475. Roy, R.; Laferrière, C. A., Synthesis of antigenic copolymers of N-acetylneuraminic acid binding to wheat germ agglutinin and antibodies. *Carbohydr. Res.* **1988**, *177*, c1-c4.

476. Gamian, A.; Chomik, M.; Laferrière, C. A.; Roy, R., Inhibition of influenza A virus hemagglutinin and induction of interferon by synthetic sialylated glycoconjugates. *Can. J. Microbiol.* **1991**, *37* (3), 233-237.
477. Roy, R.; Andersson, F. O.; Harms, G.; Kelm, S.; Schauer, R., Synthesis of Esterase-resistant 9-O-Acetylated Polysialoside as Inhibitor of Influenza C Virus Hemagglutinin. *Angew. Chem. Int. Ed. Engl.* **1992**, *31* (11), 1478-1481.
478. Roy, R.; Andersson, F. O.; Harms, G.; Kelm, S.; Schauer, R., Synthese Esterase - beständiger, 9 - O - acetylierter Polysialoside als Inhibitoren des Influenza - C - Virus - Hämagglutinins. *Angew. Chem.* **1992**, *104* (11), 1551-1554.
479. Roy, R.; Pon, R. A.; Tropper, F. D.; Andersson, F. O., Michael Addition of Poly-L-lysine to N-Acryloylated Sialosides. Syntheses of Influenza A Virus Haemagglutinin Inhibitor and Group B Meningococcal Polysaccharide Vaccines. *J. Chem. Soc., Chem. Commun.* **1993**, 264 - 265.
480. Roy, R.; Park, W. K. C.; Srivastava, O. P.; Foxall, C., Combined Glycomimetic and Multivalent Strategies for the Design of Potent Selectin Antagonists. *Bioorg. Med. Chem. Lett.* **1996**, *6* (12), 1399-1402.
481. Lees, W. J.; Spaltenstein, A.; Kingery-Wood, J. E.; Whitesides, G. M., Polyacrylamides bearing pendant α -sialoside groups strongly inhibit agglutination of erythrocytes by influenza A virus: multivalency and steric stabilization of particulate biological systems. *J. Med. Chem.* **1994**, *37* (20), 3419-3433.
482. Mammen, M.; Dahmann, G.; Whitesides, G. M., Effective inhibitors of hemagglutination by influenza virus synthesized from polymers having active ester groups. Insight into mechanism of inhibition. *J. Med. Chem.* **1995**, *38* (21), 4179-4190.
483. Sigal, G. B.; Mammen, M.; Dahmann, G.; Whitesides, G. M., Polyacrylamides bearing pendant α -sialoside groups strongly inhibit agglutination of erythrocytes by influenza virus: the strong inhibition reflects enhanced binding

through cooperative polyvalent interactions. *J. Am. Chem. Soc.* **1996**, *118* (16), 3789-3800.

484. Choi, S.-K.; Mammen, M.; Whitesides, G. M., Generation and in situ evaluation of libraries of poly (acrylic acid) presenting sialosides as side chains as polyvalent inhibitors of influenza-mediated hemagglutination. *J. Am. Chem. Soc.* **1997**, *119* (18), 4103-4111.

485. Choi, S.-K.; Mammen, M.; Whitesides, G. M., Monomeric inhibitors of influenza neuraminidase enhance the hemagglutination inhibition activities of polyacrylamides presenting multiple C-sialoside groups. *Chem. Biol.* **1996**, *3* (2), 97-104.

486. Spaltenstein, A.; Whitesides, G. M., Polyacrylamides bearing pendant. alpha.-sialoside groups strongly inhibit agglutination of erythrocytes by influenza virus. *J. Am. Chem. Soc.* **1991**, *113* (2), 686-687.

487. Sparks, M. A.; Williams, K. W.; Whitesides, G. M., Neuraminidase-resistant hemagglutination inhibitors: acrylamide copolymers containing a C-glycoside of N-acetylneuraminic acid. *J. Med. Chem.* **1993**, *36* (6), 778-783.

488. Mochalova, L.; Tuzikov, A.; Marinina, V.; Gambaryan, A.; Byramova, N.; Bovin, N.; Matrosovich, M., Synthetic polymeric inhibitors of influenza virus receptor-binding activity suppress virus replication. *Antivir. Res.* **1994**, *23* (3-4), 179-190.

489. Matrosovich, M.; Mochalova, L.; Marinina, V.; Byramova, N.; Bovin, N., Synthetic polymeric sialoside inhibitors of influenza virus receptor - binding activity. *FEBS Lett.* **1990**, *272* (1-2), 209-212.

490. Gambaryan, A.; Tuzikov, A.; Piskarev, V.; Yamnikova, S.; Lvov, D.; Robertson, J.; Bovin, N.; Matrosovich, M., Specification of receptor-binding phenotypes of influenza virus isolates from different hosts using synthetic sialylglycopolymers: non-egg-adapted human H1 and H3 influenza A and influenza

B viruses share a common high binding affinity for 6' -sialyl (N-acetyl)lactosamine). *Virology* **1997**, 232 (2), 345-350.

491. Nagy, J. O.; Wang, P.; Gilbert, J. H.; Schaefer, M. E.; Hill, T. G.; Callstrom, M. R.; Bednarski, M. D., Carbohydrate materials bearing neuraminidase-resistant C-glycosides of sialic acid strongly inhibit the in vitro infectivity of influenza virus. *J. Med. Chem.* **1992**, 35 (23), 4501-4502.

492. Nagy, J. O.; Bednarski, M. D., The chemical-enzymatic synthesis of a carbon glycoside of N-acetyl neuraminic acid. *Tetrahedron Lett.* **1991**, 32 (32), 3953-3956.

493. Roy, R.; Tropper, F., Stereospecific synthesis of aryl β -DN-acetylglucopyranosides by phase transfer catalysis. *Synth. Commun.* **1990**, 20 (14), 2097-2102.

494. Tropper, F. D.; Andersson, F. O.; Grand-Maitre, C.; Roy, R., Stereospecific synthesis of 1, 2-trans-1-phenylthio- β -D-disaccharides under phase transfer catalysis. *Synthesis* **1991**, 1991 (09), 734-736.

495. Roy, R.; Andersson, F. O.; Harms, G.; Kelm, S.; Schauer, R., Synthesis of esterase - resistant 9 - O - acetylated polysialoside as inhibitor of influenza C virus hemagglutinin. *Angew. Chem. Int. Ed. Engl.* **1992**, 31 (11), 1478-1481.

496. Paulsen, H.; Matschulat, P., Synthese von C - Glycosiden der N - Acetylneuraminsäure und weiteren Derivaten. *Liebigs Ann. Chem.* **1991**, 1991 (5), 487-495.

497. Itoh, M.; Hetterich, P.; Isecke, R.; Brossmer, R.; Klenk, H.-D., Suppression of influenza virus infection by an N-thioacetylneuraminic acid acrylamide copolymer resistant to neuraminidase. *Virology* **1995**, 212 (2), 340-347.

498. Nishimura, S.; Lee, K.; Matsuoka, K.; Lee, Y. C., Chemoenzymic preparation of a glycoconjugate polymer having a sialyloligosaccharide: Neu5Ac α (2 \rightarrow 3) Gal β (1 \rightarrow 4) GlcNAc. *Biochem. Biophys. Res. Commun.* **1994**, 199 (1), 249-254.

499. Furuike, T.; Aiba, S.; Suzuki, T.; Takahashi, T.; Suzuki, Y.; Yamada, K.; Nishimura, S.-I., Synthesis and anti-influenza virus activity of novel glycopolymers having triantennary oligosaccharide branches 1. *J. Chem. Soc. Perkin Trans. I* **2000**, (17), 3000-3005.
500. Suzuki, K.; Sakamoto, J.-I.; Koyama, T.; Yingsakmongkon, S.; Suzuki, Y.; Hatano, K.; Terunuma, D.; Matsuoka, K., Synthesis of sialic acid derivatives having a CC double bond substituted at the C-5 position and their glycopolymers. *Bioorg. Med. Chem. Lett.* **2009**, *19* (17), 5105-5108.
501. Wu, W.-Y.; Jin, B.; Krippner, G. Y.; Watson, K. G., Synthesis of a polymeric 4-N-linked sialoside which inhibits influenza virus hemagglutinin. *Bioorg. Med. Chem. Lett.* **2000**, *10* (4), 341-343.
502. Byramova, N. E.; Mochalova, L. V.; Belyanchikov, I. M.; Matrosovich, M. N.; Bovin, N. V., Synthesis of sialic acid pseudopolysaccharides by coupling of spacer-connected Neu5Ac with activated polymer. *J. Carbohydr. Chem.* **1991**, *10* (4), 691-700.
503. Tsuchida, A.; Kobayashi, K.; Matsubara, N.; Muramatsu, T.; Suzuki, T.; Suzuki, Y., Simple synthesis of sialyllactose-carrying polystyrene and its binding with influenza virus. *Glycoconjug. J.* **1998**, *15* (11), 1047-1054.
504. Thoma, G.; Patton, J. T.; Magnani, J. L.; Ernst, B.; Öhrlein, R.; Duthaler, R. O., Versatile functionalization of polylysine: synthesis, characterization, and use of neoglycoconjugates. *J. Am. Chem. Soc.* **1999**, *121* (25), 5919-5929.
505. Kamitakahara, H.; Suzuki, T.; Nishigori, N.; Suzuki, Y.; Kanie, O.; Wong, C. H., A Lysoganglioside/Poly - L - glutamic Acid Conjugate as a Picomolar Inhibitor of Influenza Hemagglutinin. *Angew. Chem. Int. Ed.* **1998**, *37* (11), 1524-1528.
506. Haldar, J.; De Cienfuegos, L. Á.; Tumpey, T. M.; Gubareva, L. V.; Chen, J.; Klibanov, A. M., Bifunctional polymeric inhibitors of human influenza A viruses. *Pharm. Res.* **2010**, *27* (2), 259-263.

507. Matsuoka, K.; Takita, C.; Koyama, T.; Miyamoto, D.; Yingsakmongkon, S.; Hidari, K. I.; Jampangern, W.; Suzuki, T.; Suzuki, Y.; Hatano, K., Novel linear polymers bearing thiosialosides as pendant-type epitopes for influenza neuraminidase inhibitors. *Bioorg. Med. Chem. Lett.* **2007**, *17* (14), 3826-3830.
508. Uemura, S.; Feng, F.; Kume, M.; Yamada, K.; Kabayama, K.; Nishimura, S.-I.; Igarashi, Y.; Inokuchi, J.-I., Cell growth arrest by sialic acid clusters in ganglioside GM3 mimetic polymers. *Glycobiology* **2007**, *17* (6), 568-577.
509. Ogata, M.; Hidari, K. I.; Kozaki, W.; Murata, T.; Hiratake, J.; Park, E. Y.; Suzuki, T.; Usui, T., Molecular design of spacer-N-linked sialoglycopolyptide as polymeric inhibitors against influenza virus infection. *Biomacromolecules* **2009**, *10* (7), 1894-1903.
510. Kolb, H. C.; Finn, M.; Sharpless, K. B., Click chemistry: diverse chemical function from a few good reactions. *Angew. Chem. Int. Ed.* **2001**, *40* (11), 2004-2021.
511. Nagao, M.; Fujiwara, Y.; Matsubara, T.; Hoshino, Y.; Sato, T.; Miura, Y., Design of glycopolymers carrying sialyl oligosaccharides for controlling the interaction with the influenza virus. *Biomacromolecules* **2017**, *18* (12), 4385-4392.
512. Tanaka, T.; Ishitani, H.; Miura, Y.; Oishi, K.; Takahashi, T.; Suzuki, T.; Shoda, S.-i.; Kimura, Y., Protecting-group-free synthesis of glycopolymers bearing sialyloligosaccharide and their high binding with the influenza virus. *ACS Macro Lett.* **2014**, *3* (10), 1074-1078.
513. Yang, Z.-Q.; Puffer, E. B.; Pontrello, J. K.; Kiessling, L. L., Synthesis of a multivalent display of a CD22-binding trisaccharide. *Carbohydr. Res.* **2002**, *337* (18), 1605-1613.
514. Courtney, A. H.; Puffer, E. B.; Pontrello, J. K.; Yang, Z.-Q.; Kiessling, L. L., Sialylated multivalent antigens engage CD22 in trans and inhibit B cell activation. *Proc. Natl. Acad. Sci. U. S. A.* **2009**, *106* (8), 2500-2505.

515. Tang, S.; Puryear, W. B.; Seifried, B. M.; Dong, X.; Runstadler, J. A.; Ribbeck, K.; Olsen, B. D., Antiviral agents from multivalent presentation of sialyl oligosaccharides on brush polymers. *ACS Macro Lett.* **2016**, *5* (3), 413-418.
516. Yamaguchi, S.; Yoshimura, A.; Yasuda, Y.; Mori, A.; Tanaka, H.; Takahashi, T.; Kitajima, K.; Sato, C., Chemical Synthesis and Evaluation of a Disialic Acid - Containing Dextran Polymer as an Inhibitor for the Interaction between Siglec 7 and Its Ligand. *ChemBioChem* **2017**, *18* (13), 1194-1203.
517. Hai, W.; Goda, T.; Takeuchi, H.; Yamaoka, S.; Horiguchi, Y.; Matsumoto, A.; Miyahara, Y., Specific recognition of human influenza virus with PEDOT bearing sialic acid-terminated trisaccharides. *ACS Appl. Mater. Interfaces* **2017**, *9* (16), 14162-14170.
518. Huang, M. L.; Cohen, M.; Fisher, C. J.; Schooley, R. T.; Gagneux, P.; Godula, K., Determination of receptor specificities for whole influenza viruses using multivalent glycan arrays. *Chem. Commun.* **2015**, *51* (25), 5326-5329.
519. Reuter, J. D.; Myc, A.; Hayes, M. M.; Gan, Z.; Roy, R.; Qin, D.; Yin, R.; Piehler, L. T.; Esfand, R.; Tomalia, D. A., Inhibition of viral adhesion and infection by sialic-acid-conjugated dendritic polymers. *Bioconjug. Chem.* **1999**, *10* (2), 271-278.
520. Wang, Q.; Dordick, J. S.; Linhardt, R. J., Chemoenzymatic synthesis of neuraminic acid containing C-glycoside polymers. *Org. Lett.* **2003**, *5* (8), 1187-1189.
521. Roy, R.; Zanini, D.; Meunier, S. J.; Romanowska, A., Solid-phase Synthesis of Dendritic Sialoside Inhibitors of Influenza A Virus Haemagglutinin. *J. Chem. Soc., Chem. Commun.* **1993**, 1869 - 1872.
522. Zanini, D.; Roy, R., Synthesis of new α -thiosialodendrimers and their binding properties to the sialic acid specific lectin from *Limax flavus*. *J. Am. Chem. Soc.* **1997**, *119*, 2088-2095.

523. Zanini, D.; Roy, R., Practical Synthesis of Starburst PAMAM α -Thiosialodendrimers for Probing Multivalent Carbohydrate–Lectin Binding Properties. *J. Org. Chem.* **1998**, *63* (10), 3486-3491.
524. Thompson, J. P.; Schengrund, C.-L., Oligosaccharide-derivatized dendrimers: defined multivalent inhibitors of the adherence of the cholera toxin B subunit and the heat labile enterotoxin of *E. coli* to GM1. *Glycoconjug. J.* **1997**, *14* (7), 837-845.
525. Clayton, R.; Hardman, J.; LaBranche, C. C.; McReynolds, K. D., Evaluation of the synthesis of sialic acid-PAMAM glycodendrimers without the use of sugar protecting groups, and the anti-HIV-1 properties of these compounds. *Bioconjug. Chem.* **2011**, *22* (10), 2186-2197.
526. Landers, J. J.; Cao, Z.; Lee, I.; Piehler, L. T.; Myc, P. P.; Myc, A.; Hamouda, T.; Galecki, A. T.; Baker Jr, J. R., Prevention of influenza pneumonitis by sialic acid–conjugated dendritic polymers. *J. Infect. Dis.* **2002**, *186* (9), 1222-1230.
527. Patel, D.; Henry, J.; Good, T., Attenuation of β -amyloid induced toxicity by sialic acid-conjugated dendrimeric polymers. *Biochim. Biophys. Acta Gen. Subj.* **2006**, *1760* (12), 1802-1809.
528. Patel, D. A.; Henry, J. E.; Good, T. A., Attenuation of β -amyloid-induced toxicity by sialic-acid-conjugated dendrimers: Role of sialic acid attachment. *Brain Res.* **2007**, *1161*, 95-105.
529. Tsvetkov, D.; Cheshev, P.; Tuzikov, A.; Chinarev, A.; Pazynina, G.; Sablina, M.; Gambaryan, A.; Bovin, N.; Rieben, R.; Shashkov, A., Neoglycoconjugates based on dendrimer poly (aminoamides). *Russ. J. Bioorg. Chem.* **2002**, *28* (6), 470-486.
530. Günther, S. C.; Maier, J. D.; Vetter, J.; Podvalnyy, N.; Khanzhin, N.; Hennet, T.; Stertz, S., Antiviral potential of 3'-sialyllactose-and 6'-sialyllactose-conjugated dendritic polymers against human and avian influenza viruses. *Sci. Rep.* **2020**, *10* (1), 1-9.

531. Zanini, D.; Roy, R., Novel Dendritic α -Sialosides: Synthesis of Glycodendrimers Based on a 3, 3 '-Iminobis (propylamine) Core. *J. Org. Chem.* **1996**, *61* (21), 7348-7354.
532. Gajbhiye, V.; Ganesh, N.; Barve, J.; Jain, N. K., Synthesis, characterization and targeting potential of zidovudine loaded sialic acid conjugated-mannosylated poly (propyleneimine) dendrimers. *Eur. J. Pharm. Sci.* **2013**, *48* (4-5), 668-679.
533. Verdile, G.; Fuller, S.; Atwood, C. S.; Laws, S. M.; Gandy, S. E.; Martins, R. N., The role of beta amyloid in Alzheimer's disease: still a cause of everything or the only one who got caught? *Pharmacol. Res.* **2004**, *50* (4), 397-409.
534. Sashiwa, H.; Makimura, Y.; Roy, R.; Shigemasa, Y., Chemical modification of chitosan: preparation of chitosan-sialic acid branched polysaccharide hybrids. *Chem. Commun.* **2000**, (11), 909-910.
535. Papp, I.; Sieben, C.; Sisson, A. L.; Kostka, J.; Bottcher, C.; Ludwig, K.; Herrmann, A.; Haag, R., Inhibition of influenza virus activity by multivalent glycoarchitectures with matched sizes. *Chembiochem* **2011**, *12* (6), 887-95.
536. Meunier, S. J.; Wu, Q.; Wang, S.-N.; Roy, R., Synthesis of hyperbranched glycodendrimers incorporating α -thiosialosides based on a gallic acid core. *Can. J. Chem.* **1997**, *75* (11), 1472-1482.
537. Sakamoto, J.-I.; Koyama, T.; Miyamoto, D.; Yingsakmongkon, S.; Hidari, K. I.; Jampangern, W.; Suzuki, T.; Suzuki, Y.; Esumi, Y.; Hatano, K., Thiosialoside clusters using carbosilane dendrimer core scaffolds as a new class of influenza neuraminidase inhibitors. *Bioorg. Med. Chem. Lett.* **2007**, *17* (3), 717-721.
538. Oka, H.; Onaga, T.; Koyama, T.; Guo, C.-T.; Suzuki, Y.; Esumi, Y.; Hatano, K.; Terunuma, D.; Matsuoka, K., Syntheses and biological evaluations of carbosilane dendrimers uniformly functionalized with sialyl α (2 \rightarrow 3) lactose moieties as inhibitors for human influenza viruses. *Bioorg. Med. Chem.* **2009**, *17* (15), 5465-5475.

539. Sakamoto, J.-I.; Koyama, T.; Miyamoto, D.; Yingsakmongkon, S.; Hidari, K. I.; Jampangern, W.; Suzuki, T.; Suzuki, Y.; Esumi, Y.; Nakamura, T., Systematic syntheses of influenza neuraminidase inhibitors: a series of carbosilane dendrimers uniformly functionalized with thioglycoside-type sialic acid moieties. *Bioorg. Med. Chem.* **2009**, *17* (15), 5451-5464.
540. Rahman, M. M.; Kitao, S.; Tsuji, D.; Suzuki, K.; Sakamoto, J.-I.; Matsuoka, K.; Matsuzawa, F.; Aikawa, S.-I.; Itoh, K., Inhibitory effects and specificity of synthetic sialyldendrimers toward recombinant human cytosolic sialidase 2 (NEU2). *Glycobiology* **2013**, *23* (4), 495-504.
541. Pukin, A. V.; Branderhorst, H. M.; Sisu, C.; Weijers, C. A.; Gilbert, M.; Liskamp, R. M.; Visser, G. M.; Zuilhof, H.; Pieters, R. J., Strong inhibition of cholera toxin by multivalent GM1 derivatives. *ChemBioChem* **2007**, *8* (13), 1500-1503.
542. Kingery-Wood, J. E.; Williams, K. W.; Sigal, G. B.; Whitesides, G. M., The agglutination of erythrocytes by influenza virus is strongly inhibited by liposomes incorporating an analog of sialyl gangliosides. *J. Am. Chem. Soc.* **1992**, *114* (18), 7303-7305.
543. Spevak, W.; Nagy, J. O.; Charych, D. H.; Schaefer, M. E.; Gilbert, J. H.; Bednarski, M. D., Polymerized liposomes containing C-glycosides of sialic acid: potent inhibitors of influenza virus in vitro infectivity. *J. Am. Chem. Soc.* **1993**, *115* (3), 1146-1147.
544. Koketsu, M.; Nitoda, T.; Sugino, H.; Juneja, L. R.; Kim, M.; Yamamoto, T.; Abe, N.; Kajimoto, T.; Wong, C.-H., Synthesis of a novel sialic acid derivative (sialylphospholipid) as an antirotaviral agent. *J. Med. Chem.* **1997**, *40* (21), 3332-3335.
545. Guo, C.-T.; Sun, X.-L.; Kanie, O.; Shortridge, K. F.; Suzuki, T.; Miyamoto, D.; Hidari, K. I.-P. J.; Wong, C.-H.; Suzuki, Y., An O-glycoside of sialic acid

derivative that inhibits both hemagglutinin and sialidase activities of influenza viruses. *Glycobiology* **2002**, *12* (3), 183-190.

546. Yadav, R.; Kikkeri, R., Exploring the effect of sialic acid orientation on ligand–receptor interactions. *Chem. Commun.* **2012**, *48* (58), 7265-7267.

547. Hendricks, G. L.; Weirich, K. L.; Viswanathan, K.; Li, J.; Shriver, Z. H.; Ashour, J.; Ploegh, H. L.; Kurt-Jones, E. A.; Fygenson, D. K.; Finberg, R. W., Sialylneolacto-N-tetraose c (LSTc)-bearing liposomal decoys capture influenza A virus. *J. Biol. Chem.* **2013**, *288* (12), 8061-8073.

548. Blixt, O.; Han, S.; Liao, L.; Zeng, Y.; Hoffmann, J.; Futakawa, S.; Paulson, J. C., Sialoside analogue arrays for rapid identification of high affinity siglec ligands. *J. Am. Chem. Soc.* **2008**, *130* (21), 6680-6681.

549. Chen, W. C.; Kawasaki, N.; Nycholat, C. M.; Han, S.; Pilotte, J.; Crocker, P. R.; Paulson, J. C., Antigen delivery to macrophages using liposomal nanoparticles targeting sialoadhesin/CD169. *PloS one* **2012**, *7* (6), e39039.

550. Cheng, H.-W.; Wang, H.-W.; Wong, T.-Y.; Yeh, H.-W.; Chen, Y.-C.; Liu, D.-Z.; Liang, P.-H., Synthesis of S-linked NeuAc- α (2-6)-di-LacNAc bearing liposomes for H1N1 influenza virus inhibition assays. *Bioorg. Med. Chem.* **2018**, *26* (9), 2262-2270.

551. Yeh, H.-W.; Lin, T.-S.; Wang, H.-W.; Cheng, H.-W.; Liu, D.-Z.; Liang, P.-H., S-Linked sialyloligosaccharides bearing liposomes and micelles as influenza virus inhibitors. *Org. Biomol. Chem.* **2015**, *13* (47), 11518-11528.

552. Zanini, D.; Roy, R., Synthesis of new α -thiosialodendrimers and their binding properties to the sialic acid specific lectin from *Limax flavus*. *J. Am. Chem. Soc.* **1997**, *119* (9), 2088-2095.

553. Groves, D. R.; Bradley, S. J.; Rose, F. J.; Kiefel, M. J.; Von Itzstein, M., How pure is your thiosialoside? A reinvestigation into the HPLC purification of thioglycosides of N-acetylneuraminic acid. *Glycoconjug. J.* **1999**, *16* (1), 13-17.

554. Sakamoto, J.-I.; Takita, C.; Koyama, T.; Hatano, K.; Terunuma, D.; Matsuoka, K., Use of a recycle-type SEC method as a powerful tool for purification of thiosialoside derivatives. *Carbohydr. Res.* **2008**, *343* (16), 2735-2739.
555. Morais, G. R.; Oliveira, I. F.; Humphrey, A. J.; Falconer, R. A., Identification of an acetyl disulfide derivative in the synthesis of thiosialosides. *Carbohydr. Res.* **2010**, *345* (1), 160-162.
556. Mandal, S.; Nilsson, U. J., Tri-isopropylsilyl thioglycosides as masked glycosyl thiol nucleophiles for the synthesis of S-linked glycosides and glycoconjugates. *Org. Biomol. Chem.* **2014**, *12* (27), 4816-4819.
557. Xue, W.; Cheng, X.; Fan, J.; Diao, H.; Wang, C.; Dong, L.; Luo, Y.; Chen, J.; Zhang, J., A novel stereoselective synthesis of 1, 2-trans-thioaldoses. *Tetrahedron Lett.* **2007**, *48* (35), 6092-6095.
558. Crich, D.; Wu, B., Stereoselective iterative one-pot synthesis of N-glycolylneuraminic acid-containing oligosaccharides. *Org. Lett.* **2008**, *10* (18), 4033-4035.
559. McAuliffe, J. C.; Rabuka, D.; Hindsgaul, O., Synthesis of O-glycolyl-linked neuraminic acids through a spirocyclic intermediate. *Org. Lett.* **2002**, *4* (18), 3067-3069.
560. Zhu, J.; Yan, F.; Guo, Z.; Marchant, R. E., Surface modification of liposomes by saccharides: Vesicle size and stability of lactosyl liposomes studied by photon correlation spectroscopy. *J. Colloid Interface Sci.* **2005**, *289* (2), 542-550.
561. Gui, L.; Lee, K. K., Influenza virus-liposome fusion studies using fluorescence dequenching and cryo-electron tomography. In *Influenza Virus*, Springer: 2018; pp 261-279.
562. van Kasteren, S. I.; Kramer, H. B.; Jensen, H. H.; Campbell, S. J.; Kirkpatrick, J.; Oldham, N. J.; Anthony, D. C.; Davis, B. G., Expanding the diversity of chemical protein modification allows post-translational mimicry. *Nature* **2007**, *446* (7139), 1105-9.

563. Marra, A.; Sinaý, P., Stereoselective synthesis of 2-thioglycosides of N-acetylneuraminic acid. *Carbohydr. Res.* **1989**, *187* (1), 35-42.
564. Vocadlo, D. J.; Withers, S. G., Detailed comparative analysis of the catalytic mechanisms of β -N-acetylglucosaminidases from families 3 and 20 of glycoside hydrolases. *Biochemistry* **2005**, *44* (38), 12809-12818.
565. Clinch, K.; Evans, G. B.; Furneaux, R. H.; Rendle, P. M.; Rhodes, P. L.; Robertson, A. M.; Rosendale, D. I.; Tyler, P. C.; Wright, D. P., Synthesis and utility of sulfated chromogenic carbohydrate model substrates for measuring activities of mucin-desulfating enzymes. *Carbohydr. Res.* **2002**, *337* (12), 1095-1111.
566. Liu, B.; Roy, R., Synthesis of clustered xenotransplantation antagonists using palladium-catalyzed cross-coupling of prop-2-ynyl α -D-galactopyranoside. *J. Chem. Soc. Perkin Trans. I* **2001**, (8), 773-779.
567. Fernandez-Megia, E.; Correa, J.; Rodríguez-Meizoso, I.; Riguera, R., A click approach to unprotected glycodendrimers. *Macromolecules* **2006**, *39* (6), 2113-2120.
568. Chen, C.-T.; Huang, W.-P., A highly selective fluorescent chemosensor for lead ions. *J. Am. Chem. Soc.* **2002**, *124* (22), 6246-6247.
569. Fine Nathel, N. F.; Morrill, L. A.; Mayr, H.; Garg, N. K., Quantification of the Electrophilicity of Benzyne and Related Intermediates. *J. Am. Chem. Soc.* **2016**, *138* (33), 10402-10405.
570. MeS, B., Synthesis of uranyl salophene metallo-macrocycles with additional functional groups. *Synthesis* **1992**.
571. Lin, C.-C.; Lin, N.-P.; Sahabuddin, L. S.; Reddy, V. R.; Huang, L.-D.; Hwang, K. C.; Lin, C.-C., 5-N, 4-O-Carbonyl-7, 8, 9-tri-O-chloroacetyl-protected sialyl donor for the stereoselective synthesis of α -(2 \rightarrow 9)-tetrasialic acid. *J. Org. Chem.* **2010**, *75* (15), 4921-4928.